

# Electronic, Structural, and Catalytic Analyses of Iron Pincer Complexes and Methods for the Direct Functionalization of Lactide

Author: Teresa Louise Mako

Persistent link: <http://hdl.handle.net/2345/bc-ir:107588>

This work is posted on [eScholarship@BC](#),  
Boston College University Libraries.

---

Boston College Electronic Thesis or Dissertation, 2017

Copyright is held by the author, with all rights reserved, unless otherwise noted.

# Electronic, Structural, and Catalytic Analyses of Iron Pincer Complexes and Methods for the Direct Functionalization of Lactide

Teresa Louise Mako

A thesis

submitted to the Faculty of

the department of Chemistry

in partial fulfillment

of the requirements for the degree of

Master of Science

Boston College  
Morrissey College of Arts and Sciences  
Graduate School

August 2017



# **Electronic, Structural, and Catalytic Analyses of Iron Pincer Complexes, and Methods for the Direct Functionalization of Lactide**

Teresa Louise Mako

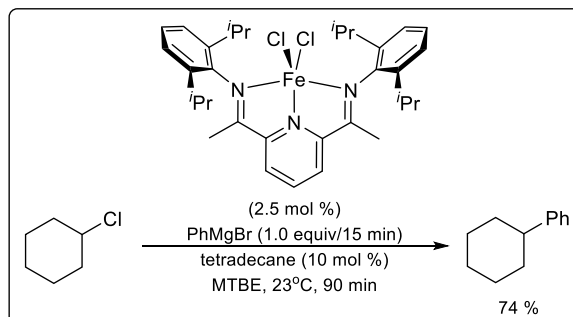
Advisor: Jeffery Byers

## **Abstracts**

### **Chapter 1. A Review of Recent Iron Catalyzed Cross Coupling Advances**

Herein, advances in iron catalyzed cross coupling from 2010-2015 are thoroughly reviewed. Newly developed protocols and the mechanistic work that has been conducted to gain understanding of these systems are discussed. Specific emphasis is placed on the techniques used for mechanistic investigations.

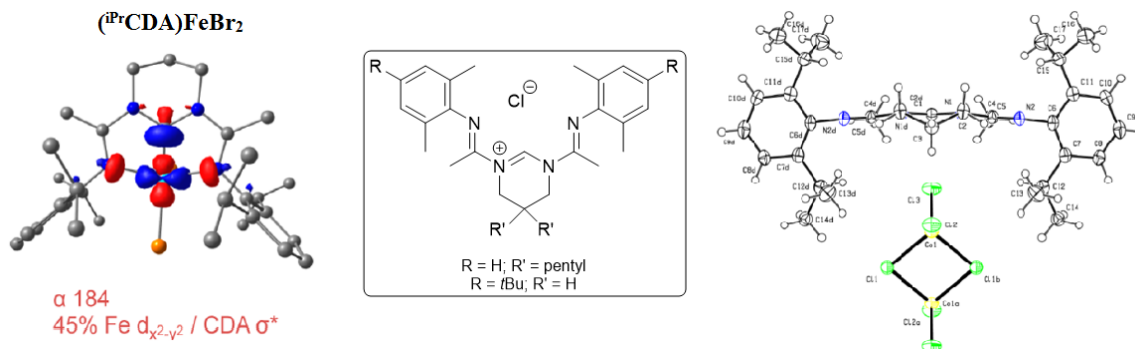
## Chapter 2. Cross Coupling Applications of Pyridyl(Diimine) Iron Complexes



Versatile and redox noninnocent pyridyl(diimine) iron complexes were explored for catalytic ability in iron catalyzed cross coupling reactions. These complexes were found active for the coupling of benzyl halides and aryl Grignard reagents, producing moderate yields. Although active for the coupling of cyclohexyl chloride and aryl Grignard reagents, the catalytic ability of these complexes was not general for alkyl halides, and the majority of substrates readily underwent  $\beta$ -hydride elimination. Mechanistic studies indicated the role of  $\text{PDiFe(I)Ph}$  and  $\text{PDiFe(0)(N}_2)_2$  as off-cycle species.

Additionally, these complexes were employed for the Suzuki-type coupling of alkyl halides with 1,1-bis(boronates), leading to the conclusion that the processes were instead base catalyzed.

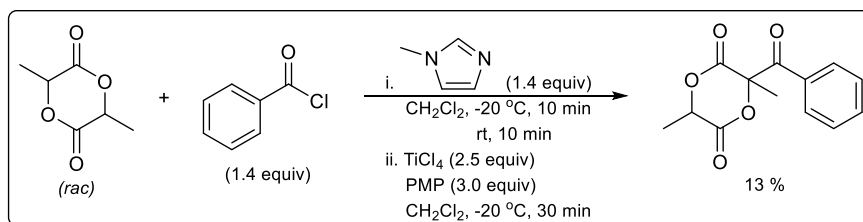
### Chapter 3. Electronic Structure Analysis and Catalytic Applications of Carbeno(Diamidine) Iron Complexes



Iron(II) pincer complexes carbeno(diamidine) iron dibromide [(CDA)FeBr<sub>2</sub>] and bis(*N*-heterocyclic carbene)pyridine iron dibromide [(CNC)FeBr<sub>2</sub>] were examined by magnetic circular dichroism and density functional theory studies to investigate the effect that NHC moieties have on electronic structure and bonding in tridentate pincer ligands. The increased Fe-C bonding and pincer-donating abilities that result from NHC incorporation have a direct impact on spin state and observed ligand fields. Additionally, the position of the NHC moiety on the tridentate ligand and the overall geometry of the molecule were found to effect the net donor ability of the pincers and the strength of the iron-pincer interactions.

Three new variations of the CDA ligand were developed and evaluated for catalytic ability in olefin hydrogenation and atom transfer radical polymerization reactions. While iron CDA complexes were found to be mediocre catalysts for both transformations, a cobalt CDA dimer complex was developed that showed promising catalytic activity for olefin hydrogenation.

## Chapter 4. The Direct Functionalization of Lactide



In an effort to provide cyclic diesters that could generate useful and biodegradable polymers, the direct functionalization of lactide was pursued. Lactide undergoes ring opening under a wide range of conditions, and thus traditional methods used for the functionalization of lactones could not be employed here. Typical routes for the formation of cyclic diesters involve multi-step syntheses and low yielding cyclization reactions. Herein, C-H activation and soft enolization have been identified as promising avenues toward the direct functionalization of lactide. Palladium catalyzed C-H activation was not amenable for lactide, however, soft enolization techniques led to low yields of the desired functionalized product.

## TABLE OF CONTENTS

<b>Table of Contents</b> .....	<b>i</b>
<b>Acknowledgements</b> .....	<b>iv</b>
<b>Nomenclature</b> .....	<b>v</b>
<b>1.0 A Review of Recent Iron Catalyzed Cross Coupling Advances</b> .....	<b>1</b>
<b>1.1 Cross Coupling History: Palladium and Nickel</b> .....	<b>1</b>
<b>1.2 Palladium Catalyzed Alkyl - Alkyl Cross Coupling</b> .....	<b>2</b>
<b>1.3 Nickel Catalyzed Alkyl-Alkyl Cross Coupling</b> .....	<b>3</b>
<b>1.4 Iron Catalyzed Kumada - Type Systems</b> .....	<b>5</b>
1.4.1 Aryl Nucleophile - Aryl Electrophile.....	7
1.4.2 Aryl Nucleophile - Vinyl Electrophile.....	10
1.4.3 Aryl Nucleophile - Alkyl Electrophile.....	11
1.4.4 Alkyl Nucleophile - Aryl Electrophile.....	21
1.4.5 Alkyl Nucleophile - Vinyl Electrophile.....	28
1.4.6 Alkyl Nucleophile - Alkyl Electrophile.....	29
1.4.7 Alkynyl Nucleophile - Alkyl Electrophile.....	31
<b>1.5 Iron Catalyzed Kumada - Mechanistic Implications</b> .....	<b>32</b>
1.5.1 Alkyl Nucleophile - Vinyl Electrophile.....	33
1.5.2 Alkyl Nucleophile - Aryl Electrophile.....	35
1.5.3 Aryl Nucleophile - Alkyl Electrophile.....	39
1.5.4 Alkyl Nucleophile - Alkyl Electrophile.....	46
1.5.5 Alkynyl Nucleophile - Alkyl Electrophile.....	47
1.5.6 Importance of Ligation.....	47
<b>1.6 Iron Catalyzed Suzuki - Type Systems</b> .....	<b>48</b>
<b>1.7 Iron Catalyzed Suzuki - Mechanistic Implications</b> .....	<b>50</b>
1.7.1 Proposed Mechanisms .....	50
1.7.2 Transmetalation Studies.....	51
<b>1.8 Additional Variations</b> .....	<b>54</b>
1.8.1 Iron Catalyzed Negishi - Type Systems.....	54
1.8.2 Iron Catalyzed Heck - Type Systems .....	56
1.8.3 Iron Catalyzed Sonogashira - Type Systems.....	58
1.8.4 Miscellaneous Systems .....	60
<b>1.9 Conclusions</b> .....	<b>63</b>
<b>1.10 References</b> .....	<b>64</b>
<b>2.0 Cross Coupling Applications of Pyridyl(Diimine) Iron Complexes</b> .....	<b>67</b>
<b>2.1 Introduction</b> .....	<b>67</b>
2.1.1 Iron PDI Complexes .....	67
2.1.2 Bis(Boronate)s as Suzuki-Miyaura Coupling Partners.....	69
<b>2.2 Kumada - Type Coupling Reactions</b> .....	<b>72</b>
2.2.1 Benzyl Halide - Aryl Grignard Reagent.....	72
2.2.2 Alkyl Halide - Aryl Grignard Reagent Optimization .....	76
2.2.3 Mechanistic Studies.....	81
2.2.4 Grignard Reagent Scope.....	84
2.2.5 Alkyl Halide Scope.....	87
2.2.6 Cyclooctyl Chloride Optimization.....	90
2.2.7 Halide Effects .....	93

2.2.8	Conclusions.....	95
<b>2.3</b>	<b>Suzuki - Type Coupling Reactions.....</b>	<b>95</b>
2.3.1	Phenyl Pinacol Borane as a Coupling Partner.....	95
2.3.2	Iron Alkoxide Catalyst Development.....	97
2.3.3	1,1-Bis(Boronates) as Coupling Partners.....	99
2.3.4	Conclusions.....	105
<b>2.4</b>	<b>Experimental.....</b>	<b>106</b>
2.4.1	General Considerations.....	106
2.4.2	Syntheses of Complexes.....	107
2.4.2	Syntheses of Substrates.....	108
2.4.2	Cross Coupling Procedures and Desired Products.....	110
<b>2.5</b>	<b>Spectroscopy.....</b>	<b>113</b>
<b>2.6</b>	<b>References.....</b>	<b>120</b>
<b>3.0</b>	<b>Electronic Structure Analyses and Catalytic Applications of Carbeno(Diamidene) Iron Complexes.....</b>	<b>122</b>
<b>3.1</b>	<b>Introduction.....</b>	<b>122</b>
3.1.1	Pyridyl(Diimine) Ligands - An Inspiration.....	122
3.1.2	Development of Carbeno(Diamidene) Ligands.....	127
3.1.2.1	Further Characterization of ( <sup>i</sup> PrCDA)Fe(II)Cl <sub>2</sub> (3.8).....	129
3.1.2.2	Characterization of ( <sup>i</sup> PrCDA)Fe(0)(CO) <sub>2</sub> (3.11).....	132
3.1.2.3	Characterization of [( <sup>i</sup> PrCDA)Fe(III)Cl <sub>2</sub> ][BF <sub>4</sub> ] (3.9).....	134
3.1.2.4	Characterization of ( <sup>i</sup> PrCDA)Fe(I)Cl (3.10).....	136
3.1.2.5	Summary and Comparisons.....	138
3.1.3	Potential Catalytic Applications.....	140
3.1.3.1	Olefin Hydrogenation.....	140
3.1.3.2	Atom Transfer Radical Polymerization.....	142
<b>3.2</b>	<b>Electronic Structure Comparison of PDI, CNC, and CDA Iron Complexes.....</b>	<b>144</b>
3.2.1	Synthesis of ( <sup>i</sup> PrCDA)FeBr <sub>2</sub> .....	144
3.2.2	Electronic Structure Comparison.....	146
3.2.3	Summary of Results.....	153
<b>3.3</b>	<b>Synthesis of Additional CDA Ligands.....</b>	<b>154</b>
<b>3.4</b>	<b>Olefin Hydrogenation.....</b>	<b>157</b>
3.4.1	Results and Discussion.....	157
3.4.2	(CDA)CoCl <sub>2</sub> Synthesis and Hydrogenation Ability.....	161
<b>3.5</b>	<b>Atom Transfer Radical Polymerization.....</b>	<b>163</b>
<b>3.6</b>	<b>Conclusions.....</b>	<b>164</b>
<b>3.7</b>	<b>Experimental.....</b>	<b>165</b>
3.7.1	General Considerations.....	165
3.7.2	Experimental Procedures.....	166
<b>3.8</b>	<b>Spectroscopy.....</b>	<b>175</b>
<b>3.9</b>	<b>References.....</b>	<b>188</b>
<b>4.0</b>	<b>The Direct Functionalization of Lactide.....</b>	<b>190</b>
<b>4.1</b>	<b>Introduction.....</b>	<b>190</b>
4.1.1	Poly(Lactic Acid) - Renewable and Biodegradable.....	190
4.1.2	Synthesis of Cyclic Diesters.....	191
4.1.3	C-H Activation.....	196
4.1.4	Soft Enolization.....	198
<b>4.2</b>	<b>C-H Activation of Lactide.....</b>	<b>199</b>
4.2.1	Results.....	199
4.2.2	Conclusions.....	204
<b>4.3</b>	<b>Soft Enolization of Lactide.....</b>	<b>204</b>
4.3.1	Results.....	204
4.3.2	Conclusions.....	208
<b>4.4</b>	<b>Experimental.....</b>	<b>209</b>
4.4.1	General Considerations.....	209

4.4.2	Experimental Procedures .....	210
4.4.2.1	C-H Activation.....	210
4.4.2.2	Soft Enolization.....	211
<b>4.5</b>	<b>Spectroscopy.....</b>	<b>213</b>
<b>4.6</b>	<b>References .....</b>	<b>216</b>
<b>5.0</b>	<b>Appendix I: X-Ray Crystallographic Analyses .....</b>	<b>217</b>
5.1	X-Ray Crystallographic Analysis of 2.21 .....	217
5.2	X-Ray Crystallographic Analysis of 3.19 .....	308
5.1	X-Ray Crystallographic Analysis of 3.33.....	329

## ACKNOWLEDGEMENTS

To Dr. Michael Neidig, Dr. Hilan Kaplan, Dr. Xiaofei Zhang, Charles Wolstenholme, Tessa Baker, Bo Li, Jessica Drake, Michael Crockett, and Aris Vasilopoulos for their scientific contributions to the research described herein.

To the ACS-PRF and to Boston College for financially supporting this research.

To Dr. Christopher Brown, Dr. Mindy Levine, and Dr. Jeffery Byers for giving me the opportunities to join their research groups and for sharing their knowledge. Special thanks to Dr. Mindy Levine for reminding me why chemistry is my passion and for providing an enjoyable research environment.

To Dr. Aman Kaur, Miao Qi, Michael Crockett, Dr. Hilan Kaplan, Jessica Drake, and Dr. Cesar Manna for their mentorship, support, and friendship during my graduate career at Boston College.

To the faculty and staff in the Boston College Chemistry Department, especially Ian Parr, Dale Mahoney, Lynne Pflaumer, Lynne O'Connell, Amarjit Nijjar, Thusitha Jayasundera, Neil Wolfman, and my committee members Amir Hoveyda and T. Ross Kelly.

To Douglas Norman for his unwavering love and boundless, patient, and invaluable support. To Syrena Fernandes for the commiseration, late night study sessions, trips to Rudy's, and for always believing in me.

To my family, who have been loyally by my side throughout this journey and who continue to support me through my ups and downs, especially my parents Laura Scoville and David Mako, and my siblings Calvin and Natalie. And to Paul, who hates the title, but loves the content.

## NOMENCLATURE

$\alpha$	alpha
$\beta$	beta
$\delta$	delta; chemical shift (NMR); isomer shift (Mössbauer)
$\mu$	micro
$\pi$	pi
$\rho$	rho
$\sigma$	sigma
$ \Delta E_Q $	quadrupole splitting
$\chi_T$	magnetic susceptibility
$\Delta G$	Gibbs free energy
$\Delta G^\ddagger$	activation energy
$10D_q$	ligand field splitting energy
Å	angstrom
Ac	acetal
acac	acetylacetonyl
add <sup>n</sup>	addition
AIBN	azobis(isobutyronitrile)
Ar	aryl
ATR	attenuated total reflectance
ATRP	atom transfer radical polymerization
BBN	9-borabicyclo(3.3.1)nonane
Boc	<i>tert</i> -butyloxycarbonyl
Bn	benzyl
BPN	2-bromopropionitrile
br	broad

Bu	butyl
CBZ	carboxybenzyl
CDA	carbenodiamidine, bis(amidino) pyrimidylidene,
CNC	2,6-bis(aryl-imidazol-2-ylidene) pyridine
conv	conversion
Cy	cyclohexyl
d	doublet (NMR)
<i>D</i>	axial zero-field splitting
DCE	1,2-dichloroethane
DBa	dibenzylideneacetone
DBN	1,8-diazabicyclo[4.3.0]non-5-ene
DBU	1,8-diazobicyclo[5.4.0]undec-7-ene
Dc	direct current
dd	doublet of doublets (NMR)
DFT	density functional theory
DMAP	4-dimethylaminopyridine
DMEDA	N,N'-dimethylethylenediamine
DMF	dimethylformamide
DMSO	dimethylsulfoxide
Dppbz	1,2-bis(diphenylphosphino)benzene
dppe	diphenylphosphino ethane
dppp	diphenylphosphino propane
dq	doublet of quartets (NMR)
dt	doublet of triplets (NMR)
<i>E</i>	equatorial field splitting (i.e. $ E/D $ )
EPR	electron paramagnetic resonance
equiv.	equivalent(s)
ESI+	electrospray ionization (positive ion mode)

Est.	estimated
Et	ethyl
Fc	ferrocene
FID	flame ionization detector
FMO	Frontier molecular orbital
g	gram(s)
GC	gas chromatography
GPC	gel permeation chromatography
<i>gem</i>	geminal
h	hour(s)
hept	heptet (NMR)
HMDS	hexamethyldisilazane, bis(trimethylsilyl)amine
HOMO	highest occupied molecular orbital
HRMS	high resolution mass spectrometry
Hz	hertz
ICP-AES	inductively coupled plasma atomic emission spectroscopy
ICP-MS	inductively coupled plasma mass spectrometry
IMes	1,3-bis(2,4,6-trimethylphenyl)-4,5-imidazol-2-ylidene
IR	infrared spectroscopy
<i>i</i> Pr	isopropyl
<i>J</i>	coupling constant in Hz (NMR)
KHMDS	potassium hexamethyldisilazide
L	liter(s)
LiHMDS	lithium hexamethyldisilazide
MA	methyl acrylate
MBO	Mayer bond order
MBP	methyl-2-bromopropionate
MCD	magnetic circular dichroism

Me	methyl
Mes	mesityl
mg	milligram(s)
MHz	megahertz
min	minute(s)
mL	milliliter(s)
MLCT	metal to ligand charge transfer
MMA	methyl methacrylate
mmol	millimole(s)
$M_n$	number average molecular weight
MO	molecular orbital
mol	mole(s)
MS	mass spectrometry
MTBE	methyl <i>tert</i> -butyl ether
$M_w$	weight average molecular weight
$M_w/M_n$	polydispersity index
NaHMDS	sodium hexamethyldisilazide
<sup>n</sup> Bu	n-butyl
NBS	N-bromosuccinimide
NHC	N-heterocyclic carbene
NMP	N-methylpyrrolidinone
NMR	nuclear magnetic resonance
ORTEP	Oak Ridge thermal ellipsoid plot
OTs	tosylate
<i>p</i>	para
PDI	pyridyldiimine, bis(imino)pyridine
PDT	product
PEG-200	poly(ethylene glycol) 200

PG	protecting group
Ph	phenyl
Pin	pinacol
Piv	pivaloyl
PLA	poly(lactic acid)
PMP	<i>N</i> -methyl-2,2,6,6-tetramethylpiperidine
psi	pounds per square inch
q	quartet (NMR)
RDS	rate determining step
s	singlet (NMR)
S	spin state
SciOPP	1,1'-(1,2-phenylene)bis[1,1-bis[3,5-bis(1,1-dimethylethyl)]phenyl]phosphine
SIMes	1,3-bis(2,4,6-trimethylphenyl)-4,5-dihydroimidazol-2-ylidene
SM	starting material
SQUID	superconducting quantum interference device
t	triplet (NMR)
<sup>t</sup> Bu	<i>tert</i> -butyl
<sup>t</sup> BuMA	<i>tert</i> -butyl methacrylate
td	triplet of doublets (NMR)
T <sub>d</sub>	tetrahedral
TD-DFT	temperature dependent density functional theory
temp	temperature
Tf	triflate
TFA	trifluoroacetic acid
T <sub>g</sub>	glass transition temperature
THF	tetrahydrofuran
TMEDA	tetramethylethylenediamine
TMP	2,2,6,6-tetramethylpiperidine

TMS	trimethylsilane; tetramethylsilane
tol	tolyl
Ts	tosyl
tt	triplet of triplets (NMR)
UV	ultraviolet
UV-vis	ultraviolet-visual spectroscopy
V	volt(s)
VTVH-MCD	variable-temperature, variable-field magnetic circular dichroism
XAFS	X-ray absorption fine structure
XANES	X-ray absorption near edge spectroscopy
Xantphos	4,5-bis(diphenylphosphino)-9,9-dimethylxanthene
+ZFS	positive zero field split
-ZFS	negative zero field split

## 1.0 A REVIEW OF RECENT IRON CATALYZED CROSS COUPLING ADVANCES<sup>1</sup>

### 1.1 CROSS COUPLING HISTORY: PALLADIUM AND NICKEL

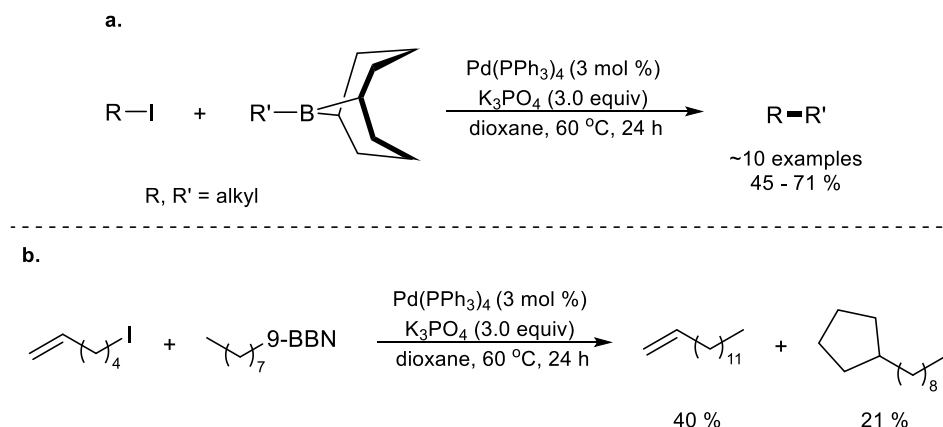
Transition metal catalyzed cross coupling of organic electrophiles and organometallic nucleophiles for the formation of carbon-carbon bonds has become a staple of synthetic chemistry since its advent in 1971 by Jay Kochi.<sup>2</sup> This preliminary report exhibited the cross coupling of vinyl bromides and alkyl Grignard reagents with catalytic amounts of FeCl<sub>2</sub>. The next year, Kumada and Corriu simultaneously published reports of similar nickel catalyzed systems.<sup>3</sup> In 1975, Murahashi et al. successfully used a palladium catalyst to couple vinyl halides and methylmagnesium bromide.<sup>4</sup> Soon after these seminal reports, cross coupling research became an extremely popular research topic, expanding into many different variations, and culminating in the presentation of the 2010 Nobel Prize in Chemistry to Richard Heck, Ei-ichi Negishi, and Akira Suzuki. The diversity in organometallic reagents and broad functional group tolerance of some methods have allowed these reactions to become extremely versatile and advantageous for a number of applications.<sup>5</sup> However, only Kumada and Suzuki systems will be discussed pertaining to the research herein.

Typically, these systems are palladium based; nevertheless, the use of alternative transition metals catalysts, specifically nickel and iron, has gained significant interest over recent years. In agricultural and pharmaceutical applications, where large-scale operations and environmentally benign techniques are desired, the use of palladium is undesirable due to cost inefficiency and toxicity.<sup>6</sup> A further limitation of palladium and nickel systems is that alkyl-alkyl and alkyl nucleophile-aryl electrophile cross couplings have proven challenging.<sup>5</sup>

## 1.2 PALLADIUM CATALYZED ALKYL - ALKYL CROSS COUPLING

Palladium systems, although robust for C(sp) and C(sp<sup>2</sup>) couplings, are plagued by the degradation of palladium-alkyl species by β-hydride elimination, therefore impeding the use of palladium for cross couplings involving sp<sup>3</sup>-hybridized carbons. Although many examples of C(sp<sup>3</sup>)-C(sp) or C(sp<sup>2</sup>) coupling exist in the literature, particularly with Suzuki coupling,<sup>5</sup> the lack of alkyl-alkyl coupling facilitated by palladium has somewhat stymied the efficacy of these techniques. Thus, in recent years, the development of systems that allow for C(sp<sup>3</sup>)-C(sp<sup>3</sup>) and C(sp<sup>3</sup>) nucleophile - C(sp<sup>2</sup>) electrophile couplings has become a prevalent topic in the literature.

Several elegant palladium catalyzed alkyl-alkyl Suzuki coupling reactions have emerged, beginning with a report by Suzuki and coworkers in 1992 that generated the coupled products of alkyl iodides and alkyl-9-BBN reagents in moderate yields (**Scheme 1.1a**).<sup>7</sup> Interestingly, when 6-iodo-1-hexene was used as a substrate with 9-octyl-9-BBN, rearrangement of the alkene to form nonylcyclopentyl as a product was observed, suggesting a radical mechanism which is contrary to the well-accepted palladium mechanism for sp<sup>2</sup> and sp cross couplings (**Scheme 1.1b**). It is important to note that for radical clock reactions such as these, the same cyclic rearrangement could reasonably occur *via* typical organometallic two electron reactions.<sup>8</sup>



**Scheme 1.1.** (a) The coupling of alkyl iodides with alkyl 9-BBN nucleophiles in the presence of catalytic amounts of Pd(PPh<sub>3</sub>)<sub>4</sub>. (b) A radical clock experiment suggesting that one electron transformations might be active for this pathway.<sup>7</sup>

In a number of studies, Fu and coworkers successfully coupled alkyl-(9-BBN) reagents with alkyl halides and pseudohalides in the presence of Pd(II) species bearing trialkylphosphine ligands such as PCy<sub>3</sub> and P<sup>t</sup>Bu<sub>2</sub>Me.<sup>9</sup> It was found that carefully chosen ligation is crucial in facilitating these reactions, and reactivity is particularly sensitive to the cone angles of the phosphine ligands. Phosphaadamantanes<sup>10</sup> and N-heterocyclic carbenes<sup>11</sup> have also been shown to form palladium complexes that are active for alkyl-alkyl cross coupling.

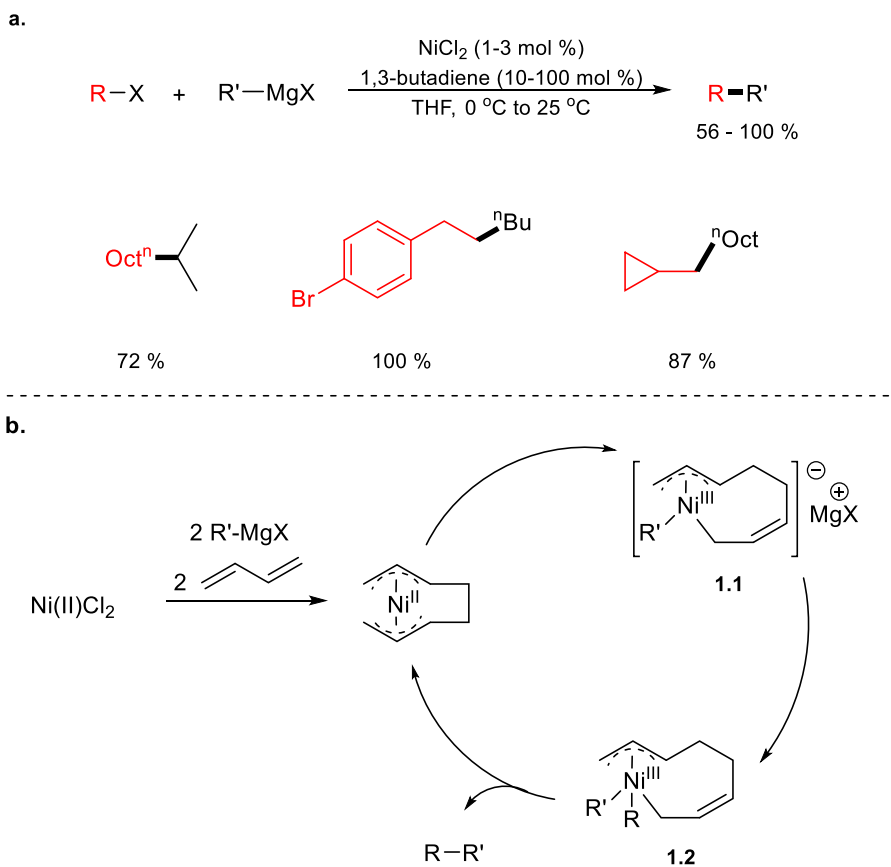
Compared to the Suzuki variation, there are significantly fewer examples of palladium catalyzed alkyl-alkyl Kumada cross coupling reactions. A single report by Kambe and coworkers achieved this transformation (*vide infra*).<sup>12</sup>

### 1.3 NICKEL CATALYZED ALKYL - ALKYL CROSS COUPLING

Nickel catalyzed systems provide a more economical alternative to palladium and considerable progress has been made with nickel complexes toward alkyl-alkyl coupling. In 2002, the first report of a nickel system that allowed for the formation of C(sp<sup>3</sup>) – C(sp<sup>3</sup>) bonds emerged from Kambe and coworkers (**Scheme 1.2a**).<sup>13</sup> 1,3-butadiene was found to provide ideal ligation for the nickel catalyst, allowing for the generation of alkyl-alkyl cross products of alkyl halides and alkyl magnesium halides in moderate to quantitative yields. Notably, this reaction likely does not proceed via a radical pathway, as shown by the use of cyclopropyl bromide as a substrate without evidence of ring opening. Furthermore, with this method, the challenging activation of C(sp<sup>3</sup>)-F bonds was achieved, leading to cross products in moderate yields.<sup>14</sup>

The use of discrete bis(η<sup>3</sup>-allyl) nickel and palladium complexes supported the hypothesis that these complexes are formed *in situ* and are an important part of the catalytic cycle.<sup>12</sup> The comparison of palladium and nickel bis(η<sup>3</sup>-allyl) species showcased the superiority of nickel in the system. For the coupling of decyl bromide and methyl magnesium bromide, the use of the bis(η<sup>3</sup>-allyl) nickel complex led to 98 % yield of undecene, the desired product, whereas the analogous palladium complex produced 90 % yield of undecene. DFT calculations<sup>15</sup> and kinetic studies were

employed to probe the reaction mechanism, and later studies indicated that the technique is tolerant of carboxylic acids.<sup>16</sup> The proposed mechanism, shown in **Scheme 1.2b**, suggests that, in the presence of 1,3-butadiene, two equivalents of Grignard reagent reduce NiCl<sub>2</sub> to form the catalytically active bis(η<sup>3</sup>-allyl) nickel species. This complex then reacts with another equivalent of the Grignard reagent to form an anionic nickel(III) complex **1.1** which, upon interaction with the alkyl halide, generates nickel species **1.2**, which produced the desired product via reductive elimination.



**Scheme 1.2. (a) The coupling of alkyl halides with alkyl Grignard reagents in the presence of catalytic amounts of nickel dichloride and 1,3-butadiene.<sup>13</sup> (b) A proposed catalytic cycle describing the nickel catalyzed system.<sup>12,13,15</sup>**

Xile Hu and coworkers have extensively studied an amido bis(amine) pincer complex termed “Nickamine” for Suzuki<sup>17</sup>- and Kumada<sup>18</sup>-type alkyl-alkyl cross coupling. Notably, the group undertook a number of excellent mechanistic studies<sup>19</sup> and structure/reactivity comparisons<sup>20</sup> of

these systems, and subsequent modification of the amido bis(amine) pincer ligand allowed for the expansion of reaction scope to include secondary alkyl halides.<sup>21</sup>

Fu and coworkers employed chiral bis(amide) ligands to achieve a stereoconvergent alkyl-alkyl Suzuki-type cross coupling.<sup>22</sup> Jarvo and coworkers used a similar system to probe the stereoselectivity of the transmetalation step of these systems, finding it to be stereoretentive.<sup>23</sup>

Although advantageous in many aspects, and despite the amazing success that has been seen in the past several decades, nickel is toxic, and along with today's economic climate and a worldwide desire for environmental protection, attention has been drawn back to iron as a non-toxic, cost effective, and abundant alternative.

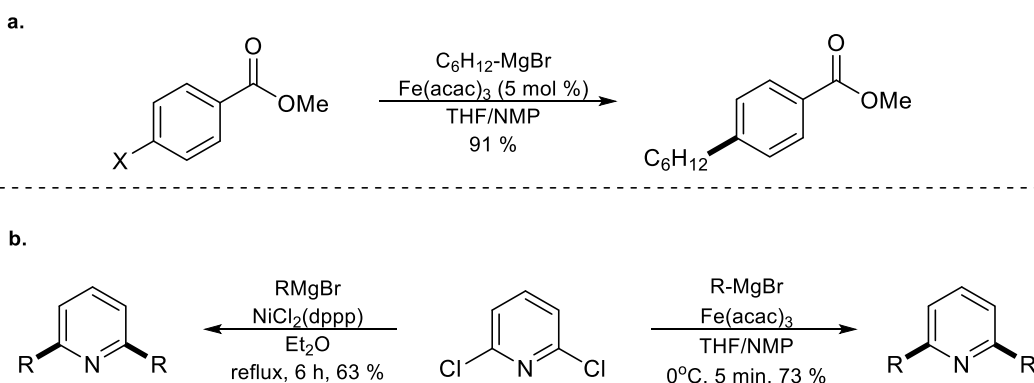
#### 1.4 IRON CATALYZED KUMADA – TYPE SYSTEMS

Until recent years, interest in palladium- and nickel- catalyzed cross coupling systems has somewhat overshadowed the analogous iron systems. Iron systems are more difficult to study than palladium due to the many potential oxidation states and common paramagnetic properties of iron complexes, which makes characterization of the species difficult; the ability of iron to undergo one and two electron transformations, leading to difficulty in predicting *in situ* generated species; and the air and water sensitivity of such complexes, for which isolation and handling are challenging.<sup>1</sup> Despite these difficulties, many scientists believe that the potential benefits of iron catalysts for cross coupling applications may far outweigh these limitations.

Iron has the benefit of being an environmentally benign, economical, and abundant transition metal, and for industrial applications, non-toxic and cost effective techniques are highly desired. Iron complexes have the ability to undergo one and two electron processes, potentially allowing for alternate reaction manifolds that could allow for wider reactivity. Additionally, iron contains smaller molecular orbitals than palladium, leading to lesser orbital overlap and decreased instance of metal-alkyl  $\beta$ -hydride elimination reactions.

Although the aforementioned Pd-alkyl  $\beta$ -hydride elimination pathway is decreased by the use of iron, it is not altogether eradicated, and alkene byproducts are still generated. Other undesired side products are generated via catalytically competitive homocoupling of the organomagnesium reagent<sup>24</sup> or the organohalide<sup>25</sup>. Ligand design has played a key role in decreasing production of byproducts from homocoupling.

Compared to other systems that use less nucleophilic transmetalation reagents, Kumada systems in general are plagued by poor functional group tolerance. However, many iron systems have overcome this limitation.<sup>26</sup> In 2002, Fürstner and coworkers discovered an iron catalyzed system that allowed for the coupling of aryl halides with alkyl Grignard reagents that tolerated the presence of ester, ether, and amide functionalities (**Scheme 1.3a**).<sup>27</sup> This report, 30 years after the seminal study, marked the first synthetically useful iron catalyzed cross coupling, although some reports were published in the intermediate years. Fürstner conducted a comparison study between similar iron and nickel systems and discovered that the iron catalyst afforded the desired product in 5 minutes at 0 °C, whereas the analogous nickel catalyzed reaction took 6 hours to reach completion at elevated temperatures (**Scheme 1.3b**). It is believed that the rate of the desired cross couple reaction out competes the detrimental reactions of the Grignard reagent with susceptible functional groups, along with homocoupling and side reactions. It was then realized that iron-based catalysts could vastly expand the scope and utility of cross coupling.



**Scheme 1.3. (a) An example of the functional group tolerance of iron-Kumada systems. (b) A comparison in reactivity between nickel- and iron catalyzed Kumada-type cross coupling, underscoring the enhanced speed of the iron catalyzed reactions.<sup>27</sup>**

The work of Fürstner and several other groups has led to a revival of iron catalyzed cross coupling. Many superb reviews have covered the progress made in this field until recent years.<sup>5,28,29,30,31</sup> Herein, the state-of-the-art chemistry that has arisen since 2010 is discussed.

It has been shown that iron systems may benefit from small amounts of co-catalyst,<sup>32</sup> and erroneous positive results have arisen from trace quantities of copper, palladium, or other metals.<sup>33</sup> Therefore, control reactions to rule out the possibility of trace metal contamination are crucial for this chemistry.

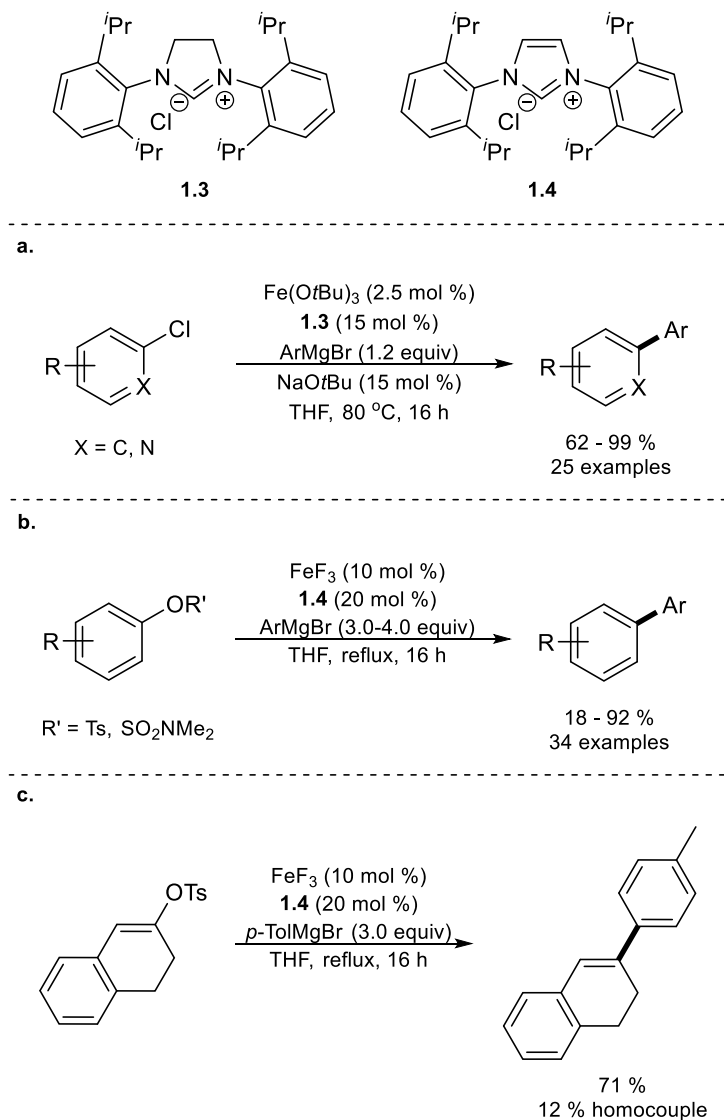
#### 1.4.1 Aryl Nucleophile - Aryl Electrophile

While aryl-aryl cross coupling is facile for palladium and nickel catalysts, iron-based catalysts suffer from homocoupling reactions of both substrates that often outcompete the desired cross reaction.<sup>34</sup> Even so, several examples of aryl-aryl coupling have appeared recently.

Duong and coworkers developed a system in which an iron alkoxide was used in conjunction with a N-heterocyclic carbene (NHC) ligand, formed from *N,N'*-(2,6-diisopropylphenyl) dihydroimidazolium chloride **1.3**, to achieve aryl-aryl coupling in up to 99 % yield (**Scheme 1.4a**).<sup>35</sup> Aryl chlorides were shown to couple readily, unlike analogous palladium and nickel systems which typically only achieve high yields with aryl bromides or iodides, which were not studied in this report. Nakamura suggests, in a similar system using iron trifluoride, due to the high affinity of iron for fluoride, the fluoride ligands enhance the selectivity of the system by inhibiting the formation of ferrate complexes that lead to detrimental homocoupling.<sup>34</sup> Duong and coworkers believe that the alkoxide ligands provide a similar benefit to the system, and the combination of  $\pi$ -donation and tunability of alkoxides allows for the fine tuning of the metal center.

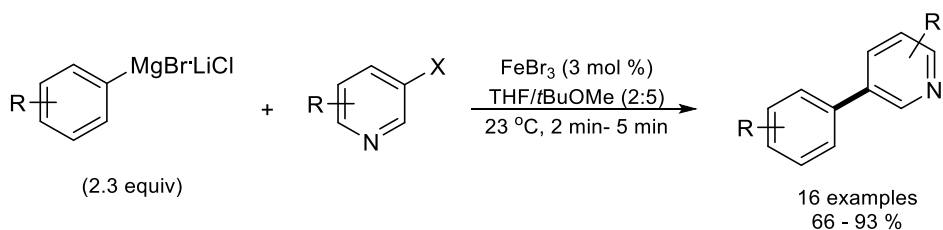
Another group inspired by Nakamura and coworkers<sup>34</sup> achieved the coupling of aryl pseudohalides with aryl Grignard reagents in the presence of catalytic amounts of iron trifluoride and an NHC precursor, *N,N'*-(2,6-diisopropylphenyl) imidazolium chloride **1.4** (**Scheme 1.4b**).<sup>36</sup> Moderate yields were attained, however, *ortho*-substitution and strongly electron withdrawing or donating substitution on either coupling partner were not well tolerated, leading to decreased yields.

A vinyl tosylate, in conjugation with an aromatic system was seen to couple in moderate yields with tolylmagnesium bromide, albeit with a significant amount of vinyl homocouple side product (Scheme 1.4c).



**Scheme 1.4.** (a) The coupling of aryl and heteroaryl chlorides with aryl magnesium bromides in the presence of catalytic amounts of Fe(OtBu)<sub>3</sub> and imidazolium salt 1.3.<sup>35</sup> (b) The coupling of aryl tosylates and sulfamates with aryl magnesium bromides in the presence of iron trifluoride and imidazolium salt 1.4.<sup>36</sup> (c) A select example of the coupling system shown in 1.4b.<sup>36</sup>

N-heteroaromatic halides have proven to be proficient coupling partners in iron catalyzed aryl-aryl cross coupling in a number of instances. Using a dicationic iron(II) center supported by a bidentate pyrimidine NHC ligand, Chen and coworkers produced the anticipated coupled products in moderate yields.<sup>37</sup> Knochel and coworkers used simple iron salts and careful solvent selection to achieve the desired coupling of N-heteroaromatic halides with aryl Grignard reagents.<sup>38</sup> In this case, reaction performance was enhanced by pre-activating the Grignard reagent with a lithium salt (**Scheme 1.5**). In later publications, Knochel and coworkers demonstrated that using isoquinoline as an additive accelerated the coupling of N-heteroaromatic halides with arylmagnesium halides by ligating to the iron tribromide precatalyst.<sup>39</sup> The isoquinoline additive increased yields of desired products by up to 52 %. The group also achieved the coupling of heteroaromatic halides with heteroaromatic Grignard reagents.<sup>40</sup>

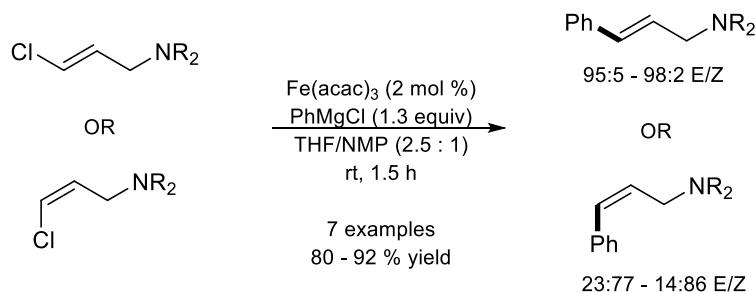


**Scheme 1.5. The coupling of lithiated aryl Grignard reagents with N-heteroaromatic halides in the presence of iron tribromide in a carefully selected solvent system.**<sup>38</sup>

#### 1.4.2 Aryl Nucleophile – Vinyl Electrophile

Like aryl-aryl coupling, very few examples of aryl-vinyl coupling have been published since 2010. Časar and coworkers observed low to moderate yields of desired product when coupling allylic and vinylic bromides with aryl Grignard reagents in the presence of an iron salt and D-glucosamine·HCl, a sustainable, biocompatible, and cost efficient ligand.<sup>41</sup> With this method, the group was able to use readily available materials to provide a key intermediate toward the synthesis of the drug sitagliptin phosphate, which is used as a treatment for type II diabetes. Shakhmaev and coworkers coupled butyl- and phenyl-magnesium bromides with vinyl chlorides in good yields with stereocontrol (**Scheme 1.6**).<sup>42</sup> Although in the majority of cases the stereochemistry of the

vinyl chloride was retained, the use of Z-allylic amine chlorides led to some loss of product stereochemistry. Finally, Jacobi von Wangelin and coworkers were able to couple vinyl bromides with *in situ* generated aryl Grignard reagents in moderate to good yields.<sup>43</sup>



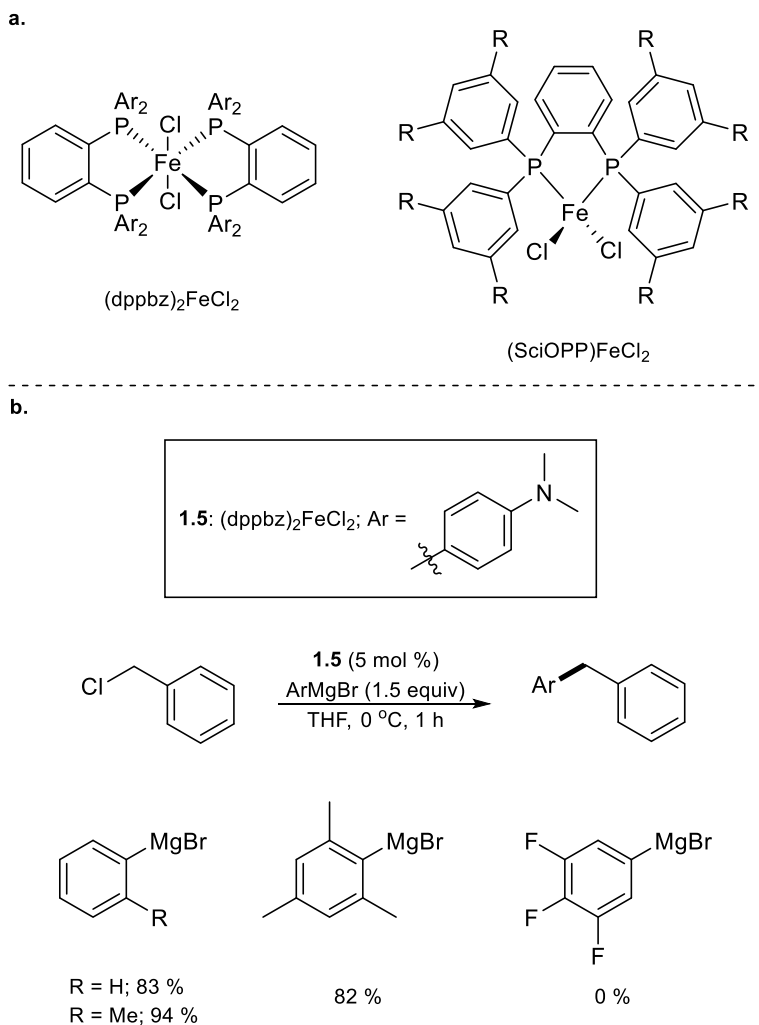
**Scheme 1.6. Moderately stereoselective coupling of E- and Z-allylic amine chlorides with phenyl magnesium chloride in the presence of catalytic amounts of Fe(acac)<sub>3</sub> and NMP as an additive.<sup>42</sup>**

### 1.4.3 Aryl Nucleophile – Alkyl Electrophile

In contrast to aryl-aryl and aryl-vinyl couplings catalyzed by iron, aryl-alkyl coupling has been far more common in recent years and a number of excellent protocols have surfaced. As previously mentioned, ligand design has become a prominent facet of the search for competent iron catalyzed cross coupling systems. Although readily available iron salts such as FeCl<sub>3</sub> and Fe(acac)<sub>3</sub> have proven to be active for such transformations, the use of ligands has generally led to higher selectivity and reactivity.

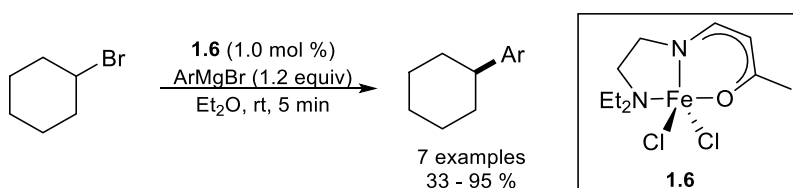
Benzylic chlorides, like aryl chlorides, suffer from facile homocoupling of the electrophile under iron catalyzed conditions. Since 2010, only one report concerning benzylic electrophiles has emerged. In 2013, Nakamura and coworkers described the cross coupling of aryl Grignard reagents with benzylic chlorides in the presence of iron(II) bisphosphine complexes.<sup>44</sup> A variety of (dppbz)<sub>2</sub>FeCl<sub>2</sub> and (SciOPP)FeCl<sub>2</sub> complexes (**Scheme 1.7a**) were screened for catalytic activity, and **1.5** was identified as the most effective precatalyst to attain the desired cross-reaction (**Scheme 1.7b**). Good yields of cross coupled products were obtained, and the reaction was found to be particularly efficient for electron-rich aryl Grignard reagents. *Ortho*-substitution was well

tolerated, but electron withdrawing substituents led to a markedly decreased yield. In cases where multiple electron withdrawing substituents were present, no desired product was formed. The same electronic trend was seen with the electrophile, yet sterically encumbered benzyl halides were not tolerated. The reaction was limited to primary benzyl chlorides with secondary benzyl chlorides leading only to homocoupling of the electrophile. Electrophiles other than benzyl chlorides were not reported.



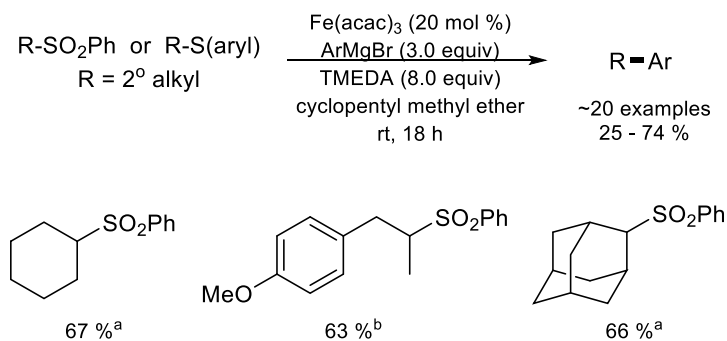
**Scheme 1.7. (a) (dppbz)<sub>2</sub>FeCl<sub>2</sub> and (SciOPP)FeCl<sub>2</sub> complexes are commonly used for iron catalyzed cross couplings. (b) (dppbz)<sub>2</sub>FeCl<sub>2</sub> complex 1.5 facilitated the coupling of benzyl chlorides with aryl magnesium bromides to achieve good yields.<sup>44</sup>**

In 2011, Yamaguchi, Asami, and coworkers replaced the commonly used acetylacetonato (acac) ligand with a  $\beta$ -aminoketonato ligand to enhance the stability of a coordinatively unsaturated iron center (**Scheme 1.8**).<sup>45</sup> The resulting complex, **1.6**, was catalytically active for the coupling of cyclohexyl bromide with aryl Grignard reagents in good yields. The substrate scope of the alkyl halide was not extensively explored, but it was found that cyclohexyl iodide was as equally competent as cyclohexyl bromide, and cyclohexyl chloride was inferior. It was also found that acyclic secondary alkyl halides and primary alkyl halides led to decreased yields, and tertiary alkyl halides were inactive.



**Scheme 1.8. The coupling of cyclohexyl bromide with aryl Grignard reagents in the presence of catalytic amounts of 1.6.**<sup>45</sup>

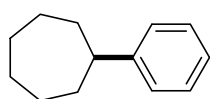
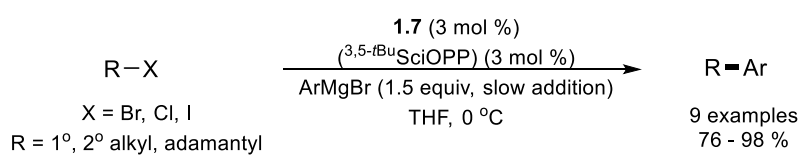
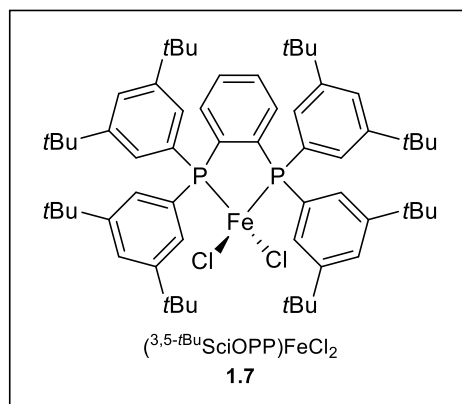
A method was developed by Denmark and Cresswell in which aryl Grignard reagents were coupled with alkyl aryl-sulfones or alkyl aryl-thioesters with  $\text{Fe}(\text{acac})_3$  as the precatalyst (**Scheme 1.9**).<sup>46</sup> Optimal conditions required three equivalents of the nucleophile and eight equivalents of TMEDA. Only heteroatom-devoid, electron rich Grignard reagents were tolerated, and the reaction was not amenable to alkyl, alkenyl, or alkynyl magnesium halides. Electrophiles containing aryl-sulfone pseudohalides were much more reactive than aryl thioesters, and the thioester required a nitrogen-containing aryl group to afford good yields. Secondary cyclic and acyclic alkyl halides coupled successfully in this system, however, primary and tertiary electrophiles were not reported. Denmark and Cresswell speculate that TMEDA acts as an ancillary ligand during the cross coupling, but Bedford suggests that the role is instead to sequester iron, causing it to be less reactive toward detrimental side reactions.<sup>47</sup>



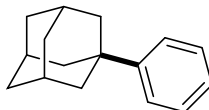
**Scheme 1.9.** The coupling of 2° alkyl pseudohalides with excess arylmagnesium bromide in the presence of catalytic amounts of Fe(acac)<sub>3</sub> and a large excess of TMEDA. <sup>a</sup>Coupled with 2-(*OiPr*)PhMgBr. <sup>b</sup>Coupled with PhMgBr.<sup>46</sup>

Nakamura and coworkers carried out an efficient cross coupling of primary and secondary alkyl chlorides with aryl magnesium halides in the presence of well-defined (SciOPP)FeCl<sub>2</sub> complex **1.7 (Scheme 1.10a)**.<sup>48</sup> It was demonstrated that, in this instance, iron SciOPP complexes were far superior to iron dppbz complexes and that an additional equivalent of ligand was required to attain high yields. Sterically hindered nucleophiles, such as mesityl magnesium bromide, were well tolerated here. In a similar system, an iron-NHC complex, generated *in situ* from imidazolium salt **1.4** and iron trichloride facilitated the reaction of primary and secondary alkyl halides with aryl Grignard reagents to generate the desired product in good to excellent yields (**Scheme 1.10b**).<sup>49</sup> Contrary to the SciOPP system, findings show that the reaction was not tolerant of mesityl magnesium bromide. Both methodologies allowed for the coupling of electron poor and electron rich nucleophiles, albeit requiring the slow addition of the reagent. Tertiary electrophile adamantyl chloride, was shown to undergo cross coupling in both systems, producing 81 % yield in the SciOPP system and 90 % yield in the NHC system. Unfortunately, other tertiary alkyl halides led to low yields. The use of *t*-butyl chloride led to 12 % of the desired cross product when coupled with phenyl magnesium bromide, and the majority of the electrophile was converted into the side products isobutene and isobutene. It is hypothesized that adamantyl chloride is favored in this system because of the hindrance of β-hydride elimination by steric constraint.

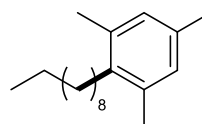
a.



92 %

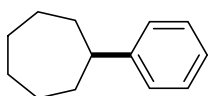
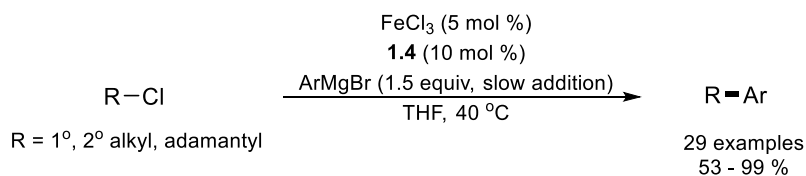


81 %

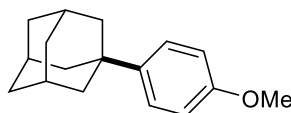


93 % (X = I)  
76 % (X = Br)

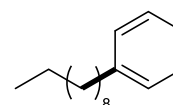
b.



96 %



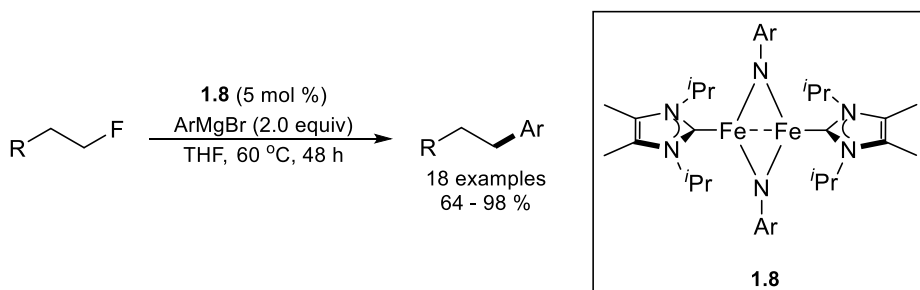
90 %



84 %

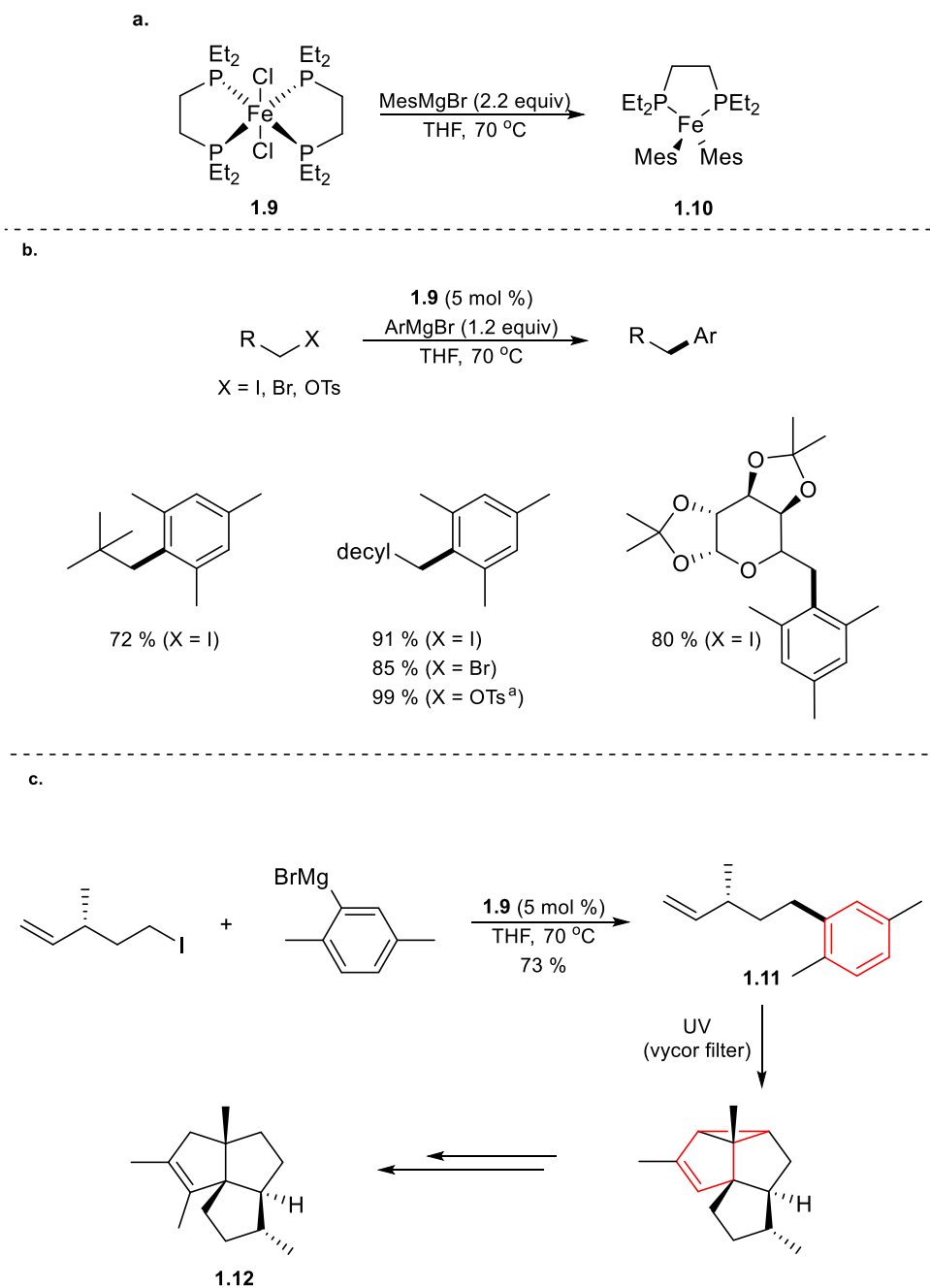
**Scheme 1.10. (a) The coupling of 1°, 2°, and adamantyl halides with aryl magnesium bromides in the presence of catalytic amounts of iron SciOPP complex 1.7 and SciOPP ligand.<sup>48</sup> (b) A similar system instead using an NHC ligand formed *in situ* from imidazolium salt 1.4.<sup>49</sup>**

Similar to reactivity expressed by nickel and palladium systems, some iron catalyzed cross coupling reactions favor alkyl iodides or bromides over alkyl chlorides, with alkyl fluorides being generally unreactive. An advancement was made when Deng and coworkers, however, were able to develop conditions for the coupling of aryl Grignard reagents with primary alkyl fluorides (**Scheme 1.11**).<sup>50</sup> This transformation was attained by the use of iron NHC complex **1.8**, and is a promising report for the future of iron catalyzed cross coupling, even though secondary alkyl, tertiary alkyl, and aryl fluorides were unreactive.



**Scheme 1.11. The coupling of alkyl fluorides with aryl Grignard reagents in good to excellent yields in the presence of iron NHC **1.8**.**<sup>50</sup>

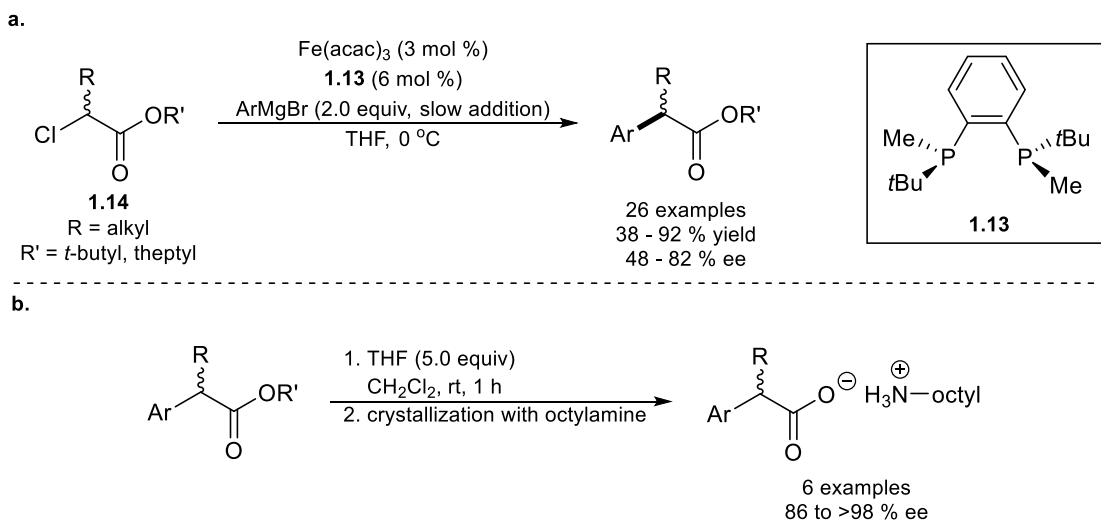
Fürstner and coworkers aimed to couple sterically hindered aryl Grignard reagents with alkyl halides, and thus performed stoichiometric studies to determine why these reagents are typically inactive.<sup>51</sup> Upon reacting mesitylmagnesium bromide with iron complex **1.9**, iron dimesityl dppe complex **1.10** was formed (**Scheme 1.12a**). Iron-ate complex  $[\text{Mes}_3\text{Fe}]^-$ , which has been shown by the Neidig group to undergo unproductive side reactions,<sup>52</sup> was not formed. With these findings, Fürstner and coworkers were able to develop a protocol for the coupling of a variety of sterically hindered aryl Grignard reagents with primary alkyl halides (**Scheme 1.12b**). Although the reaction was tolerant of the steric hindrance presented by neopentyl iodide, secondary alkyl halides were altogether unproductive. Alkyl iodides performed better than alkyl bromides, and alkyl tosylates required an iodide source, converting the tosylate to an iodide *in situ*. This method was used to form **1.11**, an intermediate toward the synthesis of **1.12**, a member of the silphiperfolene family of natural products. **1.11** undergoes an intramolecular arene-alkyl *meta*-photocycloaddition *en route* to the formation of **1.12** (**Scheme 1.12c**).



**Scheme 1.12.** (a) Active species **1.10** is formed from the treatment of iron dichloride di(bisphosphine) **1.9** with mesitylmagnesium bromide without the formation of detrimental iron-ate complex  $[\text{Mes}_3\text{Fe}]^-$ . (b) The coupling of primary alkyl halides with sterically hindered aryl Grignard reagents in the presence of catalytic amounts of **1.9**. (c) Abridged total synthesis of silphiperfol-6-ene **1.12**, using the developed methodology to form **1.11**, a crucial intermediate.<sup>51</sup>



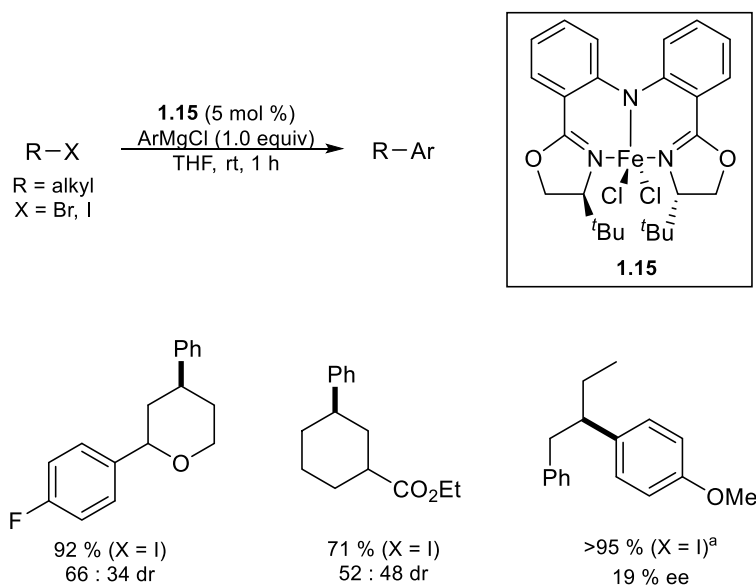
hydrolysis and subsequent crystallization in the presence of octylamine, optical purity could be enhanced (**Scheme 1.14b**). Alkyl halides containing bulky *t*-butyl ester and theptyl ester functionalities led to superior yields of coupled product. The majority of electronic variations of the nucleophiles were tolerated, however extremely electron poor 3,4,5-trifluorophenylmagnesium bromide produced significantly lower yields. Sterically constrained *ortho*-substituted Grignard reagents were not tolerated unless the *ortho*-substituent was an extended aromatic system. Control reactions showed that nickel and palladium precatalysts did not lead to the desired product.



**Scheme 1.14.** (a) The stereoconvergent cross coupling of  $\alpha$ -chloroesters (**1.14**) with arylmagnesium halides in the presence of  $\text{Fe}(\text{acac})_3$  and chiral bisphosphine ligand **1.13**. (b) Stereochemical enhancement *via* ester hydrolysis of the desired product followed by crystallization with octylamine.<sup>55</sup>

Chiral iron bis(oxazolinyphenylamido) pincer complex **1.15** was utilized by Hu and coworkers in an attempt to afford enantiomerically enriched products from the coupling of alkyl bromides and iodides with aryl Grignard reagents (**Scheme 1.15**).<sup>57</sup> Unfortunately, the highest enantiomeric excess observed for the coupling of prochiral substrates was only 19 %, and, when chiral electrophiles were used, the maximum diastereomeric ratio reached was 66 : 34. However, the protocol was shown to be very general, allowing for the cross coupling of primary and secondary alkyl iodides and bromides, and tolerant of ester, ether, and ketone functionalities. The group

effectively performed late-stage couplings of natural product-derived species effectively. It was found that *para*-methoxyphenylmagnesium chloride coupled readily but required decreased temperatures, yet other variations of the nucleophilic partner were not examined. In a later report, Hu used a similar complex for extensive mechanistic studies, which will be discussed in **Chapter 1.5**.<sup>58</sup>



**Scheme 1.15.** The coupling of alkyl bromides and iodides with phenyl or *p*-methoxyphenyl magnesium chloride in the presence of iron pincer complex **1.15**.<sup>57</sup>

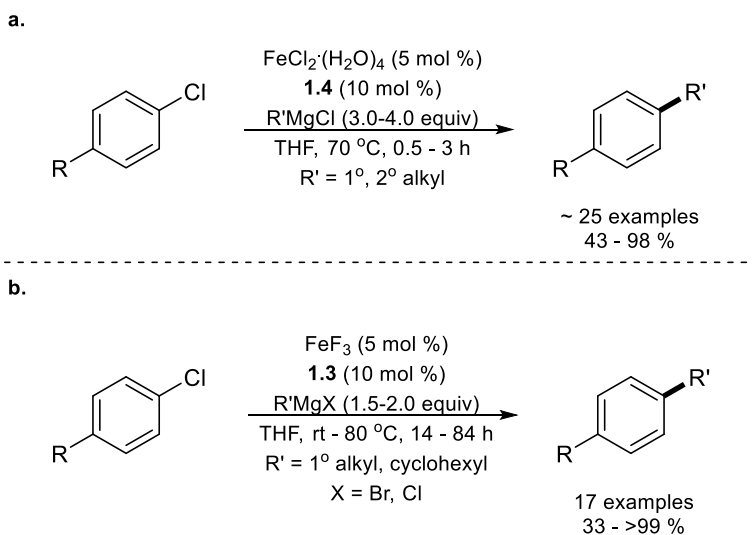
In 2011, Knochel and coworkers reported a diastereoselective cross coupling of aryl Grignard reagents with enantiomerically enriched cyclic alkyl iodides bearing bulky protecting groups adjacent to the coupling site.<sup>59</sup> Catalytic amounts of iron dichloride led to good diastereoselectivities, yet stoichiometric amounts of iron and *p*-fluorostyrene were required to obtain good yields. The role of the additive, *p*-fluorostyrene, was suggested to encourage the reductive elimination step and subsequent product formation.

#### 1.4.4 Alkyl Nucleophile – Aryl Electrophile

Since the early 2000's Kumada-type alkyl nucleophile – aryl electrophile cross couplings catalyzed by iron species have been common in the literature.<sup>60</sup> In the past several years, the rational design of ligands, as well as the use of pseudohalides and directing groups, have greatly expanded these methodologies. A current limitation of these reactions is that excess Grignard reagent is typically needed, occasionally in up to four equivalents.

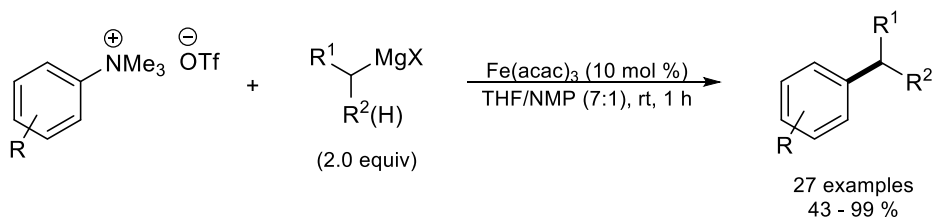
Imidazolium salt **1.4** was shown by Perry and coworkers to promote the cross coupling of primary and secondary alkyl Grignard reagents with aryl chlorides in good yields (**Scheme 1.16a**).<sup>61</sup> The focus of this research was the coupling of un-activated aryl halides, and thus steric and electronic variations of the electrophile were not heavily examined. Primary alkyl Grignard reagents and cyclohexyl magnesium bromide reacted as expected, however, acyclic secondary alkyl Grignard reagents led to a mixture of branched and linear products. This occurs in many instances where acyclic secondary alkyl Grignard reagents are used, likely as a result of  $\beta$ -hydride elimination followed by chain walking and re-insertion before the reductive elimination step that leads to the desired product. In this instance, the chain walking could be lessened with the use of six equivalents of Grignard reagent, albeit with decreased yield.

In a similar fashion, Nakamura and coworkers coupled primary alkyl, secondary alkyl, and methyl Grignard reagents with aryl halides in the presence of imidazolium salt **1.3** and iron trifluoride (**Scheme 1.16b**).<sup>62</sup> As with the Perry system, chain walking occurred for acyclic secondary alkyl Grignard reagents, yet good yields were still achieved in most cases.



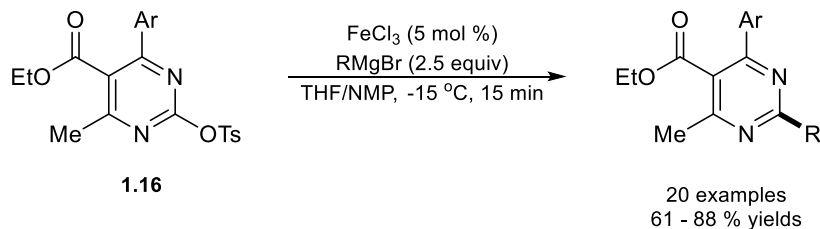
**Scheme 1.16. The coupling of aryl chlorides with primary and secondary alkyl halides in the presence of catalytic amounts of (a)  $\text{FeCl}_2 \cdot 4\text{H}_2\text{O}$  and **1.4**,<sup>61</sup> and (b)  $\text{FeF}_3$  and **1.3**.<sup>62</sup>**

The use of aryl pseudohalides rather than traditional coupling partners has been a topic of interest for several groups in recent years. Z.-X. Wang and coworkers coupled a series of aryl trimethylammonium triflates, with primary and acyclic secondary Grignard reagents in relatively good yields (**Scheme 1.17**).<sup>63</sup> The reaction was tolerant of electron rich and electron poor electrophiles. Interestingly, the addition of a small amount of NMP led to the best results, whereas a well-defined ligand system detracted from the yield of desired products. Control experiments were undertaken in order to determine if trace metals were involved in the catalytic system. It was found that 99.9 %  $\text{Fe}(\text{acac})_3$  gave similar results to 98 %  $\text{Fe}(\text{acac})_3$ , and that the addition of 0.1 mol % copper to reactions catalyzed by  $\text{Fe}(\text{acac})_3$  had no effect on reaction outcome, leading the authors to conclude that it was indeed an iron catalyzed process.



**Scheme 1.17.** The coupling of aryl trimethylammonium triflates with primary and acyclic secondary alkyl Grignard reagents in the presence of catalytic amounts of  $\text{Fe}(\text{acac})_3$  and NMP.<sup>63</sup>

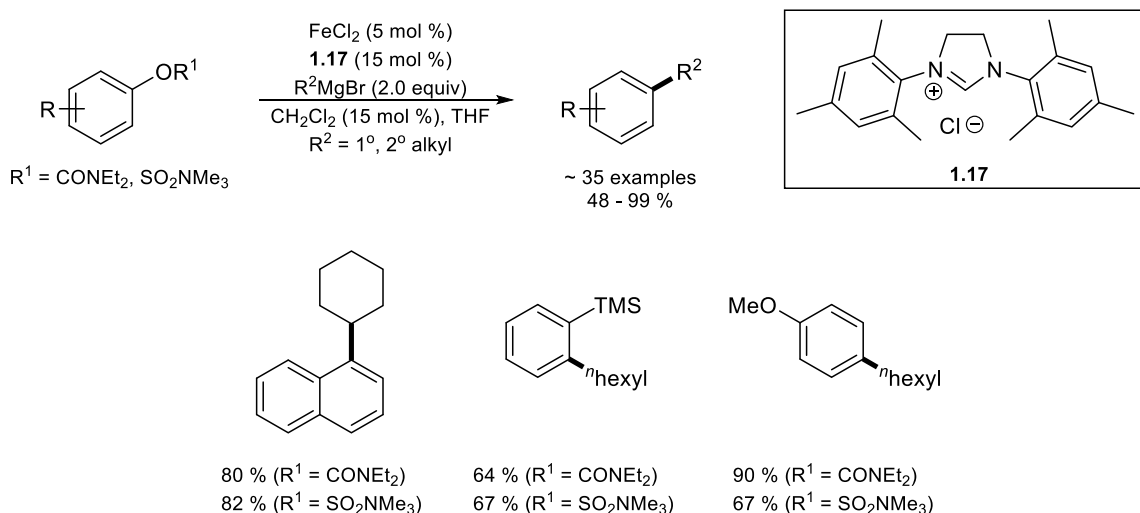
With a focus on the synthesis of bio-active molecules, X.-C. Wang and coworkers developed an iron catalyzed system for the coupling of N-heterocyclic aryl tosylates with alkyl Grignard reagents in good yields (**Scheme 1.18**).<sup>64</sup> The reaction conditions, iron trichloride with NMP as a co-solvent, were originally developed by Cahiez and Avedissian for similar cross coupling applications.<sup>65</sup> The aim of X.-C. Wang and coworkers was specific to the coupling of ethyl 4-methyl-6-aryl-2-(tosyloxy) pyrimidine-5-carboxylate, **1.16**, with alkyl and aryl Grignard reagents.<sup>64</sup> Whereas good yields were achieved in such instances, the use of pyrimidine and pyridine-based electrophiles resulted in low yields of the coupled product.



**Scheme 1.18.** The coupling of N-heterocyclic aryl tosylates (**1.16**) and alkyl Grignard reagents in the presence of catalytic amounts of iron trichloride with NMP as an additive.<sup>64</sup>

Aryl sulfamates and carbamates were found to be suitable pseudohalides by Garg and coworkers for cross coupling with primary and secondary alkyl halides in the presence of iron dichloride and imidazolium salt *N,N'*-(2,4,6-trimethylphenyl)dihydro-imidazolium chloride, **1.17** (**Scheme 1.19**).<sup>66</sup> Electron donating substitution on aryl carbamates led to an increase in yield, and *ortho*-substitution was well tolerated, even in the case of a bulky TMS group. Curiously, the reaction

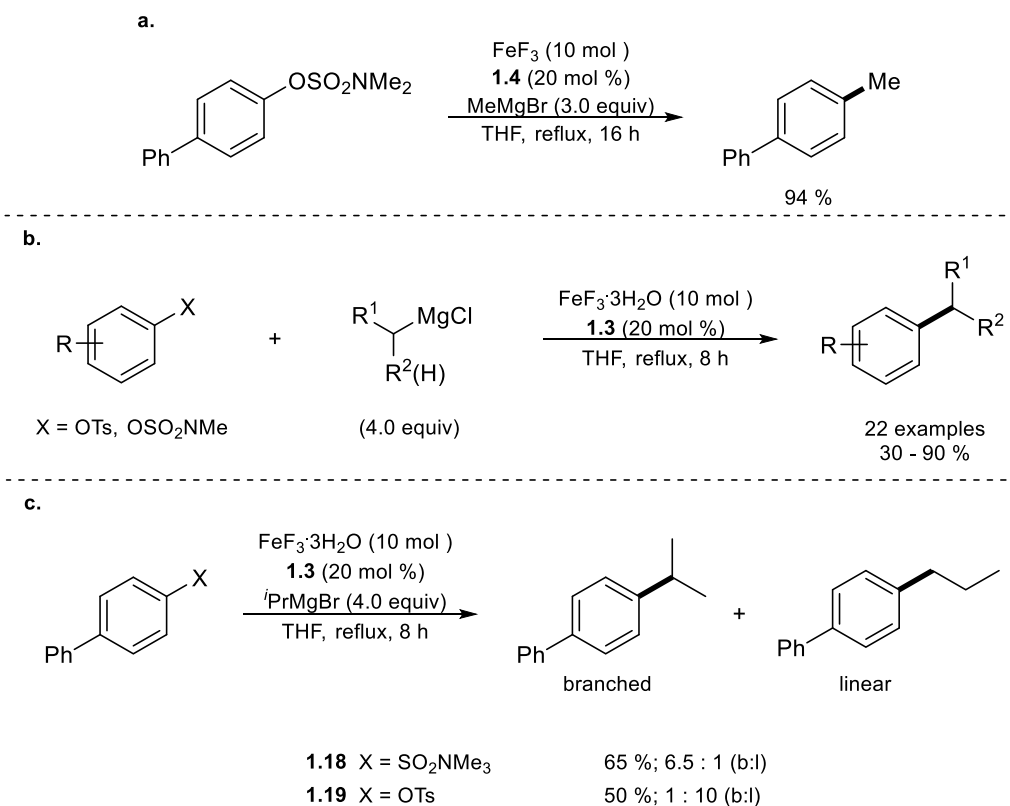
required substoichiometric amounts of methylene chloride to attain high yields, although a rationale was not provided.



**Scheme 1.19.** The coupling of alkyl Grignard reagents with aryl carbamates and sulfamates in the presence of catalytic amounts of iron dichloride, imidazolium salt **1.17**, and methylene chloride.<sup>66</sup>

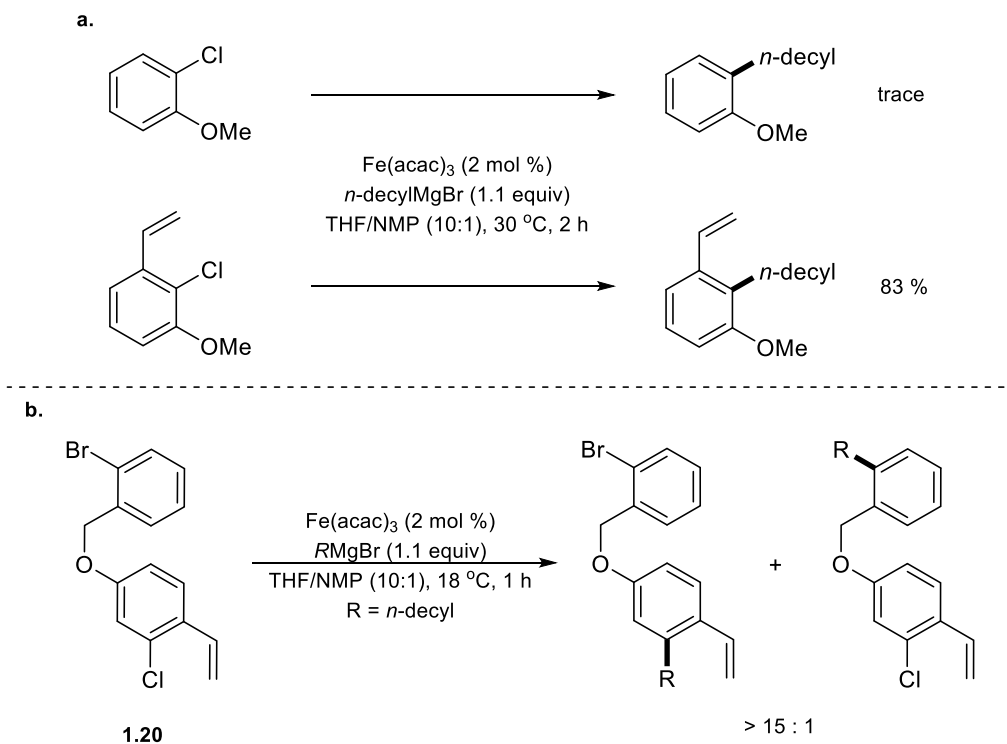
Cook and coworkers found that the same system they developed for the iron catalyzed cross coupling of aryl Grignard reagents with aryl and vinyl tosylates in the presence of **1.4** and iron trifluoride also facilitates the cross coupling of aryl sulfamates with methyl magnesium bromide (**Scheme 1.20a**).<sup>36</sup> The reaction scope was expanded through the use of NHC ligands in combination with iron trifluoride trihydrate to allow for the coupling of aryl sulfamates and tosylates with alkyl Grignard reagents (**Scheme 1.20b**).<sup>67</sup> Although only moderate yields were reached, electron withdrawing and electron donating groups appended to the aryl electrophile were well tolerated, along with *para*- and *meta*-substitution. Secondary alkyl magnesium halides produced less product than their primary counterparts, again due to the proclivity of secondary Grignard reagents to undergo chain walking. Remarkably, coupling biphenyl sulfamate **1.18** with isopropyl magnesium bromide led to predominantly branched product in a 6.5:1 ratio of branched to linear, but when biphenyl tosylate **1.19** was subjected to the same reaction conditions, the linear product dominated with a 1:10 ratio of branched to linear (**Scheme 1.20c**). Additionally, the selectivity for

sulfamate **1.18** was reversed to favor the linear product (1:5 branched to linear) when iron trichloride was used as the iron source rather than iron trifluoride trihydrate. Cook hypothesized that in the case of aryl sulfamates, the enhanced affinity of fluoride for iron blocks coordination sites that would be necessary for  $\beta$ -hydride elimination, leading to a majority of branched product. When iron trichloride was used, the facile dissociation of the ligand allows open coordination sites for  $\beta$ -hydride elimination. No explanation was provided for the difference in product distribution between sulfamates and tosylates.



**Scheme 1.20.** (a) The coupling of biphenyl sulfamate with methylmagnesium bromide in the presence of iron trifluoride and **1.4**.<sup>36</sup> (b) The coupling of aryl sulfamates and tosylates with primary and secondary alkyl Grignard reagents in the presence of iron trifluoride trihydrate and **1.3**.<sup>67</sup> (c) The coupling of biphenyl tosylate and biphenyl sulfamate with *iso*-propylmagnesium bromide to form a mixture of branched and linear products. When biphenyl sulfamate **1.18** was used, a 6.5:1 branched to linear distribution was achieved whereas the coupling of biphenyl tosylate **1.19** led to a 1:10 branched to linear ratio.<sup>67</sup>

The group of Jacobi von Wangelin demonstrated that directing groups could be utilized to enhance the formation of coupled product in certain situations.<sup>68</sup> In the presence of Fe(acac)<sub>3</sub> and NMP, *o*-chloroanisole was found to couple with *n*-decylmagnesium bromide sparingly, however, when an olefin was installed *ortho* to the chloride, the reaction proceeded smoothly to 83 % yield (**Scheme 1.21a**). A further demonstration of the chemoselectivity afforded by the installation of a directing group was seen when **1.20** was subjected to the reaction conditions. Containing both aryl bromide and aryl chloride functionalities, it is expected that the aryl bromide moiety of **1.20** would react preferably (**Scheme 1.21b**). However, with a vinyl group installed adjacent to the chloride substituent, a 15:1 selectivity toward the aryl chloride was observed. It was suspected that the olefin acts as a binding site for the iron center, allowing for close proximity to the aryl chloride. Over 30 examples demonstrating this reactivity were reported with modest to good yields. The reaction tolerated both primary and cyclic secondary Grignard reagents, yet acyclic secondary Grignard reagents were not examined.

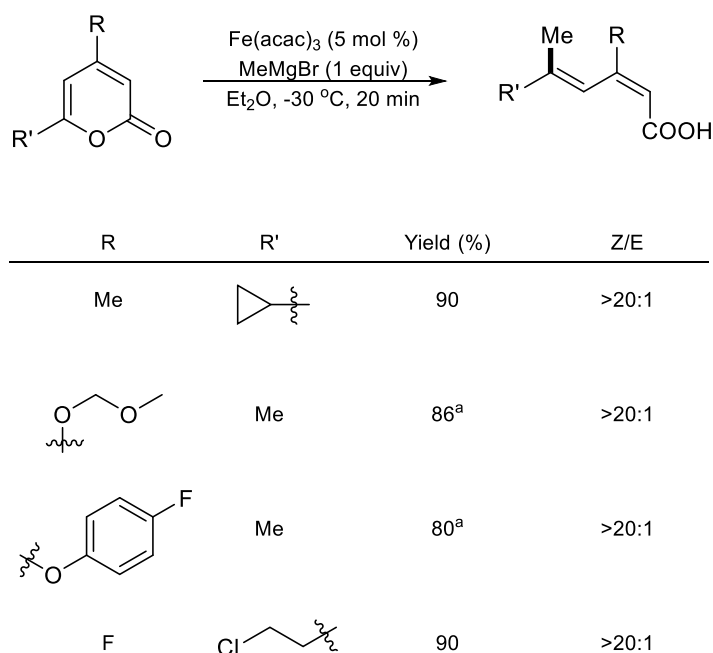


**Scheme 1.21. (a) The coupling of aryl chlorides and  $n$ -decylmagnesium bromide with and without the presence of an *ortho*-vinyl directing group in the presence of  $\text{Fe}(\text{acac})_3$  and NMP. (b) The selective coupling of an aryl chloride bearing an *o*-vinyl substituent over an aryl bromide in an  $\text{Fe}(\text{acac})_3$ /NMP catalytic system.<sup>68</sup>**

Another chemoselective iron catalyzed aryl-alkyl coupling was pursued by a Genentech Inc. research group.<sup>69</sup> In this instance, it was found that N-heteroaromatic dihalides could be selectively functionalized by a one-pot sequential addition of nucleophiles. The identities of the halogen substituents facilitated this selectivity; the most reactive site coupled first, forming a directing group for the subsequent functionalization. A variety of substitution patterns and electronic profiles were found to produce high yields and 20:1 selectivities.

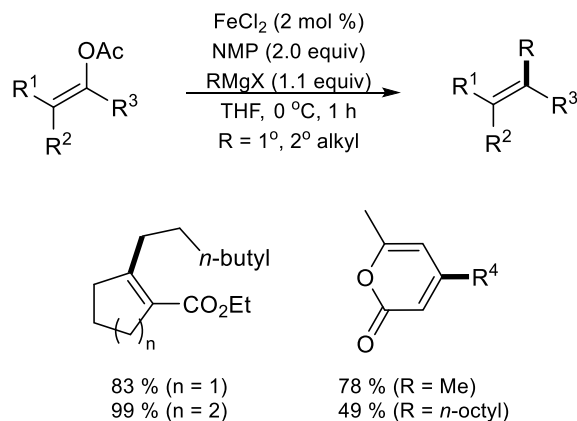
### 1.4.5 Alkyl Nucleophile – Vinyl Electrophile

E/Z stereoretentive vinyl halide coupling with aryl Grignard reagents has been known since the initial report of iron catalyzed cross coupling by Kochi and coworkers in 1971.<sup>2</sup> Even so, a substantial amount of progress has been made in this area before and after 2010. In 2010 Fürstner and coworkers realized a fundamentally different type of cross coupling in which an unsaturated cyclic ester acts as the electrophile rather than a vinyl halide (**Scheme 1.22**).<sup>70</sup> This substrate undergoes ring opening upon oxidative addition to the metal center, and can subsequently be coupled to methyl magnesium bromide to yield dienyl carboxylates. More than 15 examples with good yields and high E/Z stereoselectivities were revealed. Alas, the system was only examined with methyl magnesium bromide as the coupling partner. The group went on to use this method for the total synthesis of granulatamide B, a cytotoxic tryptamine derivative.



**Scheme 1.22.** The coupling of unsaturated cyclic esters with methyl magnesium bromide via ring opening oxidative addition in the presence of Fe(acac)<sub>3</sub>. <sup>a</sup>Solvent: Et<sub>2</sub>O/toluene (1:1).<sup>70</sup>

The Tanabe group reported the iron catalyzed cross coupling of enol tosylates with alkyl Grignard reagents lacking  $\beta$ -hydrogens in good yields and stereoselectivities.<sup>71</sup> Jacobi von Wangelin and coworkers report that vinyl acetates also smoothly react with alkyl Grignard reagents in  $\text{FeCl}_2/\text{NMP}$  conditions (**Scheme 1.23**).<sup>72</sup> With over 30 examples, it was found that primary and secondary alkyl magnesium halides were tolerated, along with a wide range of substitution patterns of the vinyl acetate. Electron withdrawing groups, however, were found to reduce the yield.



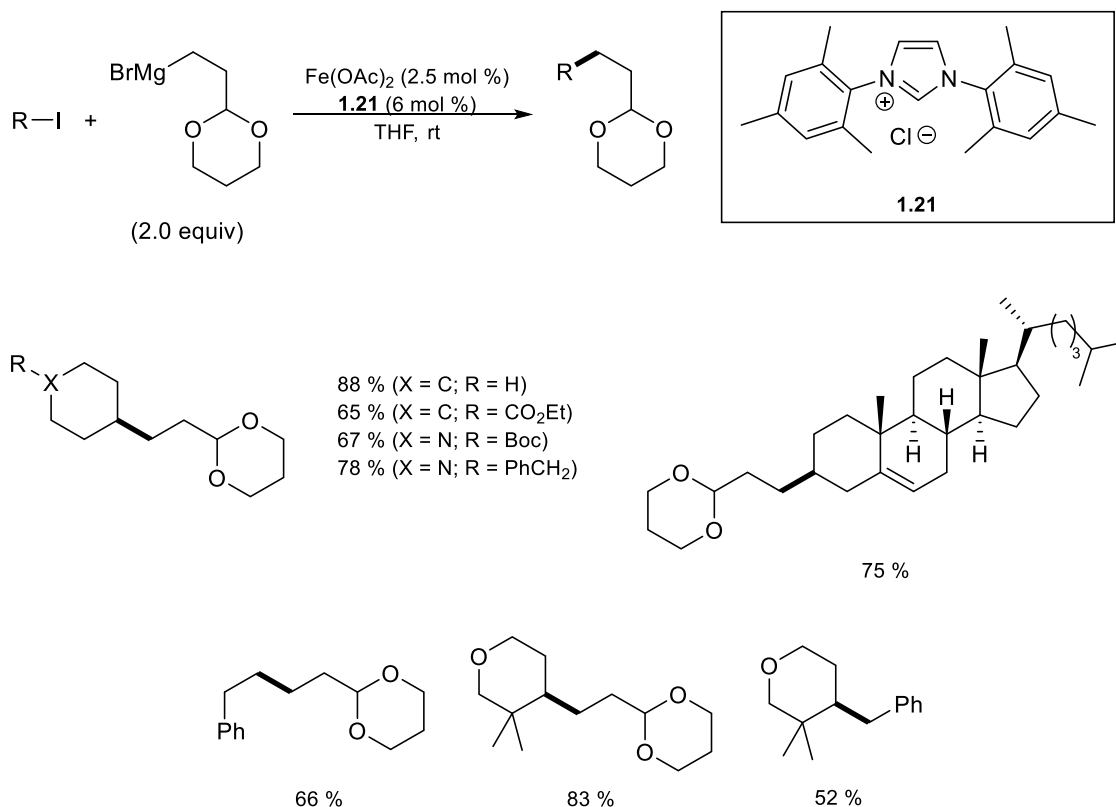
**Scheme 1.23. The coupling of vinyl acetates with alkyl Grignard reagents catalyzed by an  $\text{FeCl}_2/\text{NMP}$  system.<sup>72</sup>**

Although using NMP as an additive has led to increased reaction yields and selectivities, it is a reproductive toxin and undesirable for pharmaceutical and industrial applications.<sup>73</sup> Thus, Caheiz and coworkers attempted to identify a simple ligand system to replace NMP.<sup>74</sup> It was found that iron(II) thiolates are competent catalysts for the coupling of vinyl halides with primary and secondary alkyl Grignard reagents, providing comparable yields to those seen with NMP systems. Tertiary alkyl magnesium halides can be coupled using this system, albeit small amounts of NMP are required to achieve high yields.

#### 1.4.6 Alkyl Nucleophile – Alkyl Electrophile

As with palladium and nickel, iron-Kumada systems that facilitate alkyl-alkyl coupling are rare. Chai and coworkers published the first report of such a system in 2007,<sup>75</sup> but only a handful

of reports have followed. The Cárdenas group found that an *in situ* generated iron(II) NHC complex facilitated the coupling of primary and secondary alkyl iodides with (1,3-dioxan-2-ylethyl) magnesium bromide or benzyl magnesium bromide in moderate to good yields (**Scheme 1.24**).<sup>76</sup> A wide ligand screen was conducted, including a variety of phosphine and amine ligands, all of which proved inferior to NHC precursor *N,N'*-(2,4,6-trimethylphenyl) imidazolium chloride (**1.21**). Unlike many iron catalyzed cross coupling systems, alkyl chlorides were completely unreactive, and alkyl bromides led to significantly lower yields than alkyl iodides. However, a variety of primary and secondary alkyl iodides were tolerated, including ester-, amide-, and piperidine-containing electrophiles.

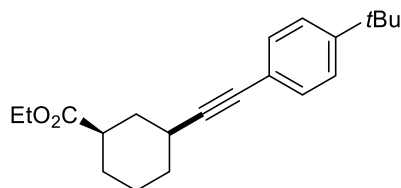
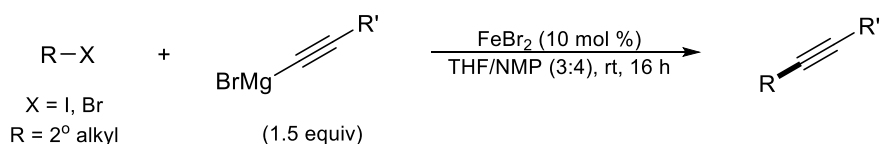


**Scheme 1.24.** The coupling of alkyl iodides with (1,3-dioxan-2-ylethyl) magnesium bromide or benzyl magnesium bromide in the presence of catalytic amounts of  $Fe(OAc)_2$  and imidazolium salt **1.21**.<sup>76</sup>

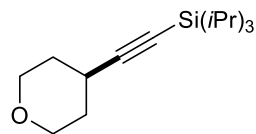
In 2012, the only other instance of alkyl-alkyl coupling was published by Ghosh and coworkers, in which iron catalyzed cross coupling of alkyl and aryl Grignard reagents with polychlorinated solvents such as dichloromethane, chloroform, and carbon tetrachloride was observed.<sup>77</sup> In all cases, multiple coupling products were produced. However, when coupling chloroform and phenyl magnesium bromide, 96 % yield of triphenylmethane was observed.

#### 1.4.7 Alkynyl Nucleophile – Alkyl Electrophile

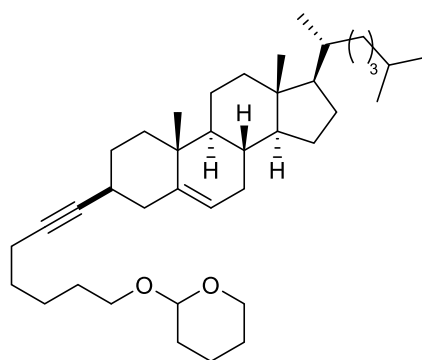
There are only two examples in the literature of alkynyl – alkyl cross coupling facilitated by an iron-based catalyst. In 2011, Nakamura and coworkers were able to couple cyclic 2° alkyl chlorides, bromides, and iodides with alkynyl magnesium bromides at elevated temperatures in the presence of SciOPP ligand **1.7**.<sup>78</sup> The group provides 12 examples of the coupling in good yields. Subsequently, Hu and coworkers reported an FeBr<sub>2</sub>/NMP system for the coupling of alkyl halides and alkynyl Grignard reagents (**Scheme 1.25**).<sup>79</sup> Sixty examples were reported with moderate to good yields, tolerating a variety of substitution patterns and functional groups. Although still limited to 2° alkyl halides, this system was able to couple both cyclic and acyclic variants. A broad range of functionality of the alkynyl Grignard reagent was tolerated, including the presence of ethers, esters, amides, piperidines, carbazoles, and silanes.



91 % (6.5:1 dr)



96 %



50 % (7:1 dr)

**Scheme 1.25.** The coupling of alkyl halides with alkynyl Grignard reagents in the presence of catalytic amounts of  $\text{FeBr}_2$  with NMP as an additive.<sup>79</sup>

## 1.5 IRON CATALYZED KUMADA - MECHANISTIC IMPLICATIONS

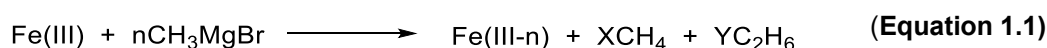
The development of iron catalyzed cross coupling has been hindered by difficulty in understanding the mechanisms of these systems. Unlike palladium, iron is more likely to undergo one and two electron transformations, and many of the species are paramagnetic. Thus, the species present during a reaction are difficult to predict and identify. Additionally, it has been proposed that multiple pathways could be in operation in one system. Several credible mechanisms

have been proposed and interestingly, it seems that the mechanism of iron catalysis relies on the identities of the coupling partners.

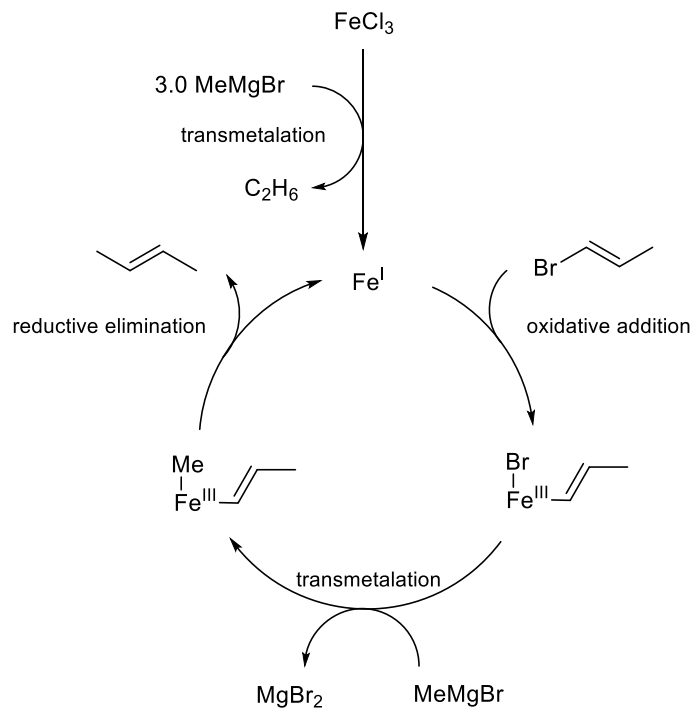
### 1.5.1 Alkyl Nucleophile – Vinyl Electrophile

In the 1970's, Kochi made significant strides toward understanding these systems. Initially attempting alkyl-alkyl coupling, low yields of desired product were observed.<sup>2</sup> Upon combining ethylmagnesium bromide and *tert*-butyl bromide in the presence of iron(III) chloride, ethane, ethane, isopropane, and isopropene were formed. However, the addition of styrene, a radical trapping agent, hindered the formation of isopropane and isopropene, suggesting an *n*-propyl radical had been formed and subsequently trapped. When attempting to couple methylmagnesium bromide and propenyl bromide under the same conditions, styrene did not affect the reaction. Even at this early stage in the development of iron catalyzed cross coupling, it was clear that different substrates result in different reaction mechanisms. Kochi also found that when coupling 1-alkenylhalides with Grignard reagents, the stereogenicity of the double bond was retained.

Upon analysis of the headspace of a reaction between ethylmagnesium bromide and a 1-alkenylhalide in the presence of Fe(III) chloride, Kochi and coworkers realized that the generation of methane and ethane was directly related to the reduction of the iron center, and were thus able to hypothesize the oxidation state of the active iron species.<sup>80</sup> Using **Equation 1.1** it was determined that  $n \approx 2$ , and therefore Fe(I) was tentatively assigned as the catalytically active species.



Upon comparison of the EPR of a known  $S = \frac{1}{2}$  Fe(I) species to that of the product from the reaction of Fe(III) trichloride with excess ethylmagnesium bromide, the oxidation state of the catalytically active species was further supported.<sup>81</sup> Thus, a mechanism similar to that of the accepted palladium-Kumada system, was proposed (**Scheme 1.26**).



**Scheme 1.26. A catalytic cycle proposed by Kochi for the iron catalyzed cross coupling of alkyl Grignard reagents and vinyl halides.<sup>81</sup>**

According to this mechanism, once the catalytically active species is formed, it oxidatively adds the 1-alkenyl bromide. The resulting iron(III) species undergoes transmetalation with methylmagnesium bromide to produce a species that can reductively eliminate to generate the desired product and restart the cycle.

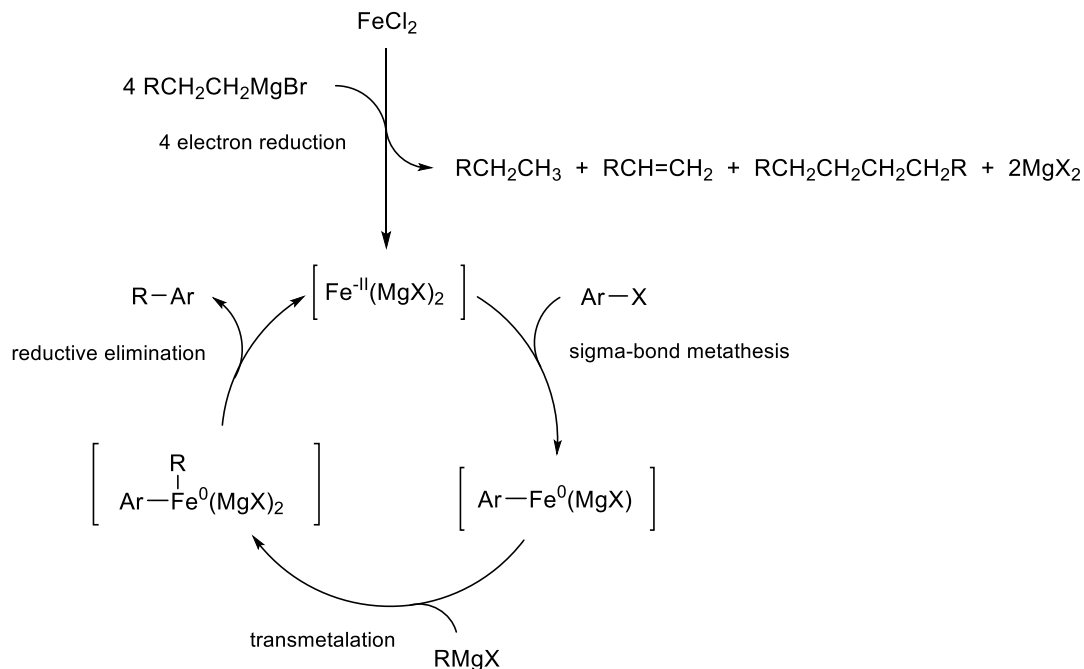
Almost 40 years later, the Neidig group was able to isolate  $S = 3/2$  species  $[\text{MgCl}(\text{THF})_5][\text{FeMe}_4] \cdot \text{THF}$  from the reaction of 4 equivalents of methylmagnesium bromide with iron trichloride in THF at  $-80\text{ }^\circ\text{C}$ .<sup>82</sup> Upon warming this species to room temperature, ethane and an  $S = 1/2$  species were generated, suggesting that  $[\text{MgCl}(\text{THF})_5][\text{FeMe}_4] \cdot \text{THF}$  is an intermediate in the formation of the active species of Kochi's proposed mechanism. It is important to note that this species only accounts for 50 % of the iron present at  $-80\text{ }^\circ\text{C}$ , suggesting that EPR silent species could be present. Therefore, bimetallic and multimetallic pathways cannot be ruled out.

### 1.5.2 Alkyl Nucleophile – Aryl Electrophile

In 2002, Fürstner and coworkers proposed a fundamentally different mechanism for iron catalyzed  $sp^3$  Grignard reagent –  $sp^2$  halide cross coupling.<sup>83</sup> Although contrary to Kochi's mechanism in that it was proposed based on aryl halide rather than vinyl halide coupling partners, it can be assumed that the similarity between these two classes of substrates places these proposals in competition with one another.

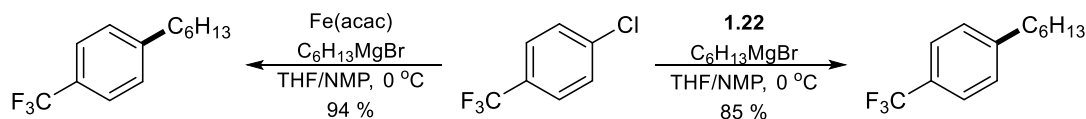
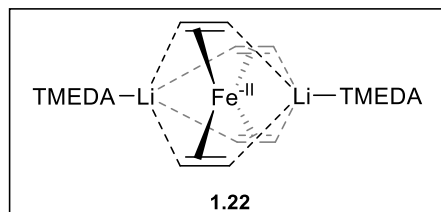
Fürstner was inspired by work done by Bogdanović and coworkers in which a number of transition metal salts were treated with magnesium powder or organic Grignard reagents to form inorganic Grignard reagents.<sup>84</sup> Although the iron-based inorganic Grignard reagents were never isolated, their structures were assumed based on the results from analogous nickel and platinum experiments. It was suggested that, overall, a four electron reduction of iron takes place to form a species likely composed of metal clusters of the form  $[Fe^{-II}(MgX)_2]$  that can oxidatively add  $ArCl$  to generate  $[ArFe^0(MgCl)]$ .

Fürstner's proposed mechanism, shown in **Scheme 1.27** is based on an  $Fe(-II)/Fe(0)$ , rather than an  $Fe(I)/Fe(III)$ , redox couple.<sup>85</sup> It was proposed that the iron salt precatalyst is reduced by an alkyl Grignard reagent to form an iron-ate species along with alkane, alkene, and alkyl homocouple byproducts.



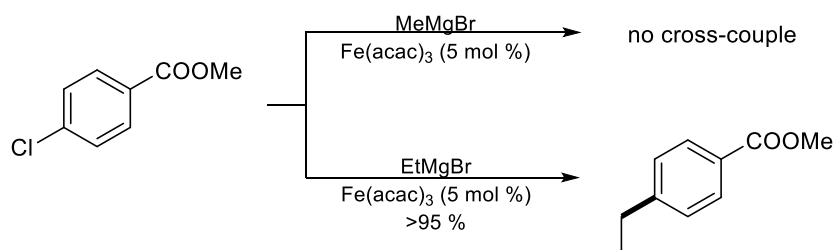
**Scheme 1.27.** A catalytic cycle proposed by Fürstner for the iron catalyzed cross coupling of alkyl Grignard reagents with aryl electrophiles, involving low valent iron species.<sup>83,85</sup>

The stoichiometry of the organic byproducts generated by the reduction of the iron precatalyst strongly suggested that four equivalents of Grignard reagent were required to generate the active species and that a four electron reduction occurred. Additionally, it was found that iron(0) powder was not catalytically competent unless reduced by excess  $\text{RMgX}$ , and that a formally  $\text{Fe}(-\text{II})$  species **1.22** originally reported by Jonas *et al.*<sup>86</sup> was active for aryl electrophile – alkyl Grignard coupling. The similarity in reaction outcome between **1.22** and the typical  $\text{RMgBr}/\text{Fe}(\text{acac})_3$  system further supported this hypothesis (**Scheme 1.28**).<sup>87</sup>



**Scheme 1.28.** A comparison of the cross coupling of an aryl halide with an alkyl Grignard reagent in the presence of well-defined species **1.22**<sup>86</sup> or  $\text{Fe}(\text{acac})_3/\text{NMP}$ , producing similar results.<sup>87</sup>

Whilst screening Grignard reagents, it was determined that nucleophiles containing  $\beta$ -hydrogens were required for this reaction, which is corroborated by the observation that alkene byproducts are formed from the reduction of the iron precatalyst (**Scheme 1.29**).<sup>88</sup> This finding is interesting because Grignard reagents lacking  $\beta$ -hydrogens worked quite well for Kochi's alkyl Grignard – vinyl halide coupling, suggesting that even the slight difference between aryl  $\text{C}(\text{sp}^2)$  and vinyl  $\text{C}(\text{sp}^2)$  electrophiles leads to an alternate mechanistic manifold.



**Scheme 1.29.** Studies indicating that alkyl Grignard reagents bearing  $\beta$ -hydrogen atoms are required to produce coupled product under conditions set forth by Fürstner.<sup>88</sup>

Upon conducting stoichiometric reactions of iron trichloride and methyl lithium in diethyl ether under rigorous conditions, an iron “super-ate” complex of the form  $[(\text{Me}_4\text{Fe})(\text{MeLi})][\text{Li}(\text{OEt}_2)]_2$  was isolated and identified.<sup>88,89</sup> This complex was not active for the coupling of aryl chlorides,

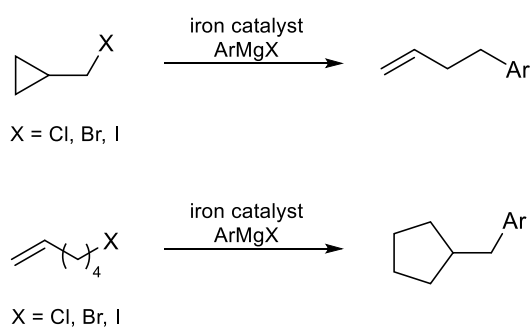
similar to previous results, but that it was catalytically competent for the cross coupling of acid chlorides and enol triflates. Therefore, Fürstner and coworkers suggest that several interconnected redox cycles may be present in these systems, and that Kochi's proposed mechanism cannot be ruled out.<sup>85</sup> However, it is important to note that the aforementioned work by Neidig and coworkers showed that low valent complexes formed from the reaction of alkyl magnesium reagents and iron salts are different from the analogous reaction with alkyl lithium reagents.<sup>82</sup>

Since this work, Fürstner's proposed Fe(-II)/Fe(0) couple has been studied by numerous groups.<sup>90</sup> Wolf and coworkers studied iron(-I) anthracene complexes and determined that the initial oxidation state of the iron species is less important than the identity of the ligand.<sup>91</sup> It was found by Werner and Bauer that a species formed from reacting Fe(acac)<sub>3</sub> with phenylmagnesium bromide effectively catalyzed the cross coupling of aryl chlorides and hexylmagnesium bromide.<sup>92</sup> The group used X-ray Absorption Fine Structure (XAFS) and X-ray Absorption Near Edge Spectroscopy (XANES) measurements of the reaction mixture to determine that the majority of iron in solution exists as nanoparticles with an average oxidation state of iron(II). The authors believe that this oxidation state is due to a geometric averaging of iron(III) and iron(I) species. No evidence was found to support the low valent iron species proposed by Fürstner. When employing such techniques, it is important to consider that XANES and XAFS measurements only provide an average picture for all of the iron species present in solution. Therefore, these data presented by Werner and Bauer do not indicate that the nanoparticles in solution are part of the catalytic cycle, nor that low valent iron species are not present.

Norrby and coworkers examined Hammond plots and other linear free energy relationships of electronically diverse aryl triflates in coupling reactions catalyzed by Fe(acac)<sub>3</sub>.<sup>93</sup> The relative reaction rates for these transformations were well correlated with the normal  $\sigma$ -values, with electron deficient aryl triflates reacting significantly faster than other aryl triflates. A  $\rho$ -value of +3.8 was obtained, suggested that during the rate determining step, significant negative charge builds up. This is more consistent with a traditional oxidative addition rather than a radical process, supporting the mechanisms proposed by both Fürstner and Kochi. It was assumed that reductive elimination occurs by a two-electron process as well, but no experiments to determine this were conducted.

### 1.5.3 Aryl Nucleophile – Alkyl Electrophile

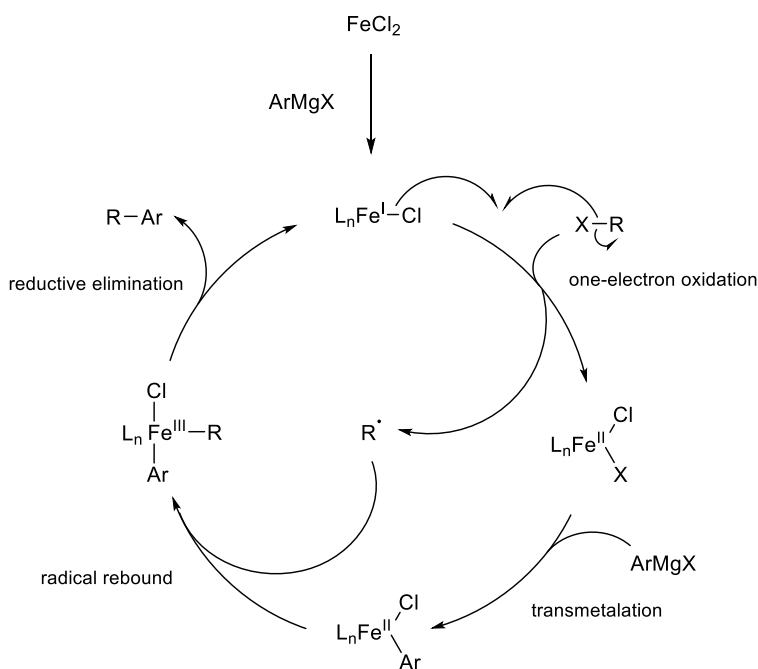
A large number of chemists are in agreement that a carbon-centered radical is present during the oxidative addition step in iron catalyzed aryl-alkyl coupling reactions. In numerous studies, radical clock alkyl halide substrates have been shown to undergo ring opening or ring closing under the cross coupling conditions, suggesting the presence of a radical (**Scheme 1.30**).<sup>48,50,51,56,76,79,94</sup> However, these kinds of experiments may not be appropriate for probing these types of reactions. It is possible for the ring opening and closing of such substrates to proceed through traditional two-electron pathways such as migratory insertion and  $\beta$ -hydride elimination. Supporting this, some palladium systems that are known to proceed via two-electron processes have shown such behavior.<sup>8</sup> Thus, additional methods must be used to probe these reactions for the presence of radicals.



**Scheme 1.30. Radical clock substrates that implicate radical intermediates in aryl Grignard-alkyl halide cross coupling reaction catalyzed by iron.**<sup>48,50,51,56,76,79,94</sup>

Fürstner<sup>88</sup> and Nakamura<sup>49</sup> have independently determined that enantiomerically enriched or diastereomerically pure alkyl halides undergo racemization as a result of C-X bond homolysis. Norrby and coworkers have employed linear free energy relationships that correlate well with radical reactions,<sup>31</sup> and Tonzetich and coworkers have inhibited cross coupling reactions with radical scavengers.<sup>94</sup> The combination of these results suggest that these pathways do indeed involve radical species.

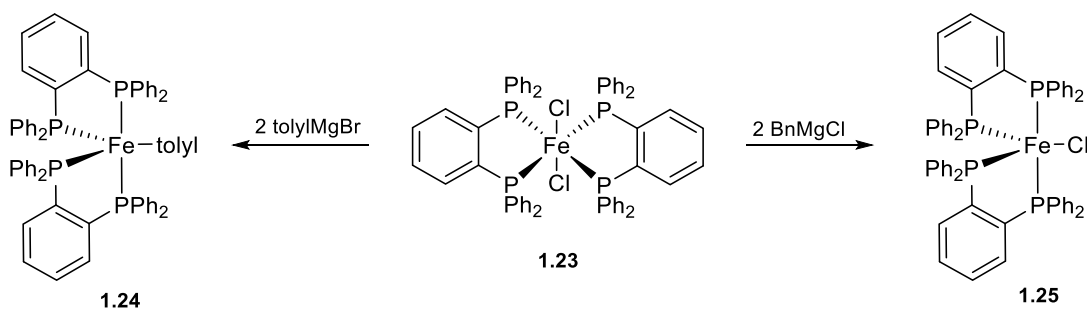
Bedford and Nakamura have provided the two most well-accepted mechanisms for aryl Grignard – alkyl halide coupling reactions catalyzed by iron. The Bedford system, **Scheme 1.31**, involves an Fe(I)/Fe(II)/Fe(III) redox manifold in which oxidative addition occurs via two sequential one-electron transformations.<sup>31,52,90,95,96</sup> The existence of an iron(I) intermediate was initially proposed due to the formation of one-half equivalent of Grignard homocouple product per each iron(II) precursor early in the reaction.<sup>31,95</sup> In this mechanism, iron dichloride is reduced by the aryl Grignard reagent to product an iron(I) halide. This species abstracts the halide from the substrate, forming an iron(II) dihalide and a carbon centered radical. The iron species undergoes transmetalation with another equivalent of aryl Grignard reagent, and the carbon centered radical recombines to form an iron(III) species that undergoes reductive elimination to generate the desired product.



**Scheme 1.31. A catalytic cycle proposed by Bedford for the iron catalyzed cross coupling of aryl Grignard reagents with alkyl electrophiles.**<sup>90,95,96</sup>

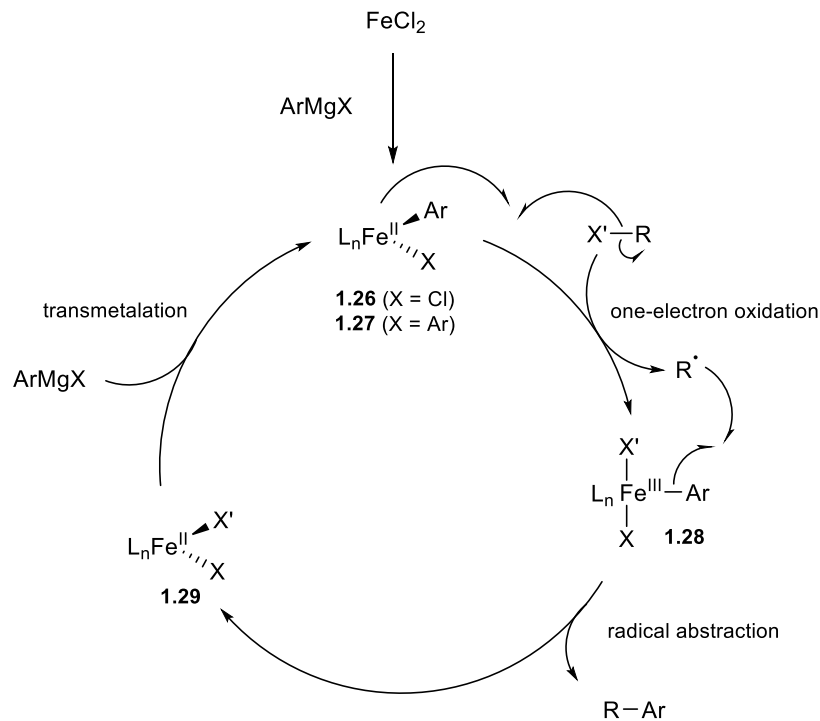
The Bedford group conducted stoichiometric experiments between  $(\text{dppbz})_2\text{Fe}(\text{II})\text{Cl}_2$ , **1.23**, and aryl Grignard reagents in order to gain insight into the reaction mechanism (**Scheme 1.32**).<sup>95</sup> In the presence of tolylmagnesium bromide,  $(\text{dppbz})_2\text{Fe}(\text{I})$  complex **1.24** was generated by way of

reduction and transmetalation. Alternatively, in the presence of benzylmagnesium chloride, an alkyl Grignard reagent, reduced complex **1.25** was generated, indicating that no transmetalation had occurred. Both **1.24** and **1.25** were found to be catalytically competent, but only **1.25** facilitated the cross coupling reaction with rates comparable to the catalytic system in question. Studies of Suzuki-type systems by the Bedford group indicate that they also proceed via an  $S = \frac{1}{2}$  iron(I) intermediate (*vide infra*), and this data was used to support the analogous Kumada-type mechanism.<sup>97</sup>



**Scheme 1.32.** The stoichiometric reaction of **1.23** with tolylmagnesium bromide to form iron(I) tolyl species **1.24**, and a similar reaction of **1.23** with benzylmagnesium chloride to form iron(I) chloride species **1.25**.<sup>95</sup>

Another mechanism for the coupling of aryl Grignard reagents with alkyl halides catalyzed by iron was originally proposed by the Nakamura group, and significant evidence has been found to support this cycle (**Scheme 1.33**).<sup>48,52,56,94,98,99</sup> In this mechanism, the activation of the iron(II) dichloride precatalyst by an aryl Grignard reagent to form aryl iron(II) chloride species **1.26** or diaryl iron(II) species **1.27** occurs without reduction of the metal center.<sup>98</sup> Either of these species can then abstract a halogen atom from the alkyl halide substrate, forming **1.28** and a carbon-centered radical. The C-C bond forming step then occurs when the alkyl radical abstracts an aryl fragment from **1.28**, leading to the desired species and iron species **1.29**, which then undergoes transmetalation with another equivalent of aryl halide to regenerate the active species.



**Scheme 1.33. A catalytic cycle proposed by Nakamura for the iron catalyzed cross coupling of aryl Grignard reagents with alkyl halides that proceeds via a Fe(II)/Fe(III) redox couple.<sup>98</sup>**

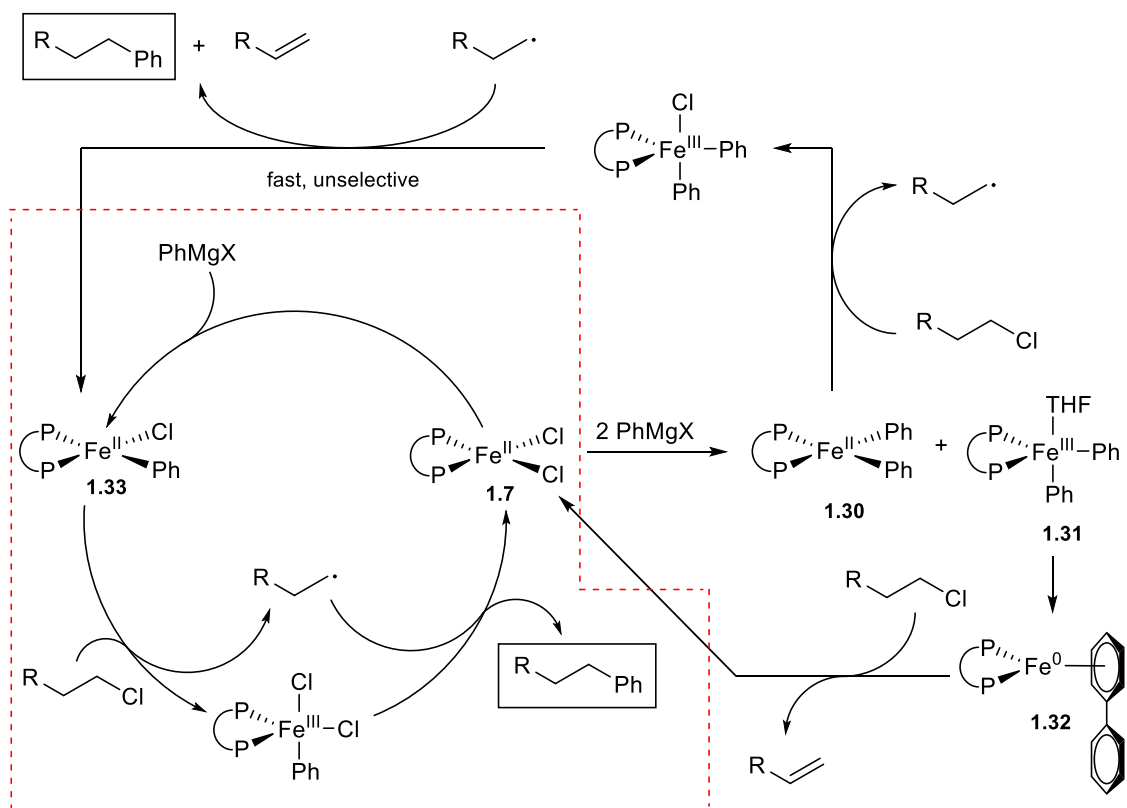
In an extensive study of this system, Neidig and coworkers applied *in situ* Mössbauer, EPR, and MCD spectroscopies to probe Kumada- and Suzuki-type iron catalyzed reactions and determine a plausible mechanism (**Scheme 1.34**).<sup>52,99</sup> Rapid freeze trapping, and subsequent study by these three techniques, of a reaction mixture containing isotopically pure (SciOPP)  $^{57}\text{FeCl}_2$  (**1.7**) and two equivalents of phenylmagnesium bromide revealed two high spin iron(II) organometallic species, **1.30** and **1.31**, as the major species present. Additionally, EPR studies indicated the presence of an  $S = \frac{1}{2}$  iron(I) species, as was observed by Bedford,<sup>97</sup> yet spin counting revealed that this species only made up 5 % of the total iron in solution, with the remaining 95 % attributed to EPR silent iron(II) and integer spin species. Spin counting was not conducted in studies by Bedford.

Addition of an alkyl halide to the mixture containing **1.30** and **1.31** led to the desired cross product and the conversion of **1.30** and **1.31** to **1.7**. The small amount of iron(I) complex observed did not react, indicating that it is likely off-cycle.

With extended reaction times or heating of the mixture of **1.30** and **1.31**, iron(0) complex **1.32** was formed, likely from the reductive elimination of biphenyl from both iron(II) species. The treatment of **1.32** with a stoichiometric quantity of alkyl halide led to the desired cross product at a significantly slower rate than the catalytic reaction, and with the production of a significant amount of alkene byproduct. This led the authors to conclude that **1.30**, **1.31**, and **1.32** are also off-cycle.

Upon addition of one equivalent of phenylmagnesium bromide to **1.7**, aryl iron(II) halide species **1.33** was formed and found to be much more active for the generation of the desired cross product than **1.7**. It is common for reactions of this type to require the slow addition of Grignard reagents, and these data suggest this promotes the formation of active species **1.33** over species **1.30** and **1.31** which lead to undesired reaction products. In similar studies with Suzuki-type systems, slow addition was not required because the transmetalation step is slower, precluding the formation of species akin to **1.30** and **1.31**.<sup>99</sup>

These studies by the Neidig group may not be applied generally to all Kumada-type coupling systems, but the elucidation of *in situ* generated species has been shown to be vital to gain understanding of the possible mechanistic manifolds.

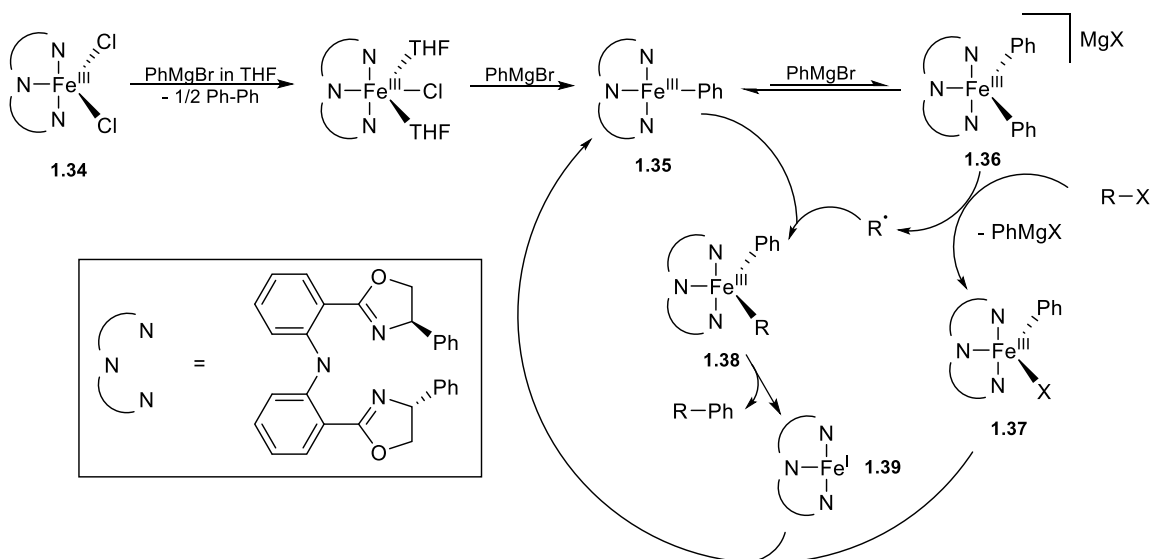


**Scheme 1.34.** A catalytic cycle proposed by Nakamura was expanded by Mössbauer, EPR, and MCD studies conducted by Neidig and coworkers.<sup>52,99</sup>

In 2015, Hu and coworkers conducted mechanistic studies that led them to propose an alternate mechanism, shown in **(Scheme 1.35)**.<sup>58</sup> For the coupling of alkyl halides and aryl Grignard reagents in the presence of **1.34**, the reaction rate was found to be first order in nucleophile, second order in catalyst, and independent of alkyl halide. Radical clock substrates and stereochemical probes were used to suggest the presence of a carbon-centered radical, but the group ruled out a radical rebound mechanism. When a linear radical clock substrate was used, the selectivity for linear product over cyclic product improved with increasing catalyst concentration. With radical rebound mechanisms, the reaction is expected to be zero order in catalyst, which is inconsistent with the data Hu and coworkers provided.

The mechanism proposed by the group is different from those previously suggested as it involves a bimetallic oxidative addition pathway, which is more consistent with the kinetic data

acquired. Precatalyst **1.34** is sequentially reduced and transmetalated by the aryl Grignard reagent to form **1.35** and half an equivalent of biphenyl. **1.35** is converted to biaryl iron(II) ate complex **1.36** which abstracts the halogen atom from the electrophile to form **1.37** and an alkyl radical. The alkyl radical then adds to **1.35** via a one electron oxidation, thus completing the overall oxidative addition of the alkyl halide, and forming species **1.38** which reductively eliminates the desired product and forms iron(I) species **1.39**. The interaction of **1.37** with **1.39** allows for the regeneration of active species **1.35**. While the Hu group's mechanistic studies are consistent with this hypothesis, other mechanisms cannot be ruled out.



**Scheme 1.35.** A catalytic cycle proposed by Hu for the iron catalyzed cross coupling of aryl Grignard reagents and alkyl halides in the presence of iron precatalyst **1.34**.<sup>58</sup>

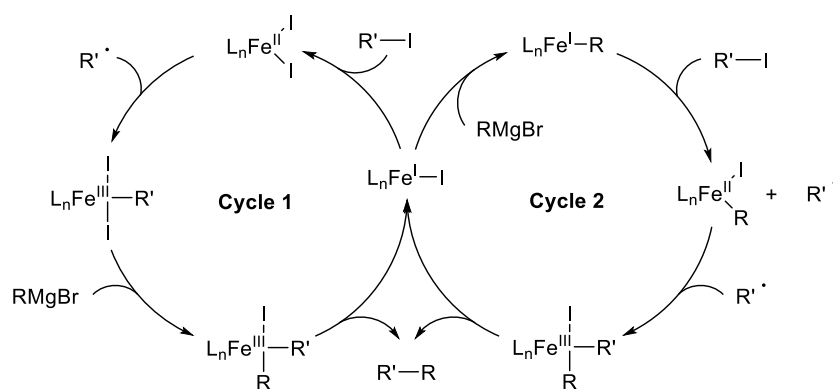
Fürstner and coworkers proposed a catalytic system involving an Fe(-II)/Fe(0) couple for aryl nucleophile – alkyl electrophile cross coupling similar to their work with alkyl Grignard reagents and aryl halides,<sup>88</sup> and Cahiez and coworkers have proposed an Fe(0)/Fe(I)/Fe(II) cycle.<sup>100</sup> However, minimal evidence was provided for either of these mechanisms.

#### 1.5.4 Alkyl Nucleophile – Alkyl Electrophile

Due to the scarcity of iron catalyzed alkyl-alkyl cross coupling in the literature, it is no surprise that few mechanistic studies of these systems exist. Cárdenas and coworkers proposed two possible mechanisms based on the observations that cyclic radical clock species undergo ring opening during the reactions, and that an  $S = \frac{1}{2}$  species is seen by EPR (**Scheme 1.36**).<sup>76</sup> The amount of homocoupled product formed upon formation of this species led the group to suggest an iron(I) active species.

Proposed **Cycle 1** suggests that an iron(I) iodide abstracts another iodide atom from the alkyl iodide substrate to form an iron(II) diiodide and an alkyl radical. Upon radical recombination, an alkyl iron(III) diiodide is generated that can undergo transmetalation with the alkyl Grignard reagent. Thus, a dialkyl iron(III) iodide species is formed that reductively eliminates the desired product.

**Cycle 2** also begins with an iron(I) iodide, but here, transmetalation is the first step, forming an iron(I) alkyl. This species abstracts an iodide from the alkyl electrophile to produce an alkyl radical and an alkyl iron(II) iodide. Similar to **Cycle 1**, the alkyl radical recombines with this species to generate the dialkyl iron(III) iodide, which undergoes reductive elimination to form the desired product and regenerate the catalytically active species.



**Scheme 1.36.** Two catalytic cycles proposed by Cárdenas for the iron catalyzed cross coupling of alkyl Grignard reagents with alkyl halides.<sup>76</sup>

Contrary to Cárdenas' suggestions, Tonzetich and coworkers conducted mechanistic studies on a similar system, only differing in the NHC ligand used and the formation of the complex *a priori* rather than *in situ*, and the findings suggest a mechanism more akin to what is proposed by Nakamura for alkyl electrophile - aryl nucleophile systems (**Scheme 1.33**).<sup>94</sup> These mechanistic studies involved the isolation of presumed reaction intermediates and the demonstration that the complexes were catalytically active.

The lack of data for these systems preclude drawing any conclusions, and there is no evidence to suggest whether or not more than one mechanism is at play in alkyl-alkyl coupling systems of this type.

#### 1.5.5 Alkynyl Nucleophile – Alkyl Electrophile

Nakamura and coworkers suggested a mechanism for alkynyl Grignard reagent – alkyl electrophile Kumada- type cross coupling that is akin to their proposal for aryl nucleophile – alkyl electrophile systems, **Scheme 1.33**.<sup>98,78</sup> This mechanism suggests the formation of a neutral (SciOPP)iron(II) bis(alkyne) as the catalytically active species. Recently, Neidig and coworkers pursued extensive studies of this system, employing EPR, MCD, Mössbauer, and X-ray spectroscopies.<sup>101</sup> Corroborating Nakamura's initial hypothesis, a (SciOPP)iron(II) bis(alkyne) species was identified as the active species, and (SciOPP)iron(I) and alkynylated ferrate species were determined to be off-cycle. The latter data suggest that mechanisms more similar to those proposed by Bedford<sup>95,96</sup> and Fürstner<sup>83</sup> may not be applicable to this system. The Neidig group also found that steric bulk of the alkyne and solvent selection were critical for this system.<sup>101</sup>

#### 1.5.6 Importance of Ligation

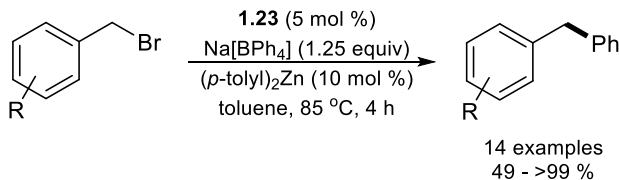
Neidig and coworkers conducted an extensive study of the electronic and structural differences between phosphine ligands and the effect that these differences might have on cross coupling applications.<sup>102</sup> Ligands containing *o*-phenylene backbones, SciOPP and dppbz, were

compared to those containing ethyl backbones, <sup>t</sup>Bu<sub>2</sub>dppe and dppe using MCD and DFT calculations of MO diagrams and Mayer bond orders (MBOs). The presence of an ethyl backbone resulted in a small decrease in  $10D_q(T_d)$  and a higher-lying ligand-based acceptor orbital relative to SciOPP and dppbz ligation. Additionally, SciOPP and dppbz were shown to have nearly identical electronic and structural properties, despite the evidence for differences in reactivity in cross coupling applications.<sup>44,48</sup> The bisphosphine ligand Xantphos was also examined, and a significantly decrease in the magnitude of  $10D_q(T_d)$  along with a lower iron-phosphine MBO was observed. Of the five ligands examined, Xantphos is the only ligand thus far that has been able to facilitate iron catalyzed Kumada- and Suzuki-type alkyl-alkyl cross coupling.<sup>34</sup> It is clear that rational ligand design is important for developing these methodologies.

## 1.6 IRON CATALYZED SUZUKI – TYPE SYSTEMS

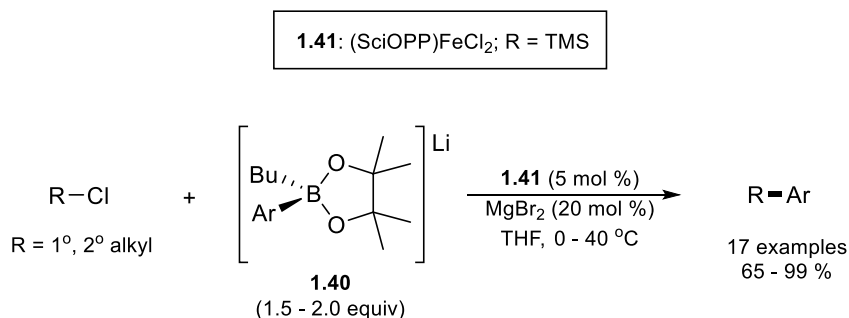
The organoboron transmetalation reagents used in Suzuki-type cross couplings are arguably more ideal than other options for industrial and pharmaceutical use due to the ease in which they are synthesized and handled. However, efficient protocols for iron catalyzed Suzuki-type couplings are uncommon.<sup>1</sup> In recent years, progress has been made in this area due to the use of highly activated borates and Zn or Mg additives.<sup>97,98,103-107</sup>

In 2009, Bedford and coworkers reported the catalytic coupling of tetraphenyl borates with benzyl bromides in the presence of well-characterized precatalyst **1.23**, and ditolyl zinc (**Scheme 1.37**).<sup>103</sup> It was hypothesized that the zinc additive stabilizes the active iron species and prevents catalyst decomposition, although no evidence was provided to support this claim. In the absence of the borate and with stoichiometric amounts of ditolyl zinc, the reaction was seen to proceed with the zinc reagent acting as the nucleophile.



**Scheme 1.37.** The coupling of benzyl bromide and sodium tetraphenyl borate in the presence of catalytic amounts of **1.23** and ditolyl zinc.<sup>103</sup>

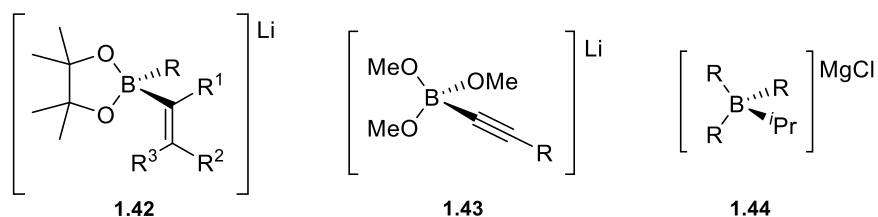
A limitation of this system is that three of the four aromatic equivalents on the borate nucleophile act as spectators in the cross coupling reactions. Nakamura and coworkers addressed this limitation by employing activated borate species such as **1.40**, formed from treating aryl boronic esters with butyl lithium (**Scheme 1.38**).<sup>98</sup> In the presence of iron(II) SciOPP complex **1.41**, alkyl-aryl coupling was accomplished in good yields. However, the desired product was only formed in high yields when sub-stoichiometric amounts of magnesium bromide were present. It was hypothesized that the additive aids in the inherently slow transmetalation step, although the precise role is not clear. Electron-donating and electron-withdrawing substitution on the aryl borate were well tolerated, yet sterically hindered substrates were not examined. Secondary and primary alkyl halides reacted smoothly, and alkyl chlorides were superior to alkyl bromides as coupling partners.



**Scheme 1.38.** The coupling of alkyl chlorides and activated aryl borate **1.40** in the presence of catalytic amounts of **1.41** and magnesium dibromide.<sup>98</sup>

Under the conditions described in **Scheme 1.38**, the aryl fragment of borate **1.40** was selectively transferred while the alkyl fragment remained inert.<sup>98</sup> However, alkynyl, alkyl and vinyl transfer could be achieved utilizing different variations of the transmetalating reagent. Vinyl borate

**1.42**<sup>104</sup> was successfully coupled under conditions similar to those in **Scheme 1.38** and, remarkably, alkynyl borate **1.43**<sup>105</sup> and alkyl borate **1.44**<sup>106,107</sup> produced the desired cross products without the need for a magnesium additive (**Scheme 1.39**). However, in order for **1.44** to undergo efficient cross coupling, Xantphos, an ancillary phosphine ligand with a larger bite angle than SciOPP, was required.



**Scheme 1.39. Vinyl borate 1.42**<sup>104</sup>, **alkynyl borate 1.43**<sup>105</sup>, and **alkyl borate 1.44**<sup>106,107</sup> can act as nucleophilic coupling partners for iron catalyzed Suzuki-type cross coupling.

Bedford and coworkers reported the formation of the activated borate species *in situ* with the addition of *t*-butyl- or *n*-butyl- lithium to a boronic ester.<sup>97</sup> Using commercially available dppe and dppp ligands, excellent yields were achieved for the coupling of alkyl and benzyl bromides with the *in situ* generated borates. The group published an additional report wherein it was found that 2-halobenzylhalides underwent cross coupling at both the aryl and benzyl positions.<sup>108</sup> This is hypothetically due to the initial coupling of the benzyl halide allowing for coordination of the substrate to the iron center, which when in close proximity can activate the aryl halide more readily.

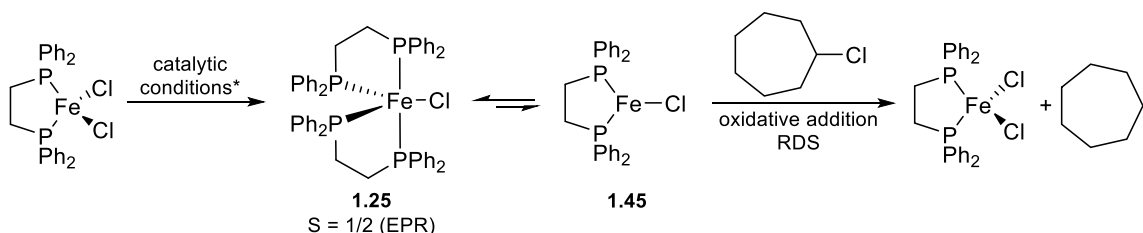
## 1.7 IRON CATALYZED SUZUKI - MECHANISTIC IMPLICATIONS

### 1.7.1 Proposed Mechanisms

The groups of Nakamura and Bedford have proposed Suzuki-type mechanisms that are identical to their previously discussed Kumada-type mechanisms. In both systems, catalytic amounts of magnesium dihalide are required to achieve good yields,<sup>97,98</sup> and both groups suggest

that this additive facilitates transmetalation. Nakamura and coworkers propose this similarity in pathways with scant mechanistic evidence,<sup>98</sup> whereas Bedford and coworkers show that **1.25**, the supposed active species generated *in situ* (**Scheme 1.40**), can be formed by stoichiometric reactions of FeCl<sub>2</sub>(dppe) and borate **1.40** with or without added MgX<sub>2</sub>.<sup>97</sup> **1.25** is formed to a lesser extent when MgX<sub>2</sub> is not present, and from this Bedford and coworkers conclude the transmetalation role of the additive, even though transmetalation is not thought to occur in the formation of **1.25**.

Kinetic studies by Bedford indicate that **1.25** is likely in equilibrium with(dppe)iron(I)Cl species **1.45**, and that **1.45** can oxidatively add the alkyl halide to regenerate (dppe)iron(II)Cl<sub>2</sub> and form an alkyl radical, which is supported by radical clock studies.<sup>97</sup> It is believed that this is the rate determining step (RDS) of the catalytic cycle because the equilibrium between **1.25** and **1.45** favors **1.25**, there is an inverse dependence on dppe, and a first order dependence of alkyl halide.



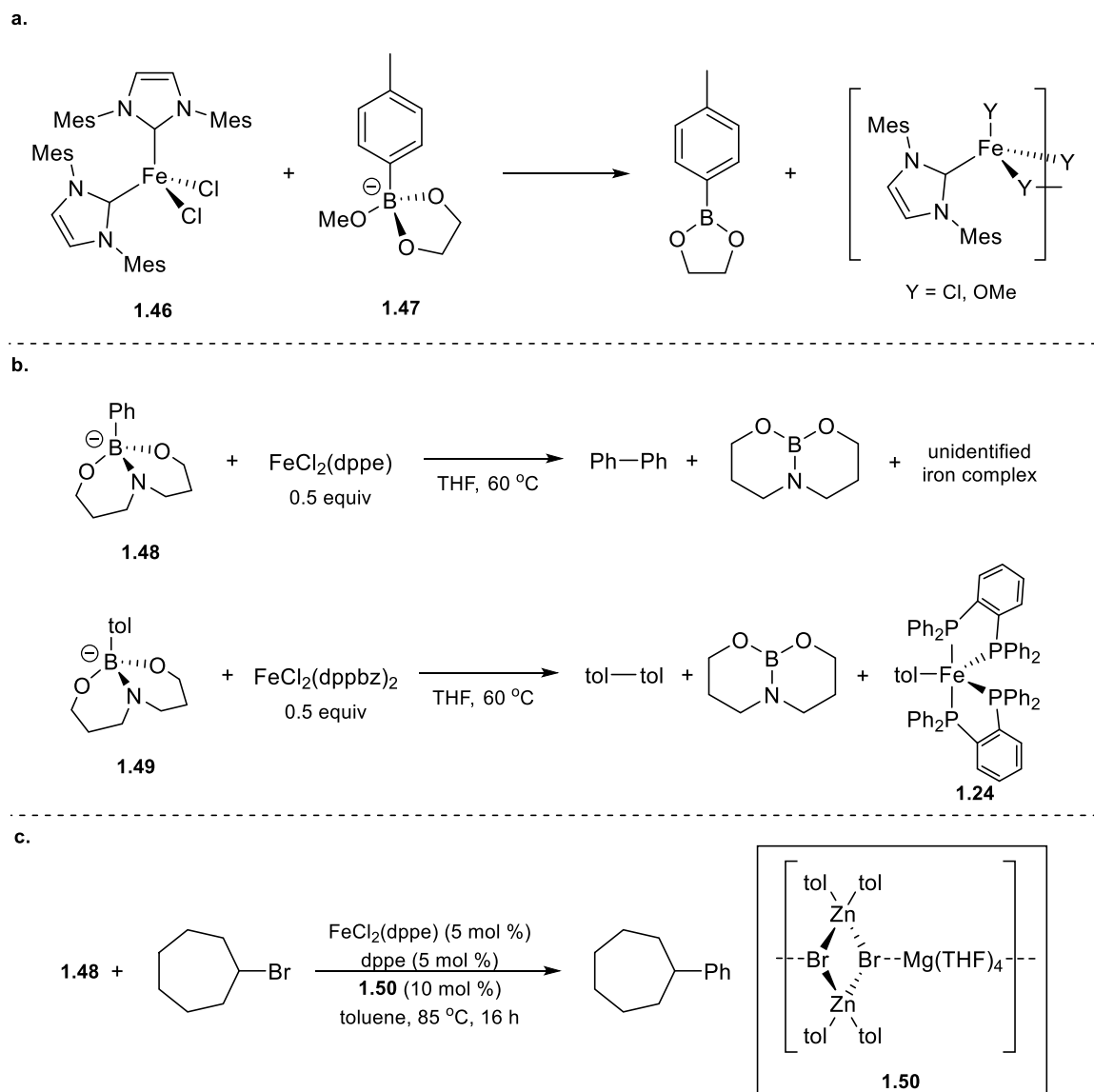
**Scheme 1.40.** The identification of **1.25** during the catalytic process, and its hypothesized equilibrium with **1.45**. **1.45** is thought to be active for oxidative addition of cycloheptyl chloride to regenerate FeCl<sub>2</sub>(dppe) and to form an alkyl radical. With or without magnesium dibromide additive.<sup>97</sup>

### 1.7.2 Transmetalation Studies

The transmetalation step in iron catalyzed cross coupling reactions is an interesting topic of study due to the vast number of mechanisms proposed for Kumada systems, but is also considered by some to be the key step in cross coupling reactions. Probing the transmetalation step could provide insight that allows for rational design of systems and improved mechanistic understanding.

Ingelson and coworkers have provided several mechanistic studies of transmetalating reagents of iron catalyzed Suzuki systems. In a stoichiometric reaction between iron(II) NHC **1.46** and borate **1.47**, the methoxide moiety was selectively transferred to the metal center to form a multimeric species (**Scheme 1.41a**).<sup>109</sup> Reflective of the high oxophilicity of iron, this suggests that borates bearing oxygen-containing groups may not be preferable transmetalating reagents. In fact, when using borate **1.48**, transmetalation was shown to occur at elevated temperatures by the formation of biphenyl (**Scheme 1.41b**).<sup>110</sup> The iron species in this instance, (dppe)FeCl<sub>2</sub> was transformed into an unidentifiable species. Upon the reaction of analogous borate **1.49** with (dppbz)<sub>2</sub>FeCl<sub>2</sub>, bitolyl was produced along with iron species **1.24** (**Scheme 1.41b**). The presence of a tolyl substituent on the iron center of **1.24** further supports the conclusion that transmetalation had occurred.

With this in mind, the group attempted to use **1.48** as the nucleophilic partner for the coupling of cycloheptylbromide in the presence of (dppe)FeCl<sub>2</sub>.<sup>110</sup> Interestingly, this reaction did not proceed to the desired cross product without zincate additive **1.50** (**Scheme 1.41c**). Additionally, the borate commonly used by Bedford,<sup>97</sup> (tBu)(Ph)B(pin), was found to transmetalate with (dppe)FeCl<sub>2</sub> readily, yet Bedford shows that the cross product is only generated in the presence of MgBr<sub>2</sub>.<sup>110</sup> These findings indicate that the additive might not act to facilitate transmetalation as Bedford suggests, and that these systems are very sophisticated. Considerable research is needed before a strong understanding can be grasped.



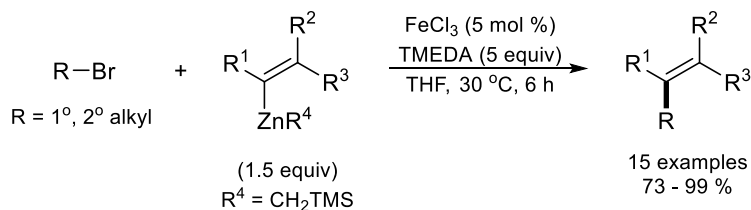
**Scheme 1.41. (a) A stoichiometric reaction between 1.46 and 1.47 in which the methoxide group of the borate is selectively transferred to the metal center.<sup>109</sup> (b) Stoichiometric reactions between 1.48 and FeCl<sub>2</sub>(dppe), and between 1.49 and FeCl<sub>2</sub>(dppbz)<sub>2</sub>, leading to transmetalation products, including iron species 1.24.<sup>110</sup> (c) The use of 1.48 as a nucleophilic partner to couple with cycloheptylbromide in the presence of catalytic amounts of FeCl<sub>2</sub>(dppe), requiring the presence of zincate 1.50.**

## 1.8 ADDITIONAL VARIATIONS

Despite the multitude of iron-based Kumada-type studies described since 1971, and the recent emergence of Suzuki-type systems, other variants of iron catalyzed cross coupling have been scarce. However, some excellent studies have been reported since 2010.

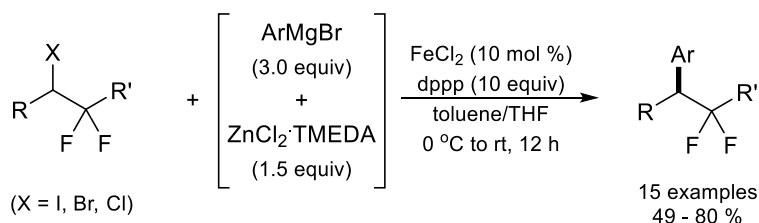
### 1.8.1 Iron Catalyzed Negishi - Type Systems

Negishi cross couplings, characterized by the use of organozinc nucleophiles, have been examined by several groups in recent years. Nakamura and coworkers stereoretentively coupled alkyl halides with vinyl zinc species in high yields (**Scheme 1.42**).<sup>111</sup> The coupling occurred in a highly chemoselective fashion, with tolerance of electron withdrawing groups installed on the vinyl zinc reagent. Primary and secondary alkyl chlorides, bromides, and iodides were tolerated, however, no tertiary alkyl halides were screened.



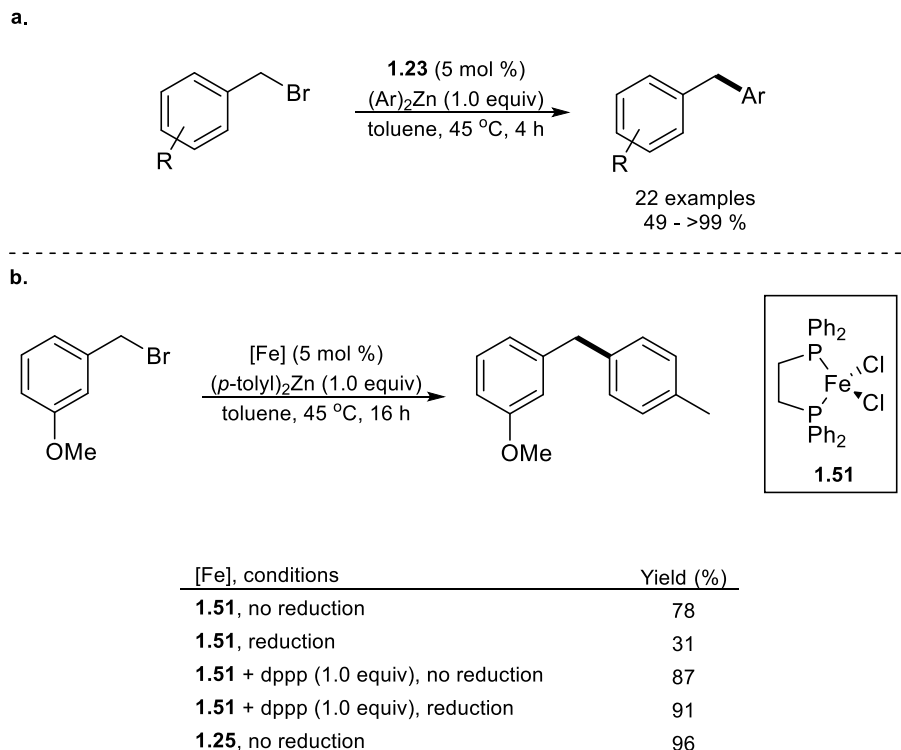
**Scheme 1.42.** The coupling of primary and secondary alkyl halides with vinyl zinc nucleophiles in the presence of catalytic amounts of FeCl<sub>3</sub> and excess TMEDA.<sup>111</sup>

Bis(diphenylphosphino) propane (dppp) was shown by the Qing group to be an efficient ligand for the iron-based coupling of zinc-activated aryl Grignard reagents with alkyl halides bearing  $\beta$ -fluorides.<sup>112</sup> As shown in **Scheme 1.43**, moderate yields of the desired *gem*-difluoromethylenated products were achieved. The zinc additive is required for this reaction to proceed, and it was hypothesized that diphenyl zinc is likely formed *in situ*, and is a competent transmetalation reagent.



**Scheme 1.43.** The coupling of alkyl halides bearing  $\beta$ -fluoride substitution with an *in situ* generated aryl zinc species facilitated by catalytic amounts of iron dichloride and dppp.<sup>112</sup>

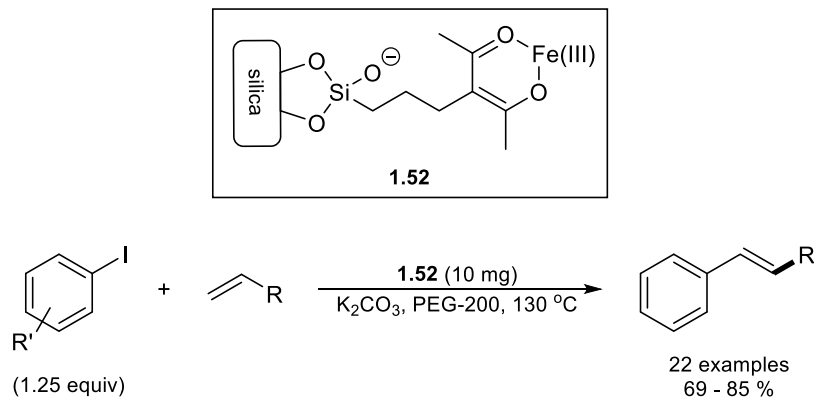
Well-defined iron species  $\text{FeCl}_2(\text{dppbz})_2$  **1.23** was utilized by the Bedford group for the coupling of benzyl bromides and chlorides with aryl zinc reagents, producing moderate to good yields (**Scheme 1.44a**).<sup>103</sup> The use of iron species **1.23** was required in order to prevent the facile homocoupling of the aryl and benzyl substrates. While *para*-substituted electrophiles and nucleophiles were shown to be well tolerated, few other substitution patterns were examined. A subsequent report examined the role of the bisphosphine ligand, revealing commercially available bis(diphenylphosphino) ethane (dppe) as an efficient ligand in the forms of iron(II) $\text{Cl}_2(\text{dppe})$  **1.51**, and a di-ligated iron(I) variant, **1.25**.<sup>96</sup> As shown in **Scheme 1.44b**, high yields of the desired cross product between diaryl zinc species and benzyl halides were seen with **1.51**, especially when it was reduced to iron(I) in the presence of an extra equivalent of dppe, presumably because **1.25** is formed *in situ*. As expected, **1.25** led to efficient catalysis without the need of excess ligand or reduction of the complex.



**Scheme 1.44.** (a) The coupling of benzyl bromides and diaryl zinc species in the presence of catalytic amounts of **1.23**.<sup>103</sup> (b) The coupling of *m*-methoxybenzyl bromide with ditolylzinc in the presence of **1.51** and **1.25** in varying conditions.<sup>96</sup>

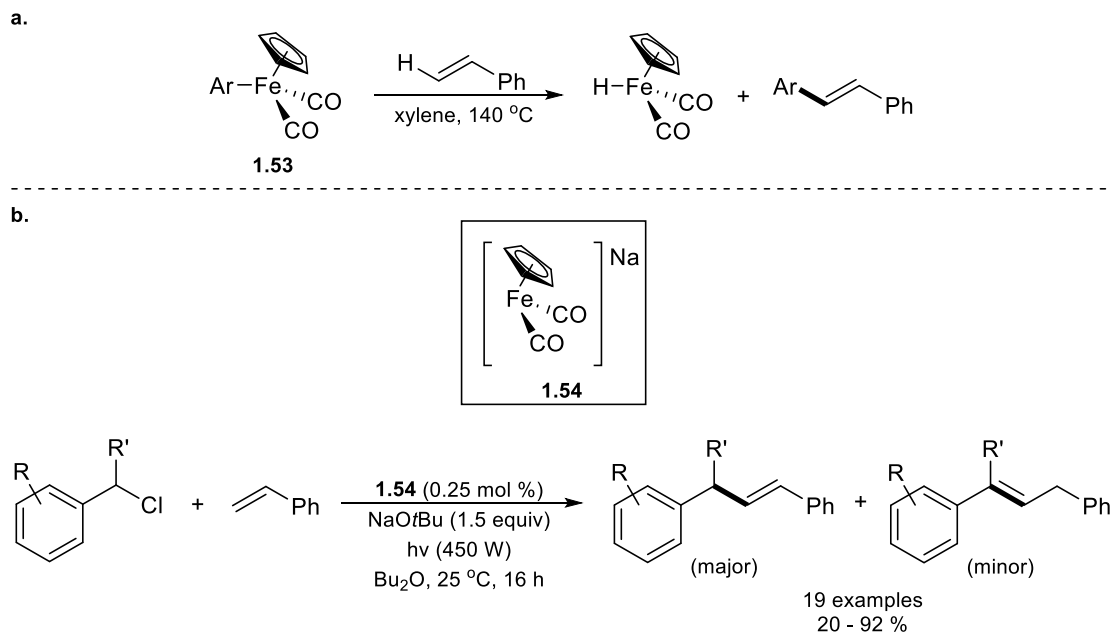
## 1.8.2 Iron Catalyzed Heck – Type Systems

Iron catalyzed Heck-type systems are rare, and the first report was disclosed by Vogel and coworkers in 2008.<sup>113</sup> Following this, only two reports have surfaced. Azizi and coworkers appended an iron(II) center bearing an acetylacetonate (acac)-type ligand to a silica support to form a heterogeneous species **1.52** that was shown to efficiently couple aryl iodides with alkenes (**Scheme 1.45**).<sup>114</sup> A variety of substituted aryl iodides, containing both electron-withdrawing and electron-donating groups, were coupled with styrene, methyl methacrylate and methacrylate in moderate to good yields. The heterogeneous catalyst could be isolated from the reaction and reused multiple times before a decrease in yield was seen. The combination of a heterogeneous iron catalyst and polyethylene glycol solvent allowed for an environmentally benign system.



**Scheme 1.45.** The coupling of aryl iodides and terminal olefins in the presence of heterogeneous iron catalyst **1.52**.<sup>114</sup>

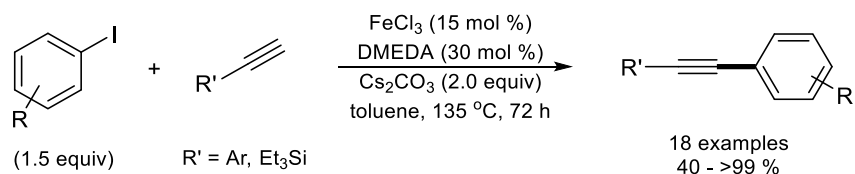
The only other report of an iron catalyzed Heck-type system was inspired by a report by Oshima and coworkers wherein styrene could be arylated by a stoichiometric quantity of iron species **1.53** (**Scheme 1.46a**).<sup>115</sup> Mankad and coworkers developed a catalytic system with a similar, anionic complex, **1.54**, for the *E*-selective coupling of benzyl chlorides with styrene in the presence of UV irradiation (**Scheme 1.46b**).<sup>116</sup> The presence of UV irradiation allowed for CO dissociation from **1.54**, forming the catalytically active species. Moderate yields were achieved, albeit 6 equivalents of styrene were required and an olefin migration product was also formed. Other olefins were not screened, and moderate steric and electronic variation of the benzyl chloride was tolerated.



**Scheme 1.46. (a) Arylation of styrene by a stoichiometric reaction with complex 1.53.<sup>115</sup> (b) *E*-selective coupling of benzyl chlorides with styrene in the presence of catalytic amounts of 1.54 and facilitated by UV irradiation.<sup>116</sup>**

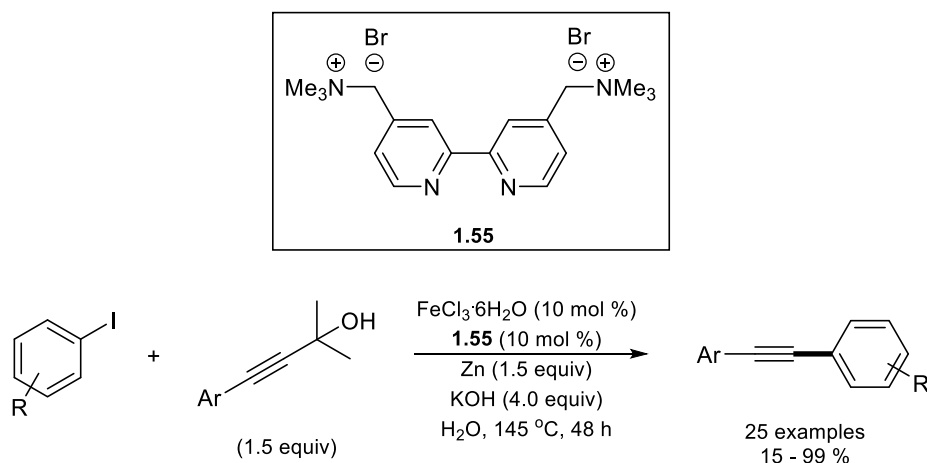
### 1.8.3 Iron Catalyzed Sonogashira – Type Systems

In 2008, Bolm and coworkers published the first instance of an iron catalyzed Sonogashira-type coupling reaction (**Scheme 1.47**).<sup>117</sup> In this report, aryl iodides and aryl alkynes or silyl alkynes were successfully coupled in good yields. Most substitution of the aryl iodide was permitted, however aryl bromides and tosylates led to decreased yields. Alkyl-substituted alkynes led to greatly diminished yields.



**Scheme 1.47. The coupling of aryl iodides with aryl or silyl alkynes in the presence of catalytic amounts of iron trichloride supported by DMEDA.<sup>117</sup>**

Following this seminal report, Tsai and coworkers utilized iron trichloride hydrate and a cationic bipyridyl ligand **1.55** to facilitate a Sonogashira-type coupling in aqueous media.<sup>118</sup> The conditions were optimized with phenylacetylene and then creatively expanded to the coupling of masked terminal alkynes (**Scheme 1.48**). These 4-aryl-2-methylbut-3-yn-ols, when treated with base, forming an alkynyl anion *in situ* via elimination. It was found that the masked alkynes could couple with aryl iodides in a wide range of yields. The reaction was tolerant of electron-withdrawing and electron-donating *para*-substitution of the aryl iodide, as well as moderate steric hindrance. Alkyl-substituted masked alkynes did not undergo the coupling reaction, and the zinc additive was required for the reactions to proceed with good yields.

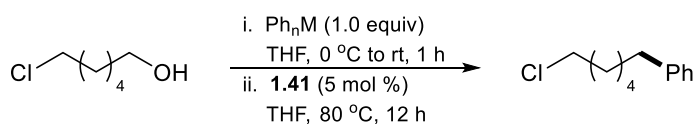


**Scheme 1.48. The coupling of aryl iodides and masked aryl-alkynes in the presence of iron trichloride hexahydrate and cationic bipyridyl ligand 1.55.**<sup>118</sup>

Finally, Chen and coworkers applied iron catalyzed Sonogashira-type methodologies to the synthesis of 2-aryl-benzo[b]furans. Modest yields with moderate functional group tolerance were achieved.<sup>119</sup>

#### 1.8.4 Miscellaneous Systems

In addition to commonly used transmetalating reagents, iron catalyzed cross coupling reactions involving other metalloids nucleophiles have been developed. Studies conducted by the Nakamura group determined the effectiveness of certain metalloids as transmetalating reagents in iron catalyzed reactions. When examining *in situ* generated phenylaluminum complexes prepared from Grignard reagents, it was found that the ratio of Grignard reagent impacts the ability of the reagent to participate in the desired reaction.<sup>120</sup> Another study screened a variety of Mg, Zn, B, and Al reagents for the coupling of hydroxylated primary alkyl chlorides in the presence of iron SciOPP complex **1.41** (Scheme 1.49).<sup>121</sup> It was found that an adduct of tetraphenylaluminum and magnesium chloride far surpassed other reagents, leading to a 91 % yield of desired product (entry 6). PhMgBr and Ph<sub>2</sub>B(pin)Li both led to extremely low yields despite being competent transmetalating reagents in aforementioned systems.



Entry	Ph <sub>n</sub> M	Yield (%)		
		Desired	Alkene	Alkane
1	PhMgBr <sup>a</sup>	4	12	17
2	Ph <sub>2</sub> Zn·2MgCl <sub>2</sub>	6	0	0
3	Ph <sub>3</sub> Zn·MgBr	13	23	20
4	Ph <sub>2</sub> B(pin)Li <sup>b</sup>	0	9	0
5	Ph <sub>3</sub> Al·3MgCl <sub>2</sub>	0	0	0
6	Ph <sub>4</sub> Al·MgCl	91	6	0

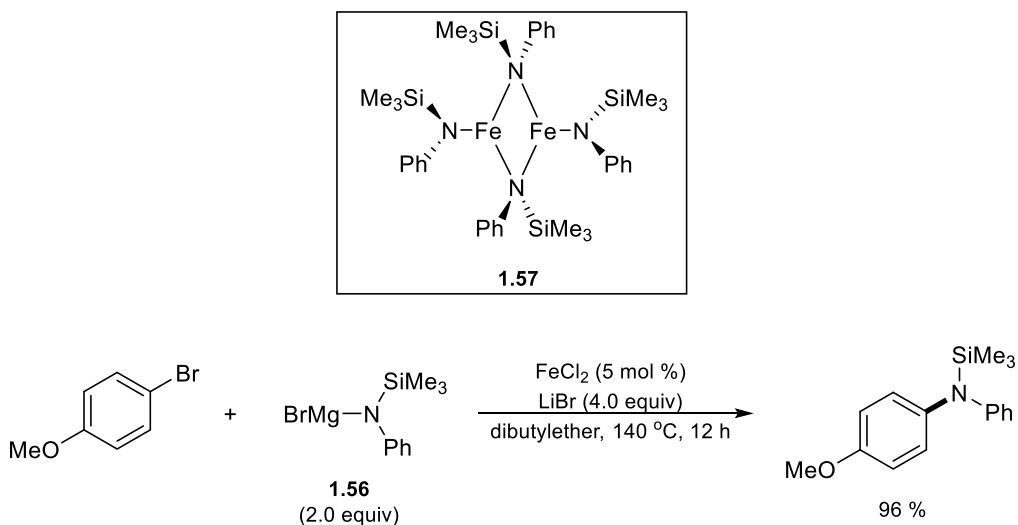
**Scheme 1.49. A screen of transmetalating reagents for the coupling of hydroxylated primary alkyl chlorides in the presence of catalytic amount of iron SciOPP complex 1.41. <sup>a</sup>2.0 equivalents of nucleophile used. <sup>b</sup>20 mol % MgBr<sub>2</sub> added as a co-catalyst.<sup>121</sup>**

Knochel and coworkers coupled aryl and heteroaryl electrophiles with benzyl manganese chloride in the presence of an iron catalyst.<sup>122</sup> The manganese-based nucleophile was formed *in situ* by first generating the benzyl Grignard reagent and transmetalating it with the lithium chloride

adduct of manganese dichloride. Fourteen examples of this coupling with moderate yields were reported. Similarly, aryl Grignard reagents were combined with copper chloride to generate organocuprates *in situ*, which subsequently were able to cross couple with alkynyl bromides in the presence of an iron catalyst.<sup>123</sup> The identity of the organocuprate was not identified, and evidence of its existence was not reported. Titanium additives were used by the Liu group for the iron catalyzed coupling of two distinct aryl Grignard reagents with low to moderate yields.<sup>124</sup>

Bedford and coworkers screened group 13 aryl nucleophiles for effectiveness as coupling partners for benzyl chlorides in the presence of iron complex **1.23**.<sup>107</sup> Aluminum and indium nucleophiles led to the desired cross product, yet boron, gallium, and thallium nucleophiles were found to require a zinc additive. A substrate scope revealed that, although aluminum and indium gave similar results for most substrates, only aluminum nucleophiles were able to couple with alkyl halides.

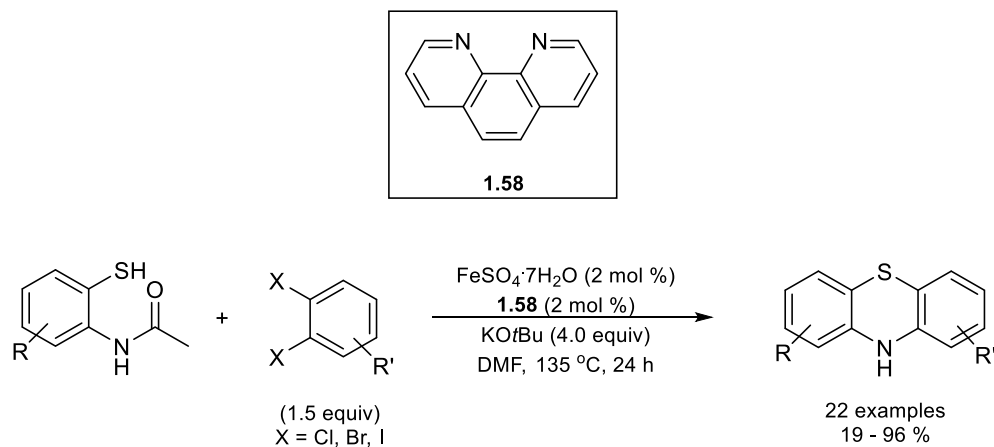
Iron catalyzed examples of C-N and C-S bond forming Buchwald-Hartwig-type reactions have also been examined. Nakamura disclosed that phenyl(trimethylsilyl)amino magnesium bromide, **1.56**, was an effective coupling partner for aryl bromides in the presence of iron dichloride and a stoichiometric amount of lithium bromide as an additive (**Scheme 1.50**).<sup>125</sup> A modest range of electron-donating and electron-withdrawing groups were tolerated on the aryl bromide, and it was suggested that iron(II) diamide dimer **1.57** was the *in situ* generated precatalyst. Because of the proclivity of Buchwald-Hartwig type reactions to provide erroneous results due to the presence of trace transition metal impurities and provide erroneous results,<sup>32,33</sup> Nakamura and coworkers evaluated their iron source by Inductively Coupled Plasma Mass Spectrometry (ICP-MS) and Inductively Coupled Plasma Atomic Emission Spectroscopy (ICP-AES).<sup>125</sup> Trace amounts of Pd, Cu, Co, and Ni were present in the iron source, but control experiments run with catalytic amounts of PdCl<sub>2</sub>, CuCl<sub>2</sub>, and CoCl<sub>2</sub> showed low activity.



**Scheme 1.50.** The coupling of *p*-methoxyphenyl bromide with phenyl(trimethylsilyl)amino magnesium bromide (**1.56**) in the presence of stoichiometric amounts of lithium bromide and catalytic amounts of iron dichloride. The reaction is thought to proceed *via* **1.57**, an *in situ* generated species.<sup>125</sup>

A similar sulfonation route by Lee and coworkers coupled vinyl halides with alkyl and aryl thiols facilitated by iron trichloride and Xantphos.<sup>126</sup> A high purity (99.99 %) iron source was used and moderate yields were achieved.

Hu and coworkers recently reported a one-pot synthesis of phenothiazines from 1,2-dihaloarenes and *N*-(2-mercaptophenyl) acetamide (**Scheme 1.51**).<sup>127</sup> The reaction is thought to proceed *via* C-S coupling with the thiol group of the nucleophile and subsequent C-N coupling with the amine group adjacent to the thiol. The system, catalyzed by iron sulfate heptahydrate supported by 1,10-phenanthroline (**1.58**), was not tolerant of substitution of the 1,2-dihaloarenes, and 1,2-dichloroarenes were inefficient coupling partners, however, moderate substitution of the nucleophile was tolerated.



**Scheme 1.51. Coupling of 1,2-dihaloarenes with *N*-(2-mercaptophenyl) acetamides in the presence of catalytic amounts of iron sulfate heptahydrate and 1,10-phenanthroline (1.58).<sup>127</sup>**

## 1.9 CONCLUSIONS

Since the revival of iron catalyzed cross coupling in the early 2000's, numerous systems have been developed that provide useful alternatives to palladium catalyzed systems, and protocols have been established for processes that are difficult to catalyze with palladium. These systems have shown remarkable reactivity and chemoselectivity, however, the growth of this field has been limited by the lack of enantioselective variants and procedures involving transmetalating partners other than Grignard reagents. The advancement of iron catalyzed cross coupling is dependent on the development of more general cross coupling methods and a better mechanistic understanding. Significant challenges remain, yet recent advancements and mechanism studies have shown encouraging and promising results for the future of iron catalyzed cross coupling.

## 1.10 REFERENCES

- <sup>1</sup> Mako, T. L.; Byers, J. A. *Inorg. Chem. Front.* **2016**, *3*, 766.
- <sup>2</sup> Tamura, M.; Kochi, J. K. *J. Am. Chem. Soc.* **1971**, *93*, 1487.
- <sup>3</sup> (a) Tamao, K.; Sumitani, K.; Kumada, M. *J. Am. Chem. Soc.* **1972**, *94*, 4374. (b) Corriu, R. J. P.; Masse, J. P. *J. Am. Chem. Soc., Chem. Commu.* **1972**, 144.
- <sup>4</sup> Yamamura, M.; Moritano, I.; Murahashi, S.-I. *Organomet. Chem.* **1975**, *91*, C39.
- <sup>5</sup> Jana, R.; Pathak, T. P.; Sigman, M. S. *Chem. Rev.* **2011**, *111*, 1417.
- <sup>6</sup> Czaplik, W. M.; Mayer, M.; Cvengros, J.; von Wangelin, A. J. *ChemSusChem*. **2009**, *2*, 396.
- <sup>7</sup> Ishiyama, T.; Abe, S.; Miyaura, N.; Suzuki, A. *Chem. Lett.* **1992**, 691.
- <sup>8</sup> (a) Kambe, N.; Iwasaki, T.; Terao, J. *Chem. Soc. Rev.* **2011**, *40*, 4937. (b) Yang, Y.; Huang, X. *Synlett* **2008**, 1366.
- <sup>9</sup> (a) Netherton, M. R.; Dai, C.; Neuschuetz, K.; Fu, G. C. *J. Am. Chem. Soc.* **2001**, *123*, 10099. (b) Kirchhoff, J. H.; Dai, C.; Fu, G. C. *Angew. Chem. Int. Ed.* **2002**, *41*, 1945. (c) Netherton, M. R.; Fu, G. C. *Angew. Chem. Int. Ed.* **2002**, *41*, 3910.
- <sup>10</sup> Brenstrum, T.; Gerristma, D. A.; Adjabeng, G. M.; Frampton, C. S.; Britten, J.; Robertson, A. J.; McNulty, J.; Capretta, A. *J. Org. Chem.* **2004**, *69*, 7635.
- <sup>11</sup> Arentsen, K.; Caddick, S.; Cloke, F. G. N.; Herring, A. P.; Hitchcock, P. B. *Tetrahedron Lett.* **2004**, *45*, 3511.
- <sup>12</sup> Terao, J.; Yoshitaka, N.; Kuniyasu, H.; Kambe, N. *Chem. Commun.* **2007**, 825.
- <sup>13</sup> Terao, J.; Watanabe, H.; Ikumi, A.; Kuniyasu, H.; Kambe, N. *J. Am. Chem. Soc.* **2002**, *124*, 4222.
- <sup>14</sup> Terao, J.; Ikumi, A.; Kuniyasu, H.; Kambe, N. *J. Am. Chem. Soc.* **2003**, *125*, 5646.
- <sup>15</sup> (a) Chass, G. A.; Kantchev, E. A. B.; Fang, D.-C. *Chem. Commun.* **2010**, *46*, 2727. (b) Li, Z.; Jianh, Y.-Y.; Fu, Y. *Chem. Eur. J.* **2012**, *18*, 4345. (c) Iwasaki, T.; Tsumura, A.; Omori, T.; Kuniyasu, H.; Terao, J.; Kambe, N. *Chem. Lett.* **2011**, *40*, 1024.
- <sup>16</sup> Iwasaki, T.; Higashikawa, K.; Reddy, V. P.; Ho, W. W. S.; Fujimoto, Y.; Fukase, K.; Terao, J.; Kuniyasu, H.; Kambe, N. *Chem. Eur. J.* **2013**, *19*, 2956.
- <sup>17</sup> Di Franco, T.; Boutin, N.; Hu, X. *Synthesis* **2013**, *45*, 2949.
- <sup>18</sup> (a) Csok, Z.; Vechorkin, O.; Harkins, S. B.; Scopelliti, R.; Hu, X. L. *J. Am. Chem. Soc.* **2008**, *130*, 8156. (b) Vechorkin, O.; Csok, Z.; Scopelliti, R.; Hu, X. L. *Chem. Eur. J.* **2009**, *15*, 3889.
- <sup>19</sup> (a) Breitenfeld, J.; Ruiz, J.; Wodrich, M. D.; Hu, X. *J. Am. Chem. Soc.* **2013**, *135*, 12004. (b) Breitenfeld, J.; Hu, X. *CHIMIA* **2014**, *68*, 235.
- <sup>20</sup> Ren, P.; Vechorkin, O.; von Allmen, K.; Scopelliti, R.; Hu, X. *J. Am. Chem. Soc.* **2011**, *133*, 7084.
- <sup>21</sup> (a) Perez Garcia, P. M.; Di Franco, T.; Epenoy, A.; Scopelliti, R.; Hu, X. *J. ACS Catal.* **2016**, *6*, 258.
- <sup>22</sup> Lu, Z.; Wilsily, A.; Fu, G. C. *J. Am. Chem. Soc.* **2011**, *133*, 8154.
- <sup>23</sup> Taylor, B. L. H.; Jarvo, E. R. *J. Org. Chem.* **2011**, *76*, 7573.
- <sup>24</sup> Nagano, T.; Hayashi, T. *Org. Lett.* **2005**, *7*, 491.
- <sup>25</sup> Xu, X.; Cheng, D.; Pei, W. *J. Org. Chem.* **2006**, *71*, 6637.
- <sup>26</sup> (a) Jin, M.; Adak, L.; Nakamura, M. *J. Am. Chem. Soc.* **2015**, *137*, 7128. (b) Bauer, G.; Cheung, C. W.; Hu, X. *Synthesis* **2015**, 1726. (c) Chen, X.; Quan, Z.-J.; Wang, X.-C. *Appl. Organomet.* **2015**, *29*, 296. (d) Gärtner, D.; Stein, A. L.; Grupe, S.; Arp, J.; Jacobi von Wangelin, A. *Angew. Chem. Int. Ed.* **2015**, *54*, 10545.
- <sup>27</sup> Fürstner, A.; Leitner, A.; Méndez, M.; Krause, H.; *J. Am. Chem. Soc.* **2002**, *124*, 13856.
- <sup>28</sup> (a) Bolm, C.; Legros, J.; Le Paih, J.; Zani, L. *Chem. Rev.* **2004**, *104*, 6217. (b) Fürstner, A.; Martin, R. *Chem. Lett.* **2005**, *34*, 624. (c) Ito, S.; Nakamura, M. *Organomet. News* **2007**, *83*. (d) Czaplik, W. M.; Mayer, M.; Cvengros, J.; Jacobi von Wangelin, A. *ChemSusChem* **2009**, *2*, 396. (e) Czaplik, W. M.; Mayer, M.; Grupe, S.; Jacobi von Wangelin, A. *Pure Appl. Chem.* **2010**, *82*, 1545. (f) Knochel, P.; Thaler, T.; Diene, C. *Isr. J. Chem.* **2010**, *50*, 547. (g) Mesganaw, T.; Garg, N. K. *Org. Process Res. Dev.* **2013**, *17*, 29. (h) Nakamura, E.; Hatakeyama, T.; Ito, S.; Ishizuka, K.; Ilies, L.; Nakamura, M. *Org. React.* **2014**, *83*, 1. (i) Bedford, R. B.; Brenner, P. B. *Top. Organomet. Chem.* **2015**, *50*, 19. (j) Kuzmina, O. M.; Steib, A. K.; Moyeux, A.; Cahiez, G.; Knochel, P. *Synthesis* **2015**, 1696.
- <sup>29</sup> Sherry, B. D.; Fürstner, A. *Acc. Chem. Res.* **2008**, *41*, 1500.
- <sup>30</sup> Bedford, R. B. *Acc. Chem. Res.* **2015**, *48*, 1485.
- <sup>31</sup> Hedström, A.; Izakian, Z.; Vreto, I.; Wallentin, C.-J.; Norrby, P.-O. *Chem. - Eur. J.* **2015**, *21*, 5946.
- <sup>32</sup> (a) Talifer, M.; Xia, N.; Oualli, A. *Angew. Chem. Int. Ed.* **2007**, *46*, 934. (b) Wu, X.; Darcel, C. *Eur. J. Org. Chem.* **2009**, 5753. (c) Guo, D.; Huang, H.; Zhou, Y.; Xu, J.; Jian, H.; Chem, K.; Liu, H. *Green Chem.* **2010**, *12*, 276.
- <sup>33</sup> Thomé, I.; Nijs, A.; Bolm, C. *Chem. Soc. Rev.* **2012**, *41*, 979.
- <sup>34</sup> (a) Hatakeyama, T.; Nakamura, M. *J. Am. Chem. Soc.* **2007**, *129*, 9844. (b) Hatakeyama, T.; Hashimoto, S.; Ishizuka, K.; Nakamura, M. *J. Am. Chem. Soc.* **2009**, *131*, 11949.

- <sup>35</sup> Chua, Y.-Y.; Duong, H. A. *Chem. Commun.* **2014**, 50, 8424.
- <sup>36</sup> Agrawal, T.; Cook, S. P. *Org. Lett.* **2014**, 16, 5080.
- <sup>37</sup> Zhang, Y.; Liu, B.; Wu, H. Y.; Chen, W. Z. *Chin. Sci. Bull.* **2012**, 57, 2368.
- <sup>38</sup> Kuzmina, O. M.; Steib, A. K.; Flubacher, D.; Knochel, P. *Org. Lett.* **2012**, 14, 4818.
- <sup>39</sup> Kuzmina, O. M.; Steib, A. K.; Markiewicz, J. T.; Flubacher, D.; Knochel, P. *Angew. Chem. Int. Ed.* **2013**, 52, 4945.
- <sup>40</sup> Kuzmina, O. M.; Steib, A. K.; Fernandez, S.; Boudot, W.; Markiewicz, J. Y.; Knochel, P. *Chem. – Eur. J.* **2015**, 21, 8232.
- <sup>41</sup> Sova, M.; Frlan, R.; Gobec, S.; Stavber, G.; Časar, Z. *Appl. Organomet. Chem.* **2015**, 29, 528.
- <sup>42</sup> Shakhmaev, R. N.; Sunagatullina, A. S.; Zorin, V. V. *Russ. J. Org. Chem.* **2014**, 50, 322.
- <sup>43</sup> Czaplík, W. M.; Mayer, M.; Jacobi von Wangelin, A. *ChemCatChem* **2011**, 3, 135.
- <sup>44</sup> Kawamura, S.; Nakamura, M. *Chem. Lett.* **2013**, 42, 183.
- <sup>45</sup> Yamaguchi, Y.; Ando, H.; Nagaya, M.; Hinago, H.; Ito, I.; Asami, M. *Chem. Lett.* **2011**, 40, 983.
- <sup>46</sup> Denmark, S. E.; Cresswell, A. J. *J. Org. Chem.* **2013**, 78, 12593.
- <sup>47</sup> Bedford, R. B.; Brenner, P. B.; Carter, E.; Cogswell, P. M.; Haddow, M. F.; Harvey, J. N.; Murphy, D. M.; Nunn, J.; Woodall, C. H. *Angew. Chem. Int. Ed.* **2014**, 53, 1804.
- <sup>48</sup> Hatakeyama, T.; Fujiwara, Y.; Okada, Y.; Itoh, T.; Hashimoto, T.; Kawamura, S.; Ogata, K.; Takaya, H.; Nakamura, M. *Chem. Lett.* **2011**, 40, 1030.
- <sup>49</sup> Ghorai, S. K.; Jin, M.; Hatakeyama, T.; Nakamura, M. *Org. Lett.* **2012**, 14, 1066.
- <sup>50</sup> Mo, Z.; Zhang, Q.; Deng, L. *Organometallics*, **2012**, 31, 6518.
- <sup>51</sup> Sun, C.; Krause, H.; Fürstner, A. *Adv. Synth. Catal.* **2014**, 356, 1281.
- <sup>52</sup> Daifuku, A. L.; Al-Afyouni, M. H.; Snyder, B. E. R.; Kneebone, J. L.; Neidig, M. L. *J. Am. Chem. Soc.* **2014**, 136, 9132.
- <sup>53</sup> Parmar, D.; Henkel, L.; Dib, J.; Reuping, M. *Chem. Commun.* **2015**, 51, 2111.
- <sup>54</sup> Czaplík, W. M.; Mayer, M.; Grupe, S.; Jacobi von Wangelin, A. *Pure. Appl. Chem.* **2010**, 82, 1545.
- <sup>55</sup> Jin, M.; Adak, L.; Nakamura, M. *J. Am. Chem. Soc.* **2015**, 137, 7128.
- <sup>56</sup> Jin, M.; Nakamura, M. *J. Chem. Lett.* **2011**, 40, 1012.
- <sup>57</sup> Bauer, G.; Cheung, C. W.; Hu, X. *Synthesis*, **2015**, 1726.
- <sup>58</sup> Bauer, G.; Woodrich, M. D.; Scopelliti, R.; Hu, X. *Organometallics* **2015**, 34, 289.
- <sup>59</sup> Steib, A. K.; Thaler, T.; Komeyama, K.; Mayer, P.; Knochel, P. *Angew. Chem. Int. Ed.* **2011**, 50, 3303.
- <sup>60</sup> Sherry, B. D.; Fürstner, A. *Acc. Chem. Res.* **2008**, 41, 1500.
- <sup>61</sup> Perry, M. C.; Gillett, A. N.; Law, T. C. *Tetrahedron Lett.* **2012**, 53, 4436.
- <sup>62</sup> Agata, R.; Iwamoto, T.; Nakagawa, N.; Isozaki, T.; Hatakeyama, T.; Takaya, H.; Nakamura, M. *Synthesis* **2015**, 1733.
- <sup>63</sup> Guo, W.-J.; Wang, Z.-X. *Tetrahedron* **2013**, 69, 9580.
- <sup>64</sup> Chen, X.; Quan, Z.-J.; Wang, X.-C. *Appl. Organomet. Chem.* **2015**, 29, 296.
- <sup>65</sup> Cahiez, G.; Avedissian, H. *Synthesis* **1998**, 1199.
- <sup>66</sup> Silberstein, A. L.; Ramgren, S. D.; Garg, N. K. *Org. Lett.* **2012**, 14, 3796.
- <sup>67</sup> Agrawal, T.; Cook, S. P. *Org. Lett.* **2013**, 15, 96.
- <sup>68</sup> Güllak, S.; Geishoff, T. N.; Jacobi von Wangelin, A. *Adv. Synth. Catal.* **2013**, 355, 2197.
- <sup>69</sup> Malhotra, S.; Seng, P. S.; Koenig, G.; Deese, A. J.; Ford, K. A. *Org. Lett.* **2013**, 15, 3698.
- <sup>70</sup> Sun, C.-L.; Fürstner, A. *Angew. Chem. Int. Ed.* **2013**, 52, 13071.
- <sup>71</sup> Hishikado, H.; Nakatsuji, H.; Ueno, K.; Nagase, R.; Tanabe, Y. *Synlett* **2010**, 14, 2087.
- <sup>72</sup> Gärtner, D.; Stein, A. L.; Grupe, S.; Arp, J.; Jacobi von Wangelin, A. *Angew. Chem. Int. Ed.* **2015**, 10545.
- <sup>73</sup> Reprotoxic Category 2, R61, *Official Journal of the European Union*, December 31, 2008, European regulation No 1272/2008.
- <sup>74</sup> Cahiez, G.; Gager, O.; Buendia, J.; Patinote, C. *Chem. – Eur. J.* **2012**, 18, 5860.
- <sup>75</sup> Dongol, K. G.; Koh, H.; Sau, M.; Chai, C. L. L. *Adv. Synth. Catal.* **2007**, 349, 1015.
- <sup>76</sup> Guisán-Ceinos, M.; Tato, F.; Bruñuel, E.; Calle, P.; Cárdenas, D. J. *Chem. Sci.* **2013**, 4, 1098.
- <sup>77</sup> Gartia, Y.; Pulla, S.; Ramidi, P.; Farris, C. C.; Nima, Z.; Jones, D. E.; Biris, A. S.; Ghosh, A. *Catal. Lett.* **2012**, 142, 1397.
- <sup>78</sup> Hatakeyama, T.; Okada, Y.; Yoshimoto, Y.; Nakamura, M. *Angew. Chem. Int. Ed.* **2011**, 50, 10973.
- <sup>79</sup> Cheung, C. W.; Ren, P.; Hu, X. *Org. Lett.* **2014**, 16, 2566.
- <sup>80</sup> Nuemann, S. M.; Kochi, J. K. *J. Org. Chem.* **1975**, 40, 599.
- <sup>81</sup> Smith, R. S.; Kochi, J. K. *J. Org. Chem.* **1976**, 41, 502.
- <sup>82</sup> Al-Afyouni, M. H.; Fillman, K. L.; Brennessel, W. W.; Neidig, M. L. *J. Am. Chem. Soc.* **2014**, 136, 15457.
- <sup>83</sup> (a) Fürstner, A.; Leitner, A.; Méndez, M.; Krause, H. *J. Am. Chem. Soc.* **2002**, 124, 13856. (b) Fürstner, A.; Leitner, A. *Angew. Chem. Int. Ed.* **2002**, 41, 609.
- <sup>84</sup> (a) Aleandri, L. E.; Bogdanović, B.; Bons, P.; Durr, C.; Gaidies, A.; Hartwig, T.; Hockett, S. C.; Legarden, M.; Wilczok, U.; Brand, R.A. *Chem. Mater.* **1995**, 7, 1153. (b) Bogdanović, B.; Schwickardi, M. *Angew. Chem. Int. Ed.* **2000**, 39, 4610.
- <sup>85</sup> Sherry, B. D.; Fürstner, A. *Acc. Chem. Res.* **2008**, 41, 1500.

- <sup>86</sup> Jonas, K.; Schieferstein, L.; Krüger, C.; Tsay, Y.-H. *Angew. Chem. Int. Ed.* **1979**, *18*, 550.
- <sup>87</sup> Martin, R.; Fürstner, A. *Angew. Chem. Int. Ed.* **2004**, *43*, 3955.
- <sup>88</sup> Fürstner, A.; Martin, R.; Krause H.; Seidel, G.; Goddard R.; Lehmann, C. W. *J. Am. Chem. Soc.* **2008**, *130*, 8773.
- <sup>89</sup> Fürstner, A.; Krause, H.; Lehmann, C. W. *Angew. Chem. Int. Ed.* **2006**, *45*, 440.
- <sup>90</sup> Bedford, R. B. *Acc. Chem. Res.* **2015**, *48*, 1485.
- <sup>91</sup> Weber, K.; Schnöckelborg, E.-M.; Wolf, R. *ChemCatChem* **2011**, *3*, 1572.
- <sup>92</sup> Schoch, R.; Besens, W.; Werner, T.; Bauer, M. *Chem. –Eur. J.* **2013**, *19*, 15816.
- <sup>93</sup> Kleimark, J.; Hedström, A.; Larsson, P.-F.; Johansson, C.; Norrby, P.-O. *ChemCatChem* **2009**, *1*, 152.
- <sup>94</sup> Przojski, J. A.; Veggeberg, K. P.; Arman, H. D.; Tonzetich, Z. J. *ACS Catal.* **2015**, *5*, 5938.
- <sup>95</sup> Adams, C. J.; Bedford, R. B.; Carter, E.; Gower, N. J.; Haddow, M. F.; Harvey, J. N.; Huwe, M.; Cartes, M. A.; Mansell, S. M.; Mendoza, C.; Murphy, D. M.; Neeve, E. C.; Nunn, J. *J. Am. Chem. Soc.* **2012**, *134*, 10333.
- <sup>96</sup> Bedford, R. B.; Carter, E.; Cogswell, P. M.; Gower, N. J.; Haddow, M. E.; Harvey, J. N.; Murphy, D. M.; Neeve, E. C.; Nunn, J. *Angew. Chem. Int. Ed.* **2013**, *52*, 1285.
- <sup>97</sup> Bedford, R. B.; Brenner, P. B.; Carter, E.; Carvell, T. W.; Cogswell, P. M.; Gallagher, T.; Harvey, J. N.; Murphy, D. M.; Neeve, E. C.; Nunn, J.; Pye, D. R. *Chem. – Eur. J.* **2014**, *20*, 7935.
- <sup>98</sup> Hatakeyama, T.; Hashimoto, T.; Kondo, Y.; Fujiwara, Y.; Seike, H.; Takaya, H.; Tamada, Y.; Ono, T.; Nakamura, M. *J. Am. Chem. Soc.* **2010**, *132*, 10674.
- <sup>99</sup> Daifuku, S. L.; Kneebone, J. L.; Snyder, B. E. R.; Neidig, M. L. *J. Am. Chem. Soc.* **2015**, *137*, 11432.
- <sup>100</sup> Cahiez, G.; Habiak, V.; Duplais, C.; Moyeux, A. *Angew. Chem. Int. Ed.* **2007**, *46*, 4364.
- <sup>101</sup> Kneebone, J. L.; Brennessel, W. W.; Neidig, M. L. *J. Am. Chem. Soc.* **2017**, *139*, 6988.
- <sup>102</sup> Kneebone, J. L.; Fleischauer, V. E.; Daifuku, S. L.; Shaps, A. A.; Bailey, J. M.; Iannuzzi, T. E.; Neidig, M. L. *Inorg. Chem* **2016**, *55*, 272-282.
- <sup>103</sup> Bedford, R. B.; Huwe, M.; Wilkinson, M. C. *Chem. Commun.* **2009**, 600.
- <sup>104</sup> Hashimoto, T.; Hatakeyama, T.; Nakamura, M. *J. Org. Chem.* **2012**, *77*, 1168.
- <sup>105</sup> Nakagawa, N.; Hatakeyama, T.; Nakamura, M. *Chem. Lett.* **2015**, *44*, 486.
- <sup>106</sup> Hatakeyama, T.; Hashimoto, T.; Kathriarachchi, K. K. A. D. S.; Zenmyo, T.; Seike, H.; Nakamura, M. *Angew. Chem. Int. Ed.* **2012**, *51*, 8834.
- <sup>107</sup> Bedford, R. B.; Brenner, P. B.; Carter, E.; Clifton, J.; Cogswell, P. M.; Gower, N. J.; Haddow, M. F.; Harvey, J. N.; Kehl, J. A.; Murphy, D. M.; Neeve, E. C.; Neidig, M. L.; Nunn, J.; Snyder, B. E. R.; Taylor, J. *Organometallics* **2014**, *33*, 5767.
- <sup>108</sup> Bedford, R. B.; Gallagher, T.; Pye, D. R.; Savage, W. *Synthesis* **2015**, 1761.
- <sup>109</sup> Dunsford, J. J.; Cade, I. A.; Fillman, K. L.; Neidig, M. L.; Ingleson, M. J. *Organometallics* **2014**, *33*, 370.
- <sup>110</sup> Dunsford, J. J.; Clark, E. R.; Ingleson, M. J. *Dalton Trans.* **2015**, *44*, 20577.
- <sup>111</sup> Hatakeyama, T.; Nakagawa, N.; Nakamura, M. *Org. Lett.* **2009**, *11*, 4496.
- <sup>112</sup> Lin, X.; Zheng, F.; Qing, F.-L. *Organometallics* **2012**, *31*, 1578.
- <sup>113</sup> Loska, R.; Volla, C. M. R.; Vogel, P. *Adv. Synth. Catal.* **2008**, *350*, 2859.
- <sup>114</sup> Hajjipour, A. R.; Azizi, G. *Green Chem.* **2013**, *15*, 1030.
- <sup>115</sup> Yashuda, S.; Yorimitsu, H.; Oshima, K. *Organometallics* **2010**, *29*, 2634.
- <sup>116</sup> Waldhart, G. W.; Mankad, N. P. *J. Org. Chem.* **2015**, *793*, 171.
- <sup>117</sup> Carril, M.; Correa, A.; Bolm, C. *Angew. Chem. Int. Ed.* **2008**, *47*, 4862.
- <sup>118</sup> Hung, T.; Huang, C.; Tsai, F. *ChemCatChem* **2012**, *4*, 540.
- <sup>119</sup> Yang, J.; Shen, G.; Chen, D. *Synth. Commun.* **2013**, *43*, 837.
- <sup>120</sup> Kawamura, S.; Ishizuka, K.; Takaya, H.; Nakamura, M. *Chem. Commun.* **2010**, *46*, 6054.
- <sup>121</sup> Kawamura, S.; Kawabata, T.; Ishizuka, K.; Nakamura, M. *Chem. Commun.* **2012**, *48*, 9376.
- <sup>122</sup> Benischke, A. D.; Breuillac, A. J. A.; Moyeux, A.; Caheiz, G.; Knochel. *Synlett* **2016**, *27*, 471.
- <sup>123</sup> Castatgnolo, D.; Botta, M. *Eur. J. Org. Chem.* **2010**, 3224.
- <sup>124</sup> Liu, K. M.; Wei, J.; Duan, X. F. *Chem. Commun.* **2015**, *51*, 4655.
- <sup>125</sup> Hatakeyama, T.; Imayoshi, R.; Yoshimoto, Y.; Ghorai, S. K.; Jin, M.; Takaya, H.; Norisuye, K.; Sohrin, Y.; Nakamura, M. *J. Am. Chem. Soc.* **2012**, *134*, 20262.
- <sup>126</sup> Lin, Y.-Y.; Wang, Y.-J.; Lin, C.-H.; Cheng, J.-H.; Lee, C.-F. *J. Org. Chem.* **2012**, *77*, 6100.
- <sup>127</sup> Hu, W.; Zhang, S. *J. Org. Chem.* **2015**, *80*, 6128.

## 2.0 CROSS COUPLING APPLICATIONS OF PYRIDYL(DIIMINE) IRON COMPLEXES

### 2.1 INTRODUCTION

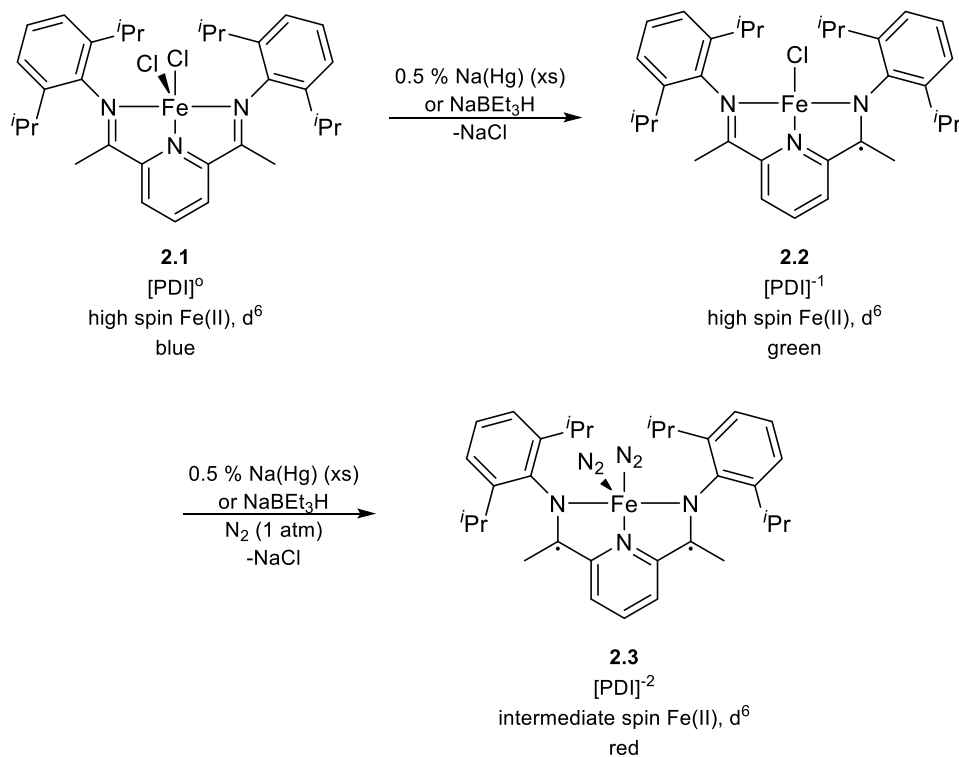
#### 2.1.1 Iron PDI Complexes

Despite the progress that has been made with iron catalyzed cross coupling in recent years (see **Chapter 1**), alkyl-alkyl cross coupling procedures are still rare. It is the goal of the research described herein to develop a system that readily facilitates this reactivity and to conduct mechanistic investigations that may lead to rational system design and further advancements in the field.

Although much work done with iron systems utilized simple iron salts as catalysts, many aforementioned studies have shown that ligation is important for imparting selectivity and promoting reactivity (see **Chapter 1.5.6**).<sup>1,2</sup> Pyridyl diamine (PDI) ligands, developed by the groups of Brookhart<sup>3</sup> and Gibson<sup>4</sup>, are attractive alternatives to facilitate iron systems due to the tunability of the ligands and versatility of the complexes (discussed further in **Chapter 3**).<sup>5</sup> Originally developed for olefin polymerization, it was found that in most cases, linear high molecular weight polymer was produced, indicating that the  $\beta$ -hydride elimination events leading to termination are reversible.<sup>4</sup> Iron-catalyzed alkyl-alkyl cross coupling systems could benefit from this characteristic if the detrimental  $\beta$ -hydride elimination side products undergo reinsertion to continue the catalytic cycle.

Low oxidation state species bearing PDI ligation have exhibited interesting redox properties.<sup>6</sup> Paul Chirik and coworkers discovered that when iron(II) complex **2.1** is reduced in the presence of sodium-mercury amalgam or sodium triethylborohydride in a nitrogen atmosphere,

species **2.2** is formed (**Scheme 2.1**). The reduction occurs on the ligand rather than on the iron center, the latter remaining in the iron(II) oxidation state. This redox relationship was corroborated by techniques including X-ray crystal structure analysis, Mössbauer spectroscopy, and calculations.<sup>7,8,9</sup> Upon reduction of **2.2** under the same conditions produces **2.3**, in which both of the imine arms of the PDI ligand have been reduced.<sup>6</sup> Again, the oxidation state of the metal center remains unchanged.

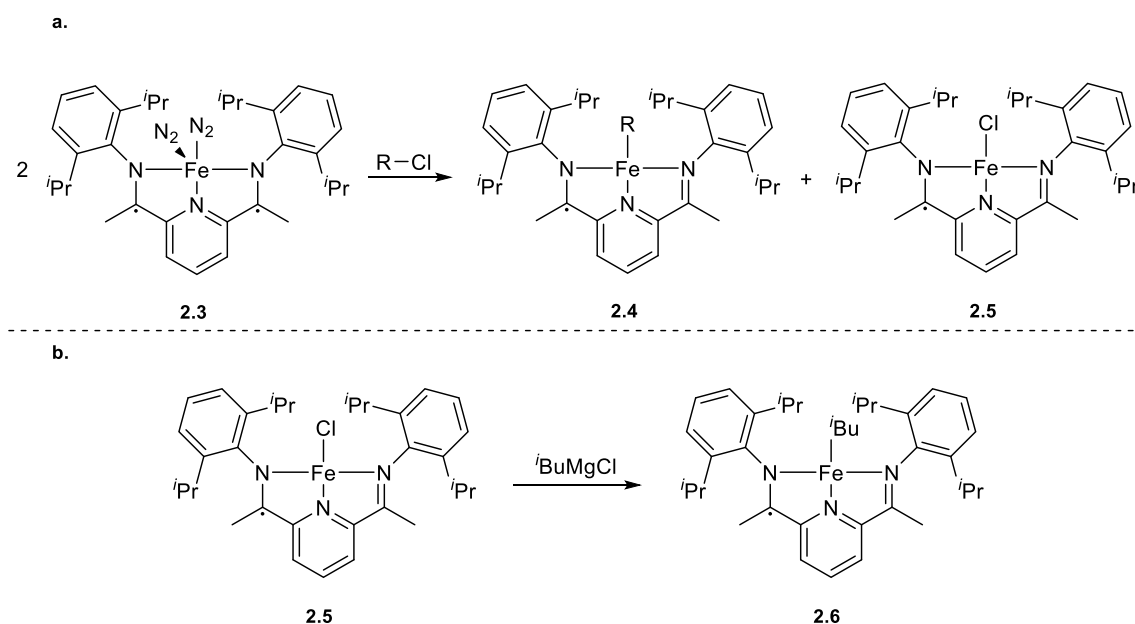


**Scheme 2.1.** The reduction of **2.1** to form high spin iron(II) complex **2.2** bearing a singly reduced ligand, and the reduction of **2.2** to form an intermediate spin iron(II) complex, **2.3**, bearing a doubly reduced PDI ligand.<sup>6</sup>

Redox-active ligands can be useful for catalytic applications such as cross coupling because the oxidation state of the metal center is maintained.<sup>10</sup> This would prevent the formation of low formal oxidation state complexes, such as [Ar<sub>3</sub>Fe]<sup>-</sup>,<sup>11</sup> which has been shown to lead to undesired biaryl side products. Furthermore, the formation of iron(0) is avoided, which could form insoluble aggregates and has been shown to be inactive for some cross coupling applications.<sup>12</sup>

Another benefit to catalytic applications is that PDI ligands have been shown to promote reversible transfer of one to three electrons between the ligand and metal center.<sup>7</sup>

The Chirik group undertook mechanistic studies which indicate how an iron PDI complex might behave in a Kumada-type system, although no cross-coupling applications have been pursued by the group. As shown in **Scheme 2.2a**, upon the treatment of PDI complex **2.3** with an alkyl chloride, a bimetallic oxidative addition occurs to form species **2.4** and **2.5**, both iron(II) species with a singly reduced ligand.<sup>9</sup> **2.5** was then treated with *isobutylmagnesium chloride* and transmetalation generated species **2.6** (**Scheme 2.2b**).<sup>13</sup>



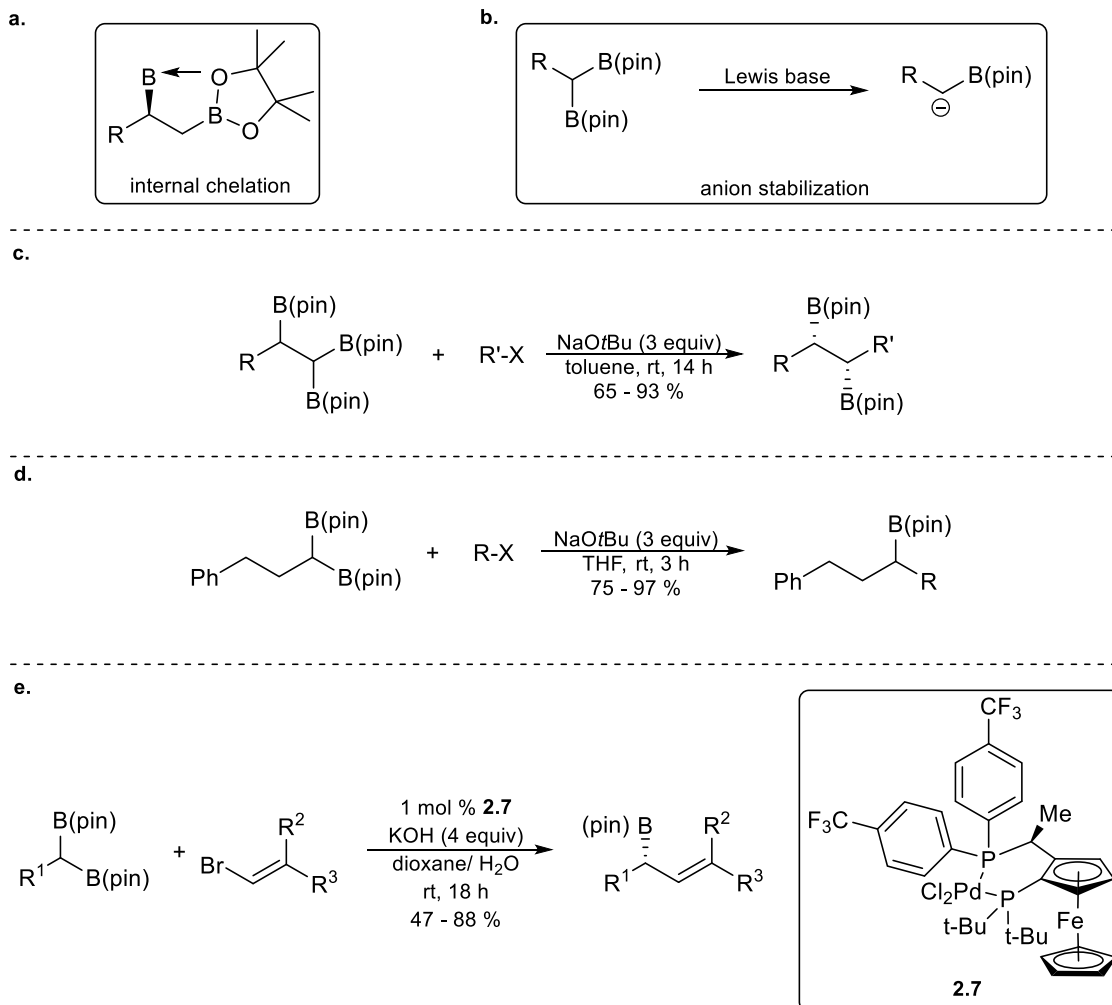
**Scheme 2.2.** (a) Treatment of **2.3** with an alkyl chloride to form **2.4** and **2.5** from a bimetallic oxidative addition.<sup>9</sup> (b) Transmetalation of **2.5** with *iso*-butylmagnesium chloride to form **2.6**.<sup>13</sup>

### 2.1.2 Bis(Boronate)s as Suzuki-Miyaura Coupling Partners

A final goal of this research is to develop a milder version of iron catalyzed Suzuki-type cross coupling that does not involve the use of highly activate borate species and pyrophoric reagents such as *t*-butyl lithium (**Chapter 1.6**).<sup>14</sup> Careful catalyst selection and a thorough

understanding of the key transmetalation step of iron-based Suzuki-type coupling reactions could aid in the development of these systems.

Multi-boronate species have been shown by the Morken group to be promising coupling partners in palladium-catalyzed and metal-free coupling reactions.<sup>15</sup> Internal chelation that occurs in 1,2-bis(boronate)s and 1,1,2-tris(boronate)s enhances the Lewis acidity of the substrate (**Scheme 2.3a**), and has led to efficient base mediated cross coupling applications with stereocontrol promoted by the internal chelation (**Scheme 2.3c**).<sup>16</sup> The treatment of 1,1-bis(boronate)s with a Lewis base generates very reactive  $\alpha$ -boryl carbanions (**Scheme 2.3b**), which are proficient for metal-free cross coupling applications.<sup>17</sup> 1,1-bis(boronate)s have been coupled with primary and secondary alkyl halides in the presence of sodium *t*-butoxide (**Scheme 2.3d**).<sup>18</sup> Additionally, 1,1-bis(boronate)s have also undergone cross coupling with vinyl bromides catalyzed by **2.7** and other palladium species (**Scheme 2.3e**).<sup>19</sup> Thus, these substrates seem promising for the development of more mild variations of iron catalyzed Suzuki cross coupling.



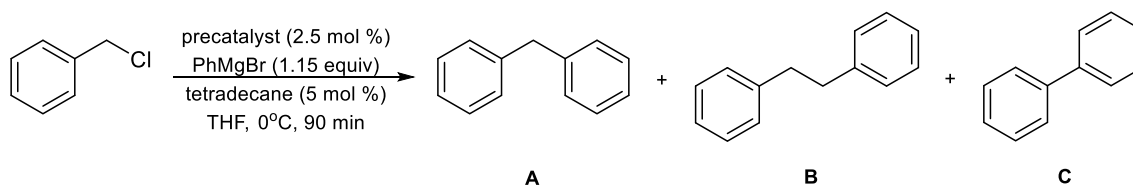
**Scheme 2.3.** a) The inherent internal chelation of 1,2-bis(boronate)s.<sup>16</sup> b) The anion stabilization that occurs upon deborylation of 1,1-bis(boronate)s.<sup>17</sup> c) The coupling of 1,1,2-tris(boronate)s with alkyl halides in the presence of sodium *t*-butoxide.<sup>16</sup> d) The coupling of 1,1-bis(boronate)s with alkyl halides in the presence of sodium *t*-butoxide.<sup>18</sup> e) The coupling of 1,1-bis(boronate)s with vinyl bromides in the presence of catalytic amounts of **2.7**.<sup>17,19</sup>

## 2.2 KUMADA – TYPE COUPLING REACTIONS

### 2.2.1 Benzyl Halide – Aryl Grignard Reagent

Initial studies of iron(II) PDI complexes for Kumada-type cross coupling applications probed the catalytic activity of the system for the coupling of benzyl chloride and phenylmagnesium bromide. These studies were conducted to determine if PDI ligation would decrease the amount of detrimental homocoupling of both substrates that is common for aryl-benzyl coupling reactions catalyzed by iron (see **Chapter 1.4.3**).

A variety of (PDI)FeCl<sub>2</sub> complexes were probed for catalytic activity. Benzyl chloride and 2.5 mol % of the precatalyst were combined in a reaction vessel under inert conditions, along with 5 mol % of tetradecane as an internal standard, and THF (**Scheme 2.4**). 1.15 equivalents of phenylmagnesium bromide were then added, and, after 90 minutes, a mixture of products was generated. Desired product, diphenylmethane, **A**, was formed, along with homocouple products of benzyl chloride and phenylmagnesium bromide, **B** and **C**, respectively, and toluene, which is formed from the dehalogenation of the electrophile.



**Scheme 2.4.** The coupling of benzyl chloride and phenylmagnesium bromide in the presence of catalytic amounts of a precatalyst, with tetradecane as an internal standard.

A screen of the ligands depicted in **Figure 2.1**, under the reaction conditions shown in **Scheme 2.4**, was conducted. It was found that (<sup>2,6-*i*Pr</sup>PhPDI)FeCl<sub>2</sub>, **2.1**, facilitated the reaction at a higher rate than the other complexes, reaching 100 % conversion of benzyl chloride in 30 minutes (**Graph 2.1**, *grey line*). (<sup>2,6-Me</sup>PhPDI)FeCl<sub>2</sub>, **2.8** (*red line*), had the next highest rate, reaching >95 % conversion in 120 minutes. Interestingly, (CyPDI)FeCl<sub>2</sub>, **2.9** (*blue line*), and (<sup>4-F</sup>PhPDI)FeCl<sub>2</sub>, **2.10**

(green line), proceeded at similar rates to iron dichloride (purple line). When no catalyst was used, only trace conversion of benzyl chloride was seen (yellow line).

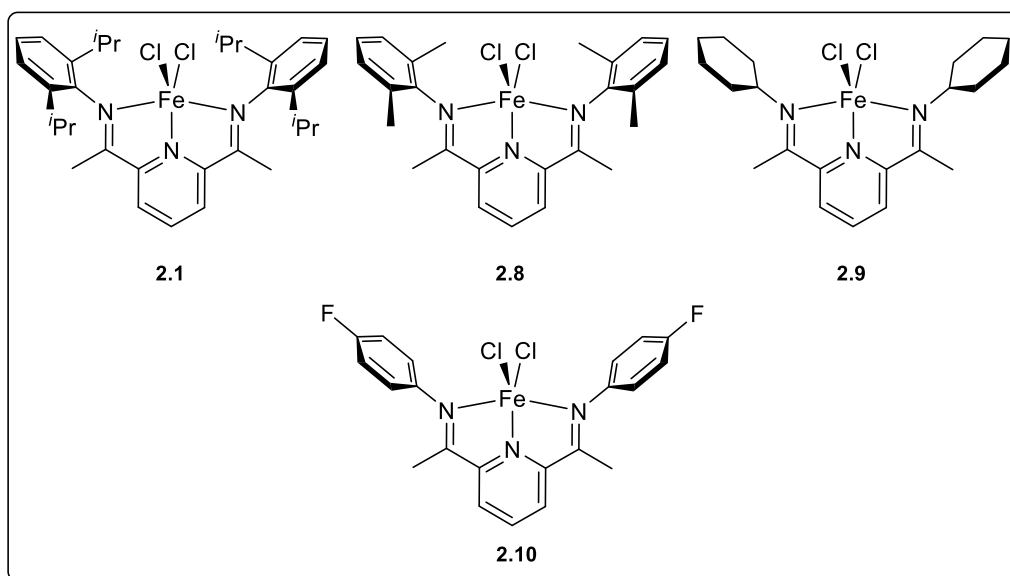
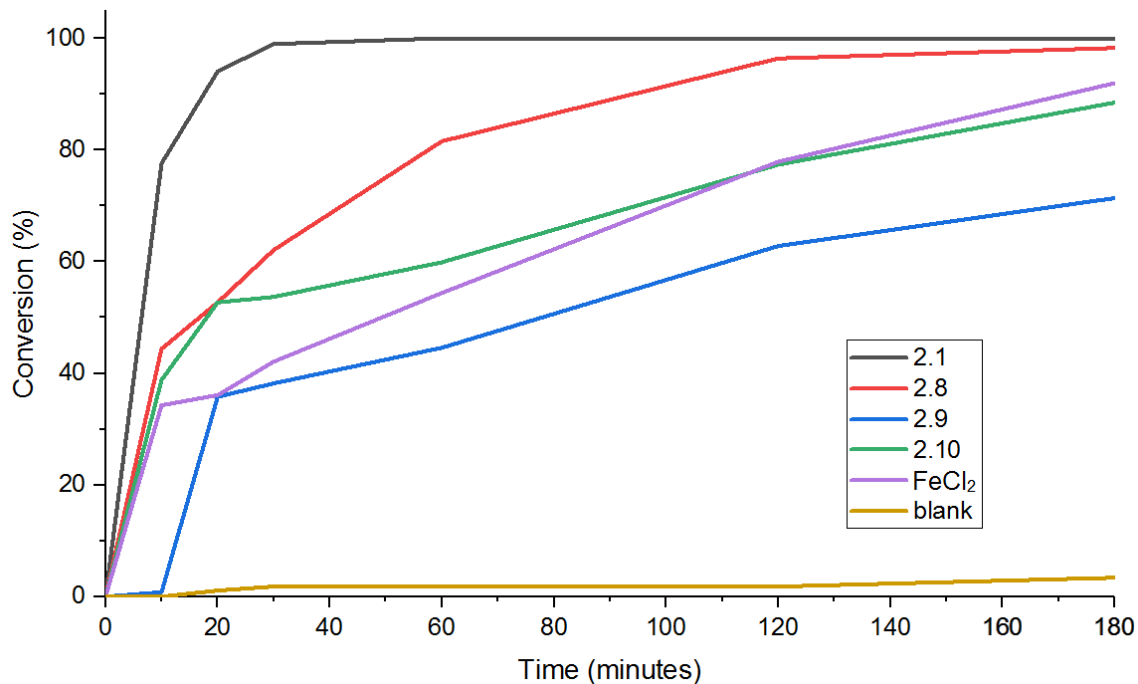


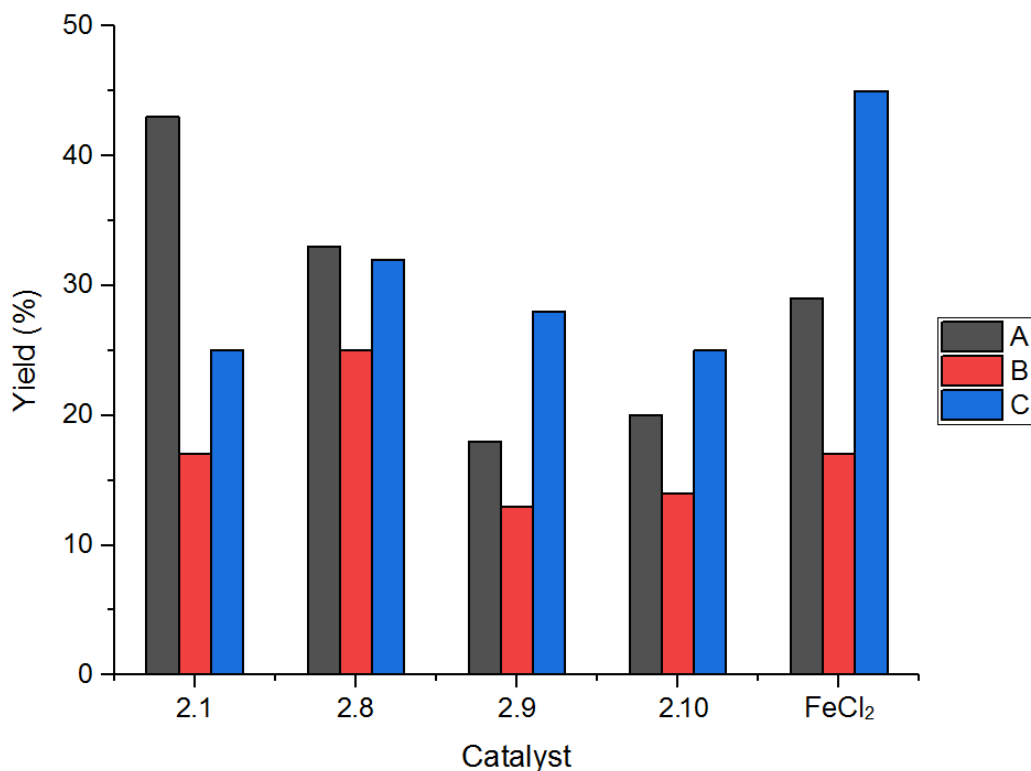
Figure 2.1. Iron(II) PDI complexes employed in the coupling of benzyl chloride and phenylmagnesium bromide.



Graph 2.1. Ligand screen – conversion of benzyl chloride (%) vs time (min). All conversions were determined by gas chromatography.

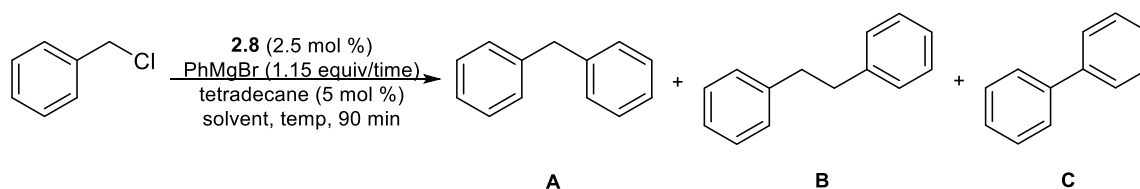
The same set of reactions was analyzed for percent yields of each of the products (**Graph 2.2**), as determined by GC calibration curves. In all cases, less than 45 % of the desired product was observed. The use of **2.1** resulted in 43 % of desired product, **A** (*grey bar*) and 17 % and 25 % of the homocoupled products **B** (*red bar*) and **C** (*blue bar*), respectively. Catalysis by **2.8** led to a decreased yield of **A**, 33 %, and increased amounts of **B**, 25 %, and **C**, 32 %. For **2.9** and **2.10** catalyzed reactions, 20 % or less of **A** was seen. The use of iron dichloride led to the greatest yield of biphenyl, **C**, at 45 % yield.

While the mass balances associated with these yields are low (e.g. complex **2.1**: 0.77 mmol total product per 1.0 mmol benzyl chloride; 0.93 mmol total product per 1.15 mmol phenylmagnesium bromide), it is important to note that toluene, an observed byproduct generated by benzyl chloride, was identified, yet quantification by GC was difficult due to overlap with the solvent region. Benzene is also a likely byproduct, formed when quenching the reaction, and thus any unreacted Grignard reagent, with acid. Therefore, the discrepancies in mass balance have been attributed to these two products.



**Graph 2.2 Ligand screen – comparison of the yields of products A (grey), B (red), and C (blue). All yields were determined by gas chromatography.**

Further optimizations of the cross coupling of benzyl chloride with phenyl magnesium bromide were conducted. As shown in **Table 2.1**, studies were done varying temperature, solvent, and the addition time of the Grignard reagent. By adding phenylmagnesium bromide over 15 minutes rather than all at once, in the presence of catalyst **2.8**, the yield of **A** increased from 33 % to 44 % (entries 1 and 2). When conducting the experiment in methyl *t*-butyl ether (MTBE) rather than THF, an increase to 52 % was seen (entry 3). Finally, as shown by entry 5, a decrease of the reaction temperature to – 10 °C led to a boost in the yield of **A** to 74 %. Unfortunately, this yield is lower than the state of the art chemistry,<sup>20</sup> and the homocoupling of the substrates is not adequately hindered.

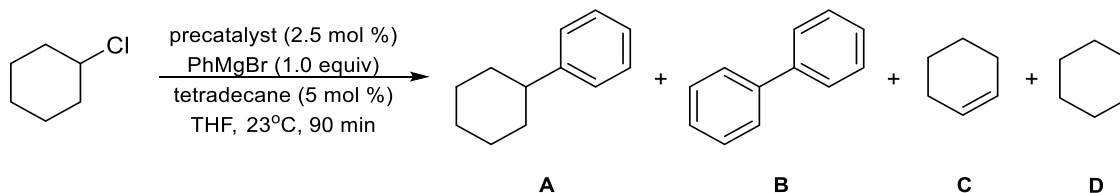


Entry	Add <sup>n</sup> Time	Solvent	Temp (°C)	Conv (%)	% Yield (GC)		
					<b>A</b>	<b>B</b>	<b>C</b>
1	0 min	THF	0	100	33	25	32
2	15 min	THF	0	100	44	27	27
3	15 min	MTBE	0	100	52	18	19
4	60 min	MTBE	0	58	14.5	10	20
5	15 min	MTBE	-10	100	74	25	27

**Table 2.1. Continued optimization of the cross coupling of benzyl chloride with phenyl magnesium bromide in the presence of catalytic amounts of 2.8. All yields were determined by gas chromatography.**

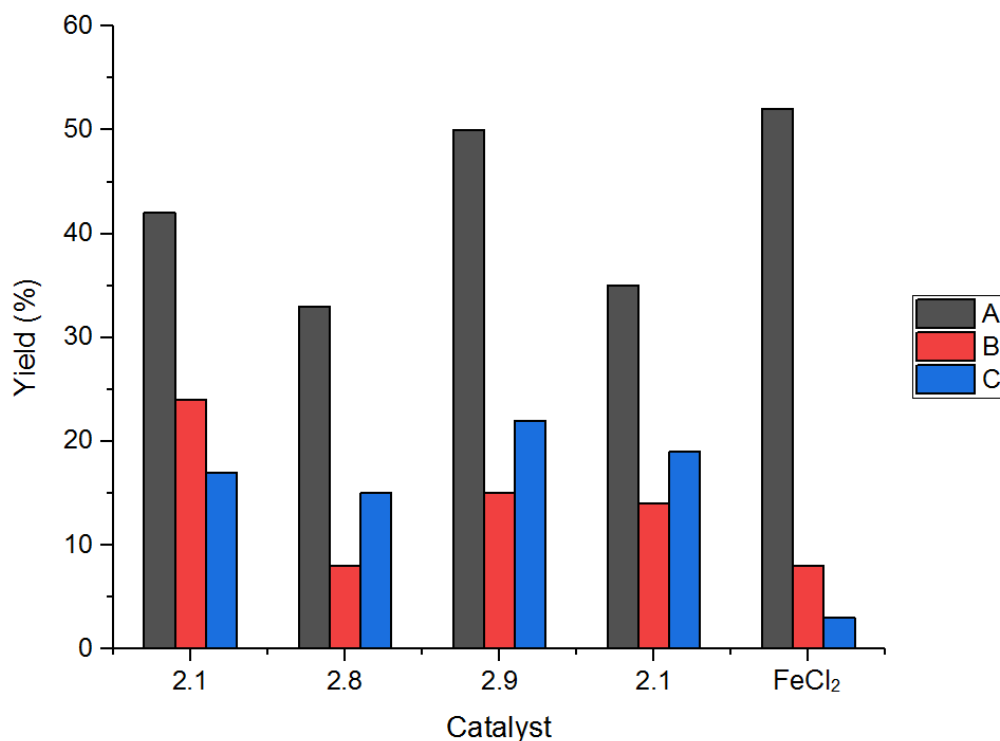
### 2.2.2 Alkyl Halide – Aryl Grignard Reagent Optimization

As with the previous system, the initial experiments probing the coupling of cyclohexyl chloride with phenylmagnesium bromide screened various iron(II) PDI complexes (**Scheme 2.5**). The coupling of these two substrates resulted in the formation of cyclohexyl benzene (**A**), biphenyl (**B**), cyclohexene (**C**), and cyclohexane (**D**). In some cases, like with benzene and toluene, **C** and **D** were difficult to quantify by GC, yet when able, their data are reported herein. Another important note is that homocoupling of cyclohexyl chloride is not observed for the reactions discussed in this section.



**Scheme 2.5. The cross coupling of cyclohexyl chloride with phenylmagnesium bromide to form cyclohexyl benzene (A), biphenyl (B), cyclohexene (C), and cyclohexane (D).**

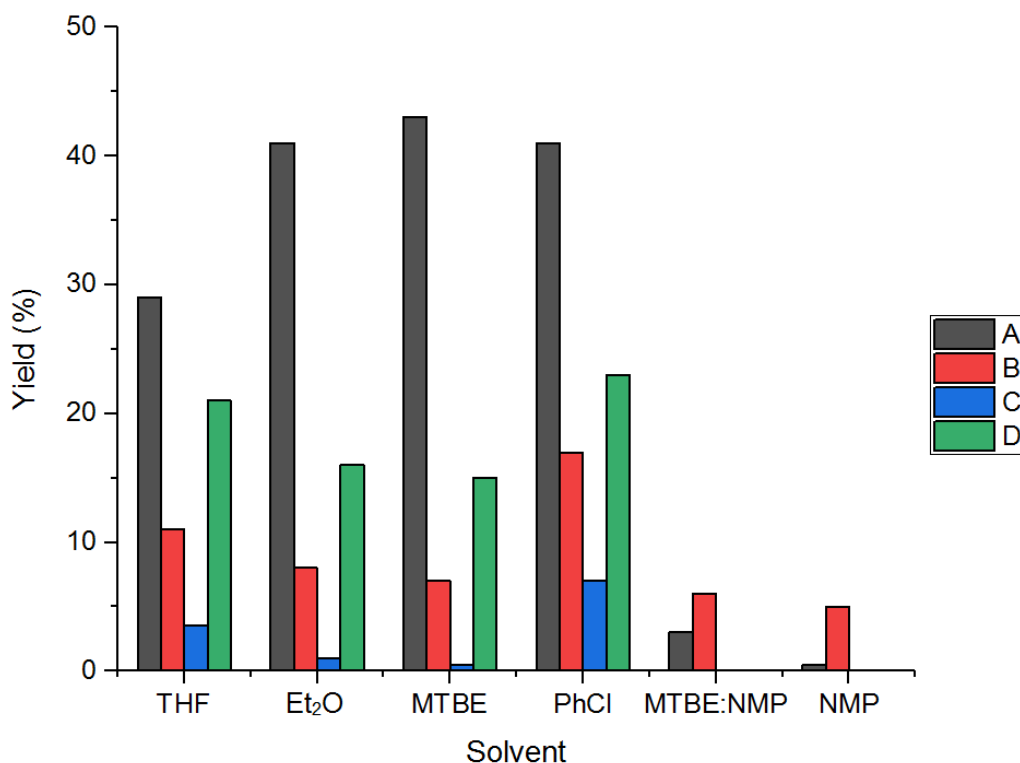
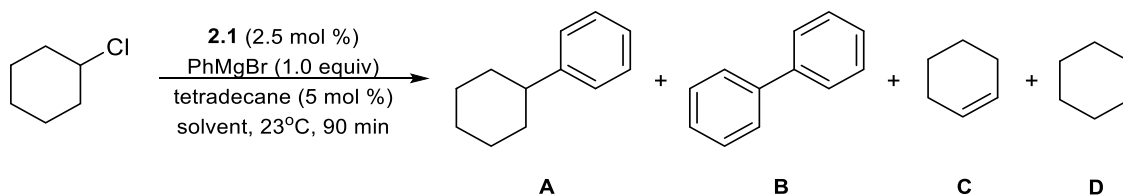
In all instances, cyclohexyl chloride had fully converted, and desired product **A** was the main species present in the reaction mixture (**Graph 2.3**). Unfortunately, under these conditions, iron dichloride provided the greatest amount of **A** (52 %), however, **2.9** was comparable (50 % **A**). **2.1** was the next most active, forming 42 % **A**, and further studies were conducted with this complex due to the difficulty in synthesis of the ligand of **2.9**.



**Graph 2.3. Ligand screen – comparison of the yields of products A (grey), B (red), and C (blue). All yields were determined by gas chromatography.**

While the aforementioned results were not favorable for the PDI ligand, optimization of the system was continued, in the hopes that increase the productivity of iron(II) PDI complexes could be increased and the efficacy of iron dichloride could be stymied. Thus, a solvent screen was conducted for the reaction of cyclohexyl chloride and phenylmagnesium bromide in the presence of complex **2.1**. As shown by **Graph 2.4**, using diethyl ether or MTBE rather than THF led to an increase in yield of desired product by more than 10 %. Chlorobenzene also led to an increased yield of **A**, yet more of side product **B** was formed than with any other solvent. It has been shown

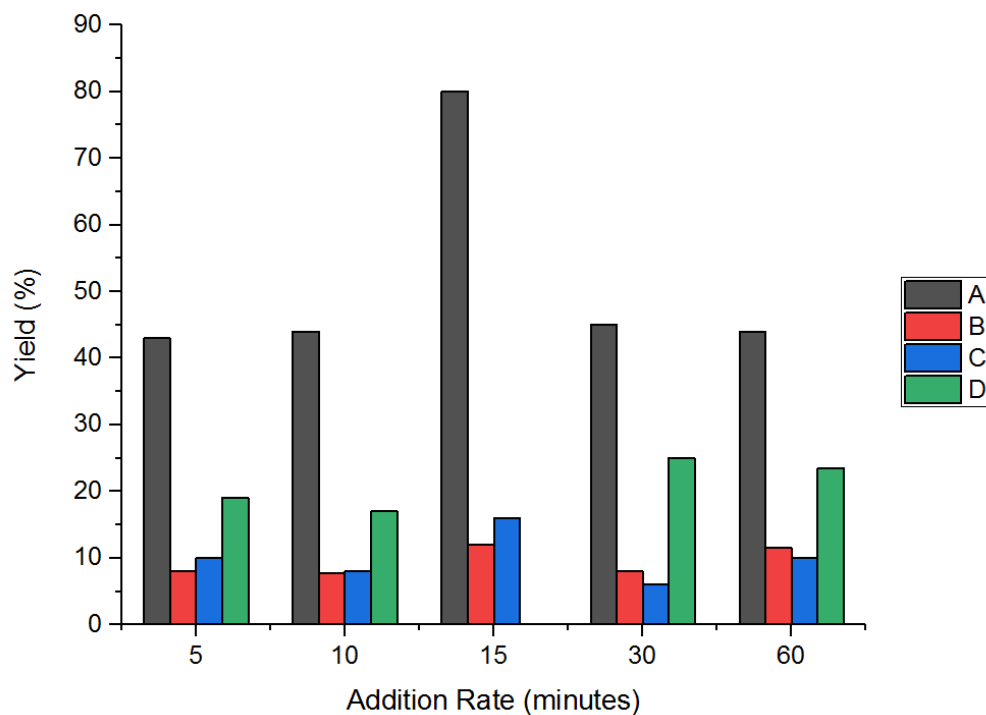
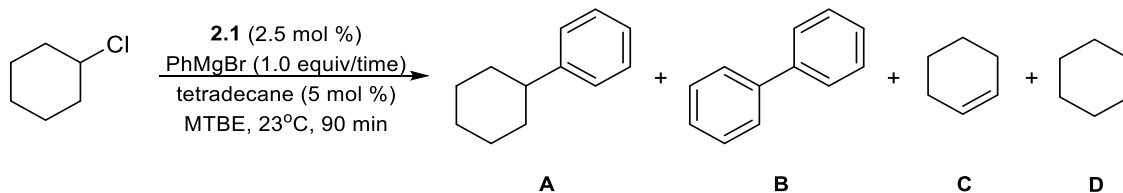
by various groups that the addition of *N*-methylpyrrolidinone (NMP) to an iron catalyzed Kumada-type system will increase the desired yield (see **Chapter 1**),<sup>21</sup> yet in this case, the addition of NMP shut down the reaction, leading to only trace amounts of **A**. Often when NMP is used, it is with a ligand-less system. It was hypothesized that, in this case, the NMP strongly coordinates to the metal center, preventing the iron center from interacting with either of the substrates.



**Graph 2.4. Solvent screen – comparison of the yields of products A (grey), B (red), C (blue), and D (green). All yields were determined by gas chromatography.**

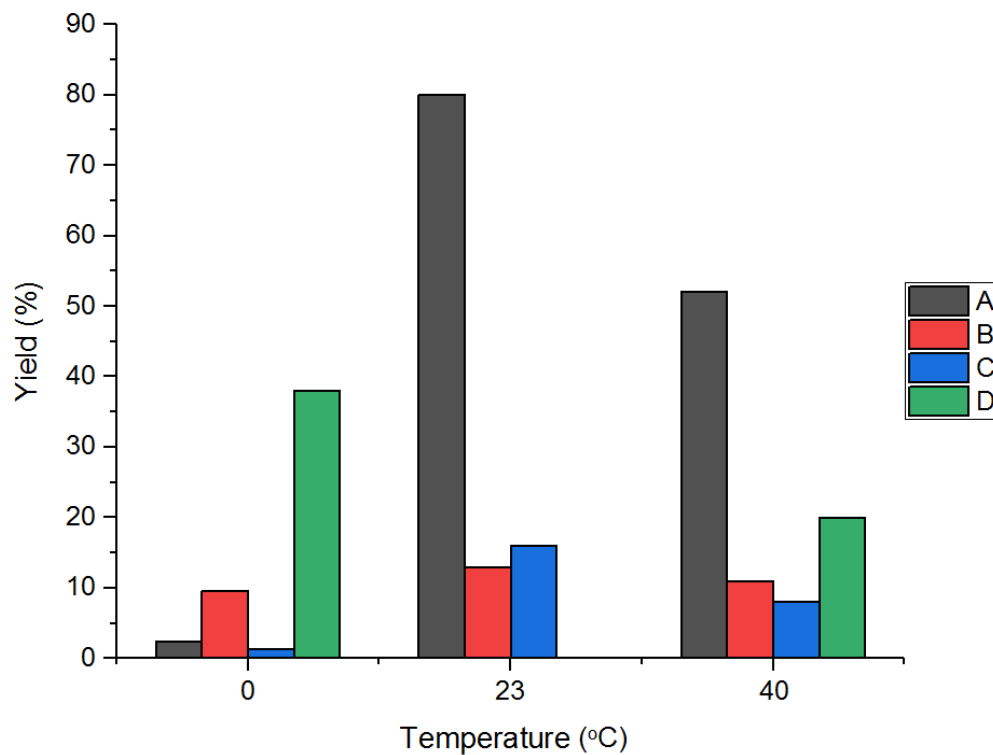
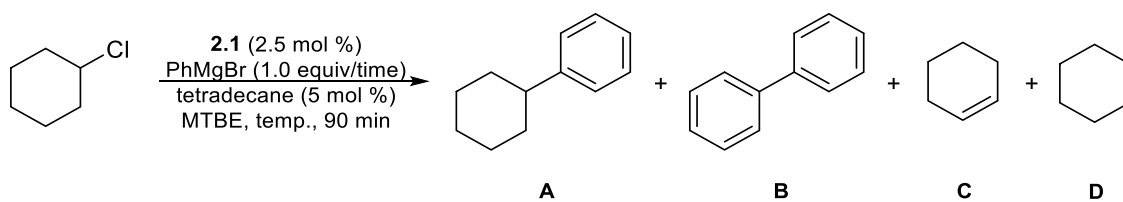
Next, the rate that the Grignard reagent was added to the reaction was varied, as this has been shown to increase yields in previous studies (see **Chapter 1**).<sup>22</sup> Indeed, adding

phenylmagnesium bromide over a 15-minute time period greatly increased the yield of **A** to 80 % (**Graph 2.5**). All other addition times, 5-, 10-, 30-, and 60-minute, led to yields less than 50 %.



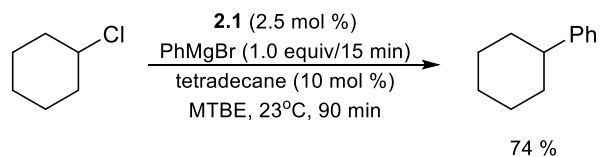
**Graph 2.5. Screen of Grignard addition rates – comparison of the yields of products A (grey), B (red), C (blue), and D (green). All yields were determined by gas chromatography.**

Finally, the temperature of this reaction was screened, and it was found that room temperature, 23 °C, was the optimal temperature (**Graph 2.6**). At 0 °C, only trace amounts of desired product were observed; and at 40 °C, 53 % **A** was formed.



**Graph 2.6. Temperature screen – comparison of the yields of products A (blue), B (orange), C (grey), and D (yellow). All yields were determined by gas chromatography.**

Thus, the optimal conditions shown in **Scheme 2.6** were obtained. Upon column chromatography of the product mixture, the desired product was isolated in a 74 % yield.



**Scheme 2.6. Optimized conditions and isolated yield of cyclohexyl benzene.**

### 2.2.3 Mechanistic Studies

Brief mechanistic studies were carried out on this system. Another ongoing project in the Byers group involved examining the effect of PDI ligand lability on catalytic systems using complexes **2.11**<sup>23</sup> and **2.12**<sup>24</sup> (Figure 2.2). **2.11**, a bidentate version of the PDI ligand, represents an iron(II) PDI complex in which an imine ligand has dissociated to open up a coordination site during catalysis. Conversely, **2.12** is a rigidly tridentate ligand that does not allow for ligand lability.

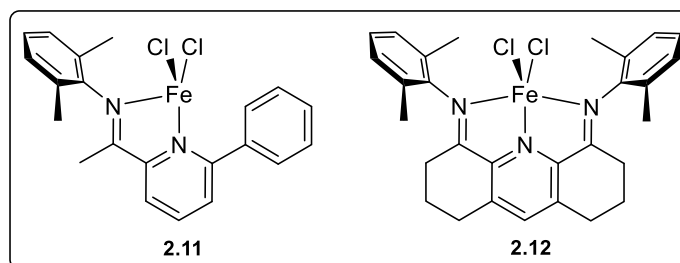
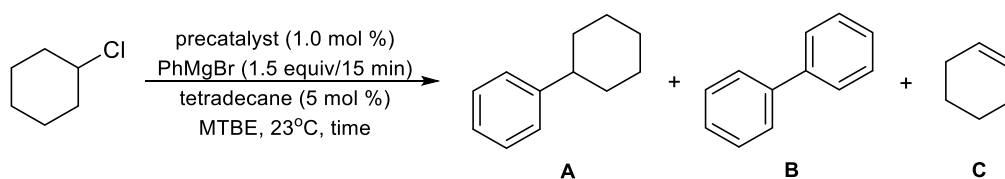


**Figure 2.2. Bidentate complex 2.11 and rigidly tridentate complex 2.12, employed for ligand lability studies.**

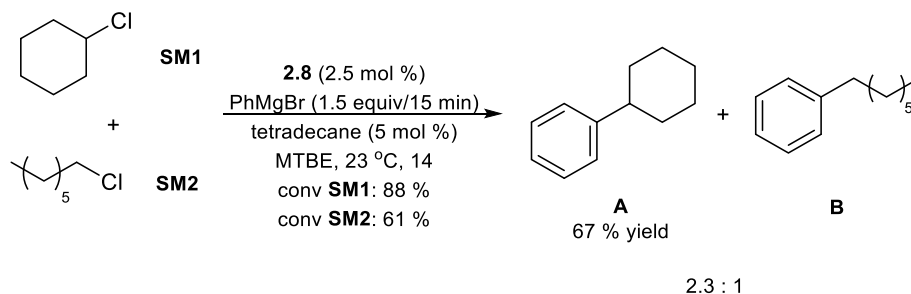
As shown in **Table 2.2**, when using **2.11**, 70 % of desired product **A** is formed under the optimized catalytic conditions after 3 hours. This is much more comparable to the results from **2.8** than when **2.12** is used, as this results in 71 % of **A** only after 18 hours. It seems that the existence of an open coordination site on the iron center facilitates the desired reaction at a faster rate. This rate is similar to what is seen with **2.8**, and thus it is likely that ligand lability plays a role in the catalytic cycle.



Entry	precatalyst	Time (h)	% conv.	Yield <b>A</b> (%)	Yield <b>C</b> (%)
1	<b>2.8</b>	1.5	100	81	13
2	<b>2.11</b>	3	100	70	15
3	<b>2.12</b>	18	96	71	15

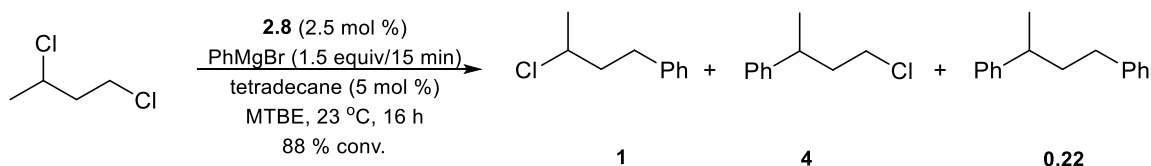
**Table 2.2. Comparison of bidentate and rigidly tridentate iron PDI analogues to determine lability of the pyridyl diimine ligand during catalysis. All yields were determined by gas chromatography.**

Both intermolecular and intramolecular comparisons of primary and secondary alkyl chlorides were conducted. In both instances, phenyl magnesium bromide was the limiting reagent as compared to C-Cl bonds, in order to prevent sites from reaching full conversion. Intermolecularly, cyclohexyl chloride, **SM1**, and octyl chloride, **SM2**, were combined in a reaction vessel under the optimal conditions, with 1.5 equivalents of Grignard reagent (**Scheme 2.7**). After 14 hours, **SM1** had reached 88 % conversion, and had generated 67 % of desired product **A**, whereas **SM2** had converted 61 %. A GC calibration curve was not calculated for desired product **B**, but a 2.3:1 ratio of **A**:**B** was observed, indicating that cyclic secondary alkyl chlorides have a higher reaction rate under these conditions than primary alkyl chlorides.



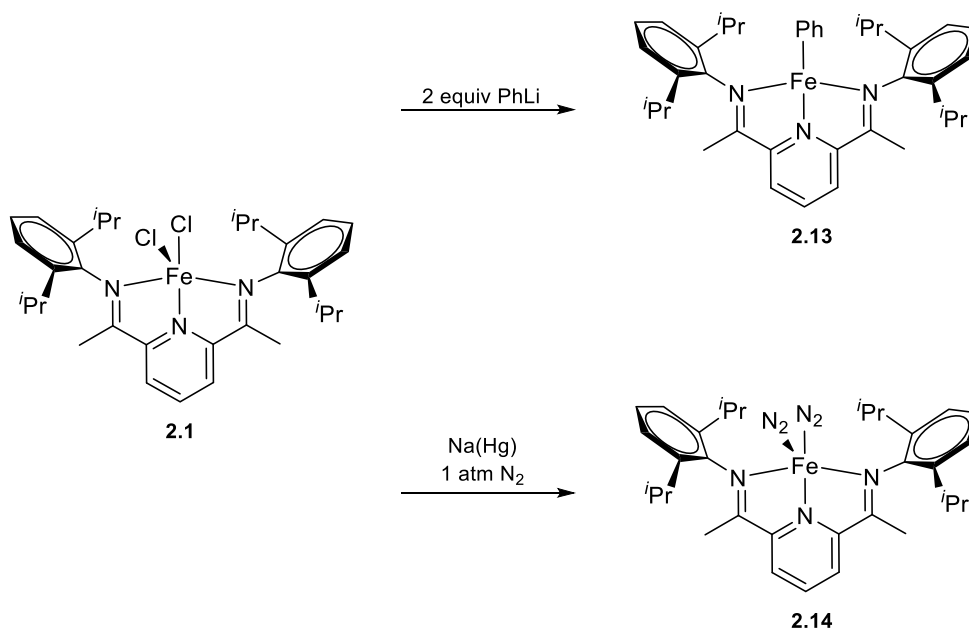
**Scheme 2.7. Intermolecular competition experiment between secondary and primary alkyl chlorides. All conversions and yields were determined by gas chromatography.**

Intramolecularly, 1,3-dichlorobutane was subjected to the same reaction conditions. A 4:1 ratio of 2° coupling to 1° coupling was observed, showing that acyclic secondary alkyl chlorides react more preferentially than primary alkyl halides (**Scheme 2.8**). A small amount of doubly arylated product was also observed.



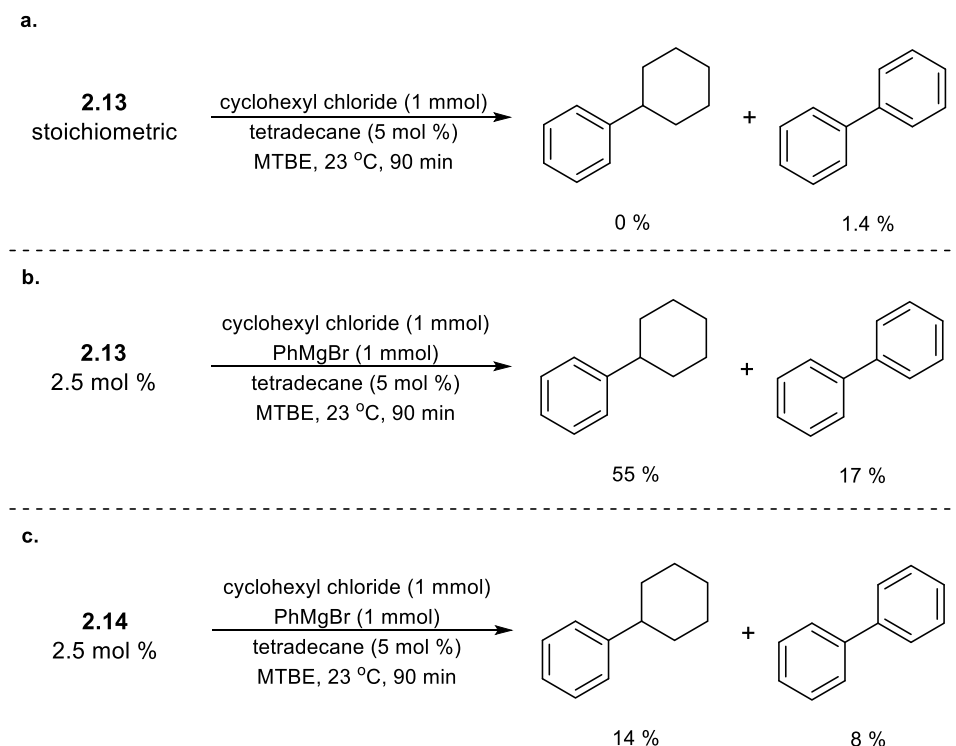
**Scheme 2.8.** Intramolecular competition experiment between secondary and primary alkyl halides. Product ratios were determined by gas chromatography.

Some additional mechanistic studies were carried out by group member Jessica Drake. Iron(II) complex **2.1** was reduced to iron(I) complex  $(^{2,6}\text{-MePhPDI})\text{FePh}$ , **2.13**, and iron(0) species  $(^{2,6}\text{-MePhPDI})\text{FeN}_2$ , **2.14**, following conditions demonstrated by Chirik and coworkers (*vide supra*),<sup>6</sup> as shown in **Scheme 2.9**.



**Scheme 2.9.** Synthesis of reduced iron species **2.13** and **2.14** by Jessica Drake following methods reported by Chirik.<sup>6</sup>

These complexes were subsequently used in stoichiometric and catalytic reactions to determine the catalytic competency of both species. A stoichiometric amount of **2.13** was combined with one equivalent of cyclohexyl chloride in MTBE, producing only trace amounts of biphenyl and no conversion of the electrophile (**Scheme 2.10a**). **2.13** was then used as a catalyst under the optimal reaction conditions, producing 55 % of the desired cyclohexyl benzene, and 17 % biphenyl (**Scheme 2.10b**). **2.14** was subjected to the same reaction conditions, forming cyclohexyl benzene and biphenyl in 14 and 8 % yields, respectively (**Scheme 2.10c**). It is clear from these studies that both **2.13** and **2.14** are off-cycle species, because there are less catalytically competent than **2.1**.

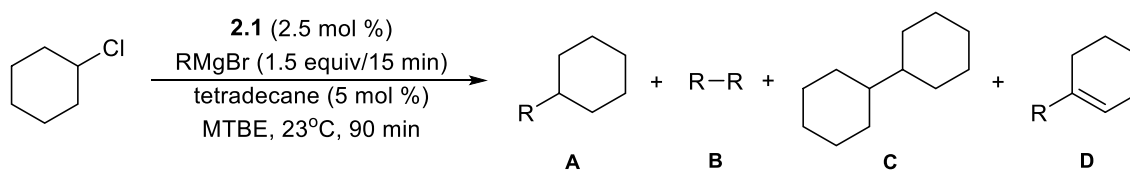


**Scheme 2.10. Stoichiometric and catalytic reactions of 2.13 and 2.14, carried out by Jessica Drake.**

## 2.2.4 Grignard Reagent Scope

A brief screening of Grignard reagents revealed that the system is applicable to both electron rich and electron poor arylmagnesium bromides (**Table 2.3**). *p*-Fluorophenylmagnesium

bromide led to a conversion of 65 % in 90 minutes, indicating a decreased reaction rate, yet produced the desired product in a 4.2:1 ratio of **A** to **B** (entry 2). *p*-Methoxyphenylmagnesium bromide gave the same product distribution, but reached 100 % conversion (entry 3). High conversions of the substrate were seen when using alkyl Grignard reagents, yet with 2-ethylhexylmagnesium bromide and octylmagnesium bromide, more electrophile homocouple product, **C**, was produced than **A** (entry 4 and 5, respectively), which did not occur when aryl Grignard reagents were used. This reaction was not found to be general for other C(sp<sup>2</sup>) Grignard reagents (entry 6), nor applicable for C(sp) nucleophiles (entry 7). When alkyl Grignard reagents were employed, the large majority of the observed products were attributed to reductions and β-hydride eliminations of both electrophile and nucleophile (**Table 2.3**).



Entry	R	Conv. SM	<b>A</b> : <b>B</b> : <b>C</b>	<b>A</b> : Reduction/β-H elim	<b>A</b> : <b>D</b>
1	Phenyl	100 %	6.2 : 1 : 0	-	-
2	<i>p</i> -fluorophenyl	65 %	4.2 : 1 : 0	-	-
3	<i>p</i> -methoxyphenyl	100 %	4.2 : 1 : 0	-	-
4*	2-ethylhexyl	90 %	1 : 0 : 1.2	1 : 12	1 : 2
5*	octyl	92 %	1 : 1 : 3	1 : 28	1 : 1
6	cyclohexyl	71 %	N/A	1 : 11	2 : 1
7	Vinyl	0 %	-	-	-
8	Alkynyl	0 %	-	-	-

**Table 2.3. Grignard reagent screen – the coupling of cyclohexyl chloride with RMgBr in the presence of catalytic amounts of 2.1. All conversions and ratios were determined by gas chromatography. \*1.0 equivalents of Grignard reagent were used.**

What is striking about the results of the alkyl-alkyl coupling, is that multiple isomers of the products of β-hydride elimination were observed. In the case of octylmagnesium bromide, standard

samples of octene isomers were compared to those seen in the GC trace, and the identities of the isomers were assigned (**Figure 2.3**). 1-Octene was the most prevalent, with *trans*- and *cis*-2-octene formed in a significant amount. Trace quantities of 3-octene and 4-octene were observed. This suggests the ability of the catalyst to promote chain walking *via* reinsertion of the product of  $\beta$ -hydride elimination. It was initially hoped that this ability, previously described by Brookhart and Gibson<sup>3,4</sup>, would allow for the productive reinsertion of such products toward formation of desired product, however, in this instance, it seems to be detrimental.

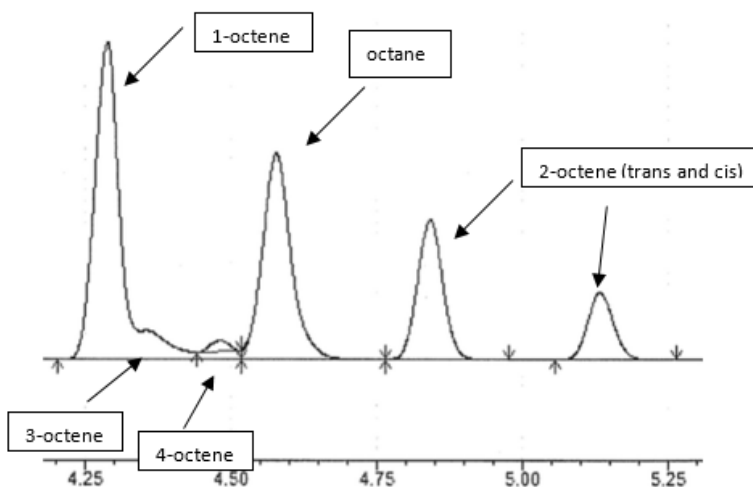


**Figure 2.3.** The GC distribution of octene isomers observed from the coupling of cyclohexyl chloride and octylmagnesium bromide in the presence of catalytic amounts of **2.1**.

Also notable is the formation of a species that was determined to be the desired product with one degree of unsaturation, **D** (**Table 2.3**). As shown in **Figure 2.4**, five **D** isomers, identified by GC/MS, were formed upon the reaction of cyclohexyl chloride and octylmagnesium bromide in the presence of **2.1**. A 1:1 ratio of **A** to the summed peaks of **D** was observed. The formation of **D** suggests that a species may be formed that undergoes  $\beta$ -hydride elimination to release this product.

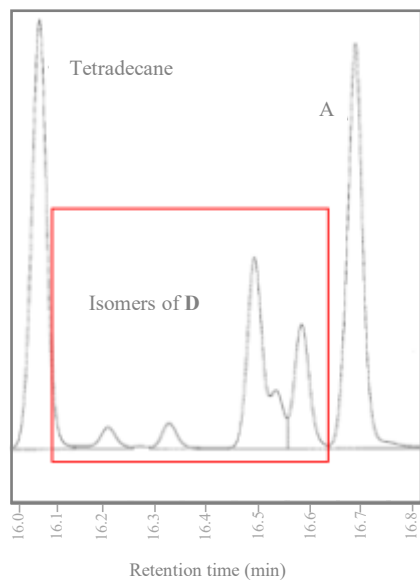
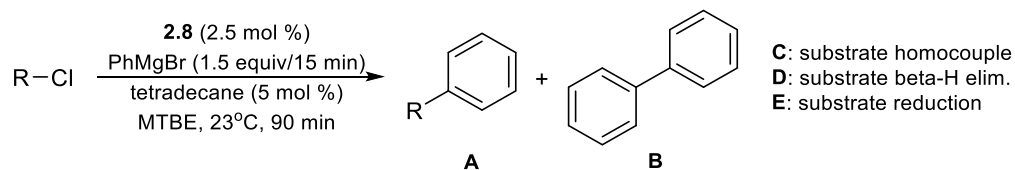


**Figure 2.4.** The GC distribution of **D** isomers observed from the coupling of cyclohexyl chloride and octylmagnesium bromide in the presence of catalytic amounts of **2.1**. The peaks were identified by GC/MS.

### 2.2.5 Alkyl Halide Scope

With optimal conditions in hand, the scope of the alkyl halide was examined. Aside from the desired product **A**, biphenyl, **B**, and the homocouple product of the substrate, **C**, were formed, along with compounds that are attributed to  $\beta$ -hydride elimination of an iron-alkyl species, **D**, and the reduction of the substrate, **E** (**Scheme 2.11**).



**Scheme 2.11.** Products formed from the coupling of an alkyl chloride with phenyl magnesium bromide under the optimized conditions.

Upon conducting a substrate scope, it was found that electrophiles other than cyclohexyl chloride perform poorly under the optimized reaction conditions (**Scheme 2.6**). Other cyclic

secondary alkyl chlorides, cyclooctyl chloride (entry 2) and 2-chloropentane (entry 6) produced 5 % and 30 % desired product, respectively, as estimated by GC comparison with the internal standard, tetradecane (**Table 2.4**). For cyclooctyl chloride, the majority of the product was cyclooctane, resulting from  $\beta$ -hydride elimination of the *in situ* generated iron-alkyl species. The major product seen in the GC trace for the coupling of 2-chloropentane was the desired product, yet **D** and **E** formation would have been concealed by the solvent region of the trace. As aforementioned, benzyl chloride (entry 4) coupled at -10 °C to form the desired product in 74 % yield by calibration curve, yet similar substrate 1,1-diphenylmethane (entry 5) led to an estimated 20 % of **A** under the same conditions, with the major of product being 1,1-diphenylmethane homocouple. The tertiary alkyl halides shown in entries 7 – 10, while fully converted, generated no desired product. (2-chloropropan-2-yl) benzene (entry 7) formed **C** and oligomers, while (2-chloropropan-2-yl) cyclohexane (entry 8) and 2-chloro-2-methylhexane (entry 9) both selectively generated **D** and **E**. With *t*-butyl chloride (entry 10) no product was seen, likely because the formation of **D** and **E** formed was obscured by the solvent region of the GC trace. Tertiary substrate 1-chloroadamantane (entry 11) was shown to form 57 % of desired product, with 100 % of the converted substrate transforming into **A**. Unfortunately, the same results were observed when using iron dichloride as the catalyst (entry 12).

Entry	Substrate	Time	Conv. (%)	Desired PDT	Est. Yield	Major PDT
1		1 h	100		81 %	<b>A</b>
2		1 h	100		5 %	<b>D</b>
3		2 h	93		13 %	<b>C</b>
4*		1 h	95		74 %	<b>A</b>
5*		18 h	100		20 %	<b>C</b>
6		16 h	100		30 %	<b>A</b>
7		16 h	100		0	<b>C, olig</b>
8		16 h	98		0	<b>D, E</b>
9		16 h	100		0	<b>D, E</b>
10		16 h	0		0	n/a
11		16 h	57		57 %	<b>A</b>
12		16 h	54		54 %	<b>A</b>

**Table 2.4. Scope of alkyl halide electrophile under optimized conditions. All conversions and yields were determined by gas chromatography as compared to tetradecane.**

\*Conducted at -10 °C.

As shown in **Chapter 2.2.2**, a similar compound, chlorobenzene, could be used as a solvent without the production of a large amount of biphenyl, which could be formed from the homocoupling of phenylmagnesium bromide or the cross coupling of chlorobenzene with the Grignard reagent. Indeed, it was found that attempting to use chlorobenzene as a substrate resulted in no conversion. Intriguingly, 2-chloronaphthalene did react to form the desired product in a small amount, as well as both nucleophile and electrophile homocoupled products.

### **2.2.6 Cyclooctyl Chloride Optimization**

As mentioned previously, the conditions optimized for cyclohexyl chloride were not general. Thus, optimization for the coupling of cyclooctyl bromide, a more challenging substrate, was attempted. Members of the Byers group, in collaboration with Nathan Szymczak from the University of Michigan, were attempting to use complexes **2.15** and **2.16**, previously developed for olefin hydroboration,<sup>25</sup> for the polymerization of ethylene (**Figure 2.5**). Additionally, PDI iron bis-alkoxide species **2.17** and **2.18** are complexes commonly used in the Byers group for the polymerization of lactide and epoxides.<sup>26</sup> Easy access to these complexes allowed for their use in cyclooctyl bromide optimization attempts.

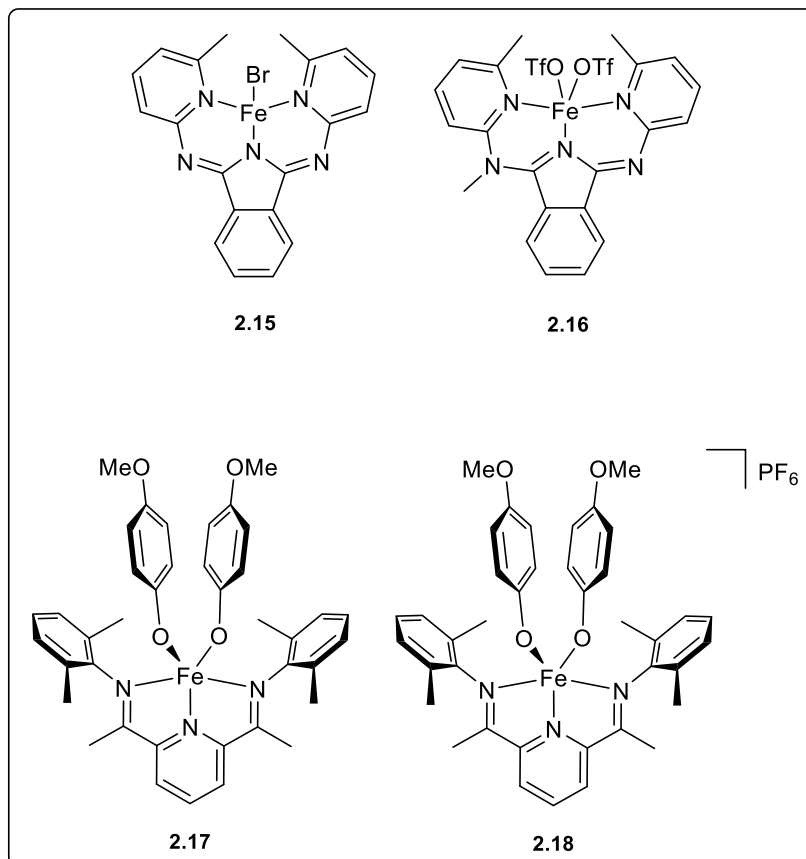
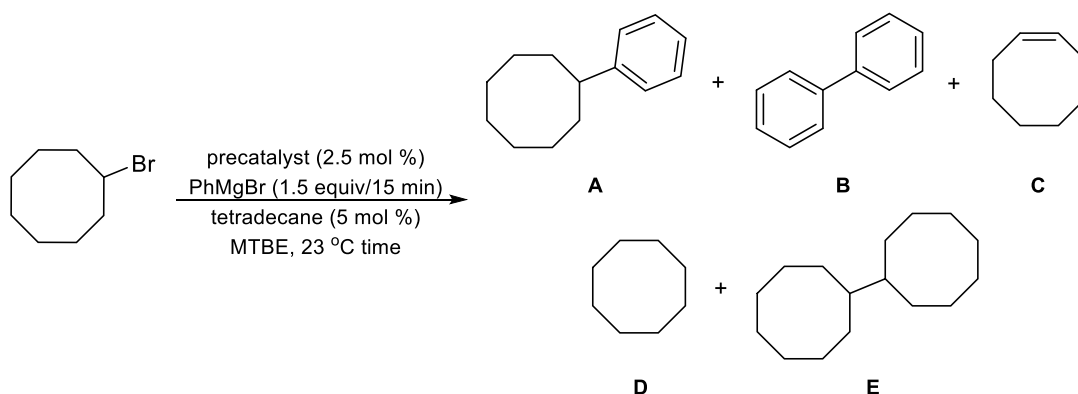


**Figure 2.5. Iron complexes 2.15 and 2.16, developed by Nathan Szymczak and coworkers,<sup>25</sup> and complexes 2.17 and 2.18, developed by Ashley Biernesser in the Byers group.<sup>26</sup>**

The coupling of cyclooctyl bromide and phenylmagnesium bromide led to five distinct products (**Scheme 2.12**). Desired product, **A**, and biphenyl, **B**, were produced, along with cyclooctene, **C**, and cyclooctane, **D**. Interestingly, and unlike cyclohexyl chloride, electrophile homocouple product, **E**, was produced.



**Scheme 2.12. Catalyst screen - the coupling of cyclooctyl bromide and phenyl magnesium bromide in the presence of catalytic amounts of an iron pre-catalyst in MTBE at 23°C.**

With all complexes screened, **B** and **C** were produced in a greater amount than desired product **A** (Table 2.5). When complex **2.8** and 1.0 equivalent of Grignard reagent were used, the ratio of A: B: C was an undesirable 1:3.1:4.8, with **E** as the majority product (entry 1). When 1.5 equivalents of phenylmagnesium bromide were used, the amount of **E** dropped 10 fold, yet **A** was still a minority product (entry 2). Bidentate iron complex **2.11** and rigidly tridentate complex **2.12** both decreased the amount of **B** produced, yet **B** and **C** were still in large excess (entries 3 and 4). Szymczak complexes **2.15** and **2.16** were the only catalysts to drastically reduce the amount of **B** produced, to a **B**: **A** ratio of 0.4:1 for **2.15** and a ratio of 0.9:1 ratio for **2.16** (entries 5 and 6). For both cases, **C** was unfortunately still in excess. When iron alkoxide species **2.17** and **2.18** were employed, the greatest disparities between undesired and desired products were seen (entries 7 and 8).

Entry	Precatalyst	Time	Conv.	Product Ratio				
				<b>A</b>	<b>B</b>	<b>C</b>	<b>D</b>	<b>E</b>
1*	<b>2.8</b>	60 min	83 %	1	3.1	4.8	0.8	13
2	<b>2.8</b>	120 min	100 %	1	3.6	7.7	0.7	1.3
3	<b>2.11</b>	60 min	100 %	1	2	11	0.3	0.5
4	<b>2.12</b>	30 min	100 %	1	1.6	3.2	0.4	0.8
5	<b>2.15</b>	30 min	100 %	1	0.4	1.8	0.1	0.1
6	<b>2.16</b>	30 min	100 %	1	0.9	3.4	0.2	0.4
7*	<b>2.17</b>	60 min	97 %	1	9.5	12	2.4	5.5
8*	<b>2.18</b>	60 min	99 %	1	5.4	9.4	1.3	2.8

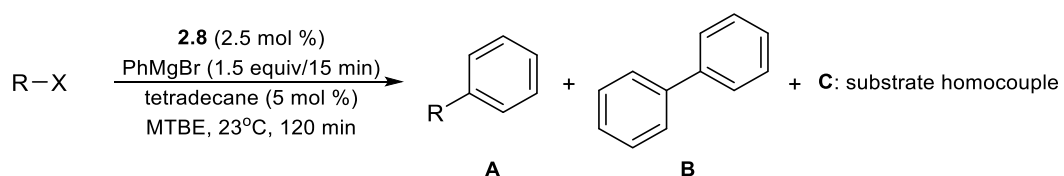
**Table 2.5. Catalyst screen – the coupling of cyclooctyl bromide and phenyl magnesium bromide in the presence of catalytic amounts of an iron precatalyst. All conversions and yields were determined by gas chromatography. The product ratios were normalized to the area of the peak of product A. \*1.0 equivalents of phenylmagnesium bromide used.**

Due to these results, and further studies that indicated that changes in temperature, solvent, and nucleophile addition rate did not ameliorate the poor yields of desired product, the optimization of this substrate was abandoned.

### 2.2.7 Halide Effects

In comparison to alkyl chlorides, alkyl bromides, iodides, and pseudohalides were studied, and an interesting trend was discovered. Decreasing C-X bond dissociation energies correlated with a decrease in the production of **A**, and an increase in the production of **C** (Table 2.6). When octyl chloride was coupled with phenylmagnesium bromide, an **A:B** ratio of 1.3:1 and an **A:C** ratio of 44:1 were observed (entry 1). When octyl bromide was used, the amount of **A** increases slightly as compared to **B**, yet the ratio of **A:C** falls almost 10 fold to 3.8:1 (entry 2), indicating a drastic increase in the amount of electrophile homocouple product. Employing octyl iodide led to a further decrease in desired product formation (entry 3). In the case of cyclohexyl substrates, no alkyl

homocouple product was formed for cyclohexyl chloride (entry 4) or cyclohexyl tosylate (entry 5), however the use of cyclohexyl tosylate noticeably decreases the amount of **A** formed. Cyclohexyl fluoride was also employed as a coupling partner, producing 13 % yield of desired product after two hours at 90 °C in toluene (entry 6). Unfortunately, the same reactivity was seen when catalyzed by iron dichloride. For benzyl halides, a slight decrease in the ratio of **A** formed was seen (entries 7 and 8). Additionally, although the use of cyclooctyl bromide rather than cyclooctyl chloride did not drastically alter the ratio of **A** to **B**, it did allow for the formation of homocouple product **C** (entry 10), whereas with cyclooctyl chloride, **C** is not observed (entry 9).



Entry	R	X	R-X Conv. (%)	A : B	A : C
1	octyl	Cl	93	1.3 : 1	44 : 1
2	octyl	Br	100	1.7 : 1	3.8 : 1
3	octyl	I	99.5	0.8 : 1	1.3 : 1
4	cyclohexyl	Cl	100	6.3 : 1	1 : 0
5	cyclohexyl	OTs	50	0.71 : 1	1 : 0
6*	cyclohexyl	F	100	1 : 1.3	1 : 0
7	benzyl	Cl	100	0.56 : 1	1.2 : 1
8	benzyl	Br	100	0.37 : 1	0.63 : 1
9	cyclooctyl	Cl	100	0.40 : 1	1 : 0
10	cyclooctyl	Br	100	0.28 : 1	0.77 : 1

**Table 2.6.** The effect of halide identity on the amount of desired and homocoupled products formed. All yields and conversions were determined by gas chromatography. \*In toluene at 90 °C, 13 % **A** formed; similar results were seen with FeCl<sub>2</sub> as the precatalyst.

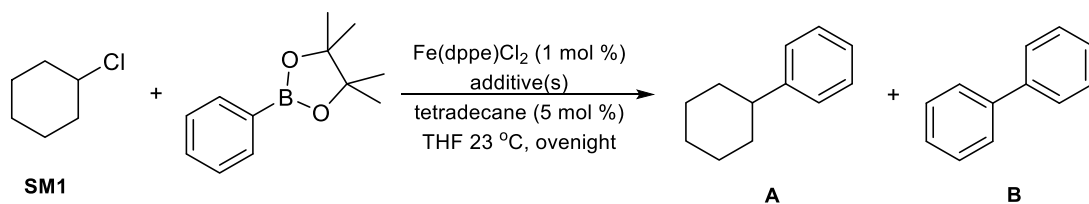
### 2.2.8 Conclusions

Despite the promising results seen for the coupling of cyclohexyl chloride and benzyl chloride with phenylmagnesium bromide in the presence of an iron(II) PDI complex, this system was not found to be general for alkyl halides. The overall goal of this chemistry was to facilitate alkyl-alkyl coupling and to develop a system that can span the many different possible substrate combinations. Neither of these goals were shown to be feasible. It is possible that this chemistry could be continued for the coupling of substituted cyclohexyl chlorides or heterocyclic analogues, yet this has not been pursued to date.

## 2.3 SUZUKI – TYPE COUPLING REACTIONS

### 2.3.1 Phenyl Pinacol Borane as a Coupling Partner

It was hypothesized that, under conditions similar to those used by the Bedford or Nakamura groups (see **Chapter 1**),<sup>14</sup> the use of an alkoxide additive to form an Fe(II) alkoxide species *in situ* could allow for the coupling of unactivated boronic esters. This might allow for iron catalyzed Suzuki-type reactions without added magnesium dibromide or the use of tBuLi to form the activated boronic ester species. Theoretically, an alkoxide ligand would allow for a more facile transmetallation step because boron is more oxophilic than halophilic. However, the use of phenylboronic acid pinacol ester as a transmetallating reagent led to no product formation (desired or undesired) under the conditions shown in **Table 2.7**, and the addition of phenyl magnesium bromide, in attempts to activate the boronic ester *in situ*, led only to the formation of biphenyl.



Entry	Additive 1 (equiv)	Additive 2 (equiv)	% conv. <b>SM1</b>	Product
1	NaOPhOMe (2)	-	0	none
2	PhMgBr (1)	-	0	<b>B</b>
3	NaOPhOMe (2)	PhMgBr (1)	0	<b>B</b>

**Table 2.7.** The attempted Suzuki-type cross coupling of cyclohexyl chloride (**SM1**) and phenylboronic acid pinacol ester in the presence of catalytic amounts of  $(\text{dppp})\text{FeCl}_2$  with alkoxide and Grignard reagent additives.

Later DFT calculations by Michael Crockett indicated that such transmetallation steps between phenylboronic acid pinacol ester and iron(II) species do benefit from the use of iron(II) bis-alkoxides rather than iron(II) dichlorides, yet the transformation is still thermodynamically disfavored (**Figure 2.6**). The use of iron(II) bis-amides, however, is thermodynamically downhill, and therefore the use of complexes of this type is currently being explored by Crockett.

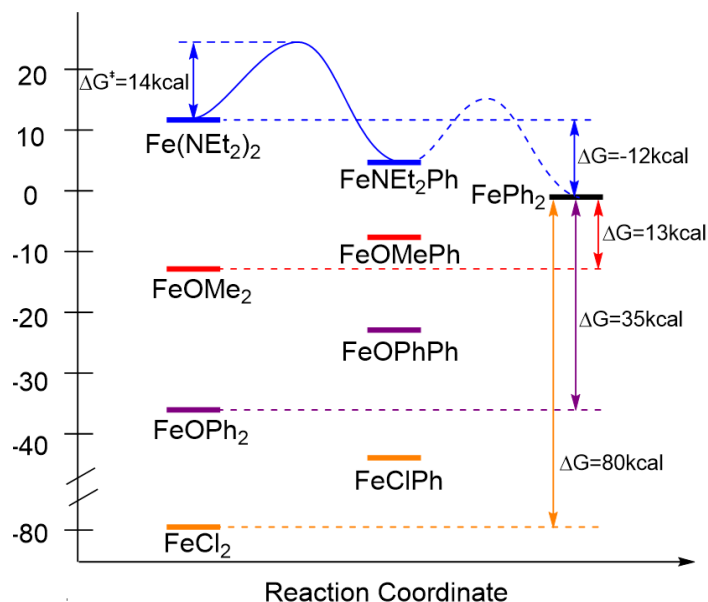
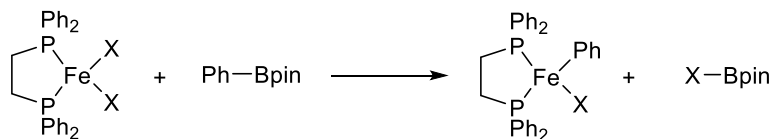


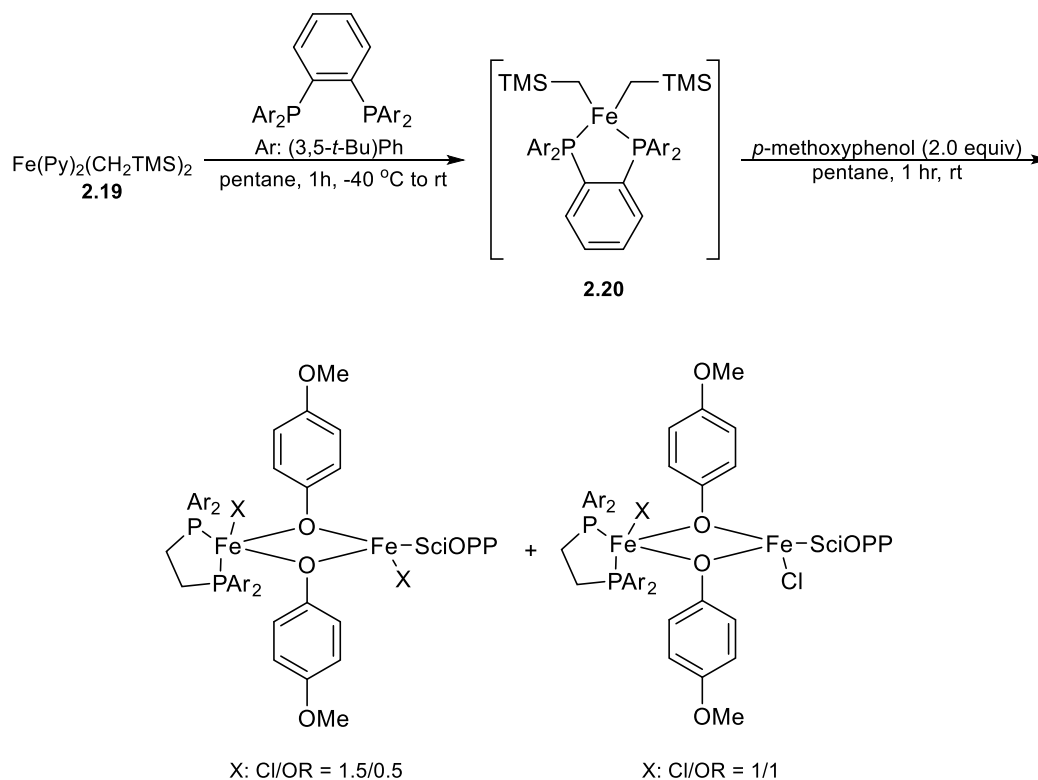
**Figure 2.6.** DFT calculations conducted by Michael Crockett. Modeled at B3LYP/6-31G\* in THF.

### 2.3.2 Iron Alkoxide Catalyst Development

As was mentioned, iron alkoxides were shown by DFT calculations to be more promising catalysts for Suzuki-type cross coupling than their iron dichloride analogues. Iron(II) bipyridyl complex **2.19**, a common precursor to iron(II) alkoxides used in the Byers group,<sup>26</sup> was treated with the SciOPP ligand often used by Nakamura (see **Chapter 1**)<sup>2</sup> in pentane at -40 °C (**Scheme 2.13**). The reaction mixture was allowed to warm to room temperature and stir for one hour. The dark orange solution was filtered through celite and concentrated to dryness to yield a yellow solid that was presumed to be **2.20**, although crystals of the compound could not be grown. NMR spectroscopy indicated that only one paramagnetic species was present in the sample.

Without further characterization, **2.20** was taken up in pentane at room temperature, and two equivalents of *p*-methoxyphenol were added. After being allowed to stir for one hour, the

resulting yellow reaction mixture was concentrated to dryness. Yellow-green crystals were obtained from recrystallization from pentane and X-ray crystallographic analysis revealed species mixture **2.21** as the reaction products (**Figure 2.7**). Unfortunately, these crystals were not used for catalysis because the small amount collected was used for X-ray crystallographic analysis.



**2.21**

**Scheme 2.13.** The synthesis of **2.21**, a mixture of bridged SciOPP alkoxy species.

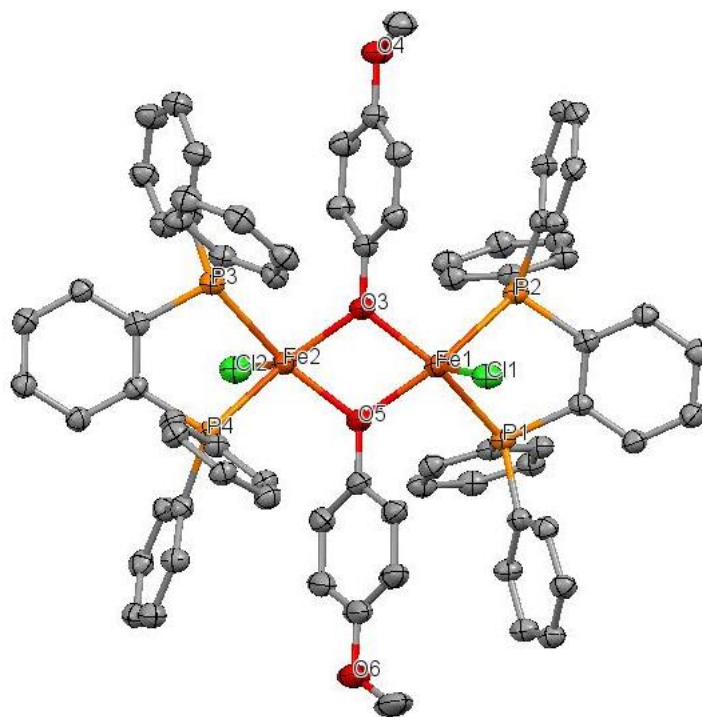


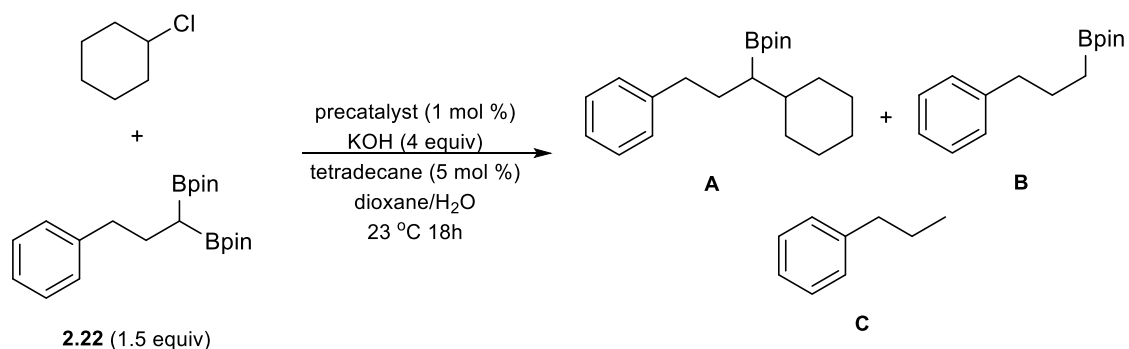
**Figure 2.7.** ORTEP plot of **2.12** at 30 % probability. Hydrogen atoms and *t*-butyl substituents have been omitted for clarity.

Attempts to synthesize (dppp)Fe bis(alkoxide) species did not proceed as smoothly. A route similar to that employed for the SciOPP ligand, beginning with **2.19**, and the salt metathesis of (dppp)FeCl<sub>2</sub> both resulted in the formation of a brown residue, with paramagnetic <sup>1</sup>H NMR signals, of which crystals could not be grown.

### 2.3.3 1,1-Bis(Boronate) Coupling Partners

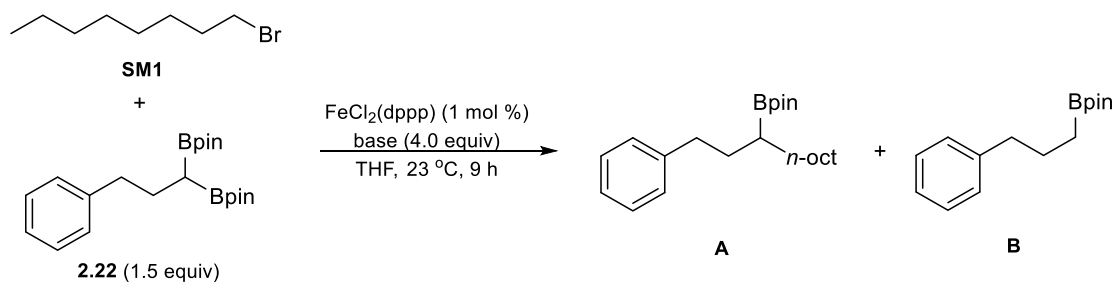
1,1-bis(boronate)s have been shown by the Morken group to be promising coupling partners in palladium-catalyzed and metal-free coupling reactions (*vide supra*). Modification of the palladium coupling reaction to an iron-catalyzed system was attempted. Following the conditions published by Morken for the palladium catalyzed coupling of 1,1-bis(boronate)s and vinyl bromides,<sup>19</sup> several iron(II)Cl<sub>2</sub> complexes were screened (**Scheme 2.14**). 2,2'-(3-phenylpropane-1,1-diyl)bis(pinacolborane), **2.22**, was employed as the nucleophilic coupling partner of cyclohexyl

chloride in the presence of catalytic amounts of an iron(II) precatalyst, with four equivalents of KOH in a water/dioxane solvent mixture. The major possible products of this reaction were the desired coupled product **A**, protodeborylation product **B**, and the result of two protodeborylation reactions, **C**. Unfortunately, all perturbations of these conditions led to the production of only protodeborylation product **B**, likely due to the presence of water.



**Scheme 2.14.** The attempted Suzuki-type cross coupling of cyclohexyl chloride (**SM1**) and 1,1-bisboronate **2.22**.

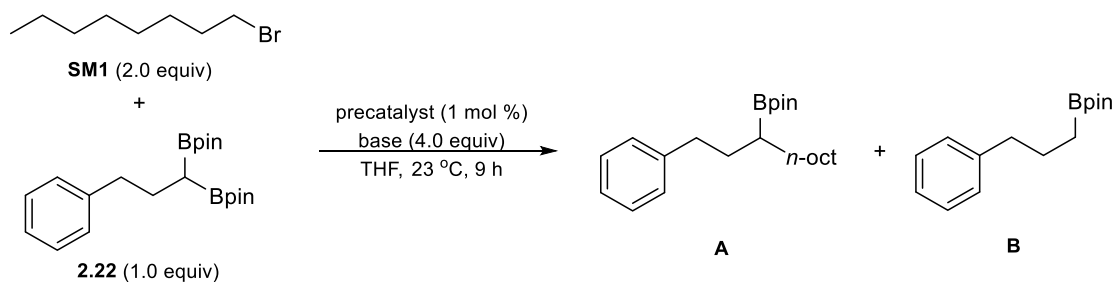
An air- and water-free system was developed in which cyclohexyl chloride and **2.22** were treated with catalytic amounts of (dppp)FeCl<sub>2</sub> and four equivalents of base in THF at room temperature. A base screen was conducted, as shown in **Table 2.8**. The use of cesium fluoride (entry 1), cesium carbonate (entry 2), aluminum isopropoxide (entry 3), magnesium dibromide (entry 4), lithium tetrafluoroborate (entry 5), or lithium methoxide (entry 6) resulted in no conversion of either starting material. Potassium ethoxide (entry 7) and potassium *t*-butoxide (entry 8) bases led to full conversion of 1-bromooctane (**SM1**) into octene, and of **2.22** into protodeborylation product **B**. Promising results were seen when lithium hexamethyldisilazide was used (entry 9), in which desired product **A** and bromopinacol borane were the major products formed.



Entry	Base	Conv <b>SM1</b> (%)	Conv <b>2.22</b> (%)	Product
1	CsF	0	0	No reaction
2	$\text{Cs}_2\text{CO}_3$	0	0	No reaction
3	$\text{Al}(\text{O}^i\text{Pr})_3$	0	0	No reaction
4	$\text{MgBr}_2$	0	0	No reaction
5	$\text{LiBF}_4$	0	0	No reaction
6	LiOMe	0	0	No reaction
7	KOEt	100	100	<b>B</b> , octene
8	KOtBu	10	100	<b>B</b> , octene
9*	LiHMDS	97	99	<b>A</b>

**Table 2.8. Base screen – the coupling of 1-bromooctane (**SM1**) and **2.22** in the presence of catalytic amounts of  $(\text{dppp})\text{FeCl}_2$  and four equivalents of base. All conversions were determined by gas chromatography. \*77 % isolated yield of desired product **A**.**

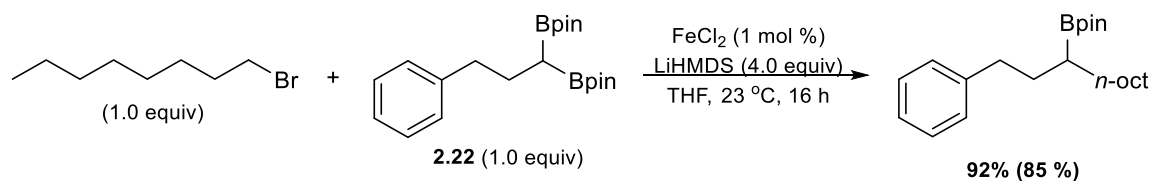
Subsequently, additional hexamethyldisilazide bases were examined under the reaction conditions (**Table 2.9**). With LiHMDS, the ratio of **A** to **B** was found to be 1.0:1 (entry 1), yet with KHMDS (entry 2) and NaHMDS (entry 3), **B** was not observed. Not all of 1-bromooctane (**SM1**) was converted into **A**, and some formation of octene and octane was observed. The use of iron dichloride resulted in a similar product ratio, but with markedly decreased conversion of **SM1** (entry 4). By increasing the reaction time to 16 hours, full conversion of **SM1** occurred.



Entry	Precatalyst	Base	Conv. <b>SM1</b> (%)	<b>A</b> : <b>B</b>	other products
1	FeCl <sub>2</sub> (dppp)	LiHMDS	97	1 : 0.1	octane/octene
2	FeCl <sub>2</sub> (dppp)	KHMDS	100	1 : 0	octane/octene
3	FeCl <sub>2</sub> (dppp)	NaHMDS	96	1 : 0	octane/octene
4	FeCl <sub>2</sub>	LiHMDS	57	1 : 0.05	octane/octene
5	none	LiHMDS	80	none	octane/octene

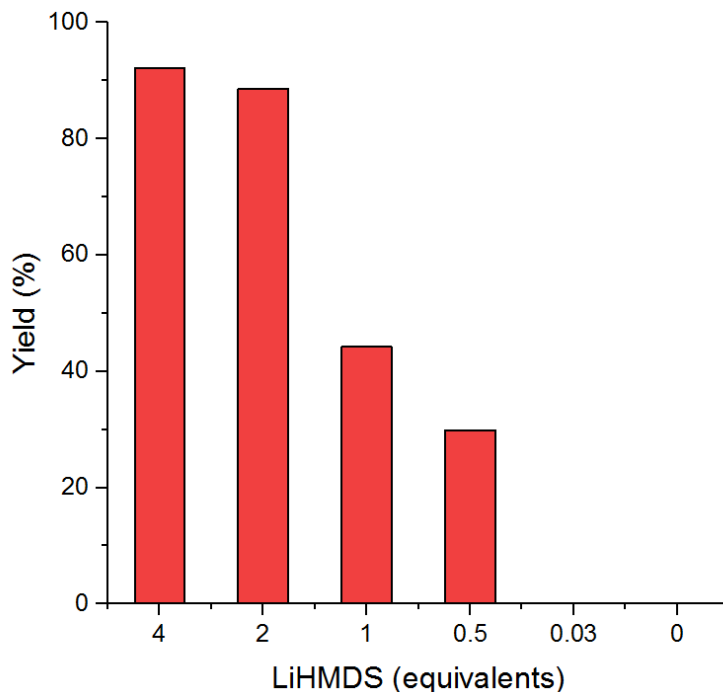
**Table 2.9.** Screen of HMDS bases and control reactions – the coupling of **SM1** and **2.22** in the presence of catalytic amounts of iron(II) and four equivalents of base. All conversions were determined by gas chromatography.

PDI and dppe ligands were screened with no improvement of the iron dichloride system. In other solvents, Et<sub>2</sub>O, CH<sub>2</sub>Cl<sub>2</sub>, etc., decreases in product yield were observed. It was also determined that an equimolar amount of starting materials was sufficient to achieve high yields. Thus, the optimal conditions were obtained, as shown in **Scheme 2.15**. Under these conditions, 92 % yield was observed by GC, and by column chromatography, an isolated yield of 85 % was achieved.



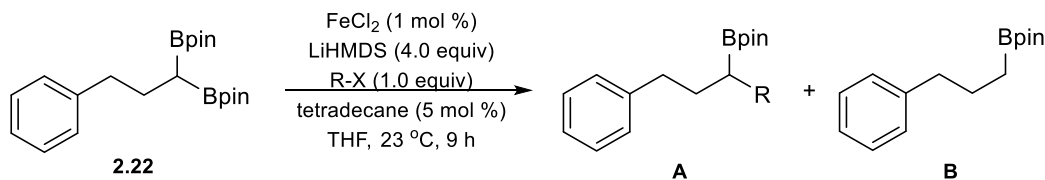
**Scheme 2.15.** Optimal conditions for the coupling of octylbromide and **2.22**, leading to 85 % isolated yield.

A screen of LiHMDS equivalents was conducted (**Graph 2.7**), revealing that the yield of desired product was highly dependent on the equivalents of base, and the use of catalytic amounts was not feasible. Under optimal conditions, 92 % **A** was produced, and decreasing the amount of base to two equivalents led to a slightly diminished yield of 89 %. However, upon reducing the amount of base to one equivalent, less than 45 % of **A** was formed. No desired product was seen when 3 mol % of LiHMDS was used.



**Graph 2.7. A screen of the equivalents of LiHMDS under the optimized conditions. All yields were determined by gas chromatography.**

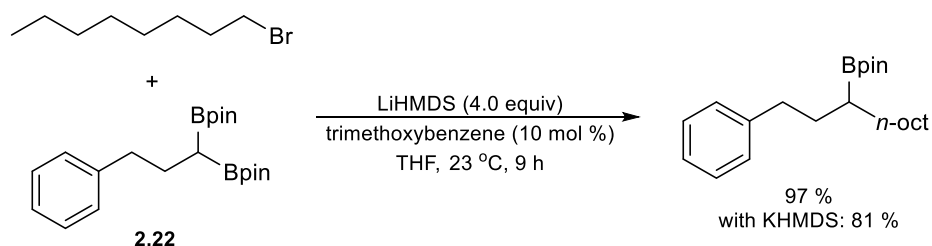
A brief substrate scope revealed that the use of octylchloride (entry 2) also led to **A** as the majority product, in similar yields to octylbromide (entry 1), as shown in **Table 2.10**. As with the attempted Kumada-type coupling reactions, the use of cyclooctyl bromide led to predominant formation of cyclooctene and cyclooctane, in this case with no desired product observed (entry 3). *t*-Butylchloride likely formed *iso*-butane and *iso*-butene which were not observable by GC, likely *iso*-butane and *iso*-butene (entry 4).



Entry	X	R	Product(s)
1	Br	octyl	A
2	Cl	octyl	A
3	Br	cyclooctyl	cyclooctene/cyclooctane
4	Cl	<i>t</i> -butyl	none

**Table 2.10. Substrate scope – the coupling of 2.22 with alkyl halides in the presence of 1 mol % iron dichloride and four equivalents of LiHMDS.**

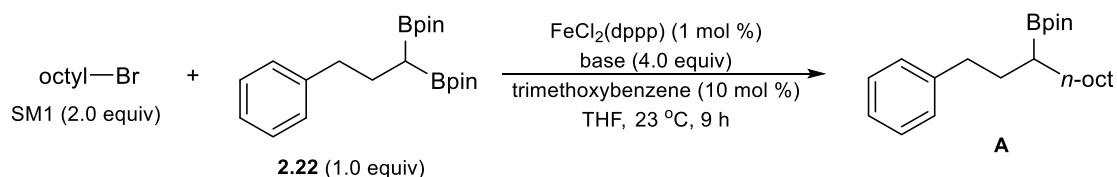
Previous control reactions had indicated that iron was required to facilitate the transformation, however, upon repeating the trials it was found that the desired product was produced in 97 % yield with LiHMDS in the absence of iron precursor (**Scheme 2.16**). When KHMDS was used, 81 % yield was observed.

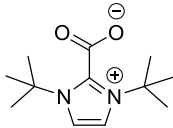
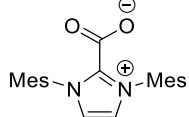


**Scheme 2.16. The control reaction of octylbromide and 2.22 in the absence of an iron source. All yields were determined by NMR in comparison to trimethoxybenzene.**

Other bases were screened, in the hopes that one could be found that required iron to produce **A** (**Table 2.11**). While triethylamine led to some substrate conversion, no desired product was formed (entry 1). When using DMAP, no conversion of **SM1** was seen (entry 2). 1,3-bis(*t*-butyl)imidazolium-2-carboxylate, IMes-CO<sub>2</sub> (entry 3) and 1,3-bis(2,4,6-trimethylphenyl)imidazolium-2-carboxylate, SIMes-CO<sub>2</sub> (entry 4), which are known to undergo thermolysis to form free NHCs *in*

*situ*,<sup>27</sup> were also examined. While significant conversion of **SM1** and **2.22** were seen for both of these bases in DMF at 100 °C, no desired product was formed.



Entry	base	Conv <b>SM1</b> (%)	Conv <b>2.22</b> (%)	Yield <b>A</b> (%)
1	Et <sub>3</sub> N	29	7	0
2	DMAP	0	6	0
3*		100	100	0
4*		35	86	0

**Table 2.11. Base screen - The attempted cross coupling reaction of octylbromide and 2.22 in the presence of 1 mol % of (dppp)FeCl<sub>2</sub>. All yields were determined by gas chromatography. \*In DMF at 100 °C.**

### 2.3.4 Conclusions

The attempted iron-based Suzuki-type cross coupling of 1,1-bis(boronate)s were found to be base catalyzed, similar to systems developed by Morken. Additionally, the coupling of aryl boronic esters in the presence of iron alkoxides was not achieved, and the brief attempts to form iron bis(phosphine) alkoxides were not successful. Further studies by group member Michael Crockett have revealed that iron amides are more amenable catalysts for these transformations, as suggested by the aforementioned calculations. This reactivity is currently being pursued by Crockett and Chet Tyrol.

## 2.4 EXPERIMENTAL

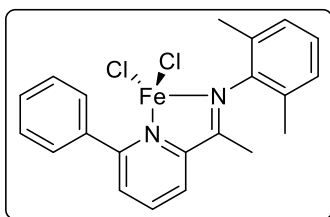
### 2.4.1 General Considerations

Unless stated otherwise, all reactions were carried out in oven-dried glassware using standard Schlenk techniques<sup>28</sup> or using an MBraun inert atmosphere (N<sub>2</sub>) drybox. Dichloromethane, pentane, toluene, diethyl ether, and tetrahydrofuran were passed through a solvent purification system under a blanket of argon and then degassed briefly under vacuum prior to use. Reagents were purchased from commercial sources and purified as necessary before use. NMR spectra were recorded at ambient temperature on a Varian VNMRS or INOVA spectrometer operating at 500 MHz for <sup>1</sup>H NMR and 125 MHz for <sup>13</sup>C NMR. The line listings for the NMR spectra of diamagnetic compounds are reported as: chemical shift in ppm (number of protons, splitting pattern, coupling constant). All chemical shifts are reported in ppm from tetramethylsilane with the peak for the residual protio version of the solvent as the internal reference. GC/FID data were obtained on a Shimadzu GC-2014 equipped with a AOC-20i Auto Injector/Auto Sampler. GC/MS data were obtained on an Agilent 7820a GC with a 5975 Mass Analyzer. High-resolution mass spectra were obtained at the Boston College Mass Spectrometry Facility. Elemental Analyses were conducted at Robertson MicroLit Laboratories. IR spectra were recorded on a Bruker ALPHA Platinum ATR infrared spectrometer. X-ray crystallographic information was obtained at the Boston College X-Ray Crystallography Center. Slow addition of reagents was facilitated by either an NE-1000 Programmable Single Syringe Pump or an NE-1600 Six Channel Programmable Syringe Pump. All aliquots removed from reaction vessels for GC analysis were taken using Teflon needles, diluted in THF, quenched with two drops of water, and dried over sodium sulfate. All isolated yields were obtained on a CombiFlashRf auto-column in 100 % hexanes. All substrates not discussed below were purchased from commercial sources. All Kumada cross coupling products were identified by GC/MS.

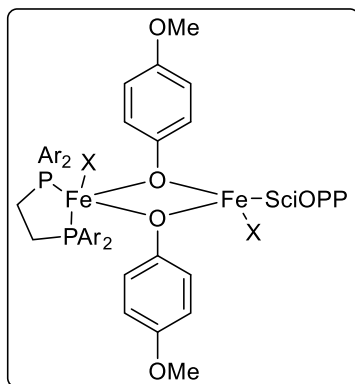
*(4E, 5E)-N<sup>4</sup>, N<sup>5</sup>-bis(2,6-dimethylphenyl)-2,3,7,8-tetrahydroacridine-4,5-(1H, 6H) diamine iron dichloride (2.12)* was synthesized according to literature procedures.<sup>24,29</sup> *(1Z, 3Z)-N1, N3-bis(6-*

*methylpyridin-2-yl)isoindoline-1,3-diimine iron monobromide (2.15)* and *(Z)-N-methyl-N-(6-methylpyridin-2-yl)-1-((6-methylpyridin-2-yl)imino)-1H-isoindol-3-amine iron bis(triflate) (2.16)* were synthesized by members of the Szymczak Group according to literature procedures.<sup>25</sup> PDI complexes **2.1**, **2.8** – **2.10** and their respective ligand precursors were prepared following literature procedures.<sup>30</sup> (PDI)Fe bis(alkoxide) species were prepared according to literature procedures.<sup>26</sup> *Bis(4,4,5,5-tetramethyl-1,3,2-dioxaborolan-2-yl) methane* and *2,2'-(3-phenylpropane-1,1-diyl)bis(4,4,5,5-tetramethyl-1,3,2-dioxaborolane (2.22)* were prepared according to literature procedures.<sup>31</sup>

## 2.4.2 Syntheses of Complexes



*(E)-N-(2,6-dimethylphenyl)-1-(6-phenylpyridin-2-yl)ethan-1-imine iron dichloride*. The *(E)-N-(2,6-dimethylphenyl)-1-(6-phenylpyridin-2-yl)ethan-1-imine* ligand<sup>32</sup> (0.029 g, 0.096 mmol) was dissolved in THF (3 mL) and a slurry of FeCl<sub>2</sub> (0.012 g, 0.091 mmol) in THF (2 mL) was added. The solution became salmon pink in color and was allowed to stir at room temperature overnight. Diethyl ether was added to fully precipitate the product, and the salmon pink solid was collected by vacuum filtration, washed with diethyl ether, and dried in vacuo. Yield = 0.035 g (89 %).<sup>32</sup>

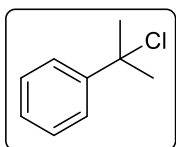


**2.21.** Step 1: In an inert atmosphere glovebox, Fe(Py)<sub>2</sub>(CH<sub>2</sub>TMS)<sub>2</sub><sup>26</sup> (0.022 g, 0.056 mmol) and the SciOPP ligand (0.050 g, 0.056 mmol) were added to a 20 mL vial and taken up in 2.5 mL of pentane. The solution became dark orange and was allowed to stir at room temperature overnight. The reaction mixture was then filtered through celite and dried in vacuo to give a yellow, oily solid. The residue was taken up in

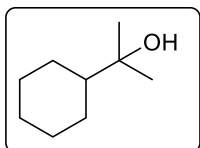
pentane and precipitated at -40 °C (solids formed were not X-ray quality crystals). Yield = 0.040 g (60 %).

Step 2: The yellow solid (0.040 g, 0.034 mmol) was taken up in pentane (5 mL) in a 20 mL vial and 4-methoxyphenol (0.009 g, 0.07 mmol) was added. The mixture was allowed to stir at room temperature overnight, at which point a yellow, slightly cloudy mixture had formed. The mixture was concentrated to dryness, then recrystallized from pentane at -40 °C.

### 2.4.3 Syntheses of Substrates

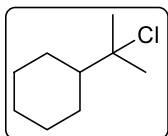


(2-chloropropan-2-yl)benzene was synthesized according to literature procedures.<sup>33</sup> In open air and at 0 °C, lithium chloride (3.7 g, 88 mmol) was dissolved in concentrated hydrochloric acid (175 mL). Once the lithium chloride was fully dissolved, 2-phenyl-2-propanol (5.0 mL, 35 mmol) was added and the solution became cloudy. The reaction mixture was allowed to warm to room temperature, and then to stir overnight. The mixture was extracted with dichloromethane (3x 50 mL), and the combined organic layers were washed with water (2x 75 mL), saturated NaHCO<sub>3</sub> (2x 75 mL), and saturated NaCl (2x 75 mL), then dried over magnesium sulfate and concentrated to yield a clear, slightly yellow oil that was dried over CaH<sub>2</sub> and distilled prior to use. Yield = 4.8 g (89 %). <sup>1</sup>H NMR (500 MHz, CDCl<sub>3</sub>) δ 7.65-7.64 (d, 2H, 7.26), 7.42-7.39 (t, 2H, 7.60), 7.34-7.31 (t, 1H, 6.73), 2.05 (s, 6H).<sup>33</sup>

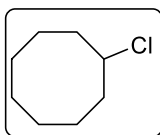


2-cyclohexylpropan-2-ol. At 0 °C, cyclohexylmagnesium bromide (1.0 M in THF, 36.2 mL, 36.2 mmol) was added slowly to a solution of acetone (2.50 mL, 34.4 mmol) in diethyl ether (10 mL). The reaction mixture was warmed to room temperature and allowed to stir overnight. The solution became pale grey and a white precipitate formed. The mixture was quenched with 30 mL water at 0 °C and extracted with ethyl acetate (3x 10 mL). The combined organic layers were washed with saturated NaCl (2x 15 mL) and saturated NaHCO<sub>3</sub> (2x 15 mL), then dried over sodium sulfate and concentrated to dryness. The remaining oil was taken up in hexanes and filtered through a plug of silica, then concentrated to yield a clear

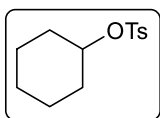
liquid. Yield = 3.8 g (78 %).  $^1\text{H NMR}$  (500 MHz,  $\text{CDCl}_3$ )  $\delta$  4.03-3.98 (dd, 1H, 9.0), 1.33-1.12 (m, 10H), 1.03 (s, 6H), matching with literature assignments.<sup>34</sup>



*(2-chloropropan-2-yl)cyclohexane*. In open air and at 0 °C, lithium chloride (1.5 g, 35 mmol) was dissolved in concentrated hydrochloric acid (70 mL). Once the lithium chloride was fully dissolved, 2-cyclohexyl-2-propanol (2.1 mL, 14 mmol) was added and the solution became cloudy. The reaction mixture was allowed to warm to room temperature, and then to stir overnight. The mixture was extracted with dichloromethane (3x 20 mL) and the combined organic layers were washed with water (2x 30 mL), saturated  $\text{NaHCO}_3$  (2x 30 mL), and saturated  $\text{NaCl}$  (2x 30 mL), then dried over magnesium sulfate and concentrated to yield a clear, slightly yellow oil that was dried over  $\text{CaH}_2$  and distilled prior to use. Yield = 2.1g (90.5 %).

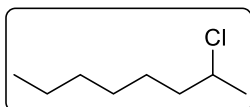


*Chlorocyclooctane*. In open air and at 0 °C, lithium chloride (4.02 g, 95 mmol) was dissolved in concentrated hydrochloric acid (190 mL). Once the lithium chloride was fully dissolved, 2-phenyl-2-propanol (5.0 mL, 38 mmol) was added and the solution became cloudy. The reaction mixture was allowed to warm to room temperature, and then to stir overnight. The mixture was extracted with dichloromethane (3x 50 mL) and the combined organic layers washed with water (2x 75 mL), saturated  $\text{NaHCO}_3$  (2x 75 mL), and saturated  $\text{NaCl}$  (2x 75 mL), then dried over magnesium sulfate and concentrated to yield a clear liquid that was dried over  $\text{CaH}_2$  and distilled prior to use. Yield = 3.9g (71 %).  $^1\text{H NMR}$  (500 MHz,  $\text{CDCl}_3$ )  $\delta$  4.25-4.20 (sept. 1H, 4.14), 2.14-2.08 (2H, m), 2.01-1.95 (2H, m), 1.79-1.72 (2H, m), 1.59-1.48 (8H, m), matching literature assignments.<sup>35</sup>



*Cyclohexyl 4-methylbenzenesulfonate*. Cyclohexanol (4.1 mL, 39 mmol) was dissolved in dichloromethane (39 mL) and the mixture was cooled to 0 °C. Pyridine (6.3 mL, 79 mmol) was then added, followed by portion-wise additions of *p*-toluenesulfonyl chloride (7.1 g, 37 mmol). The reaction mixture was allowed to stir at 0 °C for 2.5

hours, then was quenched with diethyl ether (120 mL) and water (30 mL). The organic layer was washed with HCl (2x 75 mL), saturated NaHCO<sub>3</sub> (2x 75 mL), and water (2x 75 mL), then dried over sodium sulfate, and concentrated to dryness to yield a clear oil that was dried over CaH<sub>2</sub> and distilled prior to use. Yield = 5.0 g (52 %). <sup>1</sup>H NMR (500 MHz, CDCl<sub>3</sub>) δ 7.79-7.78 (d, 2H, 6.83), 7.33-7.31 (d, 2H, 8.23), 4.51-4.46 (sept., 1H, 4.33), 1.89-1.18 (m, 10H), matching literature assignments.<sup>36</sup>

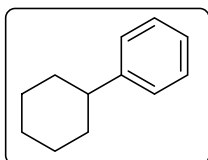


*2-chlorooctane*. To a 100 mL round bottom flask equipped with a stir bar was added: 2-octanol (3.94 mL, 25 mmol), pyridine (10 mL, 25 mmol), and diethyl ether (30 mL). The mixture was cooled to 0 °C in an ice bath, and thionyl chloride (1.80 mL, 25 mmol) was added. A flocculent white precipitate formed, and the mixture was warmed to reflux for 4 hours. The reaction mixture was cooled to room temperature and the precipitate was removed by filtration. The filtrate was washed with water (2x 10 mL) and saturated sodium chloride (2x 10 mL), then dried over sodium sulfate and concentrated to dryness to yield a slightly viscous, pale yellow oil that was dried over CaH<sub>2</sub> and distilled prior to use. Yield = 3.41 g (93 %) <sup>1</sup>H NMR (500 MHz, CDCl<sub>3</sub>) δ 4.67 – 4.52 (m, 1H), 1.72 – 1.58 (m, 1H), 1.58 – 1.49 (m, 1H), 1.40 – 1.22 (m, 11H), 0.87 (td, J = 7.2, 6.2, 2.3 Hz, 3H), matching literature assignments.<sup>37</sup>

#### 2.4.4 Cross Coupling Procedures and Desired Products

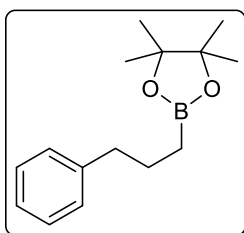
*Optimized Kumada Reaction Conditions:* The alkyl halide substrate (0.67 mmol), tetradecane (5 mol %, 0.034 mmol, ITSD), solvent (0.8 M), and catalyst (2.5 mol %, 0.017 mmol) were combined in a 50 mL pear shaped flask equipped with a second port with a glass stopcock and a 14/20 joint that was equipped with a 180° joint and stir bar, and the solution was brought to the desired temperature. Under a flow of nitrogen, the Grignard reagent was taken up into a Hamilton Syringe from its commercial sure-sealed bottle. The Grignard reagent was slowly added to the reaction mixture using a syringe pump with the correct parameters to allow the delivery of 1.0 mmol of Grignard over a 15-minute period. The reaction was allowed to continue until full starting material

conversion was indicated by GC monitoring. The reaction was quenched with 3M HCl (4 mL) and allowed to stir for about an hour, or until no more color change was visible. The aqueous layer was extracted (3x hexanes), and the combined organic layers were dried over sodium sulfate, filtered, and concentrated to dryness.

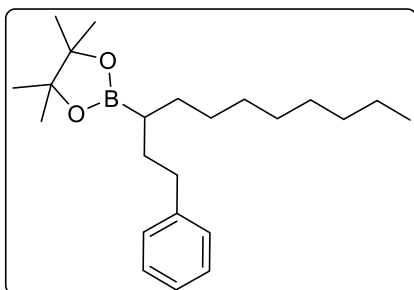


*Cyclohexylbenzene*. Isolated *via* column chromatography in 100 % hexanes; rf:0.80.  $^1\text{H NMR}$  (500 MHz, Chloroform- $d$ )  $\delta$  7.31 (t,  $J$  = 7.4 Hz, 2H), 7.27 – 7.17 (m, 3H), 2.51 (dt,  $J$  = 11.3, 6.1 Hz, 1H), 1.88 (dd,  $J$  = 20.6, 10.2 Hz, 4H), 1.77 (d,  $J$  = 13.1 Hz, 1H), 1.43 (q,  $J$  = 10.5, 10.0 Hz, 4H), 1.35 – 1.21 (m, 1H), matching literature assignments.<sup>38</sup>

*Suzuki Cross-Coupling Conditions*: Under air-free conditions, 2,2'-(3-phenylpropane-1,1-diyl)bis(4,4,5,5-tetramethyl-1,3,2-dioxaborolane) (19 mg, 0.052 mmol), the alkyl halide (0.052 mmol), tetradecane (1.0  $\mu\text{L}$ , 0.0039 mmol), catalyst (0.00052 mmol), and THF (250  $\mu\text{L}$ ) were combined in a vial and a  $t = 0$  time point was taken. The base (0.208 mmol) was then taken up in THF (500  $\mu\text{L}$ ) and added to the reaction mixture. The vial was capped and the reaction mixture was allowed to stir at room temperature overnight, taking time points as necessary.



*Protodeborylation Product*:  $^1\text{H NMR}$  (500 MHz,  $\text{CDCl}_3$ )  $\delta$  7.27-7.24 (t, 2H, 7.64), 7.18-7.16 (d, 2H, 7.30), 7.17-7.14 (t, 1H, 7.91), 2.62-2.59 (t, 2H, 7.76), 1.76-1.70 (quintet, 2H, 7.83), 1.24-1.23 (d, 12H, 3.58), 0.84-0.81 (t, 2H, 7.90).



$^1\text{H NMR}$  (400 MHz, Chloroform- $d$ )  $\delta$  7.25 – 7.16 (m, 4H), 7.14 – 7.09 (m, 1H), 2.52 – 2.46 (m, 2H), 1.91 – 1.84 (m, 2H), 1.71 – 1.65 (m, 2H), 1.27 (d,  $J$  = 11.3 Hz, 11H), 1.22 (s, 22H), 0.89 – 0.84 (m, 3H). \*note: impurity present under the

peak at 1.22 ppm. IR(neat): 765.48, 1179.75, 1210.59, 1253.11, 1313.22, 1379.22, 1432.34, 1564.81, 1620.24, 2866.30, 2925.49, 2957.27  $\text{cm}^{-1}$ .

## 2.5 SPECTROSCOPY

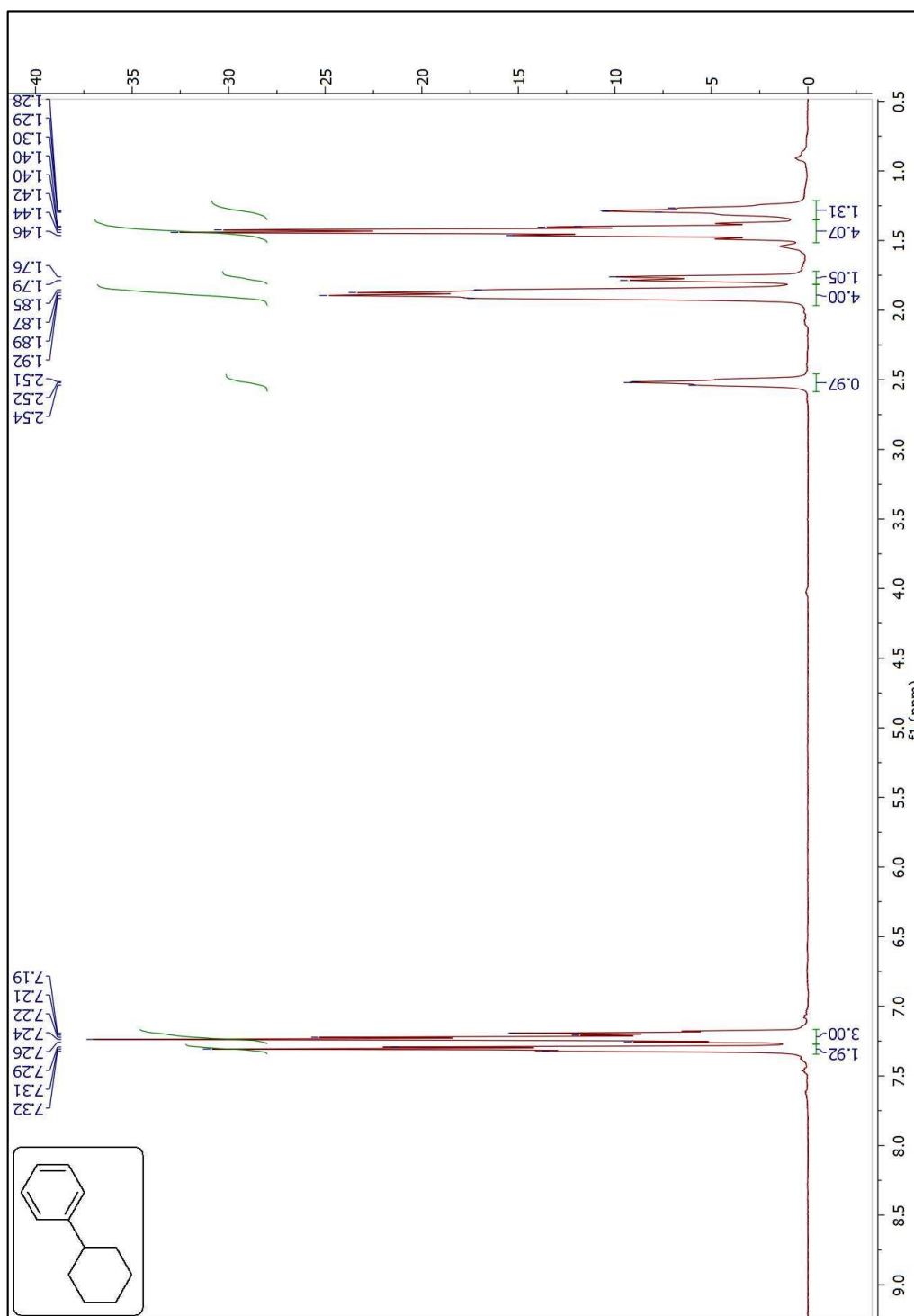
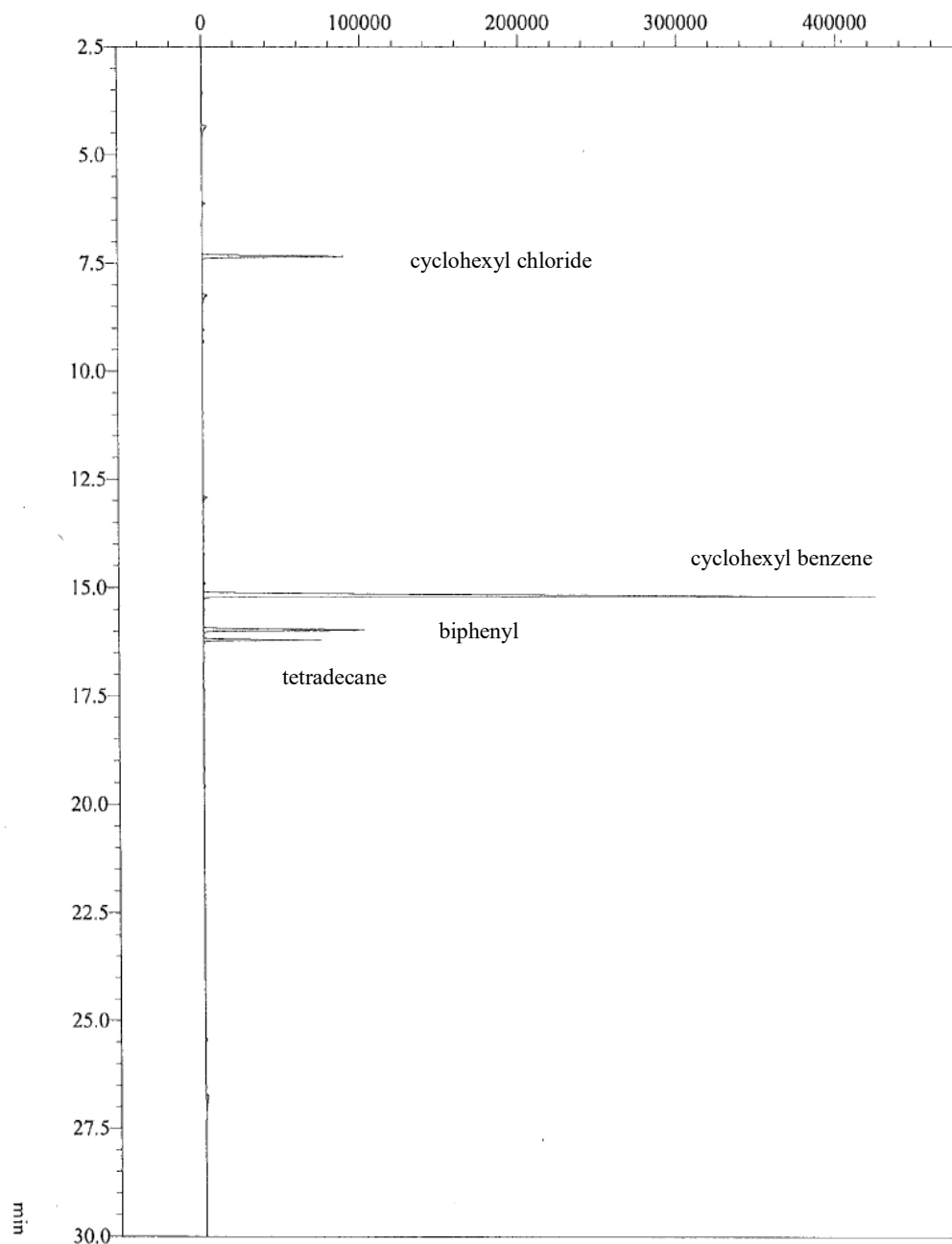


Figure 2.8.  $^1\text{H}$  NMR Spectrum of cyclohexylbenzene.

Analysis Date & Time : 12/8/2014 3:58:19 PM  
User Name : Admin  
Vial# : 22  
Sample Name : TLM-bc2-007\_60min  
Sample ID :  
Sample Type : Unknown  
Injection Volume : 1.00  
ISTD Amount : [1]=1

Data Name : C:\GCsolution\Data\Byers Lab\Mako\TLM-bc2-007\_60min.gcd  
Method Name : C:\GCsolution\Methods\Byers Lab\Mako\20-250\_10Cpermin\_30min.gem



**Figure 2.9. Representative GC trace of the cross coupling of cyclohexylchloride and phenyl magnesium bromide after 60 minutes.**

Analysis Date & Time : 12/15/2014 8:59:19 PM  
User Name : Admin  
Vial# : 60  
Sample Name : TLM-bc2-023\_90min  
Sample ID :  
Sample Type : Unknown  
Injection Volume : 1.00  
ISTD Amount : [1]=1

Data Name : C:\GCsolution\Data\Byers Lab\Mako\TLM-bc2-023\_90min.gcd  
Method Name : C:\GCsolution\Methods\Byers Lab\Mako\20-250\_10Cpermin\_30min.gcm

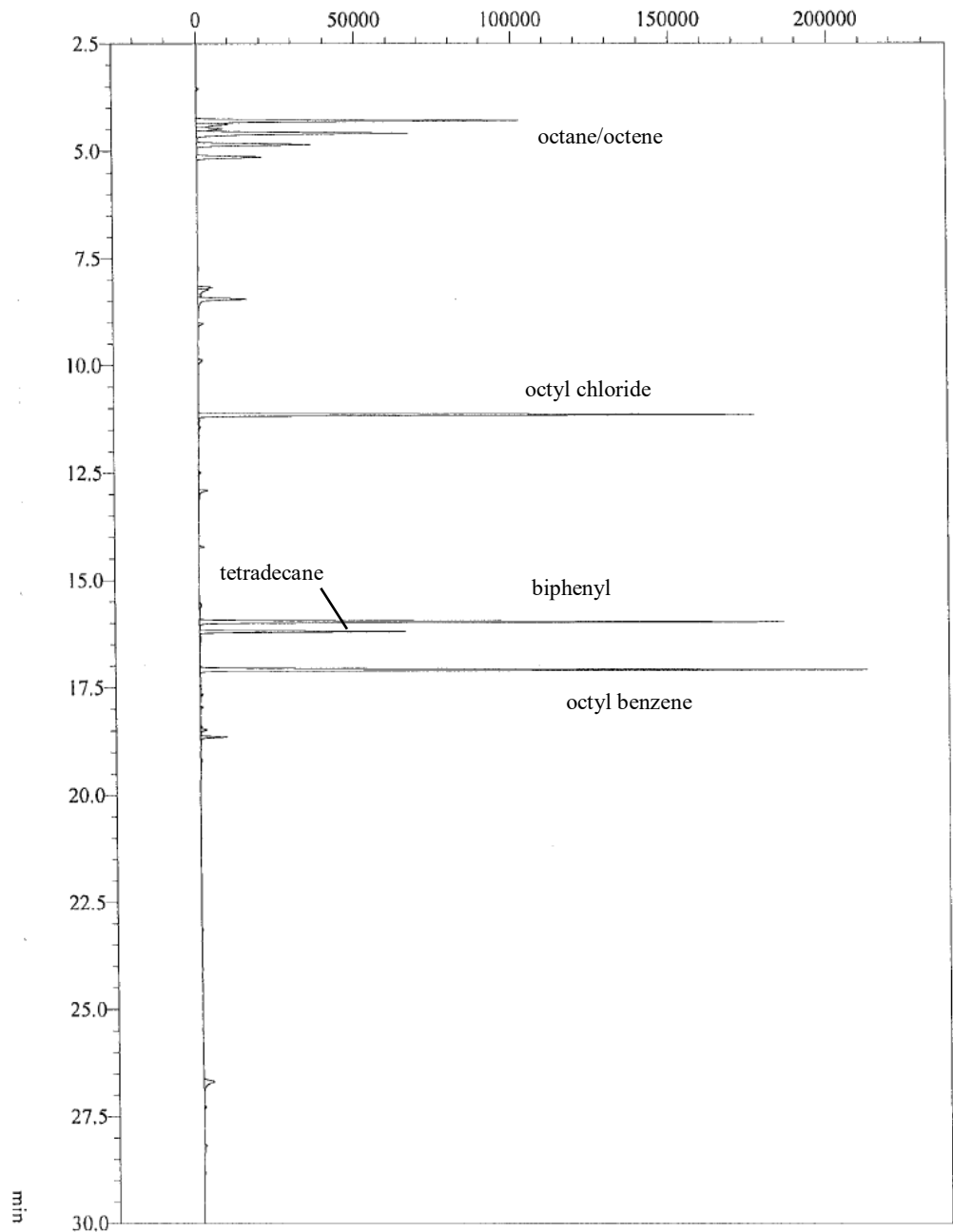


Figure 2.10. Representative GC trace of the cross coupling of octylchloride and phenyl magnesium bromide after 90 minutes.

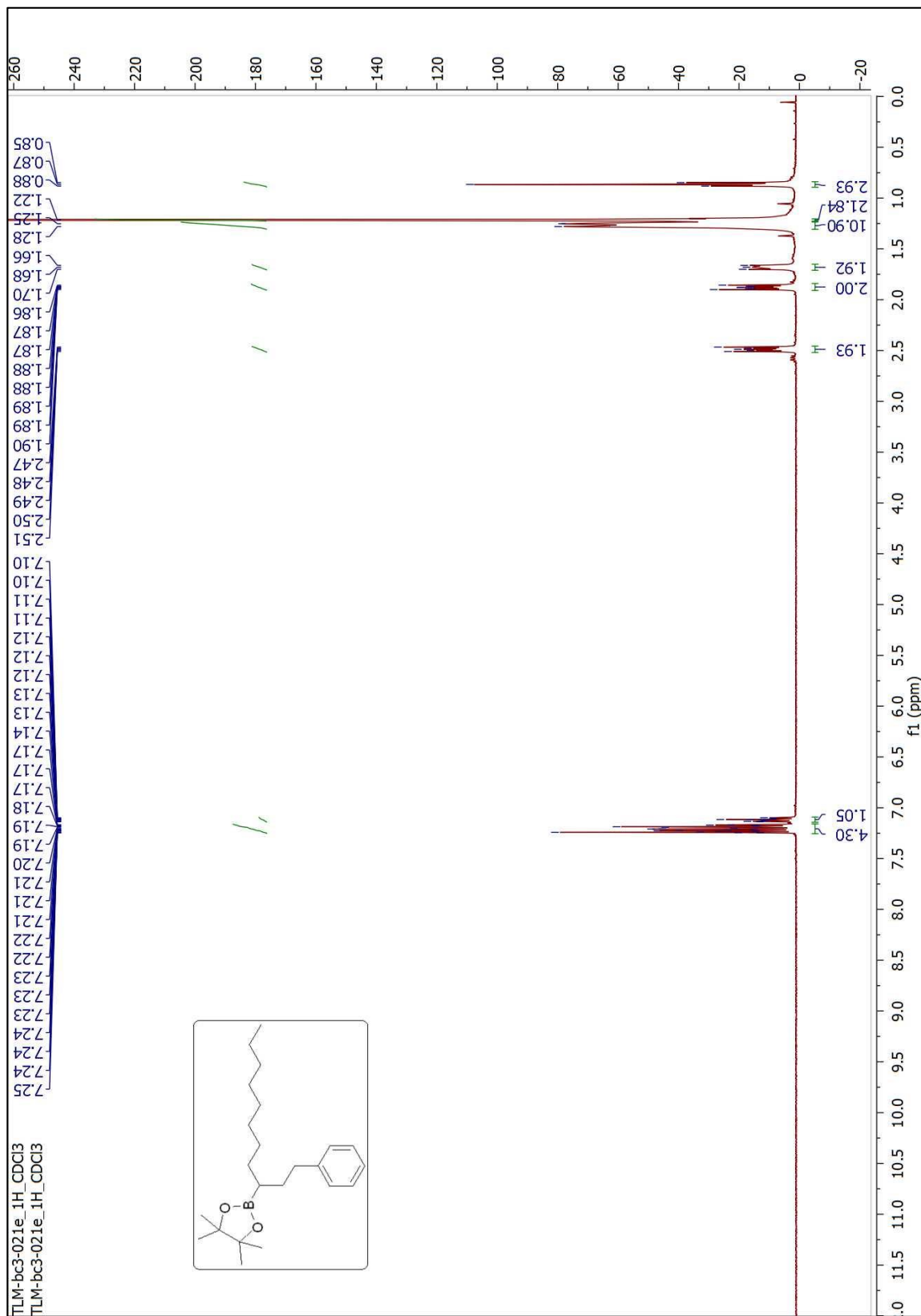


Figure 2.11. <sup>1</sup>H NMR Spectrum of 4,4,5,5-tetramethyl-2-(1-phenylundecan-3-yl)-1,3,2-dioxaborolane. Note, a small impurity exists underneath the peak at 1.22 ppm.

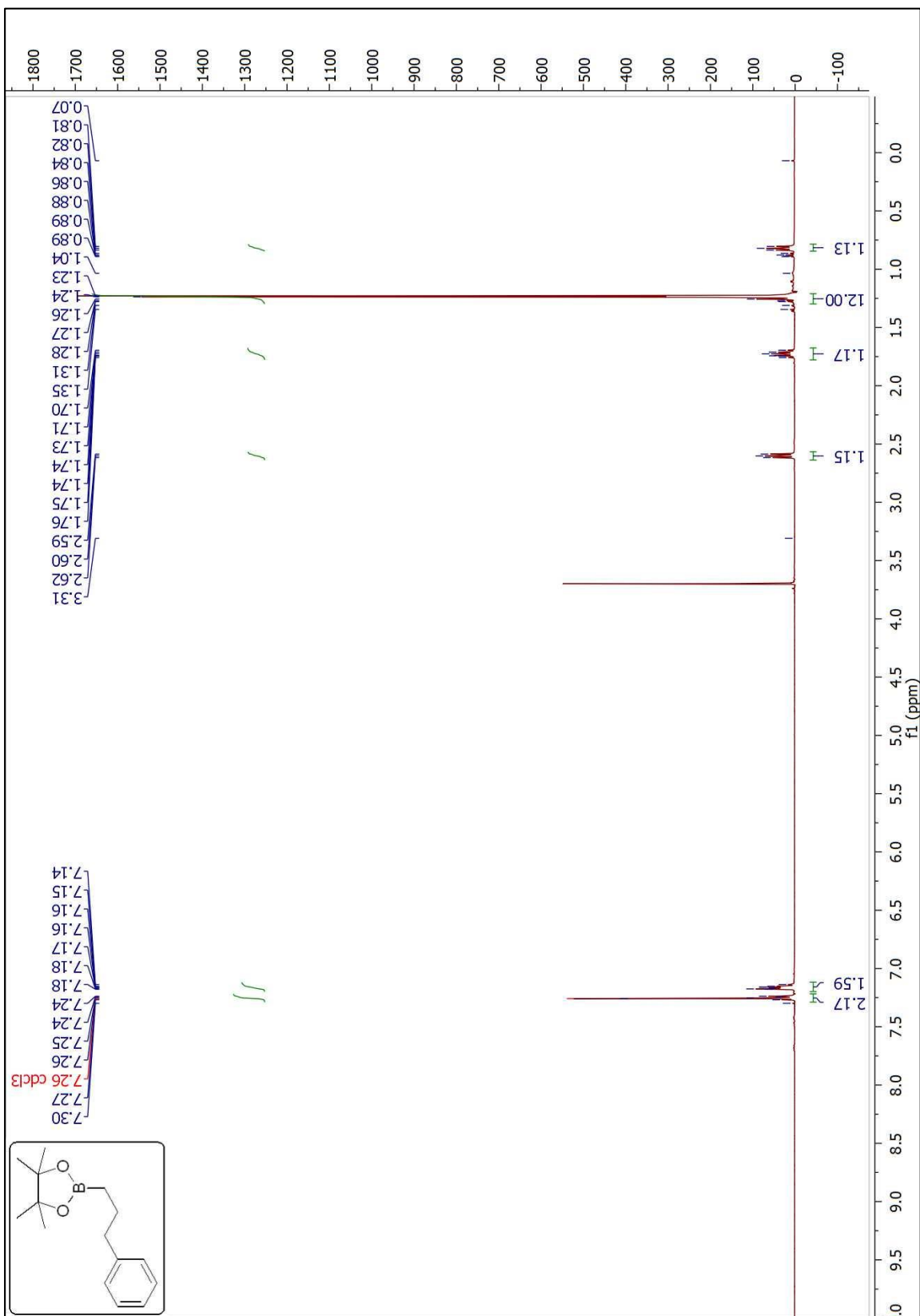


Figure 2.12.  $^1\text{H}$  NMR Spectrum of the protodeborylation product: 4,4,5,5-tetramethyl-2-(3-phenylpropyl)-1,3,2-dioxaborolane.

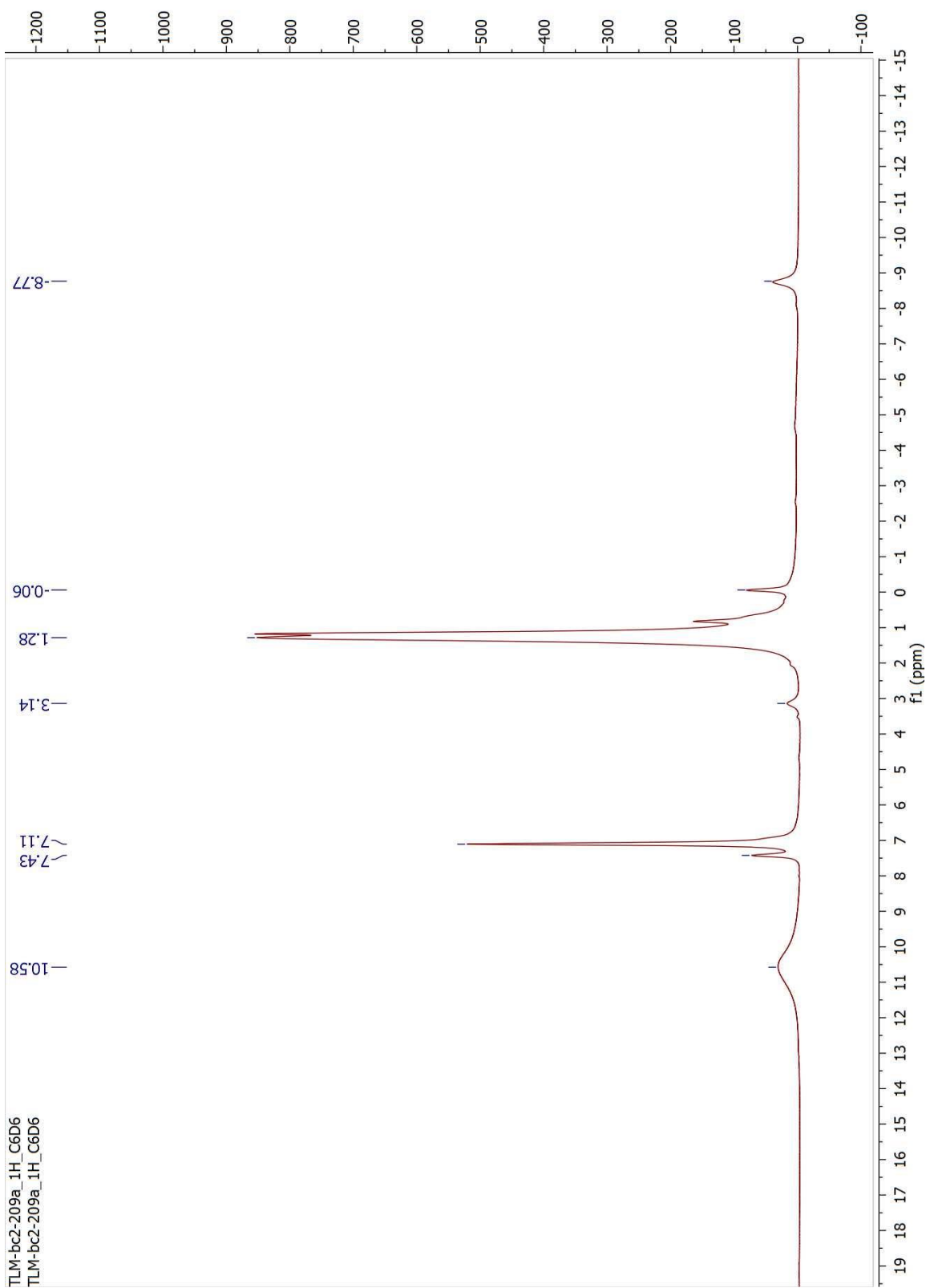


Figure 2.13.  $^1\text{H}$  NMR Spectrum of the first step in the synthesis of 2.21.

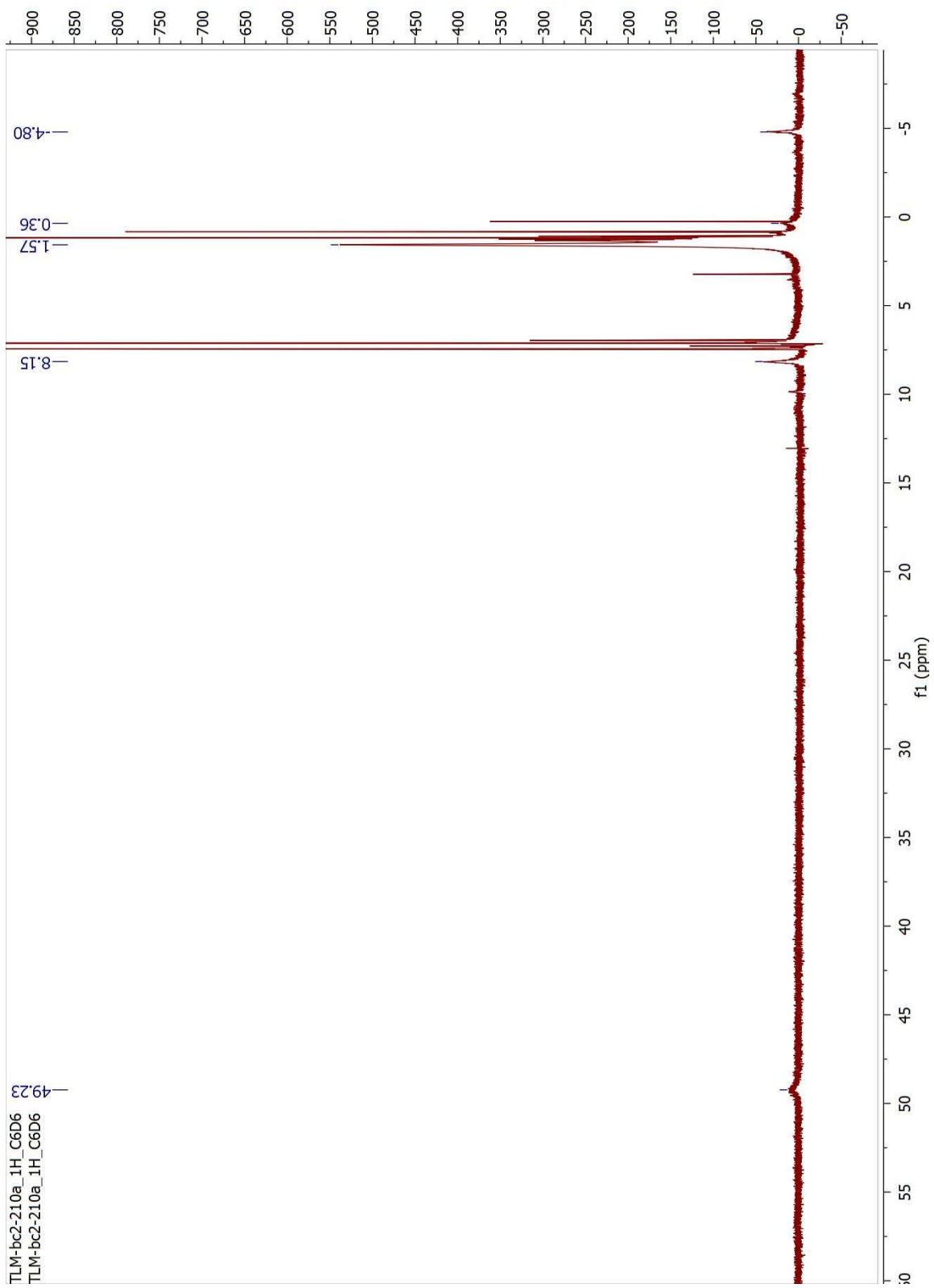


Figure 2.14.  $^1\text{H}$  NMR Spectrum of the second step in the synthesis of 2.21.

## 2.6 REFERENCES

- <sup>1</sup> (a) Kneebone, J. L.; Fleischauer, V. E.; Daifuku, S. L.; Shaps, A. A.; Bailey, J. M.; Iannuzzi, T. E.; Neidig, M. L. *Inorg. Chem.* **2016**, *55*, 272. (b) Kawamura, S.; Nakamura, M. *Chem. Lett.* **2013**, *42*, 183. (c) Ghorai, S. K.; Jin, M.; Hatakeyama, T.; Nakamura, M. *Org. Lett.* **2012**, *14*, 1066.
- <sup>2</sup> Hatakeyama, T.; Fujiwara, Y.; Okada, Y.; Itoh, T.; Hashimoto, T.; Kawamura, S.; Ogata, K.; Takaya, H.; Nakamura, M. *Chem. Lett.* **2011**, *40*, 1030.
- <sup>3</sup> Small, B. L.; Brookhart, M.; Bennett, A. M. A. *J. Am. Chem. Soc.* **1998**, *120*, 4049.
- <sup>4</sup> Britovsek, G. J. P.; Gibson, V. C.; Kimberley, B. S.; Maddox, P. J.; McTavish, S. J.; Solan, G. A.; White, A. J. P.; Williams, D. J. *Chem. Commun.* **1998**, 849.
- <sup>5</sup> (a) Gibson, V. C.; Redshaw, C.; Solan, G. A. *Chem. Rev.* **2007**, *107*, 1745. (b) Karpinić, S. S.; McGuinness, D. S.; Britovsek, G. J. P.; Patel, J. *Organometallics* **2012**, *31*, 3439. (c) Trovitch, R. J.; Lobkovsky, E.; Eckhardt, B.; Chirik, P. J. *Organometallics* **2008**, *27*, 1470. (d) Obligacion, J. V.; Chirik, P. J. *Org. Lett.* **2013**, *15*, 2680. (e) Tondreau, A. M.; Atienza, C. C. H.; Weller, K. J.; Nye, S. A.; Lewis, K. M.; Delis, J. G. P.; Chirik, P. J. *Science* **2012**, *335*, 567.
- <sup>6</sup> Bart, S. C.; Chlopek, K.; Bill, E.; Bouwkamp, M. W.; Lobkovsky, E.; Neese, F.; Wieghardt, K.; Chirik, P. J. *J. Am. Chem. Soc.* **2006**, *128*, 13901.
- <sup>7</sup> Tondreau, A. M.; Milsman, C.; Patrick, A. D.; Hoyt, H. M.; Lobkovsky, E.; Wieghardt, K.; Chirik, P. J. *J. Am. Chem. Soc.* **2010**, *132*, 15046.
- <sup>8</sup> Tondreau, A. M.; Milsman, C.; Lobkovsky, E.; Chirik, P. J. *Inorg. Chem.* **2011**, *50*, 9888.
- <sup>9</sup> Darmon, J. M.; Steiber, S. C. E.; Sylvester, K. T.; Fernández, I.; Lobkovsky, E.; Semproni, S. P.; Bill, E.; Wieghardt, K.; DeBeer, S.; Chirik, P. J. *J. Am. Chem. Soc.* **2012**, *134*, 17125.
- <sup>10</sup> Bouwkamp, M. W.; Bowman, A. C.; Lobkovsky, E.; Chirik, P. J. *J. Am. Chem. Soc.* **2006**, *128*, 13340.
- <sup>11</sup> Daifuku, A. L.; Al-Afyouni, M. H.; Snyder, B. E. R.; Kneebone, J. L.; Neidig, M. L. *J. Am. Chem. Soc.* **2014**, *136*, 9132.
- <sup>12</sup> Martin, R.; Fürstner, A. *Angew. Chem. Int. Ed.* **2004**, *43*, 3955.
- <sup>13</sup> Trovich, R. J.; Lobkovsky, E.; Chirik, P. J. *J. Am. Chem. Soc.* **2008**, *130*, 11631.
- <sup>14</sup> (a) Bedford, R. B.; Brenner, P. B.; Carter, E.; Carvell, T. W.; Cogswell, P. M.; Gallagher, T.; Harvey, J. N.; Murphy, D. M.; Neeve, E. C.; Nunn, J.; Pye, D. R. *Chem. – Eur. J.* **2014**, *20*, 7935. (b) Hatakeyama, T.; Hashimoto, T.; Kondo, Y.; Fujiwara, Y.; Seike, H.; Takaya, H.; Tamada, Y.; Ono, T.; Nakamura, M. *J. Am. Chem. Soc.* **2010**, *132*, 10674.
- <sup>15</sup> Coombs, J. R.; Zhang, L.; Morken, J. P. *J. Am. Chem. Soc.* **2014**, *136*, 16140.
- <sup>16</sup> Mlynarski, S. N.; Schuster, C. H.; Morken, J. P. *Nature* **2014**, *505*, 386.
- <sup>17</sup> Potter, B.; Syzmaniak, A. A.; Edelstein, E. K.; Morken, J. P. *J. Am. Chem. Soc.* **2014**, *136*, 17918.
- <sup>18</sup> Hong, K.; Liu, X.; Morken, J. P. *J. Am. Chem. Soc.* **2014**, *136*, 10581.
- <sup>19</sup> Potter, B.; Edelstein, E. K.; Morken, J. P. *Org. Lett.* **2016**, *18*, 3286.
- <sup>20</sup> Kawamura, S.; Nakamura, M. *Chem. Lett.* **2013**, *42*, 183.
- <sup>21</sup> (a) Caheiz, G.; Gager, O.; Buendia, J.; Patinote, C. *Chem. – Eur. J.* **2012**, *18*, 5860. (b) Guo, W.-J.; Wang, Z.-X. *Tetrahedron* **2013**, *69*, 9580. (c) Cahiez, G.; Avedissian, H. *Synthesis* **1998**, 1199.
- <sup>22</sup> (a) Ghorai, S. K.; Jin, M.; Hatakeyama, T.; Nakamura, M. *Org. Lett.* **2012**, *14*, 1066. (b) Daifuku, S. L.; Kneebone, J. L.; Snyder, B. E. R.; Neidig, M. L. *J. Am. Chem. Soc.* **2015**, *137*, 11432.
- <sup>23</sup> Synthesized by Byers group member Aman Kaur. Manna, C. M.; Kaur, A.; Yablon, L. M.; Haefner, F.; Li, B.; Byers, J. A. *J. Am. Chem. Soc.* **2015**, *137*, 14232.
- <sup>24</sup> Hoyt, J. M.; Sylvester, K. T.; Semproni, S. P.; Chirik, P. J. *J. Am. Chem. Soc.* **2013**, *135*, 4862.
- <sup>25</sup> Tseng, K.-N. T.; Kampf, J. W.; Szymczak, N. K.; *ACS Catal.* **2015**, *5*, 411.
- <sup>26</sup> (a) Biernesser, A. B.; Li, B.; Byers, J. A. *J. Am. Chem. Soc.* **2013**, *135*, 16553. (b) Biernesser, A. B.; Delle Chiaie, K. R.; Curley, J. B.; Byers, J. A. *Angew. Chem. Int. Ed.* **2016**, *55*, 5251-5254.
- <sup>27</sup> Sauvage, X.; Demonceau, A.; Delaude, L. *Adv. Synth. Catal.* **2009**, *351*, 2031-2038.
- <sup>28</sup> Burger, B. J.; Bercaw, J. E.; *New Development in the Synthesis, Manipulation and Characterization of Organometallic Compounds*; American Chemical Society: Washington DC, 1987; Vol. 357.
- <sup>29</sup> Appukuttan, V. K.; Liu, Y.; Son, B. C.; Ha, C.-S.; Suh, H.; Kim, I. *Organometallics* **2011**, *30*, 2285.
- <sup>30</sup> All PDI ligands were synthesized using the methods described in – and PDI ligands bearing cyclohexyl and 4-fluorophenyl imines were characterized according to – Görl, C.; Englemann, T.; Alt, H. G. *Applied Catalysis A: General* **2011**, *403*, 25-35. PDI ligands bearing 2,6-diisopropylphenyl and 2,6-dimethylphenyl imines and their respective iron complexes were characterized according to: Britovsek, G. J.; Bruce, M.; Gibson, V. C.; Kimberley, B. S.; Maddox, P. J.; Mastroianni, S.; McTavish, S. J. Redshaw, C.; Solan, G. A.; Strömberg, S.; White, A. J. P.; Williams, D. J. *J. Am. Chem. Soc.* **1999**, *121*, 8728-8740.

- 
- <sup>31</sup> Sun, C.; Potter, B.; Morken, J. P. *J. Am. Chem. Soc.* **2014**, *136*, 6534.
- <sup>32</sup> Manna, C. M.; Kaur, A.; Yablon, L. M.; Haeffner, F.; Li, B.; Byers, J. A. *J. Am. Chem. Soc.* **2015**, *137*, 14232.
- <sup>33</sup> Atack, T. C.; Lecker, R. M.; Cook, S. R. *J. Am. Chem. Soc.* **2014**, *136*, 9521.
- <sup>34</sup> Morioka, Y.; Matsuoka, A.; Binder, K.; Knappett, B. R.; Wheatley, A. E. H.; Naka, H. *Catal. Sci. Technol.* **2016**, *6*, 5801.
- <sup>35</sup> Combe, S. H.; Hosseini, A.; Parra, A.; Schreiner, P. R. *J. Org. Chem.* **2017**, *82*, 2407.
- <sup>36</sup> Sergeev, M. E.; Morgia, F.; Lazari, M.; Wang, C. Jr.; van Dam, R. M. *J. Am. Chem. Soc.* **2015**, *137*, 5686.
- <sup>37</sup> Caheiz, G.; Lefèvre, N.; Poizat, M.; Moyeux, A. *Synthesis* **2013**, *45*, 231.
- <sup>38</sup> Gieshoff, T. N.; Chakraborty, U.; Villa, M.; Jacobi von Wangelin, A. *Angew. Chem. Int. Ed.* **2017**, *46*, 3585.

### 3.0 ELECTRONIC STRUCTURE ANALYSES AND CATALYTIC APPLICATIONS OF CARBENO(DIAMIDINE) IRON COMPLEXES

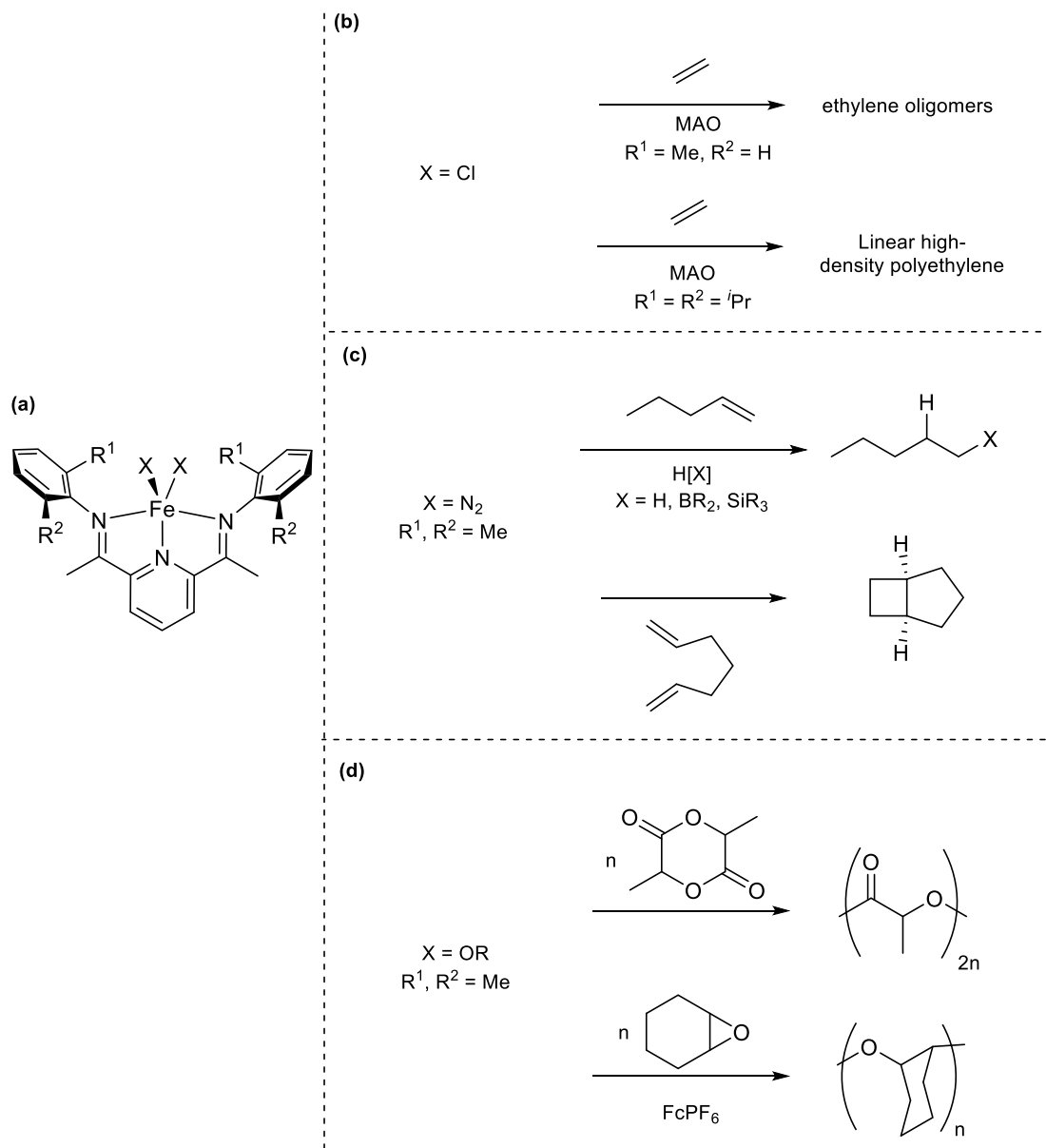
#### 3.1 INTRODUCTION

##### 3.1.1 Pyridyl(Diimine) Ligands – An Inspiration

During the past several decades, iron and cobalt complexes bearing 2,6-bis(imino) pyridine (pyridyl diimine; PDI) ligands have emerged as robust catalysts for a wide variety of transformations (**Scheme 3.1a**). Originally developed as ethylene polymerization catalysts in the late 1990's by Brookhart, Bennet, and Gibson, the catalysts showed activity that rivaled that of early transition-metal metallocene catalysts.<sup>1,2</sup> Notably, the ligands were discovered to be highly tunable; facile steric modifications of the ligand allowed for the selective formation of  $\alpha$ -olefins, oligomers, and polymers of ethylene,<sup>3</sup> shown in **Scheme 3.1b**. When acetylene was used, however, selective cyclotrimerization was seen.<sup>4</sup>

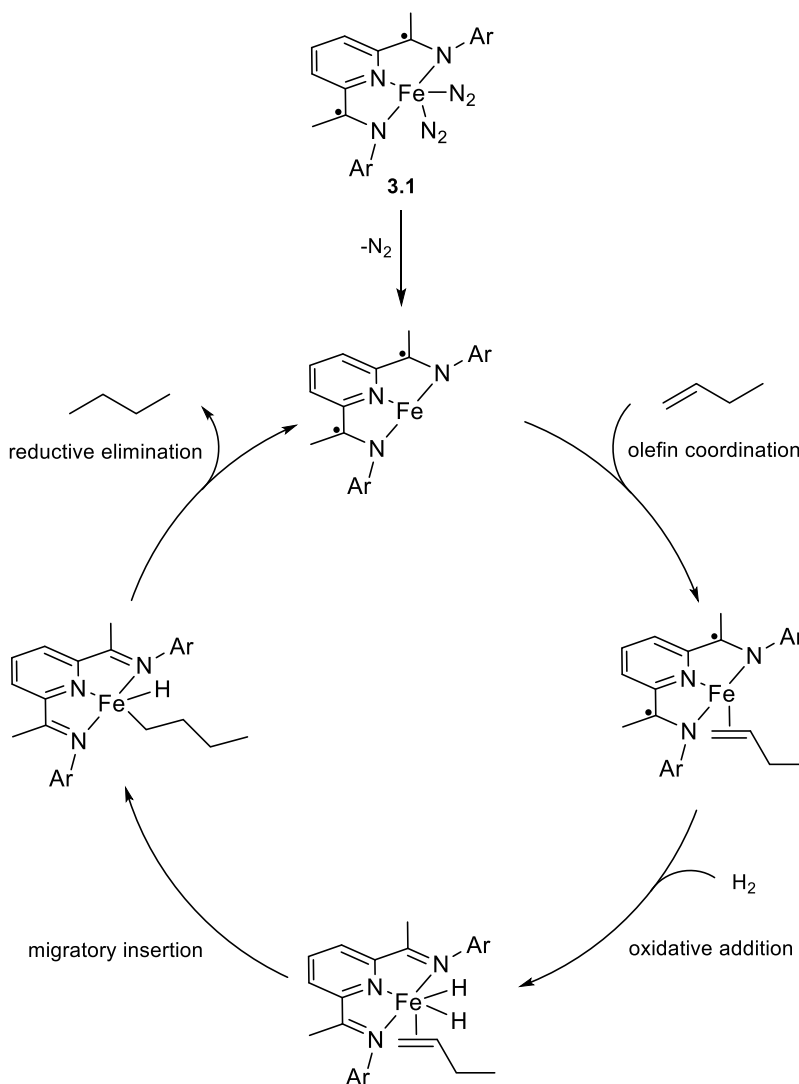
In subsequent years, Paul Chirik and coworkers expanded the reactivity scope of these iron- and cobalt-PDI complexes by examining alternative oxidation states. The iron (0) PDI dinitrogen complex that can be formed upon the sodium mercury amalgam reduction of the parent iron(II) PDI dichloride complex<sup>5</sup> was found to be active for several transformations known to proceed via low-valent intermediate species, including hydrogenation,<sup>6</sup> hydroboration,<sup>7</sup> and hydrosilylation<sup>8</sup> of alkenes, as well as [2+2] cycloadditions of alkenes<sup>9</sup> and dienes<sup>10</sup> (**Scheme 3.1c**). The Byers group later discovered that PDI iron alkoxides are active for the polymerization of lactide and epoxides (**Scheme 3.1d**).<sup>11</sup> (PDI)Fe(OR)<sub>2</sub> complexes facilitate lactide polymerization while cationic [(PDI)Fe(OR)<sub>2</sub>][PF<sub>6</sub>] species allow for the polymerization of epoxides, and *in situ* oxidation

of the former to the latter (and *vice versa*) allows for the formation of block copolymers.<sup>12</sup> Furthermore, steric modification of the PDI iron alkoxide complexes leads to *in situ* desymmetrization and the generation of stereocontrolled poly(lactic acid).<sup>13</sup>



**Scheme 3.1. Representative examples of the reactivity of iron bis(imino) pyridine complexes.**<sup>3,6-11</sup>

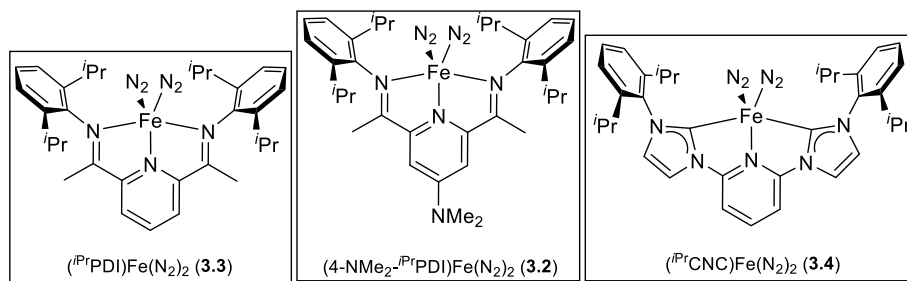
As discussed in **Chapter 2**, iron PDI complexes have unique redox properties.<sup>14</sup> An example of the utility of redox active ligands is shown in **Scheme 3.2**.<sup>5,6</sup> The reduced nature of complex **3.1** allows for the oxidative addition of molecular hydrogen, while the detrimental effects of iron(0) are avoided. When oxidative addition occurs, it is the PDI ligand, not the metal center, that undergoes the two electron oxidation. Likewise, the reductive elimination occurs via a two-electron reduction of the imine arms of the ligand.



**Scheme 3.2.** The proposed catalytic cycle for the hydrogenation of olefins by an iron (0) complex containing a redox non-innocent PDI ligand.<sup>5,6</sup> Ar = 2,6-diisopropylphenyl.

This privileged ligand class has attracted much attention in recent years, with many studies focused on slight alterations of the ligand in order to probe the relationship between structure and reactivity. A significant amount of this work has focused on the variation of the imine moieties, although a fair number of alterations to the central  $\sigma$  – donor have also emerged.<sup>15</sup> The Chirik group exhaustively screened many different variations of PDI complexes, including (4-NMe<sub>2</sub>-<sup>i</sup>PrPDI)Fe(N<sub>2</sub>)<sub>2</sub>, **3.2**, which bears substitution at the *para* position of the pyridine moiety.<sup>16</sup> A direct comparison between (<sup>i</sup>PrPDI)Fe(N<sub>2</sub>)<sub>2</sub> (**3.3**) and **3.2** revealed that the electron rich **3.2** is a more effective hydrogenation catalyst (**Table 3.1**). Ethyl 3-methylbut-2-enoate (entry 1) is 65 % converted to the hydrogenation product in 24 hours with complex **3.3**, yet is more than 95 % converted in less than a third of that time when using **3.2**. Similarly, (*E*)-prop-1-ene-1,2-diyldibenzene (entry 2) converts 12 % and 76 % for **3.3** and **3.2**, respectively, in a 24-hour time period. Isoprene (entry 3), however, showed a decrease in conversion when using the more electron rich PDI catalyst. The sterically hindered compounds shown in entries 4 – 6 exhibit trace conversions for both complexes.

Danopolous and coworkers replaced the imine arms of the PDI scaffold with N-heterocyclic carbene (NHC) moieties to form iron (0) 2,6-bis(aryl-imidazol-2-ylidene) pyridine (CNC) complexes such as **3.4**.<sup>17</sup> The enhanced electron donating capabilities of the carbene moiety led to even more favorable hydrogenation results when screened by the Chirik group (**Table 3.1**).<sup>16</sup> For entry 1, almost complete conversion was seen in one hour, and the substrates in entries 2 and 3 reach ~ 90 % conversion in 12-15 hours. 1-methylcyclohexene (entry 4) shows 20 % conversion in 24 hours, which, albeit still low yielding, is higher than the 3 % previously seen with PDI complexes. Unfortunately, the group was unable to affect the hydrogenations of 2,3-dimethyl-1*H*-indene or 2,3-dimethylbut-2-ene (entries 5 and 6, respectively) with any of these complexes.



1		65 % (24 h)	> 95 % (7 h)	> 95 % (1 h)
2		12 % (24 h)	76 % (24 h)	89 % (12 h)
3		32 % (24 h)	15 % (24 h)	95 % (15 h)
4		0 % (24 h)	3 % (24 h)	20 % (24 h)
5		3 % (48 h)	3 % (48 h)	4 % (48 h)
6		0 % (24 h)	0 % (24 h)	0 % (24 h)

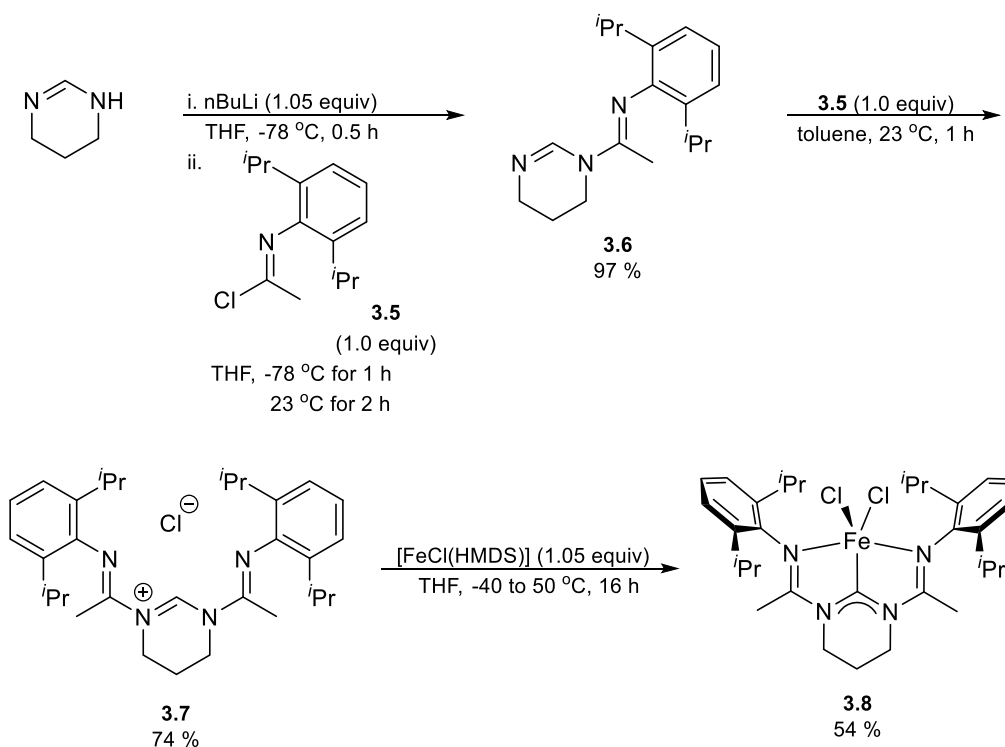
**Table 3.1. Direct comparison of PDI and CNC ligands.<sup>16</sup> Reported as: conversion (time).**

The Byers group was inspired by these discoveries to focus on the replacement of the central  $\sigma$  – donor, rather than the imine arms, with an N-heterocyclic carbene, which is notably absent from the literature.<sup>18</sup> It was hypothesized that a central NHC moiety would greatly increase the electron density of the metal center, even more so than with the CNC complexes, and lead to greater catalytic ability.

### 3.1.2 Development of Carbeno(Diamidine) Ligands

Dr. Hilan Kaplan, a former doctoral student in the Byers group, pioneered the development of an iron complex bearing a tridentate carbenodiamidine (CDA) ligand.<sup>18</sup> It is important to note that, at the advent of this project, this class of iron-NHC ligation had not been reported, although Lavoie and coworkers published similar results simultaneous to the Byers group.<sup>19</sup>

The synthesis of such ligands was achieved via the series of steps shown in **Scheme 3.3**.<sup>18</sup> Commercially available 1,4,5,6-tetrahydropyrimidine was deprotonated by *n*-butyl lithium, then treated with *N*-(2,6-diisopropylphenyl) acetimidoyl chloride, **3.5**,<sup>20</sup> to form species **3.6** in high yields. Upon treatment of **3.6** with another equivalent of **3.5**, the desired ligand **3.7** was achieved. **3.7** was metalated *via* treatment with a premixed solution of iron dichloride and NaHMDS to form complex **3.8**.



**Scheme 3.3.** Synthesis of CDA complex **3.8**.<sup>18</sup>

X-ray crystallographic analysis, shown in **Figure 3.1a**, confirmed the structure of **3.8** as a pentacoordinate complex bearing distorted square planar geometry that is very similar to that of the analogous PDI complex.<sup>18</sup> Interestingly, the crystal structure reveals that this complex contains one of the shortest iron-NHC bond lengths, 1.812 (2) Å, and is significantly shorter than that of the analogous PDI complex, 2.091 (3) Å,<sup>21</sup> reflecting the enhanced  $\sigma$ -donation from the carbene moiety. The overall geometry was found to be much more acute than the PDI compounds, indicating a less open coordination sphere around the metal center. The cyclic voltammograms of (*i*PrPDI)FeCl<sub>2</sub> and (*i*PrCDA)FeCl<sub>2</sub> (**3.8**) further elucidated the difference in electronic structure. As seen in **Figure 3.1b**, the  $E_{1/2}$  value for the central transition (assigned as Fe(II)-Fe(III)) is shifted from 0.041 V for (*i*PrPDI)FeCl<sub>2</sub> to a lower potential of -0.096 V for **1.10**, indicating a more electron-rich metal center.

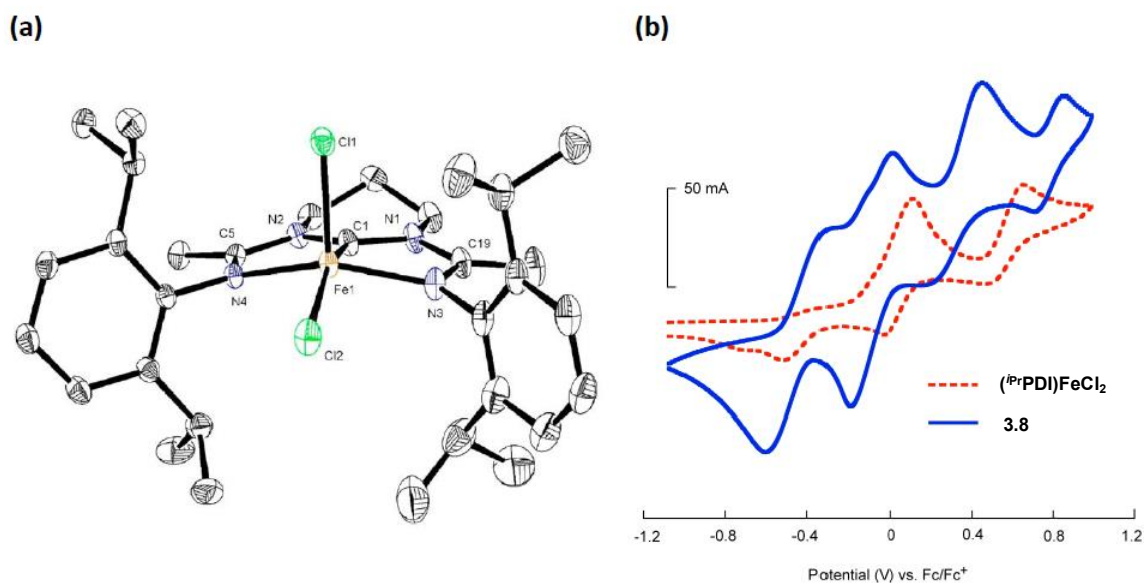
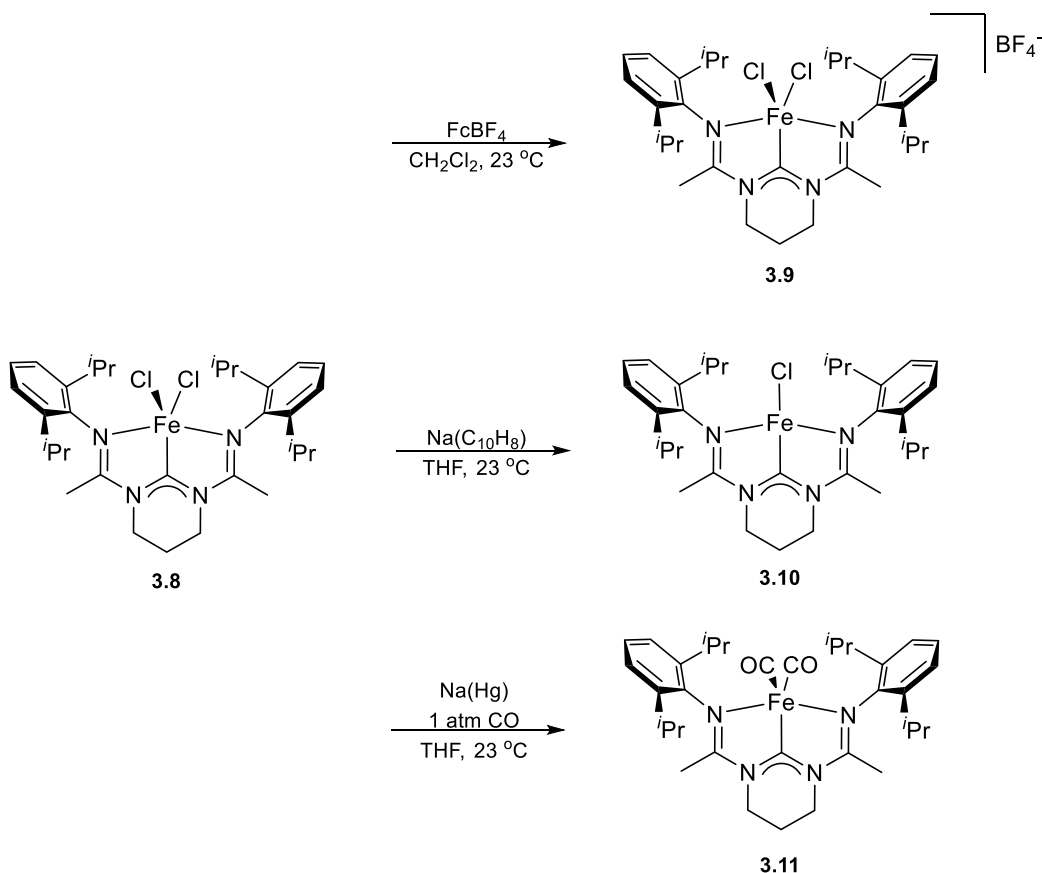


**Figure 3.1.** (a) ORTEP plot of **3.8** at the 50 % probability level. Hydrogen atoms and solvent molecules have been omitted for clarity. (b) Cyclic voltammogram comparison of **3.8** and (*i*PrPDI)FeCl<sub>2</sub>.<sup>18</sup>

It was clear from these initial studies that the new CDA iron complex exhibited exciting electronic and structural aspects that warranted further investigation. From the initial iron(II) CDA complex, three other oxidation states were synthesized. When treated with acetylferrocenium

tetrafluoroborate, **3.8** was readily converted into  $[(^i\text{PrCDA})\text{Fe(III)Cl}_2][\text{BF}_4]$  (**3.9**) (Scheme 3.4).<sup>22</sup> Reduction of **3.8** with one equivalent of sodium naphthalide yielded  $(^i\text{PrCDA})\text{Fe(I)Cl}$  (**3.10**) whereas reduction of **3.8** with excess sodium mercury amalgam in a CO atmosphere led to  $(^i\text{PrCDA})\text{Fe(0)(CO)}_2$  (**3.11**).<sup>23</sup> The structural and electronic properties of each complex were then examined.



**Scheme 3.4.** Synthesis of CDA complexes **3.9**, **3.10**, and **3.11**.<sup>22,23</sup>

### 3.1.2.1 Further Characterization of $(^i\text{PrCDA})\text{Fe(II)Cl}_2$ (**3.8**)

The solution magnetic moment of **3.8** in THF was found to be  $5.0\mu_{\text{B}}$  ( $\chi T = 3.1\text{ cm}^3\text{ K mol}^{-1}$ ) and in  $\text{CH}_2\text{Cl}_2$  to be  $4.6\mu_{\text{B}}$  ( $\chi T = 2.7\text{ cm}^3\text{ K mol}^{-1}$ ) at  $25\text{ }^\circ\text{C}$ , which are both consistent with a high spin iron(II) configuration.<sup>22</sup> Solid-state dc-magnetic susceptibility measurements of **3.8** were obtained with SQUID magnetometry from 2 K to 300 K (**Figure 3.2**), and complex temperature-dependent magnetic behavior was revealed. At low temperatures, a low magnetic moment was

observed which increased rapidly to a plateau in  $\chi T$  at intermediate temperatures. Further warming led to a gradual increase in magnetic moment. The plateau in  $\chi T$  is consistent with  $S = 1$  metal complexes, and the increase in magnetic moment suggests a spin state change to an  $S = 2$  ground state.

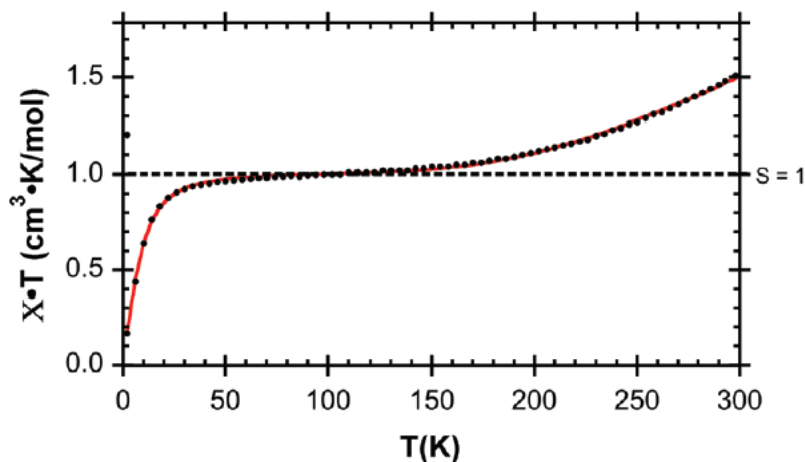


**Figure 3.2. Variable temperature solid-state dc-magnetization data for 3.8 using SQUID magnetometry. Filled symbols represent experimental data and the solid line represents simulated data.<sup>22</sup>**

Further characterization by zero field  $^{57}\text{Fe}$  Mössbauer at 90 K revealed an isomer shift of 0.31 mm/s and a quadrupole splitting of 2.14 mm/s, which is in good agreement with an intermediate spin  $S = 1$  iron(II) species (**Figure 3.3**). Increasing the temperature of the sample to 295 K led to significant changes in the spectrum. An increased isomer shift of 0.41 mm/s and a slightly decreased quadrupole splitting of 1.93 mm/s indicate a change in spin state of the complex, consistent with the SQUID magnetometry data. The presence of one set of peaks, rather than two, in the Mossbauer spectra, suggests either a rapid conversion between spin states or a quantum mechanical mixing of the two states when they are close in energy, the latter of which is less likely.

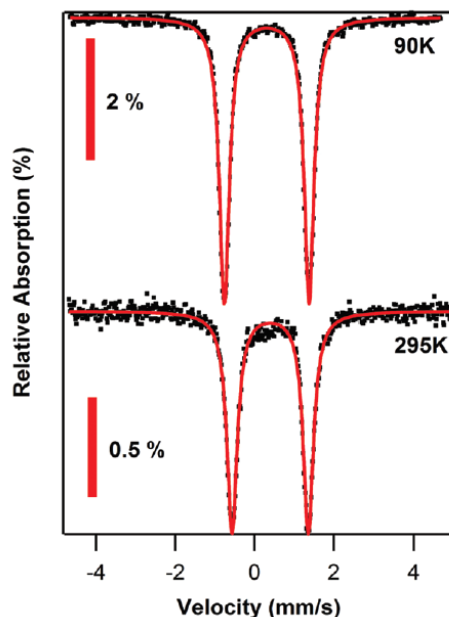


**Figure 3.3.** The zero field  $^{57}\text{Fe}$  Mössbauer spectra of 3.8 that reveals the temperature-dependence of the spin state of the complex.<sup>22</sup>

Unrestricted DFT calculations were employed to further corroborate the experimental data.<sup>22</sup> As shown in **Table 3.2**, intermediate spin state assignments are consistent with low temperature (100 K) Mössbauer measurements and bond lengths obtained from X-ray crystallographic analysis. Likewise, high spin state assignments are in good agreement with high temperature (250 K) experimental data.

Temperature/Spin State	Experimental		Calculated	
	100 K	250 K	S = 1	S = 2
Fe-C(carbene)	1.812(2)	1.882(3)	1.823	2.024
Fe-C(imine)	2.026(4)	2.104(4)	2.071	2.284
$\delta$	0.31 <sup>a</sup>	0.40 <sup>b</sup>	0.42	0.70
$ \Delta E_Q $	2.14 <sup>a</sup>	1.93 <sup>b</sup>	2.17	1.43

**Table 3.2.** Comparison of selected experimental bond lengths (Å) and Mössbauer parameters (mm/s) of 3.8 with DFT calculated values. <sup>a</sup>Measured at 90 K. <sup>b</sup>Measured at 295 K.<sup>22</sup>

### 3.1.2.2 Characterization of (*i*<sup>Pr</sup>CDA)Fe(0)(CO)<sub>2</sub> (**3.11**)

CDA complex **3.11** was revealed to be diamagnetic with C<sub>s</sub> symmetry by proton NMR spectroscopy.<sup>23</sup> X-ray crystallography of this compound indicated a distorted square planar geometry with CO ligands in the basal and axial positions (**Figure 3.4**). As previously seen with complexes of this type, the iron-carbene bond is unusually short, although not as short as parent complex **3.8**. Compared to **3.8**, **3.11** possesses contracted Fe-N(imine) and N(pyrimidine)-C(imine) bond distances as well as elongated C(imine)-N(imine) and C(pyrimidine)-N(pyrimidine) bond distances. A summary and comparison of bond lengths can be found in **Table 3.4** (*vide infra*)

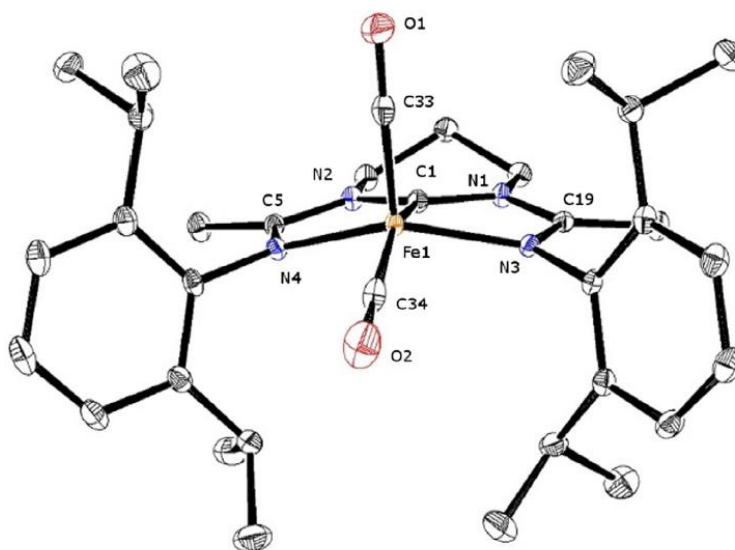


**Figure 3.4.** ORTEP plot of **3.11** with thermal ellipsoids represented at the 50% probability level. Hydrogen atoms and solvent molecules have been omitted for clarity.<sup>23</sup>

A comparison of C-O stretching frequencies of **3.11** to iron(0)(CO)<sub>2</sub> CNC and PDI complexes further supported the hypothesis that the CDA complex bears a more electron-rich iron center than the latter complexes (**Figure 3.5**).<sup>23</sup> (PDI)Fe(CO)<sub>2</sub> and (CNC)Fe(CO)<sub>2</sub> were shown to have symmetric and asymmetric stretching frequencies significantly higher than that of CDA analogue **3.11**.

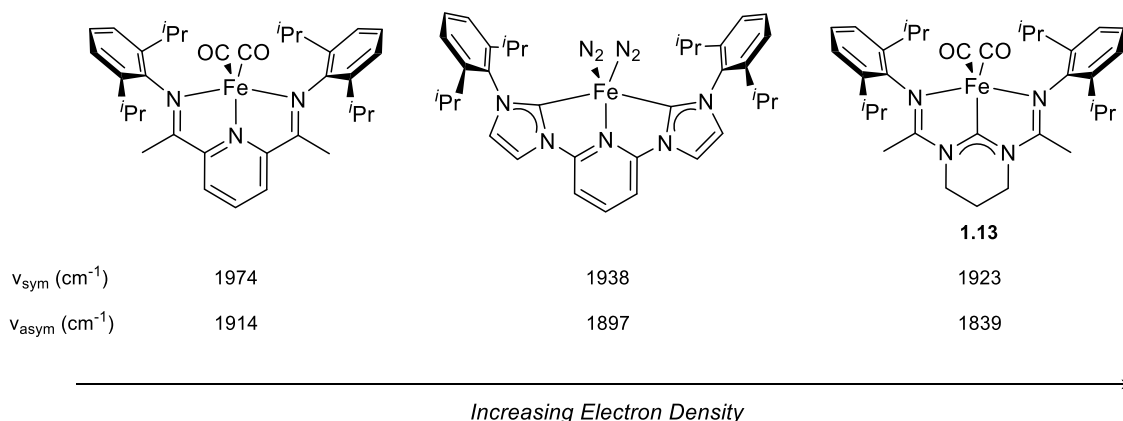


**Figure 3.5. Comparison of the IR stretching frequencies of iron(0)(CO)<sub>2</sub> PDI, CNC, and CDA carbonyl complexes.<sup>23</sup>**

The zero field <sup>57</sup>Fe Mössbauer spectrum of **3.11** revealed a single isomer shift at -0.133 mm/s and a quadrupole splitting of 1.19 mm/s at 90 K (**Figure 3.6**).<sup>23</sup> The Mössbauer fitting parameters are consistent with a low-spin iron(0) configuration, and are nearly identical to that of the equivalent PDI complex, which exhibits an isomer shift of 0.03 mm/s and a quadrupole splitting of 1.17 mm/s.

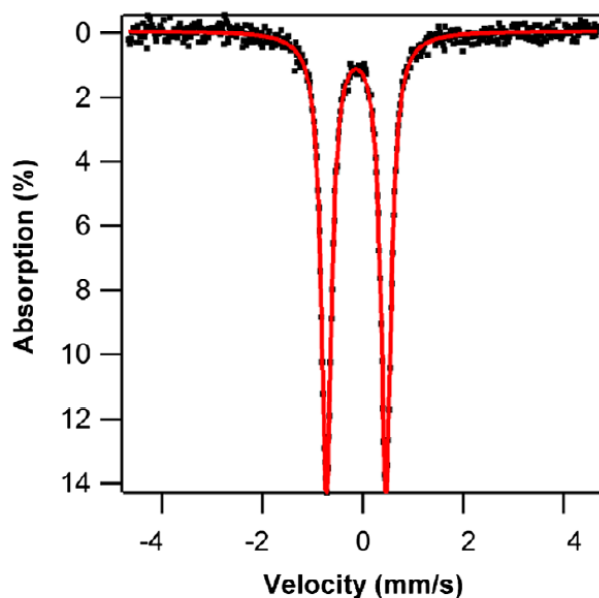


**Figure 3.6. The zero field <sup>57</sup>Fe Mössbauer spectrum of **3.11**.<sup>23</sup>**

Spin-unrestricted DFT calculations carried out by Kaplan and coworkers revealed a likely closed-shell configuration for **3.11**. The predicted bond metrics and Mössbauer parameters of **3.11** are in good agreement with a low-spin iron(0) complex with contributions from a low-spin iron(II) resonance hybrid, similar to the analogous pyridyl diimine complex.<sup>23</sup> There is a high degree of  $\pi$ -bonding between the iron center and carbeneodiamidine ligand, as expressed by the calculated molecular orbital diagram (**Figure 3.7**). The HOMO of the complex contains significant contributions from the metal  $d_{yz}$  orbital (38 %) and ligand-based  $b_2$  orbital (47 %). The large amount of electron density centered on the iron-carbene bond explains the unusually short bond length of **3.11**.

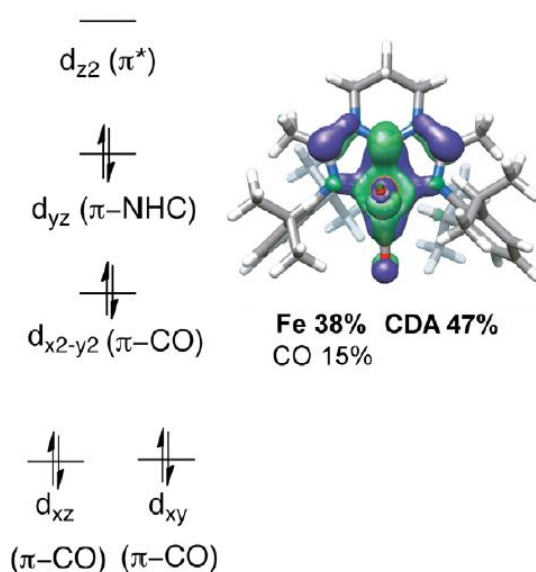


**Figure 3.7. Qualitative molecular orbital diagram of 3.11 as obtained from spin unrestricted DFT calculations by Kaplan and coworkers.<sup>23</sup>**

### 3.1.2.3 Characterization of $[(^{\text{Pr}}\text{CDA})\text{Fe}(\text{III})\text{Cl}_2][\text{BF}_4]$ (**3.9**)

Similar to **3.8**, **3.9** was shown to have temperature-dependent magnetic properties by variable temperature solid-state dc-magnetic susceptibility measurements (**Figure 3.8**).<sup>22</sup> The low-temperature plateau of  $\chi T$  is consistent with an  $S = 3/2$  assignment. Above 100 K, the magnetic moment increases to a value of  $\chi T = 3.13 \text{ cm}^3 \text{ K mol}^{-1}$ , which is lower than what is expected for an  $S = 5/2$  iron(III) assignment. The Mössbauer spectrum obtained was also consistent with an  $S = 3/2$  spin state at low temperatures, however, with increasing temperatures, the quadrupole splitting

decreased steadily, with no observed change in isomer shift. This is inconsistent for typical spin equilibrium behavior, and it was hypothesized that a quantum  $S = 3/2, 5/2$  admix could better explain this phenomenon.

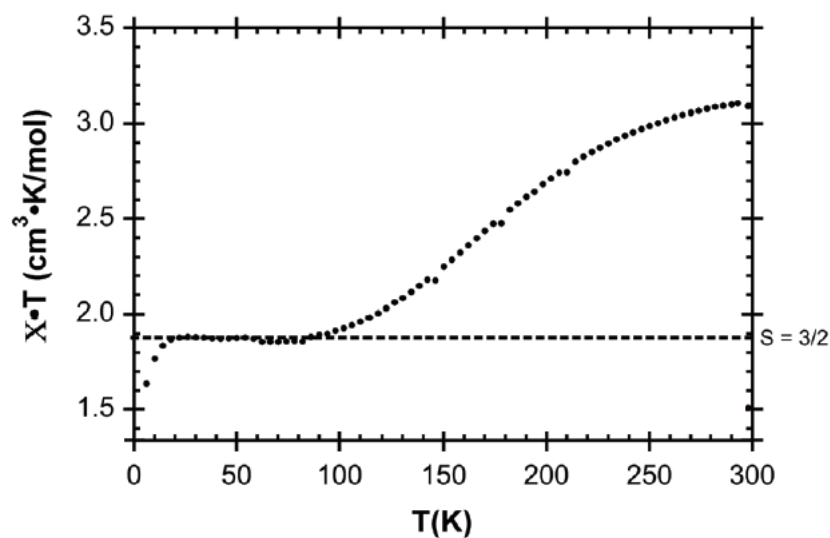


**Figure 3.8. Variable temperature solid-state dc-magnetization data for 3.9 using SQUID magnetometry.<sup>22</sup>**

Experimentally obtained bond lengths and Mössbauer parameters for **3.9** at low and high temperatures were compared to DFT calculations (**Table 3.3**).<sup>22</sup> As expected, the low temperature data were in good agreement with an intermediate-spin  $S = 3/2$  iron(III) species. At higher temperatures, the experimental values are more consistent with a high-spin  $S = 5/2$  species.

Temperature/Spin State	Experimental		Calculated	
	80 K	298 K	$S = 3/2$	$S = 5/2$
Fe-C(carbene)	1.908(2)	2.033(2)	1.904	2.105
Fe-C(imine)	2.031(9)	2.142(1)	2.102	2.262
$\delta$	0.18 <sup>a</sup>	0.21	0.32	0.33
$ \Delta E_Q $	2.21 <sup>a</sup>	1.58	2.78	1.67

**Table 3.3. Comparison of selected experimental bond lengths (Å) and Mössbauer parameters (mm/s) with calculated values for 3.9. <sup>a</sup>Measured at 100 K.<sup>22</sup>**

### 3.1.2.4 Characterization of (*i*PrCDA)Fe(I)Cl (**3.10**)

**3.10** was determined to be a distorted square planar complex with an iron-carbene bond that is the shortest bond of this type observed for the iron CDA complexes discovered thus far. Two distinctly different iron-C(imine) bond lengths were also observed (**Figure 3.9**).<sup>23</sup> The pyrimidine C-N bond distances have elongated as compared to **3.8**, and the C(imine)-N(pyrimidine) bond distances have lengthened. A comparison of bond lengths can be found in **Table 3.4** (*vide infra*).

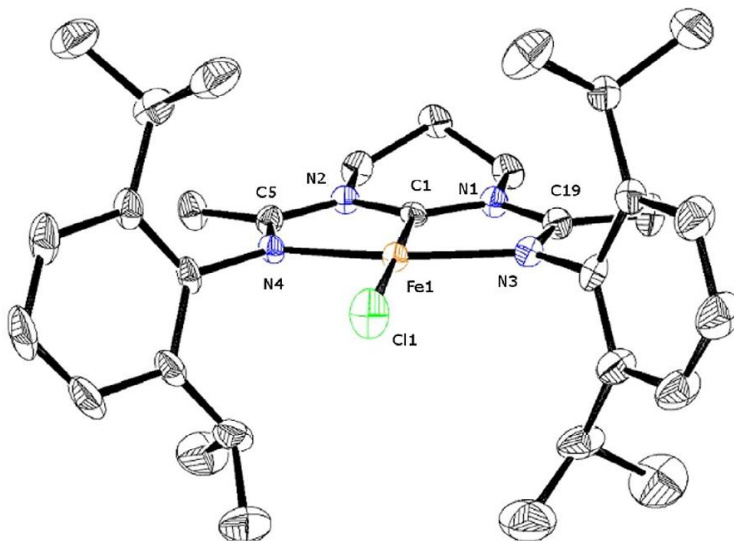


**Figure 3.9.** ORTEP plot of **3.10** with thermal ellipsoids represented at the 50% probability level. Hydrogen atoms and solvent molecules have been omitted for clarity.<sup>23</sup>

The zero-field <sup>57</sup>Fe Mössbauer spectrum at 90 K of **3.10** was shown to have contributions from three unique quadrupole doublets, which suggests the presence of three discrete iron centers in the sample (**Figure 3.10**). The major species was found to have an isomer shift of 0.25 mm/s and a quadrupole splitting of 1.94 mm/s, consistent with a low-spin iron(I)  $S = 1/2$  or an intermediate-spin iron(II)  $S = 3/2$  species. The two minor species in solution, decidedly impurities, comprised 16 % and 7 % of the iron present, with Mössbauer parameters of  $\delta = 0.96$  mm/s and  $|\Delta E| = 1.88$  mm/s, and  $\delta = -0.44$  mm/s and  $|\Delta E| = 1.88$  mm/s, respectively.

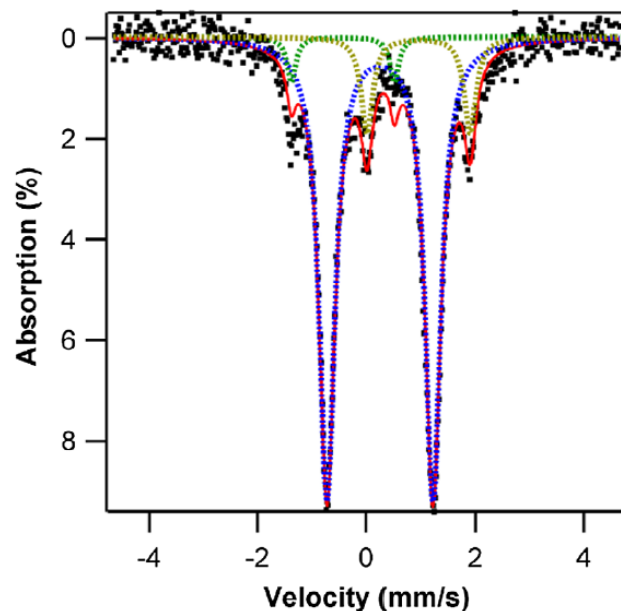


Figure 3.10. The zero field  $^{57}\text{Fe}$  Mössbauer spectrum of **3.10**.<sup>23</sup>

An EPR spectrum of **3.10** was obtained, and a mixture of species was again observed (Figure 3.11).<sup>23</sup> The major species, with a broad rhombic signal and  $g$ -values of 2.85, 2.21, and 1.91, was consistent with an  $S = 1/2$  spin-state containing a metal-based radical. This assignment of a low-spin species is consistent with Mössbauer parameters.

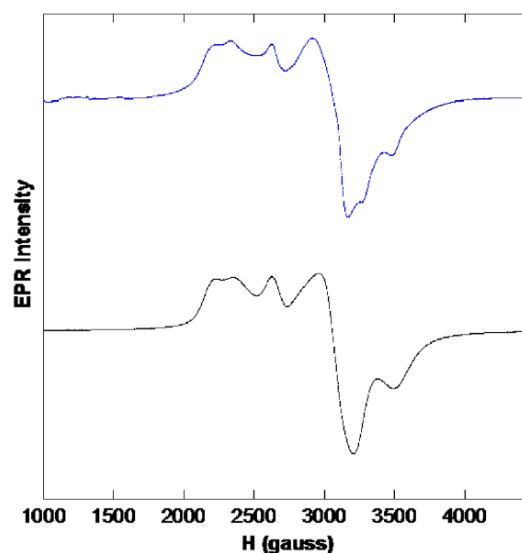
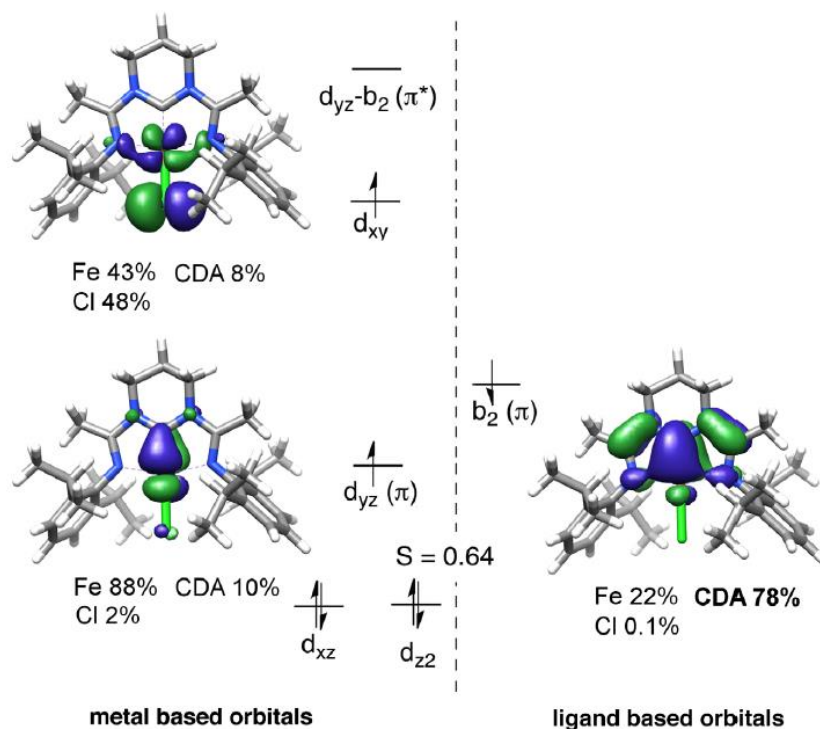


Figure 3.11. Comparison of experimental (blue) and simulated (black) EPR spectrum of **3.10** taken at 10 K.<sup>23</sup>

Unrestricted DFT calculations were carried out on **3.10**, considering both low-spin and high-spin electronic configurations.<sup>23</sup> A comparison of experimental and calculated bond lengths can be found in **Table 3.4** (*vide infra*). Better agreement is seen between the experimental bond lengths and the low-spin calculated bond lengths, which is consistent with previous data. A qualitative molecular orbital diagram for **3.10** indicates that two unpaired electrons exist on the iron center that are antiferromagnetically coupled with one unpaired electron on the CDA ligand (**Figure 3.12**). Significant electron density resides on both the metal  $d_{yz}$  orbital and the ligand-centered  $b_2$  orbital, with energy differences that suggest the aforementioned assignment, rather than a true  $\pi$ -bond.



**Figure 3.12. Qualitative molecular orbital diagram for 3.10.**<sup>23</sup>

### 3.1.2.5 Summary and Comparisons

Based on the above data, the following assignments for the analyzed CDA complexes were given: **3.8**: an intermediate-spin  $S = 1$  iron(II) at low temperatures that undergoes a spin-state change to a high-spin  $S = 2$  iron(II) species at higher temperatures; **3.9**: an intermediate-spin  $S = 3/2$  iron(III) at low temperatures that undergoes a spin-state change to a high-spin  $S = 5/2$  iron(III)

species at high temperatures; **3.10**: a low-spin iron(I) with two unpaired electrons on the metal center antiferromagnetically coupled to one unpaired electron on the ligand; **3.11**: low-spin iron(0) with minute contributions from a low-spin iron(II) resonance hybrid.<sup>22,23</sup> It is clear from these assignments that iron CDA complexes have unique electronic and magnetic structures. The single unpaired ligand-based electron and the two distinct iron-C(imine) bond lengths of **3.10** suggests similar redox non-innocent behavior as in iron PDI complexes. **Table 3.4** provides a comparison of bond lengths of the four complexes.

Bond	<b>3.8</b>	<b>3.9</b>	<b>3.10</b>	<b>3.11</b>
Fe-C(carbene)	1.812(2)	1.908(2)	1.791(3)	1.830(1)
Fe-N(imine <sub>1</sub> )	1.986(1)	2.031(9)	1.977(3)	2.028(2)
Fe-N(imine <sub>2</sub> )			2.028(2)	
C(pyrimidine)-N(pyrimidine)	1.360(3)	1.342(2)	1.390(4)	1.380(2)
C(imine)-N(imine)	1.306(2)	1.292(2)	1.308(5)	1.314(2)
C(imine)-N(pyrimidine)	1.374(3)	1.386(2)	1.369(4)	1.365(2)

**Table 3.4. A comparison of the bond lengths (Å) of CDA complexes 3.8, 3.9, 3.10, and 3.11. All crystallographic measurements were carried out at 100 K, except for 3.9, which was carried out at 80 K.**<sup>22,23</sup>

The spin density plot of **3.10** corroborates the hypothesis of redox activity by indicating the presence of two unpaired electrons on the metal center and one unpaired electron of the opposite charge delocalized throughout the CDA ligand, with the majority of the electron density residing on the carbene carbon (**Figure 3.13a**).<sup>23</sup> Spin density plots for **3.8** (**Figure 3.13b**) and **3.9** (**Figure 3.13c**) also display electron density on the CDA ligand, but to a lesser extent than **3.10**, suggesting that CDA ligands remain redox innocent for complexes in higher oxidation states.

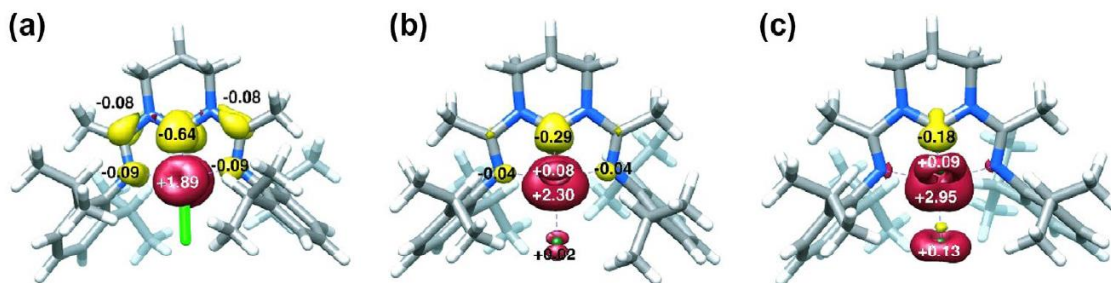


Figure 3.13. Spin density plots obtained by Mulliken population analysis for a) 3.10, b) 3.8, c) 3.9.<sup>23</sup>

### 3.1.3 Potential Catalytic Applications

Iron complexes have been utilized for a variety of catalytic applications as summarized in a review by Bolm and coworkers.<sup>24</sup> The reactions include, but are not limited to, addition reactions, substitution reactions, cycloadditions, hydrogenations, reductions, rearrangements, polymerizations, and cross-coupling reactions (see **Chapter 2**). Frequently, high-spin iron(II) and iron(III) complexes have been most effective,<sup>25</sup> and Gibson and coworkers performed a study correlating high spin states with activity for atom transfer radical polymerization (ATRP) reactions.<sup>26</sup> Low oxidation state complexes have also shown activity, yet these complexes generally have poorer air, water, and thermal stability.<sup>25</sup> Ligation in iron catalyzed systems has included phosphine-, heme-, carboxylic acid-, ammonium and phosphonium salt-, bidentate and tridentate nitrogen-, bisoxazoline-, and NHC-containing species. Notably rare in the literature are NHCs that are tridentate, such as the CDA and CNC ligands discussed above.<sup>18</sup>

#### 3.1.3.1 Olefin Hydrogenation

Olefin hydrogenation is a fundamental and extremely widely used chemical transformation, typically involving homogenous noble metal catalysts that follow predictable two-electron pathways.<sup>27</sup> The development of enantioselective olefin hydrogenations has profoundly transformed agricultural, pharmaceutical, and commodity chemical industries. Such reactions are characterized by high selectivity, exceptional atom economy, and high to quantitative yields.<sup>28</sup>

Iron PDI and CNC complexes have been screened as hydrogenation catalysts by Chirik and coworkers (**Table 3.1** *vide supra*).<sup>16</sup> The more electron-rich CNC ligands produced higher desired yields in shorter time periods for terminal, di- and tri-substituted olefins, yet tetra-substituted olefins remained unreacted. It was hypothesized by the Byers group that iron(0) CDA complex **3.8** would lead to better reactivity due to the enhanced electron density around the metal center, which is important for the key oxidative addition of H<sub>2</sub> in these transformations. As discussed in above, the Chirik group has shown that redox active ligands are beneficial for certain catalytic applications that proceed through oxidation and reduction mechanisms. The redox activity of reduced iron-CDA complexes may be equally valuable for catalytic activity.

For similar transition metal complexes that have shown reactivity toward hydrogenation of double bonds, a stepwise mechanism involving metal-ligand cooperativity has been proposed.<sup>29</sup> In such instances, oxidative addition of molecular hydrogen occurs cooperatively between the metal and the ligand. A hydride bound to the metal center and a proton centered on the ligand, as shown in **Figure 3.14**, are transferred to the unsaturated bond. In these instances, polarized double bonds are most active as the hydrogen moieties are transferred as positively and negatively charged species rather than as hydrogen atoms.

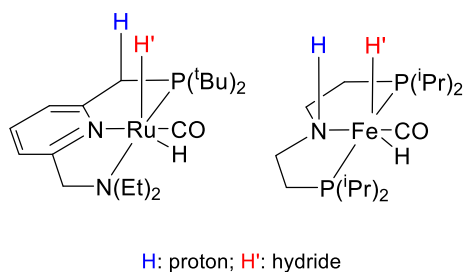
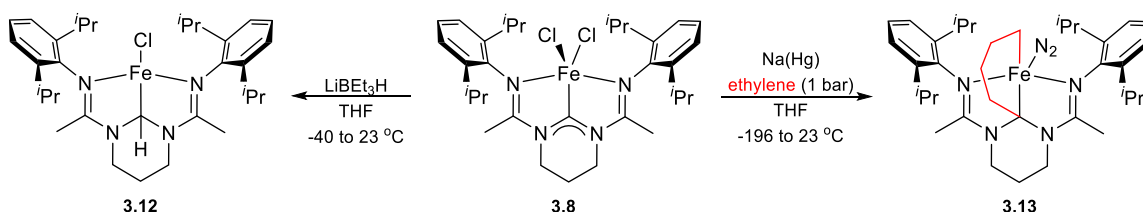


**Figure 3.14. Examples of bifunctional catalysts.**<sup>29</sup>

It has been shown by former Byers group members Dr. Hilan Kaplan and Jessica Drake that the NHC ligand participates in the reactivity of iron CDA complexes. In the presence of a hydride source, CDA species **3.8** is converted into iron(II) species **3.12**, where the hydride has been incorporated into the ligand scaffold (**Scheme 3.5**).<sup>30</sup> In the presence of excess sodium mercury amalgam and ethylene, complex **3.13** was formed in which an ethylene dimer bridged the

NHC carbon and the metal center.<sup>31</sup> Considering these observations, it is possible that iron CDA complexes will act as bifunctional catalysts.

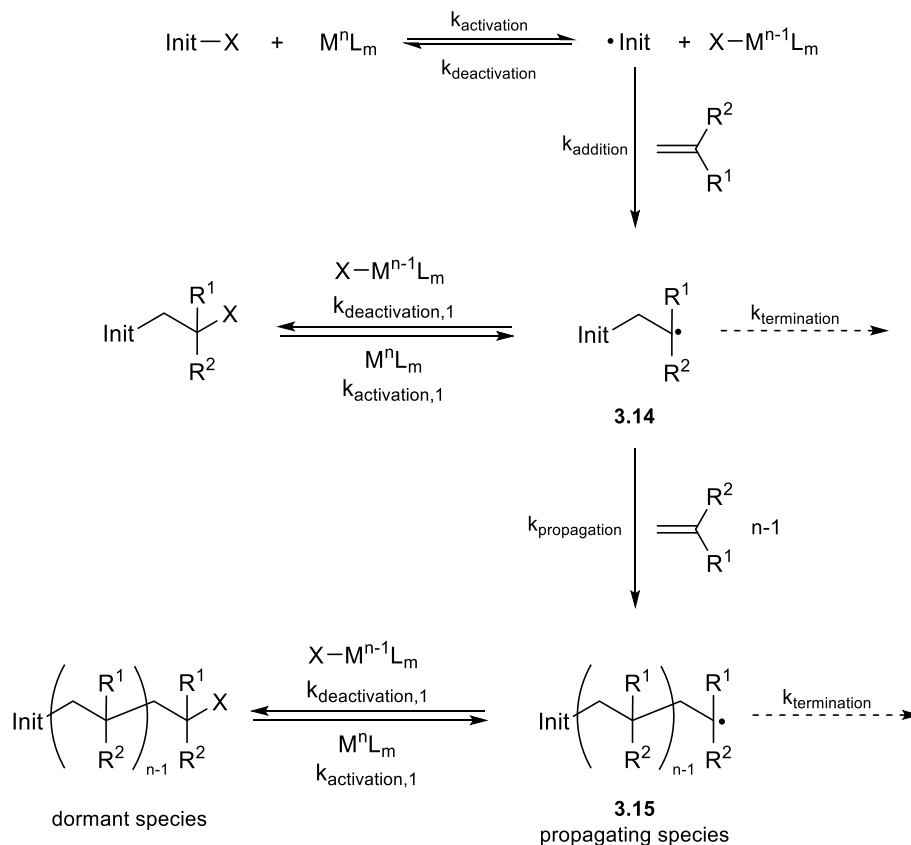


**Scheme 3.5.** The treatment of **3.8** with  $\text{LiBEt}_3\text{H}$  to form **3.12**<sup>30</sup> and the reduction of **3.8** with  $\text{Na}(\text{Hg})$  in the presence of ethylene to form **3.13**.<sup>31</sup>

The interesting electronic and redox properties of CDA ligands and the ability of iron CDA complexes to undergo temperature dependent spin transitions may enhance catalytic activity and lead to metal-ligand cooperative reaction pathways for olefin hydrogenation.

### 3.1.3.2 Atom Transfer Radical Polymerization

Atom transfer radical polymerization (ATRP) is a popular method for controlling radical polymerization of vinyl monomers that requires less rigorous conditions than ionic variations.<sup>32</sup> Krzysztof Matyjaszewski is an authority on ATRP, and has published over 100 reviews detailing the contributions his group and others have made to the field.<sup>33,34</sup> **Scheme 3.6** details the accepted mechanism of ATRP. An initiator is activated by a metal complex to generate a radical species which then adds to the vinyl monomer to generate radical species **3.14**. This species will then, ideally, propagate, leading to active species **3.15** which will continue to polymerize. Both of these species could potentially be deactivated by the oxidized metal species, leading to a dormant compound that can be reintroduced to the catalytic cycle *via* the reverse reaction. Alternatively, **3.14** and **3.15** could undergo termination steps to form species that cannot reenter the catalytic cycle. The key to ATRP is carefully controlling the rates of activation, deactivation, propagation, and termination in order to generate desired polymer lengths and dispersities.<sup>33</sup> In many cases, this can be achieved with careful catalyst choice.<sup>25,32,33,34</sup>



**Scheme 3.6. The accepted mechanism of atom transfer radical polymerization.<sup>33</sup>**

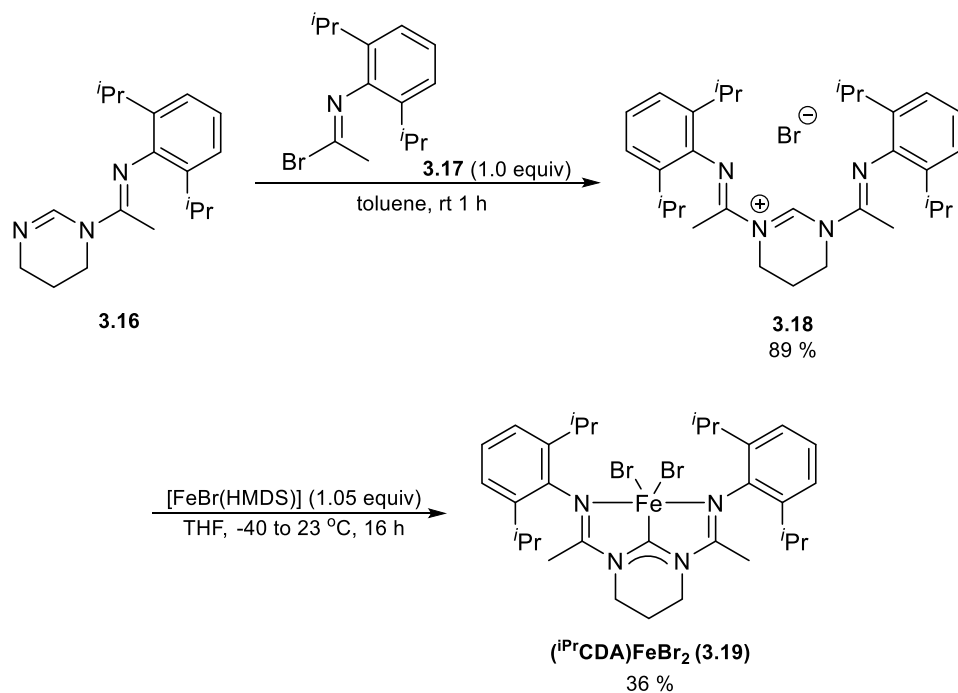
Iron PDI complexes were probed for ATRP activity by Gibson and coworkers.<sup>35</sup> It was noted that polymer dispersity and molecular weight control correlated well with oxidation potential of the complexes. Species with low oxidation potentials (-370 to -150 mV) and redox potentials (-280 to -70 mV) led to polymers with well controlled molecular weights and polydispersity indices of around 1.5, whereas those with higher oxidation potentials (180 to 260 mV) and redox potentials (330 to 410) led to uncontrolled molecular weights and broader dispersities. With a redox potential of -96 mV, unique electronic and structural properties, and similarity to iron PDI complexes, the Byers group hypothesized that **3.8** would be a promising catalyst for ATRP and similar reactions.

## 3.2 ELECTRONIC STRUCTURE COMPARISON OF PDI, CNC, AND CDA IRON COMPLEXES

Due to the aforementioned electronic uniqueness of PDI, CNC, and CDA ligands, further direct comparisons were necessary. In an effort to compare complexes that were as similar as possible in all aspects except the ligation to be examined, a CDA complex bearing ancillary bromide ligands was developed, as the CNC complexes cannot be formed with chloride ancillary ligands.<sup>36</sup> (<sup>i</sup>PrPDI)FeBr<sub>2</sub><sup>37</sup> and (<sup>i</sup>PrCNC)FeBr<sub>2</sub><sup>36</sup> were synthesized according to literature procedures.

### 3.2.1 Synthesis of (<sup>i</sup>PrCDA)FeBr<sub>2</sub>

A synthetic route was developed similar to that of the original CDA complex (**Scheme 3.7**). *N*-1-[1-(2,6-diisopropylphenylimino)ethyl]-4,5,6-trihydropyrimidine (**3.16**) was prepared according to the synthesis carried out by Dr. Kaplan.<sup>38</sup> The synthesis of *N*-(2,6-diisopropylphenyl)acetimidoyl bromide (**3.17**), while similar to that employed in the synthesis of (<sup>i</sup>PrCDA)FeCl<sub>2</sub>, required much more rigorous conditions due to the increased reactivity of the compound, and resulted in only 44 % yield, as compared to the 98 % yield achieved with the chloride analogue. Once **3.17** was obtained, the synthesis of (<sup>i</sup>PrCDA)<sup>+</sup> Br<sup>-</sup> ligand **3.18** was straightforward, again following the previously developed procedures. Difficulty arose while attempting to metalate **3.18**. Under the same conditions for the synthesis of (<sup>i</sup>PrCDA)FeCl<sub>2</sub>, a mixture of desired product and an unknown side product was formed, and the desired product was only isolable with prolonged crystallization. Even so, 21.2 % of **3.19** was obtained. The crystal structure of **3.19** is shown in **Figure 3.15**.



**Scheme 3.7. Synthesis of 3.19.**

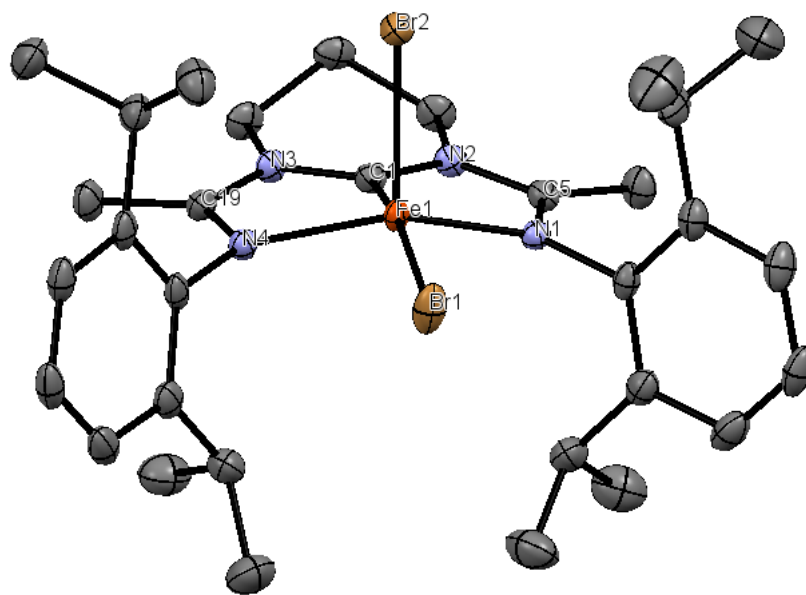
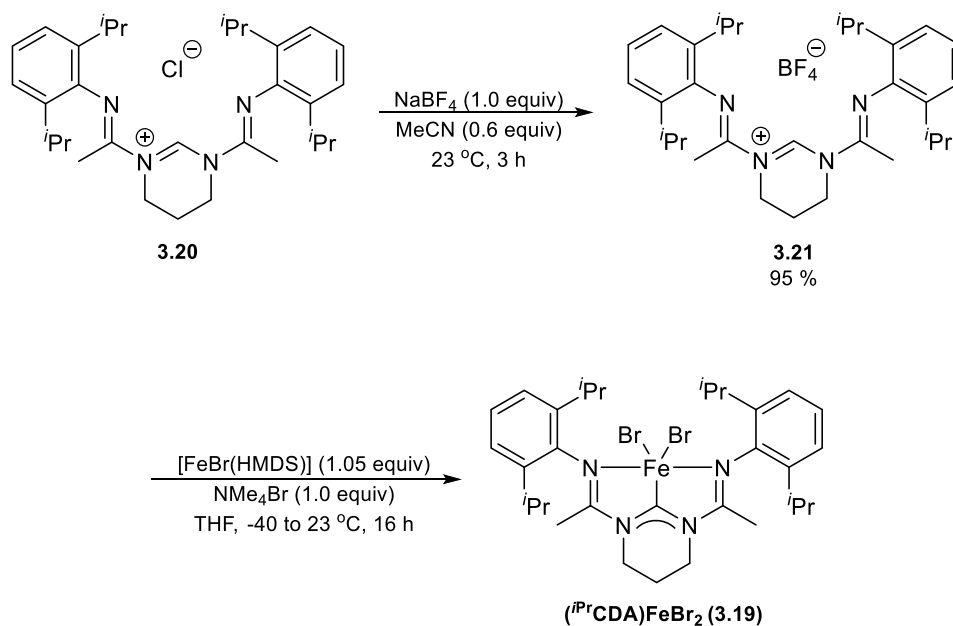


**Figure 3.15. ORTEP plot of 3.19 with thermal ellipsoids represented at the 50% probability level. Hydrogen atoms and solvent molecules have been omitted for clarity.**

The overall synthetic yield to form **3.19** was only 8 %, and in an attempt to attain higher yields and in order to ameliorate the difficulty in metalating **3.18**, an alternate synthetic route was pursued. The formation of **3.18** is much lower yielding than the formation of the analogous chloride species, so an ion-exchange route was attempted. (<sup>i</sup>PrCDA)<sup>+</sup> Cl<sup>-</sup> (**3.20**) was treated with sodium tetrafluoroborate in acetonitrile to form (<sup>i</sup>PrCDA)<sup>+</sup> BF<sub>4</sub><sup>-</sup> (**3.21**) in a 95 % yield (**Scheme 3.8**). The metalation of this species required a bromine source, and initially, tetrabutylammonium bromide was used, resulting in a mixture of desired product **3.19** and tetrabutylammonium tetrafluoroborate that could not be separated due to similar solubility profiles. The use of cetyltrimethylammonium bromide led to similar results. Finally, it was found that the use of tetramethylammonium bromide led to a product mixture that was easily separated by recrystallization in a 2:3:2 mixture of diethyl ether, methylene chloride, and tetrahydrofuran to give a 30 % yield of **3.19**.

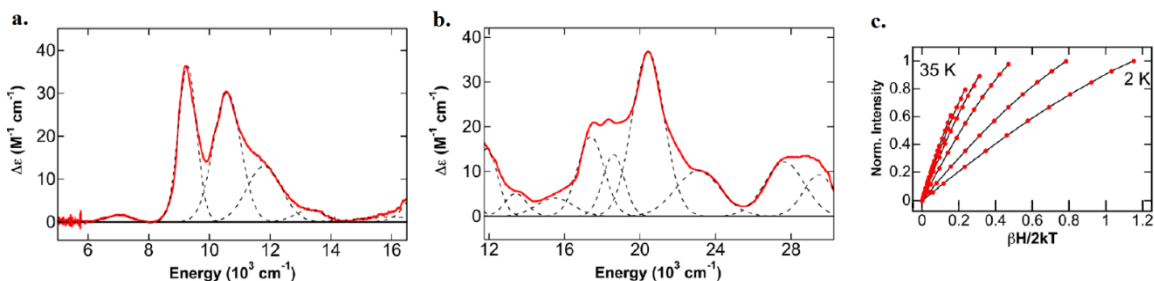


**Scheme 3.8.** An alternative route to the formation of **3.19** by way of an ion-exchange method.

### 3.2.2 Electronic Structure Comparison

With the desired iron(II) dibromide pincer complexes in hand, electronic structure comparisons were conducted in collaboration with the Neidig group from the University of

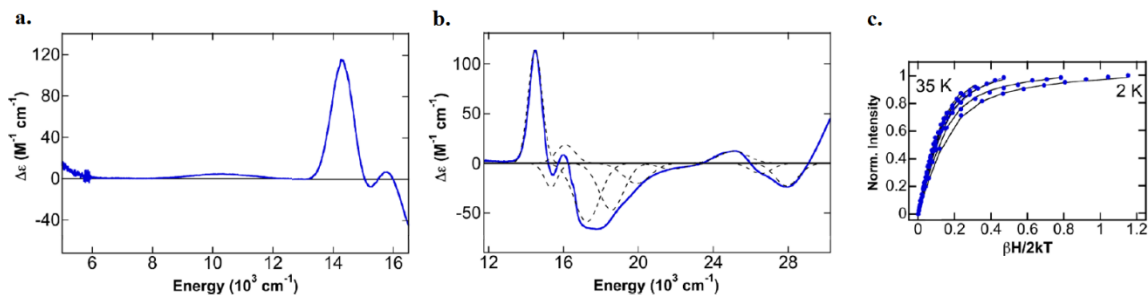
Rochester.<sup>39</sup> MCD studies were carried out in order to probe the effects of variation in NHC ligation on d-orbital splittings and electronic structure. The 5 K, 7 T, near-infrared MCD spectrum of **3.19** (**Figure 3.16a**) contains five ligand-field transitions between  $\sim 7000$  and  $\sim 13500$   $\text{cm}^{-1}$ , which exceeds the number expected for a high-spin iron(II) ( $S = 2$ ) complex, and is more consistent with an intermediate spin iron(II) ( $S = 1$ ) species. The 5 K, 7 T, UV-vis MCD spectrum of **3.19** contains a large number of charge-transfer transitions in the experimental range of  $\sim 16000$  to  $\sim 28000$   $\text{cm}^{-1}$ , and a high-energy ligand-field transition that is consistent with an  $S = 1$  complex when compared to TD-DFT calculations (**Figure 3.16b**). Furthermore, the saturation magnetization behavior of **3.19**, collected at  $9217$   $\text{cm}^{-1}$ , is well-fit to an  $S = 1$  positive zero-field split (+ZFS) non-Kramers doublet model with ground-state spin-Hamiltonian parameters of  $D = 20 \pm 4$   $\text{cm}^{-1}$  and  $|E/D| = 0.24 \pm 0.03$  with  $g_{\text{iso}} = 2.05 \pm 0.10$  (**Figure 3.16c**). This data is in agreement with the previously described SQUID magnetometry and  $^{57}\text{Fe}$  Mössbauer measurements of **3.8**.



**Figure 3.16.** a) 5 K, 7 T near-infrared MCD spectra of **3.19**, b) 5 K, 7 T UV-vis MCD spectra of **3.19**, and c) VTVH-MCD data (dots) and fit (lines) of **3.19**, collected at  $9217$   $\text{cm}^{-1}$ . Gaussian fits are shown as dashed lines. All spectra were collected in 1:1 THF/2-MeTHF.

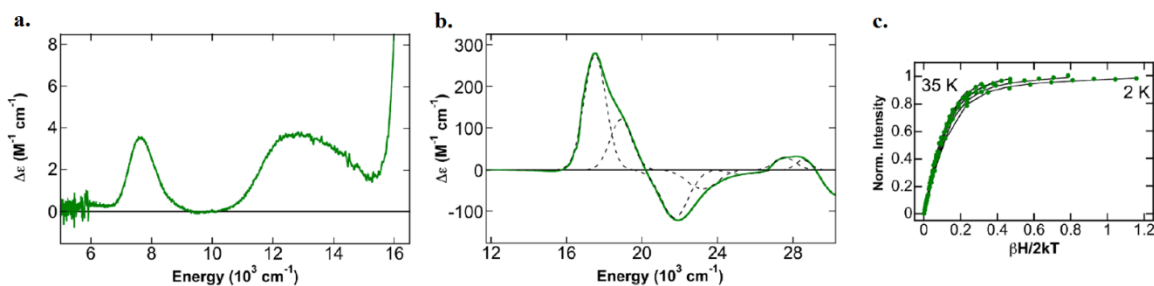
The 5 K, 7 T, near-infrared MCD spectra of  $(^{\text{Pr}}\text{PDI})\text{FeBr}_2$ , in comparison, contains only two ligand-field transitions: a low-energy tail at  $<5,000$   $\text{cm}^{-1}$  and a broad, weak transition at  $\sim 10,400$   $\text{cm}^{-1}$  (**Figure 3.17a**). These data are similar to high-spin,  $S = 2$  iron(II) pincer complexes previously studied by the Neidig group,<sup>40</sup> and are therefore consistent with this assignment. The 5 K, 7 T, UV-vis MCD spectrum of  $(^{\text{Pr}}\text{PDI})\text{FeBr}_2$  corroborates this assessment, as it contains multiple charge-transfer transitions from  $\sim 14,300$  to  $\sim 29,000$   $\text{cm}^{-1}$ , and is consistent with TD-DFT studies (**Figure 3.17b**). This ligand-field band was attributed to an MLCT transition from the Fe d orbital to the PDI

$\pi^*$  orbital. The saturation magnetization data for  $(^{iPr}PDI)FeBr_2$ , collected at  $13,899\text{ cm}^{-1}$ , is well fit to an  $S = 2$  negative zero-field split (-ZFS) non-Kramers doublet model with ground-state spin-Hamiltonian parameters of  $D = -12 \pm 1\text{ cm}^{-1}$  and  $|E/D| = 0.29 \pm 0.01$  with  $\delta = 3.0 \pm 0.2\text{ cm}^{-1}$  and  $g_{||} = 8.8 \pm 0.3$  (**Figure 3.17c**).



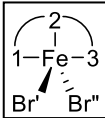
**Figure 3.17.** a) 5 K, 7 T near-infrared MCD spectra of  $(^{iPr}PDI)FeBr_2$ , b) 5 K, 7 T UV-vis MCD spectra of  $(^{iPr}PDI)FeBr_2$ , and c) VTVH-MCD data (dots) and fit (lines) of  $(^{iPr}PDI)FeBr_2$ , collected at  $13899\text{ cm}^{-1}$ . Gaussian fits are shown as dashed lines. All spectra were collected in 1:1 THF/2-MeTHF.

The 5 K, 7 T, near-infrared MCD spectrum of  $(^{iPr}CNC)FeBr_2$  exhibits two ligand-field transitions, a low-energy transition at  $7710\text{ cm}^{-1}$  and a broad transition at  $\sim 13,400\text{ cm}^{-1}$  (**Figure 3.18a**). These observed transitions indicate a larger overall ligand-field splitting than those observed for  $(^{iPr}PDI)FeBr_2$  ( $10Dq \approx 10,555\text{ cm}^{-1}$  and  $10Dq \leq 7700\text{ cm}^{-1}$ , respectively), supporting previous studies that suggest  $^{iPr}CNC$  is a stronger field ligand than  $^{iPr}PDI$ . The 5 K, 7 T, UV-vis MCD spectrum of  $(^{iPr}CNC)FeBr_2$  contains multiple transitions between  $\sim 17,000$  and  $\sim 27,000\text{ cm}^{-1}$  that were determined through TD-DFT calculations to correspond to an MLCT transition from the Fe d orbital to the CNC  $\pi^*$  orbital (**Figure 3.18b**). Additional transitions beyond  $\sim 27,000\text{ cm}^{-1}$  are consistent with contributing LCMT character. As with  $(^{iPr}PDI)FeBr_2$ , the saturation magnetization data for  $(^{iPr}CNC)FeBr_2$ , collected at  $7634\text{ cm}^{-1}$ , are well-fit to an  $S = 2$  negative zero field splitting (-ZFS) non-Kramers doublet model. Similar ground-state spin-Hamiltonian parameters of  $D = -11 \pm 2\text{ cm}^{-1}$  and  $|E/D| = 0.23 \pm 0.02$  with  $\delta = 1.6 \pm 0.2\text{ cm}^{-1}$  and  $g_{||} = 9.0 \pm 0.2$  (**Figure 3.18c**) were observed.



**Figure 3.18.** a) 5 K, 7 T near-infrared MCD spectra of (*i*PrCNC)FeBr<sub>2</sub>, b) 5 K, 7 T UV-vis MCD spectra of (*i*PrCNC)FeBr<sub>2</sub>, and c) VTVH-MCD data (dots) and fit (lines) of (*i*PrCNC)FeBr<sub>2</sub>, collected at 7634 cm<sup>-1</sup>. Gaussian fits are shown as dashed lines. All spectra were collected in 1:1 THF/2-MeTHF.

**Table 3.5** provides a comparison of experimental and calculated bond lengths and bond angles for **3.19**, (*i*PrPDI)FeBr<sub>2</sub>, and (*i*PrCNC)FeBr<sub>2</sub>. In all cases, the experimental and calculated values are in good agreement. When bond lengths and bond angles were calculated for a high-spin  $S = 2$  **3.19**, the values were not consistent with the experimental values, further supporting the assignment of an intermediate-spin  $S = 1$  species.

	( <i>i</i> PrCDA)FeBr <sub>2</sub> ( <b>3.19</b> )		( <i>i</i> PrPDI)FeBr <sub>2</sub>		( <i>i</i> PrCNC)FeBr <sub>2</sub>	
	Exp.	Calc. $S = 1$	Exp.	Calc.	Exp.	Calc.
Fe – 1	2.015(2)	2.05	2.205(2)	2.21	2.193(10)	2.19
Fe – 2	1.811(1)	1.83	2.027(2)	2.10	2.211(8)	2.28
Fe – 3	2.004(2)	2.04	2.209(2)	2.22	2.166(10)	2.17
Fe – Br'	2.4775(5)	2.57	2.4692(6)	2.54	2.5065(18)	2.59
Fe – Br''	2.4215(5)	2.46	2.3999(6)	2.45	2.4208(17)	2.49
1-Fe-3*	145.38(9)	147.0	141.13(8)	139.6	141.0(4)	138.4
Br'-Fe-Br'' *	106.44(2)	107.1	1116.054(2)	114.6	108.19(7)	111.4

**Table 3.5.** Comparison of experimental and calculated bond angles and bond lengths for **3.19**, (*i*PrPDI)FeBr<sub>2</sub>, and (*i*PrCNC)FeBr<sub>2</sub>. Measurements are reported in angstroms. \* Reported in degrees.

DFT calculations using spin-unrestricted B3LYP/def2-TZVP were employed to evaluate the molecular orbital character and energies of the three pincer complexes. The calculated molecular orbitals and depictions of  $\alpha$  Frontier molecular orbitals (FMOs) that have dominant d-orbital character for **3.19** and  $(^{Pr}CNC)FeBr_2$  are shown in **Figure 3.19**. For **3.19**, the occupied  $\alpha$  FMOs that exhibit dominant d-orbital character are  $\alpha 169$ ,  $\alpha 170$ ,  $\alpha 171$ , and  $\alpha 182$ , assigned as  $d_{yz}$ ,  $d_{xz}$ ,  $d_{xy}$ , and  $d_{z^2}$ , respectively. The unoccupied  $\alpha$  FMO that shows the same d-orbital character is  $\alpha 184$ , with the assignment  $d_{x^2-y^2}$ . For the  $\beta$  manifold, the FMOs that exhibit dominant d-character are the occupied  $\beta 179$  and  $\beta 180$  orbitals, assigned as  $d_{xy}$  and  $d_{xz}$ , respectively, and the unoccupied  $\beta 182$ ,  $\beta 183$ , and  $\beta 184$  orbitals, with the assignments  $d_{xy}$ ,  $d_{z^2}$ , and  $d_{x^2-y^2}$ , respectively. In both the  $\alpha$  and  $\beta$  manifolds,  $d_{x^2-y^2}$  is unoccupied and of the highest energy because of the direct  $\sigma^*$  interaction between the ligating atoms of the pincer ligand and the  $d_{x^2-y^2}$  Fe-based orbitals. This leads to an increased splitting in energy of  $E_g$ -derived orbitals that leads to intermediate  $S = 1$ .

$(^{Pr}PDI)FeBr_2$  and  $(^{Pr}CNC)FeBr_2$  have similar overall MO diagrams, and like **3.19**, the  $d_{x^2-y^2}$  is unoccupied and highest energy in both the  $\alpha$  and  $\beta$  manifolds, due to the direct  $\sigma^*$  interaction between the pincer ligands and the iron  $d_{x^2-y^2}$  orbital. Notable is the additional  $\sigma$  interaction between the NHC donors of  $(^{Pr}CNC)FeBr_2$  and the iron  $d_{xy}$  orbital ( $\alpha 161$ ), which is not present in  $(^{Pr}PDI)FeBr_2$ .

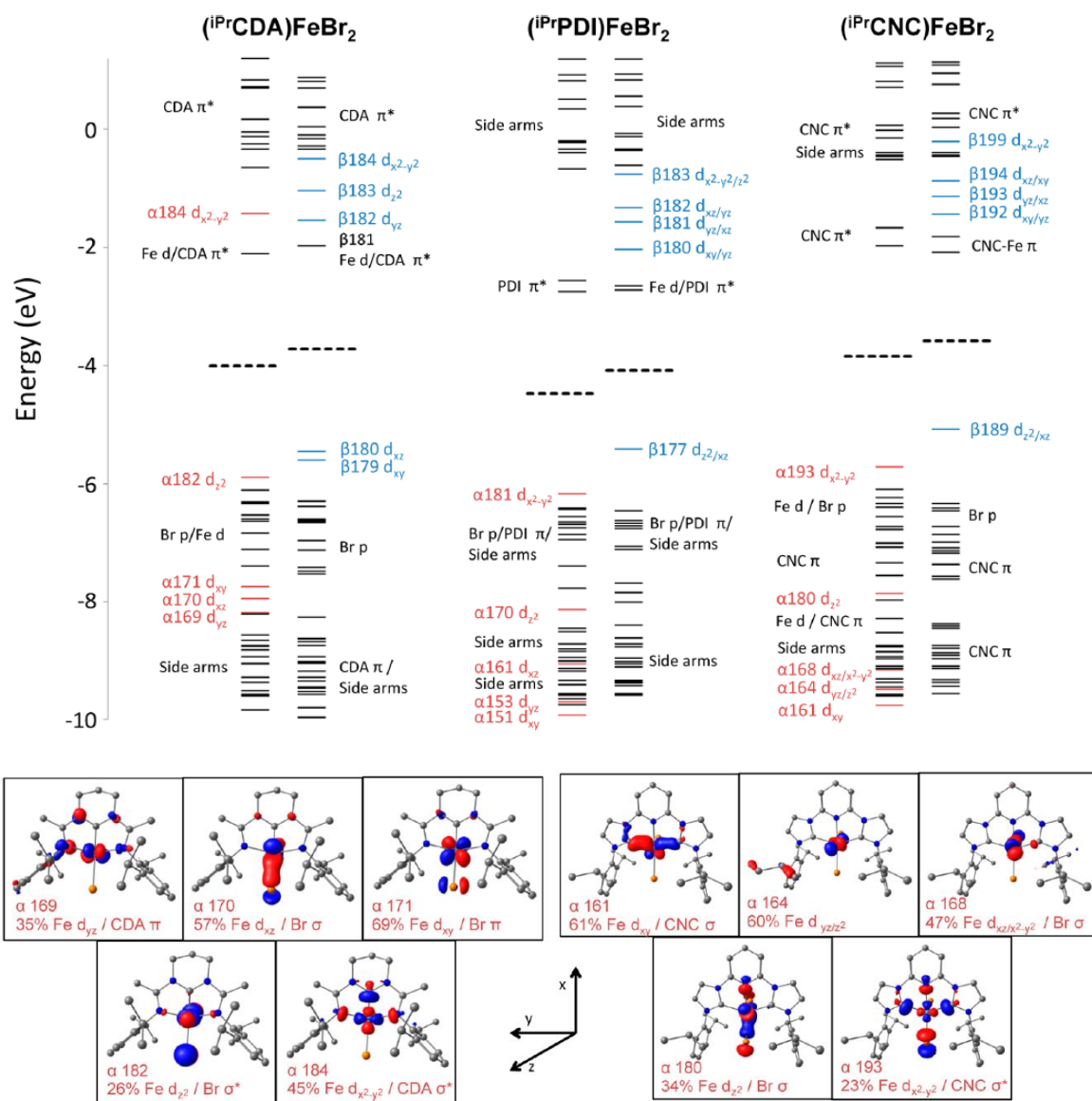


**Figure 3.19.** Calculated FMO diagrams for **3.19**, (iPrPDI)FeBr<sub>2</sub>, and (iPrCNC)FeBr<sub>2</sub>. Selected α-orbital depictions for S = 1 **3.19** and S = 2 (iPrCNC)FeBr<sub>2</sub>.

Mayer bond order (MBO) analyses were conducted for all three complexes (Table 3.6). The sum of the MBOs of the Fe-N and Fe-C ligated atoms is largest for **3.19** (MBO = 2.198), which supports the low-spin state assignment. This large MBO is mainly due to the MBO observed for Fe-C bond of 1.059, which is the largest represented in this series. Notably, the bond order of the Fe-C bond is greater than the Fe-N bonds. (iPrCNC)FeBr<sub>2</sub> exhibits the second largest summed pincer MBO of 1.542, due primarily to the large Fe-C bonds of 0.594 and 0.657, which are

comparable to the Fe-N bonds observed for **3.19**, and larger than the Fe-N<sub>imine</sub> bonds observed for (<sup>i</sup>PrPDI)FeBr<sub>2</sub> (0.393 and 0.397). The Fe-N bond to the central pyridine donor of (<sup>i</sup>PrCNC)FeBr<sub>2</sub>, however, is smaller than the analogous bond of (<sup>i</sup>PrPDI)FeBr<sub>2</sub>. The MBO analyses indicate that the order of the MBOs for Fe-pincer interactions correlate well with the order of ligand-field splitting observed by MCD for these complexes (<sup>i</sup>PrCDA > <sup>i</sup>PrCNC > <sup>i</sup>PrPDI).

Mayer Bond Order			
Complex	Spin	Fe-L	Fe-Br
<b>3.19</b>	1	0.572	0.609
		<b>1.059</b>	0.599
		0.567	
( <sup>i</sup> PrCNC)FeBr <sub>2</sub>	2	0.594	0.666
		<b>0.291</b>	0.520
		0.657	
( <sup>i</sup> PrPDI)FeBr <sub>2</sub>	2	0.393	0.584
		<b>0.447</b>	0.711
		0.397	

**Table 3.6. Mayer bond orbital analyses of **3.19**, (<sup>i</sup>PrCNC)FeBr<sub>2</sub>, and (<sup>i</sup>PrPDI)FeBr<sub>2</sub>, indicating summed Fe-pincer bond orders of 2.198, 1.542, and 1.237, respectively.**

Charge donation analyses were also conducted, indicating that **3.19** is the strongest donating pincer ligand of the series (1.613 e<sup>-</sup>), followed by (<sup>i</sup>PrCNC)FeBr<sub>2</sub> (1.034 e<sup>-</sup>), with (<sup>i</sup>PrPDI)FeBr<sub>2</sub> being the least donating (0.806 e<sup>-</sup>). This order is consistent with that of the summed MBO of the Fe-pincer bonds (**Table 3.7**). The back donation of the metal center to the pincer ligand is similar for (<sup>i</sup>PrCNC)FeBr<sub>2</sub> (0.268 e<sup>-</sup>) and (<sup>i</sup>PrPDI)FeBr<sub>2</sub> (0.309 e<sup>-</sup>), yet is significantly higher for **3.19** (0.910 e<sup>-</sup>). This is due to the amplified β donation to the CDA pincer ligand from the highly occupied β d<sub>xz</sub> on Fe, which increases the π-back bonding significantly.

complex	spin	Charge donation analysis ( $\alpha + \beta$ )		
		Donation: (pincer $\rightarrow$ FeBr <sub>2</sub> )	Back donation: (FeBr <sub>2</sub> $\rightarrow$ pincer)	Net charge donation to FeBr <sub>2</sub>
<b>3.19</b>	1	1.613 e <sup>-</sup> ( $\alpha$ : 0.872 e <sup>-</sup> ; $\beta$ : 0.741 e <sup>-</sup> )	0.910 e <sup>-</sup> ( $\alpha$ : 0.186 e <sup>-</sup> ; $\beta$ : 0.723 e <sup>-</sup> )	0.703 e <sup>-</sup>
( <sup>i</sup> PrPDI)FeBr <sub>2</sub>	2	0.806 e <sup>-</sup> ( $\alpha$ : 0.323 e <sup>-</sup> ; $\beta$ : 0.483 e <sup>-</sup> )	0.309 e <sup>-</sup> ( $\alpha$ : 0.074 e <sup>-</sup> ; $\beta$ : 0.235 e <sup>-</sup> )	0.497 e <sup>-</sup>
( <sup>i</sup> PrCNC)FeBr <sub>2</sub>	2	1.034 e <sup>-</sup> ( $\alpha$ : 0.455 e <sup>-</sup> ; $\beta$ : 0.579 e <sup>-</sup> )	0.268 e <sup>-</sup> ( $\alpha$ : 0.096 e <sup>-</sup> ; $\beta$ : 0.172 e <sup>-</sup> )	0.766 e <sup>-</sup>

**Table 3.7. Charge donation analyses of 3.19, (<sup>i</sup>PrCNC)FeBr<sub>2</sub>, and (<sup>i</sup>PrPDI)FeBr<sub>2</sub>.**

### 3.2.3 Summary of Results

The goal of this study was to examine the quantitative effects that the  $\sigma$ -donation lent by NHC moieties has as compared to nitrogen donors. In regards to the S = 2 complexes (<sup>i</sup>PrCNC)FeBr<sub>2</sub> and (<sup>i</sup>PrPDI)FeBr<sub>2</sub>, the presence of two NHC moieties in the <sup>i</sup>PrCNC pincer ligand leads to a larger ligand field ( $10D_q \approx 10,555 \text{ cm}^{-1}$ ) as opposed to the <sup>i</sup>PrPDI ligand system which contains imine moieties ( $10D_q \approx 7700 \text{ cm}^{-1}$ ). The larger ligand field of (<sup>i</sup>PrCNC)FeBr<sub>2</sub> correlates directly with the increased donor ability of NHC ligands, and both MBO and charge donation analyses corroborate a noticeable increase in  $\sigma$ -donation. Charge donation analyses also indicate comparable  $\pi$ -back bonding for both (<sup>i</sup>PrCNC)FeBr<sub>2</sub> and (<sup>i</sup>PrPDI)FeBr<sub>2</sub>, suggesting that the main contribution to the ligand field differences stems from the alteration of  $\sigma$ -donor abilities.

When replacing the central pyridine donor of (<sup>i</sup>PrPDI)FeBr<sub>2</sub> with an NHC to form **3.19**, an even more significant increase in  $\sigma$ -donation is observed, leading to a notable increase in the energy of the iron  $d_{x^2-y^2}$  orbital and overall ligand field. The high MBO of the iron-carbene bond (1.059) and the strong pincer  $\sigma$ -donation (1.613 e<sup>-</sup>) observed by charge donation analysis are

consistent with the observation that **3.19** contains a very short iron-carbene bond. This unique Fe-C interaction imparted by the CDA ligand causes **3.19** to favor an S = 1 spin state.

The difference between **3.19** and (<sup>iPr</sup>CNC)FeBr<sub>2</sub> likely results from the position of the NHC moieties and the overall geometry of the complexes. The central position of the NHC donor in **3.19** allows for not only significant  $\sigma^*$ -d<sub>x<sup>2</sup>-y<sup>2</sup> interaction, but also leads to an iron-carbene  $\pi$ -d<sub>xz</sub> interaction that is not possible with (<sup>iPr</sup>CNC)FeBr<sub>2</sub>. Additionally, MBO analysis indicates that the central pyridine donor of (<sup>iPr</sup>CNC)FeBr<sub>2</sub> is significantly weaker than the central pyridine donor of (<sup>iPr</sup>PDI)FeBr<sub>2</sub>, suggesting that the constrained geometry of (<sup>iPr</sup>CNC)FeBr<sub>2</sub> may inhibit the formation of strong interactions between the iron center and the pincer ligand.</sub>

Overall, it seems that quantitative analyses of the electronic structure and bonding abilities of NHC-containing pincer complexes could greatly expand catalyst development. The understanding of  $\sigma$ -donation and  $\pi$ -back donation characteristics as well as geometric constraints can be crucial in designing species that take full advantage of the electronic benefits of NHC donors.

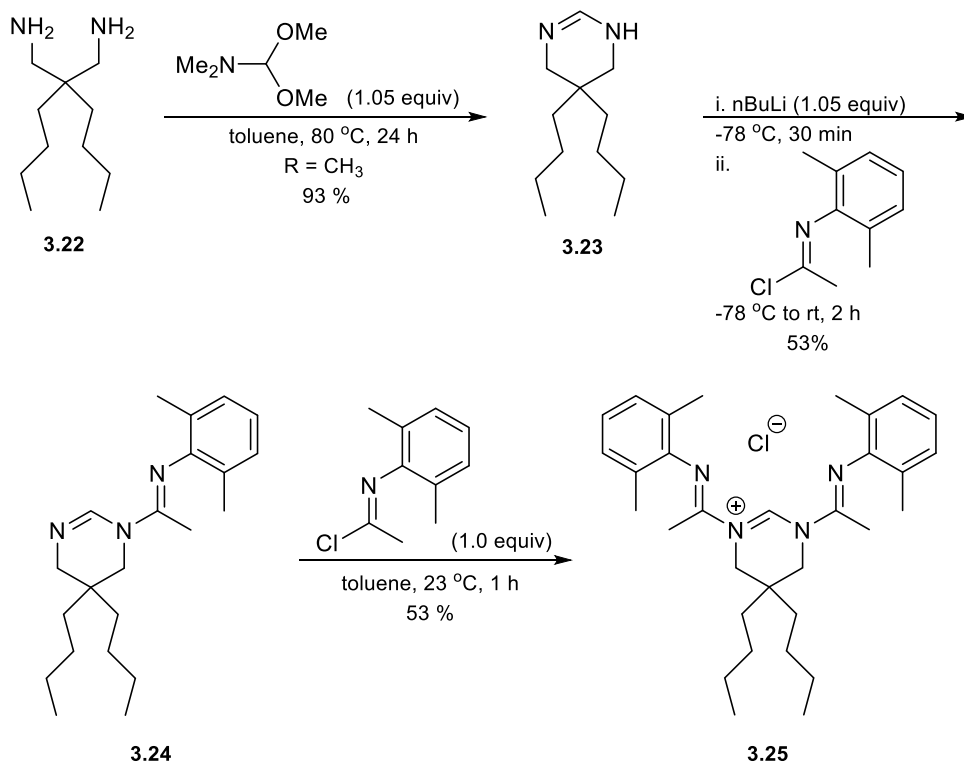
### 3.3 SYNTHESIS OF ADDITIONAL CDA LIGANDS

Initial studies by Dr. Hilan Kaplan indicated the importance of rigorous water-free conditions for catalytic applications of iron CDA complexes. Dr. Kaplan took strides to thoroughly dry the THF he used for preliminary reactions, as anything less than rigorous led to catalyst death.

Together with Charlie Wolstenholme and Dr. Xiaofei Zhang, two new variations of the CDA ligand were developed. Containing alkyl substitution at additional points along the ligand backbone, these complexes were designed to be more soluble in non-polar solvents that are easier to dry than THF, such as toluene or pentane.

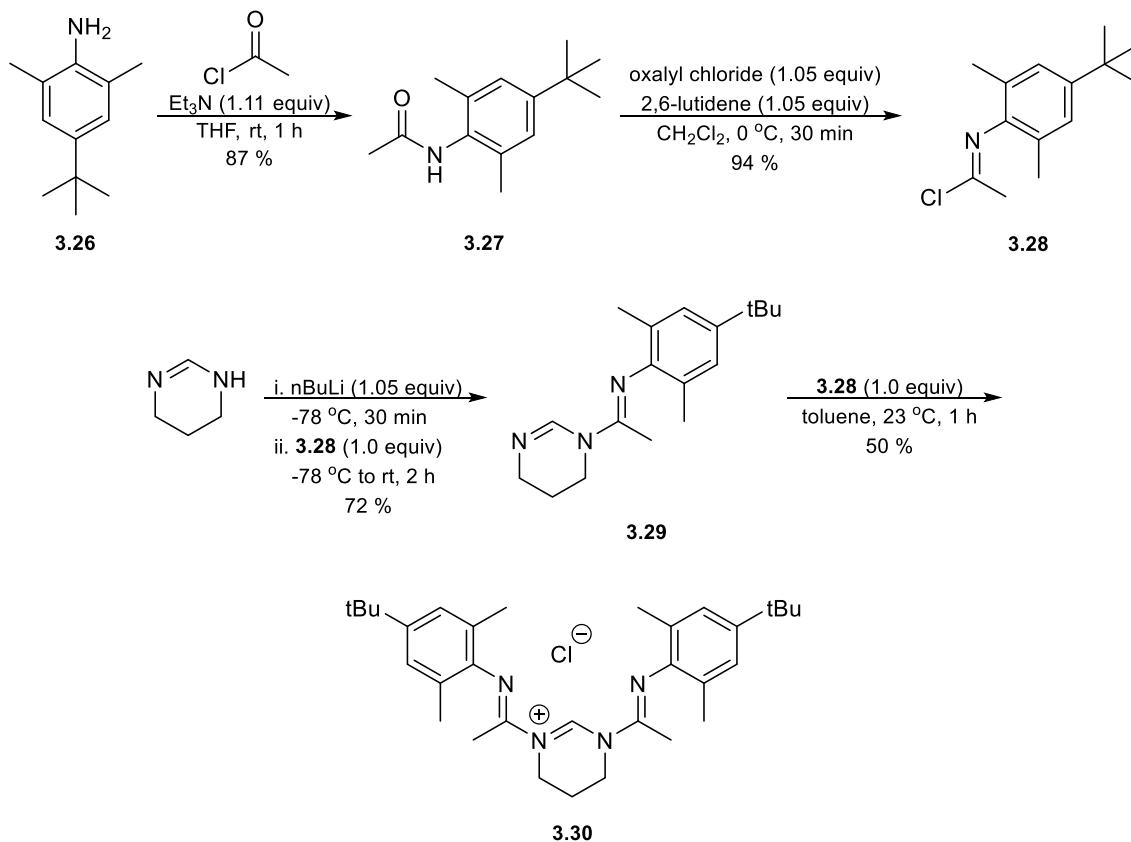
A ligand was developed that incorporated an alkyl chain on the pyrimidine backbone (**Scheme 3.9**). Beginning with diamine **3.22**, treatment with dimethylformamide dimethyl acetal yielded substituted pyrimidine **3.23**. These species could then be deprotonated with nBuLi and

treated with (*E*)-*N*-(2,6-dimethylphenyl) acetimidoyl chloride to form **3.24**. Finally, with the addition of a second equivalent of (*E*)-*N*-(2,6-dimethylphenyl) acetimidoyl chloride, CDA ligand **3.25** was formed.



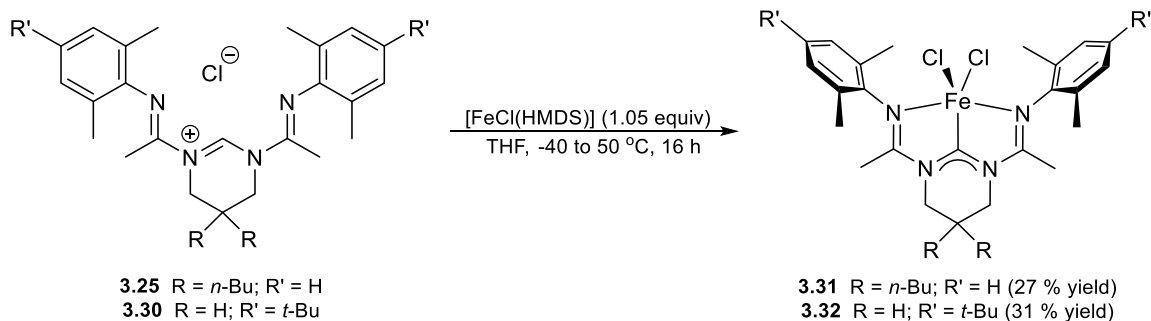
**Scheme 3.9. Synthesis of CDA ligand 3.25.**

Another CDA variation, with *p*-*tert*-butyl substitution of the aryl imines, was developed (**Scheme 3.10**). Aniline **3.26**, prepared according to literature procedures,<sup>41</sup> was treated with acetyl chloride in the presence of triethylamine to give amide **3.27** in 54 % yield. **3.27** was subsequently treated with oxalyl chloride and 2,6-lutidine to give imidoyl chloride **3.28** in 75 % yield. Then, following procedure set forth by Hilan Kaplan,<sup>38</sup> species **3.29** and ligand **3.30** were obtained.



**Scheme 3.10. Synthesis of CDA ligand 3.30.**

The new CDA ligands were metalated by treatment with premixed iron dichloride and sodium hexamethyldisilazide to form complexes **3.31** and **3.32** (Scheme 3.11). Solubility studies showed that these complexes were indeed more soluble than the original CDA complex **3.8**, being soluble in ether and toluene, and sparingly soluble in pentane.



**Scheme 3.11. Metalation of 3.25 and 3.30 with premixed iron dichloride and sodium hexamethyldisilazide to form complexes 3.31 and 3.32, respectively.**

## 3.4 OLEFIN HYDROGENATION

### 3.4.1 Results and Discussion

Initial studies of the hydrogenation ability of (<sup>Pr</sup>CDA)FeCl<sub>2</sub>, **3.8**, indicated that the complex is, in fact, active for the hydrogenation of olefins (**Table 3.8**). When allyl benzene was treated with 10 mol % **3.8** and 50 mol % sodium mercury amalgam under 80 psi hydrogen in THF, 100 % conversion of allyl benzene was observed (entry 1). However, to reach high conversion, THF that had been rigorously dried over sodium benzophenone was necessary. In cases where the THF was not adequately dried, no conversion of allyl benzene occurred. With the newly designed, more soluble CDA complexes, it was determined that full conversion could be attained in toluene, whereas the use of **3.8** led to no conversion in toluene due to insolubility (entry 2).

When complex **3.31** was employed, full conversion was observed in both THF (entry 3) and toluene (entry 4), and a lower precatalyst loading of 1 mol % was effective (entries 5 and 6). In each instance, a reaction time of 20 to 24-hours was required, with no conversion seen between 0 and 4 hours. Complex **3.37** performed comparably to **3.31** (entries 7 and 8). In the absence of iron, no conversion of allyl benzene was seen (entry 9), and in the presence of iron dichloride, only trace conversion occurred (entry 10).

pre-catalyst (x mol %)  
 50 mol % Na(Hg)  
 solvent, 23 °C, 80 psi H<sub>2</sub>  
 24 h

Entry	Precatalyst	Loading	Solvent	Conv. (%) [Yield (%, GC)]
1	<b>3.8</b>	10 mol %	THF	100*
2			toluene	0
3	<b>3.31</b>	10 mol %	THF	100
4			toluene	100
5		1 mol %	THF	100
6			toluene	100
7	<b>3.37</b>	1 mol %	THF	100
8			toluene	100 [98]
9	None	-	THF	0
10	FeCl <sub>2</sub>	10 mol %	THF	< 5

**Table 3.8. Initial screening of iron CDA complexes for the hydrogenation of allyl benzene.**

**\*Not all experiments under these conditions resulted in 100 % conversion of allyl benzene, in instances where the THF was not sufficiently dried, no conversion was observed. All conversions and yields were determined by GC.**

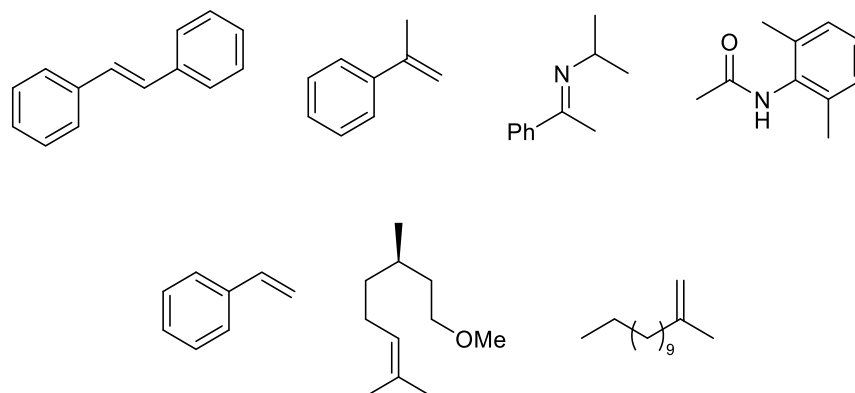
A brief substrate scope, shown in **Table 3.9**, underscored the superiority of complex **3.32** as compared to **3.8** in that the former pre-catalyst led to the complete conversion of cyclooctene and the formation of 96 % of cyclooctane (entry 2), whereas **3.8** could not initiate the conversion of cyclooctene (entry 1), even in THF. **3.32** and **3.31** were compared for the hydrogenation of cyclohexene, and, although low yields were produced in both cases, **3.31** was found to be a more effective pre-catalyst than **3.32**, producing 53 % and 32 % conversion of cyclohexene, respectively (entries 3 and 4). In THF rather than toluene, *trans*-8-octadecene was converted 35 % to the desired alkane in the presence of **3.8** (entry 5). **3.31** effectively catalyzed the hydrogenation of 1-octene with 100 % conversion (entry 6), and 1,1-diphenylmethene was converted 58 % to the desired product with complex **3.32** (entry 7).

Entry	Substrate	Precatalyst	Product	Conv. (%) [Yield (% GC)]
1		<b>3.8*</b>		0
2		<b>3.32</b>		100 [96]
3		<b>3.32</b>		32
4		<b>3.31</b>		53
5		<b>3.8*</b>		35
6		<b>3.31</b>		100
7		<b>3.32</b>		58

**Table 3.9.** The use of iron CDA complexes for the hydrogenation of cyclooctene, cyclohexene, *trans*-8-octadecene, 1-octene, and 1,1-diphenylmethene. \*Run in THF. All conversions and yields were determined by GC.

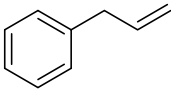
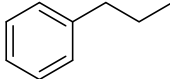
Substrates that were found to be inactive to hydrogenation by CDA catalysts included amides, imines, tri-substituted olefins, and 1,1-di-substituted olefins other than 1,1-diphenylethene. Examples are shown in **Figure 3.20**.

Inactive Substrates:



**Figure 3.20. Examples of substrates that were found inactive for hydrogenation by iron CDA complexes.**

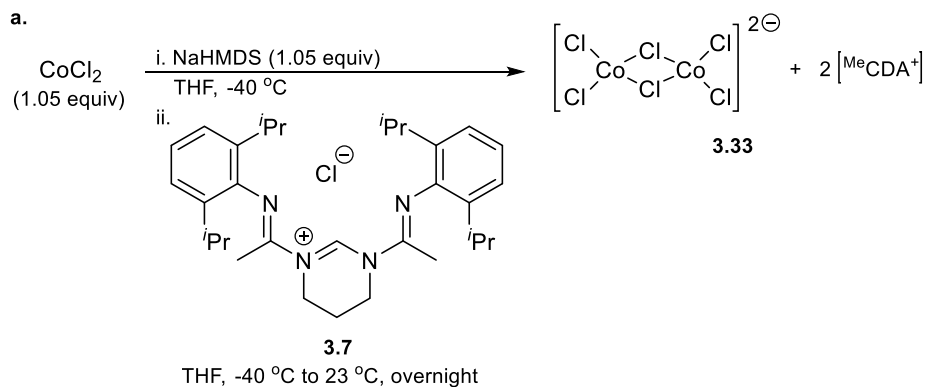
It was at this point that the CDA complexes discussed herein were synthesized anew with a different source of iron dichloride. Using the new batch of precatalysts, much lower yields were observed for many of the substrates discussed above. Control reactions were run comparing the “old” and “new” sources of iron dichloride, and it was found that the “old” source led to 20 – 30 % conversion of allyl benzene under the optimized reaction conditions in toluene (**Table 3.10**). The “new” source of iron dichloride was inert for the hydrogenation of olefins. Unfortunately, these data suggest that all previously collected results could be erroneous, although it is possible that the “new” batch of iron dichloride was the contaminated batch. Previous hydrogenations of allyl benzene by **3.8** in THF conducted by Hilan Kaplan could be repeated with the “new” iron source, yet the results of the hydrogenations in toluene could not be.

	precatalyst (x mol %) 50 mol % Na(Hg) toluene, 23 °C, 80 psi H <sub>2</sub> 24 h	
Precatalyst	Conv. (%) [Yield (%), GC]	
“old” FeCl <sub>2</sub>	26.4 ± 5.6 [21.6 ± 5.4]	
“new” FeCl <sub>2</sub>	0	

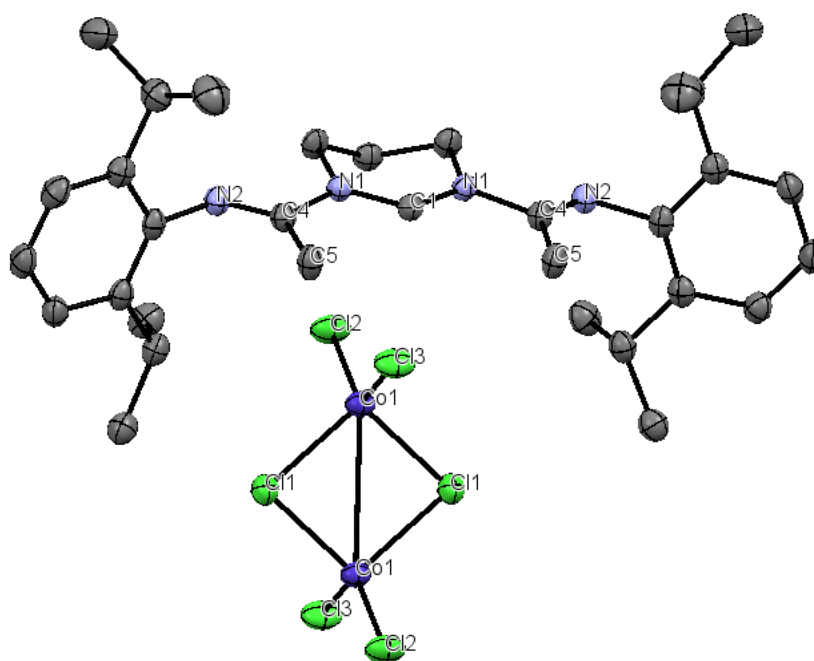
**Table 3.10.** Comparison of “old” and “new” sources of iron dichloride, suggesting that one iron dichloride source contains an impurity that led to erroneous results. All conversions and yields were determined by GC.

### 3.4.2 (CDA)CoCl<sub>2</sub> Synthesis and Hydrogenation Ability

Whilst examining the hydrogenation of olefins by iron CDA complexes, the synthesis and catalytic studies of a cobalt CDA complex were pursued. Cobalt dichloride was treated with sodium hexamethyldisilazide in THF at -40 °C. CDA ligand **3.7** was then added, and the reaction mixture was allowed to warm to room temperature and stir overnight, producing a blue-green solution (**Scheme 3.12a**). Crystals were grown from THF and pentane, and the product (**3.33**) was identified as a doubly anionic cobalt trichloride dimer co-crystallized with two equivalents of CDA ligand **3.7** by X-ray spectroscopic analysis. The crystal structure of **3.33** is shown in **Scheme 3.12b**.

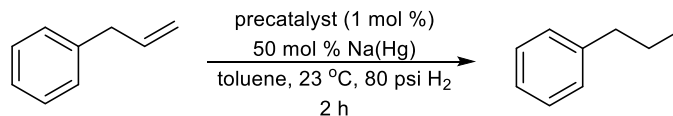


b.



**Scheme 3.12.** a) The synthesis of complex **3.33** by means similar to that for synthesizing iron CDA complexes, and b) the crystal structure of **3.33**.

Interestingly, this species was found to be very active for olefin hydrogenation. In just two hours under the optimized reaction conditions (**Table 3.11**), **3.33** facilitated full conversion of allyl benzene (entry 1). Even more notable is the fact that control reactions revealed that the simple cobalt dichloride salt led to the same reactivity (entry 2). Although the speed and efficacy of cobalt dichloride for the hydrogenation of allyl benzene indicate promising reactivity, further studies were not pursued in an effort to focus on CDA ligation.

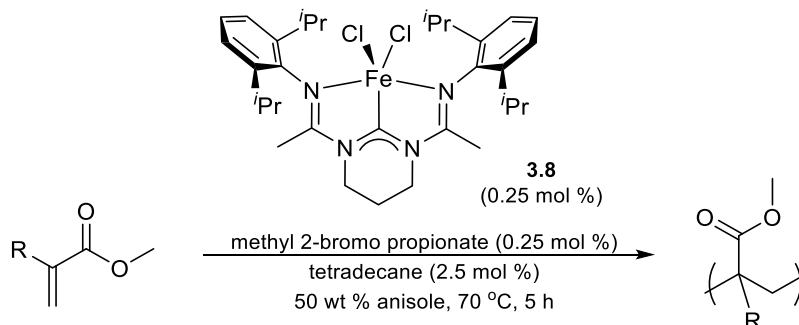


Entry	Precatalyst	Conv. (%)
1	<b>3.33</b>	100
2	CoCl <sub>2</sub>	100

**Table 3.11.** The complete conversion of allyl benzene in the presence of catalytic amounts of cobalt precatalysts, sodium mercury amalgam, and 80 psi hydrogen gas. Conversions were determined by GC.

### 3.5 ATOM TRANSFER RADICAL POLYMERIZATION

Atom transfer radical polymerization (ATRP) has been shown to be facilitated by iron PDI complexes (*vide supra*) and thus efficacy of (<sup>Pr</sup>CDA)FeCl<sub>2</sub>, **3.8**, for ATRP reactions was investigated. Initial results by Dr. Hilan Kaplan identified the conversion of methyl methacrylate (MMA) in the presence of **3.8** and 2-bromopropionitrile (BPN), yet GPC data were not collected. **Table 3.12** shows polymerizations of various monomers by **3.8**. MMA, when combined with **3.8** and methyl-2-bromopropionate (MBP) in a 400:1:1 monomer/precatalyst/initiator ratio, led to 15 % conversion of MMA, and the generation of a polymer with M<sub>n</sub> = 250 kg/mol and M<sub>w</sub>/M<sub>n</sub> = 1.79 (entry 1). Similar reactions with *t*-butyl methacrylate (*t*BuMA) and styrene led to 14 % conversion with M<sub>n</sub> = 1,662 k/mol and M<sub>w</sub>/M<sub>n</sub> = 1.47 (entry 2), and 15 % conversion with M<sub>n</sub> = 4,338 kg/mol and M<sub>w</sub>/M<sub>n</sub> = 1.88 (entry 3), respectively. No conversion of methyl acrylate (MA) was observed under these conditions (entry 4). The use of BPN as an initiator rather than MBP resulted in 58 % conversion, similar to what was seen by Dr. Kaplan, and M<sub>n</sub> = 27 kg/mol and M<sub>w</sub>/M<sub>n</sub> = 1.33 (entry 5). With a 200:1:1 ratio of monomer/precatalyst/initiator, 24 % conversion, 219 kg/mol, and M<sub>w</sub>/M<sub>n</sub> = 1.71 were observed (entry 6). Due to the non-repeatable nature of the results for the majority of substrates, it was determined that the use of CDA complexes for ATRP is not beneficial.



Entry	Monomer	Initiator	[mon]:[cat]:[init]	Conv. (% , GC)	M <sub>n</sub>	M <sub>w</sub> /M <sub>n</sub>
1	MMA	MBP	400:1:1	15	250	1.79
2	<i>t</i> BuMA			14	1,662	1.47
3	styrene			15	4,338	1.88
4	MA			-	-	-
5	MMA	BPN		58	27	1.33
6	MMA	MBP	200: 1: 1	24	219	1.71

**Table 3.12. A study of the catalytic ability of 3.8 with various monomers, initiators, and monomer/precatalyst/initiator ratios.**

### 3.6 CONCLUSIONS

Through MCD, DFT, Mayer bond order, and charge donation analyses, the electronic structures of PDI, CNC, and CDA pincer iron(II) complexes were compared. (<sup>*i*Pr</sup>PDI)FeBr<sub>2</sub> and (<sup>*i*Pr</sup>CNC)FeBr<sub>2</sub> were both found to be high-spin S = 2 species, and the (<sup>*i*Pr</sup>CNC) ligand was found to possess enhanced σ-donation to iron, hence forming a more electron-rich complex. (<sup>*i*Pr</sup>CDA)FeBr<sub>2</sub> was found to be an intermediate-spin S = 1 species with greater pincer to iron σ-donation as compared to the CNC analogue. Additionally, the central position of the NHC donor of (<sup>*i*Pr</sup>CDA)FeBr<sub>2</sub> allows for significant σ\*- d<sub>x<sup>2</sup>-y<sup>2</sup></sub> and π-d<sub>xz</sub> interactions, the latter of which is not possible for (<sup>*i*Pr</sup>CNC)FeBr<sub>2</sub>. These findings support the initial hypothesis of the Byers lab that (<sup>*i*Pr</sup>CDA)FeBr<sub>2</sub> contains a much more electron-rich metal center than its CNC and PDI counterparts.

More soluble variants of the initial (<sup>iPr</sup>CDA)FeBr<sub>2</sub> complex were synthesized with the help of Dr. Xiaofei Zhang and Charles Wolstenholme. Despite the initial promising results of the catalytic ability of (<sup>iPr</sup>CDA)FeBr<sub>2</sub> for the hydrogenation olefins in THF, these new complexes were ultimately found to be mediocre catalysts for the transformation in toluene. Erroneously high conversions attributed to contamination of the iron dichloride source were detected, and useful conversions could not be attained with the non-contaminated iron source. Additionally, the use of CDA complexes for ATRP resulted in undesired bimodal GPC distributions, and preliminary studies of [2+2] cycloadditions did not produce desired results.

The electronically and structurally uniqueness of the CDA complexes discussed herein are exciting and promising discoveries. Although the iron CDA complexes are poor catalysts for the applications discussed herein, iron CDA alkoxides are quite good catalysts for lactide polymerization,<sup>42</sup> and the potential of these complexes warrants further study.

## 3.7 EXPERIMENTAL

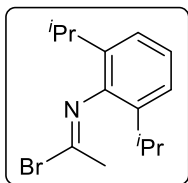
### 3.7.1 General Considerations

Unless stated otherwise, all reactions were carried out in oven-dried glassware using standard Schlenk techniques<sup>43</sup> or using an MBraun inert atmosphere (N<sub>2</sub>) drybox. Dichloromethane, pentane, toluene, diethyl ether, and tetrahydrofuran were passed through a solvent purification system under a blanket of argon and then degassed briefly under vacuum prior to use. Reagents were purchased from commercial sources and purified as necessary before use. NMR spectra were recorded at ambient temperature on a Varian VNMRS or INOVA spectrometer operating at 500 MHz for <sup>1</sup>H NMR and 125 MHz for <sup>13</sup>C NMR. The line listings for the NMR spectra of diamagnetic compounds are reported as: chemical shift in ppm (number of protons, splitting pattern, coupling constant). The line listings for the NMR spectra of paramagnetic complexes are reported as: chemical shift in ppm (number of protons, peak width at half height in Hz). All chemical

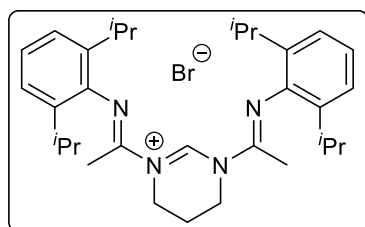
shifts are reported in ppm from tetramethylsilane with the peak for the residual protio version of the solvent as the internal reference. GC/FID data were obtained on a Shimadzu GC-2014 equipped with a AOC-20i Auto Injector/Auto Sampler. GC/MS data were obtained on a 7820a Agilent GC with a 5975 Mass Analyzer. High-resolution mass spectra were obtained at the Boston College Mass Spectrometry Facility. Elemental Analyses were conducted at Robertson MicroLit Laboratories. IR spectra were recorded on a Bruker ALPHA Platinum ATR infrared spectrometer. X-ray crystallographic information was obtained at the Boston College X-ray Crystallography Center. GPC/SEC data were obtained on an Agilent PL-GPC220 Integrated HT-GPC/SEC, and analyses were conducted using the following Mark-Houwink-Sakurada parameters: methyl methacrylate,  $K = 12.8 \times 10^{-5}$  (dL/g),  $\alpha = 0.69$ ;<sup>44</sup> *t*-butyl methacrylate,  $K = 3.3 \times 10^{-5}$  (dL/g),  $\alpha = 0.80$ ;<sup>45</sup> styrene,  $K = 14.1 \times 10^{-5}$  (dL/g),  $\alpha = 0.70$ ;<sup>46</sup> poly(methyl acrylate),  $K = 3.88 \times 10^{-5}$  (dL/g),  $\alpha = 0.82$ ;<sup>47</sup> All hydrogenation trials were run in an eight-ampule Parr Reactor that was monitored and controlled with a Parr 4848 Reactor Controller.

### 3.7.2 Experimental Procedures

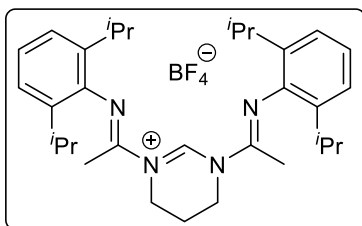
*Hydrogenation Conditions:* Into a Parr Reactor ampule equipped with a stir bar was added: sodium metal (0.002 g, 0.08 mmol), mercury (0.035 g, 0.174 mmol), the precatalyst (0.002 mmol), and toluene (2 mL). Into a separate vial was added: the substrate (0.15 mmol), tetradecane (2.0  $\mu$ L, 0.008 mmol), and toluene (1 mL), from which a  $t = 0$  time point was taken. The solution in the vial was then added to the ampule. The Parr Reactor was assembled and a flow of H<sub>2</sub> (80 psi) was applied. The reaction mixture was allowed to stir under pressure for 20-24 hours. Then, each reaction mixture was filtered through celite multiple times to remove all traces of amalgam before an aliquot was taken for GC/FID measurements.



*N*-(2,6-Diisopropylphenyl) acetimidoyl bromide (**3.17**). 2,6-Lutidene (2.78 mL, 23.9 mmol) was added to a solution of *N*-(2,6-diisopropylphenyl) acetamide (5.00 g, 22.8 mmol) that was dissolved in dichloromethane (22.8 mL). The colorless solution was cooled to 0 °C for 30 minutes, then oxalyl bromide (2.25 mL, 23.9 mmol) was added as quickly as possible (about one minute) while accounting for the vigorous gas evolution of the reaction. The originally clear yellow solution became cloudy orange. The reaction was stirred at 0 °C for 30 minutes. The solvent was removed in vacuo and the remaining yellow/orange solid was taken into a nitrogen-filled glovebox. The solid was taken up in hexanes, filtered through celite, and concentrated to dryness. This process was repeated with pentane. The remaining yellow oil was purified under inert conditions by Kugelrohr distillation. Yield = 2.8 g (44 %). <sup>1</sup>H NMR (500 MHz, CDCl<sub>3</sub>, ppm) δ 1.23-1.18 (12H, d, J = 6.86); 2.81 (3H, s); 2.85-2.75 (2H, septet, J = 6.88); 7.21-7.14 (3H, m, 4.82). <sup>13</sup>C NMR (125 MHz, C<sub>6</sub>D<sub>6</sub>, ppm) δ 23.18, 28.56, 32.86, 123.18, 124.73, 136.91, 137.28, 144.37. IR (neat): 2961, 1718, 1075, 790, 753, 541, 460 cm<sup>-1</sup>.

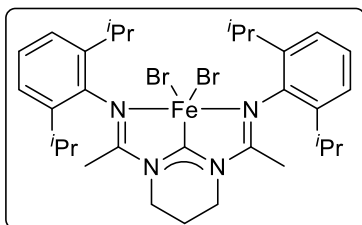


1,3-Bis((*E*)-1-((2,6-diisopropylphenyl)imino)ethyl)-3,4,5,6-tetrahydropyrimidin-1-ium bromide ((<sup>2,6-iPr</sup>Ph)CDA<sup>+</sup>Br) (**3.18**). *N*-(2,6-diisopropylphenyl) acetimidoyl bromide (0.143 g, 0.51 mmol) was dissolved in THF (5.1 mL), and *N*-1-[1-(2,6-diisopropylphenylimino)ethyl]-4,5,6-trihydropyrimidine (**3.6**) (0.145 g, 0.51 mmol) was added, and a white precipitate formed almost immediately. The solution was stirred at room temperature until high conversion was seen via <sup>1</sup>H NMR, about 1 h. The solvent was removed in vacuo and the remaining yellow and white solids were recrystallized in minimal THF and excess pentane at -40 °C to give a white solid. Yield = 0.257 g (89 %) <sup>1</sup>H NMR (125 MHz, CD<sub>2</sub>Cl<sub>2</sub>, ppm) δ 1.21-1.12 (24H, dd); 2.52-2.48 (8H, s/m); 2.81-2.76 (4H, septet); 4.35-4.32 (4H, t); 7.17-7.11 (6H, m); 9.61 (1H, s). <sup>13</sup>C NMR (500 MHz, CD<sub>2</sub>Cl<sub>2</sub>, ppm) δ 15.80, 18.51, 22.54, 23.11, 28.25, 42.24, 123.22, 124.74, 136.76, 142.07, 153.15. IR (neat): 2959, 1619, 1314, 1234, 1195, 765, 751, 446 cm<sup>-1</sup>. HRMS (ESI<sup>+</sup>) Calcd. For C<sub>32</sub>H<sub>47</sub>N<sub>4</sub> [M]<sup>+</sup>:487.38007; Found: 487.37931.



*1,3-Bis((E)-1-((2,6-diisopropylphenyl)imino)ethyl)-4,5,6-tetrahydropyrimidin-1-ium tetrafluoroborate (3.21)*. In an inert atmosphere glovebox, 1,3-bis((E)-1-((2,6-diisopropylphenyl)imino)ethyl)-4,5,6-tetrahydropyrimidin-1-ium chloride (0.500 g,

0.95 mmol) was weighed into a 20 mL vial and taken up in CH<sub>3</sub>CN (5 mL). NaBF<sub>4</sub> (0.104 g, 0.95 mmol) was taken up in CH<sub>3</sub>CN (5 mL) and this solution was transferred into the ligand solution. The reaction mixture was allowed to stir at room temperature for 24 hrs. The yellow, cloudy reaction mixture was diluted with THF (30 mL) and filtered through celite. The filtrate was concentrated to dryness, then taken up in a minimal amount of THF, then layered with an equal amount of pentane and cooled to -40 °C for several days before fluffy white crystals were isolated. Yield = 0.405 g (74 %). <sup>1</sup>H NMR (600 MHz, CD<sub>2</sub>Cl<sub>2</sub>) δ 9.31 (s, 1H), 7.22 – 7.12 (m, 6H), 4.29 (t, J = 5.9 Hz, 4H), 2.73 (p, J = 6.8 Hz, 4H), 2.47 (t, J = 5.9 Hz, 2H), 2.22 (s, 6H), 1.17 (dd, J = 36.8, 6.8 Hz, 23H). <sup>13</sup>C NMR (151 MHz, CD<sub>2</sub>Cl<sub>2</sub>) δ 152.62, 136.79, 124.92, 123.28, 67.71, 42.13, 28.16, 25.54, 23.10, 22.40, 14.55. <sup>19</sup>F NMR (470 MHz, CD<sub>2</sub>Cl<sub>2</sub>, ppm) δ -152.65. IR (neat): cm<sup>-1</sup> 776.11, 1057.60, 1196.05, 1627.65, 2869.35, 2960.77. HRMS (ESI+) Calcd. For C<sub>32</sub>H<sub>47</sub>N<sub>4</sub> [M]<sup>+</sup>:487.38007; Found: 487.37931

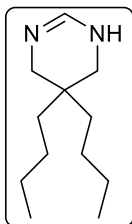


*[N,N-1,3-Bis[1-(2,6-diisopropylphenylimino)ethyl]-4,5,6-trihydropyrimid-2-ylidene] iron dibromide (3.19)*. From **3.18**: In a nitrogen-filled glovebox, a solution of NaHMDS (0.338 g, 1.84 mmol) in THF (12 mL), a solution of FeBr<sub>2</sub> (0.234 g, 1.84 mmol)

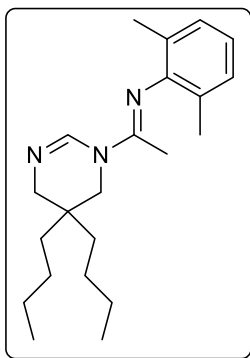
in THF (12 mL), and a solution of N, N-1,3-Bis[1-(2,6-diisopropylphenylimino)ethyl]-4,5,6-trihydropyrimidinium bromide (**4**) (0.917 g, 1.76 mmol) in THF(10 mL) were all cooled to -40 °C. An additional 12.2 mL of THF was also cooled to -40 °C for later washing. The solution of NaHMDS was added to the FeBr<sub>2</sub>, and the mixture was kept at -40 °C for 18 h with occasional agitation. This Fe(HMDS)Br solution was then warmed to room temperature, stirred for 30 minutes, then re-cooled to -40 °C. This solution was then filtered through celite into the ligand solution. This mixture was allowed to stir at room temperature overnight, then the solvent was removed in vacuo. The

remaining red and purple solids were dissolved in THF, dichloromethane, and diethyl ether (91.7 mL, 2:3:2), filtered through celite, and cooled to -40 °C for several days. The dark red/purple crystals were isolated, and purity was confirmed by IR spectroscopy and X-ray crystallography. Yield = 0.391 g (36 %). From **3.21**: Follow the same procedure as above but add one equivalent of [NMe<sub>4</sub>][Br]. IR (neat): 2959, 2866, 1612, 1560, 1389, 1322, 1291, 1206, 794, 769 cm<sup>-1</sup> (Nearly identical to previously reported (<sup>i</sup>PrCDA)FeCl<sub>2</sub>)<sup>5</sup>.

*2,2-dibutylpropane-1,3-diamine (3.22)* was prepared according to literature procedures.<sup>48</sup>

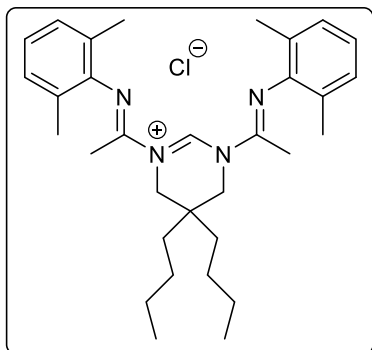


*5,5-dibutyl-1,4,5,6-tetrahydropyrimidine (3.23)*: On the Schlenk line, **3.22** (2.00 g, 10.7 mmol) was weighed into a 250 mL rbf equipped with a stirbar and a 180° joint, and then thoroughly degassed. Degassed toluene (20 mL) was added to the flask followed by DMF dimethyl acetal (0.980 mL, 11.3 mmol). The reaction was allowed to stir at 80 °C for 18 hours, and the solvent was removed in vacuo. The residue was purified by Kugelrohr distillation to give a colorless oil. Yield = 1.95 g (93 %). <sup>1</sup>H NMR (500 MHz, CDCl<sub>3</sub>) δ 7.10 (s, 1H), 2.97 (d, J = 0.9 Hz, 4H), 2.34 (s, 1H), 1.33 – 1.14 (m, 12H), 0.89 (t, J = 7.2 Hz, 6H). <sup>13</sup>C NMR (125 MHz, CD<sub>2</sub>Cl<sub>2</sub>, ppm) δ 14.02, 23.47, 25.07, 31.52, 33.80, 50.05, 147.08. IR (neat): 729.84, 1632.85, 2858.7, 2927.79 cm<sup>-1</sup>; HRMS (ESI+) Calcd. For C<sub>12</sub>H<sub>25</sub>N<sub>2</sub> [M]<sup>+</sup>: 197.20177. Found: 197.20195.



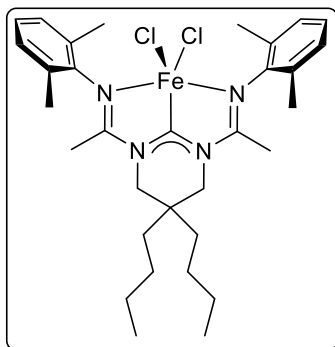
*(E)-1-(5,5-dibutyl-5,6-dihydropyrimidin-1(4H)-yl)-N-(2,6-dimethylphenyl)ethan-1-imine (3.24)*: To a solution of **3.23** (2.05 g, 10.4 mmol) in THF (90 mL, 0.1 M) at -78 °C, was added nBuLi (4.0 mL, 2.7 M, 10.9 mmol) and the solution was allowed to stir at -78 °C for 20 minutes. N-(2,6-dimethylphenyl) acetimidoyl chloride (1.97 g, 10.4 mmol) was then added and the mixture was allowed to stir for one hour at -78 °C and then for one hour at room temperature. The solvent was removed in vacuo, then the residue was taken up in

pentane and re-concentrated several times to yield an off-white solid. Yield = 1.88 g (53 %). A clean  $^1\text{H-NMR}$  of this compound could not be obtained.



*5,5-dibutyl-1,3-bis((E)-1-((2,6-dimethylphenyl)imino)ethyl)-3,4,5,6-tetrahydropyrimidin-1-ium chloride (3.25)*. In an inert atmosphere glove box, **3.24** (0.505 g, 1.79 mmol) and N-(2,6-dimethylphenyl) acetimidoyl chloride (0.426 g, 1.79 mmol) were weighed into a 20 mL vial equipped with a stir bar and taken up in toluene (15 mL). The solution was allowed to stir at room

temperature for several hours, during which a white precipitate formed in the yellow solution. The white precipitate was collected by vacuum filtration, and the solids were taken up in a minimal amount of methylene chloride and pentane was added until the solution became cloudy. The solution was cooled to  $-40\text{ }^\circ\text{C}$ . 24 hours later the solid ligand was collected *via* vacuum filtration. Yield: 0.196 g (53 %).  $^1\text{H NMR}$  (600 MHz,  $\text{CD}_2\text{Cl}_2$ )  $\delta$  9.88 (s, 1H), 7.07 (d,  $J = 7.5\text{ Hz}$ , 4H), 7.00 – 6.94 (m, 2H), 4.07 (s, 4H), 2.61 (s, 6H), 2.06 (s, 12H), 1.51 (d,  $J = 16.2\text{ Hz}$ , 2H), 1.43 – 1.30 (m, 8H), 0.94 (t,  $J = 7.0\text{ Hz}$ , 6H).  $^{13}\text{C NMR}$  (151 MHz,  $\text{CD}_2\text{Cl}_2$ )  $\delta$  206.29, 153.98, 144.65, 128.04, 126.30, 124.02, 50.25, 33.01, 32.24, 25.17, 23.12, 17.92, 15.58, 13.73. IR (neat): 854.47, 763.51, 1195.79, 1622.86, 2867.35, 2931.81, 2954.50  $\text{cm}^{-1}$ .

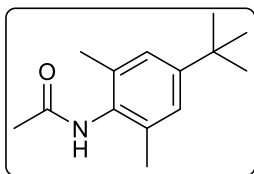


*5,5-dibutyl-1,3-bis((E)-1-((2,6-dimethylphenyl)imino)ethyl)-3,4,5,6-tetrahydropyrimidin-1-ium iron dichloride (3.31)*. In an inert atmosphere glove box, iron dichloride (0.007 g, 0.05 mmol) was weighed into a 4 mL vial and taken up in THF (0.4 mL) and allowed to stir for several minutes before it was cooled to  $-40\text{ }^\circ\text{C}$ . NaHMDS (0.009 g, 0.049 mmol) was weighed into a 4 mL vial and taken up

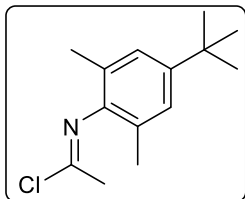
in THF (0.2 mL), then cooled to  $-40\text{ }^\circ\text{C}$ . Once both solutions were fully cooled (ca. 1 hr), the NaHMDS solution was added to the  $\text{FeCl}_2$  solution using 0.2 mL THF to transfer. The mixture was

warmed to room temperature and allowed to stir for one hour, then re-cooled to  $-40^{\circ}\text{C}$ . **3.25** (0.025 g, 0.047 mmol) was weighed into a 20 mL vial, taken up in THF (0.2 mL), and cooled to  $-40^{\circ}\text{C}$ . Once both solutions had fully cooled (ca. 1 hr), the  $\text{FeCl}_2/\text{NaHMDS}$  solution was filtered through celite into the solution of **3.25**, using 0.2 mL of THF to wash. The solution was allowed to warm to room temperature and stir overnight. Then, the red and pink solution was filtered through celite and the dark red filtrate was concentrated to dryness, then taken up in THF and pentane and allowed to crystallize at  $-40^{\circ}\text{C}$ . Yield = 0.015 g (27 %).

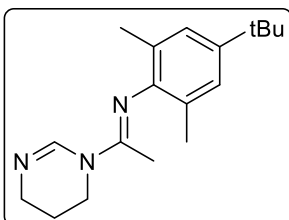
Compound **3.26** was prepared and confirmed according to literature procedures.<sup>49</sup>



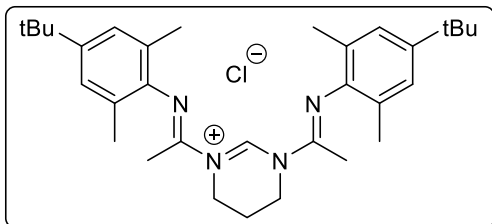
*N*-(4-(*tert*-butyl)-2,6-dimethylphenyl)acetamide (**3.27**): Under an inert atmosphere, **3.26** (1.81 mL, 9.52 mmol) was taken up in degassed THF (20 mL) and triethylamine (1.46 mL, 10.5 mmol) was added. In a separate flask, acetyl chloride (0.68 mL, 9.52 mmol) was taken up in THF (30 mL). Both mixtures were cooled to  $0^{\circ}\text{C}$  and the acetyl chloride solution was added dropwise to the solution of **3.30**. The reaction mixture was then warmed to room temperature and allowed to stir for 4 hours. The solution was then poured over water and extracted (EtOAc, 3x). The organic layers were combined, washed with brine, dried over sodium sulfate, filtered, and concentrated to dryness. The resulting yellow oily solid was recrystallized from a minimal amount of ethyl acetate and an excess of hexanes to yield a white, fluffy solid (1.81g, 87 %). Rotamer ratio = 4:1.  $^1\text{H}$  NMR (500 MHz,  $\text{CD}_2\text{Cl}_2$ , ppm)  $\delta$  (minor rotamer) 1.31 (s, 9H); 1.60 (s, 3H); 2.10 (s, 6H); 7.10 (2H). (Major rotamer) 1.31 (s, 9H); 1.60 (s, 3H); 2.10 (s, 6H); 7.10 (2H).  $^{13}\text{C}$  NMR (125 MHz,  $\text{CD}_2\text{Cl}_2$ , ppm)  $\delta$  (minor rotamer) 18.71, 31.29, 34.30, 125.57, 135.91, 151.21, 173.21. (Major rotamer) 18.66, 19.85, 31.29, 125.30, 134.81, 150.15, 168.61. IR (neat): 1522.82, 1653.37, 2956.53, 3262.83  $\text{cm}^{-1}$ . HRMS (DART+) Calcd. For  $\text{C}_{14}\text{H}_{22}\text{NO}$   $[\text{M}]^+$ :220.17014. Found: 220.17046.



*(E)*-*N*-(4-(*tert*-butyl)-2,6-dimethylphenyl)acetimidoyl chloride (**3.28**). Under an inert atmosphere, **3.27** (5.00 g, 22.8 mmol) and 2,6-lutidine (2.8 mL, 23.9 mmol) were taken up in CH<sub>2</sub>Cl<sub>2</sub> (22.8 mL, 1.0 M) and cooled to 0 °C. Oxalyl chloride (2.05 mL, 23.9 mmol) was then added as quickly as possible (about one minute) while accounting for the vigorous gas evolution. The reaction mixture was allowed to stir at 0 °C for 30 minutes. Then the solvent was removed in vacuo and the residual yellow solids were taken up in hexanes, filtered through celite, and concentrated to dryness. The same was done with pentane. The remaining yellow oil was then purified by Kugelrohr distillation to yield an off white solid that was stored in a nitrogen-filled glovebox (0.547 g, 94 %). <sup>1</sup>H NMR (500 MHz, CDCl<sub>3</sub>, ppm) δ 1.30(2, 9H), 2.07 (2, 6H), 2.61 (s, 3H); 7.03 (s, 2H). <sup>13</sup>C NMR (125 MHz, CDCl<sub>3</sub>, ppm) δ 18.12, 31.41, 34.11, 124.42, 125.01, 125.77, 143.13, 146.80. IR (neat): 765, 1708, 2963 cm<sup>-1</sup>. HRMS (ESI+) Calcd. For C<sub>14</sub>H<sub>21</sub>ClN [M]<sup>+</sup>:238.13625; Found: 238.13737.

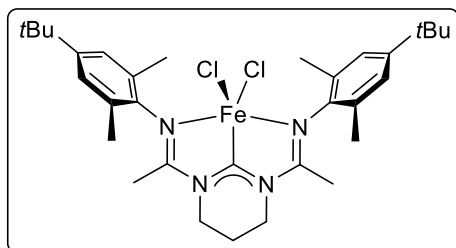


*(E)*-*N*-(4-(*tert*-butyl)-2,6-dimethylphenyl)-1-(5,6-dihydropyrimidin-1-(4H)-yl) ethan-1-imine (**3.29**). To a solution of 2,3,5,6-tetrahydropyrimidine (0.100 mL, 1.24 mmol) in THF (12.4 mL, 0.1 M) at -78 °C, was added *n*BuLi (0.52 mL, 2.5 M, 1.30 mmol) and the solution was allowed to stir at -78 °C for 20 minutes. Imidoyl chloride **3.28** (0.289 g, 1.24 mmol) was then added and the mixture was allowed to stir for one hour at -78 °C and then for one hour at room temperature. The solvent was removed in vacuo, then lyophilized with pentane to yield an off-white solid. Yield: 0.252 g, 72 %. <sup>1</sup>H NMR (500 MHz, CDCl<sub>3</sub>, ppm) δ 1.29 (s, 9H); 1.88 (s, 3H); 1.94 (m, 2H), 1.99 (s, 6H), 3.47 (t, *J* = 6.2 Hz, 2H); 3.85 (t, *J* = 6.1 Hz, 2H); 7.01 (s, 2H); 7.87 (s, 1H). <sup>13</sup>C NMR (125 MHz, CDCl<sub>3</sub>, ppm) δ 14.50, 18.47, 21.12, 31.53, 33.97, 41.12, 44.52, 124.77, 125.30, 126.57, 144.13, 145.10, 152.50. IR (neat): 995, 1184, 1332, 1616, 2937 cm<sup>-1</sup>. HRMS (ESI+) Calcd. For C<sub>18</sub>H<sub>28</sub>N<sub>3</sub> [M]<sup>+</sup>: 286.22832; Found: 286.22724.

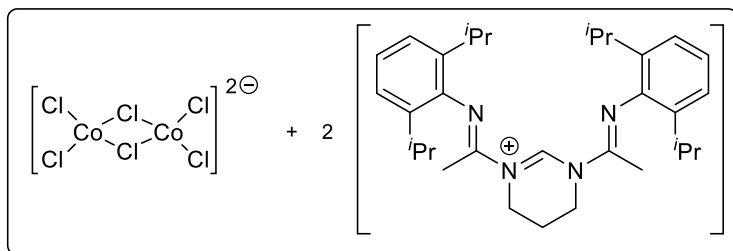


*1,3-bis((E)-1-((4-(tert-butyl)-2,6-dimethylphenyl)imino)ethyl)-3,4,5,6-tetrahydropyrimidin-1-ium chloride (3.30)*: In an inert atmosphere glovebox, **3.29** (0.124 g, 0.441 mmol) and **3.28** (0.103 g, 0.441 mmol)

were combined in toluene (100 mL) and allowed to stir for about an hour. The white precipitate was removed by filtration and rinsed with pentane. The solid was then taken up in a minimal amount of CH<sub>2</sub>Cl<sub>2</sub> (2 mL) and layered with pentane (18 mL), then cooled to -40 °C. The white solid was later collected by vacuum filtration. Yield: 0.113 g, 50 %. <sup>1</sup>H NMR (500 MHz, CD<sub>2</sub>Cl<sub>2</sub>, ppm) δ 1.30 (s, 4H); 2.05 (s, 12H); 2.44 (m, 2H); 2.57 (s, 6H); 4.32 (t, *J* = 5.8 Hz, 4H); 7.05 (s, 4H); 9.88 (s, 1H). <sup>13</sup>C NMR (125 MHz, CD<sub>2</sub>Cl<sub>2</sub>, ppm) δ 13.94, 18.61, 22.54, 31.37, 34.13 50.29, 124.87, 125.58, 141.69, 147.11, 153.23, 153.75. IR (neat): 2925, 1625 (ν<sub>CN</sub>), 1196 cm<sup>-1</sup>; HRMS (DART) Calcd. For C<sub>32</sub>H<sub>47</sub>N<sub>4</sub> [M]: 487.3812; Found: 487.3831.



*1,3-bis((E)-1-((2,6-dimethyl-4-tert-butylphenyl)imino)ethyl)-3,4,5,6-tetrahydropyrimidin-1-ium bromide, (3.32)*. Prepared in the same fashion as **3.31**. Yield = 31 %.



*[Co<sub>2</sub>Cl<sub>6</sub>][2CDA] (3.33)*. In an inert atmosphere glovebox, cobalt dichloride (0.026 g, 0.201 mmol) was weighed into a 4 mL vial and taken up in 1 mL THF.

The solution was allowed to stir vigorously for several minutes to allow the salt to dissolve, then it was cooled to -40 °C. NaHMDS (0.037 g, 0.201 mmol) was weighed into a 4 mL vial and dissolved in 1 mL THF, then cooled to -40 °C. After both solutions had cooled for one hour, the solutions were combined, using 0.5 mL THF to aid in transfer, and allowed to warm to room temperature with

stirring, then allowed to stir overnight before it was recooled to  $-40\text{ }^{\circ}\text{C}$ .  $\text{CDA}^+\text{Cl}^-$  ligand **3.7** (0.100 g, 0.191 mmol) was weighed into a 20 mL vial equipped with a stir bar and dissolved in THF (1.5 mL) before it was cooled to  $-40\text{ }^{\circ}\text{C}$ . Once both solutions had cooled completely ( $\sim 1\text{ hr}$ ), the  $\text{CoCl}_2/\text{NaHMDS}$  solution was filtered through celite into the ligand solution. The celite was washed with 1 mL THF. The reaction mixture was allowed to come to room temperature and stir overnight. Then, the solution was filtered through celite and the filtrate was collected and concentrated to dryness. The residue was taken up in a minimal amount of THF and layered with pentane, then cooled to  $-40\text{ }^{\circ}\text{C}$  for several days until yellow-green crystals formed.  $^1\text{H NMR}$  (500 MHz,  $\text{CDCl}_3$ )  $\delta$  6.33, 6.18, 2.08, 1.72, 0.42, -0.56. IR (neat): 748.28, 763.11, 782.09, 800.29, 1183.39, 1625.19, 2867.98, 2961.33  $\text{cm}^{-1}$ .

### 3.8 SPECTROSCOPY

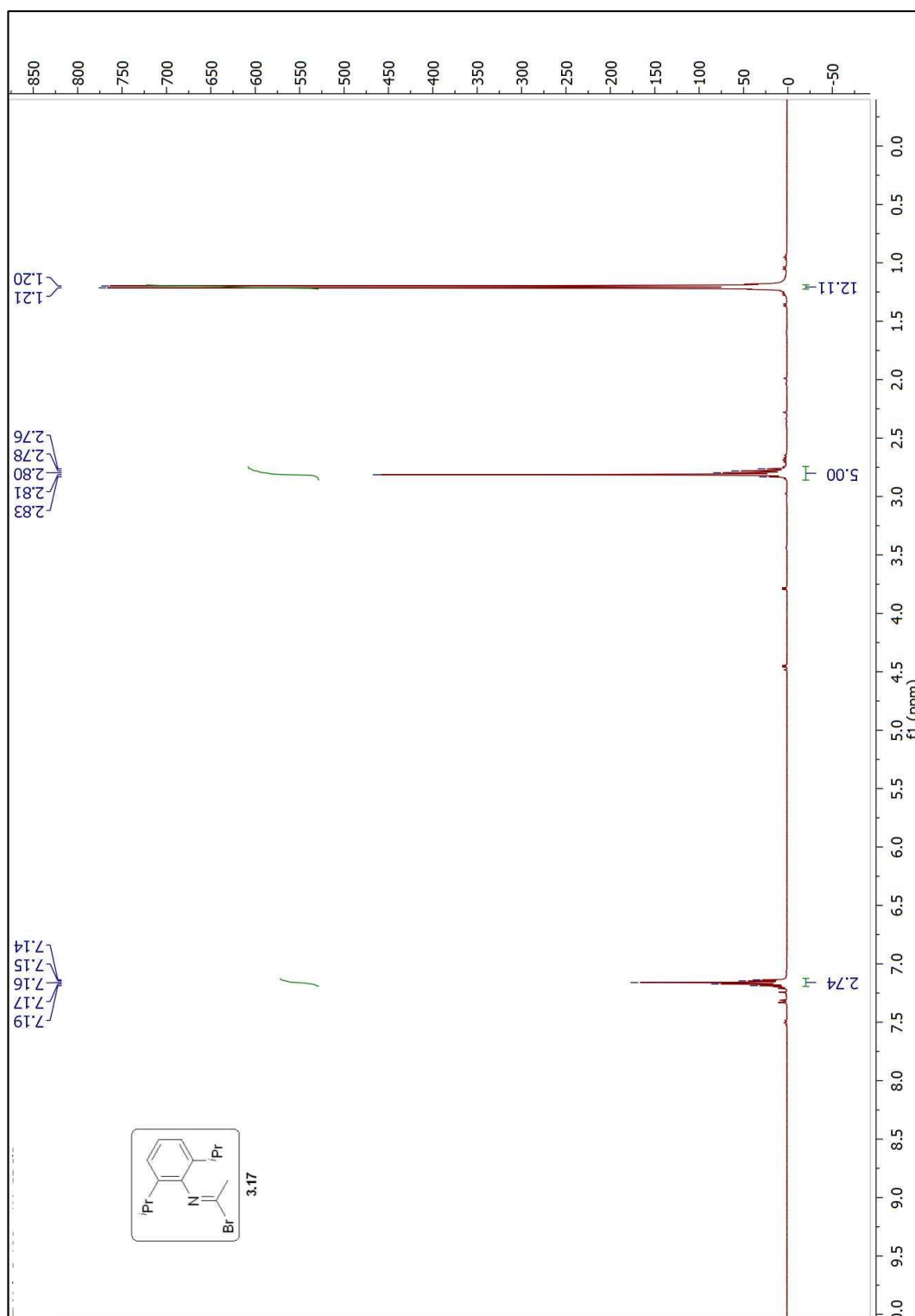


Figure 3.21  $^1\text{H}$  NMR Spectrum of 3.17.

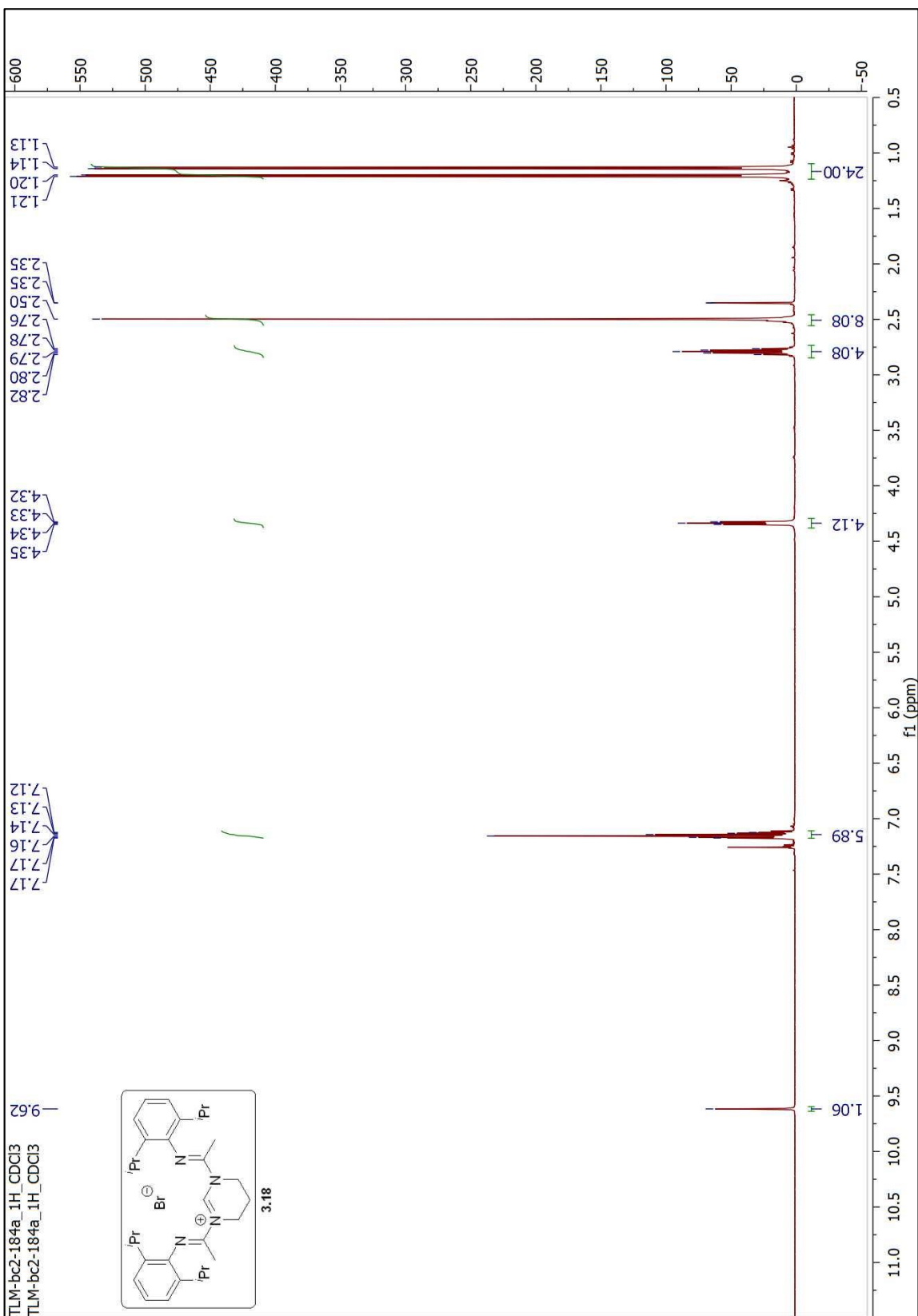


Figure 3.22 <sup>1</sup>H NMR Spectrum of 3.18.

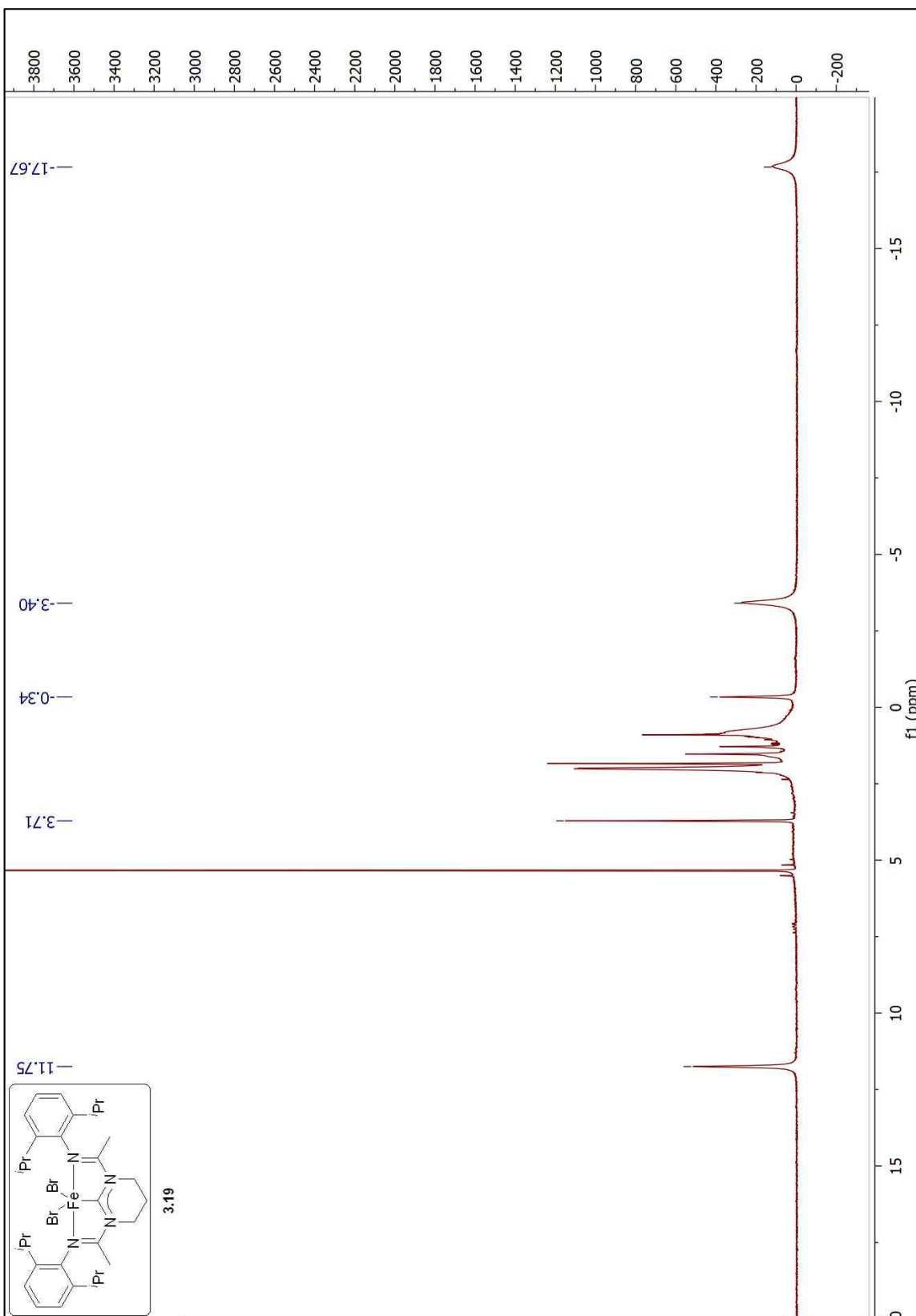


Figure 3.23  $^1\text{H}$  NMR Spectrum of 3.19.

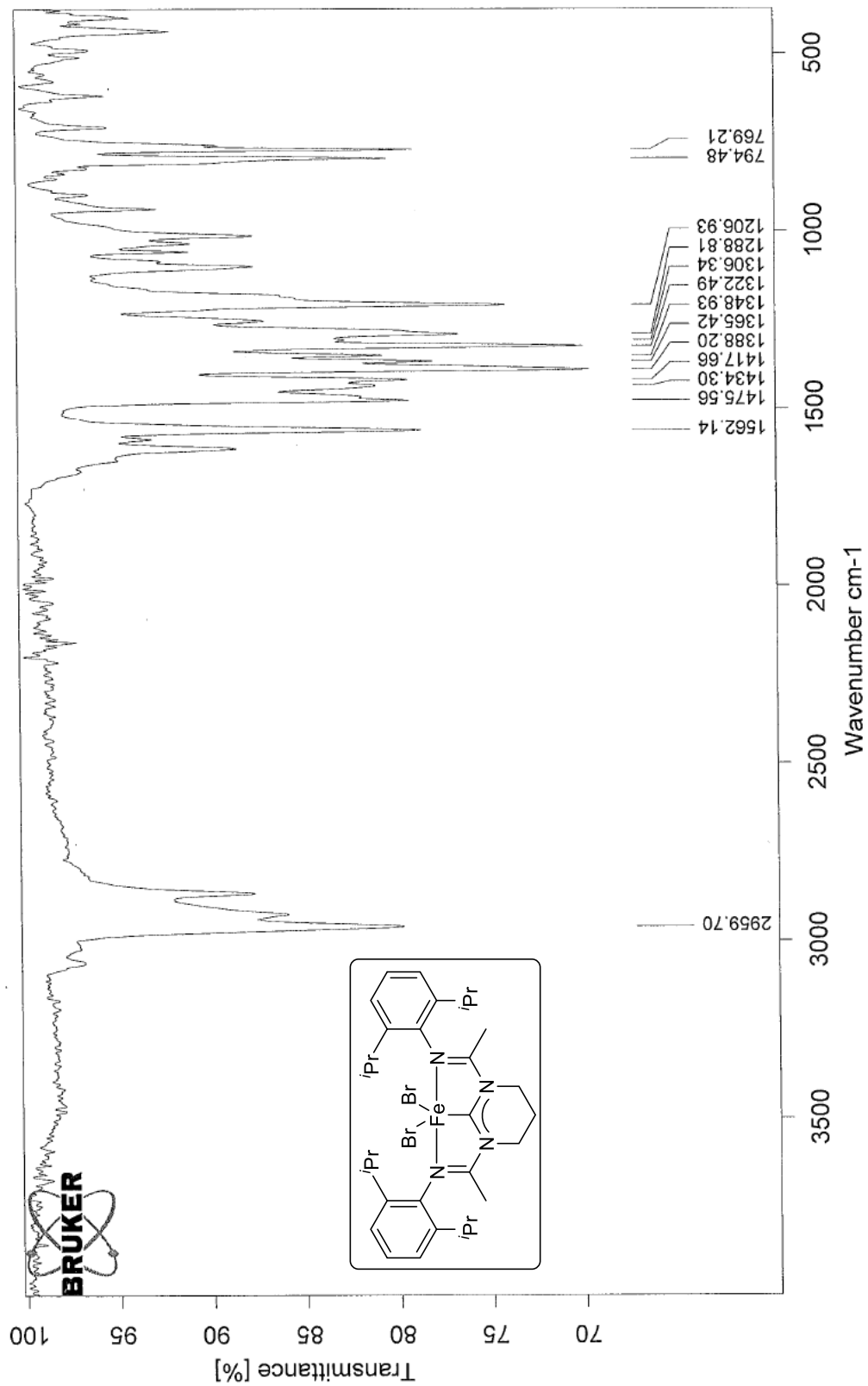


Figure 3.24 IR Spectrum of 3.19.

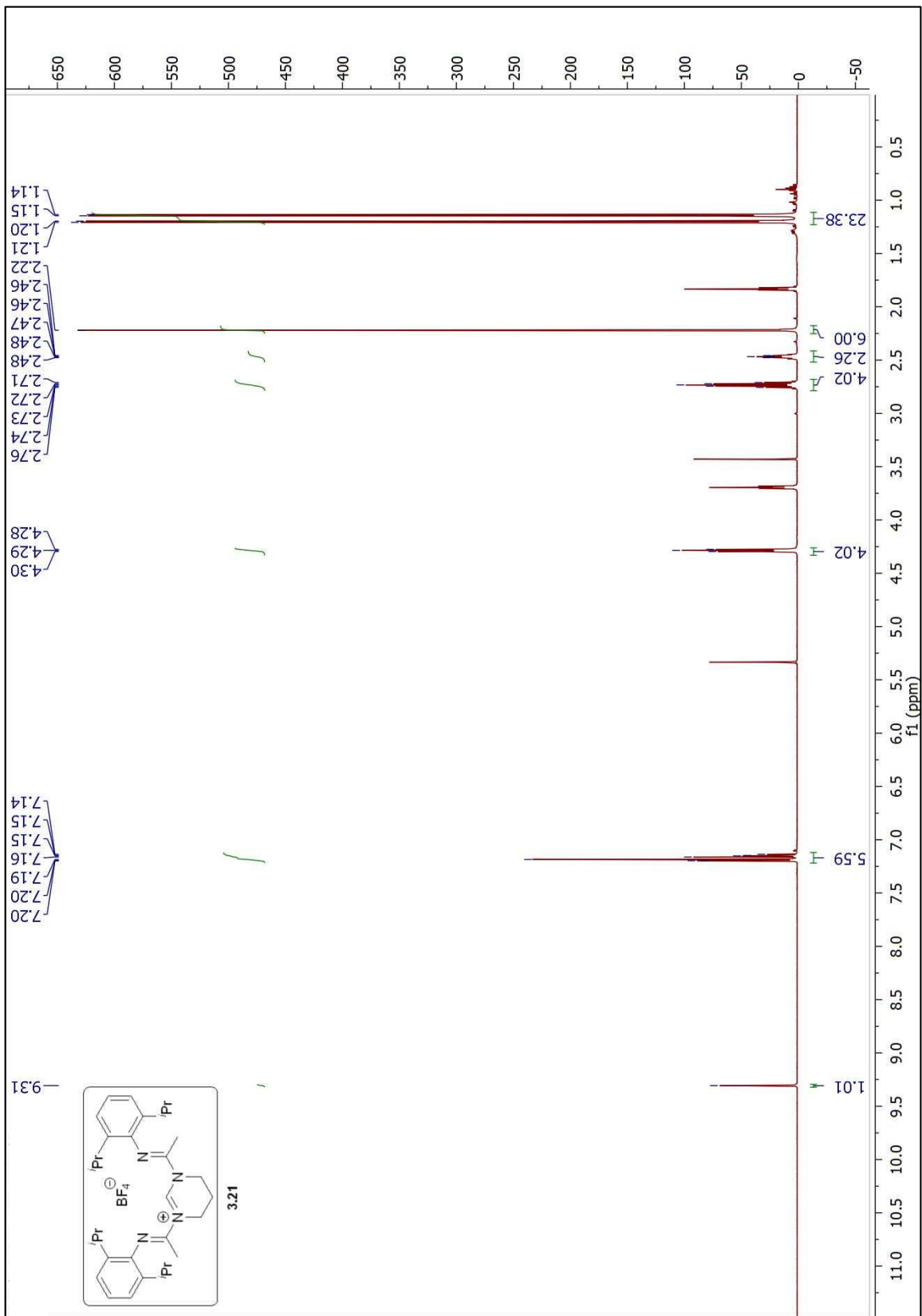


Figure 3.25  $^1\text{H}$  NMR Spectrum of 3.21.

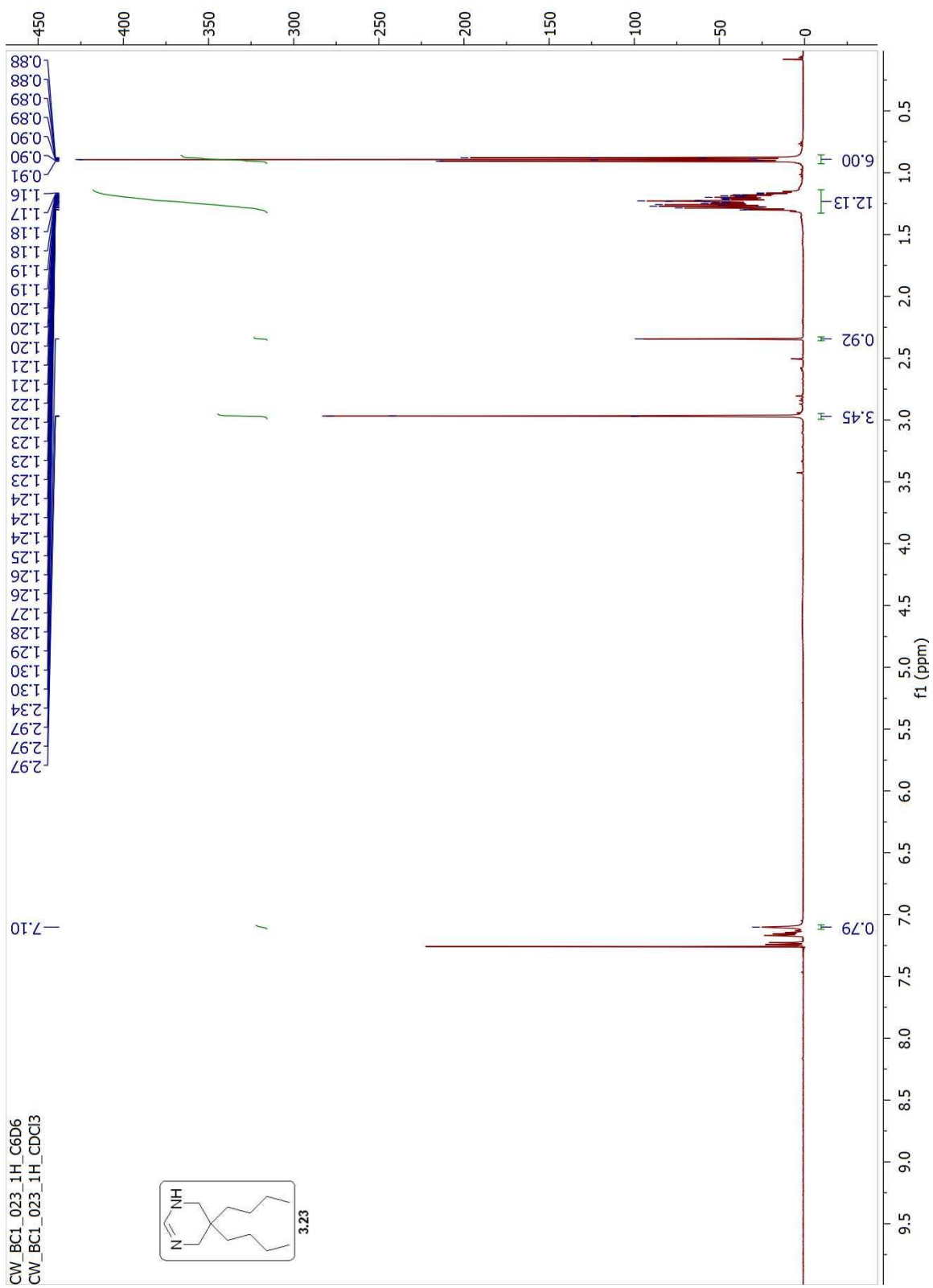


Figure 3.26  $^1\text{H}$  NMR Spectrum of 3.23.



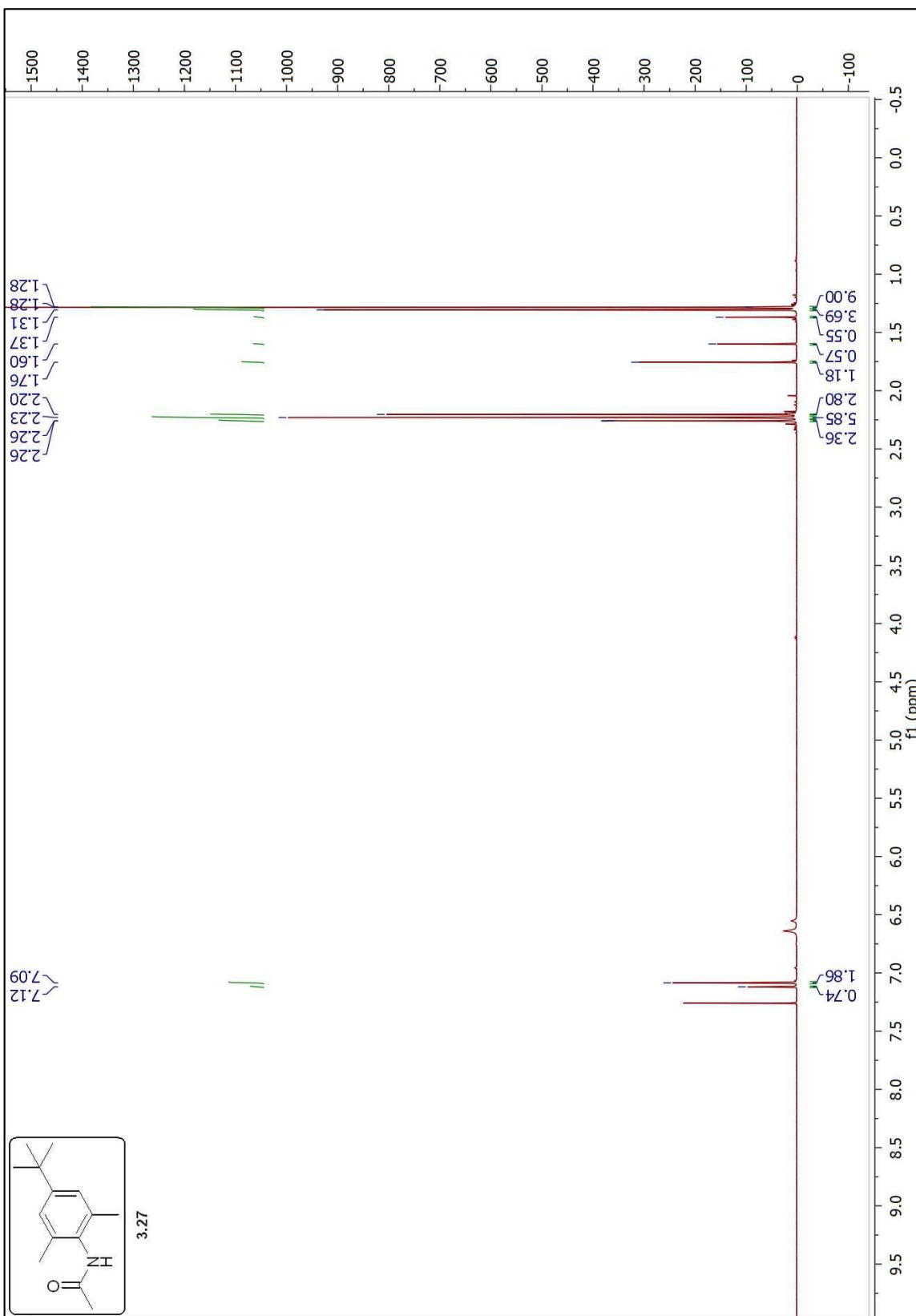


Figure 3.28 <sup>1</sup>H NMR Spectrum of 3.27.

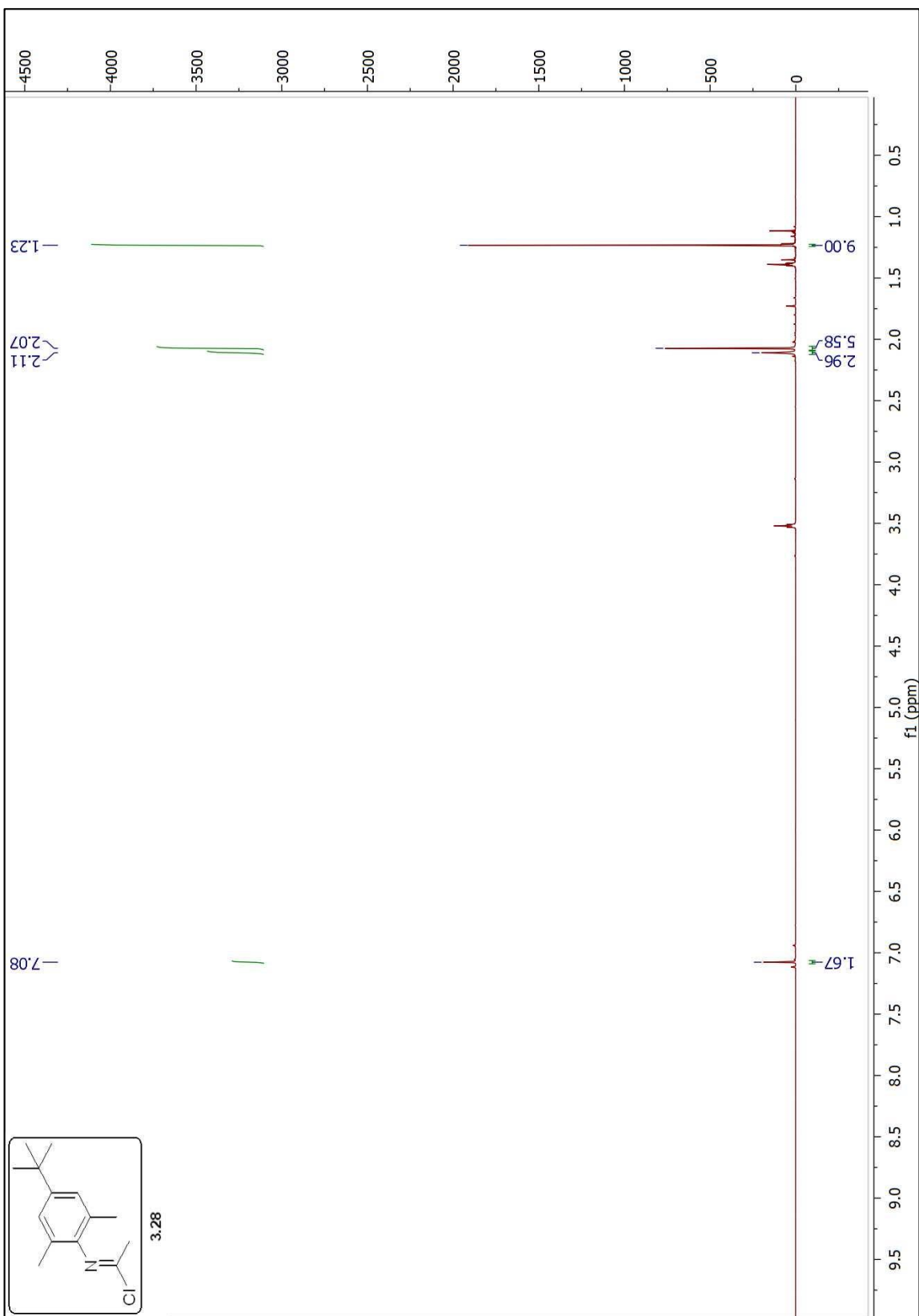


Figure 3.29  $^1\text{H}$  NMR Spectrum of 3.28.

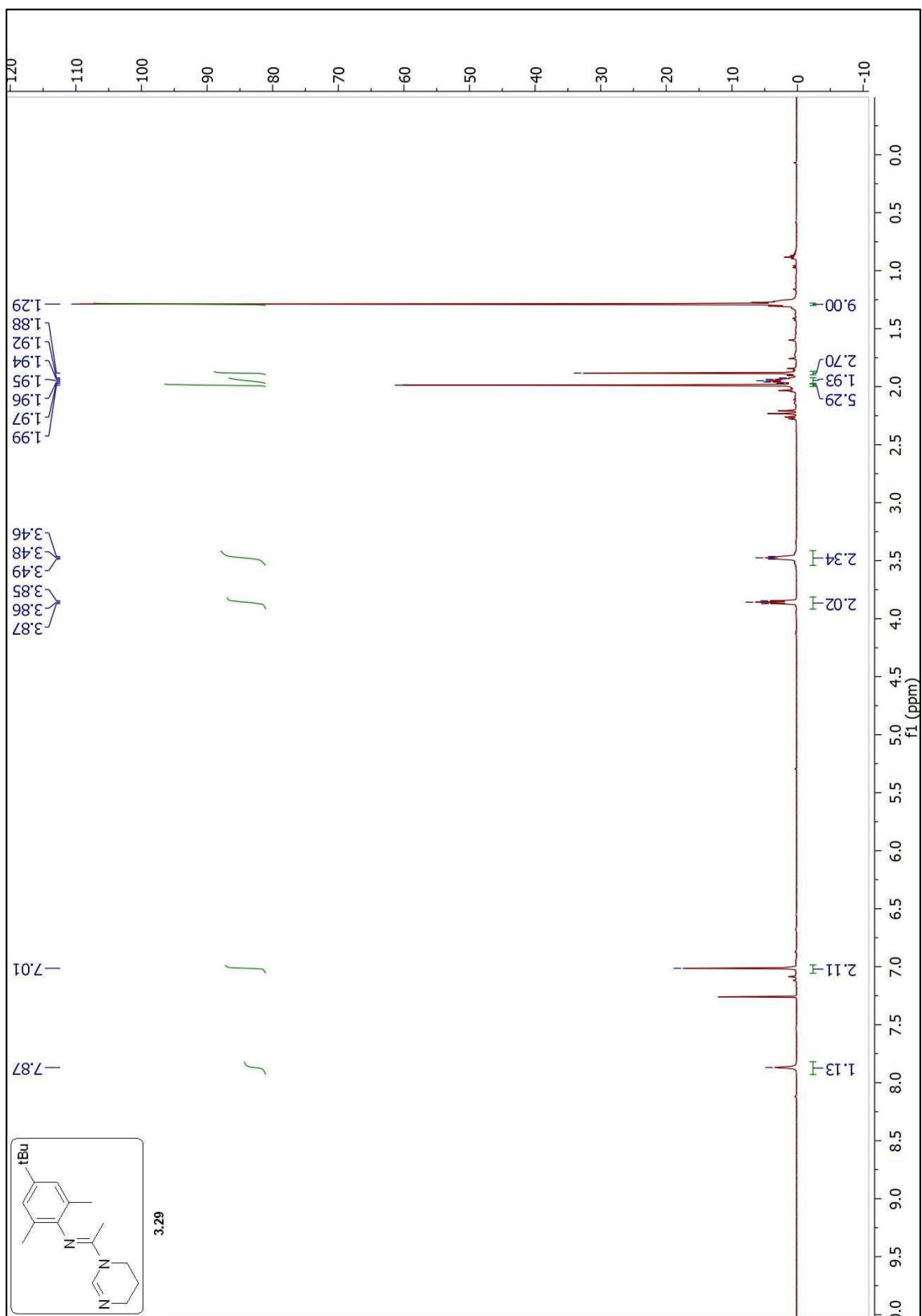


Figure 3.30  $^1\text{H}$  NMR Spectrum of 3.29.

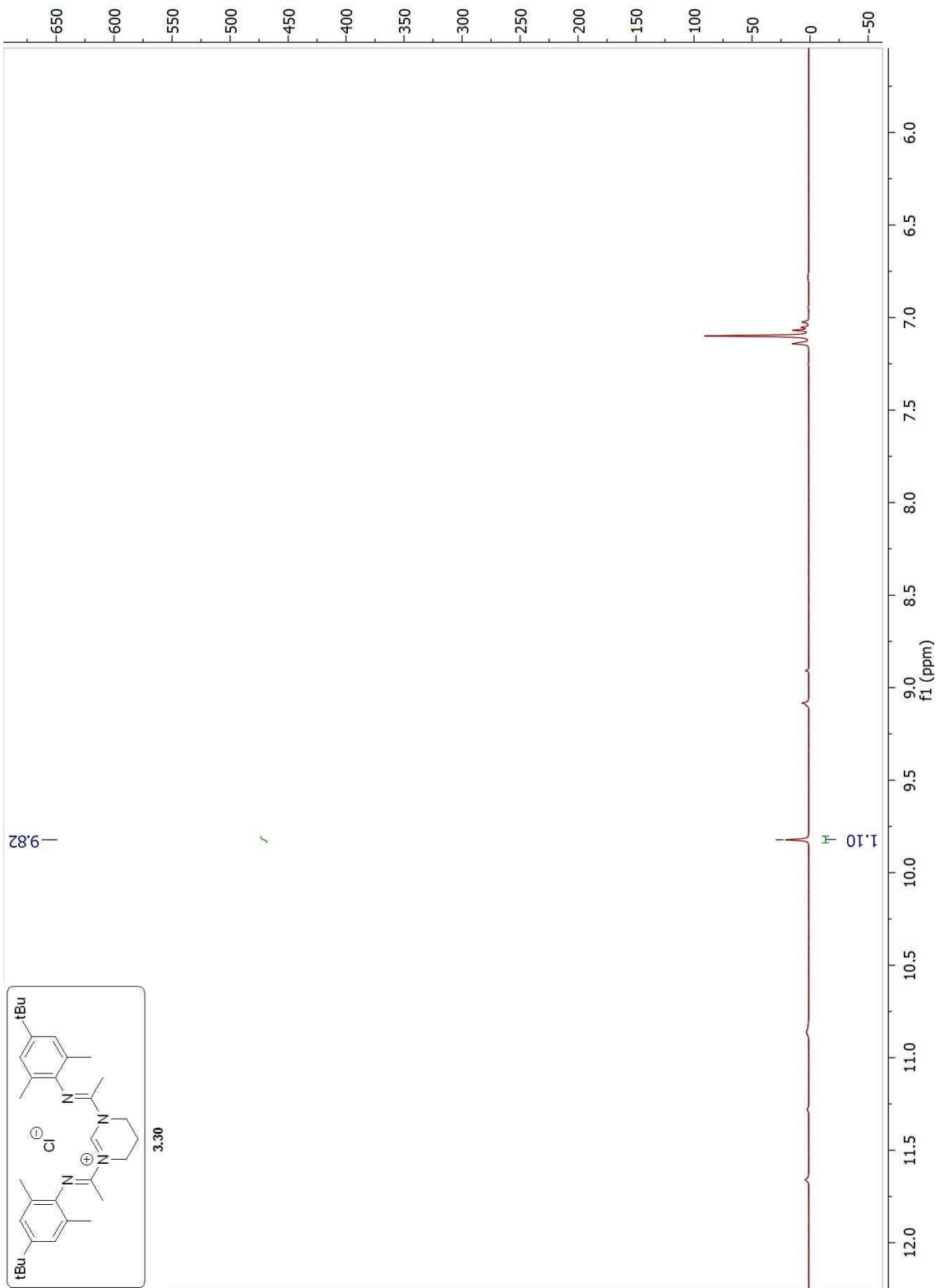


Figure 3.31. <sup>1</sup>H NMR Spectrum of 3.30.

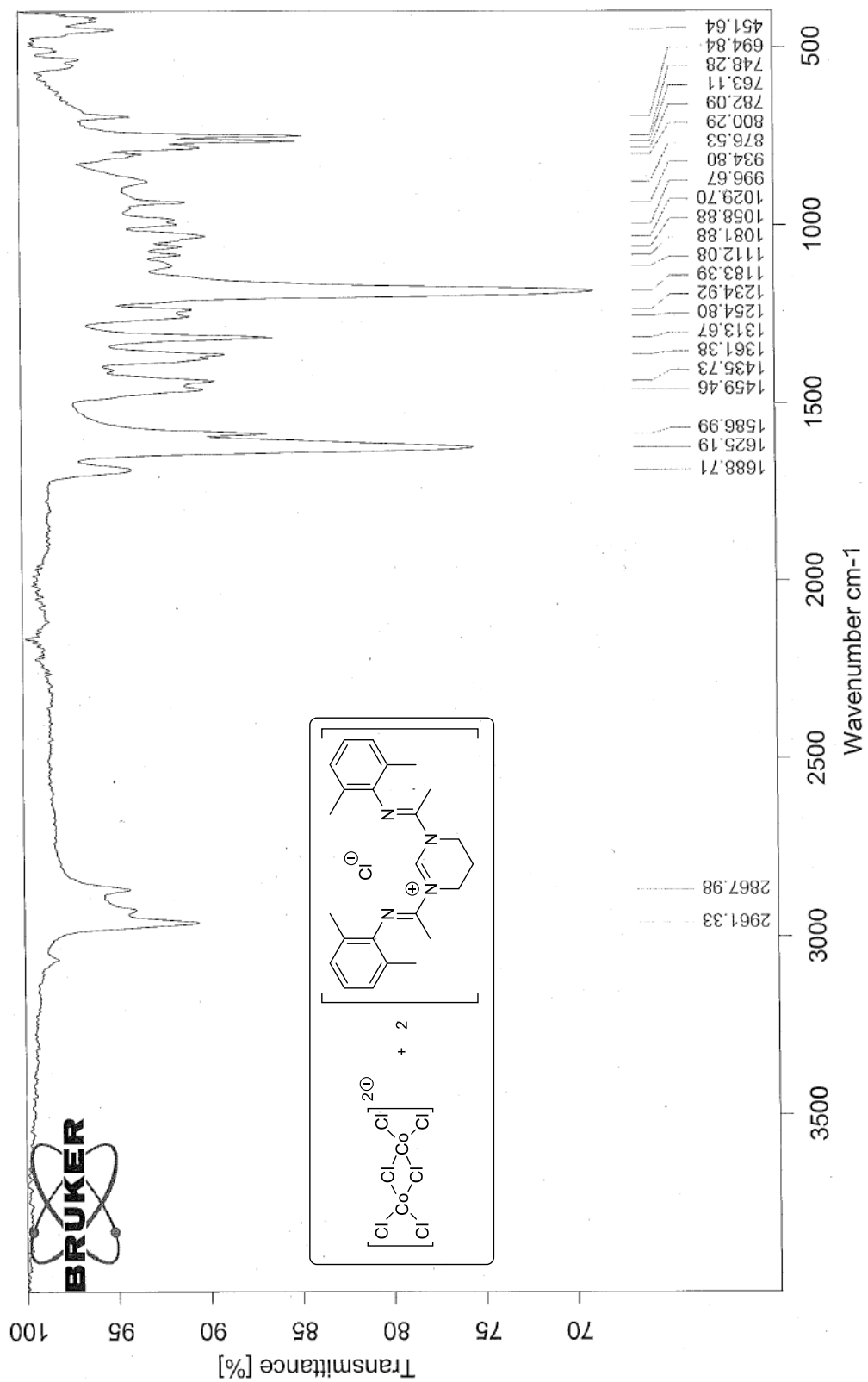


Figure 3.32 IR Spectrum of 3.34.

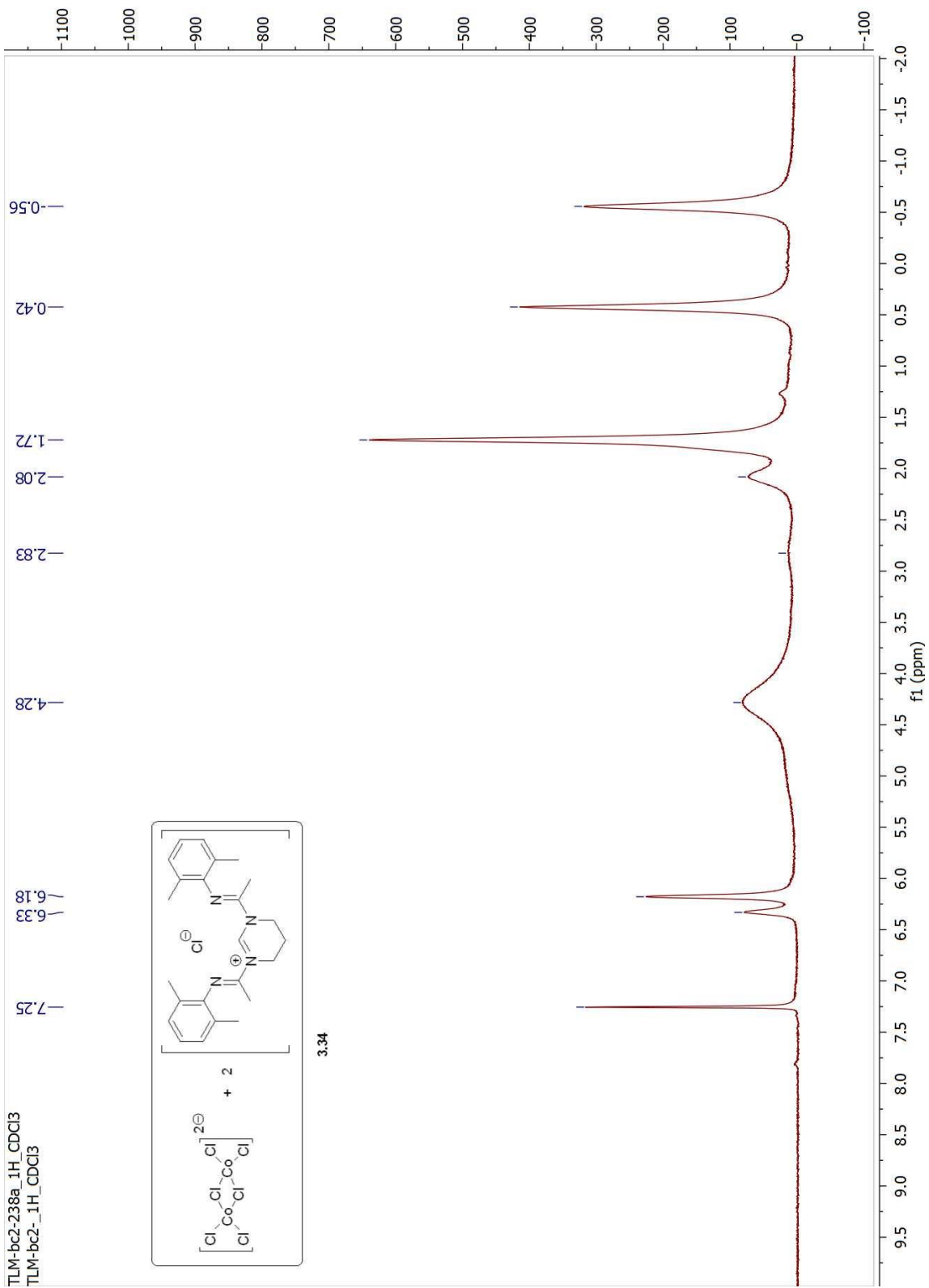


Figure 3.33  $^1\text{H}$  NMR of 3.34.

### 3.9 REFERENCES

- <sup>1</sup> Small, B. L.; Brookhart, M.; Bennet, A. M. A. *J. Am. Chem. Soc.* **1998**, *120*, 4049.
- <sup>2</sup> Britovsek, G. J. P.; Gibson, V. C.; Kimberly, B. S.; Maddox, P. J.; McTavish, S. J.; Solan, G. A.; White, A. J. P.; Williams, D. J. *Chem. Commun.* **1998**, *311*, 849.
- <sup>3</sup> Gibson, V. C.; Redshaw, C.; Solan, G. A. *Chem. Rev.* **2007**, *107*, 1745.
- <sup>4</sup> Karpiniec, S. S.; McGuinness, D. S.; Britovsek, G. J. P.; Patel, J. *Organometallics* **2012**, *31*, 3439.
- <sup>5</sup> Bart, S. C.; Lobkovsky, E.; Chirik, P. J. *J. Am. Chem. Soc.* **2004**, *126*, 13794.
- <sup>6</sup> Trovitch, R. J.; Lobkovsky, E.; Eckhard, B.; Chirik, P. J. *Organometallics* **2008**, *27*, 1470.
- <sup>7</sup> Obligacion, J. V.; Chirik, P. J. *Org. Lett.* **2013**, *15*, 2680.
- <sup>8</sup> (a) Tondreau, A. M.; Atienza, C. C. H.; Weller, K. J.; Nye, S. A.; Lewis, K. M.; Delis, J. G. P.; Chirik, P. J. *Science* **2012**, *335*, 567. (b) Tondreau, A. M.; Atienza, C. C. H.; Darmon, J. M.; Milsmann, C.; Hoyt, H. M.; Weller, K. J.; Nye, S. A.; Lewis, K. M.; Boyer, J.; Delis, J. G. P.; Lobkovsky, E.; Chirik, P. J. *Organometallics* **2012**, *31*, 4886. (c) Atienza, C. C. H.; Tondreau, A. M.; Weller, K. J.; Lewis, K. M.; Cruse, R. W.; Nye, S. A.; Boyer, J. L.; Delis, J. G. P.; Chirik, P. J. *ACS Catal.* **2012**, *2*, 2169.
- <sup>9</sup> Russell, S. K.; Lobkovsky, E.; Chirik, P. J. *J. Am. Chem. Soc.* **2011**, *133*, 8858.
- <sup>10</sup> Bouwkamp, M. W.; Bowman, A. C.; Lobkovsky, E.; Chirik, P. J. *J. Am. Chem. Soc.* **2006**, *128*, 13340.
- <sup>11</sup> Biernesser, A. B.; Li, B.; Byers, J. A. *J. Am. Chem. Soc.* **2013**, *135*, 16553.
- <sup>12</sup> Biernesser, A. B.; Delle Chiaie, K. R.; Curley, J. B.; Byers, J. A. *Angew. Chem. Int. Ed.* **2016**, *55*, 5251.
- <sup>13</sup> Manna, C. M.; Kaur, A.; Yablon, L. M.; Haeffner, F.; Bo, L.; Byers, J. A. *J. Am. Chem. Soc.* **2015**, *137*, 14232.
- <sup>14</sup> Bouwkamp, M. W.; Bowman, A. C.; Lobkovsky, E.; Chirik, P. J. *J. Am. Chem. Soc.* **2006**, *128*, 13340.
- <sup>15</sup> For a comprehensive review of PDI modifications prior to 2008: Gibson, V. C.; Redshaw, C.; Solan, G. A. *Chem. Rev.* **2007**, *107*, 1745.
- <sup>16</sup> Yu, R. P.; Darmon, J. M.; Hoyt, J. M.; Margulieux, G. W.; Turner, Z. R.; Chirik, P. J. *ACS Catal.* **2012**, *2*, 1760.
- <sup>17</sup> Danopoulos, A. A.; Tsoureas, N.; Wright, J. A.; Light, M. E. *Organometallics* **2004**, *23*, 166.
- <sup>18</sup> Kaplan, H. Z.; Li, B.; Byers, J. A. *Organometallics* **2012**, *31*, 7343.
- <sup>19</sup> Thagfi, J. A.; Lavoie, G. G. *Organometallics* **2012**, *31*, 7351.
- <sup>20</sup> Cunico, R. F.; Pandey, R. K. *J. Org. Chem.* **2005**, *70*, 5344-5346. The procedure used by Dr. Kaplan to prepare *N*-(2,6-diisopropylphenyl)acetimidoyl chloride was slightly modified from the reported synthesis.
- <sup>21</sup> Small, B. L.; Brookhart, M.; Bennett, A. M. A. *J. Am. Chem. Soc.* **1998**, *120*, 4049.
- <sup>22</sup> Drake, J. L.; Kaplan, H. Z.; Wilding, M. J. T.; Li, B.; Byers, J. A. *Dalton Trans.* **2015**, *44*, 16703.
- <sup>23</sup> Kaplan, H. Z.; Mako, T. L.; Wilding, M. J. T.; Li, B.; Byers, J. A. *J. Coord. Chem.* **2016**, *69*, 2047.
- <sup>24</sup> Bolm, C.; Legros, J.; Le Paih, J.; Zani, L. *Chem. Rev.* **2004**, *104*, 6217.
- <sup>25</sup> Xue, Z.; He, D.; Xie, X. *Polym. Chem.* **2015**, *6*, 1660.
- <sup>26</sup> (a) Shaver, M. P.; Allan, L. E. N.; Rzepa, H. S.; Gibson, V. C. *Angew. Chem. Int. Ed.* **2006**, *45*, 1241. (b) Allan, L. E. N.; Shaver, M. P.; White, A. J. P.; Gibson, V. C. *Inorg. Chem.* **2007**, *46*, 8963. (c) Shaver, M. P.; Allan, L. E. N.; Gibson, V. C. *Organometallics* **2007**, *26*, 4725.
- <sup>27</sup> Chirik, P. J. *Acc. Chem. Res.* **2015**, *48*, 1687.
- <sup>28</sup> Margarita, C.; Andersson, P. G. *J. Am. Chem. Soc.* **2017**, *139*, 1346.
- <sup>29</sup> (a) Xu, R.; Chakraborty, S.; Bellows, S. M.; Yuan, H.; Cundari, T. R.; Jones, W. D. *ACS Catal.* **2016**, *6*, 2127. (b) Zell, T.; Milstein, D. *Acc. Chem. Res.* **2015**, *48*, 1979. (c) Zhang, J.; Balaraman, E.; Leitun, G.; Milstein, D. *Organometallics* **2011**, *30*, 5716.
- <sup>30</sup> Hilan Kaplan "A General Approach to Cis-Fused Sesquiterpene Quinones and Synthesis, Characterization, and Catalytic Applications of Bis(Imino)-N-Heterocyclic Carbene Complexes of Iron" PhD diss.; Boston College, 2014, Boston College University Libraries.
- <sup>31</sup> Jessica Lin Drake, "Exploration of Second Sphere Reactivity: Carbon Dioxide Hydrogenation and Applications of Bis(Amidinato)-N-Heterocyclic Carbene Iron Complexes" Masters' Thesis; Boston College, 2015, Boston College University Libraries.
- <sup>32</sup> Abu-Surrah, A.; Ibrahim, K. A.; Abdalla, M. Y.; Issa, A. A. *J. Polym. Res.* **2011**, *18*, 59.
- <sup>33</sup> Matyjaszewski, K.; Tsarevsky, N. V. *J. Am. Chem. Soc.* **2014**, *136*, 6513.
- <sup>34</sup> Recent reviews by Matyjaszewski include: (a) Krys, P.; Matyjaszewski, K. *Eur. Polym. J.* **2017**, *89*, 482. (b) Konkolewicz, D.; Krys, P.; Matyjaszewski, K. *Acc. Chem. Res.* **2014**, *47*, 3028. (c) Konkolewicz, D.; Wang, Y.; Krys, P.; Zhong, M.; Isse, A. A.; Gennaro, A.; Matyjaszewski, K. *Polym. Chem.* **2014**, *5*, 4409. (d) Matyjaszewski, K. *Macromolecules* **2012**, *45*, 4015.
- <sup>35</sup> O'Reilly, R. K.; Gibson, V. C.; White, A. J. P.; Williams, D. J. *Polyhedron* **2004**, *23*, 2921.
- <sup>36</sup> Danopoulos, A. A.; Tsoureas, N.; Wright, J. A.; Light, M. E. *Organometallics* **2004**, *23*, 166.

- 
- <sup>37</sup> Russel, S. K.; Lobkovsky, E.; Chirik, P. J. *J. Am. Chem. Soc.* **2011**, *133*, 8858.
- <sup>38</sup> Kaplan, H. Z.; Li, B.; Byers, J. A. *Organometallics* **2012**, *31*, 7343.
- <sup>39</sup> Baker, T. M.; Mako, T. L.; Vasilopoulos, A.; Li, B.; Byers, J. A.; Neidig, M. L. *Organometallics* **2016**, *35*, 3692.
- <sup>40</sup> (a) Fillman, K. L.; Bielinski, E. A.; Schmeier, T. J.; Nesvet, J. C.; Woodruff, T. M.; Pan, C. J. Takade, M. K.; Hazari, N.; Neidig, M. L. *Inorg. Chem.* **2014**, *53*, 6606. (b) Butschke, B. I. Fillman, K. L.; Bendikov, T.; Shimon, L. J. W.; Diskin-Posner, Y.; Leitner, G.; Gorelsky, S. I.; Neidig, M. L.; Milstein, D. *Inorg. Chem.* **2015**, *54*, 4909.
- <sup>41</sup> For the synthesis of 2,6-dimethyl-4-tert-butyl-aniline from 2,6-dimethyl-4-tert-butyl-nitrobenzene: Small, B. L.; Rios, R.; Fernandez, E. R.; Gerlach, D. L.; Halfen, J. A.; Carney, M. J. *Organometallics* **2010**, *29*, 6723. For the synthesis of 2,6-dimethyl-4-tert-butyl-nitrobenzene: Liu, J.; Li, Y.; Hu, N. *J. Appl. Polym. Sci.* **2008**, *109*, 700.
- <sup>42</sup> Manna, C. M.; Kaplan, H. Z.; Li, B.; Byers, J. A. *Polyhedron* **2014**, *84*, 160.
- <sup>43</sup> Burger, B. J.; Bercaw, J. E.; *New Development in the Synthesis, Manipulation and Characterization of Organometallic Compounds*; American Chemical Society: Washington DC, 1987; Vol. 357.
- <sup>44</sup> Wagner, H. L. *J. Phys. Chem. Ref. Data.* **1987**, *16*, 165.
- <sup>45</sup> Mrkvičá, L.; Daňhelka, J. *J. Appl. Polym. Sci.* **1990**, *41*, 1929.
- <sup>46</sup> Strazielle, C.; Benoit, H. Vogl, O. *Eur. Polym. J.* **1978**, *14*, 331.
- <sup>47</sup> Mark-Houwink Parameters for Homopolymers. *Springer*. [link.springer.com/content/pdf/bbm%3A978-3-662-03910-6%2F1.pdf](http://link.springer.com/content/pdf/bbm%3A978-3-662-03910-6%2F1.pdf),
- <sup>48</sup> Qian, F.; McCusker, J. E.; Zhang, Y.; Main, A. D.; Chlebowsky, M.; Kokka, M.; McElwee-White, L. *J. Org. Chem.* **2002**, *67*, 4086.
- <sup>49</sup> (a) Liu, J.; Li, Y.; Li, Y.; Hu, N. *Journal of Applied Polymer Science.* **2008**, *109*, 700. (b) Small, B. L.; Rios, R.; Fernandez, E. R.; Gerlach, D. L.; Halfen, J. A.; Carney, M. J. *Organometallics.* **2010**, *29*, 6723.

## **4.0 THE DIRECT FUNCTIONALIZATION OF LACTIDE**

### **4.1 INTRODUCTION**

#### **4.1.1 Poly(Lactic Acid) – Renewable and Biodegradable**

200 million tons of polymers made from petrochemicals are produced annually,<sup>1</sup> and with an ever-decreasing stock of fossil fuels and the accumulation of non-biodegradable polyolefinic materials in the environment,<sup>2</sup> the development of renewable and biodegradable polymers has become highly desired, if not necessary. Conversely, naturally occurring polymers such as cellulose, starch, polysaccharides, and lignin have mechanical properties that are highly sensitive to the presence of water.<sup>1</sup> Therefore, the use of renewable feedstock chemicals, such as lactide, that produce biodegradable polymers with desirable material properties and of a degradable nature have been intensely studied over the past several decades.

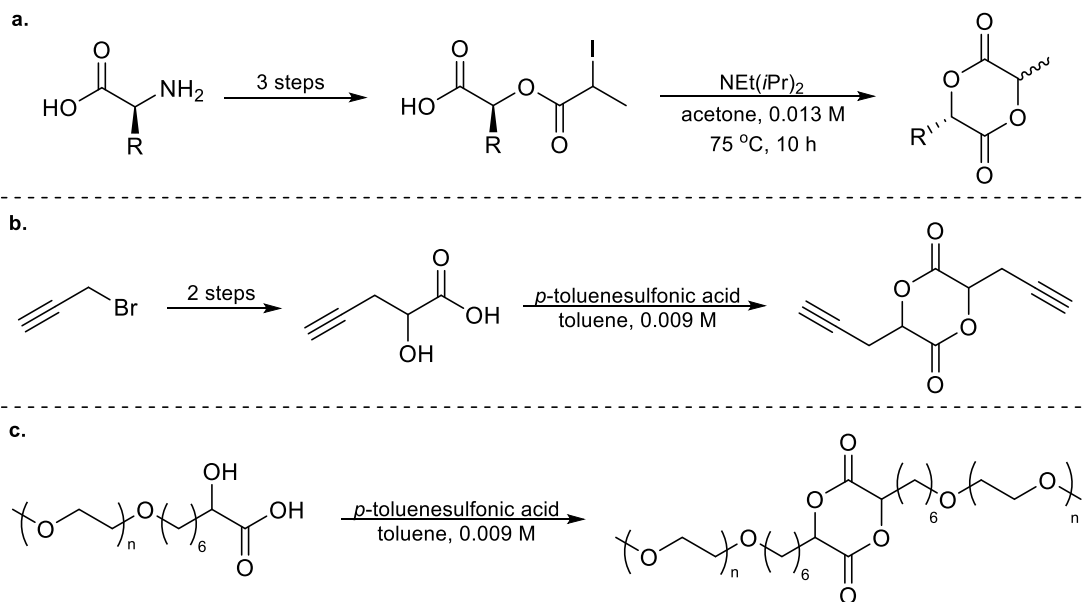
The inexpensive industrial scale production of lactic acid from fermentation processes of common materials such as corn and sugar cane,<sup>3</sup> and the subsequent facile formation of lactide, has greatly increased the use of poly(lactic acid) (PLA) in large scale operations.<sup>1</sup> PLA is a high-strength, high-modulus thermoplastic that is easily processed by methods such as injection molding, blow molding, and extrusion.<sup>3</sup> Since the 1970's, PLA and copolymers of PLA and poly(glycolic acid) have been used for medical applications such as drug and protein delivery, and bone and tissue engineering.<sup>1</sup> Additional applications of PLA include garments, agricultural films, and household items such as degradable trash bags, plates, and utensils.<sup>3</sup> Notably, the molecular weight of the polymer, degradation conditions, and polymer purity affect degradation time.

PLA also has some undesirable properties. A poor oxygen barrier and undesired thermal properties preclude its use for some industrial, medical, and household applications.<sup>4</sup> Hence, the development of polymer blends, copolymers, and cross-linked polymers of lactide have been studied in order to bring about more favorable properties. Polymer architecture can also be altered by controlling the stereoregularity of PLA.<sup>3</sup> Poly(L-lactic acid), for example, is a very crystalline material with a melt temperature of 170-183 °C, whereas poly(D,L-lactic acid) is an amorphous material with a much lower melt temperature.

The architecture of a polymer is directly affected by the architecture of the monomer, and it is the desire of the Byers group to create lactide analogues from the direct functionalization of lactide in order to impart desired material properties to the polymer. Additionally, the inherent chirality of lactide, and the ease in which its enantiomers and diastereomers are generated, will allow lactide to act as its own chiral auxiliary in any functionalization process. Ideally, when one chiral center is undergoing functionalization, the other chiral center will remain intact, imparting selectivity to the reaction.

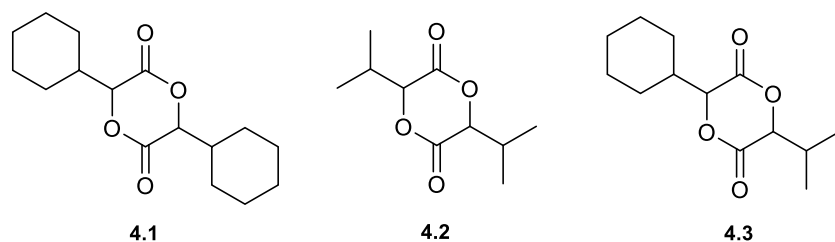
#### 4.1.2 Syntheses of Cyclic Diesters

Many syntheses of six membered cyclic diesters have been achieved in recent years. Serine, lysine, glutamic acid, and other amino acids have been transformed into cyclic diesters through straightforward syntheses such as the one shown in **Scheme 4.1a**.<sup>5</sup> Beginning with propargyl bromide, Baker and coworkers synthesized a cyclic diester with bearing alkyne groups that could be utilized after polymerization of the cyclic diester for click-type chemistry (**Scheme 4.1b**).<sup>6</sup> The Baker group then used a similar ring closure to form a cyclic diester from a polyether bearing an  $\alpha$ -hydroxy carboxylic acid end group (**Scheme 4.1c**).<sup>7</sup>



**Scheme 4.1.** Recent examples of the synthesis of cyclic diesters as mimics to lactide *via* the use of a) amino acids,<sup>5</sup> b) propargyl bromide,<sup>6</sup> and c) a polyether containing  $\alpha$ -hydroxy carboxylic acid end groups.<sup>7</sup>

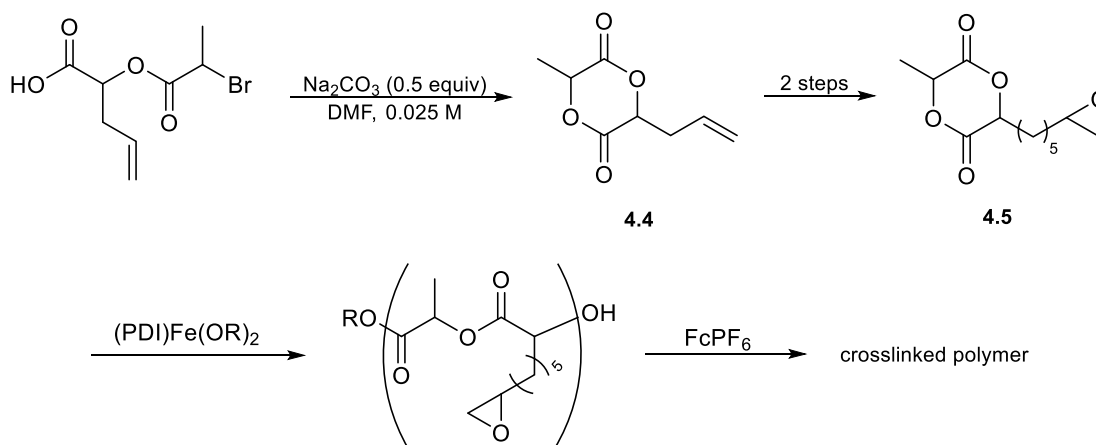
Baker and coworkers also synthesized six-membered cyclic diesters containing secondary alkyl groups, compounds **4.1**, **4.2**, **4.3**.<sup>8</sup> Kinetic studies and DSC analyses underscored the differences in polymer properties that are achieved upon the use of functionalized lactide analogues (**Table 4.1**). Upon treatment with tin(II) octanoate, *rac*-lactide polymerizes at a rate 71 times that of *rac*-**4.1** (*entries 1 and 4*). *Rac*-**4.3** and *rac*-**4.2** polymerize with relative rates of 9.9 and 3.8, respectively (*entries 2 and 3*). A stark difference in the properties of these polymers is seen in their glass transition temperatures. The polymer of *rac*-lactide has a  $T_g$  of 55 °C (*entry 1*), and the polymers of the cyclic diesters have vastly different  $T_g$  values, up to 43 °C above that of the polymer of *rac*-lactide. The polymers of *rac*-**4.3**, *rac*-**4.2**, and *rac*-**4.1** have glass transition temperatures of 73 °C (*entry 2*), 41 °C (*entry 3*), and 98 °C (*entry 4*). The  $T_g$  values of the polymers of *meso*-**4.1** and *R,R*-**4.1** were found to be 96 °C (*entry 5*) and 104 °C (*entry 6*), respectively.



Entry	Monomer	Relative Rate	T <sub>g</sub> (°C)
1	<i>Rac</i> -lactide	71	55
2	<i>Rac</i> -4.3	9.9	73
3	<i>Rac</i> -4.2	3.8	41
4	<i>Rac</i> -4.1	1	98
5	<i>Meso</i> -4.1	-	96
6	<i>R,R</i> -4.1	-	104

**Table 4.1.** Evaluation of the polymers of lactide analogues **4.1**, **4.2**, and **4.3** as compared to lactide by kinetic studies and DSC analyses.<sup>8</sup>

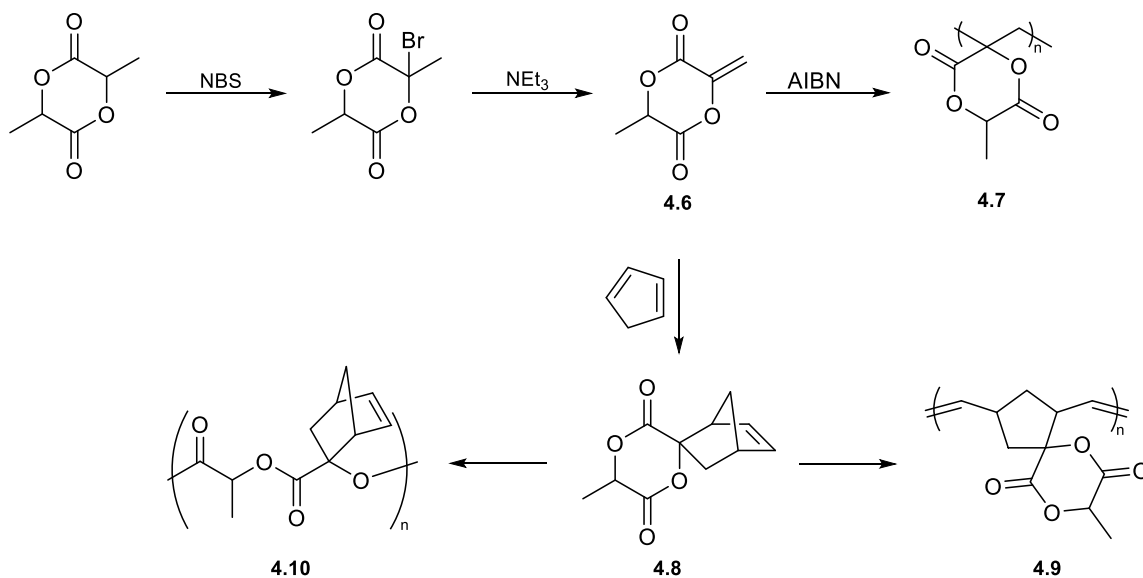
Members of the Byers group have used lactide analogue **4.4**, previously synthesized by Cheng and coworkers,<sup>9</sup> in the development of species **4.5** (**Scheme 4.2**).<sup>10</sup> This compound, containing both cyclic diester and epoxide functionalities, has been effectively used for cross-linking polymerization applications, producing properties that are vastly different from both poly(lactic acid) and polyethers.<sup>10</sup>



**Scheme 4.2.** The synthesis of **4.5** from lactide analogue **4.4**.<sup>9,10</sup>

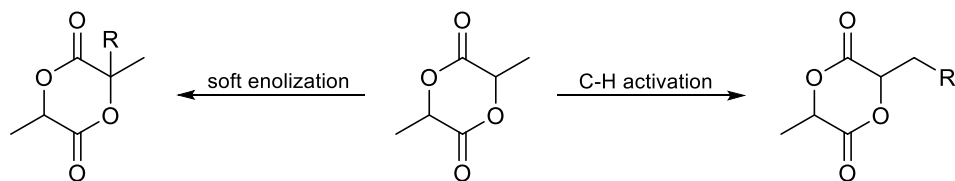
Despite the success that has been seen in the synthesis of six-membered cyclic diesters that resemble lactide over recent years, drawbacks of these techniques exist. Firstly, the key cyclization step requires a very low concentration of starting material in order to promote the formation of the six-membered ring (0.009 – 0.025M), and yields around 50 % are commonplace.<sup>5-7,10</sup> Thus these processes are not feasible for use on an industrial scale. Typically, these syntheses require multiple steps, resulting in mediocre overall yields. As a result, the beneficial properties demonstrated by polymers derived from lactide analogues have not been explored due to the limitations to scale.

Because lactide is a commodity chemical, produced cheaply and in large volumes from renewable resources,<sup>1,3</sup> it would be much more advantageous to create these lactide analogues directly from lactide itself. Unfortunately, the direct functionalization of lactide is difficult due to its proclivity for polymerization. Lactide can be polymerized under a wide range of conditions, including in acidic or basic media, in the presence of a metal species, or at high temperatures,<sup>3</sup> precluding the use of traditional methods used for the functionalization of lactones. Even so, the direct functionalization of lactide by *N*-bromosuccinimide has been reported by many research groups, beginning with the initial report in 1969 (**Scheme 4.3**).<sup>11</sup> Following the addition of bromide to the  $\alpha$ -carbon of lactide, treatment with triethylamine afforded species **4.6**, which has been polymerized in the presence of AIBN to produce polymer **4.7**.<sup>12</sup> Here, the entire mass of the polymer is derived from a biological and renewable resource. Alternatively, **4.6** can undergo a Diels-Alder reaction with cyclopentadiene to form **4.8**, from which polymers **4.9** and **4.10** have been generated from polymerizations of the alkene and of lactide, respectively.<sup>13</sup>



**Scheme 4.3.** The direct functionalization of lactide by *N*-bromosuccinimide (NBS) followed by treatment with triethylamine to produce 4.6,<sup>11</sup> which can be polymerized with AIBN to produce polymer 4.7,<sup>12</sup> or can be treated with cyclopentadiene to produce 4.8, which contains two functionalities that can be polymerized.<sup>13</sup>

In an effort to functionalize lactide at both the  $\alpha$ - and  $\beta$ -carbons of lactide, the Byers group has identified two possible routes to achieve the desired transformations: C-H activation and soft enolization (**Scheme 4.4**). It is hoped that once a successful method has been identified, the use of lactide analogues as monomers will become more facile, leading to the development of biodegradable polymers with desirable properties.



**Scheme 4.4.** Possible routes for the functionalization of lactide.

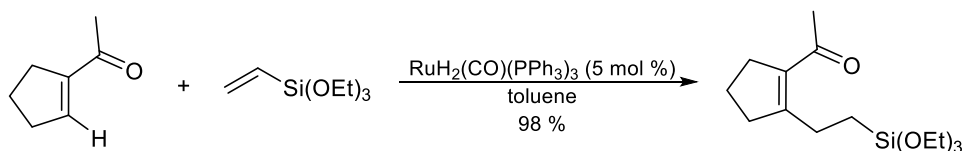
### 4.1.3 C-H Activation

The process of transforming ubiquitous and unreactive C-H bonds directly into more complicated functionalities by way of transition metal catalysis has become a powerful technique in synthetic chemistry.<sup>14</sup> Transformations of this type allow for the use of more step economical processes by circumventing traditional and lengthy functional group manipulations. Significant progress in this field has been made since the first report by Volhard in 1892,<sup>15</sup> especially for the activation of aromatic C-H bonds, and a large number of excellent reviews have been published.<sup>14,16,4,6-8</sup> The most commonly used transition metal catalysts for C-H activation are Ir, Rh, Ru, and Pd based,<sup>16,17</sup> although Ni,<sup>18</sup> Fe,<sup>19,20</sup> and other metals have also been reported. In regards to palladium systems, Pd(II) species are widely used, such as Pd(OAc)<sub>2</sub>, Pd(OTf)<sub>2</sub>, Pd(Piv)<sub>2</sub>, and Pd<sub>2</sub>(dba)<sub>3</sub>.<sup>17</sup>

The activation of aliphatic C-H bonds is particularly difficult; these bonds are robust, with a low acidity (pK<sub>a</sub> = 45-60),<sup>17</sup> high bond dissociation energies (280-410 kJ/mol),<sup>14</sup> and many conformational degrees of freedom.<sup>17</sup> However, directing groups have greatly aided the development of C(sp<sup>3</sup>)-H activation techniques.<sup>17</sup>

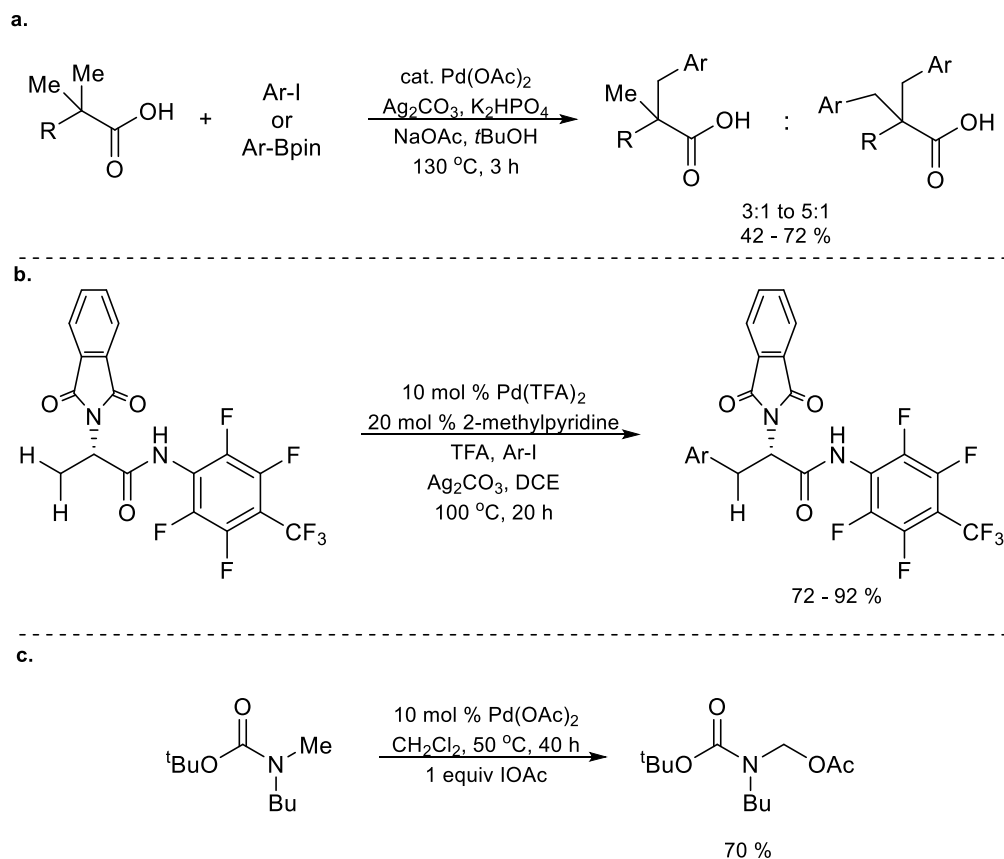
Directing groups promote cleavage of C-H bonds and control positional selectivity by coordinating to the transition metal and promoting close proximity of the target site.<sup>17</sup> Strongly coordinating directing groups are the most efficient, and include pyridines, oxazolines, sulfides, phosphines, thioamides, imines, and oximes. However, for the activation of lactide, carbonyl moieties of the molecule will ideally be used to direct its functionalization, which fall into the category of weakly coordinating directing groups. Often, weakly coordinating direction groups are functionalities that already exist on the molecule to be transformed, and thus do not need to be added and removed before and after the desired reaction. Carboxylic acids, amides, and amines are the most commonly used weakly coordinating groups for alkyl C-H bond activation, yet the groups that would be most analogous to the lactide system, esters and ketones, are rare in the literature. Ru(II) species RuH<sub>2</sub>(CO)(PPh<sub>3</sub>)<sub>3</sub> was employed by Trost and coworkers to activate a vinyl

C-H group directed by a ketone (**Scheme 4.5**).<sup>21</sup> Aryl C-H groups have been activated in the presence of an ester directing group by both  $\text{RuH}_2(\text{CO})(\text{PPh}_3)_3$ <sup>22</sup> and  $\text{CpRh}(\text{C}_2\text{H}_3\text{SiMe}_3)_2$ .<sup>23</sup>



**Scheme 4.5. Activation of a vinyl C-H bond by a ruthenium complex and directed by a ketone.**<sup>21</sup>

Several alkyl C-H activation methods that have been reported in recent years are targeted herein for the functionalization of lactide. The group of Jin-Quan Yu has developed techniques predominately utilizing carboxylic acid and amide directing groups. A method for the C-H arylation of an  $\text{sp}^3$  hybridized carbon vicinal to a carboxylic acid has been reported and is shown in **Scheme 4.6a**.<sup>24</sup> Palladium acetate was used as the precatalyst and the reaction required  $\text{Ag}_2\text{CO}_3$  as an oxidant,  $\text{K}_2\text{HPO}_4$  as a base, and high temperatures. Although successful, low yields of the desired product were obtained. A similar procedure, shown in **Scheme 4.6b**, required a pyridine-based ligand and trifluoroacetic acid for the amide-directed functionalization of a highly electronegative substrate.<sup>25</sup> The group also developed a transformation that allows for the installment of an acetate group directed by a carbamate, as shown in **Scheme 4.6c**.<sup>26</sup> Conditions similar to these methods are screened herein for lactide functionalization.

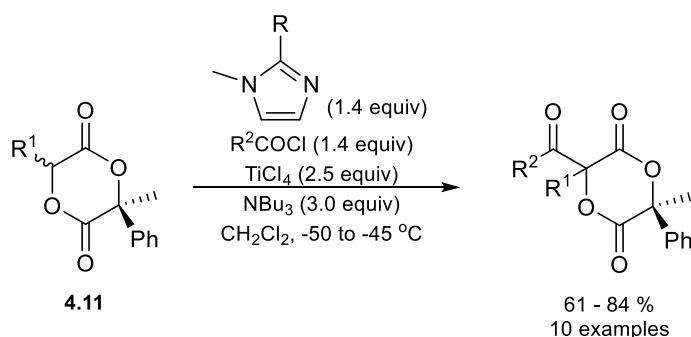


**Scheme 4.6.** Examples of alkyl C-H activation include a) ester directed arylation of an alkyl C-H bond facilitated by palladium acetate,<sup>24</sup> b) the activation of an alkyl C-H bond directed by an extremely electron poor amide in the presence of catalytic amounts of palladium triflate with 2-methylpyridine ligation,<sup>25</sup> and c) amide-directed C-H activation in the presence of palladium acetate and a hypervalent iodine source.<sup>26</sup>

#### 4.1.4 Soft Enolization

Soft enolization is also a promising technique for the functionalization of lactide. As was stated above, lactide is very sensitive to base-promoted ring opening by strong nucleophiles, which precludes direct functionalization by traditional enolization methods (e.g. the formation of lithium enolates with LDA). Alternatively, with soft enolization, the coordination of a Lewis acid to the carbonyl oxygen of lactide, however, could allow for the deprotonation of the  $\alpha$ -carbon by a weak, non-nucleophilic base.<sup>27</sup>

The Tanabe group has reported the use of a titanium-mediated Claisen condensation of a six-membered cyclic diester similar to lactide (**Scheme 4.7**).<sup>28</sup> Cyclic diester **4.11** was effectively condensed with an aliphatic acid chloride under the indicated conditions. The identity of the imidazole was dependent on the alkyl acid chloride; bulkier acid chlorides required the use of less hindered imidazoles (R = H), whereas the use of less hindered acid chlorides only produced desirable yields when bulkier imidazoles (R = Et) were employed. In many cases R<sup>1</sup> was a methyl group, providing even further similarities between **4.11** and lactide. The chirality at the site of condensation was not examined, thus it is unknown whether the chirality of the **4.11** had an effect on the reaction outcome. Because the substrate Tanabe and coworkers reported is so similar to lactide, it was hypothesized that this method would readily facilitate the desired lactide functionalization.



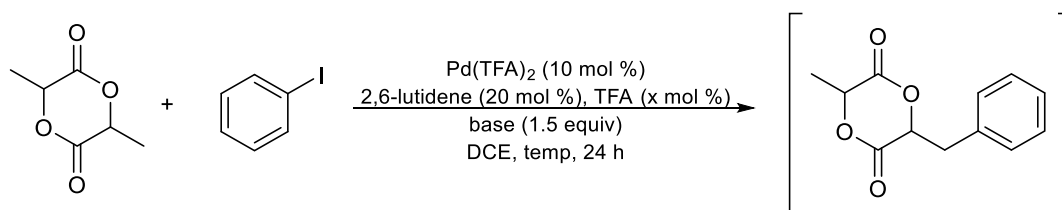
**Scheme 4.7.** The titanium-mediated Claisen condensation of lactide analogue **4.11** with an acid chloride.<sup>28</sup>

## 4.2 C-H ACTIVATION OF LACTIDE

### 4.2.1 Results

Following conditions reported by Jin-Quan Yu,<sup>26</sup> lactide was treated with phenyl iodide in the presence of catalytic amounts of Pd(TFA)<sub>2</sub>, 2,6-lutidine, TFA, and a stoichiometric amount of base in DMF (**Scheme 4.8**). When 20 mol % of TFA was used, along with Ag<sub>2</sub>CO<sub>3</sub> as the base, at

60 °C, no conversion of *meso*-lactide nor phenyl iodide was observed (*entry 1, Table 4.2*). Trace conversion of lactide and phenyl iodide was seen in the absence of TFA and with CsF as the base (*entry 2*). At 100 °C, degradation of *rac*-lactide to lactic acid and lactic acid dimer was observed, along with no conversion of phenyl iodide (*entry 3-5*).

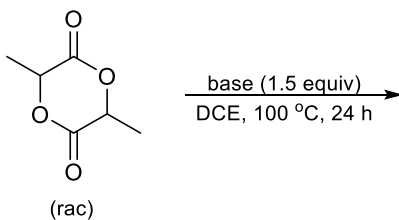


**Scheme 4.8.** Attempted activation of lactide by Pd(TFA)<sub>2</sub>.

Entry	x	base	Temp (°C)	Result
1 <sup>a</sup>	20	Ag <sub>2</sub> CO <sub>3</sub>	60	No reaction
2 <sup>a</sup>	0	CsF	60	Trace reaction
3 <sup>b</sup>	20	Ag <sub>2</sub> CO <sub>3</sub>	100	Lactic acid and dimer
4 <sup>b</sup>	0	CsF	100	Lactic acid and dimer
5 <sup>b</sup>	20	CsF	100	Lactic acid and dimer

**Table 4.2.** A screen of conditions in an attempt to generate desired reactivity. <sup>a</sup>*Meso*-lactide used. <sup>b</sup>*Rac*-lactide used.

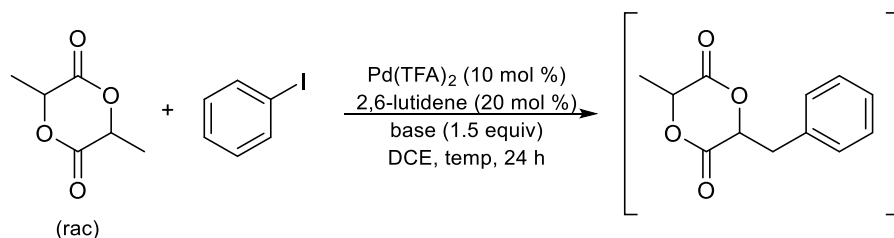
After these initial experiments had led to unfavorable results, controls reactions were conducted to determine if lactide was stable under the indicated conditions. As shown in **Table 4.3**, certain bases, CsF, K<sub>3</sub>PO<sub>4</sub>, K<sub>2</sub>CO<sub>3</sub>, and Cs<sub>2</sub>CO<sub>3</sub> are not compatible with lactide and lead to large amounts of degradation (*entries 2-5*). Bases such as AgOAc, pyridine, KOAc, and Ag<sub>2</sub>CO<sub>3</sub> did not lead to the degradation of lactide (*entries 6-9*). Upon comparison of the pK<sub>b</sub> values of the bases, those with pK<sub>b</sub> values between 9.25 and 8.8 were shown to be compatible, while those with outside this range led to lactide degradation. Silver carbonate deviates from this trend, potentially due to its very low solubility.



Entry	Base	pK <sub>b</sub>	Compatible?
1	None	-	Yes
2	CsF	10.8	No
3	K <sub>3</sub> PO <sub>4</sub>	1.55	No
4	K <sub>2</sub> CO <sub>3</sub>	3.7	No
5	Cs <sub>2</sub> CO <sub>3</sub>	3.7	No
6	AgOAc	9.25	Yes
7	Pyridine	8.8	Yes
8	KOAc	9.25	Yes
9	Ag <sub>2</sub> CO <sub>3</sub>	3.7	Yes

**Table 4.3. Lactide degradation studies in 1,2-dichloroethane and 100 °C in the presence of 1.5 equivalents of base.**

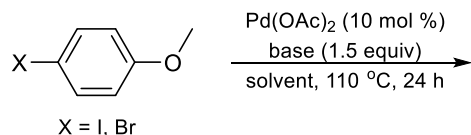
*Rac*-lactide was then subjected to the conditions shown in **Table 4.4**. When silver carbonate was used as the base, with 20 % of either 2,6-lutidine or 2-methylpyridine as a ligand, no starting material conversion occurred (*entries 1 and 2*). In the absence of the palladium precatalyst, only lactide oligomers were formed (*entry 3*). When silver acetate was used rather than silver carbonate, conversion of both starting materials was seen, and a complex mixture was observed by NMR (*entry 4*). In the absence of lactide, the same complex mixture was observed (*entry 5*), and when 4-iodoanisole was used rather than phenyl iodide, 4-acetoxyanisole was formed.



Entry	Base	Solvent	Temp (°C)	Result
1	Ag <sub>2</sub> CO <sub>3</sub>	DCE	100	No reaction
2 <sup>a</sup>	Ag <sub>2</sub> CO <sub>3</sub>	DCE	100	No reaction
3 <sup>b</sup>	AgOAc	DCE	100	Oligomers
4	AgOAc	DCE	100	Complex mixture
5 <sup>c</sup>	AgOAc	DCE	100	Complex mixture
6 <sup>d</sup>	AgOAc	Toluene	110	4-acetoxyanisole

**Table 4.4.** <sup>a</sup>2-methylpyridine used rather than 2,6-lutidine. <sup>b</sup>No palladium present. <sup>c</sup>No lactide present. <sup>d</sup>4-iodoanisole used rather than phenyl iodide.

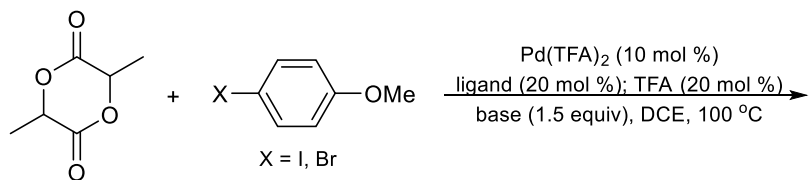
Due to the participation of phenyl iodide in unproductive side reactions involving silver acetate, a number of bases were screened to determine which were compatible with phenyl iodide under the reaction conditions in either 1,2-dichloroethane or toluene (**Table 4.5**) 4-iodoanisole and 4-bromoanisole were used as substrates, as they are easier to identify by NMR spectroscopy than phenyl iodide. 4-iodoanisole was stable when silver carbonate was used, in both DCE and toluene (*entry 3*), and with potassium acetate in toluene (*entry 4*). 4-bromoanisole was stable only in the presence of potassium acetate in DCE (*entry 7*).



Entry	X	Base	Degree of Decomposition	
			Outcome - DCE	Outcome - Toluene
1	I	Pyridine	Full	Slight
2	I	KOAc	Minimal	None
3	I	Ag <sub>2</sub> CO <sub>3</sub>	None	None
4	I	AgOAc	Moderate	Full
5	I	None	Moderate	Full
6	Br	Pyridine	Full	Full
7	Br	KOAc	None	Moderate
8	Br	Ag <sub>2</sub> CO <sub>3</sub>	Full	Slight
9	Br	AgOAc	Moderate	Full
10	Br	None	Minimal	Full

**Table 4.5. Degradation studies of 4-bromoanisole and 4-iodoanisole in the presence of palladium acetate at 110 °C.**

As shown in **Table 4.6**, regardless of the reaction conditions, no desired product was seen by NMR.



Entry	X	Ligand	Base	Result
1 <sup>a</sup>	Br	2-methylpyridine	Ag <sub>2</sub> CO <sub>3</sub>	No desired product
2	Br, I	2,6-lutidene	Ag <sub>2</sub> CO <sub>3</sub>	No desired product
3	Br, I	2,6-lutidene	KOAc	No desired product
4	Br, I	2-methylpyridine	Ag <sub>2</sub> CO <sub>3</sub>	No desired product
5	Br, I	2-methylpyridine	KOAc	No desired product
10	Br, I	N/A	2,6-lut.	No desired product
11	Br, I	N/A	2-Me-pyr.	No desired product

**Table 4.6. A screen of conditions in an attempt to generate desired reactivity. <sup>a</sup>Toluene used as solvent.**

#### 4.2.2 Conclusions

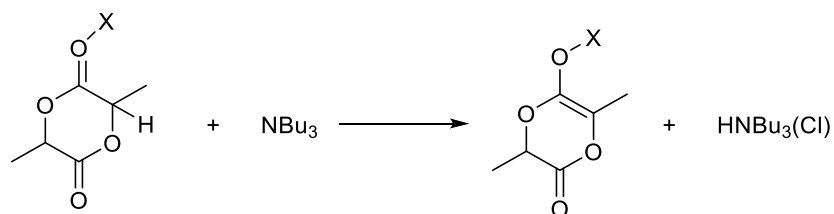
The aforementioned attempts to affect the activation of the  $\beta$ -hydrogen of lactide have proven ineffective. Certain ruthenium systems that are ketone- and ester-directed may allow for the desired transformation to occur. Alexander Wong of the Byers group is continuing this research.

### 4.3 SOFT ENOLIZATION OF LACTIDE

#### 4.3.1 Results

With Michael Crockett, calculations were run to determine the pK<sub>a</sub> of lactide with and without Lewis acid coordination, the results of which are shown in **Table 4.7**. The “adjusted pK<sub>a</sub>” values shown in **Table 4.7** take into account the pK<sub>a</sub> value of tributylamine, the deprotonating base. The

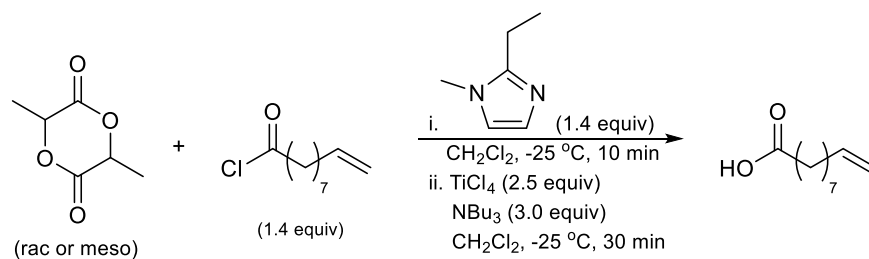
calculations place the pK<sub>a</sub> of the proton alpha to the carbonyl carbon at 31.7 in dichloromethane. With TiCl<sub>4</sub>, the desired Lewis acid mediator, the pK<sub>a</sub> dropped to -0.75, and the reaction became thermodynamically favorable. Calculations with BF<sub>3</sub> and FeCl<sub>3</sub> also indicated thermodynamically downhill reactions, while coordination to AlCl<sub>3</sub> only lowered the pK<sub>a</sub> to 26.1. FeCl<sub>3</sub> was calculated to be the most favorable, however, due to poor solubility properties, TiCl<sub>4</sub> was confirmed as the most promising Lewis acid.



X	$\Delta G$	pKa	Adjusted pKa
None	27.1	20.8	31.7
TiCl <sub>4</sub>	-15.1	-11.6	-0.75
AlCl <sub>3</sub>	19.8	15.2	26.1
BF <sub>3</sub>	-7.4	-5.7	5.2
FeCl <sub>3</sub>	-32.1	-24.7	-13.8

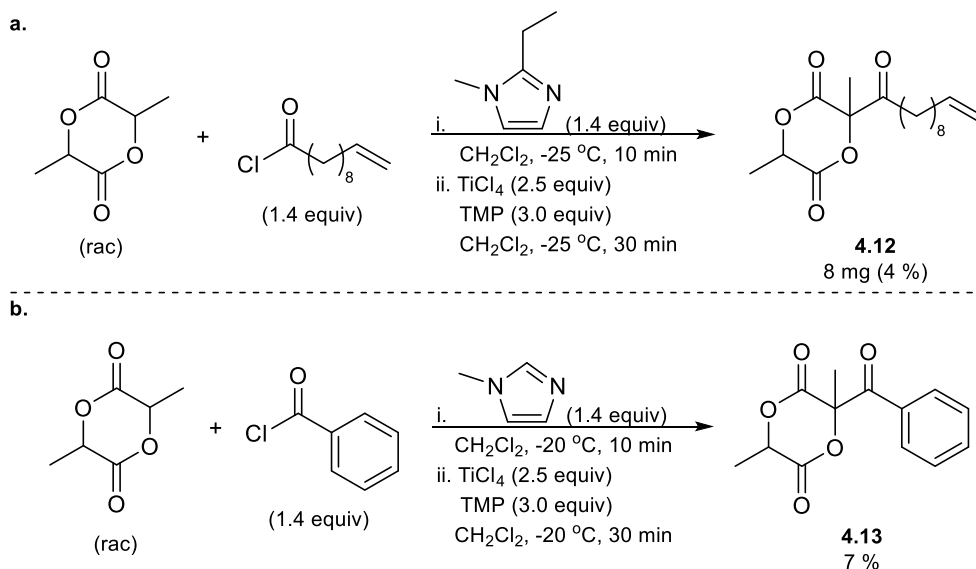
**Table 4.7. B3LYP/6-31G DFT calculations with implicit solvation of dichloromethane were performed to determine the pK<sub>a</sub> of lactide with or without Lewis acid coordination.**

Initially, a reaction was conducted following those reported by Tanabe and coworkers.<sup>28</sup> The group reports conducting the reaction at -50 °C, yet it was determined that under these conditions, titanium tetrachloride freezes. Therefore, the reaction was conducted at -25 °C. *Rac*- or *meso*-lactide, 10-undecenoyl chloride, and 1-ethyl-*N*-methylimidazole were combined in methylene chloride and treated with titanium tetrachloride and tributylamine at -50 °C (**Scheme 4.9**). Under these conditions, and also when *meso*-lactide was used, the major product observed was 10-undecenoyl carboxylic acid.



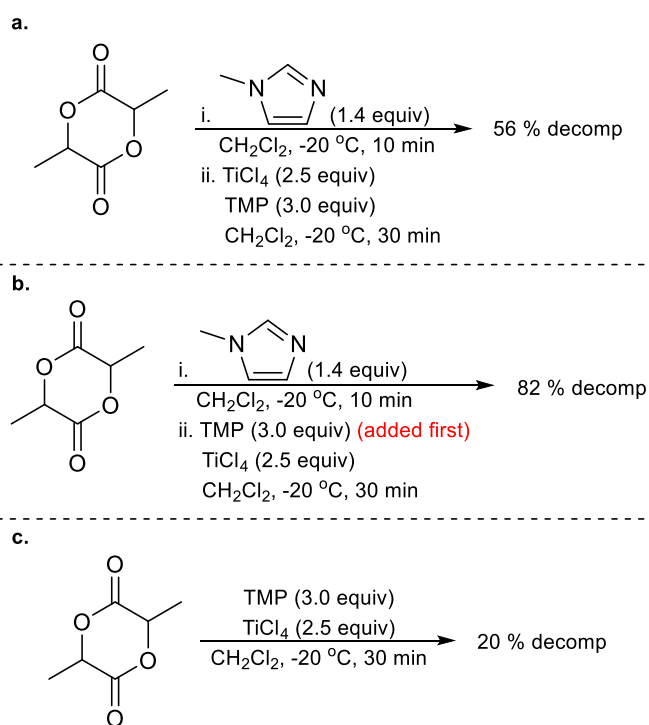
**Scheme 4.9.** Lactide was treated with 10-undecenoyl chloride (1.4 equiv), 1-ethyl-*N*-methylimidazole (1.4 equiv), titanium tetrachloride (2.5 equiv), and tributyl amine (3.0 equiv) in methylene chloride at -25 °C.

No variation of the conditions shown in **Scheme 4.9** produced the desired result. However, when tetramethylpiperidine (TMP), a less nucleophilic base with a higher  $\text{pK}_b$ , was used rather than tributylamine, 4 % of the desired product (**4.12**) was isolated (**Scheme 4.10a**). When benzoyl chloride was used as a substrate, along with *N*-methylimidazole, 7 % of the desired product (**4.13**) was isolated (**Scheme 4.10b**). In both cases, carboxylic acid and lactide degradation products were observed. Upon increasing the reaction time to five hours, no change in yield was observed, and when allowed to continue overnight at room temperature, no desired product was obtained.



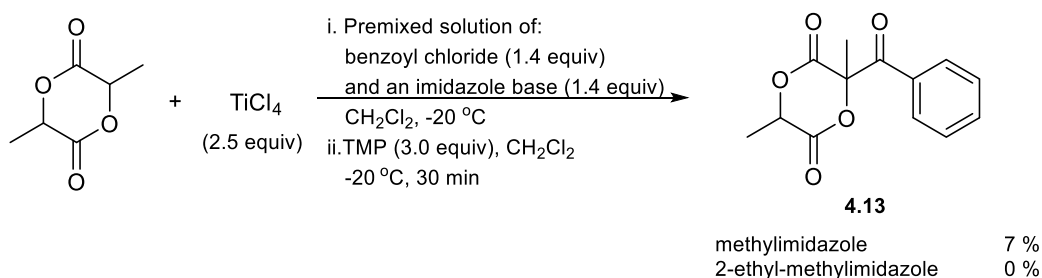
**Scheme 4.10.** a) The treatment of *rac*-lactide and 10-undecenoyl chloride with 2-ethyl-*N*-methylimidazole,  $\text{TiCl}_4$ , and TMP in  $\text{CH}_2\text{Cl}_2$  at -25 °C. b) The treatment of *rac*-lactide and benzoyl chloride with *N*-methylimidazole,  $\text{TiCl}_4$ , and TMP in  $\text{CH}_2\text{Cl}_2$  at -25 °C.

Several control reactions were performed to analyze the stability of lactide under the reaction conditions, as shown in **Scheme 4.11**. Under the original conditions, with the absence of 10-undecenoyl chloride, 56 % of the lactide degraded (**Scheme 4.11a**), and when TMP was added before TiCl<sub>4</sub>, 82 % degradation was observed (**Scheme 4.11b**). When the imidazole was omitted, only 20 % degradation was observed (**Scheme 4.11c**), indicating that *N*-methylimidazole reacts detrimentally with lactide. Thus, in subsequent reactions, the imidazole and acid chloride were premixed to ensure the formation of the adduct before the addition of lactide (**Scheme 4.12**). When TMP was added to a solution of TiCl<sub>4</sub> in CH<sub>2</sub>Cl<sub>2</sub> a color change from colorless to dark brown indicated that the TMP is reacting with the TiCl<sub>4</sub>, potentially forming compounds that degrade lactide or the formed product.



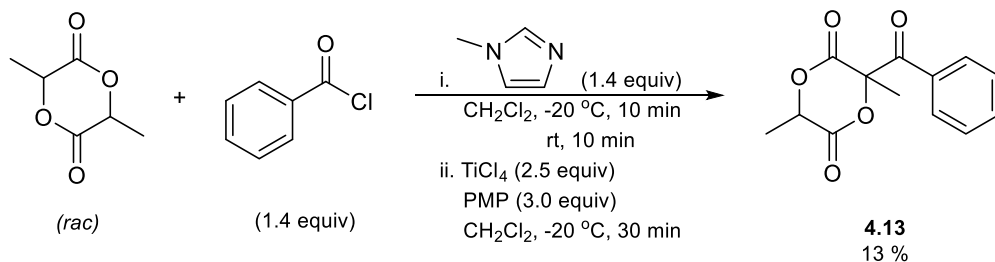
**Scheme 4.11. Investigating the stability of lactide a) in the absence of acid chloride, b) in the absence of acid chloride with TMP added before TiCl<sub>4</sub>, and c) in the presence of TMP and TiCl<sub>4</sub>.**

Accordingly, the imidazole and acid chloride were premixed and allowed to stir for 10 min at -20 °C, then for 10 min at room temperature, to ensure the formation of the imidazole adduct, before being added to a solution of lactide and TiCl<sub>4</sub> (**Scheme 4.12**). No change in yield occurred. When 2-ethyl-*N*-methylimidazole was used instead, no product was isolated, as steric hindrance prohibits the formation of the imidazole adduct with benzoyl chloride. When TMP was also added to lactide before the addition of the imidazole adduct, no product was isolated, and lactide had fully decomposed. Finally, the reaction was attempted with the slow addition of TMP, and, again, 7 % yield was observed.



**Scheme 4.12. Conditions in which a premixed solution of benzoyl chloride and *N*-methylimidazole or 2-ethyl-*N*-methylimidazole was introduced to lactide under the reaction conditions.**

The use of a bulkier base, pentamethylpiperidine (PMP), increased the yield of **4.13** to 13 % (**Scheme 4.14**). DBN and DBU were also screened, and in these cases, lactide did not convert. Iron trichloride, aluminum trichloride, copper triflate, boron trifluoride etherate, and tri(tetrafluorophenyl)borane, were screened for activity to no avail. Reducing the amounts of TiCl<sub>4</sub> and PMP to 1.0 equivalents each resulted in a decrease in yield to 7 %. It was hypothesized that the desired product may be degrading during column purification, yet when pacified silica was used, no product was isolated from the purification.



**Scheme 4.14.** The treatment of *rac*-lactide, benzoyl chloride, and *N*-methylimidazole with  $\text{TiCl}_4$  and PMP to produce 13 % of 4.13.

### 4.3.2 Conclusions

This project is still in its infancy, and further experimentation is needed to discover an effective system. Possible issues include the reaction workup, the identity of the Lewis acid, and the identity of the base. During the workup, the reaction is quenched with either water or methanol, both of which could act as nucleophiles to ring open lactide or the desired product. If the residual titanium was instead quenched with a less nucleophilic compound, such as *iso*-propanol or *tert*-butanol, this problem may be avoided. While  $\text{TiCl}_4$  decreases the  $\text{pK}_a$  of the  $\alpha$ -hydrogen, it also increases the electrophilicity of the ester carbons of lactide, increasing the chance of unproductive ring opening reactions. This dichotomy is likely hindering the desired reactivity, and an alternative Lewis acid could rectify this problem. The chemistry discussed above has highlighted the importance of base identity, and a screening of additional bases is warranted.

## 4.4 EXPERIMENTAL

### 4.4.1 General Considerations

Unless stated otherwise, all reactions were carried out in oven-dried glassware using standard Schlenk techniques<sup>29</sup> or using an MBraun inert atmosphere ( $\text{N}_2$ ) drybox.

Dichloromethane, pentane, toluene, diethyl ether, and tetrahydrofuran were passed through a solvent purification system under a blanket of argon and then degassed briefly under vacuum prior to use. NMR spectra were recorded at ambient temperature on a Varian VNMRS or INOVA spectrometer operating at 500 MHz for  $^1\text{H}$  NMR and 125 MHz for  $^{13}\text{C}$  NMR. The line listings for the NMR spectra of diamagnetic compounds are reported as: chemical shift in ppm (number of protons, splitting pattern, coupling constant). All chemical shifts are reported in ppm from TMS with the peak for the residual protio version of the solvent as the internal reference. GC/FID data were obtained on Shimadzu Gc-2014 equipped with a Shimadzu Auto Injector/Auto Sampler AOC-20i. GC/MS data were obtained on a 7820a Agilent GC with a 5975 Mass Analyzer. High-resolution mass spectra were obtained at the Boston College Mass Spectrometry Facility. Elemental Analyses were conducted at Robertson MicroLit Laboratories. IR spectra were recorded on a Bruker ALPHA Platinum ATR infrared spectrometer. X-ray crystallographic information was obtained at the Boston College X-ray Crystallography Center. All isolated yields were obtained on a CombiFlashRf auto-column. 2-ethyl-N-methylimidazole was synthesized according to literature procedures.<sup>30</sup> All other reagents were purchased from commercial sources and purified as necessary.

#### 4.4.2 Experimental Procedures

##### 4.4.2.1 C-H Activation

*Method 1 (Table 4.2, Table 4.4):* To a 7 mL vial equipped with a stir bar was added: lactide (0.100g, 0.69 mmol), phenyl iodide (77  $\mu\text{L}$ , 0.69 mmol) 2,6-lutidine (0.011 mL, 0.14 mmol), tetradecane (0.009 mL, 0.035 mmol), and 1,2-dichloroethane (2 mL). A small aliquot was taken for GC. Then, Pd(TFA)<sub>2</sub> (0.023 g, 0.07 mmol), trifluoroacetic acid (0.280 mL of a 0.5 M 1,2-dichloroethane solution) and silver carbonate (0.287 g, 1.04 mmol). The vial was capped, sealed with electrical tape, then allowed to stir at 60 OR 100 °C for 20 hours. The mixture was then allowed to cool to room temperature. It was then filtered through celite and concentrated to dryness.

*Method 2 (Table 4.3).* To a 4 mL vial equipped with a stir bar was added: lactide (0.010 g, 0.069 mmol), base (0.104 mmol), and 1,2-dichloroethane (1.0 mL). The vial was capped, sealed with electrical tape, and allowed to stir at 100 °C for 24 hours. The reaction was allowed to cool to room temperature and the solvent was removed *in vacuo*.

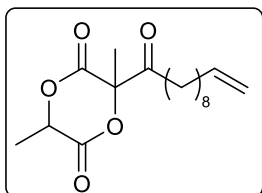
*Method 3 (Table 4.5).* To a 4 mL vial equipped with a stir bar was added: 4-iodoanisole (0.016 mg, 0.069 mmol), palladium acetate (0.002 g, 0.007 mmol), base (0.104 mmol), and toluene OR 1,2-dichloroethane (1 mL). The vial was capped, sealed with electrical tape, and allowed to stir at 100 °C for 24 hours. The reaction was allowed to cool to room temperature and the solvent was removed *in vacuo*.

*Method 4 (Table 4.6).* To a 7 mL vial equipped with a stir bar was added: lactide (0.010g, 0.069 mmol), 4-iodoanisole or 4-bromoanisole (0.069 mmol), ligand (0.014 mmol), Pd(TFA)<sub>2</sub> (0.002 g, 0.007 mmol), trifluoroacetic acid (0.028 mL of a 0.5 M 1,2-dichloroethane solution) and base (0.104 mmol) and 1,2-dichloroethane (1 mL). The vial was capped, sealed with electrical tape, then allowed to stir at 100 °C for 20 hours. The mixture was then allowed to cool to room temperature. It was then filtered through celite and concentrated to dryness.

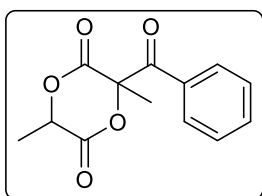
#### 4.4.2.2 Soft Enolization

*General Soft-Enolization Procedure.* To an oven dried 50 mL pear-shaped flask with a second port with a glass stopcock and 14/20 joint equipped with a stir bar and 180° joint was added lactide (0.100 g, 0.69 mmol) and CH<sub>2</sub>Cl<sub>2</sub>. The solvent was degassed and the reaction vessel was cooled to -20 °C. The acid chloride (0.97 mmol) was then added, followed by the imidazole (0.97 mmol). (If the reagents were premixed, a separate 25 mL round-bottomed flask was used to do so). TiCl<sub>4</sub> (0.191 mL, 1.74 mmol) was added, causing the solution to turn bright yellow, followed promptly by TMP (0.354 mL, 2.08 mmol), causing the solution to turn dark brown or dark violet. The reaction was monitored by TLC, for which small aliquots (~ 0.1 mL) were taken from the reaction vessel using a dessicator-dried Teflon needle. The aliquots were quenched with one drop of water and dried over sodium sulfate prior to TLC. The plate was run with 30 % ethyl acetate in hexanes and visualized by both UV light and ceric ammonium molybdate stain. A spot that is

visualized by both methods was potentially the desired product. Once it was determined that the reaction was no longer proceeding, it was quenched with 2 mL of water, then extracted (3x CH<sub>2</sub>Cl<sub>2</sub>), dried over sodium sulfate, then concentrated to dryness to yield an orange oil. The product was then isolated by column chromatography.



**3,6-dimethyl-3-(undec-10-enoyl)-1,4-dioxane-2,5-dione, 4.12.** Isolated by column chromatography in 30 % ethyl acetate in hexanes; rf: 0.31. <sup>1</sup>H NMR (500 MHz, Chloroform-d) δ 5.80 (ddt, J = 16.9, 10.1, 6.7 Hz, 1H), 5.06 – 4.90 (m, 4H), 2.32 (t, J = 7.5 Hz, 2H), 2.03 (q, J = 7.0 Hz, 3H), 1.68 (d, J = 6.7 Hz, 5H), 1.66 – 1.57 (m, 3H), 1.31 (ddd, J = 37.5, 14.5, 9.1 Hz, 16H), 0.94 (t, J = 7.3 Hz, 1H). <sup>13</sup>C NMR (125 MHz, CDCl<sub>3</sub>, ppm) δ.



**3-benzoyl-3,6-dimethyl-1,4-dioxane-2,5-dione, 4.13.** Isolated by column chromatography in 30 % ethyl acetate in hexanes; rf: 0.60. <sup>1</sup>H NMR (400 MHz, Chloroform-d) δ 8.15 (d, J = 8.1 Hz, 2H), 7.65 (t, J = 7.4 Hz, 1H), 7.51 (t, J = 7.8 Hz, 2H), 4.78 (q, J = 6.8 Hz, 1H), 2.06 (s, 3H), 1.60 (d, J = 6.7 Hz, 3H). <sup>13</sup>C NMR (125 MHz, CDCl<sub>3</sub>, ppm) δ 191.65, 166.73, 164.95, 135.12, 131.75, 130.16, 129.16, 88.07, 73.26, 22.98, 16.39. HRMS (DART) Calcd. For C<sub>13</sub>H<sub>13</sub>O<sub>5</sub> [M]<sup>+</sup>:249.07630. Found: 249.07666

## 4.5 SPECTROSCOPY

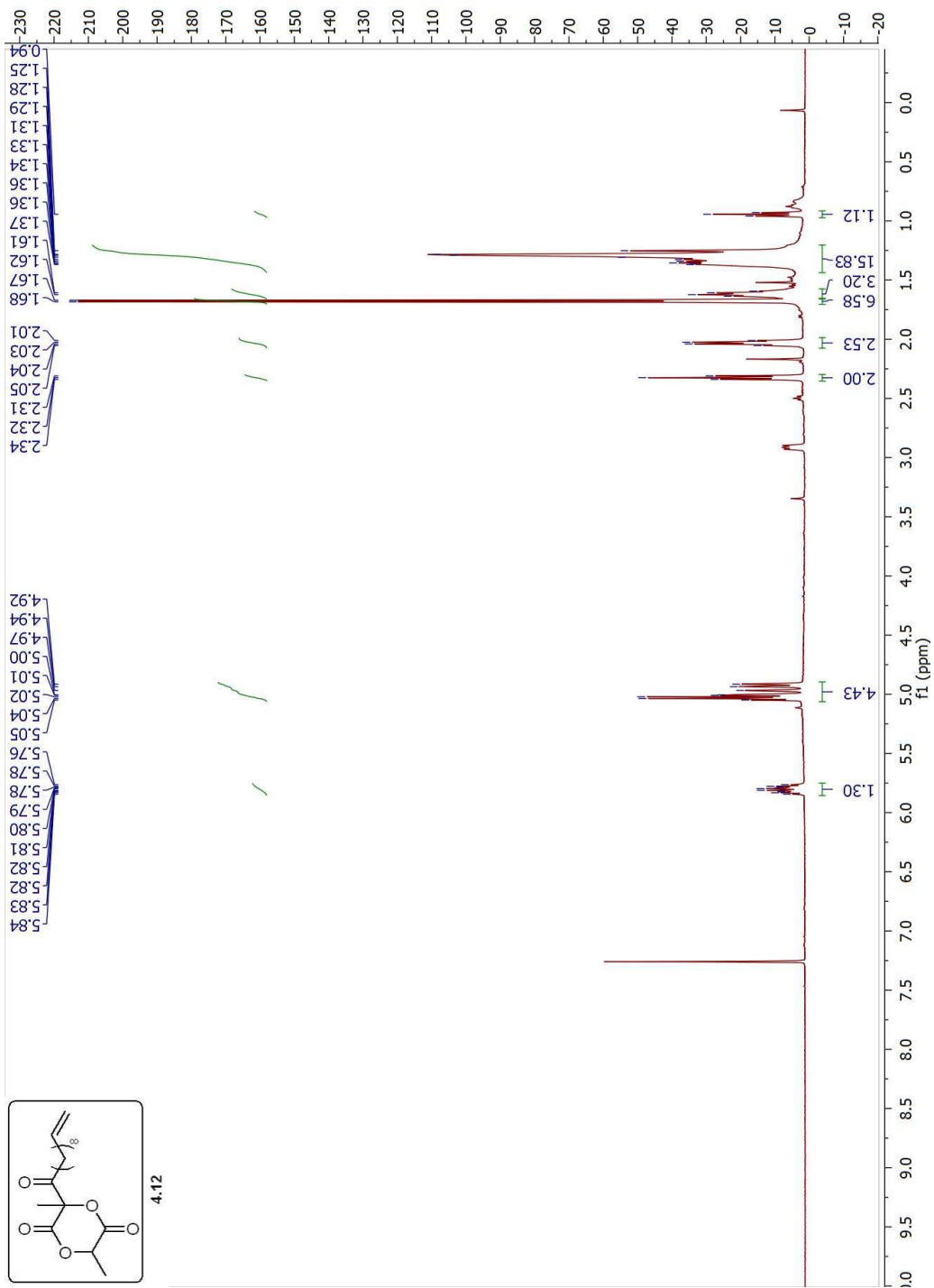


Figure 4.1.  $^1\text{H}$  NMR Spectrum of 4.12. Note, small lactide impurity leads to some incongruous integrations.

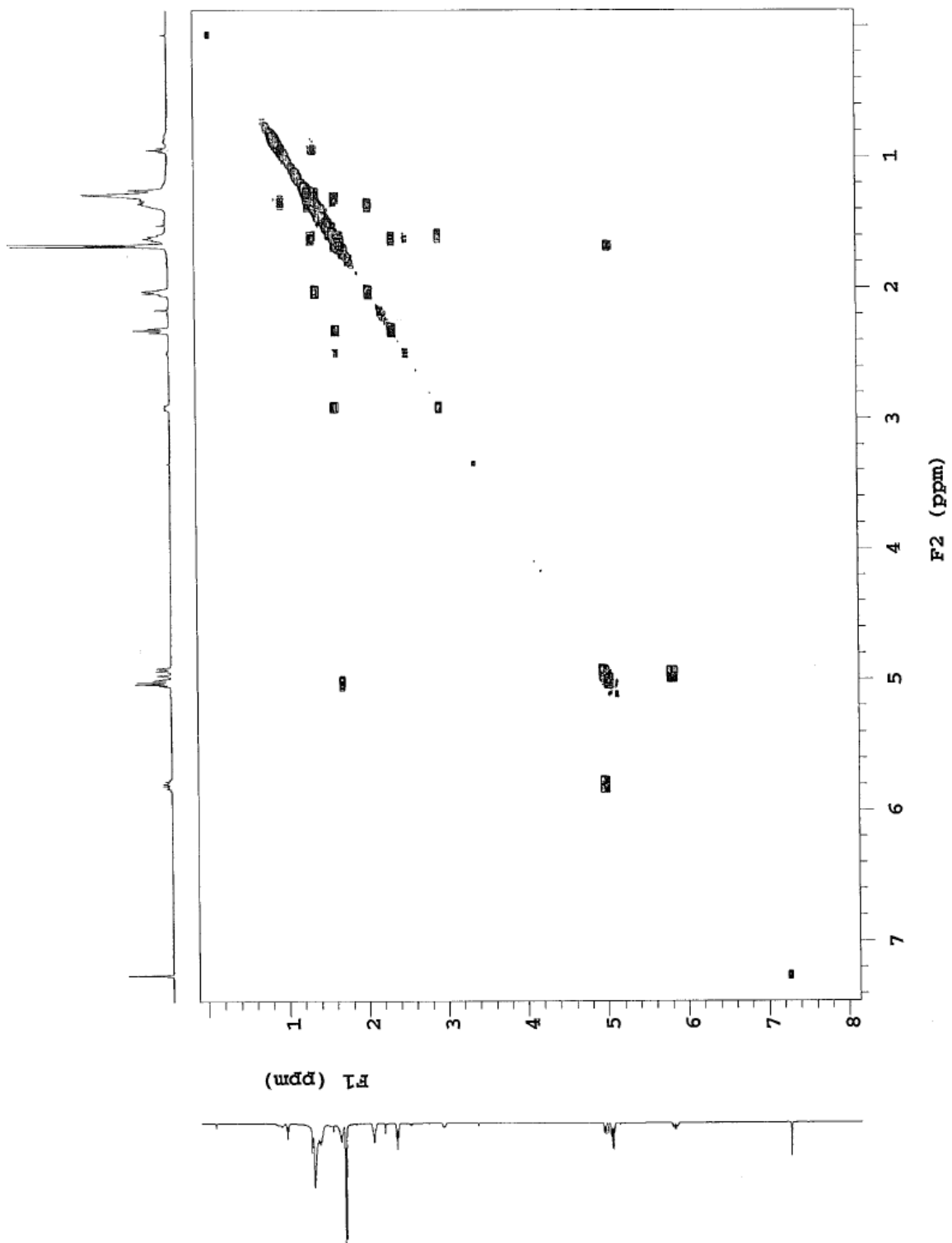


Figure 4.2. COSY NMR Spectrum of 4.12.

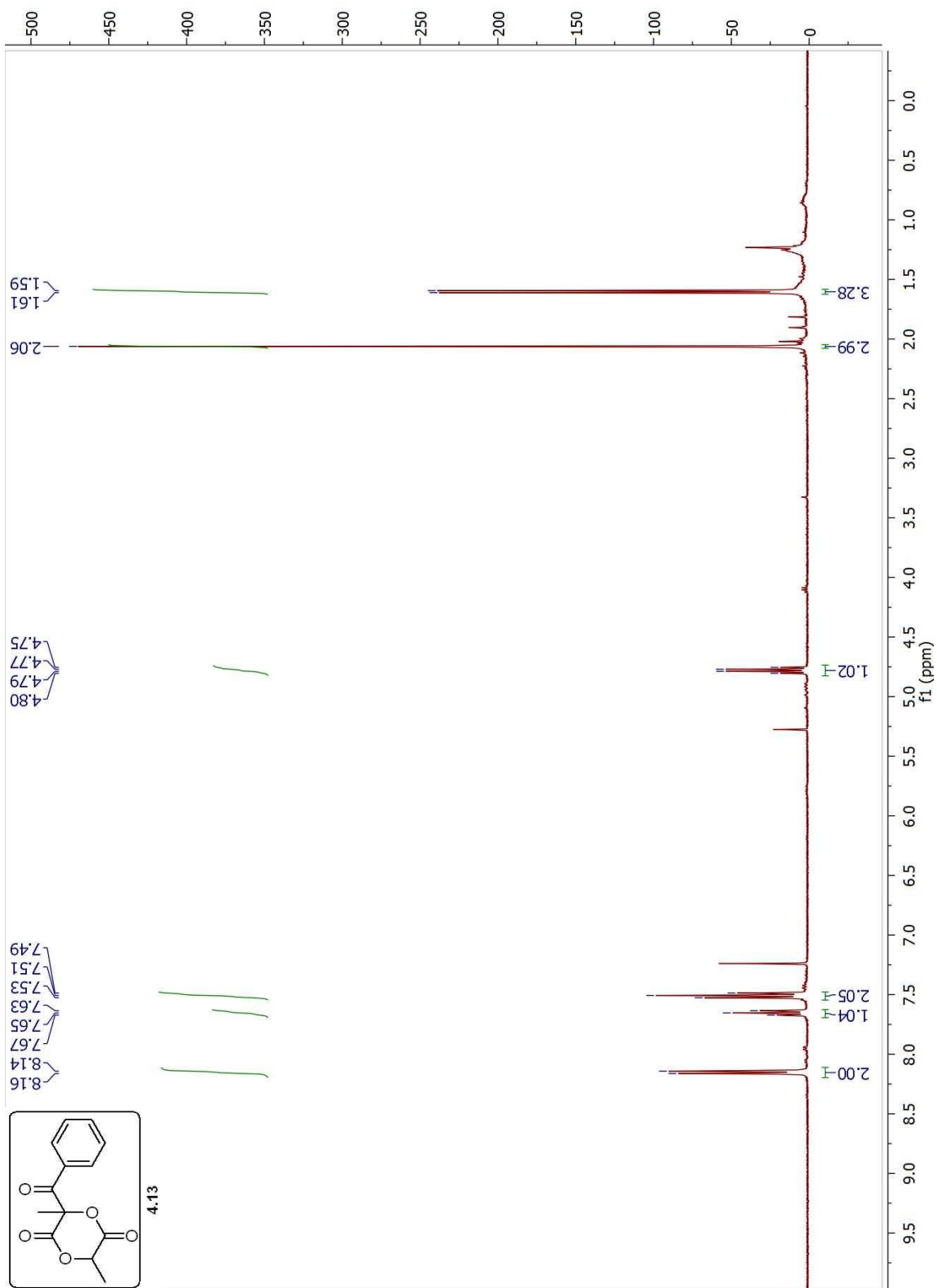


Figure 4.3.  $^1\text{H}$  NMR Spectrum of 4.13.

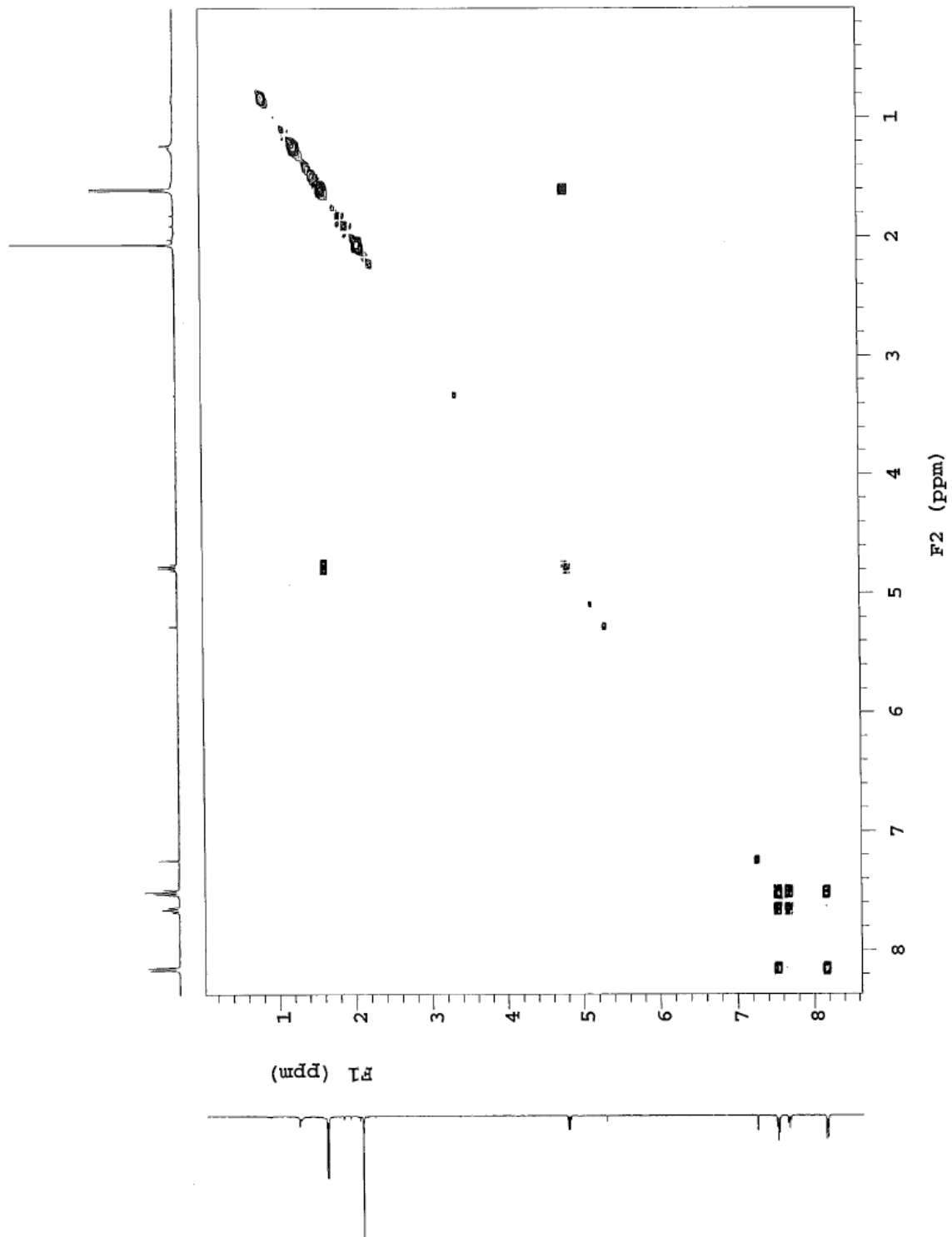


Figure 4.4. COSY NMR Spectrum of 4.13.

## 4.6 REFERENCES

- <sup>1</sup> Mecking, S. *Angew. Chem. Int. Ed.* **2004**, *43*, 1078.
- <sup>2</sup> Ajellal, N.; Carpentiere, J.-F.; Guillamue, C.; Guillaume, S. M.; Helou, M.; Poirier, V.; Sarazin, Y.; Trifonov. *Dalton Trans.* **2010**, *39*, 8363.
- <sup>3</sup> Gupta, A. P.; Kumar, V. *Eur. Polym. J.* **2007**, *43*, 4053.
- <sup>4</sup> Chen, C.; He, B.-X.; Wang, A.-L.; Yuan, G.-P.; Zhang, L. *Eur. Polym. J.* **2015**, *63*, 177.
- <sup>5</sup> Gerhardt, W. W.; Noga, D. E.; Hardcastle, K. I.; Garcia, A. J.; Collard, D. M.; Weck, M. *Biomacromolecules* **2006**, *7*, 1735.
- <sup>6</sup> Jiang, X.; Vogel, E. B.; Smith, M. R.; Baker, G. L. *Macromolecules* **2008**, *41*, 1937.
- <sup>7</sup> Jiang, X.; Smith, M. R.; Baker, G. L. *Macromolecules* **2008**, *41*, 318.
- <sup>8</sup> Jing, F.; Smith, M. R.; Baker, G. L. *Macromolecules* **2007**, *40*, 9304.
- <sup>9</sup> Zou, J.; Hew, C. C.; Themistou, E.; Li, Y.; Chen, C.-K.; Alexandridis, R.; Cheng, C. *Adv. Mater.* **2011**, *23*, 4274.
- <sup>10</sup> Delle Chiaie, K. R.; Yablon, L. M.; Biernesser, A. B.; Michalowski, G. R.; Sudyn, A. W.; Byers, J. A. *Polym. Chem.* **2016**, *7*, 4675.
- <sup>11</sup> Scheibelhoffer, A. S.; Blose, W. A.; Harwood, H. J. *Polym. Prep. (Am. Chem. Soc.; Div. Polym. Chem.)* **1969**, *10*, 1375.
- <sup>12</sup> Maudlin, T. C.; Wertz, J. T.; Boday, D. J. *ACS Macro Lett.* **2016**, *5*, 544.
- <sup>13</sup> Jing, F.; Hillmeyer, M. A. *J. Am. Chem. Soc.* **2008**, *130*, 13826.
- <sup>14</sup> Roudesly, F.; Oble, J.; Poli, G. *Journal of Molecular Catalysis A: Chemical.* **2017**, *426*, 275.
- <sup>15</sup> Volhard, J. *Justus Liebigs Ann. Chem.* **1892**, *267*, 172.
- <sup>16</sup> (a) Baudoin, O. *Acc. Chem. Res.* **2017**, *50*, 1114. (b) Mishra, N. K.; Charma, S.; Park, J.; Han, S.; Kim, I. S. *ACS Catal.* **2017**, *7*, 2821. (c) Mehta, V. P.; Garcia-Lopez, J.-A. *ChemCatChem* **2017**, *9*, 1149.
- <sup>17</sup> He, J.; Wasa, M.; Chan, K. S. L.; Shao, Q.; Yu, J.-Q. *Chem. Rev.* **2017**, *117*, 8754.
- <sup>18</sup> Joe, C. L.; Doyle, A. G. *Angew. Chem. Int. Ed.* **2016**, *55*, 4040.
- <sup>19</sup> Cheng, Q.-Q.; Yang, J.-M.; Xu, H.; Zhu, S.-F. *Synlett*, **2017**, *28*, 1327.
- <sup>20</sup> Shang, R.; Ilies, L.; Nakamura, E. *Chem. Rev.* **2017**, *117*, 9086.
- <sup>21</sup> Trost, B. M.; Imi, K.; Davies, I. W. *J. Am. Chem. Soc.* **1995**, *117*, 5371.
- <sup>22</sup> Murai, S.; Kakiuchi, F.; Sekine, S.; Tanaka, Y.; Kamatini, A.; Sonoda, M.; Chatani, N. *Nature* **1993**, *336*, 529.
- <sup>23</sup> Lenges, C. P.; Brookhart, M. *J. Am. Chem. Soc.* **1999**, *121*, 6616.
- <sup>24</sup> Giri, R.; Maugel, N.; Li, J.-J.; Wang, D.-H.; Breazzano, S. P.; Saunders, L. B.; Yu, J.-Q. *J. Am. Chem. Soc.* **2007**, *129*, 3510.
- <sup>25</sup> He, J.; Li, S.; Deng, Y.; Fu, H.; Laforteza, B. N.; Spangler, J. E.; Homs, A. H.; Yu, J.-Q. *Science*. **2014**, *343*, 1216.
- <sup>26</sup> Wang, D. H.; Hao, X.-S.; Wu, D.-F.; Yu, J.-Q. *Org. Lett.* **2006**, *8*, 3387.
- <sup>27</sup> (a) Heathcock, C. H. *Science* **1981**, *214*, 395. (b) Evans, D. A.; Nelson, J. V.; Taber, T. R. *Top. Stereochem.* **1982**, *13*, 1. (c) Hauser, C. R.; Swamer, F. W.; Adams, J. T. *Organic Reactions* **1954**, *8*, 59.
- <sup>28</sup> Nagase, R.; Oguni, Y.; Ureshino, S.; Mura, H.; Misiaki, T.; Tanabe, Y. *Chem. Commun.* **2013**, *39*, 7001.
- <sup>29</sup> Burger, B. J.; Bercaw, J. E.; *New Development in the Synthesis, Manipulation and Characterization of Organometallic Compounds*; American Chemical Society: Washington DC, 1987; Vol. 357.
- <sup>30</sup> Debdab, M.; Mongin, F.; Bazureau, J. P. *Synthesis* **2006**, *23*, 4046.

## 5.0 APPENDIX I: X-RAY CRYSTALLOGRAPHIC ANALYSES

### 5.1 X-RAY CRYSTALLOGRAPHIC ANALYSIS OF 2.21

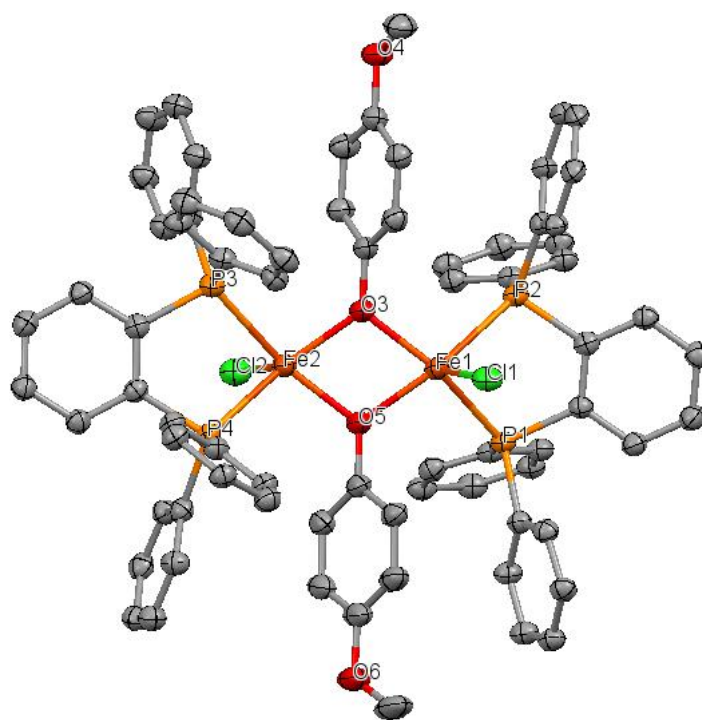


Table 1. Crystal data and structure refinement for twin5\_sq. **2.21**.

Identification code	twin5_sq	
Empirical formula	C <sub>48</sub> H <sub>58</sub> Cl <sub>4</sub> Fe <sub>6</sub> O <sub>16</sub> P <sub>12</sub>	
Formula weight	6833.46	
Temperature	100(2) K	
Wavelength	1.54178 Å	
Crystal system	Triclinic	
Space group	P-1	
Unit cell dimensions	a = 16.4468(9) Å	a = 90.980(4)°.

	$b = 16.7667(14) \text{ \AA}$	$b = 93.996(3)^\circ$ .
	$c = 45.659(3) \text{ \AA}$	$g = 117.808(2)^\circ$ .
Volume	$11092.1(13) \text{ \AA}^3$	
Z	1	
Density (calculated)	$1.023 \text{ Mg/m}^3$	
Absorption coefficient	$2.554 \text{ mm}^{-1}$	
F(000)	3684	
Crystal size	$0.300 \times 0.180 \times 0.110 \text{ mm}^3$	
Theta range for data collection	$0.971$ to $66.781^\circ$ .	
Index ranges	$-19 \leq h \leq 19$ , $-19 \leq k \leq 19$ , $0 \leq l \leq 54$	
Reflections collected	39166	
Independent reflections	39166 [R(int) = ?]	
Completeness to theta = $66.781^\circ$	99.5 %	
Absorption correction	Semi-empirical from equivalents	
Max. and min. transmission	0.7528 and 0.5651	
Refinement method	Full-matrix least-squares on $F^2$	
Data / restraints / parameters	39166 / 2094 / 2303	
Goodness-of-fit on $F^2$	1.035	
Final R indices [ $I > 2\sigma(I)$ ]	$R1 = 0.0814$ , $wR2 = 0.2258$	
R indices (all data)	$R1 = 0.1020$ , $wR2 = 0.2430$	
Extinction coefficient	n/a	
Largest diff. peak and hole	$0.930$ and $-0.499 \text{ e.\AA}^{-3}$	

Table 2. Atomic coordinates ( $\times 10^4$ ) and equivalent isotropic displacement parameters ( $\text{\AA}^2 \times 10^3$ )

for twin5\_sq.  $U(\text{eq})$  is defined as one third of the trace of the orthogonalized  $U_{ij}$  tensor.

	x	y	z	U(eq)
Fe(1)	3872(1)	5310(1)	1312(1)	46(1)
Fe(2)	3794(1)	5097(1)	2025(1)	50(1)
P(1)	4171(1)	6741(1)	1061(1)	45(1)
P(2)	5153(1)	5513(1)	985(1)	46(1)
P(3)	3715(1)	3783(1)	2316(1)	50(1)
P(4)	2410(1)	4750(1)	2329(1)	48(1)
Cl(1)	2711(3)	4366(3)	999(1)	62(1)
O(1)	3056(6)	4429(9)	1012(3)	68(3)
C(63)	2270(5)	4025(5)	824(2)	42(1)
C(64)	1430(6)	3415(6)	925(2)	54(2)
C(65)	633(6)	2969(6)	724(2)	66(2)
C(66)	682(6)	3076(7)	437(2)	67(2)
C(67)	1517(6)	3690(6)	333(2)	55(2)
C(68)	2298(5)	4159(5)	530(2)	49(2)
O(2)	-36(7)	2692(6)	228(2)	98(2)
C(69)	-888(12)	2262(12)	330(4)	122(5)
O(3)	4304(2)	4825(2)	1662(1)	61(1)
O(4)	6112(2)	2763(2)	1570(1)	69(1)
Cl(2)	4892(1)	6228(1)	2335(1)	66(1)
O(5)	3359(2)	5577(2)	1675(1)	62(1)
O(6)	1124(3)	7225(3)	1691(1)	103(2)
C(1)	3272(3)	7073(3)	967(1)	48(1)
C(2)	2488(3)	6455(3)	795(1)	50(1)
C(3)	1805(3)	6678(3)	699(1)	53(1)
C(4)	1910(3)	7523(3)	789(1)	55(1)
C(5)	2669(3)	8142(3)	966(1)	56(1)
C(6)	3353(3)	7903(3)	1056(1)	52(1)
C(7)	991(3)	6007(3)	490(1)	64(1)

C(8)	476(4)	5105(4)	631(1)	86(2)
C(9)	294(4)	6354(4)	406(2)	92(2)
C(10)	1365(4)	5885(5)	206(1)	90(2)
C(11)	2809(3)	9090(3)	1065(1)	64(1)
C(12)	3744(4)	9808(3)	989(2)	83(2)
C(13)	2774(5)	9137(4)	1397(1)	85(2)
C(14)	2066(4)	9290(4)	918(2)	85(2)
C(15)	5146(3)	7826(3)	1192(1)	48(1)
C(16)	5214(3)	8112(3)	1482(1)	54(1)
C(17)	5837(3)	8993(3)	1584(1)	56(1)
C(18)	6422(3)	9555(3)	1386(1)	57(1)
C(19)	6399(3)	9280(3)	1095(1)	56(1)
C(20)	5749(3)	8403(3)	998(1)	51(1)
C(21)	5830(3)	9319(3)	1900(1)	62(1)
C(22)	5948(4)	8699(4)	2121(1)	75(1)
C(23)	4906(3)	9323(3)	1924(1)	68(1)
C(24)	6611(4)	10283(4)	1974(1)	72(1)
C(25)	7062(3)	9937(3)	890(1)	66(1)
C(26)	6902(4)	10765(4)	869(1)	81(2)
C(27)	8057(4)	10247(4)	1022(1)	79(1)
C(28)	6932(4)	9510(4)	580(1)	85(2)
C(29)	4437(3)	6519(3)	692(1)	46(1)
C(30)	4221(3)	6896(3)	444(1)	53(1)
C(31)	4362(3)	6674(3)	168(1)	57(1)
C(32)	4718(3)	6082(3)	130(1)	56(1)
C(33)	4960(3)	5732(3)	373(1)	50(1)
C(34)	4824(2)	5949(2)	655(1)	45(1)
C(35)	6344(3)	6392(3)	1078(1)	51(1)
C(36)	6625(3)	6676(3)	1372(1)	56(1)
C(37)	7536(3)	7341(3)	1453(1)	64(1)
C(38)	8129(3)	7665(3)	1233(1)	65(1)
C(39)	7864(3)	7387(3)	935(1)	58(1)
C(40)	6960(3)	6767(3)	862(1)	54(1)
C(41)	7863(4)	7721(4)	1773(1)	73(1)
C(42)	7130(4)	7255(4)	1983(1)	84(2)
C(43)	8071(4)	8726(4)	1782(1)	86(2)

C(44)	8746(5)	7677(6)	1864(1)	106(2)
C(45)	8569(3)	7757(3)	702(1)	66(1)
C(46)	9296(8)	7454(10)	799(3)	99(4)
C(47)	9095(9)	8817(7)	738(3)	98(4)
C(48)	8171(8)	7470(10)	405(2)	103(4)
C(346)	9535(9)	8168(10)	798(3)	82(4)
C(347)	8315(9)	8382(9)	510(3)	76(4)
C(348)	8354(9)	6945(9)	451(3)	75(3)
C(49)	5264(3)	4556(3)	832(1)	48(1)
C(50)	4465(3)	3809(3)	711(1)	50(1)
C(51)	4495(3)	3050(3)	597(1)	57(1)
C(52)	5360(3)	3065(3)	610(1)	58(1)
C(53)	6164(3)	3803(3)	729(1)	57(1)
C(54)	6102(3)	4545(3)	842(1)	54(1)
C(55)	3606(4)	2240(3)	470(1)	64(1)
C(56)	2967(4)	1868(4)	715(1)	81(2)
C(57)	3771(5)	1481(4)	340(2)	94(2)
C(58)	3125(4)	2539(4)	228(1)	90(2)
C(59)	7118(4)	3842(4)	727(1)	68(1)
C(60)	7007(6)	2895(5)	655(2)	130(3)
C(61)	7600(4)	4413(6)	481(1)	101(2)
C(62)	7681(5)	4238(6)	1012(1)	112(2)
C(70)	4738(3)	4308(3)	1639(1)	53(1)
C(71)	4351(3)	3528(3)	1459(1)	58(1)
C(72)	4770(3)	2989(3)	1432(1)	56(1)
C(73)	5623(3)	3239(3)	1583(1)	57(1)
C(74)	6027(3)	4028(3)	1768(1)	65(1)
C(75)	5591(3)	4552(3)	1794(1)	61(1)
C(76)	5645(4)	1897(4)	1411(1)	81(2)
C(77)	4781(3)	3774(3)	2457(1)	56(1)
C(78)	4979(3)	3071(3)	2401(1)	60(1)
C(79)	5797(4)	3110(4)	2520(1)	69(1)
C(80)	6420(3)	3882(4)	2693(1)	70(1)
C(81)	6249(3)	4586(3)	2748(1)	64(1)
C(82)	5423(3)	4540(3)	2625(1)	61(1)
C(83)	6040(4)	2340(4)	2468(1)	79(1)

C(84)	5294(5)	1582(4)	2263(2)	98(2)
C(85)	6120(6)	1957(5)	2765(2)	111(2)
C(86)	6951(4)	2689(4)	2332(1)	89(2)
C(87)	6961(3)	5453(4)	2923(1)	74(1)
C(88)	7641(4)	5281(4)	3133(1)	87(2)
C(89)	7495(4)	6146(4)	2703(1)	89(2)
C(90)	6488(4)	5821(4)	3125(2)	93(2)
C(91)	2909(3)	2608(3)	2195(1)	54(1)
C(92)	2406(3)	2433(3)	1926(1)	57(1)
C(93)	1770(3)	1553(3)	1828(1)	64(1)
C(94)	1669(4)	863(3)	2009(1)	70(1)
C(95)	2162(4)	1010(3)	2283(1)	68(1)
C(96)	2785(3)	1904(3)	2376(1)	61(1)
C(97)	1195(3)	1350(4)	1532(1)	71(1)
C(98)	1826(5)	1656(6)	1296(2)	70(2)
C(99)	556(6)	1732(7)	1547(2)	75(2)
C(100)	573(7)	273(6)	1469(2)	82(3)
C(398)	1467(9)	2322(8)	1358(3)	67(3)
C(399)	191(10)	997(12)	1565(3)	87(4)
C(400)	1421(10)	831(9)	1331(3)	74(4)
C(101)	2031(5)	211(4)	2465(1)	84(2)
C(102)	1011(5)	-331(4)	2524(2)	105(2)
C(103)	2318(5)	-400(4)	2294(2)	102(2)
C(104)	2610(5)	508(4)	2760(1)	95(2)
C(105)	3260(3)	3905(3)	2663(1)	50(1)
C(106)	3428(3)	3535(3)	2918(1)	52(1)
C(107)	3029(3)	3574(3)	3171(1)	57(1)
C(108)	2482(3)	3991(3)	3177(1)	56(1)
C(109)	2334(3)	4391(3)	2930(1)	52(1)
C(110)	2717(3)	4337(3)	2667(1)	48(1)
C(111)	1249(3)	3822(3)	2221(1)	50(1)
C(112)	731(3)	3898(3)	1978(1)	54(1)
C(113)	-182(3)	3233(3)	1908(1)	58(1)
C(114)	-546(3)	2495(3)	2079(1)	55(1)
C(115)	-34(3)	2386(3)	2318(1)	55(1)
C(116)	866(3)	3063(3)	2386(1)	53(1)

C(117)	-766(3)	3356(3)	1648(1)	64(1)
C(118)	-286(4)	3457(4)	1367(1)	78(1)
C(119)	-1734(4)	2567(4)	1599(1)	78(2)
C(120)	-853(4)	4215(4)	1719(1)	76(1)
C(121)	-482(3)	1549(3)	2499(1)	65(1)
C(122)	-735(4)	709(3)	2300(1)	81(2)
C(123)	-1350(4)	1485(4)	2613(1)	87(2)
C(124)	175(4)	1575(4)	2757(1)	86(2)
C(125)	2194(3)	5643(3)	2484(1)	52(1)
C(126)	2960(3)	6402(3)	2617(1)	54(1)
C(127)	2861(3)	7101(3)	2750(1)	58(1)
C(128)	1987(3)	7021(3)	2744(1)	62(1)
C(129)	1200(3)	6268(3)	2615(1)	63(1)
C(130)	1326(3)	5583(3)	2484(1)	57(1)
C(131)	3718(3)	7946(3)	2891(1)	63(1)
C(132)	4242(6)	8485(5)	2642(2)	90(3)
C(133)	4288(5)	7670(5)	3092(2)	77(2)
C(134)	3442(5)	8564(5)	3074(2)	71(2)
C(432)	3900(20)	8760(20)	2744(7)	113(11)
C(433)	4739(16)	7868(16)	2854(5)	77(7)
C(434)	3740(20)	7990(20)	3217(5)	98(9)
C(135)	257(4)	6222(4)	2609(1)	77(1)
C(136)	58(9)	6540(13)	2322(3)	125(5)
C(137)	159(8)	6765(10)	2860(3)	103(4)
C(138)	-524(6)	5212(6)	2626(4)	98(4)
C(436)	300(14)	7064(13)	2442(4)	79(5)
C(437)	68(14)	6343(16)	2926(4)	77(5)
C(438)	-512(15)	5419(15)	2447(5)	91(6)
C(139)	2802(3)	5974(3)	1675(1)	61(1)
C(140)	2046(3)	5692(4)	1471(1)	64(1)
C(141)	1470(4)	6094(4)	1469(1)	76(1)
C(142)	1651(4)	6781(4)	1673(1)	81(2)
C(143)	2395(4)	7063(4)	1878(1)	79(1)
C(144)	2981(4)	6677(4)	1880(1)	69(1)
C(145)	350(5)	6926(6)	1469(2)	115(2)
Fe(3)	5233(1)	5299(1)	4665(1)	60(1)

P(5)	4032(1)	4828(1)	4235(1)	55(1)
P(6)	5698(1)	6814(1)	4423(1)	60(1)
O(7)	5410(3)	5804(2)	5079(1)	79(1)
O(8)	7825(3)	9339(2)	5459(1)	96(1)
Cl(3)	6301(4)	5051(4)	4468(1)	58(1)
O(9)	6157(12)	5182(13)	4437(4)	76(4)
C(215)	6727(10)	5006(8)	4344(3)	85(3)
C(216)	7247(12)	4702(12)	4513(4)	122(5)
C(217)	7898(15)	4470(14)	4389(5)	150(7)
C(218)	8070(12)	4384(11)	4128(4)	112(5)
C(219)	7638(13)	4812(13)	3928(4)	132(6)
C(220)	6921(11)	5093(10)	4029(3)	104(4)
O(10)	8403(14)	4148(14)	3943(5)	211(7)
C(221)	8544(15)	3713(15)	3729(5)	150(7)
C(146)	2978(3)	4936(3)	4247(1)	61(1)
C(147)	2767(4)	5452(4)	4054(1)	70(1)
C(148)	1927(4)	5468(4)	4050(1)	79(1)
C(149)	1303(4)	4945(4)	4244(1)	81(1)
C(150)	1499(4)	4428(4)	4445(1)	76(1)
C(151)	2346(4)	4440(3)	4447(1)	69(1)
C(152)	1706(5)	6044(6)	3830(2)	102(2)
C(153)	2557(8)	7116(8)	3890(2)	98(3)
C(154)	858(10)	6093(11)	3866(3)	120(5)
C(155)	1769(9)	5801(9)	3526(2)	102(4)
C(453)	761(15)	5139(15)	3613(5)	129(8)
C(454)	1350(18)	6529(17)	3965(5)	127(9)
C(455)	2357(13)	6424(14)	3612(4)	101(6)
C(156)	760(5)	3853(4)	4646(2)	95(2)
C(157)	417(13)	4407(10)	4799(4)	84(4)
C(158)	-177(9)	3197(9)	4409(4)	87(3)
C(159)	932(9)	3188(10)	4791(3)	83(3)
C(457)	630(20)	4485(18)	4885(6)	131(10)
C(458)	-30(20)	3210(20)	4516(5)	170(14)
C(459)	1229(16)	3415(15)	4890(5)	128(8)
C(160)	3632(3)	3729(3)	4038(1)	54(1)
C(161)	2697(3)	3106(3)	3981(1)	56(1)

C(162)	2432(3)	2281(3)	3831(1)	59(1)
C(163)	3115(3)	2095(3)	3740(1)	59(1)
C(164)	4059(3)	2712(3)	3793(1)	58(1)
C(165)	4299(3)	3521(3)	3944(1)	55(1)
C(166)	1406(3)	1615(4)	3763(1)	68(1)
C(167)	940(6)	2093(7)	3590(2)	88(3)
C(168)	941(6)	1370(7)	4062(2)	81(3)
C(169)	1223(7)	739(7)	3606(3)	96(3)
C(467)	762(11)	1967(11)	3832(4)	87(5)
C(468)	1240(11)	1343(11)	3412(3)	88(5)
C(469)	1153(11)	728(10)	3914(3)	84(4)
C(170)	4812(4)	2515(3)	3686(1)	68(1)
C(171)	5471(4)	2559(4)	3949(1)	85(2)
C(172)	4428(5)	1589(4)	3524(2)	91(2)
C(173)	5361(4)	3239(4)	3468(1)	82(2)
C(174)	4632(3)	5597(3)	3953(1)	55(1)
C(175)	4347(3)	5355(3)	3659(1)	61(1)
C(176)	4764(4)	5938(3)	3442(1)	66(1)
C(177)	5504(4)	6766(3)	3520(1)	64(1)
C(178)	5814(4)	7022(3)	3810(1)	64(1)
C(179)	5388(3)	6460(3)	4032(1)	56(1)
C(180)	6781(9)	7725(7)	4419(3)	65(3)
C(181)	7040(8)	8603(6)	4515(3)	70(3)
C(182)	7933(8)	9282(6)	4492(3)	77(3)
C(183)	8570(8)	9055(7)	4384(3)	77(3)
C(184)	8360(7)	8172(8)	4296(3)	75(3)
C(185)	7436(8)	7514(8)	4318(3)	65(3)
C(186)	8222(9)	10283(7)	4573(3)	99(3)
C(187)	7530(11)	10342(8)	4754(4)	120(5)
C(188)	9151(11)	10721(9)	4765(4)	131(5)
C(189)	8265(11)	10737(8)	4296(3)	119(4)
C(190)	9085(8)	7918(10)	4178(3)	85(3)
C(191)	9971(11)	8687(13)	4128(5)	148(6)
C(192)	9220(10)	7209(12)	4386(3)	111(4)
C(193)	8710(10)	7308(11)	3868(3)	101(4)
C(480)	6994(8)	7646(7)	4419(3)	50(3)

C(481)	7366(8)	8528(7)	4538(3)	68(3)
C(482)	8305(9)	9112(8)	4531(3)	80(3)
C(483)	8853(9)	8787(8)	4413(3)	79(3)
C(484)	8510(8)	7916(8)	4300(3)	73(4)
C(485)	7565(7)	7336(8)	4307(3)	58(3)
C(486)	8739(10)	10113(9)	4641(3)	101(4)
C(487)	8129(10)	10336(10)	4805(3)	98(4)
C(488)	9553(13)	10306(14)	4876(4)	152(7)
C(489)	9039(15)	10668(13)	4385(4)	160(8)
C(490)	9097(11)	7523(11)	4158(4)	99(5)
C(491)	8786(18)	6587(14)	4207(6)	196(11)
C(492)	9100(20)	7830(20)	3825(5)	270(20)
C(493)	10157(14)	8135(17)	4276(6)	197(11)
C(194)	5053(4)	7443(4)	4467(1)	75(1)
C(195)	4430(4)	7199(4)	4680(1)	81(1)
C(196)	3917(5)	7655(5)	4716(1)	99(2)
C(197)	4066(7)	8347(6)	4537(2)	124(3)
C(198)	4667(8)	8604(6)	4316(2)	128(3)
C(199)	5175(6)	8143(5)	4282(1)	105(2)
C(200)	3217(6)	7388(6)	4949(2)	113(2)
C(201)	3053(9)	6407(9)	5098(3)	89(3)
C(202)	2269(10)	7189(10)	4834(3)	95(3)
C(203)	3637(11)	8073(11)	5203(3)	95(4)
C(501)	2477(15)	6706(13)	4847(5)	148(7)
C(502)	2831(18)	8263(16)	4908(5)	190(10)
C(503)	3733(16)	7742(16)	5226(5)	142(9)
C(204)	5152(11)	9581(10)	4118(3)	91(3)
C(205)	6110(14)	10289(13)	4218(4)	142(6)
C(206)	4500(20)	9910(30)	4162(8)	232(16)
C(207)	4945(10)	9255(10)	3829(3)	86(3)
C(504)	4529(11)	9240(11)	4107(3)	97(4)
C(505)	3578(11)	9026(11)	3963(3)	109(4)
C(506)	5407(15)	9445(14)	3853(5)	136(7)
C(507)	4903(15)	10110(14)	4305(4)	129(6)
C(208)	6005(4)	6671(3)	5181(1)	71(1)
C(209)	5704(4)	7142(3)	5355(1)	77(1)

C(210)	6305(4)	8040(3)	5451(1)	77(1)
C(211)	7183(4)	8447(3)	5376(1)	78(1)
C(212)	7498(4)	7982(4)	5203(1)	81(2)
C(213)	6907(4)	7085(3)	5105(1)	73(1)
C(214)	7473(5)	9846(4)	5608(2)	114(2)

---

—

Table 3. Bond lengths [Å] and angles [°] for twin5\_sq.

---

Fe(1)-O(1)	1.918(12)
Fe(1)-O(3)	2.036(3)
Fe(1)-O(5)	2.049(3)
Fe(1)-Cl(1)	2.217(4)
Fe(1)-P(1)	2.5263(12)
Fe(1)-P(2)	2.5613(12)
Fe(2)-O(5)	2.032(3)
Fe(2)-O(3)	2.046(3)
Fe(2)-Cl(2)	2.2844(14)
Fe(2)-P(3)	2.5478(12)
Fe(2)-P(4)	2.5851(12)
P(1)-C(15)	1.829(4)
P(1)-C(1)	1.835(4)
P(1)-C(29)	1.841(4)
P(2)-C(49)	1.830(4)
P(2)-C(35)	1.833(4)
P(2)-C(34)	1.839(4)
P(3)-C(77)	1.832(4)
P(3)-C(91)	1.834(4)
P(3)-C(105)	1.846(4)
P(4)-C(125)	1.834(4)
P(4)-C(110)	1.835(4)
P(4)-C(111)	1.840(4)
O(1)-C(63)	1.370(11)
C(63)-C(68)	1.366(11)
C(63)-C(64)	1.397(11)
C(64)-C(65)	1.419(12)
C(64)-H(64)	0.9500
C(65)-C(66)	1.331(13)
C(65)-H(65)	0.9500
C(66)-O(2)	1.352(12)
C(66)-C(67)	1.399(13)
C(67)-C(68)	1.396(12)
C(67)-H(67)	0.9500

C(68)-H(68)	0.9500
O(2)-C(69)	1.364(17)
C(69)-H(69A)	0.9800
C(69)-H(69B)	0.9800
C(69)-H(69C)	0.9800
O(3)-C(70)	1.361(5)
O(4)-C(73)	1.376(5)
O(4)-C(76)	1.437(6)
O(5)-C(139)	1.360(5)
O(6)-C(142)	1.387(6)
O(6)-C(145)	1.453(9)
C(1)-C(6)	1.385(6)
C(1)-C(2)	1.392(6)
C(2)-C(3)	1.387(6)
C(2)-H(2)	0.9500
C(3)-C(4)	1.395(6)
C(3)-C(7)	1.532(6)
C(4)-C(5)	1.384(6)
C(4)-H(4)	0.9500
C(5)-C(6)	1.399(6)
C(5)-C(11)	1.549(6)
C(6)-H(6)	0.9500
C(7)-C(10)	1.523(7)
C(7)-C(8)	1.527(7)
C(7)-C(9)	1.538(7)
C(8)-H(8A)	0.9800
C(8)-H(8B)	0.9800
C(8)-H(8C)	0.9800
C(9)-H(9A)	0.9800
C(9)-H(9B)	0.9800
C(9)-H(9C)	0.9800
C(10)-H(10A)	0.9800
C(10)-H(10B)	0.9800
C(10)-H(10C)	0.9800
C(11)-C(12)	1.514(7)
C(11)-C(13)	1.522(8)

C(11)-C(14)	1.529(6)
C(12)-H(12A)	0.9800
C(12)-H(12B)	0.9800
C(12)-H(12C)	0.9800
C(13)-H(13A)	0.9800
C(13)-H(13B)	0.9800
C(13)-H(13C)	0.9800
C(14)-H(14A)	0.9800
C(14)-H(14B)	0.9800
C(14)-H(14C)	0.9800
C(15)-C(16)	1.381(6)
C(15)-C(20)	1.399(6)
C(16)-C(17)	1.395(6)
C(16)-H(16)	0.9500
C(17)-C(18)	1.393(6)
C(17)-C(21)	1.534(6)
C(18)-C(19)	1.390(6)
C(18)-H(18)	0.9500
C(19)-C(20)	1.395(6)
C(19)-C(25)	1.529(6)
C(20)-H(20)	0.9500
C(21)-C(22)	1.529(7)
C(21)-C(23)	1.533(7)
C(21)-C(24)	1.536(7)
C(22)-H(22A)	0.9800
C(22)-H(22B)	0.9800
C(22)-H(22C)	0.9800
C(23)-H(23A)	0.9800
C(23)-H(23B)	0.9800
C(23)-H(23C)	0.9800
C(24)-H(24A)	0.9800
C(24)-H(24B)	0.9800
C(24)-H(24C)	0.9800
C(25)-C(28)	1.531(7)
C(25)-C(26)	1.532(7)
C(25)-C(27)	1.541(7)

C(26)-H(26A)	0.9800
C(26)-H(26B)	0.9800
C(26)-H(26C)	0.9800
C(27)-H(27A)	0.9800
C(27)-H(27B)	0.9800
C(27)-H(27C)	0.9800
C(28)-H(28A)	0.9800
C(28)-H(28B)	0.9800
C(28)-H(28C)	0.9800
C(29)-C(34)	1.388(5)
C(29)-C(30)	1.409(5)
C(30)-C(31)	1.377(6)
C(30)-H(30)	0.9500
C(31)-C(32)	1.381(6)
C(31)-H(31)	0.9500
C(32)-C(33)	1.383(6)
C(32)-H(32)	0.9500
C(33)-C(34)	1.396(6)
C(33)-H(33)	0.9500
C(35)-C(36)	1.388(6)
C(35)-C(40)	1.399(6)
C(36)-C(37)	1.405(6)
C(36)-H(36)	0.9500
C(37)-C(38)	1.386(7)
C(37)-C(41)	1.536(7)
C(38)-C(39)	1.401(7)
C(38)-H(38)	0.9500
C(39)-C(40)	1.371(6)
C(39)-C(45)	1.542(6)
C(40)-H(40)	0.9500
C(41)-C(42)	1.515(8)
C(41)-C(44)	1.519(8)
C(41)-C(43)	1.555(8)
C(42)-H(42A)	0.9800
C(42)-H(42B)	0.9800
C(42)-H(42C)	0.9800

C(43)-H(43A)	0.9800
C(43)-H(43B)	0.9800
C(43)-H(43C)	0.9800
C(44)-H(44A)	0.9800
C(44)-H(44B)	0.9800
C(44)-H(44C)	0.9800
C(45)-C(48)	1.436(12)
C(45)-C(46)	1.545(11)
C(45)-C(47)	1.571(11)
C(46)-H(46A)	0.9800
C(46)-H(46B)	0.9800
C(46)-H(46C)	0.9800
C(47)-H(47A)	0.9800
C(47)-H(47B)	0.9800
C(47)-H(47C)	0.9800
C(48)-H(48A)	0.9800
C(48)-H(48B)	0.9800
C(48)-H(48C)	0.9800
C(49)-C(54)	1.384(6)
C(49)-C(50)	1.393(6)
C(50)-C(51)	1.390(6)
C(50)-H(50)	0.9500
C(51)-C(52)	1.408(6)
C(51)-C(55)	1.524(7)
C(52)-C(53)	1.388(7)
C(52)-H(52)	0.9500
C(53)-C(54)	1.389(6)
C(53)-C(59)	1.540(6)
C(54)-H(54)	0.9500
C(55)-C(56)	1.522(7)
C(55)-C(57)	1.540(7)
C(55)-C(58)	1.540(7)
C(56)-H(56A)	0.9800
C(56)-H(56B)	0.9800
C(56)-H(56C)	0.9800
C(57)-H(57A)	0.9800

C(57)-H(57B)	0.9800
C(57)-H(57C)	0.9800
C(58)-H(58A)	0.9800
C(58)-H(58B)	0.9800
C(58)-H(58C)	0.9800
C(59)-C(62)	1.490(8)
C(59)-C(61)	1.507(8)
C(59)-C(60)	1.538(8)
C(60)-H(60A)	0.9800
C(60)-H(60B)	0.9800
C(60)-H(60C)	0.9800
C(61)-H(61A)	0.9800
C(61)-H(61B)	0.9800
C(61)-H(61C)	0.9800
C(62)-H(62A)	0.9800
C(62)-H(62B)	0.9800
C(62)-H(62C)	0.9800
C(70)-C(71)	1.381(6)
C(70)-C(75)	1.397(6)
C(71)-C(72)	1.377(6)
C(71)-H(71)	0.9500
C(72)-C(73)	1.388(6)
C(72)-H(72)	0.9500
C(73)-C(74)	1.402(7)
C(74)-C(75)	1.379(6)
C(74)-H(74)	0.9500
C(75)-H(75)	0.9500
C(76)-H(76A)	0.9800
C(76)-H(76B)	0.9800
C(76)-H(76C)	0.9800
C(77)-C(78)	1.385(6)
C(77)-C(82)	1.393(6)
C(78)-C(79)	1.389(7)
C(78)-H(78)	0.9500
C(79)-C(80)	1.402(7)
C(79)-C(83)	1.538(7)

C(80)-C(81)	1.360(7)
C(80)-H(80)	0.9500
C(81)-C(82)	1.401(6)
C(81)-C(87)	1.537(7)
C(82)-H(82)	0.9500
C(83)-C(86)	1.519(8)
C(83)-C(84)	1.531(8)
C(83)-C(85)	1.532(8)
C(84)-H(84A)	0.9800
C(84)-H(84B)	0.9800
C(84)-H(84C)	0.9800
C(85)-H(85A)	0.9800
C(85)-H(85B)	0.9800
C(85)-H(85C)	0.9800
C(86)-H(86A)	0.9800
C(86)-H(86B)	0.9800
C(86)-H(86C)	0.9800
C(87)-C(89)	1.529(8)
C(87)-C(90)	1.539(8)
C(87)-C(88)	1.554(7)
C(88)-H(88A)	0.9800
C(88)-H(88B)	0.9800
C(88)-H(88C)	0.9800
C(89)-H(89A)	0.9800
C(89)-H(89B)	0.9800
C(89)-H(89C)	0.9800
C(90)-H(90A)	0.9800
C(90)-H(90B)	0.9800
C(90)-H(90C)	0.9800
C(91)-C(92)	1.381(6)
C(91)-C(96)	1.396(6)
C(92)-C(93)	1.392(6)
C(92)-H(92)	0.9500
C(93)-C(94)	1.386(7)
C(93)-C(97)	1.530(7)
C(94)-C(95)	1.395(7)

C(94)-H(94)	0.9500
C(95)-C(96)	1.401(6)
C(95)-C(101)	1.525(7)
C(96)-H(96)	0.9500
C(97)-C(99)	1.468(10)
C(97)-C(98)	1.477(9)
C(97)-C(100)	1.616(10)
C(98)-H(98A)	0.9800
C(98)-H(98B)	0.9800
C(98)-H(98C)	0.9800
C(99)-H(99A)	0.9800
C(99)-H(99B)	0.9800
C(99)-H(99C)	0.9800
C(100)-H(10D)	0.9800
C(100)-H(10E)	0.9800
C(100)-H(10F)	0.9800
C(101)-C(104)	1.526(9)
C(101)-C(103)	1.534(8)
C(101)-C(102)	1.537(9)
C(102)-H(10G)	0.9800
C(102)-H(10H)	0.9800
C(102)-H(10I)	0.9800
C(103)-H(10J)	0.9800
C(103)-H(10K)	0.9800
C(103)-H(10L)	0.9800
C(104)-H(10M)	0.9800
C(104)-H(10N)	0.9800
C(104)-H(10O)	0.9800
C(105)-C(110)	1.390(6)
C(105)-C(106)	1.399(6)
C(106)-C(107)	1.383(6)
C(106)-H(106)	0.9500
C(107)-C(108)	1.376(6)
C(107)-H(107)	0.9500
C(108)-C(109)	1.387(6)
C(108)-H(108)	0.9500

C(109)-C(110)	1.413(6)
C(109)-H(109)	0.9500
C(111)-C(116)	1.391(6)
C(111)-C(112)	1.395(6)
C(112)-C(113)	1.399(6)
C(112)-H(112)	0.9500
C(113)-C(114)	1.382(6)
C(113)-C(117)	1.551(6)
C(114)-C(115)	1.398(6)
C(114)-H(114)	0.9500
C(115)-C(116)	1.389(6)
C(115)-C(121)	1.534(6)
C(116)-H(116)	0.9500
C(117)-C(119)	1.521(7)
C(117)-C(118)	1.525(7)
C(117)-C(120)	1.543(7)
C(118)-H(11A)	0.9800
C(118)-H(11B)	0.9800
C(118)-H(11C)	0.9800
C(119)-H(11D)	0.9800
C(119)-H(11E)	0.9800
C(119)-H(11F)	0.9800
C(120)-H(12D)	0.9800
C(120)-H(12E)	0.9800
C(120)-H(12F)	0.9800
C(121)-C(123)	1.511(8)
C(121)-C(122)	1.528(7)
C(121)-C(124)	1.529(7)
C(122)-H(12G)	0.9800
C(122)-H(12H)	0.9800
C(122)-H(12I)	0.9800
C(123)-H(12J)	0.9800
C(123)-H(12K)	0.9800
C(123)-H(12L)	0.9800
C(124)-H(12M)	0.9800
C(124)-H(12N)	0.9800

C(124)-H(12O)	0.9800
C(125)-C(130)	1.383(6)
C(125)-C(126)	1.395(6)
C(126)-C(127)	1.392(6)
C(126)-H(126)	0.9500
C(127)-C(128)	1.378(7)
C(127)-C(131)	1.546(6)
C(128)-C(129)	1.401(7)
C(128)-H(128)	0.9500
C(129)-C(130)	1.392(6)
C(129)-C(135)	1.514(7)
C(130)-H(130)	0.9500
C(131)-C(133)	1.495(8)
C(131)-C(132)	1.517(8)
C(131)-C(134)	1.561(8)
C(132)-H(13D)	0.9800
C(132)-H(13E)	0.9800
C(132)-H(13F)	0.9800
C(133)-H(13G)	0.9800
C(133)-H(13H)	0.9800
C(133)-H(13I)	0.9800
C(134)-H(13J)	0.9800
C(134)-H(13K)	0.9800
C(134)-H(13L)	0.9800
C(135)-C(136)	1.494(12)
C(135)-C(137)	1.517(11)
C(135)-C(138)	1.585(11)
C(136)-H(13M)	0.9800
C(136)-H(13N)	0.9800
C(136)-H(13O)	0.9800
C(137)-H(13P)	0.9800
C(137)-H(13Q)	0.9800
C(137)-H(13R)	0.9800
C(138)-H(13S)	0.9800
C(138)-H(13T)	0.9800
C(138)-H(13U)	0.9800

C(139)-C(140)	1.384(7)
C(139)-C(144)	1.398(7)
C(140)-C(141)	1.397(6)
C(140)-H(140)	0.9500
C(141)-C(142)	1.373(9)
C(141)-H(141)	0.9500
C(142)-C(143)	1.373(9)
C(143)-C(144)	1.389(7)
C(143)-H(143)	0.9500
C(144)-H(144)	0.9500
C(145)-H(14D)	0.9800
C(145)-H(14E)	0.9800
C(145)-H(14F)	0.9800
Fe(3)-O(9)	1.980(17)
Fe(3)-O(7)	2.005(3)
Fe(3)-O(7)#1	2.079(3)
Fe(3)-Cl(3)	2.227(5)
Fe(3)-P(5)	2.5158(14)
Fe(3)-P(6)	2.5797(13)
P(5)-C(174)	1.826(4)
P(5)-C(146)	1.828(5)
P(5)-C(160)	1.835(4)
P(6)-C(180)	1.724(12)
P(6)-C(194)	1.828(5)
P(6)-C(179)	1.834(4)
P(6)-C(480)	1.929(11)
O(7)-C(208)	1.369(6)
O(7)-Fe(3)#1	2.079(3)
O(8)-C(211)	1.395(6)
O(8)-C(214)	1.421(8)
O(9)-C(215)	1.207(19)
C(215)-C(216)	1.39(2)
C(215)-C(220)	1.49(2)
C(216)-C(217)	1.44(2)
C(216)-H(216)	0.9500
C(217)-C(218)	1.26(2)

C(217)-H(217)	0.9500
C(218)-O(10)	1.19(2)
C(218)-C(219)	1.50(2)
C(219)-C(220)	1.55(2)
C(219)-H(219)	0.9500
C(220)-H(220)	0.9500
O(10)-C(221)	1.31(2)
C(221)-H(22D)	0.9800
C(221)-H(22E)	0.9800
C(221)-H(22F)	0.9800
C(146)-C(147)	1.380(7)
C(146)-C(151)	1.399(7)
C(147)-C(148)	1.394(7)
C(147)-H(147)	0.9500
C(148)-C(149)	1.386(8)
C(148)-C(152)	1.543(8)
C(149)-C(150)	1.396(8)
C(149)-H(149)	0.9500
C(150)-C(151)	1.383(7)
C(150)-C(156)	1.530(7)
C(151)-H(151)	0.9500
C(152)-C(154)	1.455(12)
C(152)-C(155)	1.467(12)
C(152)-C(153)	1.687(14)
C(153)-H(15A)	0.9800
C(153)-H(15B)	0.9800
C(153)-H(15C)	0.9800
C(154)-H(15D)	0.9800
C(154)-H(15E)	0.9800
C(154)-H(15F)	0.9800
C(155)-H(15G)	0.9800
C(155)-H(15H)	0.9800
C(155)-H(15I)	0.9800
C(156)-C(159)	1.434(14)
C(156)-C(157)	1.482(13)
C(156)-C(158)	1.704(19)

C(157)-H(15J)	0.9800
C(157)-H(15K)	0.9800
C(157)-H(15L)	0.9800
C(158)-H(15M)	0.9800
C(158)-H(15N)	0.9800
C(158)-H(15O)	0.9800
C(159)-H(15P)	0.9800
C(159)-H(15Q)	0.9800
C(159)-H(15R)	0.9800
C(160)-C(165)	1.388(6)
C(160)-C(161)	1.400(6)
C(161)-C(162)	1.390(6)
C(161)-H(161)	0.9500
C(162)-C(163)	1.385(7)
C(162)-C(166)	1.533(7)
C(163)-C(164)	1.408(7)
C(163)-H(163)	0.9500
C(164)-C(165)	1.378(6)
C(164)-C(170)	1.531(7)
C(165)-H(165)	0.9500
C(166)-C(169)	1.512(11)
C(166)-C(167)	1.537(10)
C(166)-C(168)	1.573(9)
C(167)-H(16A)	0.9800
C(167)-H(16B)	0.9800
C(167)-H(16C)	0.9800
C(168)-H(16D)	0.9800
C(168)-H(16E)	0.9800
C(168)-H(16F)	0.9800
C(169)-H(16G)	0.9800
C(169)-H(16H)	0.9800
C(169)-H(16I)	0.9800
C(170)-C(172)	1.528(7)
C(170)-C(171)	1.539(7)
C(170)-C(173)	1.555(7)
C(171)-H(17A)	0.9800

C(171)-H(17B)	0.9800
C(171)-H(17C)	0.9800
C(172)-H(17D)	0.9800
C(172)-H(17E)	0.9800
C(172)-H(17F)	0.9800
C(173)-H(17G)	0.9800
C(173)-H(17H)	0.9800
C(173)-H(17I)	0.9800
C(174)-C(175)	1.382(6)
C(174)-C(179)	1.419(6)
C(175)-C(176)	1.381(7)
C(175)-H(175)	0.9500
C(176)-C(177)	1.372(7)
C(176)-H(176)	0.9500
C(177)-C(178)	1.371(7)
C(177)-H(177)	0.9500
C(178)-C(179)	1.386(6)
C(178)-H(178)	0.9500
C(180)-C(181)	1.381(12)
C(180)-C(185)	1.386(15)
C(181)-C(182)	1.389(13)
C(181)-H(181)	0.9500
C(182)-C(183)	1.388(16)
C(182)-C(186)	1.545(13)
C(183)-C(184)	1.398(15)
C(183)-H(183)	0.9500
C(184)-C(185)	1.412(12)
C(184)-C(190)	1.566(15)
C(185)-H(185)	0.9500
C(186)-C(189)	1.475(17)
C(186)-C(187)	1.491(17)
C(186)-C(188)	1.546(18)
C(187)-H(18A)	0.9800
C(187)-H(18B)	0.9800
C(187)-H(18C)	0.9800
C(188)-H(18D)	0.9800

C(188)-H(18E)	0.9800
C(188)-H(18F)	0.9800
C(189)-H(18G)	0.9800
C(189)-H(18H)	0.9800
C(189)-H(18I)	0.9800
C(190)-C(191)	1.464(17)
C(190)-C(192)	1.62(2)
C(190)-C(193)	1.633(18)
C(191)-H(19A)	0.9800
C(191)-H(19B)	0.9800
C(191)-H(19C)	0.9800
C(192)-H(19D)	0.9800
C(192)-H(19E)	0.9800
C(192)-H(19F)	0.9800
C(193)-H(19G)	0.9800
C(193)-H(19H)	0.9800
C(193)-H(19I)	0.9800
C(194)-C(195)	1.385(8)
C(194)-C(199)	1.404(8)
C(195)-C(196)	1.394(9)
C(195)-H(195)	0.9500
C(196)-C(197)	1.367(11)
C(196)-C(200)	1.536(10)
C(197)-C(198)	1.391(12)
C(197)-H(197)	0.9500
C(198)-C(199)	1.392(10)
C(198)-C(204)	1.753(16)
C(199)-H(199)	0.9500
C(200)-C(202)	1.488(14)
C(200)-C(203)	1.496(14)
C(200)-C(201)	1.701(15)
C(201)-H(20A)	0.9800
C(201)-H(20B)	0.9800
C(201)-H(20C)	0.9800
C(202)-H(20D)	0.9800
C(202)-H(20E)	0.9800

C(202)-H(20F)	0.9800
C(203)-H(20G)	0.9800
C(203)-H(20H)	0.9800
C(203)-H(20I)	0.9800
C(204)-C(207)	1.375(19)
C(204)-C(206)	1.44(4)
C(204)-C(205)	1.50(2)
C(205)-H(20J)	0.9800
C(205)-H(20K)	0.9800
C(205)-H(20L)	0.9800
C(206)-H(20M)	0.9800
C(206)-H(20N)	0.9800
C(206)-H(20O)	0.9800
C(207)-H(20P)	0.9800
C(207)-H(20Q)	0.9800
C(207)-H(20R)	0.9800
C(208)-C(209)	1.376(8)
C(208)-C(213)	1.388(8)
C(209)-C(210)	1.402(7)
C(209)-H(209)	0.9500
C(210)-C(211)	1.351(8)
C(210)-H(210)	0.9500
C(211)-C(212)	1.383(8)
C(212)-C(213)	1.399(7)
C(212)-H(212)	0.9500
C(213)-H(213)	0.9500
C(214)-H(21A)	0.9800
C(214)-H(21B)	0.9800
C(214)-H(21C)	0.9800
O(1)-Fe(1)-O(3)	116.1(4)
O(1)-Fe(1)-O(5)	120.1(3)
O(3)-Fe(1)-O(5)	72.64(11)
O(3)-Fe(1)-Cl(1)	119.80(15)
O(5)-Fe(1)-Cl(1)	109.28(15)
O(1)-Fe(1)-P(1)	99.9(4)

O(3)-Fe(1)-P(1)	143.25(11)
O(5)-Fe(1)-P(1)	96.50(9)
Cl(1)-Fe(1)-P(1)	96.95(11)
O(1)-Fe(1)-P(2)	85.3(3)
O(3)-Fe(1)-P(2)	97.36(9)
O(5)-Fe(1)-P(2)	154.58(11)
Cl(1)-Fe(1)-P(2)	96.01(11)
P(1)-Fe(1)-P(2)	77.39(4)
O(5)-Fe(2)-O(3)	72.78(11)
O(5)-Fe(2)-Cl(2)	112.34(11)
O(3)-Fe(2)-Cl(2)	113.53(11)
O(5)-Fe(2)-P(3)	150.70(11)
O(3)-Fe(2)-P(3)	96.84(9)
Cl(2)-Fe(2)-P(3)	96.96(4)
O(5)-Fe(2)-P(4)	96.70(9)
O(3)-Fe(2)-P(4)	149.47(11)
Cl(2)-Fe(2)-P(4)	97.00(4)
P(3)-Fe(2)-P(4)	78.28(4)
C(15)-P(1)-C(1)	101.34(18)
C(15)-P(1)-C(29)	104.66(18)
C(1)-P(1)-C(29)	101.15(18)
C(15)-P(1)-Fe(1)	120.85(13)
C(1)-P(1)-Fe(1)	123.38(13)
C(29)-P(1)-Fe(1)	102.40(13)
C(49)-P(2)-C(35)	104.48(19)
C(49)-P(2)-C(34)	102.47(18)
C(35)-P(2)-C(34)	101.35(18)
C(49)-P(2)-Fe(1)	122.42(13)
C(35)-P(2)-Fe(1)	120.99(14)
C(34)-P(2)-Fe(1)	101.17(13)
C(77)-P(3)-C(91)	105.5(2)
C(77)-P(3)-C(105)	100.71(19)
C(91)-P(3)-C(105)	101.42(19)
C(77)-P(3)-Fe(2)	119.93(15)
C(91)-P(3)-Fe(2)	121.47(15)
C(105)-P(3)-Fe(2)	103.97(14)

C(125)-P(4)-C(110)	100.50(19)
C(125)-P(4)-C(111)	103.90(19)
C(110)-P(4)-C(111)	100.99(18)
C(125)-P(4)-Fe(2)	122.27(14)
C(110)-P(4)-Fe(2)	102.54(13)
C(111)-P(4)-Fe(2)	122.14(14)
C(63)-O(1)-Fe(1)	153.6(9)
C(68)-C(63)-O(1)	120.9(9)
C(68)-C(63)-C(64)	118.2(8)
O(1)-C(63)-C(64)	120.7(9)
C(63)-C(64)-C(65)	119.9(8)
C(63)-C(64)-H(64)	120.1
C(65)-C(64)-H(64)	120.1
C(66)-C(65)-C(64)	121.1(8)
C(66)-C(65)-H(65)	119.5
C(64)-C(65)-H(65)	119.5
C(65)-C(66)-O(2)	125.7(9)
C(65)-C(66)-C(67)	119.4(8)
O(2)-C(66)-C(67)	114.7(9)
C(68)-C(67)-C(66)	120.0(8)
C(68)-C(67)-H(67)	120.0
C(66)-C(67)-H(67)	120.0
C(63)-C(68)-C(67)	121.2(8)
C(63)-C(68)-H(68)	119.4
C(67)-C(68)-H(68)	119.4
C(66)-O(2)-C(69)	115.5(11)
O(2)-C(69)-H(69A)	109.5
O(2)-C(69)-H(69B)	109.5
H(69A)-C(69)-H(69B)	109.5
O(2)-C(69)-H(69C)	109.5
H(69A)-C(69)-H(69C)	109.5
H(69B)-C(69)-H(69C)	109.5
C(70)-O(3)-Fe(1)	124.1(3)
C(70)-O(3)-Fe(2)	128.0(3)
Fe(1)-O(3)-Fe(2)	107.27(13)
C(73)-O(4)-C(76)	116.1(4)

C(139)-O(5)-Fe(2)	127.3(3)
C(139)-O(5)-Fe(1)	125.3(3)
Fe(2)-O(5)-Fe(1)	107.31(13)
C(142)-O(6)-C(145)	114.8(5)
C(6)-C(1)-C(2)	119.9(4)
C(6)-C(1)-P(1)	123.0(3)
C(2)-C(1)-P(1)	117.2(3)
C(3)-C(2)-C(1)	120.7(4)
C(3)-C(2)-H(2)	119.7
C(1)-C(2)-H(2)	119.7
C(2)-C(3)-C(4)	118.1(4)
C(2)-C(3)-C(7)	119.0(4)
C(4)-C(3)-C(7)	122.9(4)
C(5)-C(4)-C(3)	122.6(4)
C(5)-C(4)-H(4)	118.7
C(3)-C(4)-H(4)	118.7
C(4)-C(5)-C(6)	117.9(4)
C(4)-C(5)-C(11)	123.6(4)
C(6)-C(5)-C(11)	118.5(4)
C(1)-C(6)-C(5)	120.7(4)
C(1)-C(6)-H(6)	119.6
C(5)-C(6)-H(6)	119.6
C(10)-C(7)-C(8)	110.9(5)
C(10)-C(7)-C(3)	108.2(4)
C(8)-C(7)-C(3)	110.6(4)
C(10)-C(7)-C(9)	106.8(5)
C(8)-C(7)-C(9)	107.9(5)
C(3)-C(7)-C(9)	112.4(4)
C(7)-C(8)-H(8A)	109.5
C(7)-C(8)-H(8B)	109.5
H(8A)-C(8)-H(8B)	109.5
C(7)-C(8)-H(8C)	109.5
H(8A)-C(8)-H(8C)	109.5
H(8B)-C(8)-H(8C)	109.5
C(7)-C(9)-H(9A)	109.5
C(7)-C(9)-H(9B)	109.5

H(9A)-C(9)-H(9B)	109.5
C(7)-C(9)-H(9C)	109.5
H(9A)-C(9)-H(9C)	109.5
H(9B)-C(9)-H(9C)	109.5
C(7)-C(10)-H(10A)	109.5
C(7)-C(10)-H(10B)	109.5
H(10A)-C(10)-H(10B)	109.5
C(7)-C(10)-H(10C)	109.5
H(10A)-C(10)-H(10C)	109.5
H(10B)-C(10)-H(10C)	109.5
C(12)-C(11)-C(13)	108.7(5)
C(12)-C(11)-C(14)	108.6(4)
C(13)-C(11)-C(14)	108.8(5)
C(12)-C(11)-C(5)	110.0(4)
C(13)-C(11)-C(5)	108.9(4)
C(14)-C(11)-C(5)	111.9(4)
C(11)-C(12)-H(12A)	109.5
C(11)-C(12)-H(12B)	109.5
H(12A)-C(12)-H(12B)	109.5
C(11)-C(12)-H(12C)	109.5
H(12A)-C(12)-H(12C)	109.5
H(12B)-C(12)-H(12C)	109.5
C(11)-C(13)-H(13A)	109.5
C(11)-C(13)-H(13B)	109.5
H(13A)-C(13)-H(13B)	109.5
C(11)-C(13)-H(13C)	109.5
H(13A)-C(13)-H(13C)	109.5
H(13B)-C(13)-H(13C)	109.5
C(11)-C(14)-H(14A)	109.5
C(11)-C(14)-H(14B)	109.5
H(14A)-C(14)-H(14B)	109.5
C(11)-C(14)-H(14C)	109.5
H(14A)-C(14)-H(14C)	109.5
H(14B)-C(14)-H(14C)	109.5
C(16)-C(15)-C(20)	120.1(4)
C(16)-C(15)-P(1)	118.2(3)

C(20)-C(15)-P(1)	121.2(3)
C(15)-C(16)-C(17)	121.2(4)
C(15)-C(16)-H(16)	119.4
C(17)-C(16)-H(16)	119.4
C(18)-C(17)-C(16)	117.3(4)
C(18)-C(17)-C(21)	122.7(4)
C(16)-C(17)-C(21)	120.0(4)
C(19)-C(18)-C(17)	123.1(4)
C(19)-C(18)-H(18)	118.4
C(17)-C(18)-H(18)	118.4
C(18)-C(19)-C(20)	118.0(4)
C(18)-C(19)-C(25)	120.1(4)
C(20)-C(19)-C(25)	121.9(4)
C(19)-C(20)-C(15)	120.1(4)
C(19)-C(20)-H(20)	119.9
C(15)-C(20)-H(20)	119.9
C(22)-C(21)-C(23)	110.5(4)
C(22)-C(21)-C(17)	110.7(4)
C(23)-C(21)-C(17)	107.8(4)
C(22)-C(21)-C(24)	108.0(4)
C(23)-C(21)-C(24)	108.3(4)
C(17)-C(21)-C(24)	111.6(4)
C(21)-C(22)-H(22A)	109.5
C(21)-C(22)-H(22B)	109.5
H(22A)-C(22)-H(22B)	109.5
C(21)-C(22)-H(22C)	109.5
H(22A)-C(22)-H(22C)	109.5
H(22B)-C(22)-H(22C)	109.5
C(21)-C(23)-H(23A)	109.5
C(21)-C(23)-H(23B)	109.5
H(23A)-C(23)-H(23B)	109.5
C(21)-C(23)-H(23C)	109.5
H(23A)-C(23)-H(23C)	109.5
H(23B)-C(23)-H(23C)	109.5
C(21)-C(24)-H(24A)	109.5
C(21)-C(24)-H(24B)	109.5

H(24A)-C(24)-H(24B)	109.5
C(21)-C(24)-H(24C)	109.5
H(24A)-C(24)-H(24C)	109.5
H(24B)-C(24)-H(24C)	109.5
C(19)-C(25)-C(28)	112.3(4)
C(19)-C(25)-C(26)	109.2(4)
C(28)-C(25)-C(26)	108.7(5)
C(19)-C(25)-C(27)	108.4(4)
C(28)-C(25)-C(27)	109.6(5)
C(26)-C(25)-C(27)	108.6(4)
C(25)-C(26)-H(26A)	109.5
C(25)-C(26)-H(26B)	109.5
H(26A)-C(26)-H(26B)	109.5
C(25)-C(26)-H(26C)	109.5
H(26A)-C(26)-H(26C)	109.5
H(26B)-C(26)-H(26C)	109.5
C(25)-C(27)-H(27A)	109.5
C(25)-C(27)-H(27B)	109.5
H(27A)-C(27)-H(27B)	109.5
C(25)-C(27)-H(27C)	109.5
H(27A)-C(27)-H(27C)	109.5
H(27B)-C(27)-H(27C)	109.5
C(25)-C(28)-H(28A)	109.5
C(25)-C(28)-H(28B)	109.5
H(28A)-C(28)-H(28B)	109.5
C(25)-C(28)-H(28C)	109.5
H(28A)-C(28)-H(28C)	109.5
H(28B)-C(28)-H(28C)	109.5
C(34)-C(29)-C(30)	119.2(4)
C(34)-C(29)-P(1)	119.9(3)
C(30)-C(29)-P(1)	120.8(3)
C(31)-C(30)-C(29)	120.3(4)
C(31)-C(30)-H(30)	119.9
C(29)-C(30)-H(30)	119.9
C(30)-C(31)-C(32)	120.5(4)
C(30)-C(31)-H(31)	119.8

C(32)-C(31)-H(31)	119.8
C(31)-C(32)-C(33)	119.6(4)
C(31)-C(32)-H(32)	120.2
C(33)-C(32)-H(32)	120.2
C(32)-C(33)-C(34)	120.8(4)
C(32)-C(33)-H(33)	119.6
C(34)-C(33)-H(33)	119.6
C(29)-C(34)-C(33)	119.5(4)
C(29)-C(34)-P(2)	118.3(3)
C(33)-C(34)-P(2)	122.2(3)
C(36)-C(35)-C(40)	120.4(4)
C(36)-C(35)-P(2)	117.8(3)
C(40)-C(35)-P(2)	121.7(3)
C(35)-C(36)-C(37)	119.9(4)
C(35)-C(36)-H(36)	120.1
C(37)-C(36)-H(36)	120.1
C(38)-C(37)-C(36)	117.5(4)
C(38)-C(37)-C(41)	120.7(4)
C(36)-C(37)-C(41)	121.8(4)
C(37)-C(38)-C(39)	123.8(4)
C(37)-C(38)-H(38)	118.1
C(39)-C(38)-H(38)	118.1
C(40)-C(39)-C(38)	117.0(4)
C(40)-C(39)-C(45)	122.0(4)
C(38)-C(39)-C(45)	121.0(4)
C(39)-C(40)-C(35)	121.3(4)
C(39)-C(40)-H(40)	119.4
C(35)-C(40)-H(40)	119.4
C(42)-C(41)-C(44)	111.9(5)
C(42)-C(41)-C(37)	112.9(4)
C(44)-C(41)-C(37)	109.2(5)
C(42)-C(41)-C(43)	106.3(5)
C(44)-C(41)-C(43)	108.9(5)
C(37)-C(41)-C(43)	107.4(5)
C(41)-C(42)-H(42A)	109.5
C(41)-C(42)-H(42B)	109.5

H(42A)-C(42)-H(42B)	109.5
C(41)-C(42)-H(42C)	109.5
H(42A)-C(42)-H(42C)	109.5
H(42B)-C(42)-H(42C)	109.5
C(41)-C(43)-H(43A)	109.5
C(41)-C(43)-H(43B)	109.5
H(43A)-C(43)-H(43B)	109.5
C(41)-C(43)-H(43C)	109.5
H(43A)-C(43)-H(43C)	109.5
H(43B)-C(43)-H(43C)	109.5
C(41)-C(44)-H(44A)	109.5
C(41)-C(44)-H(44B)	109.5
H(44A)-C(44)-H(44B)	109.5
C(41)-C(44)-H(44C)	109.5
H(44A)-C(44)-H(44C)	109.5
H(44B)-C(44)-H(44C)	109.5
C(48)-C(45)-C(39)	114.0(6)
C(346)-C(45)-C(39)	118.7(7)
C(48)-C(45)-C(46)	113.8(8)
C(39)-C(45)-C(46)	103.9(5)
C(346)-C(45)-C(347)	112.4(9)
C(39)-C(45)-C(347)	107.5(6)
C(48)-C(45)-C(47)	110.1(8)
C(39)-C(45)-C(47)	109.3(5)
C(46)-C(45)-C(47)	105.2(8)
C(346)-C(45)-C(348)	107.6(8)
C(39)-C(45)-C(348)	109.6(6)
C(347)-C(45)-C(348)	99.3(7)
C(45)-C(46)-H(46A)	109.5
C(45)-C(46)-H(46B)	109.5
H(46A)-C(46)-H(46B)	109.5
C(45)-C(46)-H(46C)	109.5
H(46A)-C(46)-H(46C)	109.5
H(46B)-C(46)-H(46C)	109.5
C(45)-C(47)-H(47A)	109.5
C(45)-C(47)-H(47B)	109.5

H(47A)-C(47)-H(47B)	109.5
C(45)-C(47)-H(47C)	109.5
H(47A)-C(47)-H(47C)	109.5
H(47B)-C(47)-H(47C)	109.5
C(45)-C(48)-H(48A)	109.5
C(45)-C(48)-H(48B)	109.5
H(48A)-C(48)-H(48B)	109.5
C(45)-C(48)-H(48C)	109.5
H(48A)-C(48)-H(48C)	109.5
H(48B)-C(48)-H(48C)	109.5
C(54)-C(49)-C(50)	119.9(4)
C(54)-C(49)-P(2)	122.2(3)
C(50)-C(49)-P(2)	117.8(3)
C(51)-C(50)-C(49)	120.9(4)
C(51)-C(50)-H(50)	119.5
C(49)-C(50)-H(50)	119.5
C(50)-C(51)-C(52)	117.6(4)
C(50)-C(51)-C(55)	119.6(4)
C(52)-C(51)-C(55)	122.8(4)
C(53)-C(52)-C(51)	122.3(4)
C(53)-C(52)-H(52)	118.8
C(51)-C(52)-H(52)	118.8
C(52)-C(53)-C(54)	118.2(4)
C(52)-C(53)-C(59)	122.4(4)
C(54)-C(53)-C(59)	119.3(4)
C(49)-C(54)-C(53)	121.0(4)
C(49)-C(54)-H(54)	119.5
C(53)-C(54)-H(54)	119.5
C(56)-C(55)-C(51)	108.5(4)
C(56)-C(55)-C(57)	108.7(4)
C(51)-C(55)-C(57)	112.7(5)
C(56)-C(55)-C(58)	108.5(5)
C(51)-C(55)-C(58)	109.7(4)
C(57)-C(55)-C(58)	108.6(5)
C(55)-C(56)-H(56A)	109.5
C(55)-C(56)-H(56B)	109.5

H(56A)-C(56)-H(56B)	109.5
C(55)-C(56)-H(56C)	109.5
H(56A)-C(56)-H(56C)	109.5
H(56B)-C(56)-H(56C)	109.5
C(55)-C(57)-H(57A)	109.5
C(55)-C(57)-H(57B)	109.5
H(57A)-C(57)-H(57B)	109.5
C(55)-C(57)-H(57C)	109.5
H(57A)-C(57)-H(57C)	109.5
H(57B)-C(57)-H(57C)	109.5
C(55)-C(58)-H(58A)	109.5
C(55)-C(58)-H(58B)	109.5
H(58A)-C(58)-H(58B)	109.5
C(55)-C(58)-H(58C)	109.5
H(58A)-C(58)-H(58C)	109.5
H(58B)-C(58)-H(58C)	109.5
C(62)-C(59)-C(61)	109.9(6)
C(62)-C(59)-C(60)	111.3(5)
C(61)-C(59)-C(60)	106.2(6)
C(62)-C(59)-C(53)	111.2(4)
C(61)-C(59)-C(53)	107.9(4)
C(60)-C(59)-C(53)	110.1(5)
C(59)-C(60)-H(60A)	109.5
C(59)-C(60)-H(60B)	109.5
H(60A)-C(60)-H(60B)	109.5
C(59)-C(60)-H(60C)	109.5
H(60A)-C(60)-H(60C)	109.5
H(60B)-C(60)-H(60C)	109.5
C(59)-C(61)-H(61A)	109.5
C(59)-C(61)-H(61B)	109.5
H(61A)-C(61)-H(61B)	109.5
C(59)-C(61)-H(61C)	109.5
H(61A)-C(61)-H(61C)	109.5
H(61B)-C(61)-H(61C)	109.5
C(59)-C(62)-H(62A)	109.5
C(59)-C(62)-H(62B)	109.5

H(62A)-C(62)-H(62B)	109.5
C(59)-C(62)-H(62C)	109.5
H(62A)-C(62)-H(62C)	109.5
H(62B)-C(62)-H(62C)	109.5
O(3)-C(70)-C(71)	120.9(4)
O(3)-C(70)-C(75)	121.4(4)
C(71)-C(70)-C(75)	117.8(4)
C(72)-C(71)-C(70)	122.4(4)
C(72)-C(71)-H(71)	118.8
C(70)-C(71)-H(71)	118.8
C(71)-C(72)-C(73)	119.7(4)
C(71)-C(72)-H(72)	120.2
C(73)-C(72)-H(72)	120.2
O(4)-C(73)-C(72)	124.9(4)
O(4)-C(73)-C(74)	116.2(4)
C(72)-C(73)-C(74)	118.9(4)
C(75)-C(74)-C(73)	120.4(4)
C(75)-C(74)-H(74)	119.8
C(73)-C(74)-H(74)	119.8
C(74)-C(75)-C(70)	120.9(4)
C(74)-C(75)-H(75)	119.6
C(70)-C(75)-H(75)	119.6
O(4)-C(76)-H(76A)	109.5
O(4)-C(76)-H(76B)	109.5
H(76A)-C(76)-H(76B)	109.5
O(4)-C(76)-H(76C)	109.5
H(76A)-C(76)-H(76C)	109.5
H(76B)-C(76)-H(76C)	109.5
C(78)-C(77)-C(82)	119.8(4)
C(78)-C(77)-P(3)	123.9(4)
C(82)-C(77)-P(3)	116.2(3)
C(77)-C(78)-C(79)	120.4(5)
C(77)-C(78)-H(78)	119.8
C(79)-C(78)-H(78)	119.8
C(78)-C(79)-C(80)	118.3(5)
C(78)-C(79)-C(83)	122.4(5)

C(80)-C(79)-C(83)	119.2(5)
C(81)-C(80)-C(79)	122.4(5)
C(81)-C(80)-H(80)	118.8
C(79)-C(80)-H(80)	118.8
C(80)-C(81)-C(82)	118.6(5)
C(80)-C(81)-C(87)	122.0(4)
C(82)-C(81)-C(87)	119.3(4)
C(77)-C(82)-C(81)	120.3(4)
C(77)-C(82)-H(82)	119.8
C(81)-C(82)-H(82)	119.8
C(86)-C(83)-C(84)	108.4(5)
C(86)-C(83)-C(85)	109.3(5)
C(84)-C(83)-C(85)	108.9(6)
C(86)-C(83)-C(79)	110.4(5)
C(84)-C(83)-C(79)	111.1(5)
C(85)-C(83)-C(79)	108.6(5)
C(83)-C(84)-H(84A)	109.5
C(83)-C(84)-H(84B)	109.5
H(84A)-C(84)-H(84B)	109.5
C(83)-C(84)-H(84C)	109.5
H(84A)-C(84)-H(84C)	109.5
H(84B)-C(84)-H(84C)	109.5
C(83)-C(85)-H(85A)	109.5
C(83)-C(85)-H(85B)	109.5
H(85A)-C(85)-H(85B)	109.5
C(83)-C(85)-H(85C)	109.5
H(85A)-C(85)-H(85C)	109.5
H(85B)-C(85)-H(85C)	109.5
C(83)-C(86)-H(86A)	109.5
C(83)-C(86)-H(86B)	109.5
H(86A)-C(86)-H(86B)	109.5
C(83)-C(86)-H(86C)	109.5
H(86A)-C(86)-H(86C)	109.5
H(86B)-C(86)-H(86C)	109.5
C(89)-C(87)-C(81)	108.1(5)
C(89)-C(87)-C(90)	110.9(5)

C(81)-C(87)-C(90)	111.0(4)
C(89)-C(87)-C(88)	109.9(5)
C(81)-C(87)-C(88)	112.0(5)
C(90)-C(87)-C(88)	104.9(5)
C(87)-C(88)-H(88A)	109.5
C(87)-C(88)-H(88B)	109.5
H(88A)-C(88)-H(88B)	109.5
C(87)-C(88)-H(88C)	109.5
H(88A)-C(88)-H(88C)	109.5
H(88B)-C(88)-H(88C)	109.5
C(87)-C(89)-H(89A)	109.5
C(87)-C(89)-H(89B)	109.5
H(89A)-C(89)-H(89B)	109.5
C(87)-C(89)-H(89C)	109.5
H(89A)-C(89)-H(89C)	109.5
H(89B)-C(89)-H(89C)	109.5
C(87)-C(90)-H(90A)	109.5
C(87)-C(90)-H(90B)	109.5
H(90A)-C(90)-H(90B)	109.5
C(87)-C(90)-H(90C)	109.5
H(90A)-C(90)-H(90C)	109.5
H(90B)-C(90)-H(90C)	109.5
C(92)-C(91)-C(96)	120.3(4)
C(92)-C(91)-P(3)	118.9(3)
C(96)-C(91)-P(3)	120.8(3)
C(91)-C(92)-C(93)	120.8(4)
C(91)-C(92)-H(92)	119.6
C(93)-C(92)-H(92)	119.6
C(94)-C(93)-C(92)	117.9(5)
C(94)-C(93)-C(97)	120.7(5)
C(92)-C(93)-C(97)	121.4(5)
C(93)-C(94)-C(95)	123.2(5)
C(93)-C(94)-H(94)	118.4
C(95)-C(94)-H(94)	118.4
C(94)-C(95)-C(96)	117.4(5)
C(94)-C(95)-C(101)	120.0(5)

C(96)-C(95)-C(101)	122.6(5)
C(91)-C(96)-C(95)	120.3(4)
C(91)-C(96)-H(96)	119.8
C(95)-C(96)-H(96)	119.8
C(99)-C(97)-C(98)	116.4(7)
C(99)-C(97)-C(93)	108.8(5)
C(98)-C(97)-C(93)	108.7(5)
C(99)-C(97)-C(100)	106.9(6)
C(98)-C(97)-C(100)	105.6(6)
C(93)-C(97)-C(100)	110.2(5)
C(97)-C(98)-H(98A)	109.5
C(97)-C(98)-H(98B)	109.5
H(98A)-C(98)-H(98B)	109.5
C(97)-C(98)-H(98C)	109.5
H(98A)-C(98)-H(98C)	109.5
H(98B)-C(98)-H(98C)	109.5
C(97)-C(99)-H(99A)	109.5
C(97)-C(99)-H(99B)	109.5
H(99A)-C(99)-H(99B)	109.5
C(97)-C(99)-H(99C)	109.5
H(99A)-C(99)-H(99C)	109.5
H(99B)-C(99)-H(99C)	109.5
C(97)-C(100)-H(10D)	109.5
C(97)-C(100)-H(10E)	109.5
H(10D)-C(100)-H(10E)	109.5
C(97)-C(100)-H(10F)	109.5
H(10D)-C(100)-H(10F)	109.5
H(10E)-C(100)-H(10F)	109.5
C(95)-C(101)-C(104)	112.3(5)
C(95)-C(101)-C(103)	109.3(5)
C(104)-C(101)-C(103)	108.1(6)
C(95)-C(101)-C(102)	109.5(5)
C(104)-C(101)-C(102)	108.4(6)
C(103)-C(101)-C(102)	109.2(5)
C(101)-C(102)-H(10G)	109.5
C(101)-C(102)-H(10H)	109.5

H(10G)-C(102)-H(10H)	109.5
C(101)-C(102)-H(10I)	109.5
H(10G)-C(102)-H(10I)	109.5
H(10H)-C(102)-H(10I)	109.5
C(101)-C(103)-H(10J)	109.5
C(101)-C(103)-H(10K)	109.5
H(10J)-C(103)-H(10K)	109.5
C(101)-C(103)-H(10L)	109.5
H(10J)-C(103)-H(10L)	109.5
H(10K)-C(103)-H(10L)	109.5
C(101)-C(104)-H(10M)	109.5
C(101)-C(104)-H(10N)	109.5
H(10M)-C(104)-H(10N)	109.5
C(101)-C(104)-H(10O)	109.5
H(10M)-C(104)-H(10O)	109.5
H(10N)-C(104)-H(10O)	109.5
C(110)-C(105)-C(106)	119.8(4)
C(110)-C(105)-P(3)	119.6(3)
C(106)-C(105)-P(3)	120.6(3)
C(107)-C(106)-C(105)	120.1(4)
C(107)-C(106)-H(106)	120.0
C(105)-C(106)-H(106)	120.0
C(108)-C(107)-C(106)	120.7(4)
C(108)-C(107)-H(107)	119.7
C(106)-C(107)-H(107)	119.7
C(107)-C(108)-C(109)	120.1(4)
C(107)-C(108)-H(108)	119.9
C(109)-C(108)-H(108)	119.9
C(108)-C(109)-C(110)	119.9(4)
C(108)-C(109)-H(109)	120.1
C(110)-C(109)-H(109)	120.1
C(105)-C(110)-C(109)	119.4(4)
C(105)-C(110)-P(4)	120.7(3)
C(109)-C(110)-P(4)	119.7(3)
C(116)-C(111)-C(112)	119.7(4)
C(116)-C(111)-P(4)	120.7(3)

C(112)-C(111)-P(4)	119.6(3)
C(111)-C(112)-C(113)	120.2(4)
C(111)-C(112)-H(112)	119.9
C(113)-C(112)-H(112)	119.9
C(114)-C(113)-C(112)	118.7(4)
C(114)-C(113)-C(117)	121.8(4)
C(112)-C(113)-C(117)	119.5(4)
C(113)-C(114)-C(115)	122.4(4)
C(113)-C(114)-H(114)	118.8
C(115)-C(114)-H(114)	118.8
C(116)-C(115)-C(114)	117.8(4)
C(116)-C(115)-C(121)	122.6(4)
C(114)-C(115)-C(121)	119.6(4)
C(115)-C(116)-C(111)	121.2(4)
C(115)-C(116)-H(116)	119.4
C(111)-C(116)-H(116)	119.4
C(119)-C(117)-C(118)	108.5(4)
C(119)-C(117)-C(120)	107.9(4)
C(118)-C(117)-C(120)	110.0(4)
C(119)-C(117)-C(113)	112.7(4)
C(118)-C(117)-C(113)	109.4(4)
C(120)-C(117)-C(113)	108.2(4)
C(117)-C(118)-H(11A)	109.5
C(117)-C(118)-H(11B)	109.5
H(11A)-C(118)-H(11B)	109.5
C(117)-C(118)-H(11C)	109.5
H(11A)-C(118)-H(11C)	109.5
H(11B)-C(118)-H(11C)	109.5
C(117)-C(119)-H(11D)	109.5
C(117)-C(119)-H(11E)	109.5
H(11D)-C(119)-H(11E)	109.5
C(117)-C(119)-H(11F)	109.5
H(11D)-C(119)-H(11F)	109.5
H(11E)-C(119)-H(11F)	109.5
C(117)-C(120)-H(12D)	109.5
C(117)-C(120)-H(12E)	109.5

H(12D)-C(120)-H(12E)	109.5
C(117)-C(120)-H(12F)	109.5
H(12D)-C(120)-H(12F)	109.5
H(12E)-C(120)-H(12F)	109.5
C(123)-C(121)-C(122)	109.0(5)
C(123)-C(121)-C(124)	109.4(5)
C(122)-C(121)-C(124)	108.1(5)
C(123)-C(121)-C(115)	109.8(4)
C(122)-C(121)-C(115)	108.8(4)
C(124)-C(121)-C(115)	111.6(4)
C(121)-C(122)-H(12G)	109.5
C(121)-C(122)-H(12H)	109.5
H(12G)-C(122)-H(12H)	109.5
C(121)-C(122)-H(12I)	109.5
H(12G)-C(122)-H(12I)	109.5
H(12H)-C(122)-H(12I)	109.5
C(121)-C(123)-H(12J)	109.5
C(121)-C(123)-H(12K)	109.5
H(12J)-C(123)-H(12K)	109.5
C(121)-C(123)-H(12L)	109.5
H(12J)-C(123)-H(12L)	109.5
H(12K)-C(123)-H(12L)	109.5
C(121)-C(124)-H(12M)	109.5
C(121)-C(124)-H(12N)	109.5
H(12M)-C(124)-H(12N)	109.5
C(121)-C(124)-H(12O)	109.5
H(12M)-C(124)-H(12O)	109.5
H(12N)-C(124)-H(12O)	109.5
C(130)-C(125)-C(126)	119.8(4)
C(130)-C(125)-P(4)	123.8(3)
C(126)-C(125)-P(4)	116.4(3)
C(127)-C(126)-C(125)	120.7(4)
C(127)-C(126)-H(126)	119.6
C(125)-C(126)-H(126)	119.6
C(128)-C(127)-C(126)	117.9(4)
C(128)-C(127)-C(131)	121.9(4)

C(126)-C(127)-C(131)	120.2(4)
C(127)-C(128)-C(129)	123.1(4)
C(127)-C(128)-H(128)	118.4
C(129)-C(128)-H(128)	118.4
C(130)-C(129)-C(128)	117.3(4)
C(130)-C(129)-C(135)	121.7(5)
C(128)-C(129)-C(135)	121.0(4)
C(125)-C(130)-C(129)	121.2(4)
C(125)-C(130)-H(130)	119.4
C(129)-C(130)-H(130)	119.4
C(133)-C(131)-C(132)	112.5(6)
C(133)-C(131)-C(127)	110.0(4)
C(132)-C(131)-C(127)	107.1(4)
C(133)-C(131)-C(134)	108.1(5)
C(132)-C(131)-C(134)	107.4(5)
C(127)-C(131)-C(134)	111.7(4)
C(131)-C(132)-H(13D)	109.5
C(131)-C(132)-H(13E)	109.5
H(13D)-C(132)-H(13E)	109.5
C(131)-C(132)-H(13F)	109.5
H(13D)-C(132)-H(13F)	109.5
H(13E)-C(132)-H(13F)	109.5
C(131)-C(133)-H(13G)	109.5
C(131)-C(133)-H(13H)	109.5
H(13G)-C(133)-H(13H)	109.5
C(131)-C(133)-H(13I)	109.5
H(13G)-C(133)-H(13I)	109.5
H(13H)-C(133)-H(13I)	109.5
C(131)-C(134)-H(13J)	109.5
C(131)-C(134)-H(13K)	109.5
H(13J)-C(134)-H(13K)	109.5
C(131)-C(134)-H(13L)	109.5
H(13J)-C(134)-H(13L)	109.5
H(13K)-C(134)-H(13L)	109.5
C(438)-C(135)-C(129)	115.9(9)
C(136)-C(135)-C(129)	108.9(6)

C(136)-C(135)-C(137)	109.7(8)
C(129)-C(135)-C(137)	113.8(6)
C(438)-C(135)-C(437)	112.8(12)
C(129)-C(135)-C(437)	108.1(9)
C(136)-C(135)-C(138)	106.7(8)
C(129)-C(135)-C(138)	110.9(5)
C(137)-C(135)-C(138)	106.7(7)
C(438)-C(135)-C(436)	105.0(11)
C(129)-C(135)-C(436)	107.9(9)
C(437)-C(135)-C(436)	106.6(10)
C(135)-C(136)-H(13M)	109.5
C(135)-C(136)-H(13N)	109.5
H(13M)-C(136)-H(13N)	109.5
C(135)-C(136)-H(13O)	109.5
H(13M)-C(136)-H(13O)	109.5
H(13N)-C(136)-H(13O)	109.5
C(135)-C(137)-H(13P)	109.5
C(135)-C(137)-H(13Q)	109.5
H(13P)-C(137)-H(13Q)	109.5
C(135)-C(137)-H(13R)	109.5
H(13P)-C(137)-H(13R)	109.5
H(13Q)-C(137)-H(13R)	109.5
C(135)-C(138)-H(13S)	109.5
C(135)-C(138)-H(13T)	109.5
H(13S)-C(138)-H(13T)	109.5
C(135)-C(138)-H(13U)	109.5
H(13S)-C(138)-H(13U)	109.5
H(13T)-C(138)-H(13U)	109.5
O(5)-C(139)-C(140)	120.6(5)
O(5)-C(139)-C(144)	120.8(5)
C(140)-C(139)-C(144)	118.5(4)
C(139)-C(140)-C(141)	121.0(5)
C(139)-C(140)-H(140)	119.5
C(141)-C(140)-H(140)	119.5
C(142)-C(141)-C(140)	119.8(6)
C(142)-C(141)-H(141)	120.1

C(140)-C(141)-H(141)	120.1
C(143)-C(142)-C(141)	119.7(5)
C(143)-C(142)-O(6)	115.8(6)
C(141)-C(142)-O(6)	124.5(6)
C(142)-C(143)-C(144)	121.1(6)
C(142)-C(143)-H(143)	119.4
C(144)-C(143)-H(143)	119.4
C(143)-C(144)-C(139)	119.8(5)
C(143)-C(144)-H(144)	120.1
C(139)-C(144)-H(144)	120.1
O(6)-C(145)-H(14D)	109.5
O(6)-C(145)-H(14E)	109.5
H(14D)-C(145)-H(14E)	109.5
O(6)-C(145)-H(14F)	109.5
H(14D)-C(145)-H(14F)	109.5
H(14E)-C(145)-H(14F)	109.5
O(9)-Fe(3)-O(7)	127.6(6)
O(9)-Fe(3)-O(7)#1	111.0(5)
O(7)-Fe(3)-O(7)#1	73.77(15)
O(7)-Fe(3)-Cl(3)	122.1(2)
O(7)#1-Fe(3)-Cl(3)	103.20(19)
O(9)-Fe(3)-P(5)	94.4(5)
O(7)-Fe(3)-P(5)	137.43(14)
O(7)#1-Fe(3)-P(5)	99.56(11)
Cl(3)-Fe(3)-P(5)	100.49(16)
O(9)-Fe(3)-P(6)	86.7(5)
O(7)-Fe(3)-P(6)	95.63(10)
O(7)#1-Fe(3)-P(6)	162.33(13)
Cl(3)-Fe(3)-P(6)	94.39(16)
P(5)-Fe(3)-P(6)	78.49(4)
C(174)-P(5)-C(146)	102.9(2)
C(174)-P(5)-C(160)	101.0(2)
C(146)-P(5)-C(160)	103.4(2)
C(174)-P(5)-Fe(3)	103.78(15)
C(146)-P(5)-Fe(3)	122.63(16)
C(160)-P(5)-Fe(3)	119.76(14)

C(180)-P(6)-C(194)	97.9(5)
C(180)-P(6)-C(179)	102.0(5)
C(194)-P(6)-C(179)	99.9(2)
C(180)-P(6)-Fe(3)	128.6(5)
C(194)-P(6)-Fe(3)	121.24(19)
C(179)-P(6)-Fe(3)	102.38(15)
C(208)-O(7)-Fe(3)	126.2(3)
C(208)-O(7)-Fe(3)#1	126.1(3)
Fe(3)-O(7)-Fe(3)#1	106.22(15)
C(211)-O(8)-C(214)	115.3(5)
C(215)-O(9)-Fe(3)	166.8(14)
O(9)-C(215)-C(216)	124.2(17)
O(9)-C(215)-C(220)	121.8(15)
C(216)-C(215)-C(220)	114.0(16)
C(215)-C(216)-C(217)	122.1(18)
C(215)-C(216)-H(216)	119.0
C(217)-C(216)-H(216)	119.0
C(218)-C(217)-C(216)	133(2)
C(218)-C(217)-H(217)	113.4
C(216)-C(217)-H(217)	113.4
O(10)-C(218)-C(217)	154(2)
O(10)-C(218)-C(219)	97.0(17)
C(217)-C(218)-C(219)	108.8(19)
C(218)-C(219)-C(220)	122.4(17)
C(218)-C(219)-H(219)	118.8
C(220)-C(219)-H(219)	118.8
C(215)-C(220)-C(219)	117.9(14)
C(215)-C(220)-H(220)	121.1
C(219)-C(220)-H(220)	121.1
C(218)-O(10)-C(221)	165(2)
O(10)-C(221)-H(22D)	109.5
O(10)-C(221)-H(22E)	109.5
H(22D)-C(221)-H(22E)	109.5
O(10)-C(221)-H(22F)	109.5
H(22D)-C(221)-H(22F)	109.5
H(22E)-C(221)-H(22F)	109.5

C(147)-C(146)-C(151)	119.2(5)
C(147)-C(146)-P(5)	122.0(4)
C(151)-C(146)-P(5)	118.7(4)
C(146)-C(147)-C(148)	121.3(5)
C(146)-C(147)-H(147)	119.3
C(148)-C(147)-H(147)	119.3
C(149)-C(148)-C(147)	118.0(5)
C(149)-C(148)-C(152)	121.8(5)
C(147)-C(148)-C(152)	120.2(5)
C(148)-C(149)-C(150)	122.2(5)
C(148)-C(149)-H(149)	118.9
C(150)-C(149)-H(149)	118.9
C(151)-C(150)-C(149)	118.2(5)
C(151)-C(150)-C(156)	123.1(6)
C(149)-C(150)-C(156)	118.7(5)
C(150)-C(151)-C(146)	121.0(5)
C(150)-C(151)-H(151)	119.5
C(146)-C(151)-H(151)	119.5
C(154)-C(152)-C(155)	112.3(9)
C(154)-C(152)-C(148)	115.5(7)
C(155)-C(152)-C(148)	111.6(7)
C(154)-C(152)-C(153)	105.1(9)
C(155)-C(152)-C(153)	104.2(8)
C(148)-C(152)-C(153)	107.0(6)
C(152)-C(153)-H(15A)	109.5
C(152)-C(153)-H(15B)	109.5
H(15A)-C(153)-H(15B)	109.5
C(152)-C(153)-H(15C)	109.5
H(15A)-C(153)-H(15C)	109.5
H(15B)-C(153)-H(15C)	109.5
C(152)-C(154)-H(15D)	109.5
C(152)-C(154)-H(15E)	109.5
H(15D)-C(154)-H(15E)	109.5
C(152)-C(154)-H(15F)	109.5
H(15D)-C(154)-H(15F)	109.5
H(15E)-C(154)-H(15F)	109.5

C(152)-C(155)-H(15G)	109.5
C(152)-C(155)-H(15H)	109.5
H(15G)-C(155)-H(15H)	109.5
C(152)-C(155)-H(15I)	109.5
H(15G)-C(155)-H(15I)	109.5
H(15H)-C(155)-H(15I)	109.5
C(159)-C(156)-C(157)	122.2(11)
C(458)-C(156)-C(150)	116.9(15)
C(159)-C(156)-C(150)	114.2(6)
C(157)-C(156)-C(150)	110.6(8)
C(458)-C(156)-C(457)	114.0(16)
C(150)-C(156)-C(457)	110.2(12)
C(458)-C(156)-C(459)	110.5(15)
C(150)-C(156)-C(459)	108.2(10)
C(457)-C(156)-C(459)	94.7(11)
C(159)-C(156)-C(158)	101.8(10)
C(157)-C(156)-C(158)	100.7(10)
C(150)-C(156)-C(158)	104.0(7)
C(156)-C(157)-H(15J)	109.5
C(156)-C(157)-H(15K)	109.5
H(15J)-C(157)-H(15K)	109.5
C(156)-C(157)-H(15L)	109.5
H(15J)-C(157)-H(15L)	109.5
H(15K)-C(157)-H(15L)	109.5
C(156)-C(158)-H(15M)	109.5
C(156)-C(158)-H(15N)	109.5
H(15M)-C(158)-H(15N)	109.5
C(156)-C(158)-H(15O)	109.5
H(15M)-C(158)-H(15O)	109.5
H(15N)-C(158)-H(15O)	109.5
C(156)-C(159)-H(15P)	109.5
C(156)-C(159)-H(15Q)	109.5
H(15P)-C(159)-H(15Q)	109.5
C(156)-C(159)-H(15R)	109.5
H(15P)-C(159)-H(15R)	109.5
H(15Q)-C(159)-H(15R)	109.5

C(165)-C(160)-C(161)	119.6(4)
C(165)-C(160)-P(5)	117.5(3)
C(161)-C(160)-P(5)	123.0(4)
C(162)-C(161)-C(160)	120.6(4)
C(162)-C(161)-H(161)	119.7
C(160)-C(161)-H(161)	119.7
C(163)-C(162)-C(161)	118.3(4)
C(163)-C(162)-C(166)	121.6(4)
C(161)-C(162)-C(166)	120.0(4)
C(162)-C(163)-C(164)	122.2(4)
C(162)-C(163)-H(163)	118.9
C(164)-C(163)-H(163)	118.9
C(165)-C(164)-C(163)	118.0(4)
C(165)-C(164)-C(170)	119.9(4)
C(163)-C(164)-C(170)	122.1(4)
C(164)-C(165)-C(160)	121.3(4)
C(164)-C(165)-H(165)	119.4
C(160)-C(165)-H(165)	119.4
C(467)-C(166)-C(162)	115.2(8)
C(169)-C(166)-C(162)	114.1(6)
C(467)-C(166)-C(469)	110.2(9)
C(162)-C(166)-C(469)	110.9(7)
C(169)-C(166)-C(167)	111.6(7)
C(162)-C(166)-C(167)	108.7(5)
C(169)-C(166)-C(168)	107.3(7)
C(162)-C(166)-C(168)	108.7(5)
C(167)-C(166)-C(168)	106.2(7)
C(467)-C(166)-C(468)	107.5(9)
C(162)-C(166)-C(468)	107.2(7)
C(469)-C(166)-C(468)	105.3(9)
C(166)-C(167)-H(16A)	109.5
C(166)-C(167)-H(16B)	109.5
H(16A)-C(167)-H(16B)	109.5
C(166)-C(167)-H(16C)	109.5
H(16A)-C(167)-H(16C)	109.5
H(16B)-C(167)-H(16C)	109.5

C(166)-C(168)-H(16D)	109.5
C(166)-C(168)-H(16E)	109.5
H(16D)-C(168)-H(16E)	109.5
C(166)-C(168)-H(16F)	109.5
H(16D)-C(168)-H(16F)	109.5
H(16E)-C(168)-H(16F)	109.5
C(166)-C(169)-H(16G)	109.5
C(166)-C(169)-H(16H)	109.5
H(16G)-C(169)-H(16H)	109.5
C(166)-C(169)-H(16I)	109.5
H(16G)-C(169)-H(16I)	109.5
H(16H)-C(169)-H(16I)	109.5
C(172)-C(170)-C(164)	113.2(4)
C(172)-C(170)-C(171)	108.2(5)
C(164)-C(170)-C(171)	109.6(4)
C(172)-C(170)-C(173)	107.6(5)
C(164)-C(170)-C(173)	108.8(4)
C(171)-C(170)-C(173)	109.4(5)
C(170)-C(171)-H(17A)	109.5
C(170)-C(171)-H(17B)	109.5
H(17A)-C(171)-H(17B)	109.5
C(170)-C(171)-H(17C)	109.5
H(17A)-C(171)-H(17C)	109.5
H(17B)-C(171)-H(17C)	109.5
C(170)-C(172)-H(17D)	109.5
C(170)-C(172)-H(17E)	109.5
H(17D)-C(172)-H(17E)	109.5
C(170)-C(172)-H(17F)	109.5
H(17D)-C(172)-H(17F)	109.5
H(17E)-C(172)-H(17F)	109.5
C(170)-C(173)-H(17G)	109.5
C(170)-C(173)-H(17H)	109.5
H(17G)-C(173)-H(17H)	109.5
C(170)-C(173)-H(17I)	109.5
H(17G)-C(173)-H(17I)	109.5
H(17H)-C(173)-H(17I)	109.5

C(175)-C(174)-C(179)	118.5(4)
C(175)-C(174)-P(5)	120.6(3)
C(179)-C(174)-P(5)	120.8(3)
C(176)-C(175)-C(174)	121.8(5)
C(176)-C(175)-H(175)	119.1
C(174)-C(175)-H(175)	119.1
C(177)-C(176)-C(175)	119.2(5)
C(177)-C(176)-H(176)	120.4
C(175)-C(176)-H(176)	120.4
C(178)-C(177)-C(176)	120.5(5)
C(178)-C(177)-H(177)	119.7
C(176)-C(177)-H(177)	119.7
C(177)-C(178)-C(179)	121.3(5)
C(177)-C(178)-H(178)	119.3
C(179)-C(178)-H(178)	119.3
C(178)-C(179)-C(174)	118.6(4)
C(178)-C(179)-P(6)	123.0(4)
C(174)-C(179)-P(6)	118.2(3)
C(181)-C(180)-C(185)	119.4(11)
C(181)-C(180)-P(6)	126.2(11)
C(185)-C(180)-P(6)	114.4(8)
C(180)-C(181)-C(182)	120.5(12)
C(180)-C(181)-H(181)	119.7
C(182)-C(181)-H(181)	119.7
C(183)-C(182)-C(181)	118.7(10)
C(183)-C(182)-C(186)	119.4(9)
C(181)-C(182)-C(186)	121.8(11)
C(182)-C(183)-C(184)	123.3(9)
C(182)-C(183)-H(183)	118.3
C(184)-C(183)-H(183)	118.3
C(183)-C(184)-C(185)	115.4(12)
C(183)-C(184)-C(190)	123.0(10)
C(185)-C(184)-C(190)	121.6(11)
C(180)-C(185)-C(184)	122.6(11)
C(180)-C(185)-H(185)	118.7
C(184)-C(185)-H(185)	118.7

C(189)-C(186)-C(187)	110.3(13)
C(189)-C(186)-C(182)	107.7(11)
C(187)-C(186)-C(182)	109.7(9)
C(189)-C(186)-C(188)	112.6(12)
C(187)-C(186)-C(188)	106.4(12)
C(182)-C(186)-C(188)	110.2(12)
C(186)-C(187)-H(18A)	109.5
C(186)-C(187)-H(18B)	109.5
H(18A)-C(187)-H(18B)	109.5
C(186)-C(187)-H(18C)	109.5
H(18A)-C(187)-H(18C)	109.5
H(18B)-C(187)-H(18C)	109.5
C(186)-C(188)-H(18D)	109.5
C(186)-C(188)-H(18E)	109.5
H(18D)-C(188)-H(18E)	109.5
C(186)-C(188)-H(18F)	109.5
H(18D)-C(188)-H(18F)	109.5
H(18E)-C(188)-H(18F)	109.5
C(186)-C(189)-H(18G)	109.5
C(186)-C(189)-H(18H)	109.5
H(18G)-C(189)-H(18H)	109.5
C(186)-C(189)-H(18I)	109.5
H(18G)-C(189)-H(18I)	109.5
H(18H)-C(189)-H(18I)	109.5
C(191)-C(190)-C(184)	115.0(13)
C(191)-C(190)-C(192)	111.6(13)
C(184)-C(190)-C(192)	110.6(10)
C(191)-C(190)-C(193)	106.2(12)
C(184)-C(190)-C(193)	112.6(10)
C(192)-C(190)-C(193)	99.8(12)
C(190)-C(191)-H(19A)	109.5
C(190)-C(191)-H(19B)	109.5
H(19A)-C(191)-H(19B)	109.5
C(190)-C(191)-H(19C)	109.5
H(19A)-C(191)-H(19C)	109.5
H(19B)-C(191)-H(19C)	109.5

C(190)-C(192)-H(19D)	109.5
C(190)-C(192)-H(19E)	109.5
H(19D)-C(192)-H(19E)	109.5
C(190)-C(192)-H(19F)	109.5
H(19D)-C(192)-H(19F)	109.5
H(19E)-C(192)-H(19F)	109.5
C(190)-C(193)-H(19G)	109.5
C(190)-C(193)-H(19H)	109.5
H(19G)-C(193)-H(19H)	109.5
C(190)-C(193)-H(19I)	109.5
H(19G)-C(193)-H(19I)	109.5
H(19H)-C(193)-H(19I)	109.5
C(195)-C(194)-C(199)	121.1(6)
C(195)-C(194)-P(6)	118.8(4)
C(199)-C(194)-P(6)	120.0(5)
C(194)-C(195)-C(196)	120.4(6)
C(194)-C(195)-H(195)	119.8
C(196)-C(195)-H(195)	119.8
C(197)-C(196)-C(195)	117.1(7)
C(197)-C(196)-C(200)	121.8(7)
C(195)-C(196)-C(200)	121.1(7)
C(196)-C(197)-C(198)	124.7(7)
C(196)-C(197)-H(197)	117.6
C(198)-C(197)-H(197)	117.6
C(197)-C(198)-C(199)	117.6(7)
C(197)-C(198)-C(204)	132.5(8)
C(199)-C(198)-C(204)	107.9(9)
C(198)-C(199)-C(194)	119.1(7)
C(198)-C(199)-H(199)	120.5
C(194)-C(199)-H(199)	120.5
C(202)-C(200)-C(203)	115.4(10)
C(202)-C(200)-C(196)	114.8(8)
C(203)-C(200)-C(196)	108.0(9)
C(202)-C(200)-C(201)	103.1(9)
C(203)-C(200)-C(201)	103.7(10)
C(196)-C(200)-C(201)	111.1(6)

C(200)-C(201)-H(20A)	109.5
C(200)-C(201)-H(20B)	109.5
H(20A)-C(201)-H(20B)	109.5
C(200)-C(201)-H(20C)	109.5
H(20A)-C(201)-H(20C)	109.5
H(20B)-C(201)-H(20C)	109.5
C(200)-C(202)-H(20D)	109.5
C(200)-C(202)-H(20E)	109.5
H(20D)-C(202)-H(20E)	109.5
C(200)-C(202)-H(20F)	109.5
H(20D)-C(202)-H(20F)	109.5
H(20E)-C(202)-H(20F)	109.5
C(200)-C(203)-H(20G)	109.5
C(200)-C(203)-H(20H)	109.5
H(20G)-C(203)-H(20H)	109.5
C(200)-C(203)-H(20I)	109.5
H(20G)-C(203)-H(20I)	109.5
H(20H)-C(203)-H(20I)	109.5
C(207)-C(204)-C(206)	103.7(19)
C(207)-C(204)-C(205)	119.5(15)
C(206)-C(204)-C(205)	110(2)
C(207)-C(204)-C(198)	103.7(11)
C(206)-C(204)-C(198)	99.2(18)
C(205)-C(204)-C(198)	117.8(12)
C(204)-C(205)-H(20J)	109.5
C(204)-C(205)-H(20K)	109.5
H(20J)-C(205)-H(20K)	109.5
C(204)-C(205)-H(20L)	109.5
H(20J)-C(205)-H(20L)	109.5
H(20K)-C(205)-H(20L)	109.5
C(204)-C(206)-H(20M)	109.5
C(204)-C(206)-H(20N)	109.5
H(20M)-C(206)-H(20N)	109.5
C(204)-C(206)-H(20O)	109.5
H(20M)-C(206)-H(20O)	109.5
H(20N)-C(206)-H(20O)	109.5

C(204)-C(207)-H(20P)	109.5
C(204)-C(207)-H(20Q)	109.5
H(20P)-C(207)-H(20Q)	109.5
C(204)-C(207)-H(20R)	109.5
H(20P)-C(207)-H(20R)	109.5
H(20Q)-C(207)-H(20R)	109.5
O(7)-C(208)-C(209)	120.1(5)
O(7)-C(208)-C(213)	120.2(5)
C(209)-C(208)-C(213)	119.7(5)
C(208)-C(209)-C(210)	120.0(6)
C(208)-C(209)-H(209)	120.0
C(210)-C(209)-H(209)	120.0
C(211)-C(210)-C(209)	120.4(6)
C(211)-C(210)-H(210)	119.8
C(209)-C(210)-H(210)	119.8
C(210)-C(211)-C(212)	120.3(5)
C(210)-C(211)-O(8)	124.3(6)
C(212)-C(211)-O(8)	115.3(6)
C(211)-C(212)-C(213)	120.0(6)
C(211)-C(212)-H(212)	120.0
C(213)-C(212)-H(212)	120.0
C(208)-C(213)-C(212)	119.5(6)
C(208)-C(213)-H(213)	120.2
C(212)-C(213)-H(213)	120.2
O(8)-C(214)-H(21A)	109.5
O(8)-C(214)-H(21B)	109.5
H(21A)-C(214)-H(21B)	109.5
O(8)-C(214)-H(21C)	109.5
H(21A)-C(214)-H(21C)	109.5
H(21B)-C(214)-H(21C)	109.5

---

Symmetry transformations used to generate equivalent atoms:

#1 -x+1,-y+1,-z+1

Table 4. Anisotropic displacement parameters ( $\text{\AA}^2 \times 10^3$ ) for twin5\_sq. The anisotropic displacement factor exponent takes the form:  $-2p^2 [ h^2 a^*2U^{11} + \dots + 2 h k a^* b^* U^{12} ]$

	U <sup>11</sup>	U <sup>22</sup>	U <sup>33</sup>	U <sup>23</sup>	U <sup>13</sup>	U <sup>12</sup>
Fe(1)	43(1)	47(1)	53(1)	6(1)	5(1)	24(1)
Fe(2)	50(1)	51(1)	54(1)	8(1)	8(1)	28(1)
P(1)	45(1)	44(1)	51(1)	3(1)	4(1)	25(1)
P(2)	42(1)	45(1)	53(1)	3(1)	3(1)	23(1)
P(3)	51(1)	49(1)	55(1)	3(1)	5(1)	26(1)
P(4)	46(1)	49(1)	52(1)	5(1)	3(1)	24(1)
Cl(1)	58(2)	54(2)	76(2)	4(1)	6(2)	29(2)
O(1)	50(5)	69(5)	73(4)	-15(3)	-11(4)	22(4)
C(63)	38(3)	33(3)	53(3)	-9(3)	-5(3)	18(3)
C(64)	41(3)	54(4)	62(4)	9(3)	4(3)	18(3)
C(65)	45(4)	58(5)	78(4)	20(4)	0(3)	10(4)
C(66)	48(4)	62(5)	69(4)	11(4)	-14(3)	11(4)
C(67)	59(4)	52(4)	57(4)	1(3)	1(3)	28(3)
C(68)	43(4)	43(4)	60(4)	3(3)	7(3)	20(3)
O(3)	77(2)	79(2)	54(2)	10(1)	10(1)	57(2)
O(4)	69(2)	73(2)	82(2)	-5(2)	0(2)	49(2)
Cl(2)	57(1)	57(1)	83(1)	4(1)	6(1)	26(1)
O(5)	73(2)	82(2)	58(2)	18(1)	16(1)	56(2)
O(6)	124(3)	135(4)	113(3)	53(3)	52(3)	106(3)
C(1)	46(2)	48(2)	54(2)	7(2)	6(2)	25(2)
C(2)	52(2)	43(2)	56(2)	5(2)	7(2)	23(2)
C(3)	42(2)	57(2)	60(2)	5(2)	6(2)	24(2)
C(4)	51(2)	58(2)	66(2)	7(2)	5(2)	33(2)
C(5)	54(2)	52(2)	69(3)	7(2)	5(2)	30(2)
C(6)	48(2)	45(2)	64(2)	1(2)	2(2)	24(2)
C(7)	52(2)	61(3)	75(3)	-4(2)	-5(2)	25(2)
C(8)	53(3)	73(3)	108(4)	-2(3)	-6(3)	12(2)
C(9)	68(3)	92(4)	112(5)	-12(3)	-25(3)	40(3)
C(10)	64(3)	107(5)	85(3)	-20(3)	-11(3)	30(3)

C(11)	55(2)	50(2)	96(3)	-2(2)	0(2)	32(2)
C(12)	65(3)	46(3)	139(5)	3(3)	7(3)	27(2)
C(13)	100(4)	71(3)	100(4)	-12(3)	4(3)	54(3)
C(14)	72(3)	63(3)	133(5)	-3(3)	-11(3)	44(3)
C(15)	43(2)	45(2)	62(2)	3(2)	1(2)	25(2)
C(16)	45(2)	53(2)	60(2)	6(2)	3(2)	22(2)
C(17)	48(2)	54(2)	68(2)	0(2)	-1(2)	26(2)
C(18)	48(2)	48(2)	74(2)	-1(2)	1(2)	21(2)
C(19)	47(2)	51(2)	67(2)	4(2)	4(2)	22(2)
C(20)	48(2)	49(2)	62(2)	5(2)	6(2)	27(2)
C(21)	57(2)	60(3)	66(2)	-3(2)	2(2)	25(2)
C(22)	91(4)	73(3)	64(3)	-6(2)	-2(2)	41(3)
C(23)	65(3)	62(3)	73(3)	-8(2)	7(2)	27(2)
C(24)	67(3)	68(3)	74(3)	-14(2)	3(2)	27(2)
C(25)	60(3)	55(2)	77(3)	4(2)	14(2)	21(2)
C(26)	92(4)	62(3)	90(4)	17(3)	17(3)	36(3)
C(27)	59(3)	67(3)	100(4)	3(3)	19(2)	20(2)
C(28)	86(4)	69(3)	79(3)	7(2)	26(3)	16(3)
C(29)	43(2)	44(2)	51(2)	3(2)	4(2)	20(2)
C(30)	56(2)	54(2)	57(2)	8(2)	5(2)	31(2)
C(31)	62(3)	57(2)	54(2)	8(2)	4(2)	30(2)
C(32)	59(2)	55(2)	54(2)	5(2)	8(2)	25(2)
C(33)	48(2)	47(2)	57(2)	4(2)	6(2)	22(2)
C(34)	37(2)	38(2)	54(2)	4(1)	2(1)	12(2)
C(35)	46(2)	47(2)	61(2)	2(2)	1(2)	24(2)
C(36)	49(2)	55(2)	65(2)	6(2)	5(2)	24(2)
C(37)	53(2)	64(3)	72(3)	1(2)	1(2)	26(2)
C(38)	48(2)	62(3)	78(3)	4(2)	0(2)	21(2)
C(39)	45(2)	59(2)	71(2)	8(2)	4(2)	25(2)
C(40)	46(2)	56(2)	64(2)	3(2)	2(2)	28(2)
C(41)	64(3)	74(3)	71(3)	-5(2)	-4(2)	26(2)
C(42)	93(4)	71(3)	65(3)	-3(2)	-1(3)	22(3)
C(43)	79(4)	72(3)	95(4)	-9(3)	4(3)	26(3)
C(44)	102(4)	146(6)	81(4)	-25(4)	-27(3)	74(5)
C(45)	47(2)	66(3)	87(3)	12(2)	16(2)	28(2)
C(46)	78(6)	128(10)	120(8)	30(7)	37(5)	69(7)

C(47)	100(8)	69(5)	115(8)	14(4)	46(6)	27(5)
C(48)	77(6)	130(10)	81(5)	15(5)	27(4)	27(6)
C(49)	54(2)	47(2)	48(2)	7(2)	8(2)	28(2)
C(50)	55(2)	47(2)	57(2)	6(2)	7(2)	30(2)
C(51)	73(3)	53(2)	51(2)	9(2)	7(2)	35(2)
C(52)	83(3)	60(2)	50(2)	12(2)	14(2)	47(2)
C(53)	66(2)	67(3)	55(2)	13(2)	10(2)	46(2)
C(54)	55(2)	61(2)	56(2)	8(2)	7(2)	36(2)
C(55)	79(3)	47(2)	61(2)	4(2)	6(2)	27(2)
C(56)	85(4)	58(3)	84(3)	3(2)	8(3)	20(3)
C(57)	109(5)	63(3)	103(4)	-9(3)	14(3)	35(3)
C(58)	89(4)	61(3)	90(4)	4(3)	-17(3)	14(3)
C(59)	74(3)	81(3)	73(3)	11(2)	13(2)	56(3)
C(60)	106(5)	115(5)	212(8)	4(5)	21(5)	86(5)
C(61)	66(3)	160(6)	86(4)	24(4)	13(3)	61(4)
C(62)	103(4)	198(7)	86(4)	-12(4)	-13(3)	117(5)
C(70)	58(2)	63(2)	51(2)	11(2)	10(2)	38(2)
C(71)	53(2)	64(2)	61(2)	9(2)	4(2)	30(2)
C(72)	56(2)	55(2)	60(2)	5(2)	6(2)	27(2)
C(73)	60(2)	62(2)	60(2)	6(2)	10(2)	36(2)
C(74)	58(3)	65(3)	76(3)	0(2)	-3(2)	33(2)
C(75)	63(3)	62(3)	66(3)	-3(2)	-2(2)	37(2)
C(76)	93(4)	79(3)	90(4)	-9(3)	0(3)	59(3)
C(77)	54(2)	60(2)	59(2)	5(2)	9(2)	32(2)
C(78)	61(2)	62(3)	65(3)	1(2)	7(2)	35(2)
C(79)	70(3)	77(3)	74(3)	2(2)	11(2)	47(2)
C(80)	56(3)	80(3)	85(3)	1(2)	7(2)	40(2)
C(81)	52(2)	72(3)	71(3)	1(2)	7(2)	32(2)
C(82)	56(2)	62(3)	68(3)	1(2)	7(2)	30(2)
C(83)	80(3)	83(3)	96(4)	0(3)	9(3)	57(3)
C(84)	89(4)	83(4)	141(5)	-16(3)	7(3)	58(3)
C(85)	151(7)	112(5)	116(5)	16(4)	19(4)	98(5)
C(86)	80(3)	105(4)	112(4)	-6(3)	13(3)	68(3)
C(87)	50(2)	71(3)	93(3)	-7(2)	0(2)	25(2)
C(88)	67(3)	85(4)	98(4)	2(3)	-9(3)	28(3)
C(89)	74(3)	79(4)	102(4)	6(3)	-6(3)	26(3)

C(90)	66(3)	92(4)	108(4)	-28(3)	-4(3)	28(3)
C(91)	55(2)	51(2)	61(2)	-1(2)	6(2)	28(2)
C(92)	55(2)	57(2)	59(2)	1(2)	7(2)	26(2)
C(93)	51(2)	68(3)	69(3)	-8(2)	5(2)	25(2)
C(94)	62(3)	59(3)	79(3)	-8(2)	7(2)	22(2)
C(95)	68(3)	51(2)	80(3)	1(2)	8(2)	25(2)
C(96)	63(3)	52(2)	69(3)	-1(2)	2(2)	28(2)
C(97)	54(2)	78(3)	70(3)	-11(2)	4(2)	23(2)
C(98)	54(4)	68(5)	70(4)	-9(3)	2(3)	15(4)
C(99)	72(5)	87(6)	65(5)	-4(4)	-3(4)	39(5)
C(100)	72(5)	71(5)	80(6)	-14(4)	-5(4)	16(4)
C(101)	99(4)	56(3)	102(4)	12(2)	14(3)	39(3)
C(102)	107(4)	71(4)	138(6)	32(4)	30(4)	40(3)
C(103)	125(5)	69(4)	124(5)	2(3)	11(4)	56(4)
C(104)	128(5)	62(3)	104(4)	22(3)	12(3)	50(3)
C(105)	47(2)	46(2)	53(2)	3(2)	4(2)	20(2)
C(106)	58(2)	49(2)	53(2)	5(2)	2(2)	28(2)
C(107)	61(2)	55(2)	54(2)	7(2)	1(2)	26(2)
C(108)	61(2)	55(2)	52(2)	4(2)	6(2)	27(2)
C(109)	49(2)	57(2)	50(2)	4(2)	3(2)	26(2)
C(110)	44(2)	46(2)	50(2)	4(2)	-1(2)	20(2)
C(111)	47(2)	50(2)	54(2)	1(2)	3(2)	25(2)
C(112)	53(2)	55(2)	56(2)	5(2)	1(2)	28(2)
C(113)	56(2)	61(2)	60(2)	3(2)	-2(2)	32(2)
C(114)	47(2)	54(2)	61(2)	2(2)	-1(2)	23(2)
C(115)	50(2)	51(2)	61(2)	5(2)	1(2)	22(2)
C(116)	50(2)	54(2)	57(2)	6(2)	3(2)	26(2)
C(117)	61(3)	65(3)	65(2)	2(2)	-10(2)	30(2)
C(118)	81(3)	90(4)	64(3)	7(2)	-11(2)	42(3)
C(119)	67(3)	71(3)	90(4)	4(3)	-20(2)	30(2)
C(120)	76(3)	72(3)	81(3)	5(2)	-17(3)	39(3)
C(121)	60(3)	53(2)	68(3)	13(2)	-1(2)	14(2)
C(122)	80(4)	56(3)	92(4)	14(2)	-4(3)	21(2)
C(123)	72(3)	88(4)	83(4)	18(3)	14(3)	22(3)
C(124)	72(3)	73(3)	89(3)	33(3)	-7(3)	15(3)
C(125)	56(2)	50(2)	54(2)	8(2)	7(2)	26(2)

C(126)	55(2)	54(2)	55(2)	6(2)	5(2)	27(2)
C(127)	68(2)	51(2)	56(2)	8(2)	4(2)	27(2)
C(128)	68(3)	56(2)	70(3)	4(2)	7(2)	35(2)
C(129)	66(3)	63(3)	68(3)	4(2)	7(2)	37(2)
C(130)	52(2)	52(2)	69(3)	5(2)	7(2)	27(2)
C(131)	66(3)	50(2)	70(3)	1(2)	0(2)	25(2)
C(132)	91(5)	63(4)	81(4)	-2(3)	15(4)	4(4)
C(133)	73(4)	63(4)	96(5)	-14(3)	-18(3)	37(3)
C(134)	74(4)	62(4)	80(4)	-12(3)	-6(3)	36(3)
C(135)	65(3)	73(3)	104(4)	-2(3)	9(2)	41(3)
C(136)	83(7)	178(13)	140(7)	40(7)	11(6)	82(9)
C(137)	91(7)	97(8)	138(8)	-8(6)	21(5)	59(6)
C(138)	66(5)	80(5)	164(11)	5(5)	36(5)	44(4)
C(139)	69(3)	74(3)	62(2)	25(2)	21(2)	49(2)
C(140)	62(3)	74(3)	70(3)	27(2)	20(2)	41(2)
C(141)	73(3)	100(4)	86(3)	38(3)	29(2)	60(3)
C(142)	95(4)	97(4)	89(3)	45(3)	45(3)	71(3)
C(143)	103(4)	89(4)	80(3)	30(3)	38(3)	69(3)
C(144)	89(3)	77(3)	64(3)	21(2)	25(2)	55(3)
C(145)	113(5)	152(6)	144(6)	61(5)	46(4)	108(5)
Fe(3)	70(1)	47(1)	57(1)	7(1)	0(1)	22(1)
P(5)	57(1)	49(1)	56(1)	7(1)	6(1)	23(1)
P(6)	74(1)	47(1)	56(1)	7(1)	8(1)	25(1)
O(7)	105(3)	54(2)	53(2)	7(1)	0(2)	16(2)
O(8)	79(2)	49(2)	146(4)	-17(2)	-22(2)	24(2)
Cl(3)	51(2)	51(2)	80(2)	9(1)	7(1)	28(1)
O(9)	63(7)	57(7)	100(8)	9(5)	3(5)	23(4)
C(215)	72(7)	70(7)	105(8)	13(6)	-7(6)	28(6)
C(146)	57(2)	58(2)	66(3)	1(2)	8(2)	25(2)
C(147)	73(3)	73(3)	73(3)	14(2)	14(2)	42(3)
C(148)	70(3)	90(4)	89(3)	15(3)	14(2)	47(3)
C(149)	73(3)	81(3)	100(4)	10(3)	23(3)	42(3)
C(150)	70(3)	67(3)	92(3)	10(2)	28(2)	31(2)
C(151)	75(3)	61(3)	74(3)	7(2)	19(2)	33(2)
C(152)	103(4)	134(5)	106(4)	34(4)	22(3)	85(4)
C(153)	118(7)	111(6)	96(7)	34(5)	18(5)	78(5)

C(154)	116(8)	152(12)	142(10)	56(9)	31(7)	101(8)
C(155)	111(8)	118(9)	95(5)	25(5)	1(5)	70(7)
C(156)	85(4)	79(4)	128(5)	20(3)	51(3)	39(3)
C(157)	85(9)	82(7)	100(9)	23(6)	53(8)	46(7)
C(158)	65(5)	68(6)	117(8)	17(6)	44(5)	17(5)
C(159)	71(7)	79(7)	101(8)	32(6)	48(7)	31(6)
C(160)	55(2)	49(2)	53(2)	7(2)	2(2)	21(2)
C(161)	56(2)	55(2)	55(2)	11(2)	7(2)	24(2)
C(162)	61(2)	54(2)	55(2)	11(2)	4(2)	22(2)
C(163)	68(2)	53(2)	57(2)	8(2)	7(2)	27(2)
C(164)	60(2)	56(2)	60(2)	11(2)	5(2)	29(2)
C(165)	48(2)	51(2)	65(2)	10(2)	2(2)	21(2)
C(166)	58(3)	68(3)	65(3)	10(2)	5(2)	18(2)
C(167)	60(5)	82(6)	99(7)	21(5)	-5(4)	14(4)
C(168)	60(5)	82(6)	78(5)	18(4)	10(4)	13(4)
C(169)	64(5)	78(5)	112(7)	-13(5)	8(5)	6(4)
C(170)	66(3)	63(3)	85(3)	12(2)	15(2)	35(2)
C(171)	83(4)	90(4)	100(4)	19(3)	9(3)	55(3)
C(172)	89(4)	77(3)	119(5)	-3(3)	22(3)	47(3)
C(173)	76(3)	83(4)	98(4)	22(3)	27(3)	44(3)
C(174)	57(2)	49(2)	61(2)	9(2)	9(2)	27(2)
C(175)	64(3)	57(2)	60(2)	7(2)	4(2)	29(2)
C(176)	76(3)	69(3)	55(2)	6(2)	7(2)	35(2)
C(177)	73(3)	63(3)	60(2)	13(2)	12(2)	33(2)
C(178)	75(3)	59(3)	61(2)	11(2)	12(2)	33(2)
C(179)	61(2)	52(2)	58(2)	7(2)	7(2)	28(2)
C(180)	64(5)	50(4)	71(6)	8(4)	2(4)	19(4)
C(181)	58(5)	49(4)	90(7)	5(4)	1(5)	16(4)
C(182)	58(5)	49(4)	106(7)	6(4)	1(4)	12(4)
C(183)	58(5)	47(4)	106(8)	10(4)	4(5)	10(4)
C(184)	67(5)	63(5)	83(7)	15(4)	10(4)	20(4)
C(185)	71(5)	50(5)	68(6)	12(4)	2(4)	24(4)
C(186)	82(7)	43(5)	149(9)	-5(4)	-1(6)	12(4)
C(187)	113(9)	42(6)	185(12)	-21(6)	13(8)	21(6)
C(188)	107(8)	71(8)	186(13)	-35(8)	-31(8)	25(6)
C(189)	107(10)	52(6)	162(9)	4(6)	-6(7)	10(6)

C(190)	64(5)	89(7)	88(6)	13(5)	19(4)	24(5)
C(191)	86(8)	135(10)	186(15)	30(9)	48(8)	15(7)
C(192)	87(9)	143(10)	103(8)	20(7)	13(7)	53(8)
C(193)	80(7)	124(10)	86(6)	5(6)	18(5)	38(7)
C(194)	109(4)	69(3)	62(3)	4(2)	10(2)	53(3)
C(195)	97(4)	87(4)	64(3)	-8(2)	2(3)	47(3)
C(196)	114(4)	123(5)	76(3)	-26(3)	-9(3)	73(4)
C(197)	188(7)	138(6)	94(4)	-26(4)	-3(4)	120(6)
C(198)	223(8)	126(6)	96(4)	2(4)	11(5)	132(6)
C(199)	187(7)	88(4)	79(4)	20(3)	34(4)	94(5)
C(200)	107(5)	148(6)	100(4)	-31(4)	2(3)	76(4)
C(201)	97(8)	110(7)	86(7)	3(5)	29(6)	69(6)
C(202)	106(7)	101(8)	103(8)	-6(6)	6(5)	71(7)
C(203)	121(10)	105(8)	67(6)	-5(6)	18(5)	59(8)
C(208)	95(3)	43(2)	61(3)	5(2)	-11(2)	22(2)
C(209)	93(4)	56(3)	67(3)	4(2)	-10(2)	25(2)
C(210)	87(3)	55(3)	82(3)	-1(2)	-14(3)	31(2)
C(211)	79(3)	48(2)	94(4)	-2(2)	-22(3)	24(2)
C(212)	88(4)	55(3)	94(4)	4(2)	-15(3)	31(2)
C(213)	89(3)	52(2)	71(3)	8(2)	-6(2)	27(2)
C(214)	89(4)	60(3)	184(7)	-32(4)	-24(4)	34(3)

---

-

Table 5. Hydrogen coordinates ( $\times 10^4$ ) and isotropic displacement parameters ( $\text{\AA}^2 \times 10^{-3}$ ) for twin5\_sq.

	x	y	z	U(eq)
H(64)	1393	3300	1128	65
H(65)	56	2588	796	79
H(67)	1552	3788	129	66
H(68)	2860	4579	458	58
H(69A)	-1061	1623	350	183
H(69B)	-1341	2313	191	183
H(69C)	-875	2540	522	183
H(2)	2420	5875	743	60
H(4)	1443	7679	725	66
H(6)	3879	8314	1179	62
H(8A)	242	5199	813	128
H(8B)	-41	4685	495	128
H(8C)	898	4852	676	128
H(9A)	36	6441	584	137
H(9B)	607	6930	313	137
H(9C)	-204	5911	269	137
H(10A)	1691	6471	120	136
H(10B)	1792	5637	249	136
H(10C)	852	5470	68	136
H(12A)	3775	9785	776	125
H(12B)	3832	10404	1055	125
H(12C)	4229	9699	1087	125
H(13A)	2172	8675	1449	128
H(13B)	3263	9030	1494	128
H(13C)	2866	9736	1461	128
H(14A)	1456	8830	965	127
H(14B)	2168	9887	990	127
H(14C)	2096	9282	704	127

H(16)	4830	7701	1615	64
H(18)	6857	10155	1452	69
H(20)	5716	8196	801	61
H(22A)	6540	8704	2103	113
H(22B)	5934	8914	2321	113
H(22C)	5445	8083	2082	113
H(23A)	4841	9723	1781	102
H(23B)	4400	8709	1883	102
H(23C)	4888	9540	2123	102
H(24A)	6549	10693	1835	107
H(24B)	6574	10477	2174	107
H(24C)	7208	10293	1961	107
H(26A)	7327	11188	738	121
H(26B)	6265	10575	792	121
H(26C)	7014	11063	1065	121
H(27A)	8493	10669	893	118
H(27B)	8149	10547	1217	118
H(27C)	8164	9721	1041	118
H(28A)	7370	9953	456	127
H(28B)	7043	8984	589	127
H(28C)	6300	9318	495	127
H(30)	3977	7305	468	64
H(31)	4214	6929	1	69
H(32)	4797	5916	-62	67
H(33)	5223	5340	347	61
H(36)	6203	6422	1517	68
H(38)	8752	8099	1287	78
H(40)	6748	6588	661	64
H(42A)	6573	7297	1917	125
H(42B)	6984	6618	1988	125
H(42C)	7360	7548	2181	125
H(43A)	8544	9058	1649	129
H(43B)	7506	8762	1721	129
H(43C)	8294	8993	1983	129
H(44A)	9201	7984	1723	159
H(44B)	8991	7974	2061	159

H(44C)	8615	7044	1869	159
H(46A)	9538	7672	1003	148
H(46B)	9010	6793	784	148
H(46C)	9803	7704	671	148
H(47A)	9363	9006	942	147
H(47B)	9587	9051	605	147
H(47C)	8661	9055	691	147
H(48A)	8656	7730	270	155
H(48B)	7875	6810	382	155
H(48C)	7709	7675	361	155
H(34A)	9896	8370	628	123
H(34B)	9696	8688	935	123
H(34C)	9674	7727	898	123
H(34D)	7652	8074	450	114
H(34E)	8476	8944	624	114
H(34F)	8659	8522	335	114
H(34G)	7697	6651	381	112
H(34H)	8725	7204	285	112
H(34I)	8512	6499	537	112
H(50)	3891	3819	707	60
H(52)	5394	2551	534	70
H(54)	6643	5054	927	64
H(56A)	2391	1346	637	121
H(56B)	3268	1683	873	121
H(56C)	2831	2337	794	121
H(57A)	4182	1712	182	141
H(57B)	4057	1268	494	141
H(57C)	3181	979	260	141
H(58A)	3528	2780	68	134
H(58B)	2544	2020	151	134
H(58C)	2995	3008	310	134
H(60A)	6634	2653	467	196
H(60B)	7616	2934	642	196
H(60C)	6698	2495	811	196
H(61A)	7226	4149	294	151
H(61B)	7682	5026	515	151

H(61C)	8204	4437	472	151
H(62A)	7363	3863	1172	168
H(62B)	8285	4261	1005	168
H(62C)	7763	4850	1048	168
H(71)	3775	3357	1350	70
H(72)	4478	2449	1309	68
H(74)	6605	4201	1876	78
H(75)	5874	5087	1919	73
H(76A)	5049	1532	1490	121
H(76B)	6023	1588	1433	121
H(76C)	5544	1981	1202	121
H(78)	4552	2560	2279	72
H(80)	6983	3914	2774	85
H(82)	5299	5033	2657	73
H(84A)	4700	1348	2348	147
H(84B)	5247	1818	2071	147
H(84C)	5457	1094	2238	147
H(85A)	5532	1731	2854	167
H(85B)	6268	1461	2735	167
H(85C)	6609	2433	2896	167
H(86A)	7438	3175	2460	133
H(86B)	7107	2196	2306	133
H(86C)	6897	2920	2139	133
H(88A)	7294	4837	3273	131
H(88B)	7976	5050	3019	131
H(88C)	8081	5848	3241	131
H(89A)	7954	6706	2810	134
H(89B)	7808	5906	2582	134
H(89C)	7066	6272	2577	134
H(90A)	6151	5366	3264	140
H(90B)	6956	6371	3235	140
H(90C)	6056	5961	3006	140
H(92)	2495	2918	1805	69
H(94)	1244	260	1943	83
H(96)	3126	2032	2563	73
H(98A)	2219	1360	1307	104

H(98B)	1465	1498	1105	104
H(98C)	2214	2312	1320	104
H(99A)	173	1484	1710	112
H(99B)	908	2391	1577	112
H(99C)	160	1576	1362	112
H(10D)	977	-8	1458	123
H(10E)	173	21	1629	123
H(10F)	193	152	1282	123
H(39A)	1336	2729	1479	101
H(39B)	2124	2617	1325	101
H(39C)	1098	2180	1168	101
H(39D)	107	1394	1706	130
H(39E)	-130	979	1374	130
H(39F)	-62	387	1637	130
H(40A)	2092	1114	1324	111
H(40B)	1197	216	1397	111
H(40C)	1128	808	1134	111
H(10G)	927	-845	2640	157
H(10H)	824	58	2632	157
H(10I)	631	-553	2336	157
H(10J)	2234	-914	2411	153
H(10K)	1935	-621	2107	153
H(10L)	2968	-56	2256	153
H(10M)	2505	-25	2869	143
H(10N)	3265	846	2727	143
H(10O)	2433	894	2874	143
H(106)	3816	3257	2917	63
H(107)	3135	3310	3342	68
H(108)	2204	4006	3352	67
H(109)	1977	4701	2937	62
H(112)	999	4402	1859	64
H(114)	-1167	2045	2033	66
H(116)	1226	3006	2548	63
H(11A)	340	3964	1395	118
H(11B)	-254	2900	1320	118
H(11C)	-635	3571	1205	118

H(11D)	-2052	2494	1778	118
H(11E)	-2078	2684	1436	118
H(11F)	-1697	2014	1551	118
H(12D)	-236	4734	1752	114
H(12E)	-1199	4318	1554	114
H(12F)	-1179	4137	1896	114
H(12G)	-176	745	2225	121
H(12H)	-1025	169	2414	121
H(12I)	-1167	672	2135	121
H(12J)	-1193	2022	2740	130
H(12K)	-1780	1447	2447	130
H(12L)	-1638	944	2726	130
H(12M)	738	1616	2683	130
H(12N)	333	2101	2890	130
H(12O)	-126	1023	2864	130
H(126)	3556	6443	2616	65
H(128)	1915	7499	2832	75
H(130)	807	5065	2393	68
H(13D)	3841	8650	2517	135
H(13E)	4786	9035	2723	135
H(13F)	4436	8119	2525	135
H(13G)	3921	7325	3249	116
H(13H)	4483	7294	2981	116
H(13I)	4833	8210	3179	116
H(13J)	3067	8754	2946	107
H(13K)	3085	8229	3234	107
H(13L)	4001	9099	3156	107
H(43D)	3868	8647	2531	170
H(43E)	3447	8958	2788	170
H(43F)	4524	9239	2812	170
H(43G)	4695	7329	2948	115
H(43H)	4822	7825	2645	115
H(43I)	5267	8406	2949	115
H(43J)	3605	7399	3290	147
H(43K)	4356	8442	3300	147
H(43L)	3280	8161	3276	147

H(13M)	-551	6512	2316	187
H(13N)	528	7164	2302	187
H(13O)	66	6152	2161	187
H(13P)	291	6555	3048	154
H(13Q)	596	7406	2848	154
H(13R)	-471	6686	2847	154
H(13S)	-419	4975	2812	147
H(13T)	-1128	5196	2617	147
H(13U)	-506	4841	2461	147
H(43M)	798	7623	2538	119
H(43N)	419	7014	2237	119
H(43O)	-289	7074	2448	119
H(43P)	595	6880	3023	115
H(43Q)	-488	6418	2925	115
H(43R)	-22	5810	3033	115
H(43S)	-1088	5454	2456	136
H(43T)	-383	5405	2241	136
H(43U)	-572	4869	2536	136
H(140)	1918	5218	1329	77
H(141)	953	5893	1327	92
H(143)	2510	7530	2022	95
H(144)	3502	6891	2021	83
H(14D)	580	7036	1273	173
H(14E)	8	7263	1500	173
H(14F)	-59	6280	1482	173
H(216)	7174	4643	4718	146
H(217)	8275	4361	4532	180
H(219)	7810	4913	3732	159
H(220)	6617	5314	3895	125
H(22D)	8069	3079	3717	225
H(22E)	9154	3749	3766	225
H(22F)	8514	3986	3543	225
H(147)	3204	5803	3923	84
H(149)	721	4939	4240	98
H(151)	2501	4107	4586	83
H(15A)	3154	7133	3868	146

H(15B)	2461	7498	3746	146
H(15C)	2551	7339	4089	146
H(15D)	846	6257	4072	180
H(15E)	831	6551	3741	180
H(15F)	326	5504	3810	180
H(15G)	2349	5776	3512	152
H(15H)	1248	5209	3465	152
H(15I)	1753	6255	3396	152
H(45A)	986	4770	3512	193
H(45B)	291	4762	3742	193
H(45C)	490	5390	3468	193
H(45D)	923	6156	4105	190
H(45E)	1853	7067	4069	190
H(45F)	1019	6712	3817	190
H(45G)	2530	5973	3542	152
H(45H)	2075	6601	3447	152
H(45I)	2909	6956	3699	152
H(15J)	345	4818	4662	126
H(15K)	-180	4011	4872	126
H(15L)	860	4759	4965	126
H(15M)	-364	3584	4295	130
H(15N)	-20	2836	4275	130
H(15O)	-687	2794	4520	130
H(15P)	1155	2898	4652	124
H(15Q)	1401	3480	4957	124
H(15R)	360	2732	4863	124
H(45J)	1243	4942	4971	197
H(45K)	306	4785	4790	197
H(45L)	279	4117	5040	197
H(45M)	-445	2888	4666	256
H(45N)	-316	3481	4385	256
H(45O)	93	2783	4401	256
H(45P)	1810	3898	4984	193
H(45Q)	801	3126	5040	193
H(45R)	1350	2966	4789	193
H(161)	2240	3248	4044	68

H(163)	2940	1531	3639	71
H(165)	4933	3945	3984	66
H(16A)	1072	2656	3698	133
H(16B)	1180	2228	3397	133
H(16C)	272	1698	3566	133
H(16D)	1047	1924	4170	122
H(16E)	277	976	4020	122
H(16F)	1212	1057	4180	122
H(16G)	556	349	3570	144
H(16H)	1500	866	3418	144
H(16I)	1495	433	3728	144
H(46D)	125	1497	3782	131
H(46E)	850	2143	4042	131
H(46F)	885	2494	3717	131
H(46G)	1657	1106	3360	132
H(46H)	599	880	3364	132
H(46I)	1363	1879	3302	132
H(46J)	1583	501	3867	125
H(46K)	1192	836	4127	125
H(46L)	523	280	3844	125
H(17A)	5724	3149	4056	128
H(17B)	5133	2082	4081	128
H(17C)	5976	2474	3878	128
H(17D)	4939	1501	3460	137
H(17E)	4079	1117	3656	137
H(17F)	4020	1554	3352	137
H(17G)	5616	3842	3566	122
H(17H)	5866	3138	3406	122
H(17I)	4948	3193	3296	122
H(175)	3851	4773	3604	73
H(176)	4540	5767	3241	80
H(177)	5805	7165	3371	77
H(178)	6332	7595	3859	77
H(181)	6604	8744	4597	84
H(183)	9179	9522	4369	92
H(185)	7258	6903	4260	78

H(18A)	7508	10037	4937	180
H(18B)	7706	10977	4800	180
H(18C)	6920	10048	4644	180
H(18D)	9087	10396	4946	196
H(18E)	9629	10690	4656	196
H(18F)	9325	11354	4816	196
H(18G)	8722	10694	4179	178
H(18H)	7658	10446	4185	178
H(18I)	8444	11374	4341	178
H(19A)	10381	8467	4055	222
H(19B)	9871	9062	3982	222
H(19C)	10255	9047	4313	222
H(19D)	8616	6704	4415	166
H(19E)	9595	6981	4292	166
H(19F)	9533	7513	4577	166
H(19G)	8114	6780	3890	151
H(19H)	8635	7671	3713	151
H(19I)	9155	7107	3816	151
H(481)	6980	8731	4623	81
H(483)	9493	9184	4409	95
H(485)	7312	6725	4235	70
H(48D)	7941	9956	4974	147
H(48E)	8458	10973	4875	147
H(48F)	7581	10228	4677	147
H(48G)	10008	10177	4787	228
H(48H)	9844	10941	4947	228
H(48I)	9316	9920	5041	228
H(48J)	9444	10505	4280	240
H(48K)	8498	10563	4253	240
H(48L)	9375	11308	4452	240
H(49A)	9179	6382	4114	294
H(49B)	8819	6507	4419	294
H(49C)	8146	6232	4123	294
H(49D)	9333	8483	3827	406
H(49E)	9508	7669	3718	406
H(49F)	8476	7520	3728	406

H(49D)	10342	8768	4239	296
H(49E)	10234	8075	4488	296
H(49F)	10542	7937	4175	296
H(195)	4352	6718	4801	98
H(197)	3735	8675	4565	148
H(199)	5598	8300	4135	126
H(20A)	3647	6469	5181	133
H(20B)	2635	6272	5254	133
H(20C)	2783	5914	4946	133
H(20D)	2053	6736	4670	142
H(20E)	1853	6957	4991	142
H(20F)	2275	7744	4767	142
H(20G)	4258	8158	5262	143
H(20H)	3676	8648	5144	143
H(20I)	3254	7861	5368	143
H(50A)	2387	6740	4634	221
H(50B)	2518	6153	4888	221
H(50C)	1954	6697	4940	221
H(50D)	3337	8853	4978	285
H(50E)	2650	8282	4700	285
H(50F)	2302	8115	5023	285
H(50G)	4285	8311	5200	214
H(50H)	3352	7852	5361	214
H(50I)	3916	7308	5308	214
H(20J)	6145	10448	4428	214
H(20K)	6546	10057	4187	214
H(20L)	6267	10827	4106	214
H(20M)	4600	10160	4365	348
H(20N)	4590	10384	4026	348
H(20O)	3873	9413	4126	348
H(20P)	5359	9012	3779	128
H(20Q)	4304	8774	3802	128
H(20R)	5022	9745	3702	128
H(50J)	3635	9515	3838	164
H(50K)	3321	8457	3844	164
H(50L)	3167	8971	4116	164

H(50M)	5386	9853	3705	204
H(50N)	6018	9721	3963	204
H(50O)	5289	8871	3756	204
H(50P)	4853	10582	4194	193
H(50Q)	4544	9993	4476	193
H(50R)	5552	10309	4371	193
H(209)	5088	6858	5409	92
H(210)	6094	8364	5570	92
H(212)	8115	8272	5150	97
H(213)	7123	6762	4987	88
H(21A)	6923	9796	5494	171
H(21B)	7944	10481	5631	171
H(21C)	7311	9611	5803	171

---

Table 6. Torsion angles [°] for twin5\_sq.

---

Fe(1)-O(1)-C(63)-C(68)	105(2)
Fe(1)-O(1)-C(63)-C(64)	-80(2)
C(68)-C(63)-C(64)-C(65)	-1.3(12)
O(1)-C(63)-C(64)-C(65)	-176.8(10)
C(63)-C(64)-C(65)-C(66)	4.4(15)
C(64)-C(65)-C(66)-O(2)	-179.0(10)
C(64)-C(65)-C(66)-C(67)	-4.9(16)
C(65)-C(66)-C(67)-C(68)	2.5(15)
O(2)-C(66)-C(67)-C(68)	177.2(9)
O(1)-C(63)-C(68)-C(67)	174.4(9)
C(64)-C(63)-C(68)-C(67)	-1.1(11)
C(66)-C(67)-C(68)-C(63)	0.6(13)
C(65)-C(66)-O(2)-C(69)	9.1(18)
C(67)-C(66)-O(2)-C(69)	-165.3(11)
C(15)-P(1)-C(1)-C(6)	-13.6(4)
C(29)-P(1)-C(1)-C(6)	-121.2(4)
Fe(1)-P(1)-C(1)-C(6)	125.7(3)
C(15)-P(1)-C(1)-C(2)	165.3(3)
C(29)-P(1)-C(1)-C(2)	57.7(3)
Fe(1)-P(1)-C(1)-C(2)	-55.3(4)
C(6)-C(1)-C(2)-C(3)	3.2(6)
P(1)-C(1)-C(2)-C(3)	-175.7(3)
C(1)-C(2)-C(3)-C(4)	-2.4(6)
C(1)-C(2)-C(3)-C(7)	175.3(4)
C(2)-C(3)-C(4)-C(5)	0.6(7)
C(7)-C(3)-C(4)-C(5)	-177.0(4)
C(3)-C(4)-C(5)-C(6)	0.4(7)
C(3)-C(4)-C(5)-C(11)	179.0(4)
C(2)-C(1)-C(6)-C(5)	-2.2(6)
P(1)-C(1)-C(6)-C(5)	176.7(3)
C(4)-C(5)-C(6)-C(1)	0.4(7)
C(11)-C(5)-C(6)-C(1)	-178.2(4)
C(2)-C(3)-C(7)-C(10)	-62.7(6)
C(4)-C(3)-C(7)-C(10)	114.9(5)

C(2)-C(3)-C(7)-C(8)	58.9(6)
C(4)-C(3)-C(7)-C(8)	-123.5(5)
C(2)-C(3)-C(7)-C(9)	179.6(5)
C(4)-C(3)-C(7)-C(9)	-2.8(7)
C(4)-C(5)-C(11)-C(12)	-126.6(5)
C(6)-C(5)-C(11)-C(12)	52.0(6)
C(4)-C(5)-C(11)-C(13)	114.5(5)
C(6)-C(5)-C(11)-C(13)	-67.0(6)
C(4)-C(5)-C(11)-C(14)	-5.8(7)
C(6)-C(5)-C(11)-C(14)	172.8(5)
C(1)-P(1)-C(15)-C(16)	84.7(3)
C(29)-P(1)-C(15)-C(16)	-170.5(3)
Fe(1)-P(1)-C(15)-C(16)	-56.0(4)
C(1)-P(1)-C(15)-C(20)	-88.0(3)
C(29)-P(1)-C(15)-C(20)	16.9(4)
Fe(1)-P(1)-C(15)-C(20)	131.4(3)
C(20)-C(15)-C(16)-C(17)	4.3(6)
P(1)-C(15)-C(16)-C(17)	-168.4(3)
C(15)-C(16)-C(17)-C(18)	-3.5(6)
C(15)-C(16)-C(17)-C(21)	173.9(4)
C(16)-C(17)-C(18)-C(19)	1.0(7)
C(21)-C(17)-C(18)-C(19)	-176.4(4)
C(17)-C(18)-C(19)-C(20)	0.9(7)
C(17)-C(18)-C(19)-C(25)	179.9(4)
C(18)-C(19)-C(20)-C(15)	-0.2(6)
C(25)-C(19)-C(20)-C(15)	-179.2(4)
C(16)-C(15)-C(20)-C(19)	-2.3(6)
P(1)-C(15)-C(20)-C(19)	170.1(3)
C(18)-C(17)-C(21)-C(22)	-127.1(5)
C(16)-C(17)-C(21)-C(22)	55.7(6)
C(18)-C(17)-C(21)-C(23)	112.0(5)
C(16)-C(17)-C(21)-C(23)	-65.2(5)
C(18)-C(17)-C(21)-C(24)	-6.8(6)
C(16)-C(17)-C(21)-C(24)	176.0(4)
C(18)-C(19)-C(25)-C(28)	179.9(5)
C(20)-C(19)-C(25)-C(28)	-1.1(7)

C(18)-C(19)-C(25)-C(26)	-59.5(6)
C(20)-C(19)-C(25)-C(26)	119.5(5)
C(18)-C(19)-C(25)-C(27)	58.7(6)
C(20)-C(19)-C(25)-C(27)	-122.3(5)
C(15)-P(1)-C(29)-C(34)	98.6(3)
C(1)-P(1)-C(29)-C(34)	-156.4(3)
Fe(1)-P(1)-C(29)-C(34)	-28.3(3)
C(15)-P(1)-C(29)-C(30)	-83.8(4)
C(1)-P(1)-C(29)-C(30)	21.2(4)
Fe(1)-P(1)-C(29)-C(30)	149.3(3)
C(34)-C(29)-C(30)-C(31)	2.3(6)
P(1)-C(29)-C(30)-C(31)	-175.3(3)
C(29)-C(30)-C(31)-C(32)	-0.2(7)
C(30)-C(31)-C(32)-C(33)	-1.9(7)
C(31)-C(32)-C(33)-C(34)	1.9(6)
C(30)-C(29)-C(34)-C(33)	-2.3(6)
P(1)-C(29)-C(34)-C(33)	175.3(3)
C(30)-C(29)-C(34)-P(2)	176.9(3)
P(1)-C(29)-C(34)-P(2)	-5.4(4)
C(32)-C(33)-C(34)-C(29)	0.2(6)
C(32)-C(33)-C(34)-P(2)	-179.0(3)
C(49)-P(2)-C(34)-C(29)	162.7(3)
C(35)-P(2)-C(34)-C(29)	-89.5(3)
Fe(1)-P(2)-C(34)-C(29)	35.6(3)
C(49)-P(2)-C(34)-C(33)	-18.1(4)
C(35)-P(2)-C(34)-C(33)	89.7(3)
Fe(1)-P(2)-C(34)-C(33)	-145.2(3)
C(49)-P(2)-C(35)-C(36)	-116.4(3)
C(34)-P(2)-C(35)-C(36)	137.4(3)
Fe(1)-P(2)-C(35)-C(36)	26.8(4)
C(49)-P(2)-C(35)-C(40)	63.3(4)
C(34)-P(2)-C(35)-C(40)	-42.9(4)
Fe(1)-P(2)-C(35)-C(40)	-153.5(3)
C(40)-C(35)-C(36)-C(37)	-0.4(6)
P(2)-C(35)-C(36)-C(37)	179.3(3)
C(35)-C(36)-C(37)-C(38)	-2.2(7)

C(35)-C(36)-C(37)-C(41)	176.1(4)
C(36)-C(37)-C(38)-C(39)	2.1(8)
C(41)-C(37)-C(38)-C(39)	-176.3(5)
C(37)-C(38)-C(39)-C(40)	0.7(7)
C(37)-C(38)-C(39)-C(45)	-178.4(5)
C(38)-C(39)-C(40)-C(35)	-3.4(6)
C(45)-C(39)-C(40)-C(35)	175.6(4)
C(36)-C(35)-C(40)-C(39)	3.4(6)
P(2)-C(35)-C(40)-C(39)	-176.3(3)
C(38)-C(37)-C(41)-C(42)	-177.5(5)
C(36)-C(37)-C(41)-C(42)	4.2(7)
C(38)-C(37)-C(41)-C(44)	-52.3(7)
C(36)-C(37)-C(41)-C(44)	129.4(6)
C(38)-C(37)-C(41)-C(43)	65.6(6)
C(36)-C(37)-C(41)-C(43)	-112.7(5)
C(40)-C(39)-C(45)-C(48)	6.4(9)
C(38)-C(39)-C(45)-C(48)	-174.6(8)
C(40)-C(39)-C(45)-C(46)	-118.1(7)
C(38)-C(39)-C(45)-C(46)	60.9(8)
C(40)-C(39)-C(45)-C(47)	130.0(7)
C(38)-C(39)-C(45)-C(47)	-51.0(8)
C(35)-P(2)-C(49)-C(54)	8.8(4)
C(34)-P(2)-C(49)-C(54)	114.2(3)
Fe(1)-P(2)-C(49)-C(54)	-133.7(3)
C(35)-P(2)-C(49)-C(50)	-173.3(3)
C(34)-P(2)-C(49)-C(50)	-67.9(3)
Fe(1)-P(2)-C(49)-C(50)	44.2(4)
C(54)-C(49)-C(50)-C(51)	-0.5(6)
P(2)-C(49)-C(50)-C(51)	-178.5(3)
C(49)-C(50)-C(51)-C(52)	0.3(6)
C(49)-C(50)-C(51)-C(55)	179.2(4)
C(50)-C(51)-C(52)-C(53)	-0.4(6)
C(55)-C(51)-C(52)-C(53)	-179.2(4)
C(51)-C(52)-C(53)-C(54)	0.7(6)
C(51)-C(52)-C(53)-C(59)	-176.5(4)
C(50)-C(49)-C(54)-C(53)	0.9(6)

P(2)-C(49)-C(54)-C(53)	178.8(3)
C(52)-C(53)-C(54)-C(49)	-1.0(6)
C(59)-C(53)-C(54)-C(49)	176.3(4)
C(50)-C(51)-C(55)-C(56)	-62.5(5)
C(52)-C(51)-C(55)-C(56)	116.3(5)
C(50)-C(51)-C(55)-C(57)	177.0(4)
C(52)-C(51)-C(55)-C(57)	-4.2(6)
C(50)-C(51)-C(55)-C(58)	55.9(6)
C(52)-C(51)-C(55)-C(58)	-125.3(5)
C(52)-C(53)-C(59)-C(62)	-138.6(5)
C(54)-C(53)-C(59)-C(62)	44.2(7)
C(52)-C(53)-C(59)-C(61)	100.9(6)
C(54)-C(53)-C(59)-C(61)	-76.4(6)
C(52)-C(53)-C(59)-C(60)	-14.7(7)
C(54)-C(53)-C(59)-C(60)	168.1(5)
Fe(1)-O(3)-C(70)-C(71)	-53.7(5)
Fe(2)-O(3)-C(70)-C(71)	116.1(4)
Fe(1)-O(3)-C(70)-C(75)	125.5(4)
Fe(2)-O(3)-C(70)-C(75)	-64.6(6)
O(3)-C(70)-C(71)-C(72)	-179.9(4)
C(75)-C(70)-C(71)-C(72)	0.8(7)
C(70)-C(71)-C(72)-C(73)	-1.5(7)
C(76)-O(4)-C(73)-C(72)	-7.1(7)
C(76)-O(4)-C(73)-C(74)	172.2(5)
C(71)-C(72)-C(73)-O(4)	-179.1(4)
C(71)-C(72)-C(73)-C(74)	1.7(7)
O(4)-C(73)-C(74)-C(75)	179.6(4)
C(72)-C(73)-C(74)-C(75)	-1.1(7)
C(73)-C(74)-C(75)-C(70)	0.4(8)
O(3)-C(70)-C(75)-C(74)	-179.5(4)
C(71)-C(70)-C(75)-C(74)	-0.2(7)
C(91)-P(3)-C(77)-C(78)	16.2(4)
C(105)-P(3)-C(77)-C(78)	121.4(4)
Fe(2)-P(3)-C(77)-C(78)	-125.5(4)
C(91)-P(3)-C(77)-C(82)	-165.1(3)
C(105)-P(3)-C(77)-C(82)	-60.0(4)

Fe(2)-P(3)-C(77)-C(82)	53.1(4)
C(82)-C(77)-C(78)-C(79)	2.5(7)
P(3)-C(77)-C(78)-C(79)	-178.9(4)
C(77)-C(78)-C(79)-C(80)	-1.3(7)
C(77)-C(78)-C(79)-C(83)	178.9(5)
C(78)-C(79)-C(80)-C(81)	0.4(8)
C(83)-C(79)-C(80)-C(81)	-179.7(5)
C(79)-C(80)-C(81)-C(82)	-0.8(8)
C(79)-C(80)-C(81)-C(87)	-176.3(5)
C(78)-C(77)-C(82)-C(81)	-2.8(7)
P(3)-C(77)-C(82)-C(81)	178.4(4)
C(80)-C(81)-C(82)-C(77)	2.0(7)
C(87)-C(81)-C(82)-C(77)	177.6(4)
C(78)-C(79)-C(83)-C(86)	122.8(6)
C(80)-C(79)-C(83)-C(86)	-57.1(7)
C(78)-C(79)-C(83)-C(84)	2.5(8)
C(80)-C(79)-C(83)-C(84)	-177.3(5)
C(78)-C(79)-C(83)-C(85)	-117.3(6)
C(80)-C(79)-C(83)-C(85)	62.8(7)
C(80)-C(81)-C(87)-C(89)	96.0(6)
C(82)-C(81)-C(87)-C(89)	-79.5(6)
C(80)-C(81)-C(87)-C(90)	-142.0(6)
C(82)-C(81)-C(87)-C(90)	42.4(7)
C(80)-C(81)-C(87)-C(88)	-25.2(7)
C(82)-C(81)-C(87)-C(88)	159.3(5)
C(77)-P(3)-C(91)-C(92)	-134.2(4)
C(105)-P(3)-C(91)-C(92)	121.2(4)
Fe(2)-P(3)-C(91)-C(92)	6.8(4)
C(77)-P(3)-C(91)-C(96)	47.6(4)
C(105)-P(3)-C(91)-C(96)	-57.1(4)
Fe(2)-P(3)-C(91)-C(96)	-171.4(3)
C(96)-C(91)-C(92)-C(93)	-0.2(7)
P(3)-C(91)-C(92)-C(93)	-178.4(3)
C(91)-C(92)-C(93)-C(94)	-0.9(7)
C(91)-C(92)-C(93)-C(97)	178.9(4)
C(92)-C(93)-C(94)-C(95)	1.0(8)

C(97)-C(93)-C(94)-C(95)	-178.8(5)
C(93)-C(94)-C(95)-C(96)	0.0(8)
C(93)-C(94)-C(95)-C(101)	-178.3(5)
C(92)-C(91)-C(96)-C(95)	1.2(7)
P(3)-C(91)-C(96)-C(95)	179.4(4)
C(94)-C(95)-C(96)-C(91)	-1.1(7)
C(101)-C(95)-C(96)-C(91)	177.2(5)
C(94)-C(93)-C(97)-C(99)	112.9(7)
C(92)-C(93)-C(97)-C(99)	-66.9(7)
C(94)-C(93)-C(97)-C(98)	-119.4(6)
C(92)-C(93)-C(97)-C(98)	60.8(7)
C(94)-C(93)-C(97)-C(100)	-4.0(7)
C(92)-C(93)-C(97)-C(100)	176.1(5)
C(94)-C(95)-C(101)-C(104)	-178.6(5)
C(96)-C(95)-C(101)-C(104)	3.2(8)
C(94)-C(95)-C(101)-C(103)	61.4(7)
C(96)-C(95)-C(101)-C(103)	-116.8(6)
C(94)-C(95)-C(101)-C(102)	-58.3(7)
C(96)-C(95)-C(101)-C(102)	123.5(6)
C(77)-P(3)-C(105)-C(110)	150.9(3)
C(91)-P(3)-C(105)-C(110)	-100.7(4)
Fe(2)-P(3)-C(105)-C(110)	26.1(4)
C(77)-P(3)-C(105)-C(106)	-31.6(4)
C(91)-P(3)-C(105)-C(106)	76.8(4)
Fe(2)-P(3)-C(105)-C(106)	-156.4(3)
C(110)-C(105)-C(106)-C(107)	2.1(6)
P(3)-C(105)-C(106)-C(107)	-175.4(3)
C(105)-C(106)-C(107)-C(108)	-1.4(7)
C(106)-C(107)-C(108)-C(109)	-1.0(7)
C(107)-C(108)-C(109)-C(110)	2.6(7)
C(106)-C(105)-C(110)-C(109)	-0.5(6)
P(3)-C(105)-C(110)-C(109)	177.0(3)
C(106)-C(105)-C(110)-P(4)	-175.2(3)
P(3)-C(105)-C(110)-P(4)	2.3(5)
C(108)-C(109)-C(110)-C(105)	-1.9(6)
C(108)-C(109)-C(110)-P(4)	172.9(3)

C(125)-P(4)-C(110)-C(105)	-155.6(3)
C(111)-P(4)-C(110)-C(105)	97.9(4)
Fe(2)-P(4)-C(110)-C(105)	-28.9(4)
C(125)-P(4)-C(110)-C(109)	29.7(4)
C(111)-P(4)-C(110)-C(109)	-76.8(4)
Fe(2)-P(4)-C(110)-C(109)	156.4(3)
C(125)-P(4)-C(111)-C(116)	-105.3(4)
C(110)-P(4)-C(111)-C(116)	-1.5(4)
Fe(2)-P(4)-C(111)-C(116)	111.0(3)
C(125)-P(4)-C(111)-C(112)	71.8(4)
C(110)-P(4)-C(111)-C(112)	175.7(3)
Fe(2)-P(4)-C(111)-C(112)	-71.8(4)
C(116)-C(111)-C(112)-C(113)	2.7(6)
P(4)-C(111)-C(112)-C(113)	-174.5(3)
C(111)-C(112)-C(113)-C(114)	-1.7(7)
C(111)-C(112)-C(113)-C(117)	176.4(4)
C(112)-C(113)-C(114)-C(115)	-0.4(7)
C(117)-C(113)-C(114)-C(115)	-178.5(4)
C(113)-C(114)-C(115)-C(116)	1.5(7)
C(113)-C(114)-C(115)-C(121)	180.0(4)
C(114)-C(115)-C(116)-C(111)	-0.4(7)
C(121)-C(115)-C(116)-C(111)	-178.9(4)
C(112)-C(111)-C(116)-C(115)	-1.7(6)
P(4)-C(111)-C(116)-C(115)	175.5(3)
C(114)-C(113)-C(117)-C(119)	-3.0(7)
C(112)-C(113)-C(117)-C(119)	179.0(4)
C(114)-C(113)-C(117)-C(118)	-123.8(5)
C(112)-C(113)-C(117)-C(118)	58.1(6)
C(114)-C(113)-C(117)-C(120)	116.3(5)
C(112)-C(113)-C(117)-C(120)	-61.7(6)
C(116)-C(115)-C(121)-C(123)	122.4(5)
C(114)-C(115)-C(121)-C(123)	-56.0(6)
C(116)-C(115)-C(121)-C(122)	-118.4(5)
C(114)-C(115)-C(121)-C(122)	63.2(6)
C(116)-C(115)-C(121)-C(124)	0.9(7)
C(114)-C(115)-C(121)-C(124)	-177.5(5)

C(110)-P(4)-C(125)-C(130)	-108.9(4)
C(111)-P(4)-C(125)-C(130)	-4.7(4)
Fe(2)-P(4)-C(125)-C(130)	138.9(3)
C(110)-P(4)-C(125)-C(126)	68.6(3)
C(111)-P(4)-C(125)-C(126)	172.8(3)
Fe(2)-P(4)-C(125)-C(126)	-43.6(4)
C(130)-C(125)-C(126)-C(127)	0.1(6)
P(4)-C(125)-C(126)-C(127)	-177.5(3)
C(125)-C(126)-C(127)-C(128)	-0.6(6)
C(125)-C(126)-C(127)-C(131)	-178.8(4)
C(126)-C(127)-C(128)-C(129)	1.0(7)
C(131)-C(127)-C(128)-C(129)	179.2(4)
C(127)-C(128)-C(129)-C(130)	-0.9(7)
C(127)-C(128)-C(129)-C(135)	-178.7(5)
C(126)-C(125)-C(130)-C(129)	0.0(7)
P(4)-C(125)-C(130)-C(129)	177.4(4)
C(128)-C(129)-C(130)-C(125)	0.4(7)
C(135)-C(129)-C(130)-C(125)	178.2(5)
C(128)-C(127)-C(131)-C(133)	131.7(5)
C(126)-C(127)-C(131)-C(133)	-50.2(6)
C(128)-C(127)-C(131)-C(132)	-105.7(6)
C(126)-C(127)-C(131)-C(132)	72.4(6)
C(128)-C(127)-C(131)-C(134)	11.6(7)
C(126)-C(127)-C(131)-C(134)	-170.3(5)
C(130)-C(129)-C(135)-C(136)	-82.7(10)
C(128)-C(129)-C(135)-C(136)	95.1(10)
C(130)-C(129)-C(135)-C(137)	154.7(8)
C(128)-C(129)-C(135)-C(137)	-27.6(10)
C(130)-C(129)-C(135)-C(138)	34.4(9)
C(128)-C(129)-C(135)-C(138)	-147.8(8)
Fe(2)-O(5)-C(139)-C(140)	-130.7(4)
Fe(1)-O(5)-C(139)-C(140)	46.7(6)
Fe(2)-O(5)-C(139)-C(144)	49.6(6)
Fe(1)-O(5)-C(139)-C(144)	-133.0(4)
O(5)-C(139)-C(140)-C(141)	179.8(4)
C(144)-C(139)-C(140)-C(141)	-0.4(7)

C(139)-C(140)-C(141)-C(142)	0.1(7)
C(140)-C(141)-C(142)-C(143)	-0.5(8)
C(140)-C(141)-C(142)-O(6)	-179.9(5)
C(145)-O(6)-C(142)-C(143)	178.9(5)
C(145)-O(6)-C(142)-C(141)	-1.6(8)
C(141)-C(142)-C(143)-C(144)	1.3(8)
O(6)-C(142)-C(143)-C(144)	-179.2(5)
C(142)-C(143)-C(144)-C(139)	-1.7(8)
O(5)-C(139)-C(144)-C(143)	-179.1(4)
C(140)-C(139)-C(144)-C(143)	1.2(7)
Fe(3)-O(9)-C(215)-C(216)	-19(9)
Fe(3)-O(9)-C(215)-C(220)	160(7)
O(9)-C(215)-C(216)-C(217)	178(2)
C(220)-C(215)-C(216)-C(217)	-2(2)
C(215)-C(216)-C(217)-C(218)	-9(4)
C(216)-C(217)-C(218)-O(10)	-166(4)
C(216)-C(217)-C(218)-C(219)	15(3)
O(10)-C(218)-C(219)-C(220)	167.6(18)
C(217)-C(218)-C(219)-C(220)	-13(3)
O(9)-C(215)-C(220)-C(219)	-177.5(18)
C(216)-C(215)-C(220)-C(219)	2(2)
C(218)-C(219)-C(220)-C(215)	6(2)
C(217)-C(218)-O(10)-C(221)	101(10)
C(219)-C(218)-O(10)-C(221)	-80(9)
C(174)-P(5)-C(146)-C(147)	4.5(5)
C(160)-P(5)-C(146)-C(147)	-100.3(4)
Fe(3)-P(5)-C(146)-C(147)	120.4(4)
C(174)-P(5)-C(146)-C(151)	-179.0(4)
C(160)-P(5)-C(146)-C(151)	76.2(4)
Fe(3)-P(5)-C(146)-C(151)	-63.1(4)
C(151)-C(146)-C(147)-C(148)	-1.9(8)
P(5)-C(146)-C(147)-C(148)	174.6(4)
C(146)-C(147)-C(148)-C(149)	-0.3(9)
C(146)-C(147)-C(148)-C(152)	-179.4(6)
C(147)-C(148)-C(149)-C(150)	1.5(10)
C(152)-C(148)-C(149)-C(150)	-179.4(6)

C(148)-C(149)-C(150)-C(151)	-0.4(9)
C(148)-C(149)-C(150)-C(156)	-178.5(6)
C(149)-C(150)-C(151)-C(146)	-1.9(8)
C(156)-C(150)-C(151)-C(146)	176.1(5)
C(147)-C(146)-C(151)-C(150)	3.0(8)
P(5)-C(146)-C(151)-C(150)	-173.6(4)
C(149)-C(148)-C(152)-C(154)	7.7(13)
C(147)-C(148)-C(152)-C(154)	-173.4(10)
C(149)-C(148)-C(152)-C(155)	-122.3(9)
C(147)-C(148)-C(152)-C(155)	56.7(10)
C(149)-C(148)-C(152)-C(153)	124.3(7)
C(147)-C(148)-C(152)-C(153)	-56.7(8)
C(151)-C(150)-C(156)-C(159)	-12.5(12)
C(149)-C(150)-C(156)-C(159)	165.5(10)
C(151)-C(150)-C(156)-C(157)	130.0(11)
C(149)-C(150)-C(156)-C(157)	-52.0(13)
C(151)-C(150)-C(156)-C(158)	-122.6(8)
C(149)-C(150)-C(156)-C(158)	55.4(8)
C(174)-P(5)-C(160)-C(165)	61.9(4)
C(146)-P(5)-C(160)-C(165)	168.2(3)
Fe(3)-P(5)-C(160)-C(165)	-51.1(4)
C(174)-P(5)-C(160)-C(161)	-118.1(4)
C(146)-P(5)-C(160)-C(161)	-11.9(4)
Fe(3)-P(5)-C(160)-C(161)	128.9(3)
C(165)-C(160)-C(161)-C(162)	0.2(6)
P(5)-C(160)-C(161)-C(162)	-179.8(3)
C(160)-C(161)-C(162)-C(163)	-0.1(6)
C(160)-C(161)-C(162)-C(166)	-178.5(4)
C(161)-C(162)-C(163)-C(164)	-0.3(7)
C(166)-C(162)-C(163)-C(164)	178.0(4)
C(162)-C(163)-C(164)-C(165)	0.7(7)
C(162)-C(163)-C(164)-C(170)	-178.3(4)
C(163)-C(164)-C(165)-C(160)	-0.7(6)
C(170)-C(164)-C(165)-C(160)	178.4(4)
C(161)-C(160)-C(165)-C(164)	0.3(6)
P(5)-C(160)-C(165)-C(164)	-179.8(3)

C(163)-C(162)-C(166)-C(169)	3.0(8)
C(161)-C(162)-C(166)-C(169)	-178.7(6)
C(163)-C(162)-C(166)-C(167)	-122.3(6)
C(161)-C(162)-C(166)-C(167)	56.1(7)
C(163)-C(162)-C(166)-C(168)	122.6(6)
C(161)-C(162)-C(166)-C(168)	-59.1(7)
C(165)-C(164)-C(170)-C(172)	179.8(5)
C(163)-C(164)-C(170)-C(172)	-1.2(7)
C(165)-C(164)-C(170)-C(171)	58.9(6)
C(163)-C(164)-C(170)-C(171)	-122.1(5)
C(165)-C(164)-C(170)-C(173)	-60.6(6)
C(163)-C(164)-C(170)-C(173)	118.4(5)
C(146)-P(5)-C(174)-C(175)	-76.1(4)
C(160)-P(5)-C(174)-C(175)	30.6(4)
Fe(3)-P(5)-C(174)-C(175)	155.2(3)
C(146)-P(5)-C(174)-C(179)	102.7(4)
C(160)-P(5)-C(174)-C(179)	-150.7(4)
Fe(3)-P(5)-C(174)-C(179)	-26.1(4)
C(179)-C(174)-C(175)-C(176)	-1.5(7)
P(5)-C(174)-C(175)-C(176)	177.3(4)
C(174)-C(175)-C(176)-C(177)	2.6(8)
C(175)-C(176)-C(177)-C(178)	-1.5(8)
C(176)-C(177)-C(178)-C(179)	-0.6(8)
C(177)-C(178)-C(179)-C(174)	1.7(7)
C(177)-C(178)-C(179)-P(6)	-173.5(4)
C(175)-C(174)-C(179)-C(178)	-0.6(7)
P(5)-C(174)-C(179)-C(178)	-179.4(4)
C(175)-C(174)-C(179)-P(6)	174.8(3)
P(5)-C(174)-C(179)-P(6)	-4.0(5)
C(180)-P(6)-C(179)-C(178)	-19.6(6)
C(194)-P(6)-C(179)-C(178)	80.8(4)
C(480)-P(6)-C(179)-C(178)	-31.6(6)
Fe(3)-P(6)-C(179)-C(178)	-153.9(4)
C(180)-P(6)-C(179)-C(174)	165.2(6)
C(194)-P(6)-C(179)-C(174)	-94.4(4)
C(480)-P(6)-C(179)-C(174)	153.2(5)

Fe(3)-P(6)-C(179)-C(174)	30.9(4)
C(194)-P(6)-C(180)-C(181)	17.2(13)
C(179)-P(6)-C(180)-C(181)	119.1(12)
Fe(3)-P(6)-C(180)-C(181)	-124.1(11)
C(194)-P(6)-C(180)-C(185)	-165.1(10)
C(179)-P(6)-C(180)-C(185)	-63.1(11)
Fe(3)-P(6)-C(180)-C(185)	53.6(12)
C(185)-C(180)-C(181)-C(182)	4.2(19)
P(6)-C(180)-C(181)-C(182)	-178.2(10)
C(180)-C(181)-C(182)-C(183)	-2.8(19)
C(180)-C(181)-C(182)-C(186)	174.9(12)
C(181)-C(182)-C(183)-C(184)	0(2)
C(186)-C(182)-C(183)-C(184)	-177.8(12)
C(182)-C(183)-C(184)-C(185)	1.5(19)
C(182)-C(183)-C(184)-C(190)	-179.1(12)
C(181)-C(180)-C(185)-C(184)	-3(2)
P(6)-C(180)-C(185)-C(184)	179.4(10)
C(183)-C(184)-C(185)-C(180)	-0.1(19)
C(190)-C(184)-C(185)-C(180)	-179.5(12)
C(183)-C(182)-C(186)-C(189)	74.8(16)
C(181)-C(182)-C(186)-C(189)	-102.9(15)
C(183)-C(182)-C(186)-C(187)	-165.2(13)
C(181)-C(182)-C(186)-C(187)	17.1(18)
C(183)-C(182)-C(186)-C(188)	-48.4(17)
C(181)-C(182)-C(186)-C(188)	133.9(14)
C(183)-C(184)-C(190)-C(191)	-8(2)
C(185)-C(184)-C(190)-C(191)	171.3(14)
C(183)-C(184)-C(190)-C(192)	119.5(14)
C(185)-C(184)-C(190)-C(192)	-61.1(16)
C(183)-C(184)-C(190)-C(193)	-129.8(13)
C(185)-C(184)-C(190)-C(193)	49.6(17)
C(180)-P(6)-C(194)-C(195)	-132.0(6)
C(179)-P(6)-C(194)-C(195)	124.3(5)
C(480)-P(6)-C(194)-C(195)	-130.6(6)
Fe(3)-P(6)-C(194)-C(195)	13.1(6)
C(180)-P(6)-C(194)-C(199)	49.8(7)

C(179)-P(6)-C(194)-C(199)	-53.9(6)
C(480)-P(6)-C(194)-C(199)	51.2(7)
Fe(3)-P(6)-C(194)-C(199)	-165.1(5)
C(199)-C(194)-C(195)-C(196)	-0.8(10)
P(6)-C(194)-C(195)-C(196)	-179.0(5)
C(194)-C(195)-C(196)-C(197)	-0.6(10)
C(194)-C(195)-C(196)-C(200)	179.5(6)
C(195)-C(196)-C(197)-C(198)	2.2(13)
C(200)-C(196)-C(197)-C(198)	-177.9(8)
C(196)-C(197)-C(198)-C(199)	-2.2(14)
C(196)-C(197)-C(198)-C(204)	-164.1(10)
C(197)-C(198)-C(199)-C(194)	0.5(13)
C(504)-C(198)-C(199)-C(194)	-166.2(11)
C(204)-C(198)-C(199)-C(194)	166.6(8)
C(195)-C(194)-C(199)-C(198)	0.9(11)
P(6)-C(194)-C(199)-C(198)	179.0(6)
C(197)-C(196)-C(200)-C(202)	54.2(12)
C(195)-C(196)-C(200)-C(202)	-125.9(9)
C(197)-C(196)-C(200)-C(203)	-76.1(12)
C(195)-C(196)-C(200)-C(203)	103.7(11)
C(197)-C(196)-C(200)-C(201)	170.7(8)
C(195)-C(196)-C(200)-C(201)	-9.4(10)
C(197)-C(198)-C(204)-C(207)	-127.6(13)
C(199)-C(198)-C(204)-C(207)	69.2(13)
C(197)-C(198)-C(204)-C(206)	-21(2)
C(199)-C(198)-C(204)-C(206)	175.8(17)
C(197)-C(198)-C(204)-C(205)	97.8(17)
C(199)-C(198)-C(204)-C(205)	-65.4(14)
Fe(3)-O(7)-C(208)-C(209)	132.7(4)
Fe(3)#1-O(7)-C(208)-C(209)	-63.1(6)
Fe(3)-O(7)-C(208)-C(213)	-45.9(6)
Fe(3)#1-O(7)-C(208)-C(213)	118.2(5)
O(7)-C(208)-C(209)-C(210)	-177.9(4)
C(213)-C(208)-C(209)-C(210)	0.7(7)
C(208)-C(209)-C(210)-C(211)	-0.4(8)
C(209)-C(210)-C(211)-C(212)	0.1(8)

C(209)-C(210)-C(211)-O(8)	179.3(5)
C(214)-O(8)-C(211)-C(210)	-6.1(8)
C(214)-O(8)-C(211)-C(212)	173.2(6)
C(210)-C(211)-C(212)-C(213)	-0.1(8)
O(8)-C(211)-C(212)-C(213)	-179.4(5)
O(7)-C(208)-C(213)-C(212)	177.8(4)
C(209)-C(208)-C(213)-C(212)	-0.8(7)
C(211)-C(212)-C(213)-C(208)	0.5(8)

---

Symmetry transformations used to generate equivalent atoms:

#1 -x+1,-y+1,-z+1

## 5.2 X-RAY CRYSTALLOGRAPHIC ANALYSIS OF 3.19

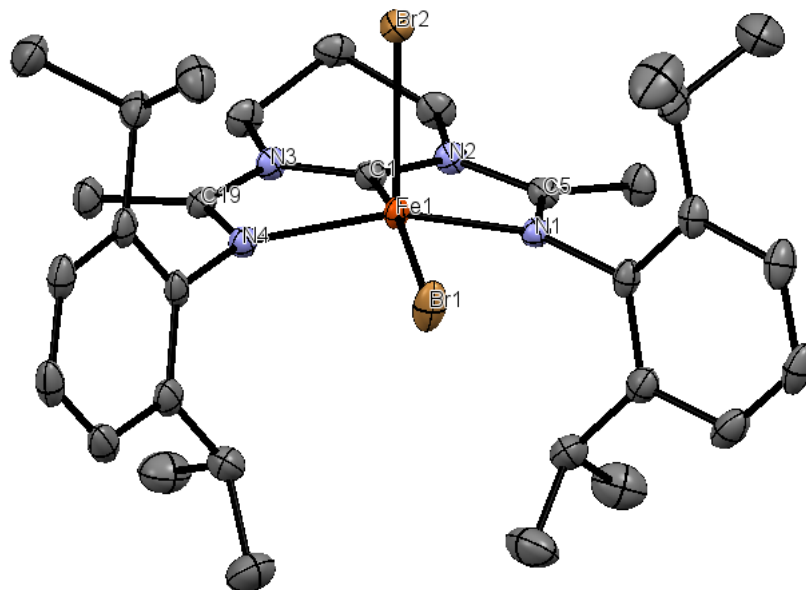


Table 1. Crystal data and structure refinement for C<sub>32</sub>H<sub>46</sub>Br<sub>2</sub>FeN<sub>4</sub>.

Identification code	C <sub>32</sub> H <sub>46</sub> Br <sub>2</sub> FeN <sub>4</sub>	
Empirical formula	C <sub>37.25</sub> H <sub>56.50</sub> Br <sub>2</sub> Cl <sub>4.50</sub> Fe N <sub>4</sub> O <sub>0.75</sub>	
Formula weight	947.56	
Temperature	100(2) K	
Wavelength	1.54178 Å	
Crystal system	Monoclinic	
Space group	P2 <sub>1</sub> /c	
Unit cell dimensions	a = 18.1054(7) Å	a = 90°.
	b = 13.2094(5) Å	b = 103.866(2)°.
	c = 18.9300(7) Å	g = 90°.
Volume	4395.4(3) Å <sup>3</sup>	
Z	4	
Density (calculated)	1.432 Mg/m <sup>3</sup>	
Absorption coefficient	7.643 mm <sup>-1</sup>	
F(000)	1946	
Crystal size	0.400 x 0.340 x 0.100 mm <sup>3</sup>	
Theta range for data collection	2.514 to 66.864°.	

Index ranges	-21<=h<=21, -15<=k<=15, -22<=l<=22
Reflections collected	54369
Independent reflections	7796 [R(int) = 0.0468]
Completeness to theta = 66.864°	99.7 %
Absorption correction	Semi-empirical from equivalents
Max. and min. transmission	0.7528 and 0.4482
Refinement method	Full-matrix least-squares on F <sup>2</sup>
Data / restraints / parameters	7796 / 0 / 499
Goodness-of-fit on F <sup>2</sup>	1.030
Final R indices [I>2sigma(I)]	R1 = 0.0353, wR2 = 0.0973
R indices (all data)	R1 = 0.0366, wR2 = 0.0986
Extinction coefficient	na
Largest diff. peak and hole	1.028 and -1.161 e.Å <sup>-3</sup>

Table 2. Atomic coordinates ( $\times 10^4$ ) and equivalent isotropic displacement parameters ( $\text{\AA}^2 \times 10^3$ )

for C<sub>32</sub>H<sub>46</sub>Br<sub>2</sub>FeN<sub>4</sub>. U(eq) is defined as one third of the trace of the orthogonalized U<sub>ij</sub> tensor.

	x	y	z	U(eq)
Br(1)	2380(1)	3072(1)	3302(1)	28(1)
Br(2)	3705(1)	4479(1)	4954(1)	23(1)
Fe(1)	2700(1)	3173(1)	4617(1)	14(1)
N(1)	1768(1)	3909(2)	4734(1)	15(1)
N(2)	2310(1)	3572(2)	5910(1)	17(1)
N(4)	3310(1)	1887(2)	4831(1)	17(1)
N(3)	3257(1)	2329(2)	5970(1)	18(1)
C(1)	2757(2)	3006(2)	5579(1)	17(1)
C(2)	2419(2)	3601(2)	6712(1)	22(1)
C(3)	3232(2)	3282(2)	7056(1)	23(1)
C(4)	3418(2)	2264(2)	6772(1)	23(1)
C(5)	1747(1)	4062(2)	5410(1)	17(1)
C(6)	1176(2)	4674(2)	5681(2)	25(1)
C(7)	1174(1)	4329(2)	4160(1)	18(1)
C(8)	543(2)	3721(2)	3864(1)	23(1)
C(9)	-27(2)	4133(2)	3306(2)	29(1)
C(10)	32(2)	5103(3)	3054(2)	31(1)
C(11)	667(2)	5679(2)	3343(2)	29(1)
C(12)	1257(2)	5305(2)	3898(2)	23(1)
C(13)	461(2)	2655(2)	4138(2)	29(1)
C(14)	298(2)	1882(3)	3521(2)	44(1)
C(15)	-156(2)	2611(3)	4564(2)	41(1)
C(16)	1954(2)	5945(2)	4188(2)	29(1)
C(17)	1764(2)	6919(3)	4536(3)	50(1)
C(18)	2370(2)	6164(3)	3590(2)	51(1)
C(19)	3556(1)	1708(2)	5524(1)	19(1)
C(20)	4101(2)	901(2)	5863(2)	26(1)
C(21)	3563(2)	1245(2)	4318(1)	20(1)

C(22)	4271(2)	1406(2)	4162(1)	22(1)
C(23)	4484(2)	763(2)	3659(2)	26(1)
C(24)	4019(2)	-11(2)	3330(2)	28(1)
C(25)	3318(2)	-152(2)	3484(2)	29(1)
C(26)	3071(2)	478(2)	3972(2)	24(1)
C(27)	4802(2)	2257(2)	4500(2)	25(1)
C(28)	4840(2)	3049(2)	3922(2)	34(1)
C(29)	5599(2)	1859(3)	4868(2)	36(1)
C(30)	2299(2)	315(2)	4140(2)	28(1)
C(31)	2373(2)	-350(3)	4822(2)	41(1)
C(32)	1719(2)	-155(3)	3503(2)	42(1)
C(1S)	941(2)	4035(3)	1775(2)	49(1)
CI(1)	363(1)	2953(1)	1590(1)	76(1)
CI(2)	1496(1)	4137(1)	1125(1)	81(1)
C(2S)	4520(2)	5772(3)	3518(2)	33(1)
CI(3)	4438(1)	7093(1)	3374(1)	54(1)
CI(4)	4572(15)	5153(11)	2740(10)	66(3)
CI(4X)	4265(14)	5142(7)	2676(4)	73(3)
O(1S)	2408(2)	6258(3)	6714(2)	51(1)
C(3S)	2277(7)	7124(9)	7086(6)	37(2)
C(4S)	2478(3)	8001(4)	6615(3)	47(1)
C(5S)	3142(3)	7570(6)	6374(3)	57(2)
C(6S)	3064(5)	6451(7)	6440(4)	71(3)
C(7S)	2906(12)	7264(17)	6667(12)	69(6)
CI(5)	2077(6)	7038(11)	6927(6)	65(3)
CI(6)	3194(3)	6150(4)	6258(3)	48(1)

---

Table 3. Bond lengths [Å] and angles [°] for C<sub>32</sub>H<sub>46</sub>Br<sub>2</sub>FeN<sub>4</sub>.

---

Br(1)-Fe(1)	2.4216(5)
Br(2)-Fe(1)	2.4776(5)
Fe(1)-C(1)	1.811(3)
Fe(1)-N(1)	2.004(2)
Fe(1)-N(4)	2.015(2)
N(1)-C(5)	1.305(3)
N(1)-C(7)	1.444(3)
N(2)-C(1)	1.360(3)
N(2)-C(5)	1.374(3)
N(2)-C(2)	1.483(3)
N(4)-C(19)	1.303(3)
N(4)-C(21)	1.444(3)
N(3)-C(1)	1.360(3)
N(3)-C(19)	1.376(3)
N(3)-C(4)	1.478(3)
C(2)-C(3)	1.520(4)
C(2)-H(2A)	0.9900
C(2)-H(2B)	0.9900
C(3)-C(4)	1.517(4)
C(3)-H(3A)	0.9900
C(3)-H(3B)	0.9900
C(4)-H(4A)	0.9900
C(4)-H(4B)	0.9900
C(5)-C(6)	1.496(4)
C(6)-H(6A)	0.9800
C(6)-H(6B)	0.9800
C(6)-H(6C)	0.9800
C(7)-C(8)	1.399(4)
C(7)-C(12)	1.402(4)
C(8)-C(9)	1.398(4)
C(8)-C(13)	1.520(4)
C(9)-C(10)	1.380(5)
C(9)-H(9)	0.9500
C(10)-C(11)	1.377(5)

C(10)-H(10)	0.9500
C(11)-C(12)	1.396(4)
C(11)-H(11)	0.9500
C(12)-C(16)	1.509(4)
C(13)-C(14)	1.527(4)
C(13)-C(15)	1.528(5)
C(13)-H(13)	1.0000
C(14)-H(14A)	0.9800
C(14)-H(14B)	0.9800
C(14)-H(14C)	0.9800
C(15)-H(15A)	0.9800
C(15)-H(15B)	0.9800
C(15)-H(15C)	0.9800
C(16)-C(17)	1.524(5)
C(16)-C(18)	1.530(5)
C(16)-H(16)	1.0000
C(17)-H(17A)	0.9800
C(17)-H(17B)	0.9800
C(17)-H(17C)	0.9800
C(18)-H(18A)	0.9800
C(18)-H(18B)	0.9800
C(18)-H(18C)	0.9800
C(19)-C(20)	1.490(4)
C(20)-H(20A)	0.9800
C(20)-H(20B)	0.9800
C(20)-H(20C)	0.9800
C(21)-C(22)	1.400(4)
C(21)-C(26)	1.402(4)
C(22)-C(23)	1.398(4)
C(22)-C(27)	1.517(4)
C(23)-C(24)	1.375(4)
C(23)-H(23)	0.9500
C(24)-C(25)	1.381(5)
C(24)-H(24)	0.9500
C(25)-C(26)	1.394(4)
C(25)-H(25)	0.9500

C(26)-C(30)	1.521(4)
C(27)-C(28)	1.528(4)
C(27)-C(29)	1.536(4)
C(27)-H(27)	1.0000
C(28)-H(28A)	0.9800
C(28)-H(28B)	0.9800
C(28)-H(28C)	0.9800
C(29)-H(29A)	0.9800
C(29)-H(29B)	0.9800
C(29)-H(29C)	0.9800
C(30)-C(32)	1.529(4)
C(30)-C(31)	1.541(5)
C(30)-H(30)	1.0000
C(31)-H(31A)	0.9800
C(31)-H(31B)	0.9800
C(31)-H(31C)	0.9800
C(32)-H(32A)	0.9800
C(32)-H(32B)	0.9800
C(32)-H(32C)	0.9800
C(1S)-Cl(1)	1.757(4)
C(1S)-Cl(2)	1.772(4)
C(1S)-H(1S1)	0.9900
C(1S)-H(1S2)	0.9900
C(2S)-Cl(4)	1.707(16)
C(2S)-Cl(4X)	1.760(8)
C(2S)-Cl(3)	1.767(3)
C(2S)-H(2S1)	0.9900
C(2S)-H(2S2)	0.9900
O(1S)-C(3S)	1.394(14)
O(1S)-C(6S)	1.428(9)
C(3S)-C(4S)	1.557(12)
C(3S)-H(3S1)	0.9900
C(3S)-H(3S2)	0.9900
C(4S)-C(5S)	1.497(8)
C(4S)-H(4S1)	0.9900
C(4S)-H(4S2)	0.9900

C(5S)-C(6S)	1.492(12)
C(5S)-H(5S1)	0.9900
C(5S)-H(5S2)	0.9900
C(6S)-H(6S1)	0.9900
C(6S)-H(6S2)	0.9900
C(7S)-Cl(5)	1.71(3)
C(7S)-Cl(6)	1.80(3)
C(7S)-H(7S1)	0.9900
C(7S)-H(7S2)	0.9900
C(1)-Fe(1)-N(1)	78.20(10)
C(1)-Fe(1)-N(4)	78.41(10)
N(1)-Fe(1)-N(4)	145.38(9)
C(1)-Fe(1)-Br(1)	165.59(8)
N(1)-Fe(1)-Br(1)	98.06(6)
N(4)-Fe(1)-Br(1)	98.28(6)
C(1)-Fe(1)-Br(2)	87.98(8)
N(1)-Fe(1)-Br(2)	102.68(6)
N(4)-Fe(1)-Br(2)	101.63(6)
Br(1)-Fe(1)-Br(2)	106.435(18)
C(5)-N(1)-C(7)	119.2(2)
C(5)-N(1)-Fe(1)	113.92(17)
C(7)-N(1)-Fe(1)	126.72(16)
C(1)-N(2)-C(5)	111.5(2)
C(1)-N(2)-C(2)	122.5(2)
C(5)-N(2)-C(2)	126.0(2)
C(19)-N(4)-C(21)	119.0(2)
C(19)-N(4)-Fe(1)	113.16(17)
C(21)-N(4)-Fe(1)	127.41(16)
C(1)-N(3)-C(19)	111.5(2)
C(1)-N(3)-C(4)	122.6(2)
C(19)-N(3)-C(4)	125.8(2)
N(3)-C(1)-N(2)	120.2(2)
N(3)-C(1)-Fe(1)	119.84(19)
N(2)-C(1)-Fe(1)	119.94(19)
N(2)-C(2)-C(3)	108.1(2)

N(2)-C(2)-H(2A)	110.1
C(3)-C(2)-H(2A)	110.1
N(2)-C(2)-H(2B)	110.1
C(3)-C(2)-H(2B)	110.1
H(2A)-C(2)-H(2B)	108.4
C(4)-C(3)-C(2)	111.6(2)
C(4)-C(3)-H(3A)	109.3
C(2)-C(3)-H(3A)	109.3
C(4)-C(3)-H(3B)	109.3
C(2)-C(3)-H(3B)	109.3
H(3A)-C(3)-H(3B)	108.0
N(3)-C(4)-C(3)	107.9(2)
N(3)-C(4)-H(4A)	110.1
C(3)-C(4)-H(4A)	110.1
N(3)-C(4)-H(4B)	110.1
C(3)-C(4)-H(4B)	110.1
H(4A)-C(4)-H(4B)	108.4
N(1)-C(5)-N(2)	114.3(2)
N(1)-C(5)-C(6)	127.1(2)
N(2)-C(5)-C(6)	118.6(2)
C(5)-C(6)-H(6A)	109.5
C(5)-C(6)-H(6B)	109.5
H(6A)-C(6)-H(6B)	109.5
C(5)-C(6)-H(6C)	109.5
H(6A)-C(6)-H(6C)	109.5
H(6B)-C(6)-H(6C)	109.5
C(8)-C(7)-C(12)	122.2(2)
C(8)-C(7)-N(1)	118.1(2)
C(12)-C(7)-N(1)	119.7(2)
C(9)-C(8)-C(7)	117.6(3)
C(9)-C(8)-C(13)	120.3(3)
C(7)-C(8)-C(13)	122.1(2)
C(10)-C(9)-C(8)	121.2(3)
C(10)-C(9)-H(9)	119.4
C(8)-C(9)-H(9)	119.4
C(11)-C(10)-C(9)	120.1(3)

C(11)-C(10)-H(10)	119.9
C(9)-C(10)-H(10)	119.9
C(10)-C(11)-C(12)	121.2(3)
C(10)-C(11)-H(11)	119.4
C(12)-C(11)-H(11)	119.4
C(11)-C(12)-C(7)	117.7(3)
C(11)-C(12)-C(16)	119.9(3)
C(7)-C(12)-C(16)	122.5(2)
C(8)-C(13)-C(14)	112.0(3)
C(8)-C(13)-C(15)	111.1(3)
C(14)-C(13)-C(15)	110.3(3)
C(8)-C(13)-H(13)	107.8
C(14)-C(13)-H(13)	107.8
C(15)-C(13)-H(13)	107.8
C(13)-C(14)-H(14A)	109.5
C(13)-C(14)-H(14B)	109.5
H(14A)-C(14)-H(14B)	109.5
C(13)-C(14)-H(14C)	109.5
H(14A)-C(14)-H(14C)	109.5
H(14B)-C(14)-H(14C)	109.5
C(13)-C(15)-H(15A)	109.5
C(13)-C(15)-H(15B)	109.5
H(15A)-C(15)-H(15B)	109.5
C(13)-C(15)-H(15C)	109.5
H(15A)-C(15)-H(15C)	109.5
H(15B)-C(15)-H(15C)	109.5
C(12)-C(16)-C(17)	112.0(3)
C(12)-C(16)-C(18)	110.8(3)
C(17)-C(16)-C(18)	111.3(3)
C(12)-C(16)-H(16)	107.5
C(17)-C(16)-H(16)	107.5
C(18)-C(16)-H(16)	107.5
C(16)-C(17)-H(17A)	109.5
C(16)-C(17)-H(17B)	109.5
H(17A)-C(17)-H(17B)	109.5
C(16)-C(17)-H(17C)	109.5

H(17A)-C(17)-H(17C)	109.5
H(17B)-C(17)-H(17C)	109.5
C(16)-C(18)-H(18A)	109.5
C(16)-C(18)-H(18B)	109.5
H(18A)-C(18)-H(18B)	109.5
C(16)-C(18)-H(18C)	109.5
H(18A)-C(18)-H(18C)	109.5
H(18B)-C(18)-H(18C)	109.5
N(4)-C(19)-N(3)	114.8(2)
N(4)-C(19)-C(20)	126.5(2)
N(3)-C(19)-C(20)	118.7(2)
C(19)-C(20)-H(20A)	109.5
C(19)-C(20)-H(20B)	109.5
H(20A)-C(20)-H(20B)	109.5
C(19)-C(20)-H(20C)	109.5
H(20A)-C(20)-H(20C)	109.5
H(20B)-C(20)-H(20C)	109.5
C(22)-C(21)-C(26)	121.5(2)
C(22)-C(21)-N(4)	120.4(2)
C(26)-C(21)-N(4)	118.1(2)
C(23)-C(22)-C(21)	117.8(3)
C(23)-C(22)-C(27)	119.2(3)
C(21)-C(22)-C(27)	123.0(2)
C(24)-C(23)-C(22)	121.4(3)
C(24)-C(23)-H(23)	119.3
C(22)-C(23)-H(23)	119.3
C(23)-C(24)-C(25)	120.0(3)
C(23)-C(24)-H(24)	120.0
C(25)-C(24)-H(24)	120.0
C(24)-C(25)-C(26)	121.0(3)
C(24)-C(25)-H(25)	119.5
C(26)-C(25)-H(25)	119.5
C(25)-C(26)-C(21)	118.2(3)
C(25)-C(26)-C(30)	120.7(3)
C(21)-C(26)-C(30)	121.1(2)
C(22)-C(27)-C(28)	109.7(2)

C(22)-C(27)-C(29)	111.6(2)
C(28)-C(27)-C(29)	111.2(3)
C(22)-C(27)-H(27)	108.1
C(28)-C(27)-H(27)	108.1
C(29)-C(27)-H(27)	108.1
C(27)-C(28)-H(28A)	109.5
C(27)-C(28)-H(28B)	109.5
H(28A)-C(28)-H(28B)	109.5
C(27)-C(28)-H(28C)	109.5
H(28A)-C(28)-H(28C)	109.5
H(28B)-C(28)-H(28C)	109.5
C(27)-C(29)-H(29A)	109.5
C(27)-C(29)-H(29B)	109.5
H(29A)-C(29)-H(29B)	109.5
C(27)-C(29)-H(29C)	109.5
H(29A)-C(29)-H(29C)	109.5
H(29B)-C(29)-H(29C)	109.5
C(26)-C(30)-C(32)	112.7(3)
C(26)-C(30)-C(31)	110.8(2)
C(32)-C(30)-C(31)	109.5(3)
C(26)-C(30)-H(30)	107.9
C(32)-C(30)-H(30)	107.9
C(31)-C(30)-H(30)	107.9
C(30)-C(31)-H(31A)	109.5
C(30)-C(31)-H(31B)	109.5
H(31A)-C(31)-H(31B)	109.5
C(30)-C(31)-H(31C)	109.5
H(31A)-C(31)-H(31C)	109.5
H(31B)-C(31)-H(31C)	109.5
C(30)-C(32)-H(32A)	109.5
C(30)-C(32)-H(32B)	109.5
H(32A)-C(32)-H(32B)	109.5
C(30)-C(32)-H(32C)	109.5
H(32A)-C(32)-H(32C)	109.5
H(32B)-C(32)-H(32C)	109.5
Cl(1)-C(1S)-Cl(2)	109.5(2)

Cl(1)-C(1S)-H(1S1)	109.8
Cl(2)-C(1S)-H(1S1)	109.8
Cl(1)-C(1S)-H(1S2)	109.8
Cl(2)-C(1S)-H(1S2)	109.8
H(1S1)-C(1S)-H(1S2)	108.2
Cl(4)-C(2S)-Cl(3)	111.1(4)
Cl(4X)-C(2S)-Cl(3)	109.5(4)
Cl(4)-C(2S)-H(2S1)	109.4
Cl(3)-C(2S)-H(2S1)	109.4
Cl(4)-C(2S)-H(2S2)	109.4
Cl(3)-C(2S)-H(2S2)	109.4
H(2S1)-C(2S)-H(2S2)	108.0
C(3S)-O(1S)-C(6S)	107.1(7)
O(1S)-C(3S)-C(4S)	103.2(9)
O(1S)-C(3S)-H(3S1)	111.1
C(4S)-C(3S)-H(3S1)	111.1
O(1S)-C(3S)-H(3S2)	111.1
C(4S)-C(3S)-H(3S2)	111.1
H(3S1)-C(3S)-H(3S2)	109.1
C(5S)-C(4S)-C(3S)	101.9(7)
C(5S)-C(4S)-H(4S1)	111.4
C(3S)-C(4S)-H(4S1)	111.4
C(5S)-C(4S)-H(4S2)	111.4
C(3S)-C(4S)-H(4S2)	111.4
H(4S1)-C(4S)-H(4S2)	109.2
C(6S)-C(5S)-C(4S)	104.6(6)
C(6S)-C(5S)-H(5S1)	110.8
C(4S)-C(5S)-H(5S1)	110.8
C(6S)-C(5S)-H(5S2)	110.8
C(4S)-C(5S)-H(5S2)	110.8
H(5S1)-C(5S)-H(5S2)	108.9
O(1S)-C(6S)-C(5S)	108.1(5)
O(1S)-C(6S)-H(6S1)	110.1
C(5S)-C(6S)-H(6S1)	110.1
O(1S)-C(6S)-H(6S2)	110.1
C(5S)-C(6S)-H(6S2)	110.1

H(6S1)-C(6S)-H(6S2)	108.4
Cl(5)-C(7S)-Cl(6)	110.2(11)
Cl(5)-C(7S)-H(7S1)	109.6
Cl(6)-C(7S)-H(7S1)	109.6
Cl(5)-C(7S)-H(7S2)	109.6
Cl(6)-C(7S)-H(7S2)	109.6
H(7S1)-C(7S)-H(7S2)	108.1

---

Symmetry transformations used to generate equivalent atoms:

Table 4. Anisotropic displacement parameters ( $\text{\AA}^2 \times 10^3$ ) for C<sub>32</sub>H<sub>46</sub>Br<sub>2</sub>FeN<sub>4</sub>. The anisotropic displacement factor exponent takes the form:  $-2p^2 [ h^2 a^2 U^{11} + \dots + 2 h k a^* b^* U^{12} ]$

	U <sup>11</sup>	U <sup>22</sup>	U <sup>33</sup>	U <sup>23</sup>	U <sup>13</sup>	U <sup>12</sup>
Br(1)	32(1)	41(1)	11(1)	-1(1)	2(1)	17(1)
Br(2)	20(1)	21(1)	25(1)	0(1)	2(1)	0(1)
Fe(1)	16(1)	16(1)	10(1)	1(1)	1(1)	4(1)
N(1)	16(1)	16(1)	13(1)	0(1)	2(1)	1(1)
N(2)	22(1)	18(1)	11(1)	0(1)	3(1)	1(1)
N(4)	18(1)	17(1)	15(1)	-1(1)	0(1)	3(1)
N(3)	21(1)	19(1)	11(1)	2(1)	-1(1)	3(1)
C(1)	20(1)	16(1)	14(1)	0(1)	1(1)	0(1)
C(2)	31(1)	25(1)	10(1)	-1(1)	4(1)	0(1)
C(3)	28(1)	25(1)	13(1)	0(1)	0(1)	-4(1)
C(4)	27(1)	27(1)	11(1)	5(1)	-1(1)	1(1)
C(5)	20(1)	15(1)	17(1)	-1(1)	5(1)	0(1)
C(6)	27(1)	29(2)	19(1)	-3(1)	7(1)	7(1)
C(7)	18(1)	23(1)	13(1)	0(1)	4(1)	7(1)
C(8)	20(1)	27(2)	20(1)	-4(1)	2(1)	4(1)
C(9)	20(1)	41(2)	22(1)	-7(1)	-1(1)	4(1)
C(10)	25(1)	45(2)	19(1)	5(1)	0(1)	14(1)
C(11)	29(2)	34(2)	24(1)	10(1)	6(1)	12(1)
C(12)	23(1)	26(1)	20(1)	4(1)	6(1)	8(1)
C(13)	24(1)	27(2)	31(2)	-2(1)	-3(1)	0(1)
C(14)	47(2)	33(2)	53(2)	-16(2)	16(2)	-9(2)
C(15)	53(2)	40(2)	31(2)	0(2)	11(2)	-9(2)
C(16)	27(1)	23(2)	35(2)	13(1)	3(1)	3(1)
C(17)	44(2)	31(2)	69(3)	-5(2)	2(2)	-3(2)
C(18)	39(2)	61(3)	53(2)	24(2)	14(2)	-5(2)
C(19)	18(1)	18(1)	18(1)	1(1)	-1(1)	1(1)
C(20)	29(1)	24(1)	21(1)	3(1)	-2(1)	9(1)
C(21)	23(1)	18(1)	15(1)	0(1)	-2(1)	10(1)
C(22)	22(1)	23(1)	16(1)	3(1)	-2(1)	11(1)

C(23)	26(1)	30(2)	19(1)	2(1)	1(1)	14(1)
C(24)	36(2)	27(2)	16(1)	-2(1)	-1(1)	17(1)
C(25)	34(2)	22(1)	22(1)	-4(1)	-7(1)	9(1)
C(26)	26(1)	22(1)	18(1)	1(1)	-4(1)	7(1)
C(27)	20(1)	27(2)	27(1)	-2(1)	4(1)	6(1)
C(28)	34(2)	31(2)	42(2)	3(1)	15(1)	5(1)
C(29)	23(2)	40(2)	40(2)	-8(1)	-2(1)	7(1)
C(30)	28(2)	21(1)	32(2)	-4(1)	1(1)	0(1)
C(31)	42(2)	38(2)	41(2)	0(2)	7(2)	-10(2)
C(32)	31(2)	47(2)	42(2)	-8(2)	-4(1)	-4(2)
C(1S)	47(2)	58(2)	40(2)	2(2)	6(2)	10(2)
CI(1)	78(1)	98(1)	54(1)	-23(1)	18(1)	-34(1)
CI(2)	63(1)	110(1)	75(1)	32(1)	27(1)	3(1)
C(2S)	38(2)	36(2)	22(1)	-1(1)	3(1)	-4(1)
CI(3)	72(1)	34(1)	47(1)	-6(1)	-1(1)	-5(1)
CI(4)	129(7)	48(3)	34(4)	-2(2)	45(4)	-2(4)
CI(4X)	155(8)	37(2)	25(1)	-10(1)	18(3)	-30(3)
O(1S)	74(2)	34(2)	41(2)	-12(2)	8(2)	-6(2)
C(3S)	46(6)	41(4)	22(5)	5(4)	5(4)	12(4)
C(4S)	53(3)	42(3)	45(3)	8(2)	9(2)	-1(2)
C(5S)	43(3)	92(5)	37(3)	3(3)	10(2)	-10(3)
C(6S)	90(6)	91(7)	33(3)	4(4)	19(3)	58(5)
C(7S)	65(13)	69(14)	65(13)	9(11)	3(10)	-39(12)
CI(5)	66(6)	89(5)	38(4)	-22(3)	5(4)	10(4)
CI(6)	34(2)	50(3)	59(3)	4(2)	10(2)	-5(2)

---

-

Table 5. Hydrogen coordinates ( $\times 10^4$ ) and isotropic displacement parameters ( $\text{\AA}^2 \times 10^{-3}$ ) for C<sub>32</sub>H<sub>46</sub>Br<sub>2</sub>FeN<sub>4</sub>.

	x	y	z	U(eq)
H(2A)	2057	3135	6862	26
H(2B)	2327	4294	6870	26
H(3A)	3587	3799	6951	28
H(3B)	3305	3243	7591	28
H(4A)	3961	2097	6974	27
H(4B)	3103	1727	6918	27
H(6A)	787	4927	5266	37
H(6B)	1431	5246	5968	37
H(6C)	935	4248	5986	37
H(9)	-463	3739	3097	35
H(10)	-365	5374	2680	37
H(11)	704	6343	3161	35
H(13)	955	2467	4478	35
H(14A)	-197	2028	3193	65
H(14B)	291	1200	3724	65
H(14C)	696	1921	3251	65
H(15A)	-34	3092	4970	62
H(15B)	-181	1925	4754	62
H(15C)	-648	2788	4242	62
H(16)	2307	5544	4574	35
H(17A)	1426	7336	4167	75
H(17B)	2234	7294	4742	75
H(17C)	1509	6756	4924	75
H(18A)	2509	5523	3394	76
H(18B)	2831	6556	3793	76
H(18C)	2037	6551	3199	76
H(20A)	4184	438	5485	39
H(20B)	3892	524	6217	39

H(20C)	4586	1210	6111	39
H(23)	4961	862	3542	31
H(24)	4180	-448	2998	34
H(25)	2999	-687	3254	34
H(27)	4586	2588	4881	30
H(28A)	5045	2739	3539	52
H(28B)	5170	3608	4145	52
H(28C)	4328	3309	3709	52
H(29A)	5560	1370	5247	54
H(29B)	5923	2425	5088	54
H(29C)	5821	1528	4504	54
H(30)	2100	991	4244	34
H(31A)	2626	-987	4756	61
H(31B)	1866	-495	4895	61
H(31C)	2675	8	5248	61
H(32A)	1680	261	3067	63
H(32B)	1221	-189	3622	63
H(32C)	1883	-840	3412	63
H(1S1)	1278	3985	2270	59
H(1S2)	620	4645	1756	59
H(2S1)	4983	5625	3905	39
H(2S2)	4075	5523	3685	39
H(3S1)	2608	7139	7585	44
H(3S2)	1739	7164	7114	44
H(4S1)	2049	8152	6194	57
H(4S2)	2621	8624	6906	57
H(5S1)	3123	7763	5865	69
H(5S2)	3628	7811	6690	69
H(6S1)	3007	6126	5959	85
H(6S2)	3524	6171	6776	85
H(7S1)	3310	7461	7097	82
H(7S2)	2830	7830	6314	82

Table 6. Torsion angles [°] for C<sub>32</sub>H<sub>46</sub>Br<sub>2</sub>FeN<sub>4</sub>.

---

C(19)-N(3)-C(1)-N(2)	169.3(2)
C(4)-N(3)-C(1)-N(2)	-8.3(4)
C(19)-N(3)-C(1)-Fe(1)	-12.0(3)
C(4)-N(3)-C(1)-Fe(1)	170.44(19)
C(5)-N(2)-C(1)-N(3)	-168.4(2)
C(2)-N(2)-C(1)-N(3)	9.4(4)
C(5)-N(2)-C(1)-Fe(1)	12.9(3)
C(2)-N(2)-C(1)-Fe(1)	-169.33(19)
N(1)-Fe(1)-C(1)-N(3)	167.7(2)
N(4)-Fe(1)-C(1)-N(3)	13.4(2)
Br(1)-Fe(1)-C(1)-N(3)	91.4(4)
Br(2)-Fe(1)-C(1)-N(3)	-88.9(2)
N(1)-Fe(1)-C(1)-N(2)	-13.6(2)
N(4)-Fe(1)-C(1)-N(2)	-167.8(2)
Br(1)-Fe(1)-C(1)-N(2)	-89.8(4)
Br(2)-Fe(1)-C(1)-N(2)	89.9(2)
C(1)-N(2)-C(2)-C(3)	22.0(3)
C(5)-N(2)-C(2)-C(3)	-160.6(2)
N(2)-C(2)-C(3)-C(4)	-54.4(3)
C(1)-N(3)-C(4)-C(3)	-24.0(3)
C(19)-N(3)-C(4)-C(3)	158.7(2)
C(2)-C(3)-C(4)-N(3)	55.4(3)
C(7)-N(1)-C(5)-N(2)	175.8(2)
Fe(1)-N(1)-C(5)-N(2)	-8.5(3)
C(7)-N(1)-C(5)-C(6)	-2.4(4)
Fe(1)-N(1)-C(5)-C(6)	173.4(2)
C(1)-N(2)-C(5)-N(1)	-1.7(3)
C(2)-N(2)-C(5)-N(1)	-179.4(2)
C(1)-N(2)-C(5)-C(6)	176.6(2)
C(2)-N(2)-C(5)-C(6)	-1.1(4)
C(5)-N(1)-C(7)-C(8)	-93.0(3)
Fe(1)-N(1)-C(7)-C(8)	91.9(3)
C(5)-N(1)-C(7)-C(12)	89.5(3)
Fe(1)-N(1)-C(7)-C(12)	-85.6(3)

C(12)-C(7)-C(8)-C(9)	-2.3(4)
N(1)-C(7)-C(8)-C(9)	-179.7(2)
C(12)-C(7)-C(8)-C(13)	178.8(3)
N(1)-C(7)-C(8)-C(13)	1.4(4)
C(7)-C(8)-C(9)-C(10)	0.4(4)
C(13)-C(8)-C(9)-C(10)	179.3(3)
C(8)-C(9)-C(10)-C(11)	1.1(4)
C(9)-C(10)-C(11)-C(12)	-0.7(4)
C(10)-C(11)-C(12)-C(7)	-1.2(4)
C(10)-C(11)-C(12)-C(16)	178.3(3)
C(8)-C(7)-C(12)-C(11)	2.7(4)
N(1)-C(7)-C(12)-C(11)	-179.9(2)
C(8)-C(7)-C(12)-C(16)	-176.7(3)
N(1)-C(7)-C(12)-C(16)	0.7(4)
C(9)-C(8)-C(13)-C(14)	53.3(4)
C(7)-C(8)-C(13)-C(14)	-127.8(3)
C(9)-C(8)-C(13)-C(15)	-70.5(3)
C(7)-C(8)-C(13)-C(15)	108.4(3)
C(11)-C(12)-C(16)-C(17)	62.5(4)
C(7)-C(12)-C(16)-C(17)	-118.1(3)
C(11)-C(12)-C(16)-C(18)	-62.3(4)
C(7)-C(12)-C(16)-C(18)	117.0(3)
C(21)-N(4)-C(19)-N(3)	-177.1(2)
Fe(1)-N(4)-C(19)-N(3)	9.8(3)
C(21)-N(4)-C(19)-C(20)	1.4(4)
Fe(1)-N(4)-C(19)-C(20)	-171.6(2)
C(1)-N(3)-C(19)-N(4)	0.2(3)
C(4)-N(3)-C(19)-N(4)	177.7(2)
C(1)-N(3)-C(19)-C(20)	-178.4(2)
C(4)-N(3)-C(19)-C(20)	-1.0(4)
C(19)-N(4)-C(21)-C(22)	-81.3(3)
Fe(1)-N(4)-C(21)-C(22)	90.7(3)
C(19)-N(4)-C(21)-C(26)	100.2(3)
Fe(1)-N(4)-C(21)-C(26)	-87.8(3)
C(26)-C(21)-C(22)-C(23)	-1.3(4)
N(4)-C(21)-C(22)-C(23)	-179.8(2)

C(26)-C(21)-C(22)-C(27)	177.2(2)
N(4)-C(21)-C(22)-C(27)	-1.3(4)
C(21)-C(22)-C(23)-C(24)	-0.5(4)
C(27)-C(22)-C(23)-C(24)	-179.1(2)
C(22)-C(23)-C(24)-C(25)	1.3(4)
C(23)-C(24)-C(25)-C(26)	-0.2(4)
C(24)-C(25)-C(26)-C(21)	-1.6(4)
C(24)-C(25)-C(26)-C(30)	-179.8(3)
C(22)-C(21)-C(26)-C(25)	2.4(4)
N(4)-C(21)-C(26)-C(25)	-179.1(2)
C(22)-C(21)-C(26)-C(30)	-179.4(2)
N(4)-C(21)-C(26)-C(30)	-0.9(4)
C(23)-C(22)-C(27)-C(28)	68.3(3)
C(21)-C(22)-C(27)-C(28)	-110.2(3)
C(23)-C(22)-C(27)-C(29)	-55.3(3)
C(21)-C(22)-C(27)-C(29)	126.2(3)
C(25)-C(26)-C(30)-C(32)	-29.1(4)
C(21)-C(26)-C(30)-C(32)	152.7(3)
C(25)-C(26)-C(30)-C(31)	93.9(3)
C(21)-C(26)-C(30)-C(31)	-84.2(3)
C(6S)-O(1S)-C(3S)-C(4S)	37.6(8)
O(1S)-C(3S)-C(4S)-C(5S)	-37.0(7)
C(3S)-C(4S)-C(5S)-C(6S)	22.2(7)
C(3S)-O(1S)-C(6S)-C(5S)	-23.9(8)
C(4S)-C(5S)-C(6S)-O(1S)	-1.0(7)

---

Symmetry transformations used to generate equivalent atoms:

### 5.3 X-RAY CRYSTALLOGRAPHIC ANALYSIS OF 3.34

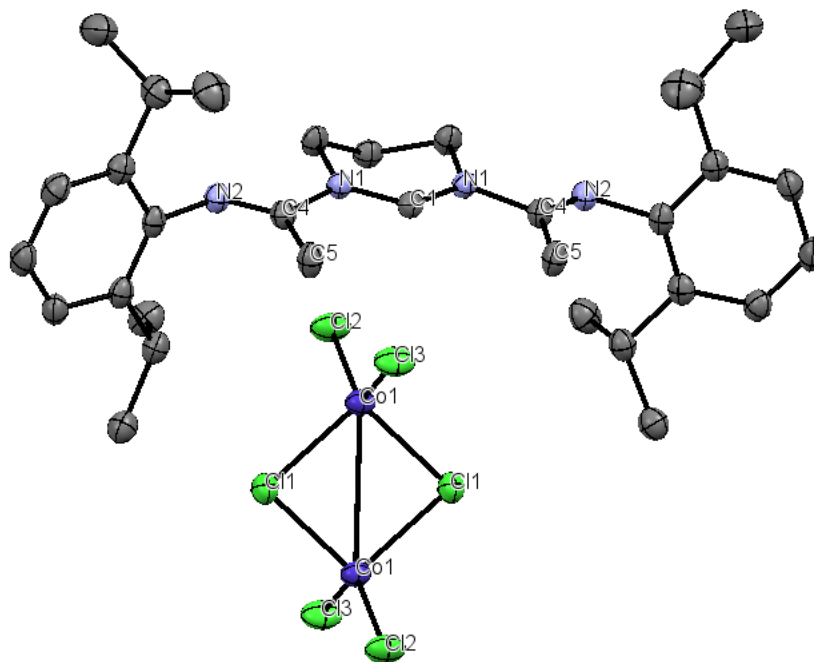


Table 1. Crystal data and structure refinement for  $\text{Co}_2\text{Cl}_6(\text{C}_{32}\text{H}_{47}\text{N}_4)_2$  (**3.34**)

Identification code	$\text{Co}_2\text{Cl}_6(\text{C}_{32}\text{H}_{47}\text{N}_4)_2$	
Empirical formula	$\text{C}_{64} \text{H}_{94} \text{Cl}_6 \text{Co}_2 \text{N}_8$	
Formula weight	1306.03	
Temperature	100(2) K	
Wavelength	1.54178 Å	
Crystal system	Orthorhombic	
Space group	Cmca	
Unit cell dimensions	$a = 31.3855(16)$ Å	$a = 90^\circ$ .
	$b = 9.1786(4)$ Å	$b = 90^\circ$ .
	$c = 23.4329(11)$ Å	$c = 90^\circ$ .
Volume	$6750.4(6)$ Å <sup>3</sup>	
Z	4	
Density (calculated)	1.285 Mg/m <sup>3</sup>	
Absorption coefficient	6.366 mm <sup>-1</sup>	
F(000)	2760	
Crystal size	0.220 x 0.060 x 0.040 mm <sup>3</sup>	
Theta range for data collection	2.816 to 66.663°.	

Index ranges	-37<=h<=37, -10<=k<=10, -27<=l<=27
Reflections collected	41549
Independent reflections	3047 [R(int) = 0.0435]
Completeness to theta = 66.663°	100.0 %
Absorption correction	Semi-empirical from equivalents
Max. and min. transmission	0.7528 and 0.5809
Refinement method	Full-matrix least-squares on F <sup>2</sup>
Data / restraints / parameters	3047 / 0 / 194
Goodness-of-fit on F <sup>2</sup>	1.027
Final R indices [ >2sigma(I)]	R1 = 0.0324, wR2 = 0.0864
R indices (all data)	R1 = 0.0365, wR2 = 0.0905
Extinction coefficient	na
Largest diff. peak and hole	0.390 and -0.164 e.Å <sup>-3</sup>

Table 2. Atomic coordinates ( $\times 10^4$ ) and equivalent isotropic displacement parameters ( $\text{\AA}^2 \times 10^3$ )

for  $\text{Co}_2\text{Cl}_6(\text{C}_{32}\text{H}_{47}\text{N}_4)_2$ .  $U(\text{eq})$  is defined as one third of the trace of the orthogonalized  $U_{ij}$  tensor.

	x	y	z	$U(\text{eq})$
Co(1)	5000	834(1)	5570(1)	25(1)
Cl(1)	4446(1)	0	5000	31(1)
Cl(2)	5000	-380(1)	6396(1)	39(1)
Cl(3)	5000	3251(1)	5499(1)	39(1)
N(1)	5371(1)	5142(2)	6641(1)	23(1)
N(2)	6092(1)	4973(2)	6572(1)	26(1)
C(1)	5000	5494(3)	6418(1)	22(1)
C(2)	5395(1)	4236(2)	7164(1)	29(1)
C(3)	5000	3312(3)	7209(1)	27(1)
C(4)	5763(1)	5485(2)	6345(1)	25(1)
C(5)	5726(1)	6391(2)	5816(1)	31(1)
C(6)	6508(1)	5190(2)	6342(1)	25(1)
C(7)	6665(1)	4253(2)	5915(1)	27(1)
C(8)	7087(1)	4428(2)	5750(1)	31(1)
C(9)	7342(1)	5500(2)	5991(1)	35(1)
C(10)	7182(1)	6398(2)	6410(1)	33(1)
C(11)	6765(1)	6249(2)	6602(1)	28(1)
C(12)	6387(1)	3052(2)	5661(1)	30(1)
C(13)	6304(1)	1857(2)	6103(1)	38(1)
C(14)	6577(1)	2357(2)	5123(1)	34(1)
C(15)	6588(1)	7206(2)	7077(1)	35(1)
C(16)	6918(1)	7580(3)	7529(1)	49(1)
C(17)	6396(1)	8593(2)	6839(1)	51(1)

Table 3. Bond lengths [Å] and angles [°] for Co<sub>2</sub>Cl<sub>6</sub>(C<sub>3</sub>H<sub>4</sub>N<sub>4</sub>)<sub>2</sub>.

---

Co(1)-Cl(3)	2.2251(8)
Co(1)-Cl(2)	2.2349(8)
Co(1)-Cl(1)	2.3206(5)
Co(1)-Cl(1)#1	2.3207(5)
Cl(1)-Co(1)#1	2.3206(5)
N(1)-C(1)	1.3175(18)
N(1)-C(4)	1.445(2)
N(1)-C(2)	1.483(2)
N(2)-C(4)	1.255(2)
N(2)-C(6)	1.425(2)
C(1)-N(1)#2	1.3175(18)
C(1)-H(1)	0.9500
C(2)-C(3)	1.505(2)
C(2)-H(2A)	0.9900
C(2)-H(2B)	0.9900
C(3)-C(2)#2	1.505(2)
C(3)-H(3A)	0.9900
C(3)-H(3B)	0.9900
C(4)-C(5)	1.498(2)
C(5)-H(5A)	0.9800
C(5)-H(5B)	0.9800
C(5)-H(5C)	0.9800
C(6)-C(11)	1.402(3)
C(6)-C(7)	1.408(3)
C(7)-C(8)	1.391(3)
C(7)-C(12)	1.526(2)
C(8)-C(9)	1.389(3)
C(8)-H(8)	0.9500
C(9)-C(10)	1.377(3)
C(9)-H(9)	0.9500
C(10)-C(11)	1.391(3)
C(10)-H(10)	0.9500
C(11)-C(15)	1.523(3)
C(12)-C(13)	1.530(3)

C(12)-C(14)	1.534(3)
C(12)-H(12)	1.0000
C(13)-H(13A)	0.9800
C(13)-H(13B)	0.9800
C(13)-H(13C)	0.9800
C(14)-H(14A)	0.9800
C(14)-H(14B)	0.9800
C(14)-H(14C)	0.9800
C(15)-C(17)	1.515(3)
C(15)-C(16)	1.521(3)
C(15)-H(15)	1.0000
C(16)-H(16A)	0.9800
C(16)-H(16B)	0.9800
C(16)-H(16C)	0.9800
C(17)-H(17A)	0.9800
C(17)-H(17B)	0.9800
C(17)-H(17C)	0.9800

Cl(3)-Co(1)-Cl(2)	124.17(3)
Cl(3)-Co(1)-Cl(1)	106.616(17)
Cl(2)-Co(1)-Cl(1)	109.532(17)
Cl(3)-Co(1)-Cl(1)#1	106.615(17)
Cl(2)-Co(1)-Cl(1)#1	109.531(17)
Cl(1)-Co(1)-Cl(1)#1	96.94(2)
Co(1)#1-Cl(1)-Co(1)	83.06(2)
C(1)-N(1)-C(4)	120.52(15)
C(1)-N(1)-C(2)	120.59(15)
C(4)-N(1)-C(2)	118.50(13)
C(4)-N(2)-C(6)	122.86(15)
N(1)#2-C(1)-N(1)	124.4(2)
N(1)#2-C(1)-H(1)	117.8
N(1)-C(1)-H(1)	117.8
N(1)-C(2)-C(3)	109.40(15)
N(1)-C(2)-H(2A)	109.8
C(3)-C(2)-H(2A)	109.8
N(1)-C(2)-H(2B)	109.8

C(3)-C(2)-H(2B)	109.8
H(2A)-C(2)-H(2B)	108.2
C(2)#2-C(3)-C(2)	110.8(2)
C(2)#2-C(3)-H(3A)	109.5
C(2)-C(3)-H(3A)	109.5
C(2)#2-C(3)-H(3B)	109.5
C(2)-C(3)-H(3B)	109.5
H(3A)-C(3)-H(3B)	108.1
N(2)-C(4)-N(1)	114.55(15)
N(2)-C(4)-C(5)	128.52(16)
N(1)-C(4)-C(5)	116.93(14)
C(4)-C(5)-H(5A)	109.5
C(4)-C(5)-H(5B)	109.5
H(5A)-C(5)-H(5B)	109.5
C(4)-C(5)-H(5C)	109.5
H(5A)-C(5)-H(5C)	109.5
H(5B)-C(5)-H(5C)	109.5
C(11)-C(6)-C(7)	122.08(16)
C(11)-C(6)-N(2)	117.30(16)
C(7)-C(6)-N(2)	120.23(16)
C(8)-C(7)-C(6)	117.47(17)
C(8)-C(7)-C(12)	121.24(17)
C(6)-C(7)-C(12)	121.24(16)
C(9)-C(8)-C(7)	121.12(18)
C(9)-C(8)-H(8)	119.4
C(7)-C(8)-H(8)	119.4
C(10)-C(9)-C(8)	120.30(18)
C(10)-C(9)-H(9)	119.8
C(8)-C(9)-H(9)	119.8
C(9)-C(10)-C(11)	121.03(18)
C(9)-C(10)-H(10)	119.5
C(11)-C(10)-H(10)	119.5
C(10)-C(11)-C(6)	117.94(18)
C(10)-C(11)-C(15)	121.53(17)
C(6)-C(11)-C(15)	120.52(16)
C(7)-C(12)-C(13)	110.56(15)

C(7)-C(12)-C(14)	113.56(15)
C(13)-C(12)-C(14)	108.94(16)
C(7)-C(12)-H(12)	107.9
C(13)-C(12)-H(12)	107.9
C(14)-C(12)-H(12)	107.9
C(12)-C(13)-H(13A)	109.5
C(12)-C(13)-H(13B)	109.5
H(13A)-C(13)-H(13B)	109.5
C(12)-C(13)-H(13C)	109.5
H(13A)-C(13)-H(13C)	109.5
H(13B)-C(13)-H(13C)	109.5
C(12)-C(14)-H(14A)	109.5
C(12)-C(14)-H(14B)	109.5
H(14A)-C(14)-H(14B)	109.5
C(12)-C(14)-H(14C)	109.5
H(14A)-C(14)-H(14C)	109.5
H(14B)-C(14)-H(14C)	109.5
C(17)-C(15)-C(16)	109.75(19)
C(17)-C(15)-C(11)	111.06(18)
C(16)-C(15)-C(11)	112.95(17)
C(17)-C(15)-H(15)	107.6
C(16)-C(15)-H(15)	107.6
C(11)-C(15)-H(15)	107.6
C(15)-C(16)-H(16A)	109.5
C(15)-C(16)-H(16B)	109.5
H(16A)-C(16)-H(16B)	109.5
C(15)-C(16)-H(16C)	109.5
H(16A)-C(16)-H(16C)	109.5
H(16B)-C(16)-H(16C)	109.5
C(15)-C(17)-H(17A)	109.5
C(15)-C(17)-H(17B)	109.5
H(17A)-C(17)-H(17B)	109.5
C(15)-C(17)-H(17C)	109.5
H(17A)-C(17)-H(17C)	109.5
H(17B)-C(17)-H(17C)	109.5

Symmetry transformations used to generate equivalent atoms:

#1  $-x+1,-y,-z+1$  #2  $-x+1,y,z$

Table 4. Anisotropic displacement parameters ( $\text{\AA}^2 \times 10^3$ ) for  $\text{Co}_2\text{Cl}_6(\text{C}_{32}\text{H}_{47}\text{N}_4)_2$ . The anisotropic

displacement factor exponent takes the form:  $-2p^2 [ h^2 a^*2U^{11} + \dots + 2 h k a^* b^* U^{12} ]$

	U <sup>11</sup>	U <sup>22</sup>	U <sup>33</sup>	U <sup>23</sup>	U <sup>13</sup>	U <sup>12</sup>
Co(1)	31(1)	24(1)	21(1)	1(1)	0	0
Cl(1)	24(1)	36(1)	32(1)	-1(1)	0	0
Cl(2)	56(1)	40(1)	22(1)	4(1)	0	0
Cl(3)	59(1)	25(1)	32(1)	-2(1)	0	0
N(1)	21(1)	27(1)	22(1)	3(1)	1(1)	0(1)
N(2)	22(1)	28(1)	28(1)	4(1)	0(1)	-1(1)
C(1)	23(1)	21(1)	22(1)	1(1)	0	0
C(2)	25(1)	37(1)	23(1)	10(1)	-1(1)	2(1)
C(3)	31(1)	29(1)	23(1)	5(1)	0	0
C(4)	23(1)	25(1)	27(1)	2(1)	1(1)	-1(1)
C(5)	22(1)	36(1)	33(1)	12(1)	2(1)	1(1)
C(6)	21(1)	28(1)	28(1)	10(1)	-2(1)	2(1)
C(7)	24(1)	28(1)	28(1)	8(1)	-4(1)	2(1)
C(8)	25(1)	38(1)	30(1)	3(1)	-1(1)	4(1)
C(9)	21(1)	49(1)	34(1)	6(1)	1(1)	-4(1)
C(10)	27(1)	37(1)	34(1)	4(1)	-3(1)	-8(1)
C(11)	27(1)	29(1)	29(1)	7(1)	-1(1)	-1(1)
C(12)	25(1)	32(1)	32(1)	4(1)	-4(1)	-1(1)
C(13)	42(1)	32(1)	40(1)	5(1)	-4(1)	-8(1)
C(14)	31(1)	34(1)	35(1)	2(1)	-4(1)	1(1)
C(15)	32(1)	33(1)	39(1)	-1(1)	4(1)	-5(1)
C(16)	47(1)	61(1)	40(1)	-13(1)	3(1)	-2(1)
C(17)	54(1)	38(1)	61(2)	-3(1)	3(1)	5(1)

Table 5. Hydrogen coordinates ( $\times 10^4$ ) and isotropic displacement parameters ( $\text{\AA}^2 \times 10^{-3}$ ) for  $\text{Co}_2\text{Cl}_6(\text{C}_{32}\text{H}_{47}\text{N}_4)_2$ .

	x	y	z	U(eq)
H(1)	5000	6038	6074	27
H(2A)	5419	4871	7504	34
H(2B)	5650	3603	7149	34
H(3A)	5000	2577	6900	33
H(3B)	5000	2789	7578	33
H(5A)	6011	6608	5668	46
H(5B)	5578	7304	5906	46
H(5C)	5563	5855	5527	46
H(8)	7204	3804	5466	37
H(9)	7628	5615	5867	42
H(10)	7359	7131	6571	39
H(12)	6107	3492	5556	36
H(13A)	6575	1396	6209	57
H(13B)	6113	1124	5940	57
H(13C)	6172	2286	6443	57
H(14A)	6644	3120	4844	50
H(14B)	6371	1676	4958	50
H(14C)	6838	1830	5223	50
H(15)	6354	6651	7269	42
H(16A)	7137	8211	7362	74
H(16B)	7051	6682	7669	74
H(16C)	6780	8088	7847	74
H(17A)	6615	9134	6628	76
H(17B)	6288	9195	7153	76
H(17C)	6161	8347	6581	76

Table 6. Torsion angles [°] for Co<sub>2</sub>Cl<sub>6</sub>(C<sub>32</sub>H<sub>47</sub>N<sub>4</sub>)<sub>2</sub>.

---

C(4)-N(1)-C(1)-N(1)#2	175.52(16)
C(2)-N(1)-C(1)-N(1)#2	2.8(3)
C(1)-N(1)-C(2)-C(3)	25.6(2)
C(4)-N(1)-C(2)-C(3)	-147.22(16)
N(1)-C(2)-C(3)-C(2)#2	-52.9(3)
C(6)-N(2)-C(4)-N(1)	179.81(15)
C(6)-N(2)-C(4)-C(5)	-0.2(3)
C(1)-N(1)-C(4)-N(2)	-173.45(18)
C(2)-N(1)-C(4)-N(2)	-0.6(2)
C(1)-N(1)-C(4)-C(5)	6.6(3)
C(2)-N(1)-C(4)-C(5)	179.46(16)
C(4)-N(2)-C(6)-C(11)	101.5(2)
C(4)-N(2)-C(6)-C(7)	-85.5(2)
C(11)-C(6)-C(7)-C(8)	-1.1(3)
N(2)-C(6)-C(7)-C(8)	-173.66(15)
C(11)-C(6)-C(7)-C(12)	176.58(16)
N(2)-C(6)-C(7)-C(12)	4.0(2)
C(6)-C(7)-C(8)-C(9)	-0.8(3)
C(12)-C(7)-C(8)-C(9)	-178.46(17)
C(7)-C(8)-C(9)-C(10)	1.2(3)
C(8)-C(9)-C(10)-C(11)	0.4(3)
C(9)-C(10)-C(11)-C(6)	-2.2(3)
C(9)-C(10)-C(11)-C(15)	178.17(17)
C(7)-C(6)-C(11)-C(10)	2.5(3)
N(2)-C(6)-C(11)-C(10)	175.34(15)
C(7)-C(6)-C(11)-C(15)	-177.80(16)
N(2)-C(6)-C(11)-C(15)	-5.0(2)
C(8)-C(7)-C(12)-C(13)	108.4(2)
C(6)-C(7)-C(12)-C(13)	-69.2(2)
C(8)-C(7)-C(12)-C(14)	-14.4(2)
C(6)-C(7)-C(12)-C(14)	168.03(16)
C(10)-C(11)-C(15)-C(17)	88.8(2)
C(6)-C(11)-C(15)-C(17)	-90.8(2)
C(10)-C(11)-C(15)-C(16)	-35.0(3)

C(6)-C(11)-C(15)-C(16)

145.36(19)

---

Symmetry transformations used to generate equivalent atoms:

#1  $-x+1, -y, -z+1$  #2  $-x+1, y, z$